UC Berkeley
UC Berkeley Electronic Theses and Dissertations

Title

Total Synthesis of (+)-6-epi-ophiobolin A and Progress Toward the Total Synthesis of Ineleganolide

Permalink

https://escholarship.org/uc/item/0bp4w9tq

Author

Thach, Danny

Publication Date

2022

Peer reviewed|Thesis/dissertation

eScholarship.org Powered by the California Digital Library
University of California

Total Synthesis of (+)-6-*epi*-ophiobolin A and Progress Toward the Total Synthesis of Ineleganolide

By

Danny Q. Thach

A dissertation submitted in partial satisfaction of the

requirements for the degree of

Doctor of Philosophy

in

Chemistry

in

the Graduate Division

of the

University of California, Berkeley

Committee in Charge:

Professor Thomas Maimone, Chair
Professor Richmond Sarpong
Professor John Dueber

Spring 2022

Abstract

Total Synthesis of (+)-6-*epi*-ophiobolin A and Progress Toward the Total Synthesis of Ineleganolide

by

Danny Q. Thach

Doctor of Philosophy in Chemistry

University of California, Berkeley

Professor Thomas Maimone, Chair

The ophiobolin sesterterpenes are notable plant pathogens which have recently elicited significant chemical and biological attention because of their intriguing carbogenic frameworks, reactive functionalities, and emerging anticancer profiles. In Chapter 1, a 14-step total synthesis of (+)-6-*epi*-ophiobolin A is disclosed. This work demonstrates a streamlined synthetic platform to complex ophiobolins from (–)-linalool by leveraging the disparate termination modes of a radical polycyclization cascade for divergent elaboration and functionalization.

In Chapter 2, the synthetic studies toward the polycyclic norcembranoid diterpene natural product ineleganolide is described. The synthetic strategy employs a Liebeskind-Srogl coupling to unite (–)-linalool- and (–)-perillaldehyde-derived fragments followed by sequential Ueno-Stork radical cyclization and intramolecular etherification to forge the 5,5,5,6 tetracyclic core of ineleganolide. Subsequent efforts to construct the pentacyclic core of ineleganolide are disclosed. Efforts to advance the late-stage intermediate to the natural product are currently ongoing.

Tables of Contents

Chapter 1: Total Synthesis of (+)-6-*epi*-ophiobolin A……1
1.1 Background and Isolation……..……..2
1.2 Biological Activity……3
1.3 Biosynthesis……...3
1.4 Previous Syntheses……6
1.5 Challenges Associated with the Synthesis of (+)-6-*epi*-ophiobolin A……8
1.6 Synthetic Strategy…….…..9
1.7 Total Synthesis of (+)-6-*epi*-ophiobolin A……11
1.7.1 Correcting the C2–C3 Relative Stereoconfiguration……..…….11
1.7.2 Synthesis of the 5-8-5 Ophiobolin Core……..14
1.7.3 Construction of the Spirocyclic-THF Ring and Completion of the Synthesis……..……15
1.8 Conclusion……19
1.9 Distribution of Credit……20
1.10 References……..21
1.11 Experimental Procedures and Characterization Data……..24

Chapter 2: Total Synthesis of (+)-6-*epi*-ophiobolin A……65
2.1 Background and Introduction……...……66
2.1.1 A Brief Overview of Furanocembranoid Natural Products……66
2.1.2 Isolation and Biological Activity of Ineleganolide……67
2.2 Biosynthesis……...…….…68
2.2.1 Biosynthesis of Furanocembranoid Diterpenes and Norditerpenes……68
2.2.2 Biosynthesis of Polycyclic Furanobutenolide Cembranoids and Norcembranoids……69
2.3 Previous Synthetic Efforts Toward Ineleganolide and Related Norcembranoids…….72
2.3.1 Pattenden's Biomimetic Semisynthesis of Ineleganolide and Sinulochmodin C……72
2.3.2 Vanderwal's Synthetic Studies Toward Ineleganolide. ……73
2.3.3 Stoltz's Synthetic Studies Toward Ineleganolide……..75
2.4 Strategic Considerations and Retrosynthesis……78
2.4.1 Strategic Design Principles……78
2.4.2 Retrosynthesis……79
2.5 Synthetic Studies Toward Ineleganolide……...…80
2.5.1 Application of the Oshima-Utimoto Reaction.……..80
2.5.2 Alternative Strategy to Access Diene Intermediate 2.301……..…86
2.5.3 Evaluation of a Liebeskind-Srogl Coupling Strategy……..…89
2.6 Conclusion……..103
2.7 Distribution of Credit……..103
2.8 References……..104
2.9 Experimental Procedures and Characterization Data…….108

Acknowledgments

Throughout my graduate studies, I have been blessed with the greatest support group a person could ask for. I am still not sure what I have done to deserve such great people in my life, but I am beyond thankful for each and every person who has been there for me through this journey. It really took a village to reach the end but I can confidently say that *"going down within this ship I couldn't have a better crew to travel with".*

Tom: I wish to express my deepest gratitude to you for dealing with me over the past 6 years. I know I may not have been the easiest student to deal with, but I am truly honored to have been under your guidance during my Ph.D. You have cultivated a research group which fosters excellence, creativity, and passion both inside and outside the laboratory and I genuinely believe there is no comparable environment for the development of scientists. Thank you for always being patient with me and, in the cases where I really needed it, pushing me to reach my potential. In the end, I couldn't imagine becoming the scientist and person I am today without you and for that I thank you.

I would like to pay special thanks to my teammates on the ophiobolin and cembranoid projects.

Dr. Zach Brill: You still are one of the most intelligent and unique people I've ever met. Thank you for defending me when people doubted me. You are going to have a bright future in industry or anything else you set your mind to. I wish you and Steph the best!

Dr. Huck (Huckyboo) Grover: The man who never sleeps. You are very likely the nicest and hardest working person I have ever had the pleasure of meeting (and you look like a normal guy…*for a vegetarian*). Thank you for putting up with me that first year, and I'm sorry for flooding 909 my first week and not being there to help you clean it up. Hope to see you soon!

Jordan Thompson: It was a pleasure watching you grow as a chemist over the past few years. You were truly one of the highlights in my Ph.D. Thank you for all the help at the end of the ophiobolin project and the early studies towards the cembranoids. Your resolve and work ethic will take you very far no matter what direction you chose. Good luck in your Ph.D, though I'm not sure you will need it.

Danny Huang (Lil' D): My partner in crime. First of all, I have never seen anyone eat a burrito as quickly as you. Thank you for taking the leap and joining the cembranoid project, it's been a true pleasure working with you over the past two years and watching you grow as a scientist and devolve as a human alongside me. You are one of the only people left in the group who I know can make the molecule, so "just look at it", and make the molecule already. All jokes aside you are a brilliant chemist with great insight and I look forward to seeing what the future has in store for you. *You're a real boy!*

To the Maimone group members past and present

Chi Ting: Cheers to the Maimone alumni who actually went into academia (so far). Thanks for all your help during my first year and your advice throughout the years. You were instrumental in

developing my synthetic logic. I can't help but think of you every time I see a slice of Zachary's deep dish or Papa Johns. Looking forward to seeing your groups work!

Kevin Hung: After almost 30 years on this planet, I don't think I've met anybody else like you. Here's to another 30.

Matt Condakes: The interactive Scifinder, with sass! I'd pay to see your reaction to the current group…*If it was streamed on Twitch*. Thank you for destroying me in my GRS practices and qual prep. It really did the trick and I was better because of it.

Xirui Hu: To this day I still consider you my mentor in chemistry and in life (even though you are avoiding me like the ~~plague~~ pandemic!). You can only move coasts so many times! I can't believe it's been so long since we have sat next to each other and I wish we would have worked next to each other sooner. Thank you for being there for me during my stressful times early on and calming me down. I miss our hot-pot and vodka sessions and I really hope we can live in the same city one day. 中国人喜欢.

Bingqi Tong: The man with the best poker face in the Maimone group. My condolences about having to share a room with you know who, but I'm glad it all worked out in the end. I'm still sorry about hitting you in the head with my flip flop during the holiday party – I still haven't found that single flop. I'm glad to hear you're doing well in Boston, you of all people deserve a bit of rest and relaxation. Thank you for our wonderful chemistry conversations and for listening to my rants over the years.

Karl Haelsig: My Taco Bell companion and generous donor of meals and booze. It's funny looking back at how we would butt heads in the early days, but I can confidently say now that all the pent up chemistry rage (and degeneracy) has bonded us for life. You have taught me so much about chemistry and life since my time here. I'll never forget you punching my fire extinguisher before immediately doing Forrest Gump impressions from the bottom of a trashcan. Thanks for being a great friend and for forcing me to watch a variety of terrible but surprisingly good movies. Though I don't know if I'll ever finish Lord of the Rings. You have taught me that with hardwork, perseverance, and a lot of 4 loko's anything is possible. Don't forget to facetime me to show me your new chinos!

Claire Harmange Magnani: Not having you around this last year has been miserable. The two of us played the bad cop/bad cop duo very well for the past 5 years. I hope you, Christopher, and Julien are doing well in the east coast!

Rachel Rosen: You are very nice lady. Thank you for always being there for me. I was a huge angry mess the first few years and a huge stress ball my last few years but you somehow put up with all of that and found a way to save me from myself. You are one of the most caring people I know and words cannot express how much you mean to me. So, with that I'll just say this: "*dibs*".

(*Insert topgunthumbsup.jpeg*)

Linus Shen: Lobster Linus, you are very interesting man. I'm sorry for screaming at you for 5 years straight. I know our time together in the Maimone lab didn't end as we would have liked,

but I like to think it wasn't totaled. I wish you the best in your future endeavors and may the traffic gods bless the roads of the Bay Area. Remember, you promised me a car in the future.

Drew and Patti Musacchio: MEHRRRR! To my significant brother Drew and my twin Patti, I will never forget all the wonderful times we shared in Berkeley. Drew, you are so hilarious. I still can't believe I first met you without your beard. I guess my brain repressed that memory. I miss all the MMA/WWE theatrics we used to have. I especially miss the time when you threw my gordita crunch into the air and I got really mad. From the Two-handed Stout® we brewed together to all the football games we watched while grilling during the year-long typhoon we had in Berkeley (2016), I will always treasure our shared love for food, drinks, football, and debauchery. I really hope we live near each other when/if Diablo 4 or Starcraft 3 comes out. To Patti, we are so similar its uncanny. You are such a big role model in my life and you (and sometimes Drew) have been here for me through some terrible times. I'm sorry I ruined Drew's pasta proposal surprise but you were going to find out eventually anyways! I couldn't have asked for a better friend and mentor. Also, thank you for giving me the underwear grant (NIGMU F32); my last week in Berkeley was brutal and I would have chafed so hard without you!

Vasil (Chad) Vasilev: Ho hoy ho hoy. You are an exceptional scientist and an even better friend. I don't know how you have put up with me for the past 5 years, but I'm thankful you have. It has been 3 years of "Dewar" jokes and we are still going strong. I'll never admit it to you, but I'm going to miss the "Oh, Danny" comments. You're going to find a lot of success in pharma and in life, and I can't wait to see it. The future is going to be *spicy*.

Beth Zhu (la): Beth. You are unequivocally the funniest person I've ever met. I can't express how proud of you I am. I have literally watched you go from learning how to TLC to making a natural product; all while becoming the most brutal and hardcore person in our group. Now that's what I call mult-tasking! When you joined, I was told you had the "heart of a lion" and after 4 years of knowing you, I have to say that was an understatement. You have a bright future ahead of you. Don't forget about our friendship when you own Wuxi.

Yi Xie: Man, did we get off on the wrong foot. I'm glad we worked it out by the end. You're a smart guy and I can see how passionate you are about chemistry. Best of luck on your project, I know you can do it! Don't forget about our friendship when Beth owns Wuxi.

Paolo Machicao: I can't understate how insane you are to leave your cushy job to go back and do a total synthesis Ph.D., but I respect it. You are such a kind human being...almost to a fault. Just remember to take care of yourself. Best of luck in 907.

Lukas Spessert: I hope you know all the jokes come from a good place. You're a good guy and a good friend. Don't sacrifice future for now. You can do both.

Dr. Helge Berneaud (broritto): "*You sweet, sweet man".* Thank you for all the homecooked meals during my first year. You are such a calm person and I will never forget all the wild nights. I still can't believe we got that tattoo but I'm so glad we did! I'm thankful that after all these years, our friendship is still as tight as your skinny jeans. I promise I will visit you in Germany at some point! Good luck in your postdoc!

Dr. Jun Xuan: Shanpowwww~, I miss talking to you about chemistry and basketball. You were a huge resource for the lab during your time here. Best of luck in your career and I can't wait to see your total synthesis papers!

Dr. Mikiko Okumura: Big black tube. I know you had your reservations about most of our group, but thanks for being a good friend to me. I love that we can just argue about chemistry and move on. Your point blank assertiveness about your opinions in chemistry is refreshing and something I think may be disappearing. Thanks for being a part time spy for us! Best of luck in your career!

Dr. Naifeng Hu: You have the patience of a monk! I think we both know what I'm talking about. You are so close to the end and I know it will work out! Best of luck with your project, you're an incredible person.

Dr. Kuan Yu: Char siu bao (just joking!), We've only known each other for a year but you're a very smart and kind person. I suspect you will have a very successful time in the Maimone group and I'm looking forward to seeing it. Thanks for the food and best wishes to you and your family.

Kincade, Shang, Vanessa, and Kelvin: Good luck with your projects! Trust the process and never give up (take your COSYs and HSQCs on your crude material!).

Luiz Novaes, **Tobi Pinkert, Malte Moeller, Marco Pierau, and Sebastian Clementson:** It feels like yesterday Luiz was extracting nimbolide, Malte was extracting ophiobolin, and Tobi was drinking straight whiskey in the group room. Marco, I was never able to clean my shoes after we wrestled on the roof of Latimer, let alone forget what your favorite grocery to eat was. Sebastian, I regret not getting to know you better. You were such a wonderful person and I was in a bad spot in my Ph.D. I'm glad you got out of that room and it seems like you're in a much better place now. Congrats on your new family!

To my Berkeley Cell Mates

Ed Miller (Spesh): I could write a whole chapter about this guy. You are one of the most weird, hilarious, infuriating, intelligent and kind people I have had the pleasure of meeting. We've spent our entire Ph.D.'s together and I wouldn't have it any other way. Thanks for always being there for me during my dark days even though you would just ignore my rants and respond with *"[smacks lips]…yeah that sucks man"* . I'm still processing the trauma of your GRS introduction.

"do you have water where you're from"
"that's a dumb looking chair"
"I'm the blackpearl….too much [redacted]for my own good"

Jeffrey S. Derrick: Even though you were "The leaky cauldron" for the first few years, I will never forget the circumstances which spurred our lifelong friendship – stall-mates in the bathroom during first year orientation. Thank you for helping me tame Ed for the past 5 years. You are one of best scientists I've ever met and I have tremendous respect for you as a friend, human being, and chemist. The image of you incapacitated for 48 hours after your qual and the time you "*squandered*" all your "*power*" in our bathroom is permanently etched into my brain. There are

too many memories to recount, and unfortunately, I can't include most of your quotes if I want to graduate. Never forget the *Brita Fiasco* of 2016. Good luck at Merck and I'll be seeing you in NJ!

Trevor Roberts: Even though your palette was completely unrefined when I first met you, I knew you were a great human being. I will never forget walking into Spatz's restroom to see you watery-eyed staring at your airpods in the toilet. My knee has permanent scar-tissue from that day, and because of that I'll relive that moment every time I sit or stand. Thank you for being Mr. Stinky's father in my place. Your life is going to improve dramatically in San Diego and I am beyond happy for you! The next time we see each other it'll be a *"barn fight"*!

John Lee: To our honorary roommate, even though you have an *American* name you are the definition of a loyal and kind friend. Thank you for all the vodka/coke-zero nights and for not charging interest on the trips I owe you for (still). Thank you for putting up with me and my living situation this past year. You are truly a wonderful person and I know you are going to achieve everything you want in life (not sure about quitting the vape though).

"Holy [redacted] dude, I'm [redacted]!"

Cindy Hong: Mama Hong, thank you for being there for me as a friend when I was in the pits (over and over again). Our love for kimchi soup, taco bell, and binge drinking has united us forever. Because of you, I gag when I see a mimosa. Looking forward to seeing you in NJ!

Eugene Kapustin: "*Vaha-ppened to my acknowledgment?*" John Lee told me not to include you in the acknowledgment. Cyka!

David Dunsky: The J.Crew model himself. Living with you my first year was a true blessing. You are an incredible person and friend. I'm still not sure what possessed you to choose me as your friend, but I'm thankful every day that we are in each other's lives. Best of luck finding *"Jewish Brisket"* in NYC, you deserve nothing but the best in life.

Suhong Kim: You are an incredibly bright and driven scientist and it has been a pleasure to be your friend over the years. I look forward to hanging out with you in NJ!

Steven Hanna: I will never forget the times we fixed the pressure reactor in the catalysis center at 3AM…only for it to break as soon as we left the room. Thank you for giving me all the Hartwig phosphine ligands and our discussions about hydroformylation reactions.

Dom Wong: Thank you for taking me in like family during the first several years. *The Daily Pint*, may it rest in peace, was my (and many others) escape from the stresses of grad school. I will never forget all the late nights of beer and good food with you. I wish you and your family the best and hopefully we can grab some Café Su Da in the future!

Hasan Celik: I'll miss our conversations about the NFL and life. Best of wishes to you and your family.

Mazda CX-5 (Cardi B): What a journey this last year has been. We tried our best but I guess that's life. I'll likely never forget this past year.

To my mentors at UT Austin

John Thompson and **Yan Xu:** Without the two of you, I can honestly say I wouldn't be the chemist I am now. Thank you for providing me with perspective, training, and a passion for science.

Tao Xu: To Professor Buzzed Chemist, your advice about graduate school was simultaneously great and terrible. I can't wait to visit you in Tsingtao and pop open that cigar you've been saving me. I'll bring the Live Oak!

To my Family and Friends

To my Family: Thank you for always being there for me during this journey. It's crazy to imagine that 28 years ago, we had to choose between food or shelter. Fast forward to the present and we have surpassed our family's wildest expectations. Mom, Dad, Patrick and Karen, thank you for sacrificing everything for decades to get me to this point. I can't say it all worked out the way we imagined but I can confidently say it worked out. Mom and Dad, every day that goes by I'm amazed you have held on this long to see my complete my Ph.D. I'm sorry I put my studies before family for the most of my Ph.D., but I'm glad you can see the fruits of your labor.

Cong, Don, Kevin, and Angie: To my second family, thank you for being there for me through thick and thin. Not a day has gone by where I didn't think about the wonderful friendships I have with y'all. We made it out of the hood together and in the process have formed an unbreakable bond (*chemistry pun*). I will never forget where we came from and I have a feeling neither will you. We have a long and bright future ahead of us, so let's go get this bag.

James and Tam: James you have been a mentor and brother to me since my time at UT. You are a brother to me and words cannot describe how much of a positive influence you have been on me. You and Tam are too good to me and I can't underscore how much you guys mean to me. I have a feeling our friendship will continue to grow for the foreseeable future.

Wei and Saad: Graduate school has undoubtedly changed me, but I'm glad you guys are still great people who I have the honor of calling friends. Congrats on all your successes.

Minh Phamily: I haven't been able to see you much over the past six years but every time I'm home it's like we're back in high school again. Hopefully we can see more of each other in the future.

Jessica, Jennifer, and Vincent: As much as we joke about how we hate each other and are trying to distance ourselves, it warms my heart that our friendship has lasted this long. I'm sure our friendship will continue to get stronger...from a distance.

List of Abbreviations

4ÅMS	4 Å molecular sieves
ABSA	4-Acetamidobenzenesulfonyl azide
Ac	acetate
Acac	acetylacetone
AIBN	azobisisobutyronitrile
BHT	butylated hydroxytoluene
bpy	bipyridine
BRSM	Based on recovered starting material
Bz	benzoyl
CAN	cerium ammonium nitrate
COD	cyclooctadiene
CSA	camphorsulfonic acid
dba	dibenzylideneacetone
DCC	*N,N'*-dicyclohexylcarbodiimide
DCE	dichloroethane
DCM	dichloromethane
DDQ	2,3-Dichloro-5,6-dicyano-1,4-benzoquinone
DEAP	diethyl allyl phosphate
DIBAL	diisobutylaluminum hydride
DMA	dimethylacetamide
DMAP	dimethylamino pyridine
DMAPP	dimethylallyl pyrophosphate
DME	dimethoxyethane
DMP	Dess-Martin periodinane
DMS	dimethyl sulfide
DMSO	dimethyl sulfoxide
dtbpy	di-*tert*-Butyl bipyridine
ent	enantiomeric
EtH	ethyl-hexanoate
EVE	ethyl vinyl ether
Fur	furyl
HG	Hoveyda-Grubbs
HMPA	bis(trimethylsilyl)amide
HRMS	high-resolution mass spectrometry
IBX	2-iodoxybenzoic acid
IPP	isopentenyl pyrophosphate
KHMDS	potassium bis(trimethylsilyl)amide
LAH	Lithium aluminum hydride
LDA	lithium diisopropylamine
LED	light emitting diode
LHMDS	lithium bis(trimethylsilyl)amide
m-CPBA	*meta*-chloroperoxybenzoic acid
MeCN	acetonitrile

MsCl	Methanesulfonyl chloride
TsCl	4-Toluenesulfonyl chloride
Naph	naphthalenide
NBS	*N*-bromosuccinimide
NIS	*N*-iodosuccinimide
Phen	1,10-phenanthroline
PhMe	toluene
PIDA	(diacetoxyiodo)benzene
PIFA	(Bis(trifluoroacetoxy)iodo)benzene
PPTS	pyridinium p-toluenesulfonate
pyr	pyridine
RCM	ring closing metathesis
TBAF	tetrabutylammonium fluoride
TBHP	*tert*-butyl hydroperoxide
TBS	*tert*-butyldimethylsilyl
Tc	thiophene-2-carboxylate
TEMPO	(2,2,6,6-Tetramethylpiperidin-1-yl)oxyl
Tf	Triflate or trifluoromethanesulfonate
THF	tetrahydrofuran
TLC	thin layer chromatography
TMP	2,2,6,6-Tetramethylpiperidine
TMS	trimethylsilyl
TMSCN	trimethylsilylcyanide
TPP	tetraphenylporphyrin
TsOH	*p*-Toluenesulfonic acid

Chapter 1

Total Synthesis of (+)-6-*epi*-ophiobolin A

Chapter 1

Total Synthesis of (+)-6-*epi*-ophiobolin A

1.1 Background and Isolation

Terpenoids represent the largest and most diverse group of naturally occurring small molecules with more than 80,000 unique members identified to date.[1] Despite the vast chemical diversity present within the terpene chemical space, these natural products all arise from the enzymatic assembly of simple C_5-units and subsequent oxidative tailoring. Compared to prominent (C_{10})-mono-, (C_{15})-sesqui-, (C_{20})-di-, and (C_{30})-tri-terpene natural products, C_{25}-sesterterpenes are among the rarest group of terpenoids comprising roughly only 2% of known members (slightly more than 1000 have been characterized).[2]

The sesterterpenoids are derived from enzymatic cyclization of C_{25}-geranylfarnesyl pyrophosphate (GFPP). These natural products are typically isolated from fungi, bacteria, plants, insects, and marine organisms, and induce a wide array of biological activities including antibacterial, antifungal, antinematodal, and anticancer activity.[3-5] As a result of the structural complexity and intriguing biological profiles, this class of terpenoids has historically attracted considerable attention from the biological and synthetic communities.

The ophiobolins are a class of sesterterpene metabolites typified by a 5-8-5 tricyclic skeleton and are produced predominantly by pathogenic fungi of the genera *Bipolaris, Drechslera* and *Aspergillus.*[3] These fungal pathogens are associated with the brown spot disease found on rice and were responsible for the potato and corn blight epidemics of 1943 and 1972, respectively.[6-8] In 1957 Orsenigo and coworkers isolated ophiobolin A (**1.1**), the first naturally occurring sesterterpene.[9] Nearly a decade later, Nozoe and coworkers disclosed the structure of ophiobolin

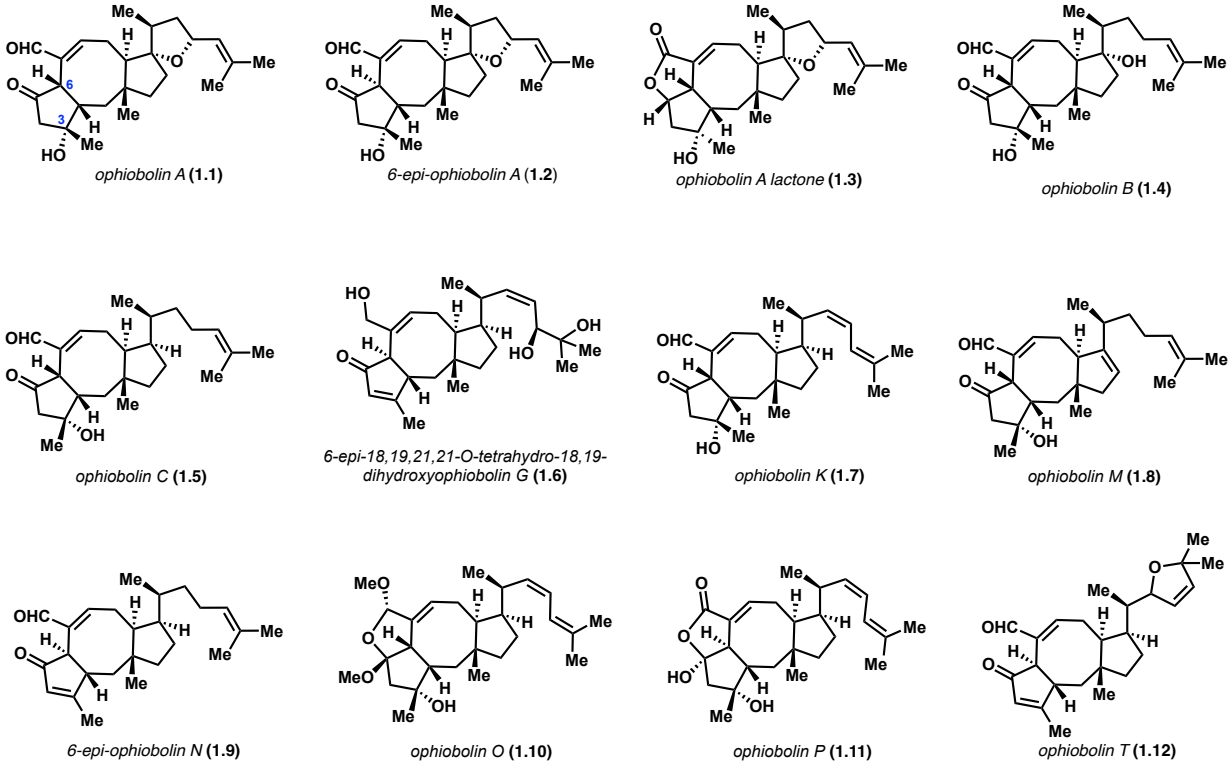


Figure 1: Structural Diversity of the Ophiobolins

A which was unambiguously assigned by X-ray crystallographic analysis of an intermediate resulting from the bromoetherification of the pendant alkene side chain.[10]

In 1984, (+)-6-*epi*-ophiobolin A (**1.2**) was isolated from the fungal pathogen *Bipolaris sp*. by the Kim group.[11] Three years later, the groups of Canales and Gray isolated **1.2** alongside 3-anhydro-6-*epi*-ophiobolin A from *Drechslera Maydis* as part of an effort to identify the toxins involved in the South corn leaf blight of 1972.[12]

Throughout the ophiobolin family of natural products there exists a conserved 5-8-5 tricyclic core bearing the same relative stereochemical configurations at the C2, C10, C11, C14 and C15 centers. Notably, although the core skeleton of the ophiobolins is conserved, the ophiobolins often possess a variety of side chain oxidation patterns. Additionally, the C21 position can exist in the alcohol, aldehyde, or carboxyl oxidation state. Lastly, many ophiobolins are found with a member epimeric at C6, and many exist with or without the C3 hydroxyl group.[5]

Initially studied due to ophiobolin A's promising phytotoxic profile, the ophiobolin natural products, which now comprises over 50 members, are now known to inhibit the growth of a variety of human cancer cells among a variety of other biological properties.[3, 4, 13, 14]

1.2 Biological Activity

Structurally diverse ophiobolins possess a wide array of biological activities. For example, ophiobolin C (**1.5**), K (**1.7**), and M (**1.8**) possess strong nematocidal activity, whereas ophiobolin P (**1.11**) and T (**1.12**) show anti-bacterial properties (see Figure 1).[3, 5, 13] Although most ophiobolins exhibit some biological activity, ophiobolin A remains the flagship member of this ever-growing family of sesterterpene natural products due to its marked anticancer activity[15-18] and phytotoxic, antimicrobial,[19] and anti-inflammatory[20] properties. Notably, ophiobolin A has been identified as a strong antagonist of calmodulin and induces non-apoptotic cell death in Glioblastoma cells,[16] while ophiobolin O possesses anti-proliferative effect on breast cancer cells.[21]

Early studies revealed that ophiobolin A is an inhibitor of calmodulin-dependent cyclic nucleotide phosphodiesterase in both bovine brain calmodulin and plants.[22] Subsequent UV-spectroscopic studies by Au revealed that the interaction of ophiobolin A and calmodulin results in the formation of a new chromophore, likely the result of Schiff base formation between a lysine residue of calmodulin and the 1,4-dicarbonyl moiety of ophiobolin A. Site-directed mutagenesis studies on calmodulin identified the specific lysine residue (Lys 75) in calmodulin crucial to the inhibitory effects of ophiobolin A.[23] These initial findings led to the hypothesis that OPA-induced cell death arises via the inhibition of calmodulin.

More recently, ophiobolin A was screened against a panel of 60-cell lines as part of a search for new anticancer agents by the National Cancer Institute (NCI). The NCI-60 panel of cell lines, which includes breast cancer, melanoma, glioma, and leukemia cells, provided mean concentrations resulting in 50% growth inhibition (GI_{50}) of 72 nM.[13] Whereas the mean concentrations resulting in 50% lethality (LC_{50}) was shown to be 629 nM.[17] Importantly, comparing the LC_{50} data reported by the NCI-60 to the calmodulin mRNA expression levels for the same cell lines shows no correlation between calmodulin mRNA expression and the toxicity of ophiobolin A.[17] These findings suggest that although ophiobolin A does indeed inhibit calmodulin, it is likely not the sole biological target that leads to its anticancer activity.

In 2013, Kiss and coworkers reported ophiobolin A's potent antiproliferative effects against glioblastoma multiforme, a highly aggressive and lethal form of brain cancer due to the tumor cells' resistance to apoptotic cell death mechanisms.[16] The inhibitory effects of ophiobolin

A on glioblastoma cell function were postulated to result from membrane vacuolization and decreased large-conductance potassium activated calcium channel activity.

Kornienko and coworkers disclosed a study which showed that the condensation of benzyl amine and ophiobolin leads to the formation of a pyrrole-ophiobolin adduct which is biologically inactive.[18] However, the formation of a bis-ketal adduct of ophiobolin A does not inhibit its anticancer activity likely due to the ability of the bis-ketal to unveil the 1,4 dicarbonyl moiety.[18] Kornienko postulated that the Paal-Knorr reactivity of ophiobolin on lysine residues of proteins may explain the biological activity of ophiobolin A.

Subsequent genetic studies by O'Shea and coworkers revealed that inactivation of the pathways involved in the biosynthesis of phosphatidylethanolamine (PE) suppressed ophiobolin A's biological activity (Figure 2).[24] The authors posit that the PE-OPA pyrrole adduct would result in the conversion of the small/polar head group of membrane bound PE to a hydrophobic/bulky group that can disrupt and destabilize the cellular bilayers and lead to cell leakage and ultimately paraptosis-like cell death. This hypothesis finds credence in subsequent experiments which showed that liposomes composed of only phosphatidylcholine (PC) instead of PE lead to no disruption of the lipid bilayer or leakage.

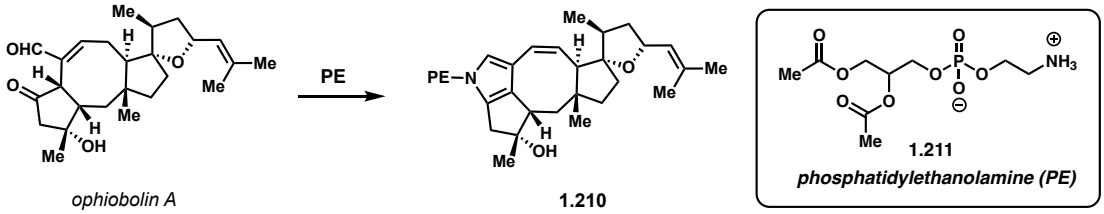


Figure 2. Paal-Knorr Condensation of ophiobolin A with phosphatidylethanolamine (PE)

In 2017, Kiss and coworkers expanded on their previous study, which showed that ophiobolin A could induce paraptosis-like cell death associated with vacuolization in glioblastoma cells, by providing evidence in support of their previous hypothesis that ophiobolin A leads to the physical swelling of the endoplasmic reticulum (ER) and mitochondria and results in vacuolization of glioma, breast, and cervical cancer cells.[17]

Taken together, the studies by Kiss, Kornienko, and O'Shea suggest that the process of cancer cell death likely proceeds through enlargement of the mitochondria and endoplasmic reticulum (ER) due to disruption of the membrane lipid bilayers resulting in paraptosis-like cell death, a non-apoptotic cell death associated with ER-vacuolization. [13, 16-18, 24-29] In all of these studies, the reactive aldehyde groups is suspected as the key pharmacophore of the natural product.

Additionally, the Najumudeen group discovered that covalent inhibition of calmodulin (via Schiff Base or pyrrole formation) leads to disruption of K-ras4B/calmuodulin interactions and results in cancer stem cell (CSC) inhibition.[30] It is understood that cancer stem cell inhibition has a direct role on cancer therapy remission.[31] In the same vein, given the fact that the Ras-nanoclusters occur on lipid membrane platforms possessing approximately 20% phosphatidylethanolamine, the interaction of ophiobolin A with intermembrane PE, in conjunction with calmodulin inhibition dependent K-ras clustering could lead to the observed anti-cancer stem cell activity of **1.1** and is consistent with the aforementioned cellular effects of ophiobolin A on the ER and mitochondria. These findings suggest that **1.1** may serve as a new agent to prevent cancer therapy remission.

Lastly, a recent study by the Choi group suggests that ophiobolin A may covalently modify free thiol groups, such as glutathione, likely via thio-Michael addition to the α,β-unsaturated aldehyde moiety of **1.1**.[32] In this scenario, the covalent modification of cysteine residues on proteins could then lead misfolding of proteins in the ER, leading to ER stress and dilation and ultimately paraptosis-like to cell death.

Although ophiobolin C which lacks the C14 oxidation is inactive, **1.2** possesses analogous phytotoxic and cytotoxic effects to **1.1**. Notably, studies have shown that **1.2** is less potent than its epimeric congener ophiobolin A. It has been hypothesized that this discrepancy in potency arises due to the slower rates of pyrrole formation for **1.2** compared to **1.1**, but this has not been proven or studied to date. To this end, the relationship between **1.2** and **1.1** and their cytotoxic effects appears to be cell line specific.

1.3 Biosynthesis

In 2013, as part of a fungal genome mining expedition, the Oikawa group identified the first gene cluster associated with a sesterterpene synthase.[33] Using characteristic sequences from the fusicoccadiene synthase (PaFS), a related natural product possessing a 5-8-5 tricycle, they were able to apply bioinformatics analysis to identify that the *A. clavatus* genome encodes ophiobolin F synthase (AcOS).

The proposed biosynthesis begins with the union of DMAPP and IPP C_5-fragments via the prenyltransferase (PT) domain of AcOS to assemble the C_{25}-linear chain GFPP. At this point GFPP is preorganized within the terpene cyclase domain of AcOS and undergoes the C1–C11 cyclization reaction to provide the macrocyclic 12-geranyl-humulen-9-yl cation (**1.212**) and subsequent transannular C10–C14 cyclization to give dolabelladien-15-yl tertiary cation (**1.213**). The resultant carbocation intermediate can then undergo a 1,5-hydride shift to provide a stabilized carbocation on C8 (**1.214**). This allylic cation then undergoes another cyclization reaction to close the A-ring of the ophiobolins and thereby provide the C3 carbocation that is subsequently attacked by water to install the C3 hydroxyl group completing the biosynthesis of ophiobolin F (**1.215**), the proposed biosynthetic progenitor to all ophiobolin natural products. Oxidative tailoring of **1.215**, likely mediated by P450-monooxygenases,[34] installs the various oxidations on C5, C21, C14 and C17 to access diverse family of ophiobolin natural products. Unsurprisingly, given the acidity of

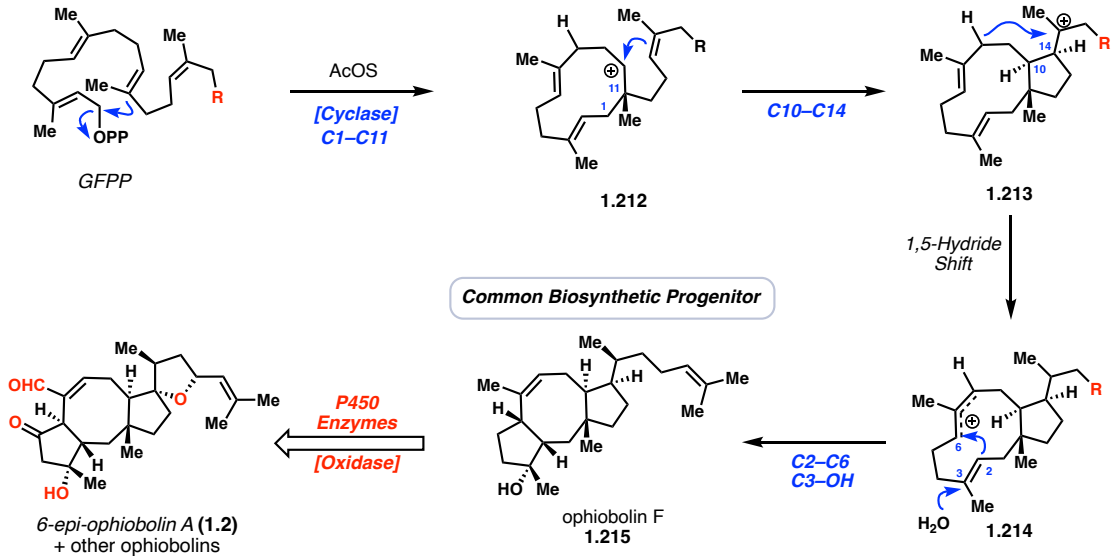


Figure 3: Biosynthesis of the Ophiobolins

the C6 C–H, throughout the ophiobolin family, many members commonly epimerize at C6 to give the "6-epi" series.

1.4 Previous Syntheses

In 1989, Kishi and coworkers disclosed a 37-step synthesis of (+)-ophiobolin C starting from cyclopentene **1.216**.[35] This compound was elaborated in a 3-step sequence to afford ketone **1.27**. A Luche reduction/acylation sequence with **1.218** followed by subjecting the resulting intermediate to elevated temperatures (230 ºC) facilitated a tandem Brook rearrangement/Ireland-Claisen rearrangement to yield **1.219** in 72% yield upon acidification. Cyclopentene **1.219** was then converted to aldehyde **1.220** in a nine-step sequence. Exposure of **1.220** to lithiate **1.221** then provided vinyl silane **1.222**. Following several functional group manipulations (steps e-h), the 5,8,5-fused tricyclic core of ophiobolin C was constructed via the use of the Nozaki–Hiyama–Kishi reaction providing tricycle **1.223** in 73% yield. Next, a 3-step sequence transposed the allylic alcohol group to arrive at intermediate **1.224**. Following silylation of the primary alcohol of **1.224**, the C3-methyl group was then installed to provide **1.225**. Finally, oxidation of the primary alcohol group followed by Wittig reaction and global deprotection/oxidation completed the synthesis of (+)-ophiobolin C (**1.5**).

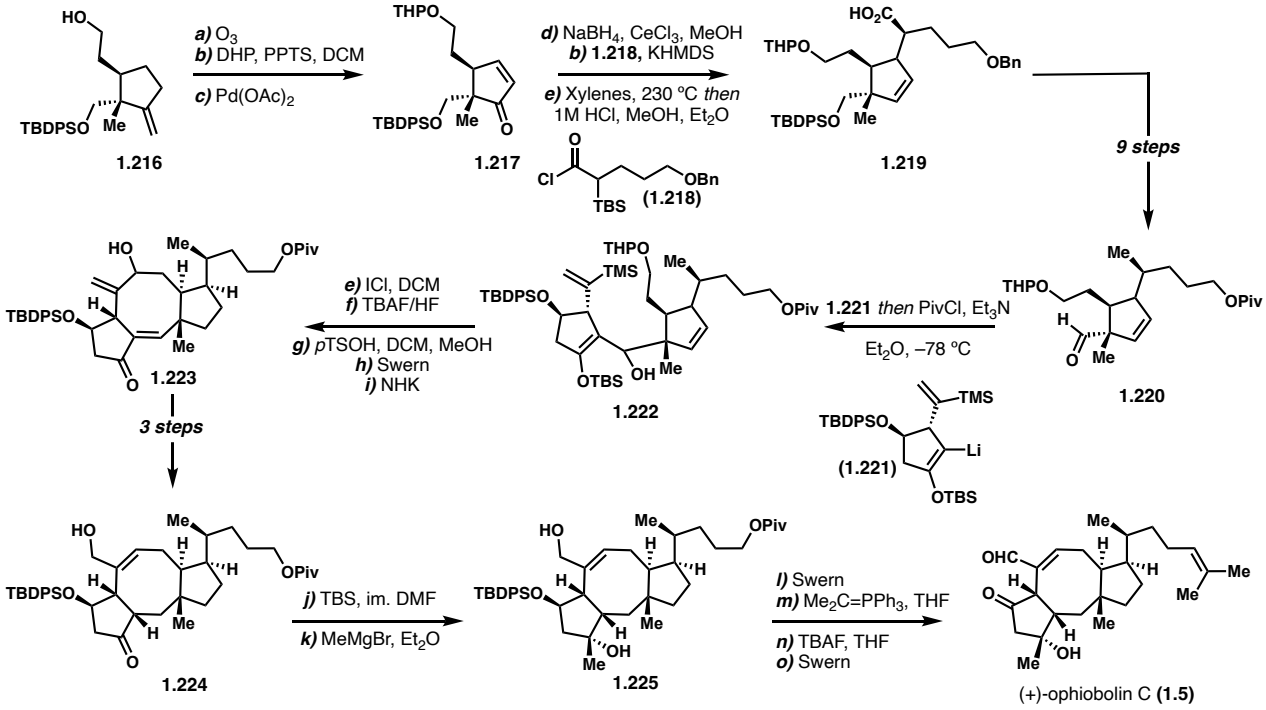


Figure 4: Kishi's Synthesis of (+)-Ophiobolin C

In 2011, Nakada and coworkers synthesized ophiobolin A starting from chiral monoester **1.225**, which was prepared via enzymatic resolution of the corresponding racemic diester.[36, 37] This material was first converted to iodide **1.226** in 15-steps. Addition of the lithiate derived from **1.226** into lactone **1.232** and subsequent Sakurai-type cyclization in the presence of BF_3•OEt_2 afforded the 5,5-fused spirocyclic compound **1.227** in 38% yield over two steps. A 4-step sequence involving hydroboration, pivoylation, deprotection, and oxidation yielded aldehyde **1.228** in 86% yield. Aldehyde **1.228** was then coupled with **1.234** and dehydrated with Burgess reagent to give

enone **1.229** in 83% yield. Enone **1.229** was then converted to homoallylic alcohol **1.230** via a 12-step sequence in 22% overall yield. Ring closing metathesis (RCM) of **1.230** followed by benzylation of the homoallylic alcohol group and cleavage of the O-TBS group afforded **1.231** in

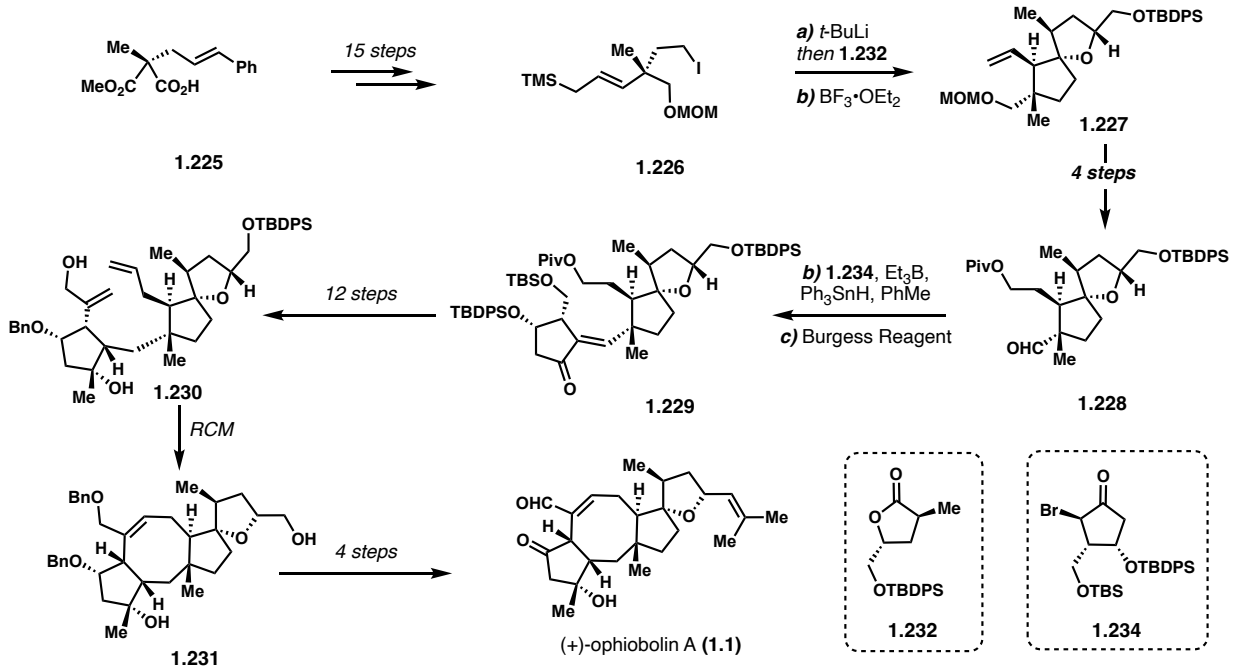


Figure 5: Nakada's Synthesis of (+)-Ophiobolin A

63% yield. Finally, installation of the isoprenyl functionality and global-deprotection/oxidation led to the natural product **1.1** in 47 overall steps.

In 2016, the Maimone group disclosed an elegant and expedient synthetic route to (–)-6-*epi*-ophiobolin N (**1.9**) in 9 steps from the monoterpene feedstocks (–)-linalool and farnesol (Figure 6).[38] Inspired by the biosynthetic processes which construct the hallmark 5-8-5 tricyclic core of the ophiobolins in one biosynthetic step, the Maimone group sought to reverse engineer this bond-forming logic to develop a strategy to access the tricyclic skeleton of the ophiobolins in rapid fashion.

This synthetic logic was borne out by the development of a radical polycyclization cascade which could forge the 8- and 5-membered rings of the tricyclic core in a single step from a monocyclic intermediate bearing the requisite side chain via an 8-*endo*/5-*exo*-trig radical cyclization cascade. Ultimately, the synthetic strategy to access the enantiomeric form of 6-*epi*-ophiobolin N relies on the union of a chiral cyclopentenone fragment derived from linalool (C_6) with a 1-carbon homologated farnesol-derived fragment ($C_{15} + C_1$) to access the radical cyclization intermediate. The proposed 8-*endo*/5-*exo*-radical polycyclization cascade then provides the 5-8-5 tricyclic core of the ophiobolins.

In the forward sense, the synthesis of (–)-6-*epi*-ophiobolin N commenced with the enantioselective cyclopropanation of farnesol using Charette's chiral dioxaborolane reagent (**1.233**),[39] followed by iodination under Appel conditions. Lithiation of the resulting iodide triggers a reductive fragmentation which, following *in-situ* transmetallation with CuI, undergoes a conjugate addition to the linalool derived cyclopentenone **1.234** (prepared in two steps) to provide a diastereomeric mixture (3:1) of diketone **1.236** following quenching of the resultant enolate with

trichloroacetyl chloride. The conjugate addition of the farnesol-derived cuprate proceeded with strong facial bias leading to predominantly the isomer arising from the nucleophilic approach *anti* to the bulky OTBS group.

It is important to note that although the diastereoselectivity of the conjugate addition is ultimately inconsequential in the synthesis of (–)-6-*epi*-ophiobolin N and other *anhydro*-ophiobolins due to the ablation of the C3 stereochemistry, the stereochemical outcome of this transformation represents a significant challenge when considering the synthesis of higher complexity ophiobolin congeners. Specifically, higher complexity ophiobolin congeners such as **1.1** and **1.2** which possess the C3-hydroxyl group require the relative C2–C3 stereochemistry present in the minor diastereomer of **1.235**. A discussion of these challenges and others will be provided in the future sections (see section 1.4).

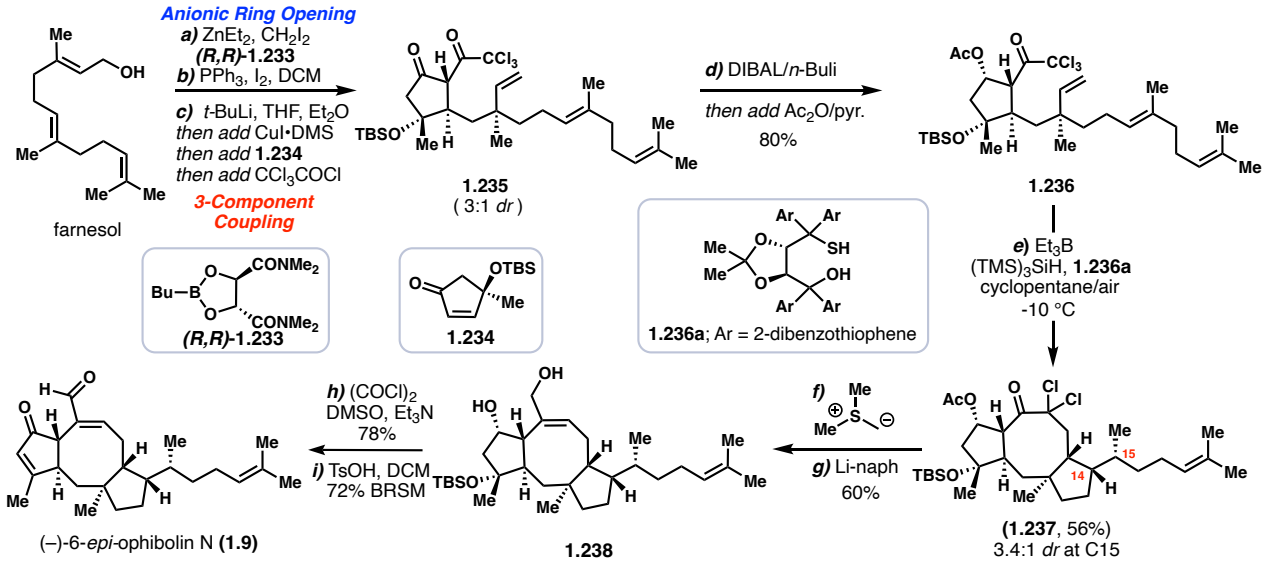


Figure 6: Maimone's Synthesis of (–)-6-*epi*-ophiobolin N

The diastereoselective reduction of the C5 carbonyl followed by *in situ* acetylation provides the radical cyclization precursor **1.236**. This intermediate was then subjected to reductive radical generating conditions which led to the 8-*endo*/5-*exo* radical cyclization cascade to form the archetypal 5-8-5-fused tricyclic core of the ophiobolins possessing the correct relative stereochemical configurations at C-10, -11, -14, and -15. Importantly, by judicious choice of reagents, termination of the C15 tertiary radical by hydrogen-atom transfer (HAT) from a chiral thiol hydrogen-atom donor (HAD, **1.236a**) led to the formation of the tricyclic intermediate possessing the correct configuration at C15 (see **1.237**, *dr* = 3.4:1).

At this juncture, all that remained was the installation of the final carbon-unit and several functional group interconversions. Corey-Chaykovsky epoxidation, reductive dechlorination with concomitant epoxide opening provided the diol intermediate **1.238**. A double Swern-oxidation followed by elimination of the C3 hydroxyl then completes the asymmetric synthesis of (–)-6-*epi*-ophioblin N (**1.9**) as the unnatural enantiomer in 9 steps from inexpensive feedstock monoterpenes.

1.5 Challenges Associated with the Synthesis of (+)-6-*epi*-ophiobolin A

As mentioned in the previous section, the application of a unique 8-*endo*/5-*exo* radical polycyclization cascade of diketone **1.236** enabled the expedient construction of the ophiobolin 5-8-5-fused tricyclic core. Several steps were needed to convert this intermediate to the unnatural

enantiomer of 6-*epi*-ophiobolin N. Although the radical cascade strategy developed served as a powerful tool for the construction of the tricyclic core, several structural and stereochemical challenges must first be addressed for the successful extension of this synthetic strategy to higher complexity congeners in their natural absolute configuration, such as (+)-6-*epi*-ophiobolin A.

First, while the polycyclization cascade enabled expedient access to the lower complexity ophiobolins such as 6-*epi*-ophiobolin N, the reductive nature of the radical cyclization provides tricyclic intermediates possessing little oxidation on the side chain and complicates efforts towards the synthesis of higher complexity congeners such as ophiobolin A which possesses an additional stereochemically dense spirocyclic tetrahydrofuran (THF) ring (Figure 7).

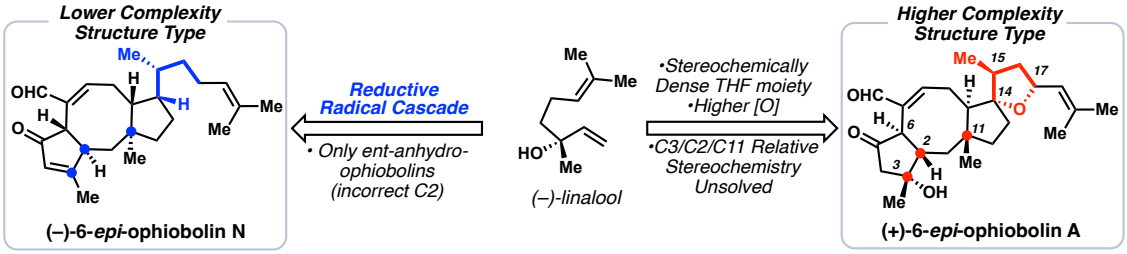


Figure 7: Overview of Synthetic Challenges Toward **1.2**

The inclusion of the the THF ring in **1.2** poses a significant challenge relative to the basic, unoxidized ophiobolin sidechain. For instance, Nakada's convergent strategy required 17 steps to construct the core of the 5,5-spirocyclic THF of ophiobolin A.[36] This challenging sector of the ophiobolins needed several additional steps to install the remaining pendant alkene side chain. To this end, our goal to develop an expedient synthesis of **1.2** necessitates an efficient strategy to construct this stereochemically dense sector found in the most complex ophiobolin subtypes.

In addition to the challenges associated with the construction of functionalized spirocyclic-THF ring of **1.2**, and with the goal of developing a general strategy to all ophiobolin structural types, several pivotal stereochemical challenges must first be addressed. Namely, the relative stereochemistry between the C3, C2, and C11 centers formed selectively in the three-component coupling of the 6-*epi*-ophiobolin N synthesis (see **1.235**, Figure 6), is not observed in any naturally occurring ophiobolin member. As a result of this stereochemical outcome, only 3-*anhydro*-ophiobolins with the ablated C3 stereogenic center in their non-natural enantiomeric series could be synthesized from the commercially available (–)-linalool. Additionally, it was unclear at the outset of our synthetic planning stage, whether the cyclization would proceed with the desired stereochemical outcome at carbons C2, C3, and C11 in this new diastereomeric system.

Ultimately, the successful extension of the radical polycyclization strategy developed in the (–)-6-*epi*-ophiobolin N synthesis to the total synthesis of (+)-6-*epi*-ophiobolin A would enable access to the majority of ophiobolins, not just the anhydro variants, and, importantly, provide the natural enantiomer of the ophiobolins for biological evaluation.

1.6 Synthetic Strategy

The ability to dictate and/or possibly control the product distribution of a chemical reaction via the manipulation of termination modes of radical intermediates generated as the result of carbon–carbon bond forming reactions is what sets radical chemistry apart from conventional polar reactivity. Importantly, the ability to control the product distribution of radical reactions by controlling the modes of radical termination is therefore a powerful synthetic strategy.

During the Maimone group's synthetic studies toward (–)-6-*epi*-ophiobolin N, the authors discovered that by switching between atom-transfer, photoredox, and canonical radical generating conditions, the radical cyclization could be programmed to give various substitution patterns on the farnesol-derived side chain.[38]

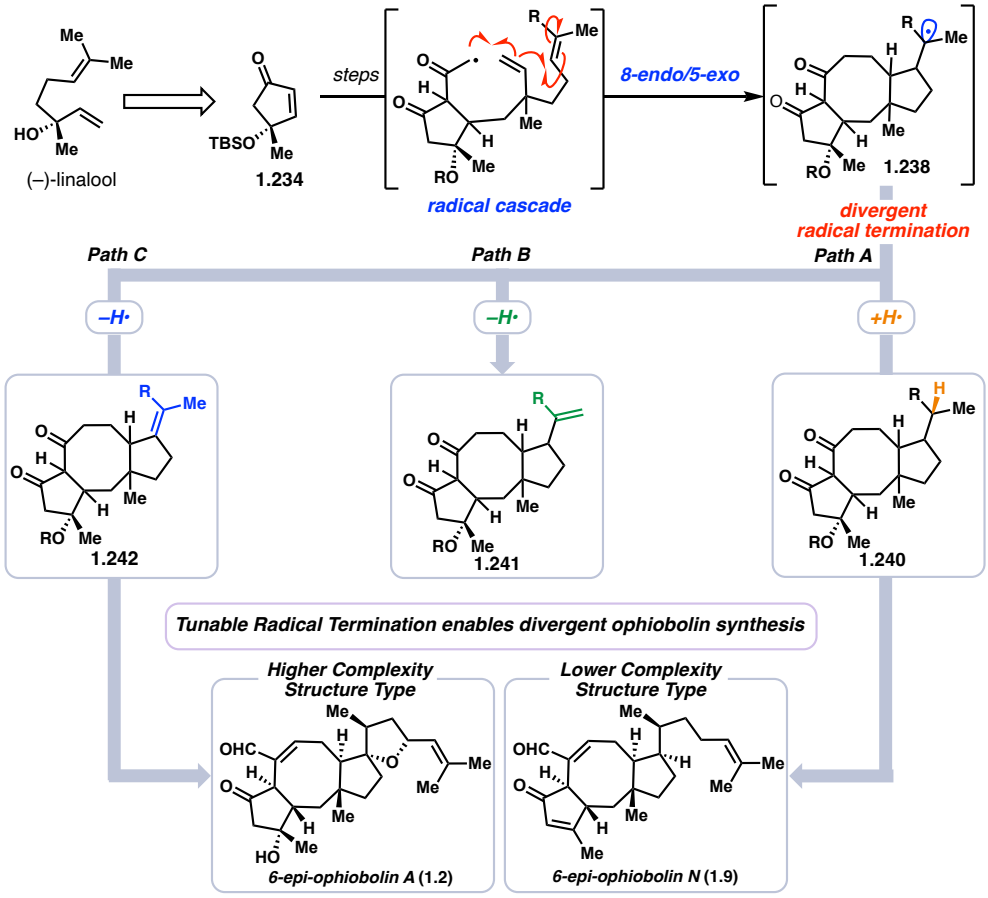


Figure 8: Programmable Radical Polycyclization Cascade

We envisioned that the ability to leverage the disparate modes of radical termination to access 5-8-5 carbocyclic frameworks containing chemically distinct functional handles could enable divergent elaboration toward higher complexity ophiobolin structure types such as (+)-6-*epi*-ophiobolin A (Figure 8). At the outset of our synthetic planning stage, it was unclear whether the cyclization would proceed with the desired stereochemical outcome in this new diastereomeric substrate which possesses the requisite relative stereochemistry between C2, C3, and C11. Additionally, we envisioned that a redox neutral radical polycyclization (Path C, Figure 8) which would provide a 5,8,5-fused tricyclic intermediate possessing the C14–C15 alkene (see **1.242**, Figure 8) could serve as versatile synthetic handle for the construction of the spirocyclic THF ring of **1.2**. Importantly, the successful implementation of such a strategy could result in a unified synthetic platform to access all known ophiobolin structural types in rapid fashion.

Retrosynthetically, we envision that 6-*epi*-ophiobolin A could, in analogy to the synthesis of **1.9**, be accessed from tetracyclic intermediate **1.243** via a 4-step endgame sequence involving Corey-Chaykovsky epoxidation, reductive epoxide opening, and oxidation/deprotection. The intermediate **1.243** could in turn be prepared from the 5-8-5-fused tricyclic intermediate **1.244**.

As mentioned above, we envisaged that an intermediate possessing the 5,5-spirocyclic THF intermediate (**1.243**), could be constructed via a 3-step sequence involving allylic oxidation (C14–

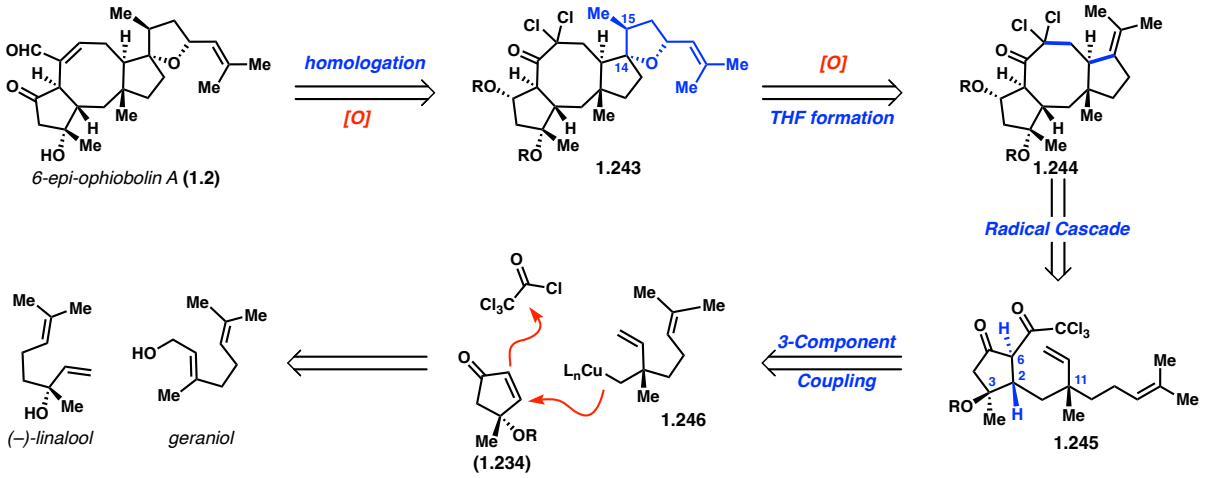


Figure 9: Retrosynthesis of (+)-6-*epi*-ophiobolin A.

O), hydroformylation (1-carbon homologation), and vinylation of the tricyclic intermediate **1.244** possessing an exocyclic alkene.

The tricyclic intermediate (**1.244**) could ultimately arise from a redox-neutral radical cyclization of monocyclic diketone intermediate **1.245**. In analogy to the synthesis of **1.9**, we sought to employ a strategy which united a geraniol-derived cuprate (**1.246**) with the chiral linalool-derived cyclopentenone (**1.234**) in conjugate fashion. Importantly, the successful execution of this strategy initially hinges on the successful reversal of the relative stereochemical outcome of the conjugate addition reaction, which provides the incorrect C2–C3 configurations.

1.7 Total Synthesis of (+)-6-*epi*-ophiobolin A

1.7.1 Correcting the C2–C3 Relative Stereoconfiguration

Our synthetic approach seeks to leverage a polycyclization cascade to access all ophiobolin structure types (in their natural enantiomeric series) by leveraging the termination modes of radical intermediates to provide expedient access to 5-8-5-fused tricyclic cores possessing suitable handles for further elaboration.

As mentioned in the previous sections, there are several stereochemical and chemical challenges which must be addressed to access higher complexity ophiobolins such as (+)-6-*epi*-ophiobolin A. The most immediate challenge presented in our pursuit of **1.2** pertains to the relative C2–C3 stereochemistry found in naturally occuring ophiobolins. In the previous studies by the Maimone group, it was shown that the relative C2–C3 stereoconfiguration found in naturally occurring ophiobolins is preferentially formed as the minor diastereomer (see **1.248**, Figure 10B) in the conjugate addition reaction, which unites the two chiral terpene-derived fragments.

Our initial efforts toward the synthesis of **1.2** began with the evaluation of a synthetic strategy to access the radical polycyclization precursor **1.249**. We began with the synthesis of the iodide **1.247** which is accessed from geraniol using a two-step sequence reported by Charette and coworkers. In contrast to the synthesis the depicted enantiomer of **1.9**, which uses the (*R,R*) enantiomer of Charette's dioxaborolane cyclopropanation ligand (**1.233**),[39] the synthesis of the naturally occurring enantiomer of **1.2** would require the use of the (*S,S*)-**1.233** (Figure 10C).

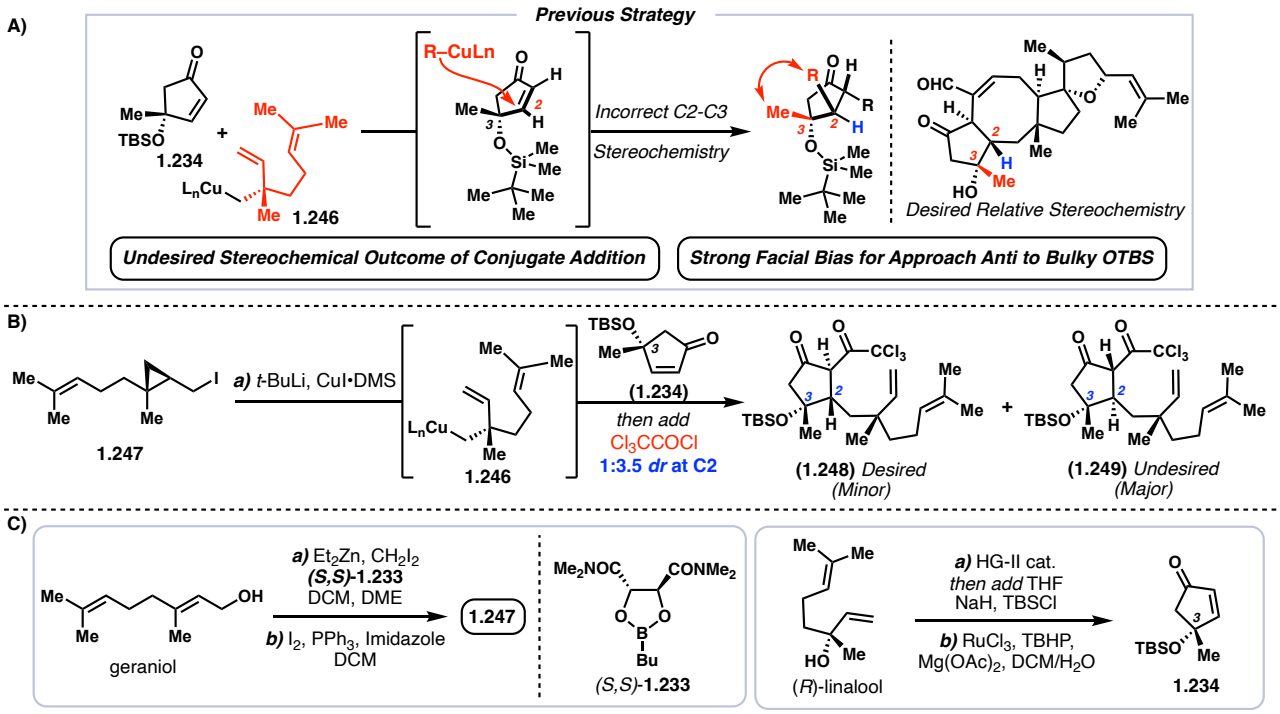


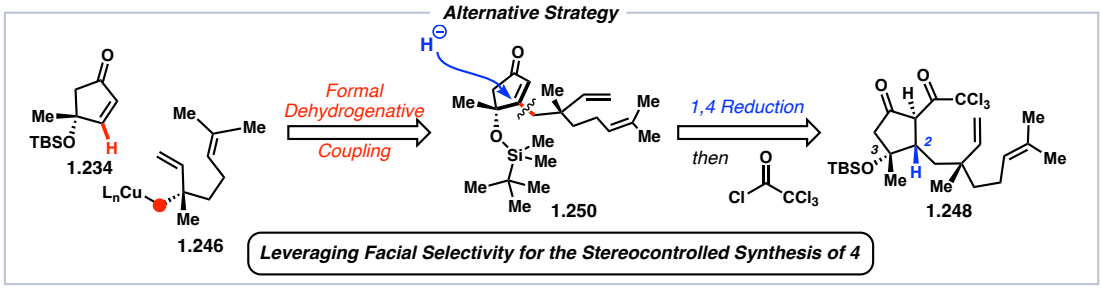
Figure 10: Conjugate Addition of Cuprate **1.246** to Cyclic Enone **1.234**

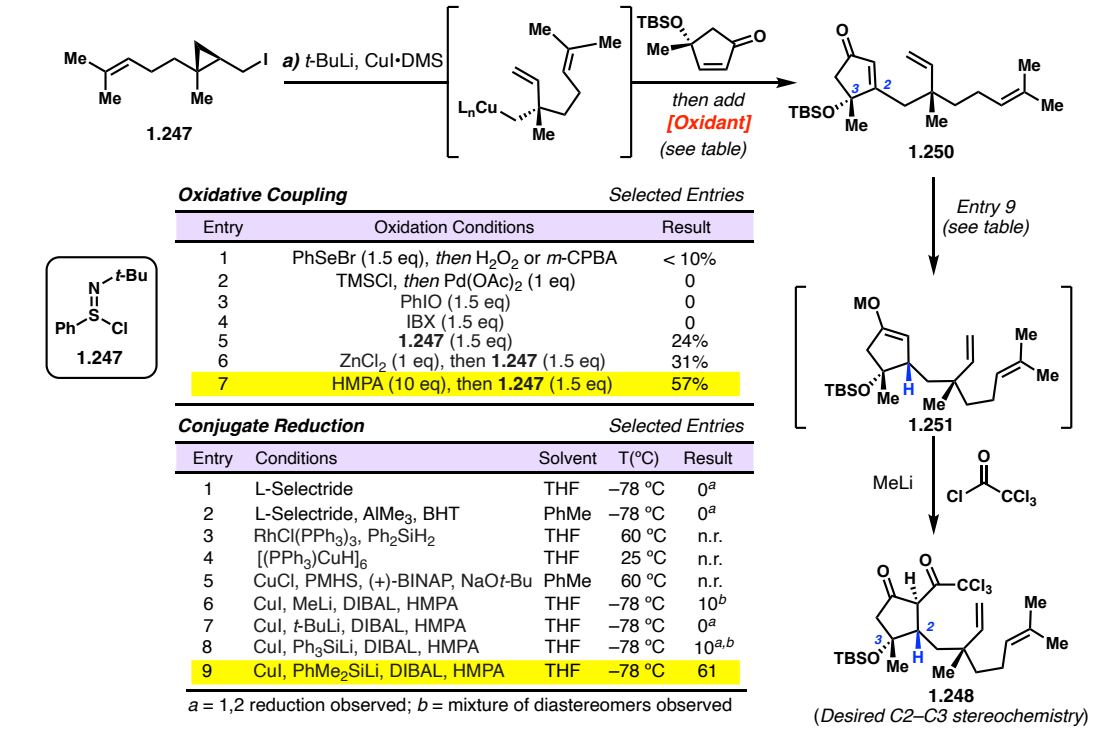
Conjugate addition of cuprate **1.246**, generated *in situ* from iodide **1.247** via lithiation-triggered anionic cyclopropane fragmentation, to the linalool-derived cyclopentenone **1.234** provided diastereomers **1.248** and **1.249** (1:3.5) after acylating the *in-situ* formed enolate with trichloroacetyl chloride. Notably, the ratio between the desired diastereomer **1.248** and undesired diastereomer **1.249** was slightly diminished relative the three-component coupling used in the synthesis of **1.9** (Figure 10C).

Despite the subtle change in diastereoselectivity observed in the conjugate addition reaction, presumed to be the result of the change in stereoconfiguration on C11, we recognized that the observed stereochemical outcome of the reaction is due largely to the intrinsic facial bias provided by cyclopentenone **1.234** (see Figure 10A). Accordingly, extensive efforts were devoted to reversing the facial selectivity of the conjugate addition reaction. Although the use of strong titanium- and aluminum-based Lewis acids have been shown to override the facial selectivity of nucleophilic attack at the β-position of cyclic α,β-unsaturated ketones possessing OTBS groups to favor the *syn*-approach, our studies revealed that titanium and aluminum based Lewis acids led to poor yields and minimal change in diastereoselctivity.[40] Additionally, the use of bulky Lewis acids such as Maruoka's aluminum tris(2,6-diphenylphenoxide) (ATPH) which can effectively reverse facial selectivity through coordination from the less hindered face, were ineffective in this context.[41, 42]

Given the strong facial preference for nucleophilic attack *anti* to the bulky OTBS group of **1.234**, we hypothesized that conjugate reduction of cyclic enone **1.234** possessing the geraniol-derived side chain preinstalled would deliver the hydride *anti* to the OTBS group as well. Thus the desired diastereomer was envisioned as arising from a two-step sequence involving first conjugate addition and *in situ* dehydrogenation, followed by a second conjugate reduction step. The enolate resulting from 1,4-hydride addition could then be quenched with trichloroacetyl chloride to afford the radical polycyclization precursor **1.248**.

To explore the feasibility of this two-step sequence, we began by examining a formal oxidative coupling reaction, which would proceed through conjugate addition followed by *in situ* oxidation to reinstall the *α,β*-unsaturation (see **1.250**, Figure 11). We initially began by quenching the enolate formed following conjugate addition with phenylselenium bromide which we hoped could reinstall the desired unsaturation via oxidation and selenoxide elimination. However, our attempts to quench the enolate with PhSeBr led to only trace amounts of the α-selenoketone product. We next explored the Saegusa oxidation, but found it only provided trace amounts of the desired enone **1.250**.[43] Alternatively, the use of hypervalent iodine oxidants such as IBX or PhIO led to decomposition of the reaction mixture.[44-46] Ultimately, we found that *N-tert*-butyl-phenyl-sulfinimidoyl chloride (**1.247**, Mukaiyama's Reagent) was uniquely capable of facilitating the *in situ* desaturation to provide the **1.250** in 24% yield, a process which likely proceeds through *syn*-elimination.[47, 48] We suspected that the poor efficiency of this reaction may be due to speciation effects of the resulting metal-enolate following conjugate addition. With this in mind, our attempts to transmetallate enolate **1.251** with $ZnCl_2$ led to the complete suppression of the reaction. However, the addition of HMPA (10 equiv.) proved beneficial and provided the **1.250** in 57% yield.





Oxidative Coupling — *Selected Entries*

Entry	Oxidation Conditions	Result
1	PhSeBr (1.5 eq), *then* H_2O_2 or *m*-CPBA	< 10%
2	TMSCl, *then* $Pd(OAc)_2$ (1 eq)	0
3	PhIO (1.5 eq)	0
4	IBX (1.5 eq)	0
5	**1.247** (1.5 eq)	24%
6	$ZnCl_2$ (1 eq), then **1.247** (1.5 eq)	31%
7	HMPA (10 eq), then **1.247** (1.5 eq)	57%

1.247

Conjugate Reduction — *Selected Entries*

Entry	Conditions	Solvent	T(°C)	Result
1	L-Selectride	THF	–78 °C	0[a]
2	L-Selectride, $AlMe_3$, BHT	PhMe	–78 °C	0[a]
3	$RhCl(PPh_3)_3$, Ph_2SiH_2	THF	60 °C	n.r.
4	$[(PPh_3)CuH]_6$	THF	25 °C	n.r.
5	CuCl, PMHS, (+)-BINAP, NaO*t*-Bu	PhMe	60 °C	n.r.
6	CuI, MeLi, DIBAL, HMPA	THF	–78 °C	10[b]
7	CuI, *t*-BuLi, DIBAL, HMPA	THF	–78 °C	0[a]
8	CuI, Ph_3SiLi, DIBAL, HMPA	THF	–78 °C	10[a,b]
9	CuI, $PhMe_2SiLi$, DIBAL, HMPA	THF	–78 °C	61

a = 1,2 reduction observed; *b* = mixture of diastereomers observed

Figure 11: Oxidative Coupling Strategy to **1.248**

With enone **1.250** in hand, we were poised to investigate the planned conjugate reduction to set the C2 stereocenter and access the requisite relative C2–C3 configuration as found in the ophiobolins. We suspected that this conjugate reduction would be extremely challenging because of the C3-siloxy group and quaternary center adjacent to the β–position of the enone system of **1.250**. Unsurprisingly, subjecting **1.250** to well-precedented hydride reagents capable of conjugate reduction led to either exclusive carbonyl 1,2-reduction or no reaction at all. Attempts to reduce **1.250** under single electron conditions led to decomposition, likely proceeding through a vinylogous spin-center shift mechanism based on the observance of the C3-deoxygenation product of **1.250**. After extensive experimentation, we identified that stoichiometric quantities of $PhMe_2SiCu$–H (generated *in situ* from DIBAL and $PhMe_2SiCu$), as reported by Daniewski and co-workers, led to a highly diastereoselective 1,4-reduction with only trace quantities of carbonyl reduction observed.[49] Analysis of the crude reaction mixture revealed that the aluminum enolate formed following conjugate reduction did not efficiently undergo the corresponding acylation by quenching with trichloroacetyl chloride. However, we found that the addition of methyl lithium to the aluminum enolate prior to the trichloroacetyl chloride quench provided the radical cyclization precursor **1.248** in 61% yield.

The development of a protocol for the oxidative union of geraniol- and linalool-derived fragments and subsequent conjugate reduction thus resulted in a two-step sequence to access the radical cyclization precursor with the desired relative C2–C3 configuration present in all ophiobolins which contain a C3 hydroxyl group.

1.7.2 Synthesis of the 5-8-5 Ophiobolin Core

With access to intermediate **1.248**, we were poised to evaluate the radical polycyclization cascade to construct the 5-8-5 tricyclic core of the ophiobolins. We postulated that a redox-neutral radical cyclization to access a tricyclic scaffold bearing an exocyclic tetrasubstituted alkene moiety would allow for facile construction of the spirocyclic THF ring of 6-*epi*-ophiobolin A.

We quickly found that subjecting **1.248** to copper-mediated atom-transfer radical cyclization conditions (CuCl/bpy, EtOH, Et_3N, 60 ºC) led to formation of the 5-8-5 tricyclic intermediate **1.253** (*ca.* 35%) alongside substantial quantities of hydrodechlorinated **1.248**, which downstream studies revealed to be incompatible with late-stage operations. Ultimately, we identified that optimization of the copper source (CuBr/dtbpy), base (di-*tert*-butyl pyridine), and solvent (DMF) provided tricycle **1.253** in 55% yield (Figure 12).

Importantly, the radical cyclization proceeded efficiently and yielded a tricyclic intermediate with the correct C10–C11 relative stereochemistry (see X-ray, Figure **12**) as a single diastereomer. Additionally, we didn't observe formation of other olefin regioisomers in the crude reaction mixture, likely due to the thermodynamic preference for the internal alkene.

With **1.253** secured, we turned our attention to formation of the formidable spirocyclic-THF ring system. Our downstream studies revealed that the free 1,3-diketone moiety of **1.253** would be incompatible with various late-stage operations thus necessitating the selective protection of this sector of the molecule. To this end, a two-step protocol involving dual reduction of the C5 and C7 ketones followed by a one-pot acylation (C5–OH) and DMP oxidation (C7-OH) provided keto acetate (**1.254**) in 49% over two steps.

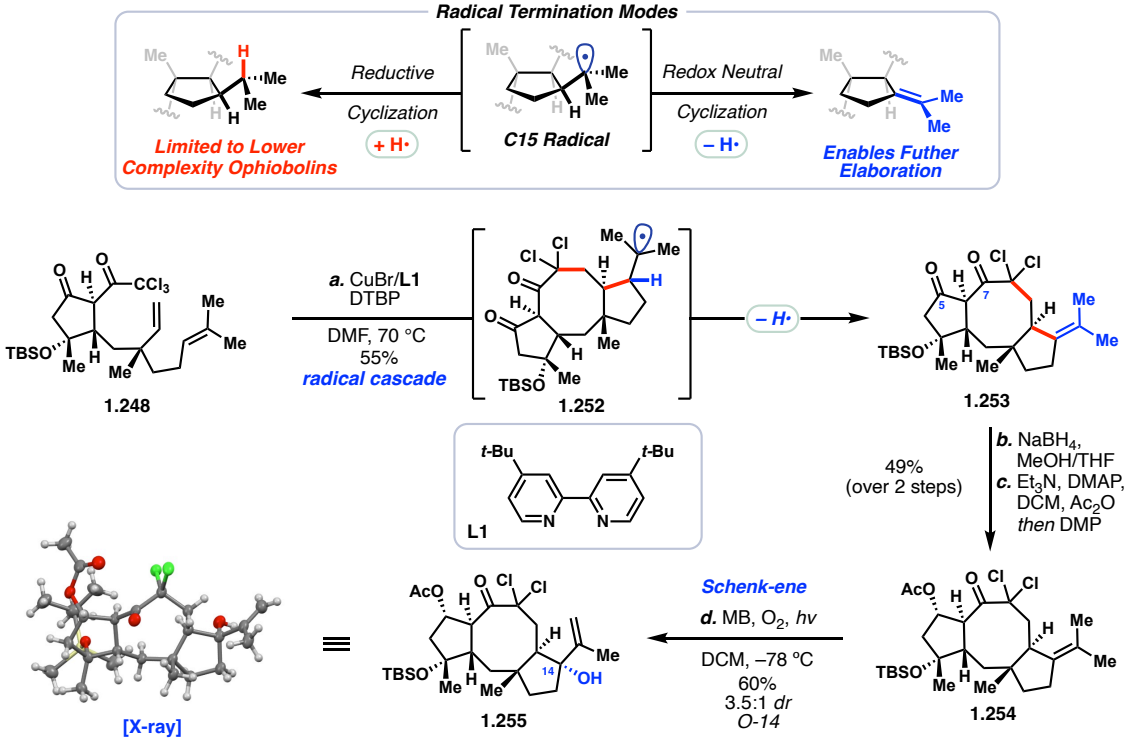


Figure 12: Construction and Functionalization of the 5-8-5-fused Tricyclic core.

From tricycle **1.254**, we envisioned that construction of the spirocyclic THF ring could begin by allylic oxidation of the tetrasubstituted alkene to install the correct oxidation at C14 present in ophiobolin A and B. The corresponding allylic alcohol could then be used to install the remaining 5 carbons to complete the spirocyclic THF ring.

Subjecting **1.254** to singlet oxygen generating conditions (O_2, methylene blue, *hv*) provided a separable mixture of tertiary alcohol diastereomers at C14 (**1.255**) in 56% yield. Single-crystal X-ray diffraction of the **1.255** confirmed this stereochemical assignment of the C14 hydroxyl as well as previously generated stereocenters from the radical polycyclization cascade.

1.7.3 Construction of the Spirocyclic-THF Ring and Completion of the Synthesis

With the tricyclic core possessing all but two stereogenic centers (C15 and C17) the final hurdle towards the completion 6-*epi*-ophiobolin A was the construction of the stereochemically dense spirocyclic THF ring.

We envisioned that the THF ring (**1.256**, Figure 13) could be constructed via the addition of a 4-carbon vinyl nucleophile to an oxocarbenium intermediate (**1.257**) generated *in situ* from an activated cyclic acetal precursor. We postulated that the C15 β-Methyl group could guide the approach of the vinyl nucleophile to provide the desired *trans*-relationship between the C15–C17 stereocenters. This cyclic acetal intermediate could in turn arise from the hydroformylation of the 1,1 disubstituted alkene of **1.258** (see **1.255**) to set the C15 stereogenic center and provide the spirocyclic THF following *in situ* lactolization and protection of the resulting lactol intermediate.[50]

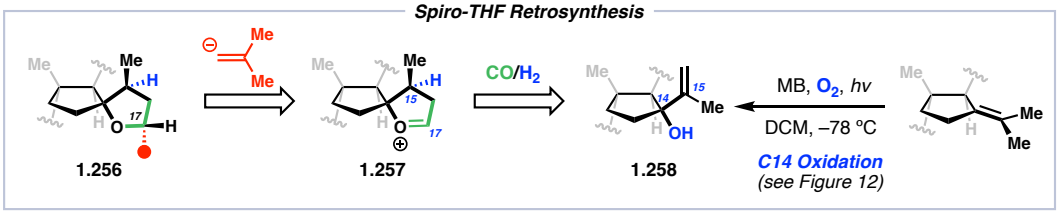


Figure 13: Retrosynthesis of the Spirocyclic THF Ring of **1.2**.

We began by surveying reaction conditions for the hydroformylation reaction of allylic alcohol **1.255**. Considerable time and effort were spent on evaluating various catalyst-ligand combinations in a variety of solvents and temperatures to affect a diastereoselective hydroformylation reaction and construction of the C15 stereocenter. We found that a major side product formed in this reaction was the hydrodechlorination of **1.255** prior to any hydroformylation reaction, which we note is incompatible with late-stage elaboration to **1.2**. Notably, although our brief attempts to employ Co- or Pd-catalyzed hydroformylations led largely to hydrodechlorination, and no reaction, respectively, we found that Rh-catalyzed hydroformylation typically led to full consumption of **1.255** with varying product distributions. As such, efforts to optimize the hydroformylation reaction focused on using $Rh(CO)_2(acac)$ as the catalyst with varying supporting ligands.

Figure **14** depicts a select group of ligands which were evaluated in the Rh-catalyzed hydroformylation reaction of **1.255**. Across the board, we found that phosphine ligands either provided no selectivity for the desired C15 stereocenter or selectively produced the incorrect C15 configuration. Worth noting is that most ligands evaluated in the hydroformylation reaction, regardless of identity, provided predominantly hydrodechlorination of the starting material and occasionally the product was observed as the major product. In fact, only a handful of ligands were found to be competent in the hydroformylation reaction and provided only minimal to no observed formation of the reductive dechlorination products ($\mathbf{L_4}$, $\mathbf{L_5}$, $\mathbf{L_{17}}$, $\mathbf{L_{18}}$, and $\mathbf{L_{20}}$) with $\mathbf{L_4}$ providing a near quantitative yield of a roughly 1:1 mixture of C15 epimers.

In an effort to improve the diastereoselectivity of this transformation, we varied the pressure of syngas and the ratios of CO/H_2, however this had little affect on diastereoselection. It was observed, however, that lowering the ratio of hydrogen gas led to slightly lower amounts of reductive dechlorination at the expense of reaction rates. Replacement of toluene as solvent led to either complete loss of catalytic activity (EtOAc, Et_2O, THF) or led to almost exclusively reductive dechlorination (DMF). Importantly, we observed a slight improvement in diastereoselectivity in favor of the desired C15 diastereomer when using $\mathbf{L_4}$ as the ligand in DMF (1 : 1.2 to ~ 1 : 1 dr), albeit with substantial amounts of dechlorination. Interestingly, although the diastereoselectivity across many catalyst/ligand systems in toluene is unaffected by lowering the reaction temperature, the use of ligand $\mathbf{L_4}$ in DMF at 40 ºC instead of 80 ºC led to a reversal in diastereoselectivity (2 :1 dr) favoring the desired diastereomer at C15, albeit in a combined yield of <10%. Additionally, under these conditions, substantial quantities of hydrodechlorination was observed. Interestingly, we only observed improvements in selectivity with ligand $\mathbf{L_4}$ and slight improvement with $\mathbf{L_6}$. In the case of $\mathbf{L_6}$ analysis of the reaction mixture proved challenging on preparative scale due to the prohibitively low yield.

Extensive efforts to improve the yield of this reaction, such as switching to other formamide-type solvents, additives, and changing ligands were unsuccessful, all leading to either poorer yields and selectivities or no product formation.

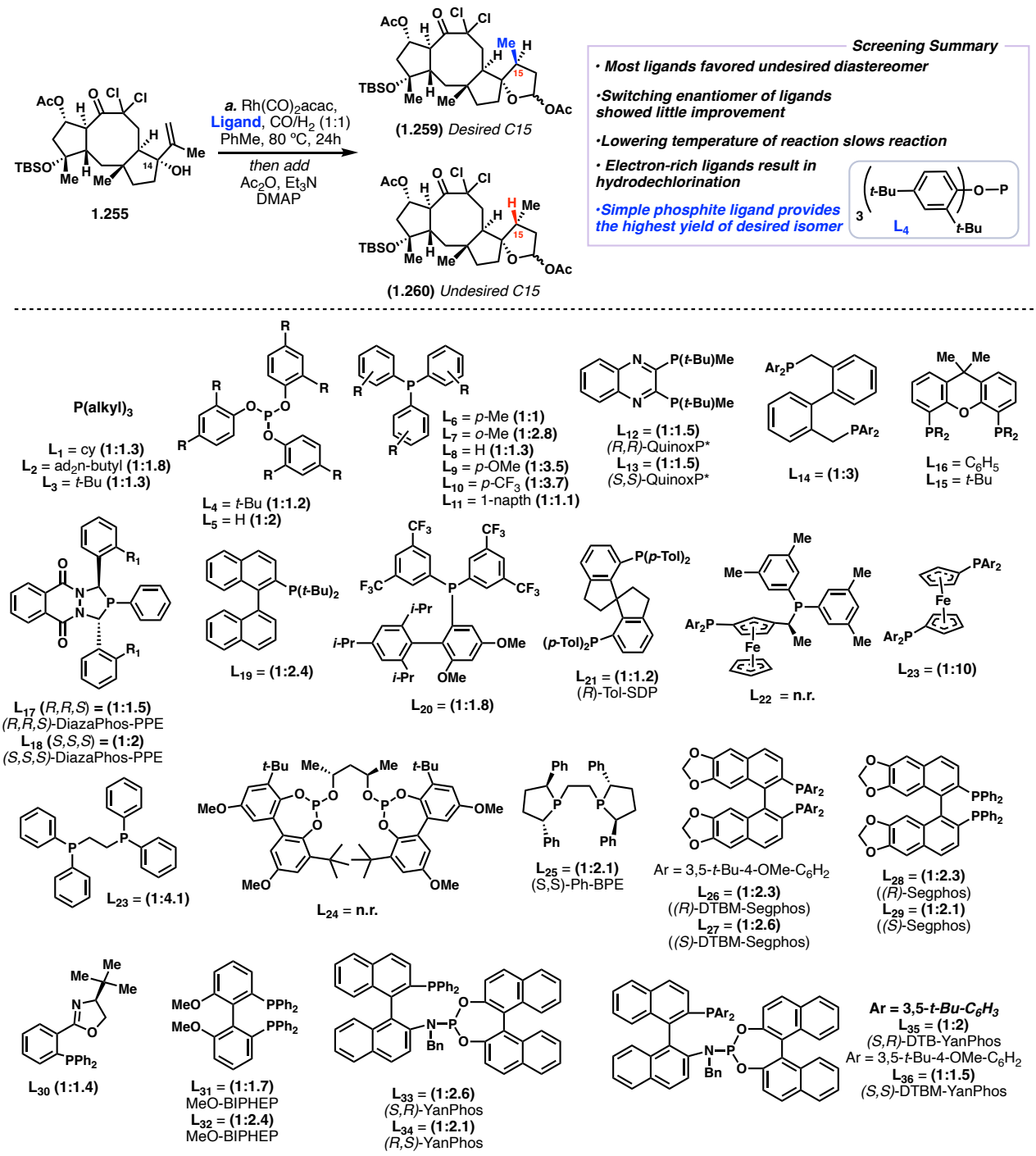
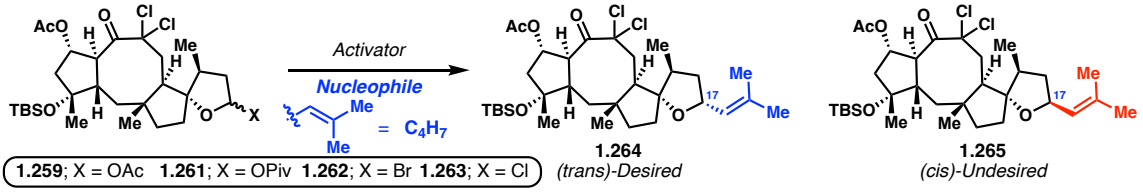


Figure 14: Representative Ligands Evaluated in the Hydroformylation Reaction of **1.255**

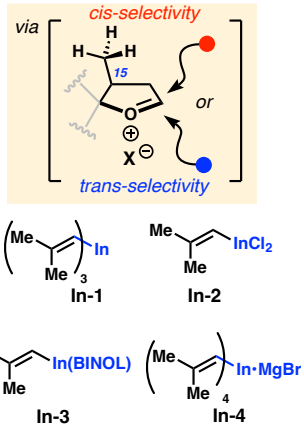
Abandoning the conditions using **L4**/DMF, we then turned to the use of chiral phosphine ligands used in asymmetric hydroformylation reactions with the hope that the enantiomeric ligands could provide differential diastereoselectivities. However, we observed that the use of chiral ligands (**L17**/**L18**, **L26**/**L27**, **L28**/**L29**, **L31**/**L32**, **L33**/**L34**, and **L35**/**L36**) as either enantiomer did not result in a substantial change in diastereoselectivity, all favoring the undesired C15 diastereomer.[50-56]

We also considered whether the C14-hydroxyl group could serve as a directing group for the hydroformylation reaction. It was unclear whether this hydroxyl group was at fault for the

observed diastereoselectivity of this reaction, which favored the undesired isomer **1.260**. On the other hand, we were inspired by the studies from the Breit group which showed that the use of *ortho*-diphenylphosphino benzoic esters (*o*-DPPB) as a directing group could enable a diastereoselective hydroformylation event.[57, 58] To our surprise, the C14-hydroxyl group of **1.255** was incredibly resistant to functionalization. Our attempts to install a trimethylsilyl group or even an acetate group on the tertiary allylic alcohol were unsuccessful, ultimately thwarting our attempts to probe the role of the C14 hydroxyl group in the transformation.



Entry	X =	Lewis Acid	Nucleophile	Solvent/*T*(°C)	Yield (**1.265**:**1.266**)
1	OAc	BF_3•OEt_2	$MgBr(C_4H_7)$	DCM/–78 °C	36% (3:1)[b]
2	OAc	TMSOTf	$MgBr(C_4H_7)$	DCM/–78 °C	60% (1:20)
3	OAc	$TMSNTf_2$	$MgBr(C_4H_7)$	DCM/–78 °C	27% (20:1)
4	OAc	TMSBr	$MgBr(C_4H_7)$	DCM/–78 °C	17% (1:1)[a]
5	OPiv	BF_3•OEt_2	$MgBr(C_4H_7)$	DCM/–78 °C	10% (3:1)[b]
6	Cl	BF_3•OEt_2	$MgBr(C_4H_7)$	DCM/–78 °C	(0%)[a]
7	Br	BF_3•OEt_2	$MgBr(C_4H_7)$	DCM/–78 °C	(0%)[a]
8	OAc	BF_3•OEt_2	$ZnBr(C_4H_7)$	DCM/Et_2O/–78 °C	11% (2:1)
9	OAc	BF_3•OEt_2	$CeCl_2(C_4H_7)$	DCM/–78 °C	10% (1:1.5)
10	OAc	BF_3•OEt_2	$CuTc(C_4H_7)$	THF/–78 °C	21% (1:1)
11	OAc	BF_3•OEt_2	$Al(C_4H_7)_3$	DCM/–78 °C	13% (1:1.8)
12	OAc	BF_3•OEt_2	**In-1**	DCM/–78 °C	54% (1:1)
13	OAc	BF_3•OEt_2	**In-2**	DCM/–78 °C	< 10% (1:1)
14	OAc	BF_3•OEt_2	**In-3**	DCM/–78 °C	18% (>20:1)
15	OAc	BF_3•OEt_2	**In-4**	DCM/–78 °C	64% (>20:1)



a = elimination to dihydrofuran observed; *b* = acetate deprotection

Figure 15: Completion of the Spirocyclic THF Ring

Although it is unclear at this stage what factors govern this hydroformylation reaction to provide the observed diastereoselectivity in favor of the undesired C15 isomer (**1.260**), we were relieved to have identified that ligand **L4** (see above) could provide near quantitative yields of a roughly 1:1 mixture of C15 epimers, which following *in situ* acetylation provided 44% of our desired C15 tetracyclic intermediate **1.259**. Despite the lack of diastereoselectivity, we could obtain suitable amounts of **1.259** from this sequence, which allowed us to proceed with the completion of the spirocyclic THF ring and ultimately the completion of (+)-6-*epi*-ophiobolin A.

We next turned our attention to the installation of the remaining four carbons on the THF ring of **1.2**. As mentioned above, we postulated that the addition of a 2-methylpropenyl nucleophile to the oxocarbenium intermediate generated from **1.259** (yellow box, Figure 15) would provide a *trans*-relationship between C15 and C17 due to the steric influence of the C15 methyl group. Our intial attempts revealed that modest diastereoselectivity could be obtained using 2-methylpropenyl grignard in the presence of BF_3•OEt_2 as a Lewis acid to activate the lactol-acetate **1.259** albeit in only 36% yield (3 : 1 dr) alongside deacetylation of **1.259** (*ca*. 60%).

The use of different Lewis acids (entries 2-4) led to either elimination of the acetate to a dihydrofuran, deacetylation, or decomposition. We presumed these undesired deacetylation to the arises from the lability of the acetoxy group of intermediate **1.259**. We then evaluated a variety of leaving groups (**1.261**-**1.263**, Figure 15) and found that although switching to pivalate (**1.261**) provided a slight decrease in the amount of deacetylation, the reaction did not proceed in good yield. Additionally the use of halide groups **1.262** and **1.263** in place of the carboxy leaving groups

led to exclusive elimination to a cyclic vinyl-ether. We then evaluated various organometallic nucleophiles and found that zinc-, cerium-, aluminum- and copper-based organometallics performed poorly in this reaction with respect to both yield and diastereoselectivity. We were cognizant of the relatively mild nature of organoindium nucleophiles commonly used in various alkylation and vinylation reactions. We therefore surveyed a variety of organoindium and organoindate nucleophiles. Although tri-vinyl indium reagent **In-1** (Figure 15) provided 54% of a 1:1 mixture of C17-diastereomers, the use of a dichloro-indium nucleophile (**In-2**) led to a diminished yield. The use of a BINOL-ligated indium nucleophile (**In-3**) provided exquisite selectivity favoring the desired C17 stereoconfiguration, albeit in only 18% yield. Ultimately, we found that the use of the tetra-organoindate nucleophile (**In-4**) could deliver the desired product (**1.264**) in 64% yield as nearly a single diastereomer.[59-63] We presume that the anionic nature of this species and increased steric bulk surrounding the tetra-coordinate indium center accounts for the desired reactivity and selectivity of this reagent in the vinylation reaction, relative to other nucleophiles.

With tetracycle **1.264** in hand, the synthesis of (+)-6-*epi*-ophiobolin A was completed via a four-step endgame sequence. First, Corey-Chaykovsky epoxidation of the C7 carbonyl with concomitant deprotection of the C5 acetate in 62% yield (**1.266**). Subjecting epoxide **1.266** to lithium naphthalenide resulted in the dehalogenation of geminal dichloride and *in situ* opening of the epoxide moiety to provide diol **1.268**. Next, silyl ether deprotection promoted by TBAF generated triol intermediate **1.269** in 96% yield. Finally, Swern oxidation of the triol intermediate generated the target in 85% yield, thus completing a 14-step total synthesis of **1.2** from (–)-linalool and geraniol.

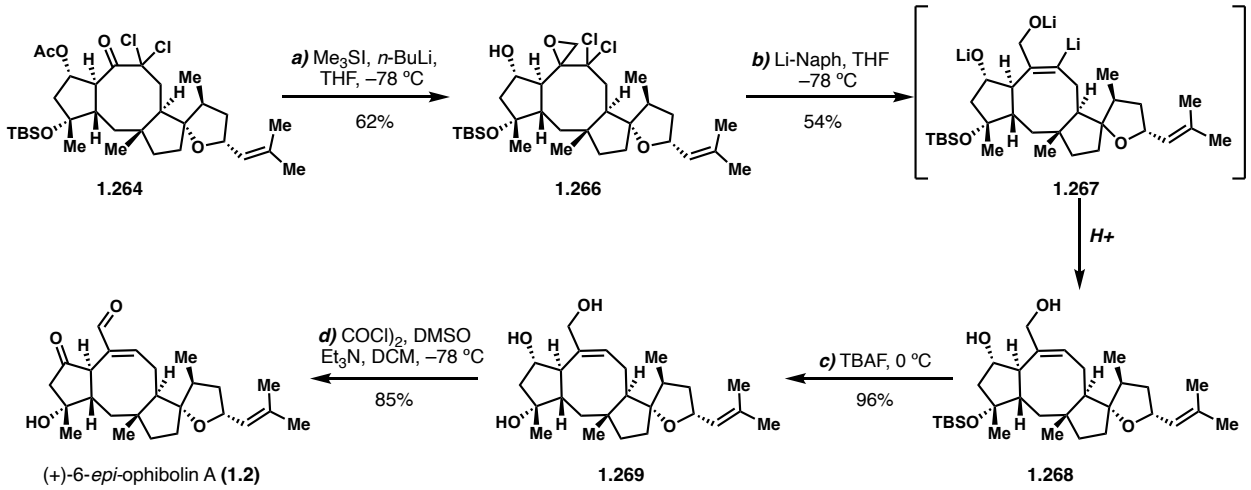


Figure 16: Total Synthesis of (+)-6-*epi*-ophiobolin A

1.8 Conclusion

We have successfully leveraged the divergent termination modes of a radical polycyclization cascade strategy to access (+)-6-*epi*-ophiobolin A in 14 steps from (–)-linalool. As a result, we have demonstrated that a radical cascade strategy has the potential to serve as a unified synthetic platform to access nearly all ophiobolin structural types by subtle manipulation of the synthetic sequence. Several stereochemical challenges were solved to enable to the synthesis of **1.2**. Namely, we developed a two-step sequence to correct the relative C2–C3 stereochemistry of **1.249**. Additionally, we developed a 3-step sequence to access the stereochemically dense

spirocyclic THF ring of **1.2**. Ultimately, these studies highlight the power of radicals in organic synthesis and we hope these studies may serve to better our understanding of the biological activity of the ophiobolins.

1.9 Distribution of Credit

The synthetic strategy outlined in this chapter to access (+)-6-*epi*-ophiobolin A were a result of a collaborative process between Dr. Huck Grover, Dr. Zachary Brill, Jordan K. Thompson, Kenneth V. Esguerra and myself under the guidance Professor Thomas Maimone. The optimization of the dehydrogenative coupling, conjugate reduction, hydroformylation, and vinylation reactions were done by myself. Dr. Zachary Brill and myself obtained synthetic samples of **1.2**. Jordan K. Thompson and Kenneth V. Esguerra assisted in the preparation of starting materials. The X-ray crystal structure of **1.255** was obtained by Dr. Jeffery S. Derrick, following my submission of a suitable crystalline sample.

1.10 References

1. Tetali, S. D., *Planta* **2019,** *249,* 1-8.
2. Chai, H. Z.; Yin, R.; Liu, Y. F.; Meng, H. Y.; Zhou, X. Q.; Zhou, G. L.; Bi, X. P.; Yang, X.; Zhu, T. H.; Zhu, W. M.; Deng, Z. X.; Hong, K., *Sci Rep* **2016,** *6,* 11.
3. Au, T. K.; Chick, W. S. H.; Leung, P. C., *Life Sci.* **2000,** *67,* 733-742.
4. Li, K. K.; Gustafson, K. R., *Nat. Prod. Rep.* **2021,** *38,* 1251-1281.
5. Tian, W.; Deng, Z. X.; Hong, K., *Mar. Drugs* **2017,** *15,* 21.
6. Kim, H.; Kim, J.; Kim, B.; Kim, H.; Cho, K.; Kim, H. J.; Kim, J. C.; Kim, B. S.; Kim, H. G.; Cho, K. Y., *Plant Pathology Journal* **1999,** *15,* 14-20.
7. Kumar, K. V. K.; Reddy, M. S.; Kloepper, J. W.; Lawrence, K. S.; Zhou, X. G.; Groth, D. E.; Zhang, S.; Rao, R. S.; Wang, Q.; Raju, M. R. B.; Raju, S. K.; Fernando, W. G. D.; Sudini, H.; Du, B.; Miller, M. E., *Commercial Potential of Microbial Inoculants for Sheath Blight Management and Yield Enhancement of Rice*. Springer: New York, 2011; p 237-264.
8. Evidente, A.; Cimmino, A.; Masi, M., *Phytochem. Rev.* **2019,** *18,* 843-870.
9. Orsenigo, M., *Phytopathology* **1957,** *29,* 189-196.
10. Itai, A.; Nozoe, S., *Chem. Pharm. Bull.* **1980,** *28,* 1043-1050.
11. Kim, J. M.; Hyeon, S. B.; Isogai, A.; Suzuki, A., *Agricultural and Biological Chemistry* **1984,** *48,* 803-805.
12. Canales, M. W.; Gray, G. R., *Phytochemistry* **1988,** *27,* 1653-1663.
13. Masi, M.; Dasari, R.; Evidente, A.; Mathieu, V.; Kornienko, A., *Bioorg. Med. Chem. Lett.* **2019,** *29,* 859-869.
14. Evidente, A.; Kornienko, A.; Lefranc, F.; Cimmino, A.; Dasari, R.; Evidente, M.; Mathieu, V.; Kiss, R., *Curr. Med. Chem.* **2015,** *22,* 3502-3522.
15. Rodolfo, C.; Rocco, M.; Cattaneo, L.; Tartaglia, M.; Sassi, M.; Aducci, P.; Scaloni, A.; Camoni, L.; Marra, M., *PLoS One* **2016,** *11,* 19.
16. Bury, M.; Girault, A.; Megalizzi, V.; Spiegl-Kreinecker, S.; Mathieu, V.; Berger, W.; Evidente, A.; Kornienko, A.; Gailly, P.; Vandier, C.; Kiss, R., *Cell Death Dis.* **2013,** *4,* 11.
17. Morrison, R.; Lodge, T.; Evidente, A.; Kiss, R.; Townley, H., *Int. J. Oncol.* **2017,** *50,* 773-786.
18. Dasari, R.; Masi, M.; Lisy, R.; Ferderin, M.; English, L. R.; Cimmino, A.; Mathieu, V.; Brenner, A. J.; Kuhn, J. G.; Whitten, S. T.; Evidente, A.; Kiss, R.; Kornienko, A., *Bioorg. Med. Chem. Lett.* **2015,** *25,* 4544-4548.
19. Li, E. G.; Clark, A. M.; Rotella, D. P.; Hufford, C. D., *Journal of Natural Products-Lloydia* **1995,** *58,* 74-81.
20. Posa, A.; Szabo, R.; Szalai, Z.; Kupai, K.; Deim, Z.; Murlasits, Z.; Bencsik, O.; Szekeres, A.; Vagvolgyi, C.; Balogh, L.; Juhasz, B.; Szilvassy, Z.; Varga, C., *Hum. Exp. Toxicol.* **2017,** *36,* 594-602.
21. Lv, C. T.; Qin, W. X.; Zhu, T. H.; Wei, S. J.; Hong, K.; Zhu, W. M.; Chen, R. H.; Huang, C. G., *Mar. Drugs* **2015,** *13,* 431-443.
22. Leung, P. C.; Graves, L. M.; Tipton, C. L., *Int. J. Biochem.* **1988,** *20,* 1351-1359.
23. Au, T. K.; Leung, P. C., *Plant Physiol.* **1998,** *118,* 965-973.
24. Chidley, C.; Trauger, S. A.; Birsoy, K.; O'Shea, E. K., *eLife* **2016,** *5,* 20.

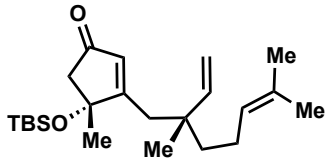
25. Reisenauer, K. N.; Tao, Y. F.; Das, P.; Song, S. X.; Svatek, H.; Patel, S. D.; Mikhail, S.; Ingros, A.; Sheesley, P.; Masi, M.; Boari, A.; Evidente, A.; Kornienko, A.; Romo, D.; Taube, J., *Sci Rep* **2021,** *11,* 10.
26. Evidente, A.; Kornienko, A.; Cimmino, A.; Andolfi, A.; Lefranc, F.; Mathieu, V.; Kiss, R., *Nat. Prod. Rep.* **2014,** *31,* 617-627.
27. Byun, H. S.; He, L. L.; Bittman, R., *Tetrahedron* **2000,** *56,* 7051-7091.
28. Morrison, R.; Gardiner, C.; Evidente, A.; Kiss, R.; Townley, H., *Pharm. Res.* **2014,** *31,* 2904-2917.
29. Bury, M.; Novo-Uzal, E.; Andolfi, A.; Cimini, S.; Wauthoz, N.; Heffeter, P.; Lallemand, B.; Avolio, F.; Delporte, C.; Cimmino, A.; Dubois, J.; Van Antwerpen, P.; Zonno, M. C.; Vurro, M.; Poumay, Y.; Berger, W.; Evidente, A.; De Gara, L.; Kiss, R.; Locato, V., *Int. J. Oncol.* **2013,** *43,* 575-585.
30. Najumudeen, A. K.; Jaiswal, A.; Lectez, B.; Oetken-Lindholm, C.; Guzman, C.; Siljamaki, E.; Posada, I. M. D.; Lacey, E.; Aittokallio, T.; Abankwa, D., *Oncogene* **2016,** *35,* 5248-5262.
31. Hirsch, H. A.; Iliopoulos, D.; Tsichlis, P. N.; Struhl, K., *Cancer Research* **2009,** *69,* 7507-7511.
32. Kim, I. Y.; Kwon, M.; Choi, M. K.; Lee, D.; Lee, D. M.; Seo, M. J.; Choi, K. S., *Oncotarget* **2017,** *8,* 106740-106752.
33. Chiba, R.; Minami, A.; Gomi, K.; Oikawa, H., *Org. Lett.* **2013,** *15,* 594-597.
34. Narita, K.; Chiba, R.; Minami, A.; Kodama, M.; Fujii, I.; Gomi, K.; Oikawa, H., *Org. Lett.* **2016,** *18,* 1980-1983.
35. Rowley, M.; Tsukamoto, M.; Kishi, Y., *J. Am. Chem. Soc.* **1989,** *111,* 2735-2737.
36. Tsuna, K.; Noguchi, N.; Nakada, M., *Angew. Chem.-Int. Edit.* **2011,** *50,* 9452-9455.
37. Tsuna, K.; Noguchi, N.; Nakada, M., *Chem.-Eur. J.* **2013,** *19,* 5476-5486.
38. Brill, Z. G.; Grover, H. K.; Maimone, T. J., *Science* **2016,** *352,* 1078-1082.
39. Charette, A. B.; Juteau, H.; Lebel, H.; Molinaro, C., *J. Am. Chem. Soc.* **1998,** *120,* 11943-11952.
40. Jeroncic, L. O.; Cabal, M. P.; Danishefsky, S. J.; Shulte, G. M., *J. Org. Chem.* **1991,** *56,* 387-395.
41. Ooi, T.; Maruoka, K., *J. Synth. Org. Chem. Jpn.* **1996,** *54,* 200-211.
42. Saito, S.; Sone, T.; Murase, M.; Yamamoto, H., *J. Am. Chem. Soc.* **2000,** *122,* 10216-10217.
43. Ito, Y.; Hirao, T.; Saegusa, T., *J. Org. Chem.* **1978,** *43,* 1011-1013.
44. Gnaim, S.; Vantourout, J. C.; Serpier, F.; Echeverria, P. G.; Baran, P. S., *ACS Catal.* **2021,** *11,* 883-892.
45. Tohma, H.; Kita, Y., *Adv. Synth. Catal.* **2004,** *346,* 111-124.
46. Nicolaou, K. C.; Mathison, C. J. N.; Montagnon, T., *J. Am. Chem. Soc.* **2004,** *126,* 5192-5201.
47. Mukaiyama, T.; Matsuo, J.; Yanagisawa, M., *Chem. Lett.* **2000,** 1072-1073.
48. Mukaiyama, T.; Matsuo, J.; Kitagawa, H., *Chem. Lett.* **2000,** 1250-1251.
49. Daniewski, A. R.; Liu, W., *J. Org. Chem.* **2001,** *66,* 626-628.
50. Airiau, E.; Chemin, C.; Girard, N.; Lonzi, G.; Mann, A.; Petricci, E.; Salvadori, J.; Taddei, M., *Synthesis* **2010,** 2901-2914.
51. Du, X. J.; Tang, Y. H.; Zhang, X.; Lei, M., *Chinese Chemical Letters* **2013,** *24,* 1083-1086.

52. Margalef, J.; Langlois, J.; Garcia, G.; Godard, C.; Dieguez, M., *Advances in Catalysis, Vol 69* **2021,** *69,* 181-215.
53. Klosin, J.; Landis, C. R., *Accounts Chem. Res.* **2007,** *40,* 1251-1259.
54. Deng, Y. C.; Wang, H.; Sun, Y. H.; Wang, X., *ACS Catal.* **2015,** *5,* 6828-6837.
55. Brezny, A. C.; Landis, C. R., *Accounts Chem. Res.* **2018,** *51,* 2344-2354.
56. Eilbracht, P.; Barfacker, L.; Buss, C.; Hollmann, C.; Kitsos-Rzychon, B. E.; Kranemann, C. L.; Rische, T.; Roggenbuck, R.; Schmidt, A., *Chem. Rev.* **1999,** *99,* 3329-3365.
57. Breit, B.; Grunanger, C. U.; Abillard, O., *Eur. J. Org. Chem.* **2007,** *2007,* 2497-2503.
58. Breit, B., *Directed Metallation* **2007,** *24,* 145-168.
59. Araki, S.; Shimizu, T.; Jin, S. J.; Butsugan, Y., *J. Chem. Soc.-Chem. Commun.* **1991,** 824-825.
60. Shen, Z. L.; Wang, S. Y.; Chok, Y. K.; Xu, Y. H.; Loh, T. P., *Chem. Rev.* **2013,** *113,* 271-401.
61. Hirashita, T.; Hayashi, Y.; Mitsui, K.; Araki, S., *Tetrahedron Lett.* **2004,** *45,* 3225-3228.
62. Araki, S.; Jin, S. J.; Butsugan, Y., *J. Chem. Soc.-Perkin Trans. 1* **1995,** 549-552.
63. Lee, P. H.; Lee, S. W.; Seomoon, D., *Org. Lett.* **2003,** *5,* 4963-4966.

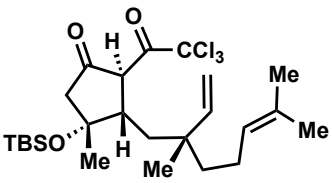
1.11 Experimental Procedures and Characterization Data

General Procedures:

All reactions were performed in flame- or oven-dried glassware under a positive pressure of nitrogen or argon, unless otherwise noted. Air- and moisture-sensitive liquids were transferred via syringe. When indicated, solvents or reagents were degassed by sparging with argon for 10 minutes in an ultrasound bath at 25 °C. Volatile solvents were removed under reduced pressure rotary evaporation below 35 °C. Analytical and preparative thin-layer chromatography (TLC) were performed using glass plates pre-coated with silica gel (0.25-mm, 60-Å pore size, Merck TLC Silicagel 60 F_{254}) impregnated with a fluorescent indicator (254 nm). TLC plates were visualized by exposure to ultraviolet light (UV) and then were stained by submersion in an ethanolic anisaldehyde solution or a basic potassium permanganate solution, followed by brief heating on a hot plate. Flash column chromatography was performed with silica gel purchased from Silicycle (SiliaFlash®, 60 Å, 230-400 mesh, 40-63 μm). Pentanes, triethylamine (Et_3N), trichloroacetyl chloride, and oxalyl chloride were distilled over calcium hydride prior to use. Indium chloride, $Rh(CO)_2(acac)$, 2-methyl-1-propenyl magnesium bromide were purchased from Sigma Aldrich and used without any further purification. The mixture of carbon monoxide/hydrogen gas (1:1) was purchased from Praxair Specialty Gases. Iodide **1.247**,[1] *N-tert*-butylbenzenesulfinimidoyl chloride,[2] $PhMe_2SiLi$,[3] and lithium naphthalenide[4] were prepared according to literature procedures. All other reagents were used as received from commercial sources, unless stated otherwise. Proton nuclear magnetic resonance (^{1}H NMR) spectra and carbon nuclear magnetic resonance (^{13}C NMR) spectra were recorded on Bruker AV-500, Bruker AV-600, or Bruker AV-700 spectrometers at 23 °C. Proton chemical shifts are expressed as parts per million (ppm, δ scale) and are referenced to residual solvent ($CDCl_3$: δ 7.26, C_6D_6: δ 7.16), unless stated otherwise. Carbon chemical shifts are expressed as parts per million (ppm, δ scale) and are referenced to the solvent ($CDCl_3$: δ 77.16, C_6D_6: δ 128.06), unless stated otherwise. Data is represented as follows: chemical shift, multiplicity (s = singlet, d = doublet, dd = doublet of doublets, ddd, doublet of doublet of doublet, dt = triplet of doublets, t = triplet, q = quartet, m = multiplet, br = broad), coupling constant (*J*) in Hertz (Hz), and integration. Infrared (IR) spectra were recorded on a Bruker Alpha FT- IR spectrometer as thin films and are reported in frequency of absorption (cm^{-1}). Only selected resonances are reported. High-resolution mass spectra (HRMS) were obtained by the mass spectrometry facility at the University of California, Berkeley using a Finnigan LTQFT mass spectrometer (Thermo Electron Corporation). X-ray diffraction data for **27** was collected at the Small Molecule X-ray Crystallography Facility (CheXray) at University of California, Berkeley using a Rigaku XtaLAB P200 equipped with a MicroMax 007HF rotating anode and Pilatus3 R 200K-A hybrid pixel array detector. Data were collected using CuKα radiation (λ = 1.5418 Å).



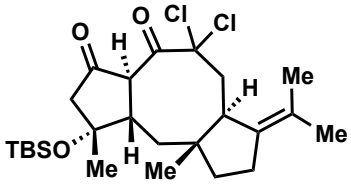
1.250: Freshly prepared cyclopropyl iodide **1.247** (3.10 g, 11.1 mmol, 1.3 equiv) was azeotropically dried with benzene three times at 15 °C in the absence of light and transferred to a 500 mL round bottom flask under an argon atmosphere. To this flask was added Et_2O (41 mL) and pentane (56 mL). The solution was then cooled to –78 °C and *tert*-Butyllithium (1.7 M in pentane, 9.3 mL, 15.9 mmol, 1.85 equiv) was added dropwise over 10 minutes. The resulting white suspension was stirred at –78 °C for 2.5 hours. In a separate flask, Me_2S (1.3 mL, 18.3 mmol, 2.1 equiv) was added to a suspension of CuI (979 mg, 5.1 mmol, 0.6 equiv) in THF (11 mL) and the mixture was stirred until a clear colorless solution formed. This solution was then added dropwise to the solution containing the lithiate of **1.247**. The resulting light yellow-white suspension was stirred for 35 minutes at –78 °C. A solution of enone **1.234** (1.94 g, 8.57 mmol, 1.0 equiv) in Et_2O (6 mL) was then added dropwise to the reaction mixture. The resulting light-orange suspension was stirred for 4 hours, slowly warming from –78 °C to –40 °C. Upon consumption of **1.234** as indicated by TLC, the reaction mixture was cooled to –78 °C and freshly distilled HMPA (14.9 mL, 85.7 mmol, 10.0 equiv) was added. The reaction mixture was stirred for 10 minutes, followed by the dropwise addition of a solution of Mukaiyama's reagent (*N*-*tert*-butylbenzenesulfinimidoyl chloride) (2.77 g, 12.9 mmol, 1.5 equiv) in Et_2O (20 mL). The resulting brown suspension was stirred for 2 hours, slowly warming to 0 °C, and then warmed to 25 °C and stirred for an additional 1 hour. The reaction mixture was then quenched with saturated aqueous $NaHCO_3$ (30 mL). Then NH_4OH (0.5 mL) and H_2O (30 mL) were added, and the mixture was extracted with Et_2O (3 x 50 mL), washed with H_2O (3 x 50 mL) and brine (1 x 30 mL), dried over $MgSO_4$, and concentrated under reduced pressure. The crude product was purified with two consecutive rounds of column chromatography (silica gel, 2% Et_2O in hexanes→15% Et_2O in hexanes; then 20% $AgNO_3$ adsorbed silica gel, 2% Et_2O in hexanes → 50% Et_2O in hexanes). The resulting mixture was then suspended in pentanes and cooled to –78 ºC to yield a yellow solid. The supernatant was then decanted, the solid washed with pentanes, and the material concentrated *in vacuo* to yield 1.84 g of enone **1.250** (4.9 mmol, 57%) as a yellow oil. **1.250:** $[\alpha]_D^{25}$ –8.4° (c = 0.01 g/mL, $CHCl_3$); R_f = 0.28 (12% Et_2O in hexanes); ^1H NMR (500 MHz, C_6D_6) δ 6.16 (s, 1 H), 5.61 (dd, *J* = 17.6, 10.8 Hz, 1 H), 5.14 (app t, *J* = 7.2 Hz, 1 H), 4.92 (dd, *J* = 10.8, 1.2 Hz, 1 H), 4.84 (dd, *J* = 17.6, 1.2 Hz, 1 H), 2.55-2.50 (m, 2 H), 2.32 (d, *J* = 17.3 Hz, 1 H), 2.18 (dd, *J* = 17.5, 1.5 Hz, 1 H), 1.98-1.91 (m, 2 H), 1.67 (s, 3 H), 1.55 (s, 3 H), 1.42-1.32 (m, 2 H), 1.08 (s, 3H), 0.90 (s, 3 H), 0.88 (s, 9 H), -0.01 (s, 3 H), -0.07 (s, 3 H); ^{13}C NMR (175 MHz, C_6D_6) δ 202.9, 179.5, 146.2, 131.2, 128.9, 125.9, 113.1, 80.3, 51.9, 42.4, 39.7, 37.7, 28.2, 25.9, 25.9, 23.2, 23.0, 18.2, 17.7, -2.4, -2.8; IR ν_{max} (cm^{-1}) 2956, 2929, 2857, 1715, 1618, 1472, 1375, 1252, 1155, 1004, 835, 775; HRMS (ESI) calcd for $C_{23}H_{40}O_2SiNa$ [M + Na^+] *m/z* 399.2690, found 399.2710.



1.248: A solution of $PhMe_2SiLi$ (1M in THF, 2.0 mL, 2.0 mmol, 1.25 equiv) was added slowly to a suspension of CuI (305 mg, 1.6 mmol, 1.0 equiv) in THF (13.5 mL) at –10 °C. The resulting dark purple suspension was then cooled to –50 °C and HMPA (10 mL) was added, followed by the slow addition of DIBAL (1M in hexanes, 4.8 mL, 4.8 mmol, 3.0 equiv). The black reaction mixture was stirred for an additional 30 minutes at –50 °C then cooled to –78 °C wherein a solution of enone **1.250** (600 mg, 1.60 mmol, 1.0

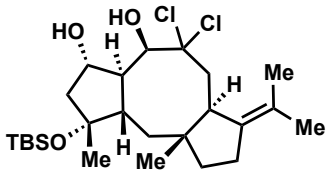
equiv) in THF (3.5 mL) was added slowly dropwise, rinsing the remaining enone with THF (2 x 1 mL). The resulting suspension was then stirred for 3 hours, slowly warming to –30 °C during this period. Upon consumption of the starting material as indicated by TLC, the reaction was cooled back to –78 °C, and methyllithium (1.6 M in Et_2O, 3.8 mL, 6.0 mmol, 3.8 equiv) was slowly added. After stirring the reaction mixture at –78 °C for 30 minutes, trichloroacetyl chloride (1.1 mL, 9.6 mmol, 6.0 equiv) was added. The resulting dark yellow solution was stirred for 3 hours, slowly warming to 0 °C, and then cooled to –40 °C. The reaction mixture was then diluted with Et_2O and TMEDA (1 mL) was added. The reaction was then quenched with saturated aqueous $NaHCO_3$ (20 mL) and aqueous Rochelle's salt solution (1M, 20 mL). After stirring at 25 °C for 3 hours, the biphasic reaction mixture was poured into a separatory funnel containing H_2O (20 mL), Et_2O (50 mL), and NH_4OH (1 mL). After extracting with Et_2O (3 x 40 mL), the combined organic layers were then washed with H_2O (3 x 100 mL), brine (50 mL), dried over $MgSO_4$, and concentrated under reduced pressure. The dark brown colored crude material was purified by column chromatography (1% Et_2O in hexanes → 8% Et_2O in hexanes) to provide 510 mg of diketone **1.248** (0.976 mmol, 61%) as an orange oil: $[\alpha]_D^{25}$ +46.3° (c = 0.0078 g/mL, $CHCl_3$); R_f = 0.53 (25% Et_2O in hexanes). **1.248** ^{1}H NMR (600 MHz, C_6D_6) δ 5.64 (dd, *J* = 17.5, 10.7 Hz, 1H), 5.20 (app t, *J* = 7.1 Hz, 1 H), 5.11 (dd, *J* = 10.7, 1.2 Hz, 1H), 4.96 (dd, *J* = 17.5, 1.3 Hz, 1H), 4.47 (d, *J* = 10.8 Hz, 1H), 2.40 (ddd, *J* = 10.8, 4.8, 2.7 Hz, 1H), 2.26 (dd, *J* = 17.5, 1.0 Hz, 1H), 2.04 – 1.96 (m, 3H), 1.94 (d, *J* = 17.5 Hz, 1H), 1.68 (s, 3H), 1.58 (s, 3H), 1.39 – 1.33 (m, 3H), 1.00 (s, 3H), 0.93 (s, 3H), 0.86 (s, 9H), -0.06 (d, *J* = 28.7 Hz, 6H). ^{13}C NMR (151 MHz, C_6D_6-d_6) δ 205.6, 185.7, 145.2, 130.8, 124.8, 113.6, 78.8, 62.5, 53.8, 49.5, 42.3, 40.9, 39.0, 25.4, 25.3, 24.4, 23.1, 21.2, 18.0, 17.3, -2.8, -3.2; IR ν_{max} (cm^{-1}) 2955, 2928, 2857, 1767, 1735, 1461, 1380, 1255, 1092, 1004, 837, 775; HRMS (ESI) calcd. for $C_{25}H_{41}O_3Cl_3SiNa$ [M + Na^+] *m/z* 545.1788, found 545.1815.

Technical Notes: #1) The 1M $PhMe_2SiLi$ solution in THF should be a deep black/brown-colored solution. #2) The solution containing DIBAL, HMPA and $PhMe_2SiLi$ should be a dark brownish-red solution. This can be judged by tilting the flask so that the solution coats the side of the flask and leaves a red residue on the slide of the flask.

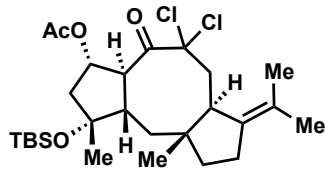


1.253: A solution of diketone **1.248** (500 mg, 0.96 mmol, 1.0 equiv) in degassed DMF (25 mL) was added to a round-bottom flask containing CuBr (96 mg, 0.67 mmol, 0.7 equiv), 4,4'-di-*tert*-butyl-bipyridine (231 mg, 0.86 mmol, 0.9 equiv), and 2,6-di-*tert*-butyl-pyridine (0.21 mL, 0.96 mmol, 1.0 equiv). The resulting blue-green colored solution was stirred at 70 °C for 1 hour, then cooled to 25 °C. EtOAc (25 mL) was added, followed by a 5% solution of NH_4OH in saturated aqueous NH_4Cl (5 mL) and H_2O (5 mL). The resulting biphasic mixture was stirred for 25 minutes, then poured into a separatory funnel containing H_2O (20 mL) and EtOAc (50 mL). The aqueous layer was extracted with EtOAc (2 x 75 mL), and the combined organic layers were washed with H_2O (3 x 30 mL) and brine (1 x 20 mL), dried over $MgSO_4$, and concentrated under reduced pressure. The resulting crude material was purified by column chromatography (1% Et_2O in hexanes → 10% Et_2O in hexanes) to provide 256 mg of tricycle **1.253:** (0.527 mmol, 55%) as a yellow oil. **1.253**: $[\alpha]_D^{25}$ +22.8° (c = 0.0017 g/mL, $CHCl_3$); R_f = 0.40 (25% Et_2O in hexanes); ^{1}H NMR (500 MHz, C_6D_6) δ 4.71 (d, *J* = 11.0 Hz, 1 H), 2.89 (d, *J* = 10.8 Hz,

1 H), 2.83 (d, *J* = 16.1 Hz, 1 H), 2.59 (dd, *J* = 16.2, 10.7 Hz, 1 H), 2.33-2.26 (m, 2 H), 2.13-2.06 (m, 2 H), 1.89-1.80 (m, 1 H), 1.72-1.62 (m, 2 H), 1.70 (s, 3 H), 1.49 (s, 3 H), 1.40-1.28 (m, 2H), 0.89 (s, 3 H), 0.83 (s, 9 H), 0.64 (s, 3 H), -0.08 (s, 3 H), -0.09 (s, 3 H); ^{13}C NMR (150 MHz, C_6D_6) δ 205.4, 194.0, 131.6, 124.5, 88.9, 77.4, 61.5, 57.2, 55.8, 50.8, 48.1, 41.3, 38.9, 36.7, 26.0, 23.2, 22.8, 22.4, 18.0, 17.9, -2.41, -2.64; IR ν_{max} (cm^{-1}) 2954, 2929, 2856, 1762, 1718, 1461, 1380, 1257, 1206, 1067, 1004, 836, 797; HRMS (ESI) calcd. for $C_{25}H_{40}O_3Cl_2SiK$ [M + K^+] *m/z* 525.1755, found 525.1766.

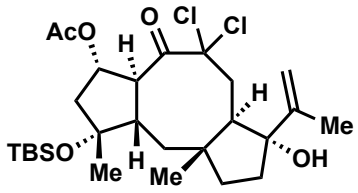


SI-1: Tricycle **1.253** (255 mg, 0.53 mmol, 1.0 equiv) was dissolved in a mixture of MeOH (6.2 mL) and THF (1.5 mL) and cooled to –40 °C wherein $NaBH_4$ (291 mg, 7.9 mmol, 15 equiv) was added. Upon completion of the reaction, as indicated by TLC (~1 hr), H_2O (5 mL) was added, and the resulting mixture was extracted with Et_2O (3 x 25 mL), washed with brine (10 mL), dried over $MgSO_4$, and concentrated under reduced pressure. The resulting crude material was purified by column chromatography (1% Et_2O in CH_2Cl_2 → 5% Et_2O in CH_2Cl_2) to provide 181 mg (0.370 mmol, 70%) of diol **SI-1** as a white foam. **SI-1:** $[\alpha]_D^{25}$ +15.0° (c = 0.0021 g/mL, $CHCl_3$); R_f = 0.45 (50% Et_2O in hexanes); ^{1}H NMR (700 MHz, C_6D_6) δ 4.42 (d, *J* = 13.5, 6.7, 6.6, 4.2 Hz, 1 H), 3.45 (dd, *J* = 7.5, 4.1 Hz, 1 H), 3.14 (d, J = 16.7 Hz, 1 H), 2.83 (d, *J* = 4.0 Hz, 1 H), 2.78 (d, *J* = 4.3 Hz, 1 H), 2.66 (d, *J* = 7.4 Hz, 1 H), 2.40 (dd, *J* = 16.7, 8.1 Hz, 1 H), 2.15 (q, *J* = 7.3 Hz, 1 H), 2.13-1.94 (m, 4 H), 1.93 (s, 3 H), 1.93-1.88 (m, 1 H), 1.57 (s, 3 H), 1.40-1.31 (m, 3 H), 1.25 (ddd, *J* = 12.4, 12.2, 7.7 Hz, 1 H), 1.15 (dd, *J* = 14.2, 12.1 Hz, 1 H), 1.10 (s, 3 H), 0.96 (s, 9 H), 0.59 (s, 3 H), 0.07 (s, 3 H), 0.06 (s, 3 H); ^{13}C NMR(175 MHz, C_6D_6) δ 140.5, 123.8, 104.2, 84.3, 80.2, 73.5, 55.1, 51.6, 47.5, 47.3, 46.9, 46.3, 43.8, 31.8, 29.2, 26.2, 23.2, 22.0, 21.2, 18.6, -1.85, -2.13; IR ν_{max} (cm^{-1}) 3405, 2955, 2929, 2856, 1647, 1462, 1377, 1256, 1083, 989, 835, 774; HRMS (ESI) calcd. for $C_{25}H_{44}O_3Cl_2SiNa$ [M + Na^+] *m/z* 513.2329, found 513.2339

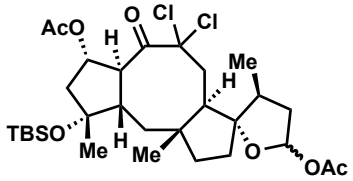


1.254: Et_3N (0.04 mL, 0.33 mmol, 2.0 equiv) and Ac_2O (0.02 mL, 0.16 mmol, 1.0 equiv) were sequentially added to a solution of diol **SI-1** (80 mg, 0.16 mmol, 1.0 equiv) and DMAP (10 mg, 0.08 mmol, 0.5 equiv) in CH_2Cl_2 (3 mL) at 0 °C. The resulting colorless solution was stirred for 15 minutes at 0 °C, then warmed to 25 °C and stirred for an additional 1 hour. Upon completion of the reaction as indicated by TLC, the reaction mixture was cooled back to 0 °C and DMP (692 mg, 1.93 mmol, 10 equiv) was added. The resulting white suspension was stirred for 15 minutes at 0 °C, then warmed to 25 °C and stirred for an additional 1 hour. Saturated aqueous $NaHCO_3$ (3 mL) and saturated aqueous $Na_2S_2O_3$ (3 mL) were then added, and the resulting biphasic mixture was stirred at 25 °C for 15 minutes. The mixture was then extracted with CH_2Cl_2 (3 x 20 mL), washed with brine (10 mL), dried over $MgSO_4$, and concentrated under reduced pressure. The resulting crude material was purified by column chromatography (2% Et_2O in hexanes → 12% Et_2O in hexanes) to yield 60.5 mg of ketone **1.254** (0.114 mmol, 70%) as a white foam. **1.254:** $[\alpha]_D^{25}$ –42.4° (c = 0.01 g/mL, $CHCl_3$); R_f = 0.45 (20% Et_2O in hexanes); ^{1}H NMR (600 MHz, C_6D_6-d_6) δ 5.47 (dt, *J* = 6.2, 5.1 Hz, 1 H), 4.24 (dd, *J* = 11.3, 5.2 Hz, 1 H), 2.91 (d, *J* = 10.7 Hz, 1 H), 2.87 (d, *J* = 15.9 Hz, 1 H), 2.66 (dd, *J* = 15.9, 10.6 Hz, 1 H), 2.10 (dd, *J* = 14.4, 6.4 Hz, 1 H), 1.94-1.86 (m, 1 H), 1.84 (dd,

J = 11.8, 3.5 Hz, 1 H), 1.82-1.78 (m, 2 H), 1.76 (s, 3 H), 1.72 (s, 3 H), 1.72-1.67 (m, 1 H), 1.58 (dd, *J* = 14.2, 3.5 Hz, 1 H), 1.50 (s, 3 H), 1.34 (ddd, *J* = 13.4, 12.8, 6.4 Hz, 1 H), 1.28 (dd, *J* = 11.8, 6.5 Hz, 1 H), 0.96 (s, 9 H), 0.90 (s, 3 H), 0.66 (s, 3 H), 0.05 (s, 3 H), 0.00 (s, 3H); ^{13}C NMR (150 MHz, C_6D_6-d_6) δ 205.1, 169.9, 141.1, 123.0, 93.6, 84.0, 79.4, 56.8, 55.9, 51.8, 47.1, 46.8, 45.7, 43.7, 42.8, 28.6, 26.2, 24.7, 22.3, 21.6, 20.8, 20.5, 18.6, -1.8, -2.3; IR ν_{max} (cm^{-1}) 2930, 2955, 1744, 1379, 1361, 1239, 1122, 1024, 836, 805; HRMS (ESI) calcd. for $C_{27}H_{44}O_4Cl_2SiNa$ [M + Na^+] *m/z* 553.2278, found 553.2292.

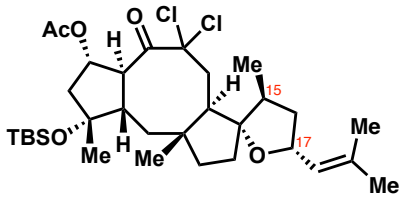


1.255: A solution of ketone **1.254** (190 mg, 0.36 mmol, 1.0 equiv) in CH_2Cl_2 (24 mL) under an atmosphere of O_2 (1 atm) was cooled to –78 °C, and a solution of methylene blue (1.1 mg, 0.004 mmol, 0.01 equiv) in CH_2Cl_2 (0.15 mL) was added. While bubbling O_2 through the resulting blue solution, the reaction mixture was irradiated with a sunlamp for 20 minutes. Upon completion of the reaction, as indicated by TLC, PPh_3 (283 mg, 1.08 mmol, 3.0 equiv) was added. The reaction mixture was warmed to 25 °C over 2 hours, then concentrated under reduced pressure. The resulting crude material was purified by column chromatography (4% Et_2O in hexanes→ 50% Et_2O in hexanes) to provide 80.2 mg of desired allylic alcohol **1.255** (0.146 mmol, 41%) as a white foam along with 14% of 14-*epi*-**1.255**. **1.255**: $[\alpha]_D^{25}$ –55.5° (c = 0.004 g/mL, $CHCl_3$); R_f = 0.22 (20% Et_2O in hexanes); ^{1}H NMR (500 MHz, C_6D_6) δ 5.46 (ddd, *J* = 7.5, 5.2, 3.6 Hz, 1 H), 4.85 (s, 1 H), 4.79 (s, 1 H), 4.20 (dd, *J* = 11.3, 5.2 Hz, 1 H), 2.68 (d, *J* = 15.2 Hz, 1 H), 2.47 (dd, *J* = 15.2, 10.6 Hz, 1 H), 2.37 (d, *J* = 10.6 Hz, 1 H), 1.97-1.89 (m, 2 H), 1.85-1.76 (m, 3 H), 1.71 (s, 3 H), 1.67-1.57 (m, 2 H), 1.62 (s, 3 H), 1.22 (ddd, *J* = 11.9, 6.2, 2.0 Hz, 1 H), 1.09-1.03 (m, 1 H), 1.03 (s, 9 H), 0.91 (s, 3 H), 0.59 (s, 3 H), 0.07 (s, 3 H), 0.06 (s, 3 H); ^{13}C NMR (175 MHz, C_6D_6) δ 205.0, 170.0, 147.9, 113.2, 93.5, 89.7, 84.0, 79.5, 56.9, 55.8, 54.2, 49.2, 46.9, 44.4, 42.8, 42.3, 35.7, 26.2, 24.7, 22.6, 20.4, 20.3, 18.7, -1.8, -2.3; IR ν_{max} (cm^{-1}) 3518, 2956, 2856, 1743, 1379, 1361, 1251, 1122, 1029, 836, 773; HRMS (ESI) calcd for $C_{27}H_{44}O_5Cl_2SiNa$ [M + Na^+] *m/z* 569.2227, found 569.2239



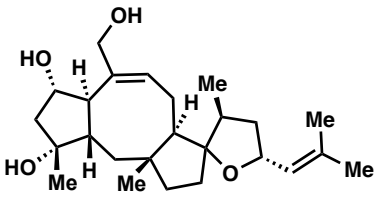
1.259: A 10 mL reaction tube containing allylic alcohol **1.255** (30 mg, 0.05 mmol, 1.0 equiv.), $Rh(CO)_2(acac)$ (4 mg, 0.015 mmol, 0.3 equiv), and tris(2,4-di-*tert*-butylphenyl)phosphite (20.2 mg, 0.03 mmol, 0.6 equiv) was evacuated and backfilled with Argon three times and then degassed toluene (3 mL) added. The resulting light yellow-colored solution was placed in a Parr pressure reactor with a vent needle puncturing the septum before closing the apparatus. The Parr reactor was then pressurized to 100 psi with a 1:1 mixture of CO/H_2. The reactor was then placed in an oil bath and heated to 80 °C with stirring for 24 hours. After cooling to 25 °C, the resulting brown solution was removed from the Parr reactor and the reaction was degassed with argon for 10 minutes. The reaction tube was then cooled to 0 ºC and DMAP (3.6 mg, 0.3 mmol, 0.6 equiv.), Et_3N (0.07 mL, 0.52 mmol, 10 equiv.), and Ac_2O (0.02 mL, 0.26 mmol, 5.0 equiv.) were added sequentially. The resulting solution was stirred for 15 minutes at 0 ºC then warmed to 25 ºC and stirred for 1 hour. Upon completion of the reaction as indicated by TLC, the reaction was quenched with saturated aqueous $NaHCO_3$ (3 mL) and extracted with Et_2O (3 x 6 mL), washed with brine (3 mL), dried over $MgSO_4$ and

concentrated under reduced pressure. The resulting crude oil was purified by column chromatography (the silica gel was pretreated with 3% triethylamine in hexanes; gradient of 10% Et_2O in hexanes (containing 3% Et_3N) → 40% Et_2O in hexanes (containing 3% trimethylamine,) to provide 32.5 mg (0.052 mmol, 96%) of a mixture of 4 inseparable lactol acetates. ^1H NMR analysis of this mixture indicated 46% of material with the correct C15 configuration and this mixture was was carried forward without further purification. The diagnostic ^1H signals for the desired C15 diastereomers are as follows: $R_f = 0.53$ (40% Et_2O in hexanes). **1.259:** ^1H NMR (500 MHz, C_6D_6) δ 6.30 (dd, J = 5.9, 3.0 Hz, 1H), 6.22 (d, J = 4.5 Hz, 1H). IR ν_{max} (cm^{-1}) 2927, 2854, 1741, 1463, 1377, 1361, 1321, 1232, 1251, 1193, 1021, 993, 833. HRMS (ESI) calcd for $C_{30}H_{48}O_7Cl_2SiNa$ [M + Na^+] *m/z* 641.2439, found 641.2439.



1.264: To an oven-dried reaction tube containing $InCl_3$ (29.7 mg, 0.134 mmol, 2.8 equiv.) was added 1 mL of THF. The resulting solution was then cooled to –78 ºC and 2-methyl-1-propenyl magnesium bromide (0.5M in THF, 1.07 mL, 0.54 mmol, 11.2 equiv.) was added dropwise to the stirring solution. The suspension was then stirred at –78 ºC for 45 minutes then warmed to 0 ºC and stirred for an additional 15 minutes. In a separate flask, the aforementioned mixture of lactol acetate diastereomers (30 mg total, 46% of the desired lactol acetate **1.259**, 0.048 mmol of total isomers, 1.0 equiv.), was azeotropically dried with benzene (3x) and dissolved in DCM (2 mL). The resulting solution was then cooled to –78 ºC and freshly distilled BF_3•OEt_2 (0.017 mL, 0.134 mmol, 2.8 equiv.) was added and the mixture stirred for 5 minutes at –78 ºC. The solution containing the preformed organoindate was then added dropwise at –78 ºC and the reaction mixture stirred for 8 hours. Upon completion of the reaction, as indicated by TLC, the reaction was diluted with 2 mL of CH_2Cl_2 and quenched with saturated aqueous NH_4Cl (2 mL) at –78 ºC and warmed to room temperature. The mixture was then extracted with DCM (3 x 3 mL), washed with brine, dried over $MgSO_4$, and concentrated under reduced pressure. The resulting crude material was purified with two consecutive rounds of column chromatography (2% Et_2O in hexanes → 40% Et_2O in hexanes; then 0% CH_2Cl_2 in hexanes →100% CH_2Cl_2) to give 19.1 mg of coupled product **1.264** (64% yield). It should be noted that although an analytically pure sample was obtained for analytical purposes after successive preparative TLC's, the mixture of C15 diastereomers can only be efficiently separated at the stage of compound **1.269**. Repeated chromatography also leads to the formation of undesired byproducts. **1.264**: $[\alpha]_D^{25}$ +21.1° (c = 0.001 g/mL, $CHCl_3$); $R_f = 0.38$ (25% Et_2O in hexanes); ^1H NMR (600 MHz, C_6D_6) δ 5.47-5.41 (m, 2 H), 4.57 (q, J = 7.3 Hz, 1 H), 4.22 (dd, J = 11.4, 5.1 Hz, 1 H), 2.80 (d, J = 14.6 Hz, 1 H), 2.65-2.55 (m, 1 H), 2.51 (d, J = 10.6 Hz, 1H), 2.04 (s, 1H), 1.97-1.95 (d, J = 13.2 Hz, 1H), 1.88-1.85 (m, 1H), 1.79 (s, 1H), 1.77 (d, J = 6.7 Hz, 1H), 1.73-1.71 (m, 2H), 1.70 (s, 3 H), 1.62 (s, 3 H), 1.51 (s, 3 H), 1.41-1.38 (m, 2H), 1.34 (m, 1H), 1.25 (dd, J = 12.5, 6.5 Hz, 2H), 0.99 (s, 9 H), 0.93 (s, 3H), 0.67 (d, J = 6.8 Hz, 3 H), 0.64 (s, 3 H), 0.06 (s, 3 H), 0.03 (s, 3 H); IR ν_{max} (cm^{-1}) 2957, 2925, 2852, 1742, 1719, 1379, 1240, 1123, 1026; ^{13}C NMR (151 MHz, C_6D_6) δ 205.4, 170.0, 133.0, 128.4, 96.9, 93.3, 84.1, 79.5, 72.4, 56.7, 55.9, 53.2, 48.1, 46.86, 45.0, 43.5, 42.6, 40.6, 36.2, 30.8, 26.2, 25.8, 24.8, 22.8, 20.4, 18.6, 18.2, 15.9, -1.8, -2.3; IR ν_{max} (cm^{-1}) 2957, 2925, 2852, 1742, 1719, 1379, 1240, 1123, 1026; HRMS (ESI) calcd for $C_{32}H_{52}O_5Cl_2SiNa$ [M + Na^+] *m/z* 637.2853, found 637.2878. *The ^{13}C spectrum provided in C_6D_6 contains signals which overlap with the solvent signal. We have attached an additional ^{13}C

spectrum in $CDCl_3$ in which all signals are clearly displayed. ^{13}C NMR (151 MHz, $CDCl_3$) δ 206.3, 171.1, 134.7, 126.8, 96.6, 92.3, 84.2, 79.6, 72.6, 72.2, 56.7, 56.0, 53.2, 46.9, 46.7, 45.1, 43.4, 42.9, 39.9, 35.9, 21.1, 26.1, 25.4, 22.7, 20.9, 18.5, 18.4, 16.5, -1.8, -2.3.

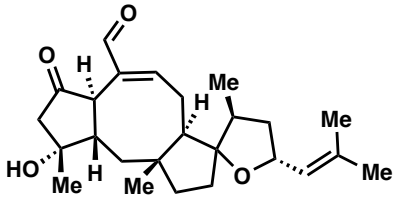


1.269: *Step 1*. In a reaction tube, trimethylsulfonium iodide (49.7 mg, 0.64 mmol, 20 equiv.) was azeotropically dried with benzene three times. The reaction vessel was evacuated and backfilled with argon (3x) and THF (0.7 mL) added. The suspension was cooled to 0 ºC and *n*-Butyllithium (2.5M in hexanes, 0.09 mL, 0.22 mmol, 7.0 equiv.) was added dropwise to the stirring suspension and stirred at 0 ºC for 15 mintues then cooled to –20 ºC. In a separate flask, the indate addition products (19.1 mg in total, 46% of the desired C15 diastereomer **1.264**, 0.031 mmol in total, 1.0 equiv.) was dissolved in THF (0.3 mL) and cooled to –20 ºC. The suspension was then added dropwise to the solution of tetracycles and stirred for 10 minutes. Upon completion of the reaction, as indicated by TLC, the reaction mixture was diluted with Et_2O and quenched with saturated aqueous NH_4Cl (1 mL), extracted with Et_2O (3 x 5 mL), washed with brine (3 mL), dried over $MgSO_4$, and concentrated under reduced pressure. The crude material was purified by column chromatography (2% Et_2O in hexanes →20% Et_2O in hexanes) to yield 11.3 mg (0.019 mmol, 62%) of *spiro*-epoxide diastereomers **SI-2** as a clear oil; R_f = 0.51 (40% Et_2O in hexanes) which were used without further purification.

Step 2. To a reaction tube containing degassed THF (0.6 mL) was added lithium naphthalenide (1M in THF, 0.66 mL, 0.66 mmol, 35 equiv.) at –78 ºC. To this dark green solution was added the diastereomeric mixture of spiro-epoxides **SI-2** (11.3 mg in total, 0.019 mmol, 1 equiv) dropwise as a solution in THF (1.0 mL). The reaction mixture was stirred at –78 ºC for 15 minutes and then quenched with saturated aqueous NH_4Cl (1 mL), extracted with Et_2O, washed with brine, dried over $MgSO_4$, and concentrated under reduced pressure. The resulting crude material was purified by column chromatography (2% Et_2O in CH_2Cl_2 → 40% Et_2O in CH_2Cl_2) to provide 5.4 mg of diols **SI-3** (0.01 mmol, 54%) as a clear oil; R_f = 0.28 (50% Et_2O in CH_2Cl_2) which were used without further purification.

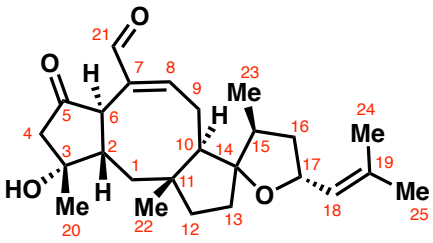
Step 3. TBAF (1 M in THF, 0.05 mL, 0.05 mmol, 5 equiv) was added dropwise to a solution of the previously obtained mixture of diols **SI-3** (5.4 mg in total, 46% of the desired C-15 diastereomers, 0.01 mmol in total, 1.0 equiv) in THF (0.5 mL) at 0 °C. The resulting solution was then warmed to 25 °C and stirred for 29 hours. After completion of the reaction as indicated by TLC, the reaction mixture was quenched with 1M HCl (0.5 mL) and MeOH (0.05 mL), extracted with EtOAc (3 x 2 mL), dried over $MgSO_4$, and concentrated under reduced pressure. The crude mixture was then purified by column chromatography (3:1 silica-florisil 10% Et_2O in CH_2Cl_2 →100% Et_2O) to yield 1.9 mg (96%) of diastereomerically pure triol **1.269**: $[\alpha]_D^{25}$+16.8° (c = 0.0019 g/mL, $CHCl_3$); R_f = 0.37 (100% Et_2O); ^1H NMR (600 MHz, $CDCl_3$-*d*) δ 5.66 (dd, *J* = 7.3, 3.6 Hz, 1H), 5.16 (d, *J* = 8.4 Hz, 1H), 4.58 (m, *J* = 7.8 Hz, 2H), 4.11 – 3.94 (m, 2H), 3.22 (appt s, 1H), 2.55 (dd, *J* = 13.3, 4.1 Hz, 1H), 2.45 (s, 1H), 2.39 (d, *J* = 17.8 Hz, 1H), 2.19 (q, *J* = 6.7 Hz, 1H), 2.01 (td, *J* = 12.1, 11.0, 6.6 Hz, 1H), 1.95 (d, *J* = 3.9 Hz, 2H), 1.84 – 1.74 (m, 4H), 1.71 (s, 3H), 1.69 – 1.67 (m, 3H), 1.66 – 1.62 (m, 2H), 1.34 (ddd, *J* = 17.5, 12.8, 9.3 Hz, 2H), 1.26 (s, 3H), 1.03 (d, *J* = 7.0 Hz, 3H), 0.87 (s, 3H);^{13}C NMR (151 MHz, $CDCl_3$-*d*) δ 138.4, 135.1, 129.2, 127.0, 96.3, 81.7, 75.4, 71.8, 68.5, 54.9, 54.0, 53.6, 48.8, 44.6, 42.6, 42.0, 41.4, 35.3, 31.4, 29.8, 26.7, 26.1, 22.3, 18.3, 16.7; IR ν_{max} (cm^{-1}) 3350, 2923, 2853,

1453, 1377, 1262, 1215, 1119, 1071, 928, 815; HRMS (ESI) calcd. for $C_{25}H_{40}O_4Na$ [M + Na^+] *m/z* 427.2819, found 427.2821



6-*epi*-ophiobolin A (1.2): In a reaction vial, a solution of DMSO (5.0 µL, 0.071 mmol, 15 equiv.) in CH_2Cl_2 (0.1 mL) was added dropwise to a solution of oxalyl chloride (4.0 µL, 0.050 mmol, 10 equiv.) in CH_2Cl_2 (0.3 mL) at –78 °C. After stirring at -78 °C for 30 minutes, a solution of triol **1.269** (1.9 mg, 0.0047 mmol, 1.0 equiv.) in CH_2Cl_2 (0.2 mL) was added dropwise, rinsing the material with additional CH_2Cl_2 (2 x 0.1 mL). The resulting cloudy solution was stirred for an additional 30 minutes at –78 °C, followed by addition of Et_3N (12.6 µL, 0.094 mmol, 20 equiv.). The reaction mixture was then stirred for 3 hours, slowly warmed to 0 °C, and then quenched with H_2O (1 mL), extracted with CH_2Cl_2 (3 x 2 mL), washed with brine (1 mL), dried over $MgSO_4$, and concentrated under reduced pressure. The crude mixture was purified by column chromatography (2% Et_2O in CH_2Cl_2 → 40% Et_2O in CH_2Cl_2) to provide 1.6 mg (85%) of 6-*epi*-ophiobolin A (**1.2**): $[\alpha]_D^{25}$+ 37.4° (c = 0.0012 g/mL, $CHCl_3$); R_f = 0.60 (50% Et_2O in CH_2Cl_2); ^{1}H NMR (700 MHz, $CDCl_3$) δ 9.22 (s, 1H), 6.88 (d, *J* = 7.2, 1H), 5.14 (d, *J* = 8.7, 1H), 4.61 (q, *J* = 7.2 Hz, 1H), 3.35 (d, J = 8.8 Hz, 1H), 3.06 (d, *J* = 16.7 Hz, 1H), 2.78 (d, *J* = 19.8 Hz, 1H), 2.61 (dd, *J* = 14.2, 4.3 Hz, 1H), 2.40 (dd, *J* = 16.7, 1.5 Hz, 1H), 2.34 (ddd, *J* = 19.8, 14.1, 7.1 Hz, 1H), 2.21 (q, *J* = 6.8 Hz, 1H), 2.12 (ddd, *J* = 12.4, 10.7, 4.3 Hz, 1H), 1.87 (appt t, *J* = 12.9 Hz, 1H), 1.83 – 1.77 (m, 2H), 1.77-1.73 (m, 1H), 1.71 (d, *J* = 1.4 Hz, 3H), 1.71 – 1.68 (m, 2H), 1.68 (d, *J* = 1.3 Hz, 3H), 1.42 (s, 3H), 1.38 (ddd, *J* = 11.1, 9.6, 5.6 Hz, 1H), 1.34 – 1.26 (m, 1H), 1.04 (d, *J* = 7.0 Hz, 3H), 0.85 (s, 3H); ^{13}C NMR (176 MHz, $CDCl_3$) δ 216.3, 194.0, 157.7, 142.5, 135.3, 126.8, 95.9, 76.7, 72.0, 54.8, 53.4, 49.5, 48.1, 42.6, 42.2, 42.0, 41.6, 35.2, 31.0, 29.5, 25.8, 22.8, 18.2, 16.1; IR ν_{max} (cm^{-1}) 3439, 2932, 1741, 1682, 1640, 1456, 1378, 1214, 1071, 786, 734; HRMS (ESI) calcd. for $C_{25}H_{46}O_4Na$ [M + Na^+] *m/z* 423.2506, found 423.2513.

(+)-6-*epi*-ophiobolin A ^{1}H spectra comparison:

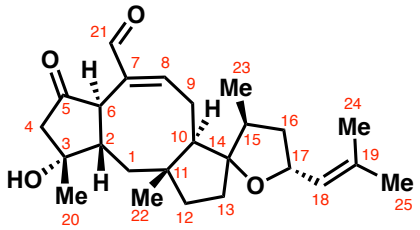


(+)-6-*epi*-ophiobolin A

Position	^{1}H (δ) Natural Sample (300 MHz, $CDCl_3$) *[ref. 5]*	^{1}H (δ) Synthetic Sample (700 MHz, $CDCl_3$)
1	-	1.87 (appt t, *J* = 12.9 Hz, 1H)* 1.77-1.73 (m, 1H)*
2	-	2.12 (ddd, *J* = 12.4, 10.7, 4.3 Hz, 1H)*
3	-	-
4a	2.38 (m, 1H)	2.40 (dd, *J* = 16.7, 1.5 Hz, 1H)
4b	3.04 (d, *J* = 16.8 Hz, 1H)	3.06 (d, *J* = 16.7 Hz, 1H)
5	-	-
6	3.35 (br d, *J* = 10.5 Hz, 1H)	3.35 (d, *J* = 8.8 Hz, 1H)
7	-	-
8	6.87 (m, 1H)	6.88 (d, *J* = 7.2, 1H)
9	2.77 (m, 1H)	2.78 (d, *J* = 19.8 Hz, 1H) 2.34 (ddd, *J* = 19.8, 14.1, 7.1 Hz, 1H)*
10	2.60 (dd, *J* = 13.8, 4.2 Hz, 1H)	2.61 (dd, *J* = 14.2, 4.3 Hz, 1H)
11	-	-
12	-	1.34 – 1.26 (m, 1H)* 1.38 (ddd, *J* = 11.1, 9.6, 5.6 Hz, 1H)*
13	-	1.71 – 1.68 (m, 2H)*
14	-	-
15	-	2.21 (q, *J* = 6.8 Hz, 1H)*
16	-	1.83 – 1.77 (m, 2H)*
17	4.60 (ddd, *J* = 9.0, 7.0, 7.0 Hz, 1H)	4.61 (q, *J* = 7.2 Hz, 1H),
18	5.13 (dq, *J* = 9.0, 1.5 Hz, 1H)	5.14 (d, *J* = 8.7, 1H)
19	-	-
20	1.41 (s, 3H)	1.42 (s, 3H)
21	-	9.22 (s, 1H)
22	0.84 (s, 3H)	0.85 (s, 3H)
23	1.03 (d, *J* = 6.9 Hz, 3H)	1.04 (d, *J* = 7.0 Hz, 3H)
24	1.66 (d, *J* = 1.2, 3H)	1.68 (d, *J* = 1.3 Hz, 3H)
25	1.70 (d, *J* = 1.2, 3H)	1.71 (d, *J* = 1.4 Hz, 3H)

*Indicates tentative assignment.

(+)-6-*epi*-ophiobolin A ^{13}C spectra comparison:

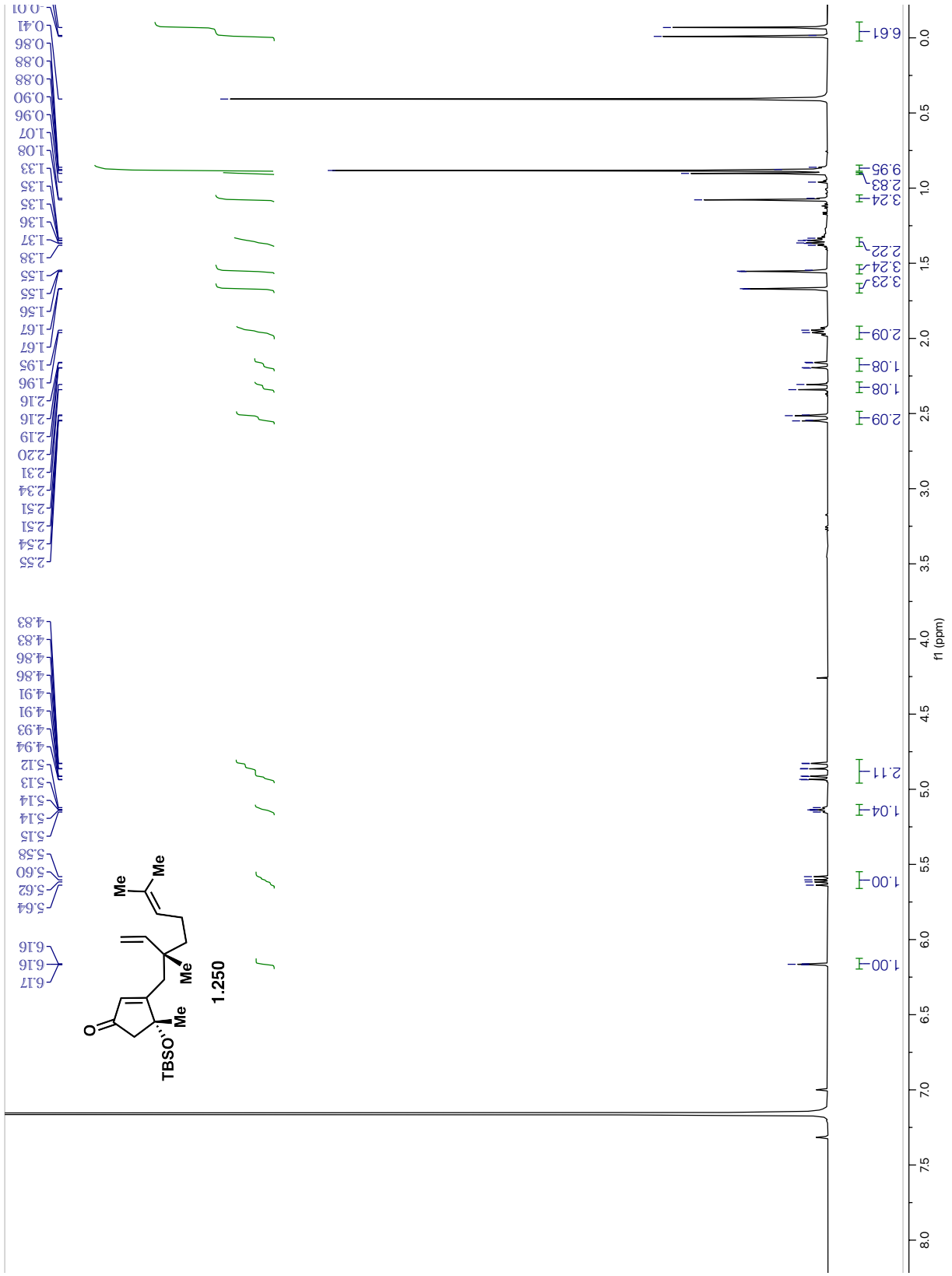


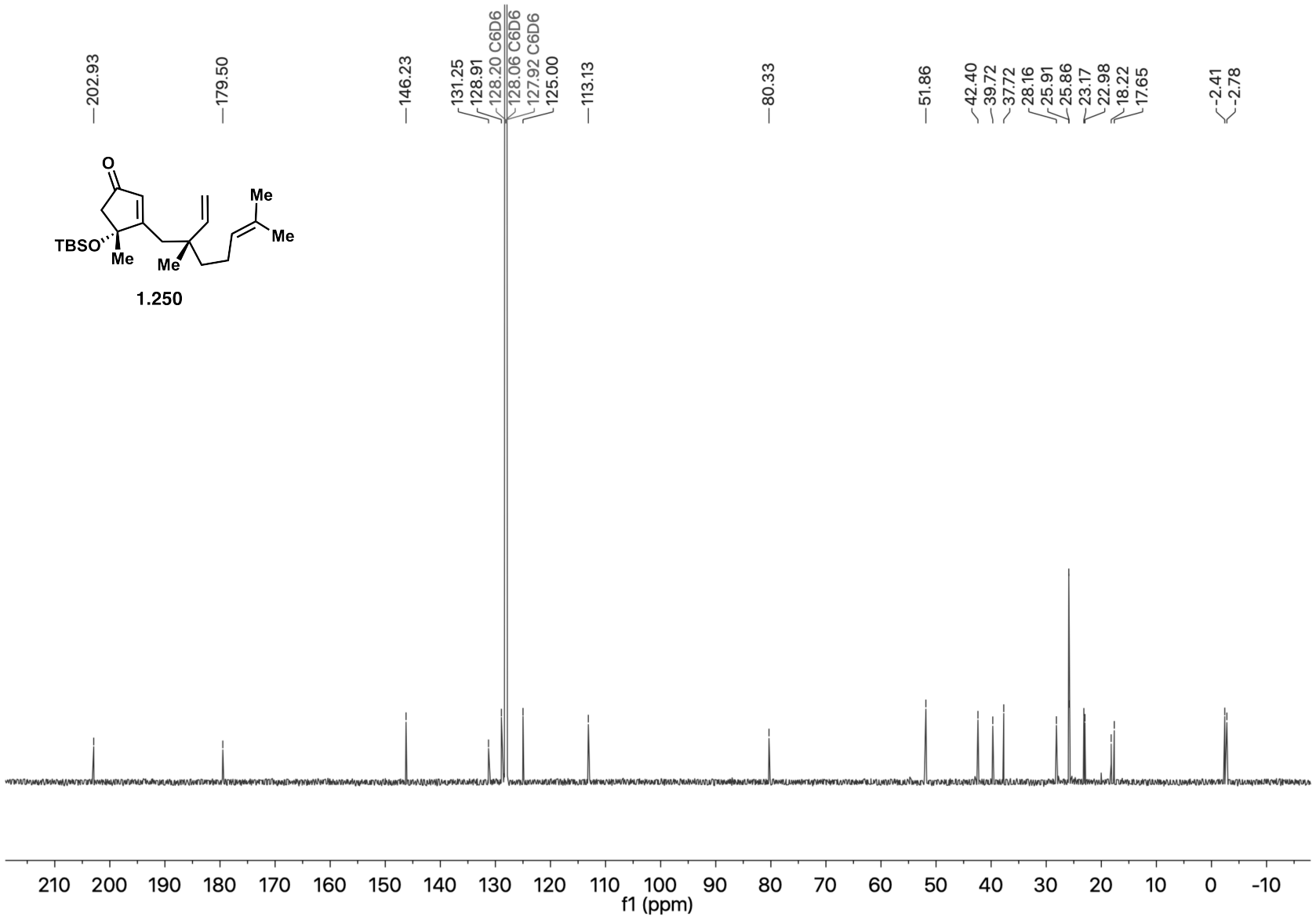
(+)-6-*epi*-ophiobolin A

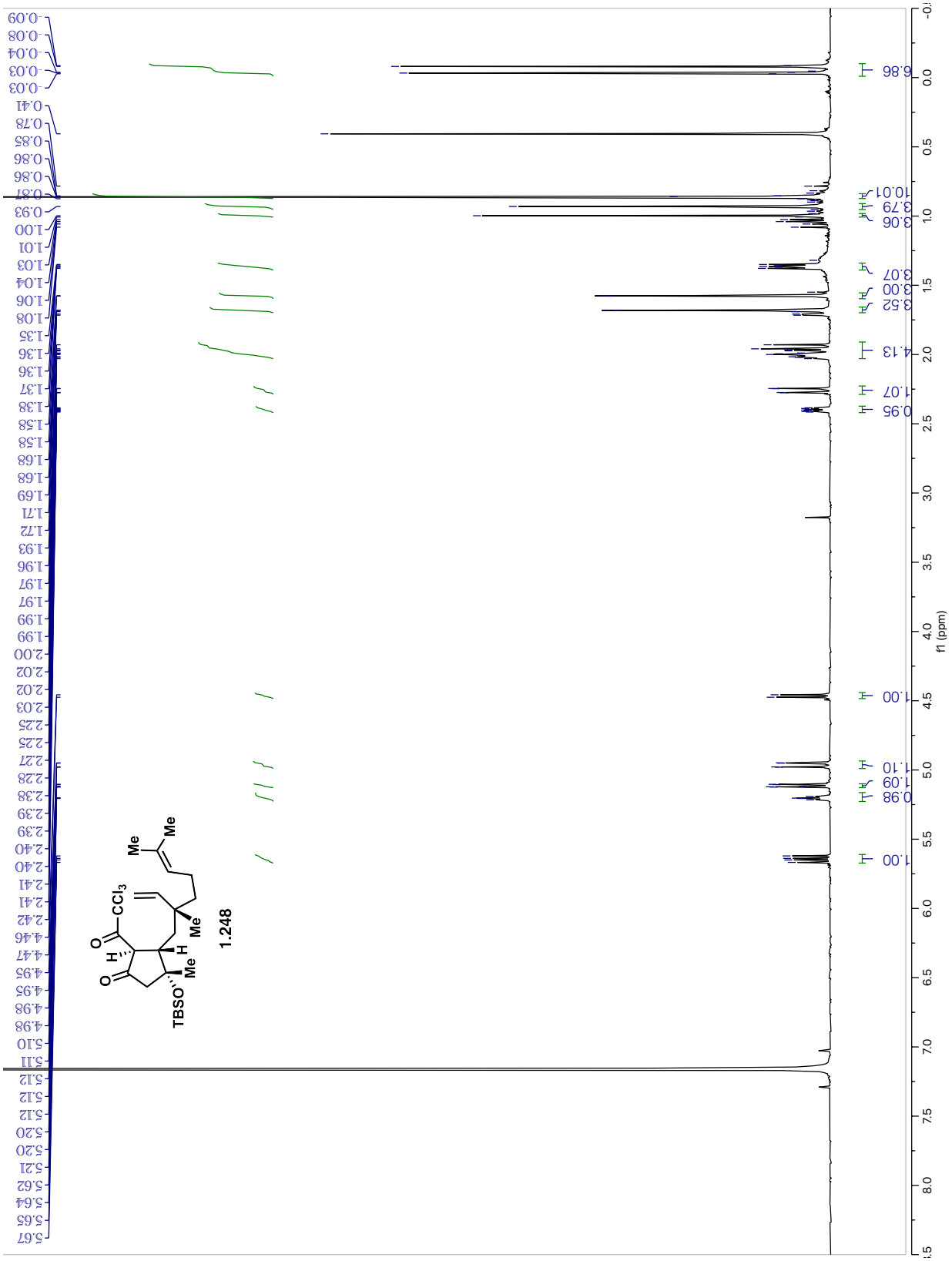
Position	^{13}C (δ) Natural Sample (75 MHz, $CDCl_3$) *[ref. 5]*	^{13}C (δ) Synthetic Sample (176 MHz, $CDCl_3$)
1	42.1	42.2
2	49.5	49.5
3	76.6	76.7
4	54.7	54.8
5	216.6	216.3
6	48.0	48.1
7	142.5	142.5
8	157.7	157.7
9	29.4	29.5
10	53.3	53.4
11	41.5	41.6
12	42.0	42.0
13	42.6	42.6
14	96.0	95.9
15	35.2	35.2
16	31.0	31.0
17	72.0	72.0
18	126.8	126.8
19	135.2	135.3
20	25.7	25.8
21	194.0	194.0
22	22.8	22.8
23	16.1	16.1
24	18.1	18.2
25	25.8	25.8

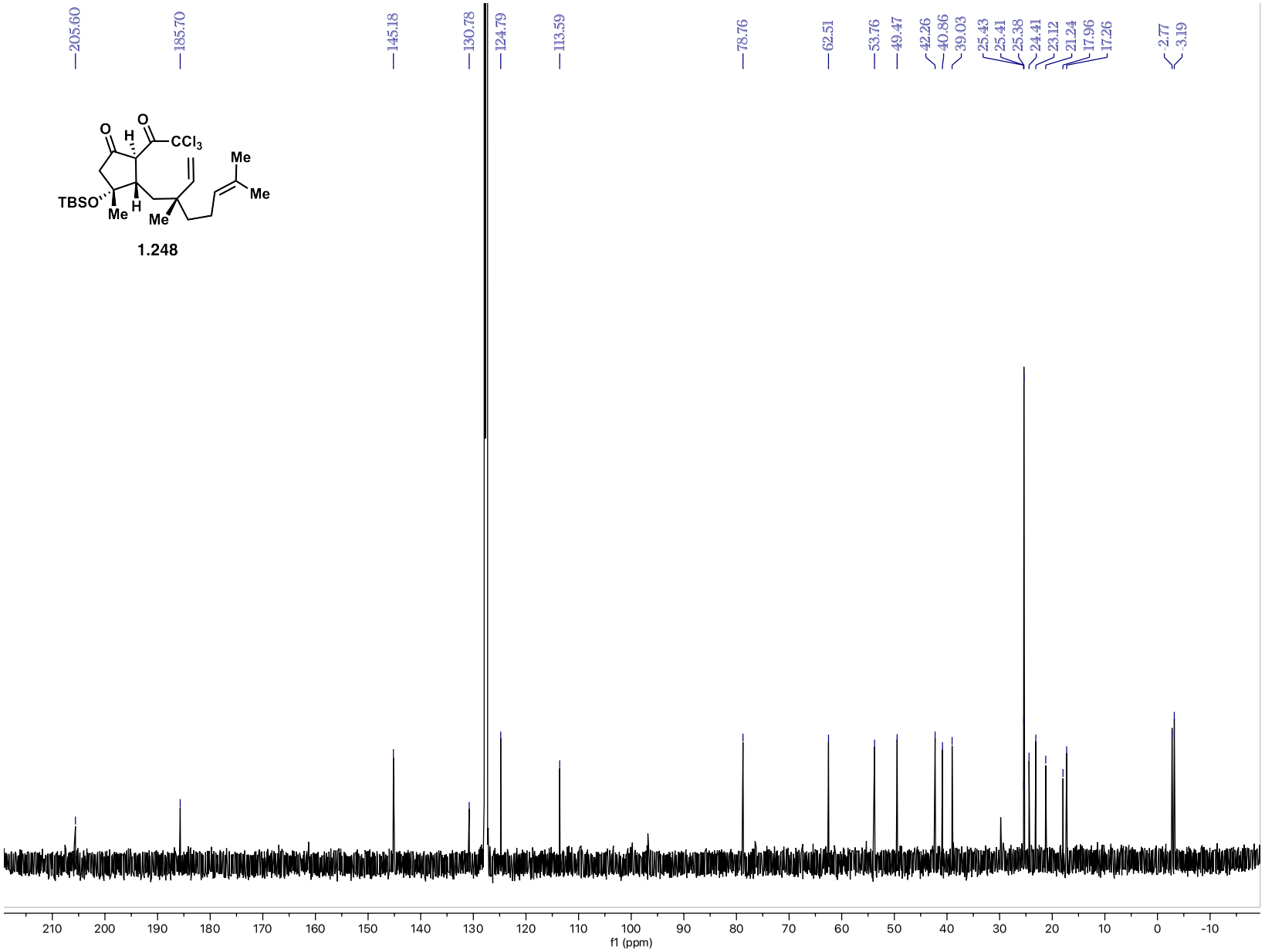
References:

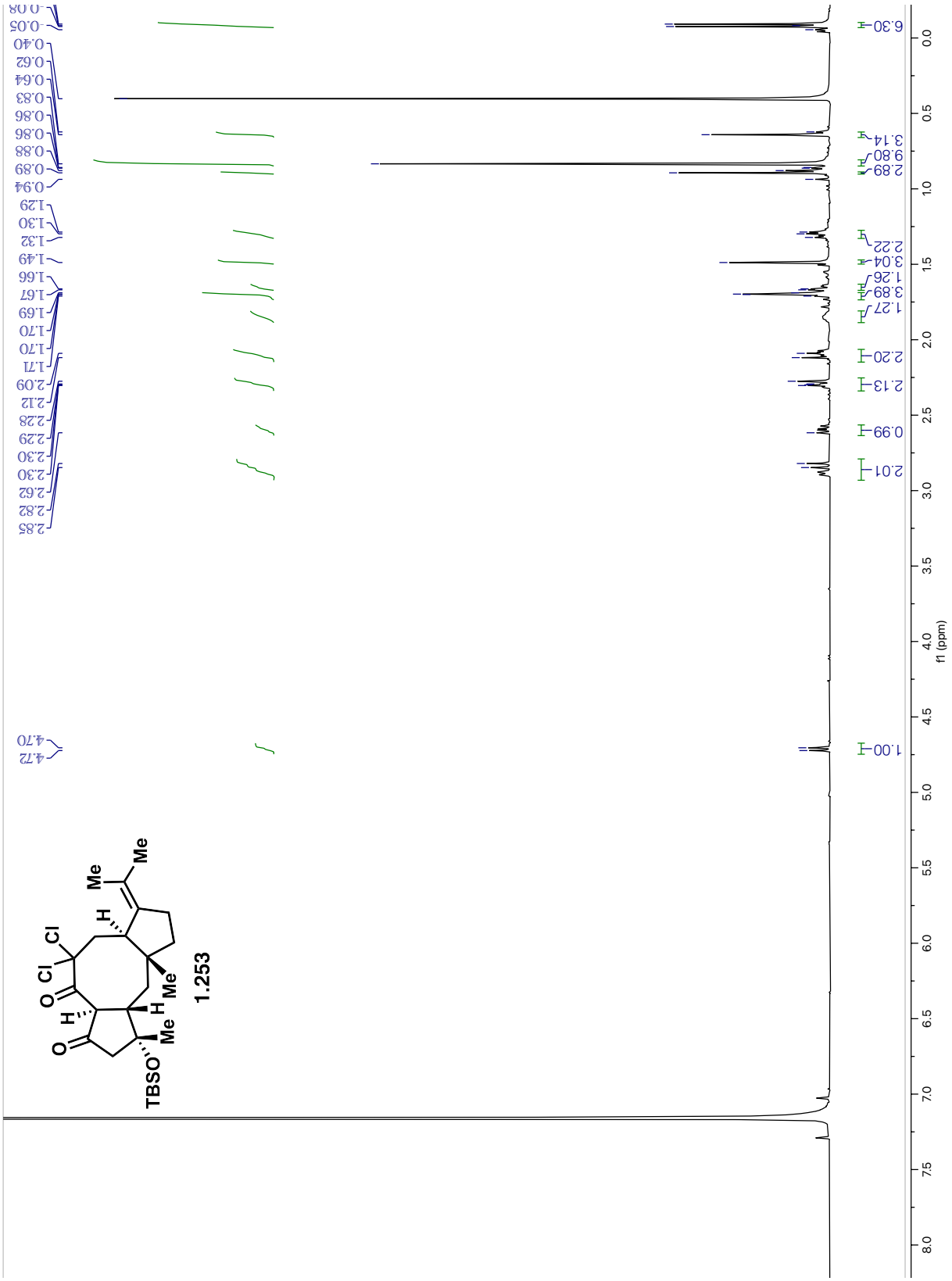
1) Charette, A. B.; Lebel, H. *Org. Synth*. **1999**, *76*, 86-100.
2) Matsuo, J.-i.; Iida, D.; Tatani, K.; Mukaiyama, T. *Bull. Chem. Soc. Jpn*. **2002**, *75*, 223-224.
3) Lettan, R. B.; Milgram, B. C.; Scheidt, K. A. *Org. Synth*. **2007**, *84*, 22-31.
4) Morra, N. A.; Pagenkopf, B. L. *Org. Synth.* **2008**, *85*, 53-63.
5) Li, E.; Clark, A. M.; Rotella, D. P.; Hufford, C. D. *J. Nat. Prod.* **1995**, *58*, 74-81.

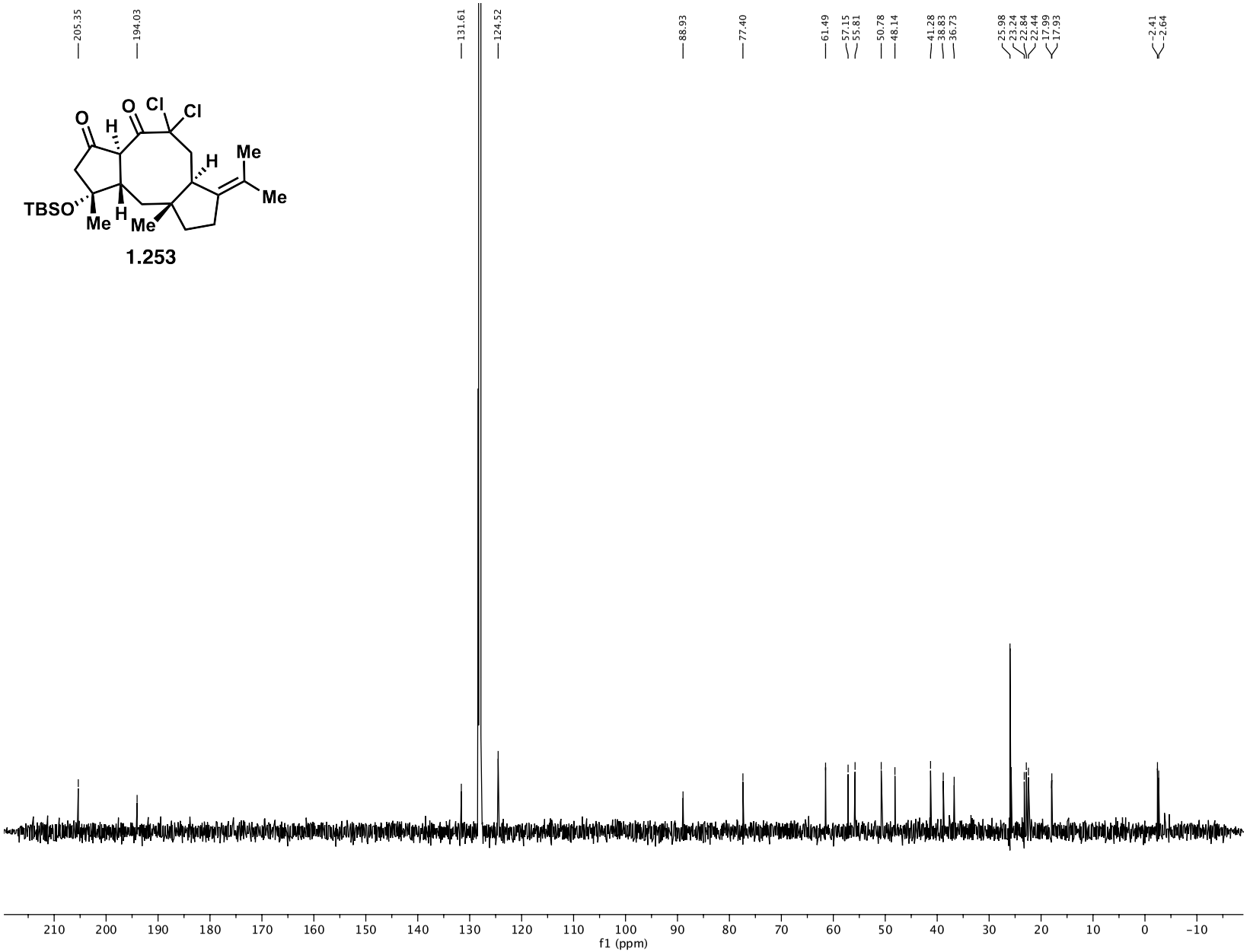

TBSO
O
Me
Me
Me
Me
1.250
f1 (ppm)

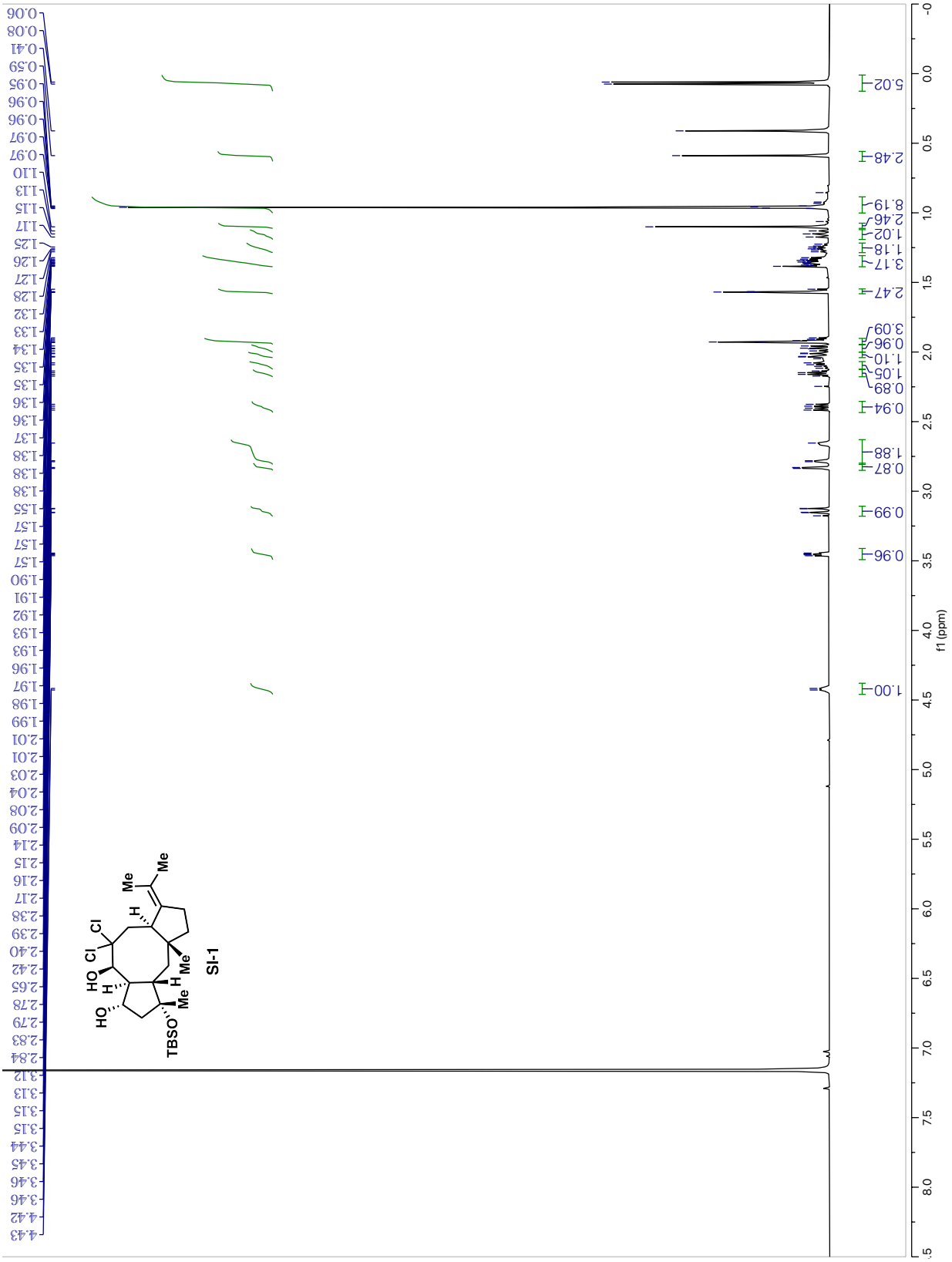

202.93
179.50
146.23
131.25
128.91
128.20 C6D6
128.06 C6D6
127.92 C6D6
125.00
113.13
80.33
51.86
42.40
39.72
37.72
28.16
25.91
25.86
23.17
22.98
18.22
17.65
-2.41
-2.78
O
TBSO
Me
Me
Me
Me
1.250
210 200 190 180 170 160 150 140 130 120 110 100 90 80 70 60 50 40 30 20 10 0 -10
f1 (ppm)

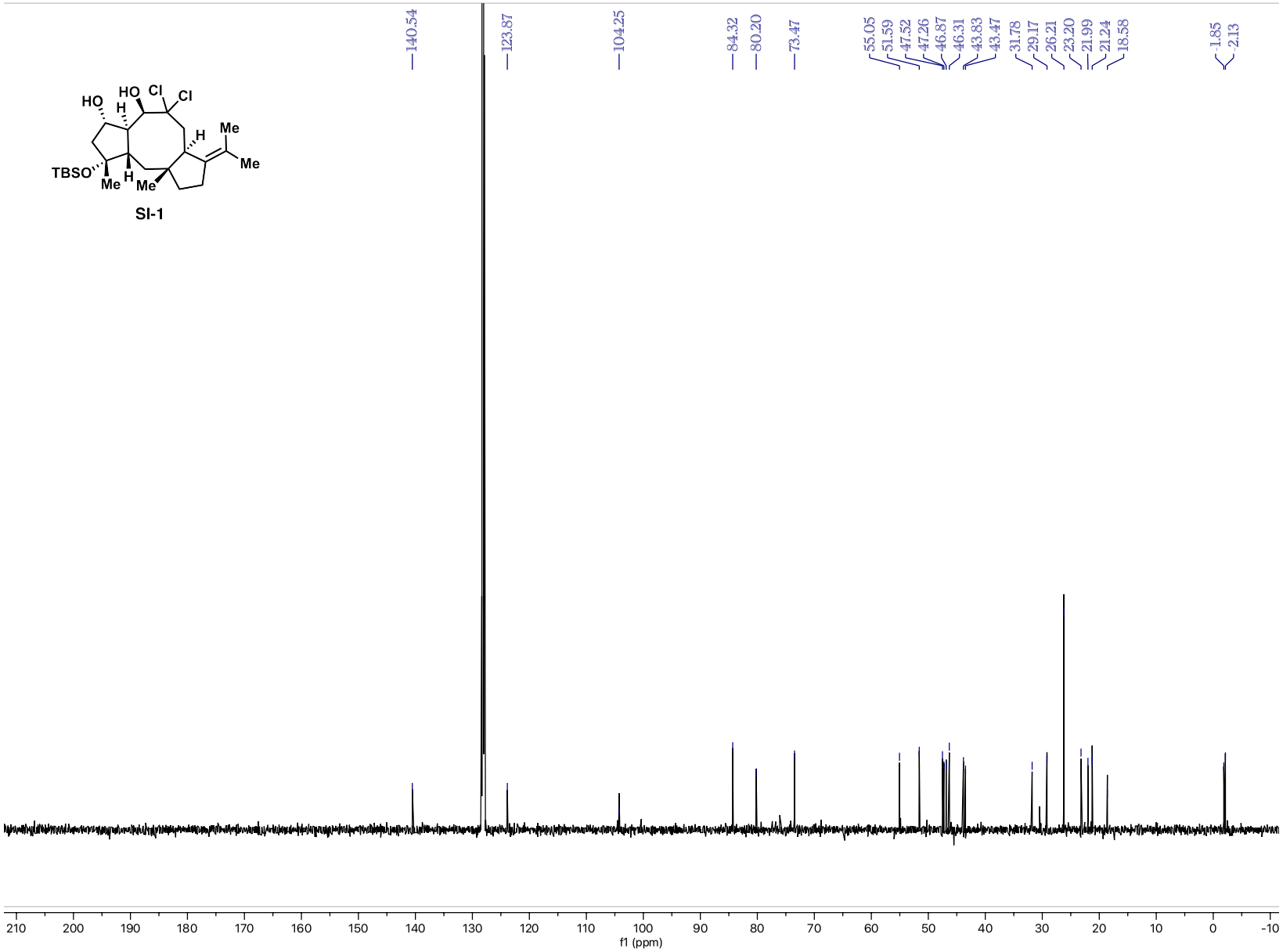

1.248
f1 (ppm)

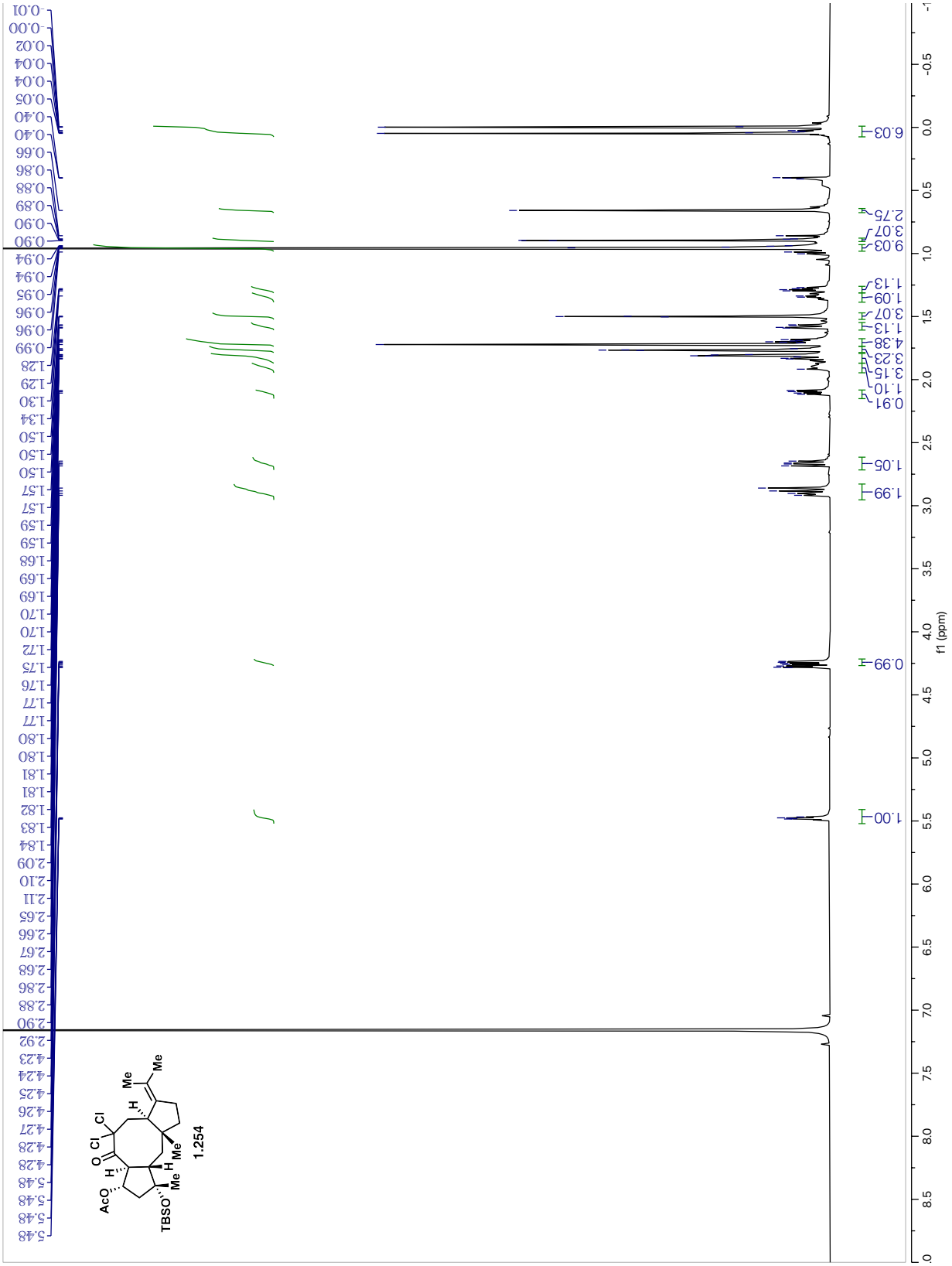

205.60
185.70
145.18
130.78
124.79
113.59
78.76
62.51
53.76
49.47
42.26
40.86
39.03
25.43
25.41
25.38
24.41
23.12
21.24
17.96
17.26
2.77
3.19
O
H
O
CCl3
Me
Me
TBSO
Me
H
Me
1.248
210
200
190
180
170
160
150
140
130
120
110
100
90
80
70
60
50
40
30
20
10
0
-10
f1 (ppm)

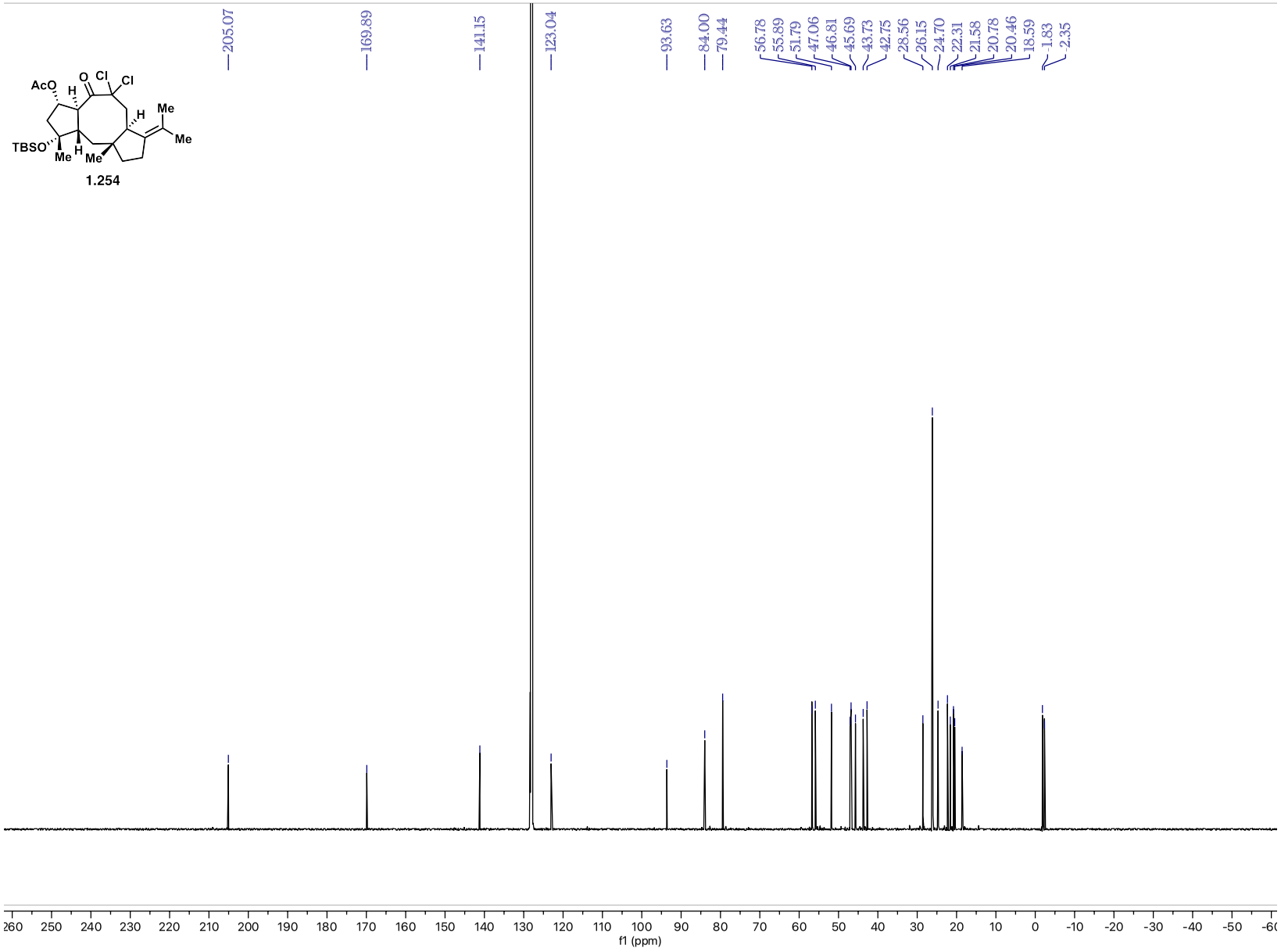

1.253
TBSO
Me
Me
H
Me
Me
H
O
O
Cl
Cl
f1 (ppm)

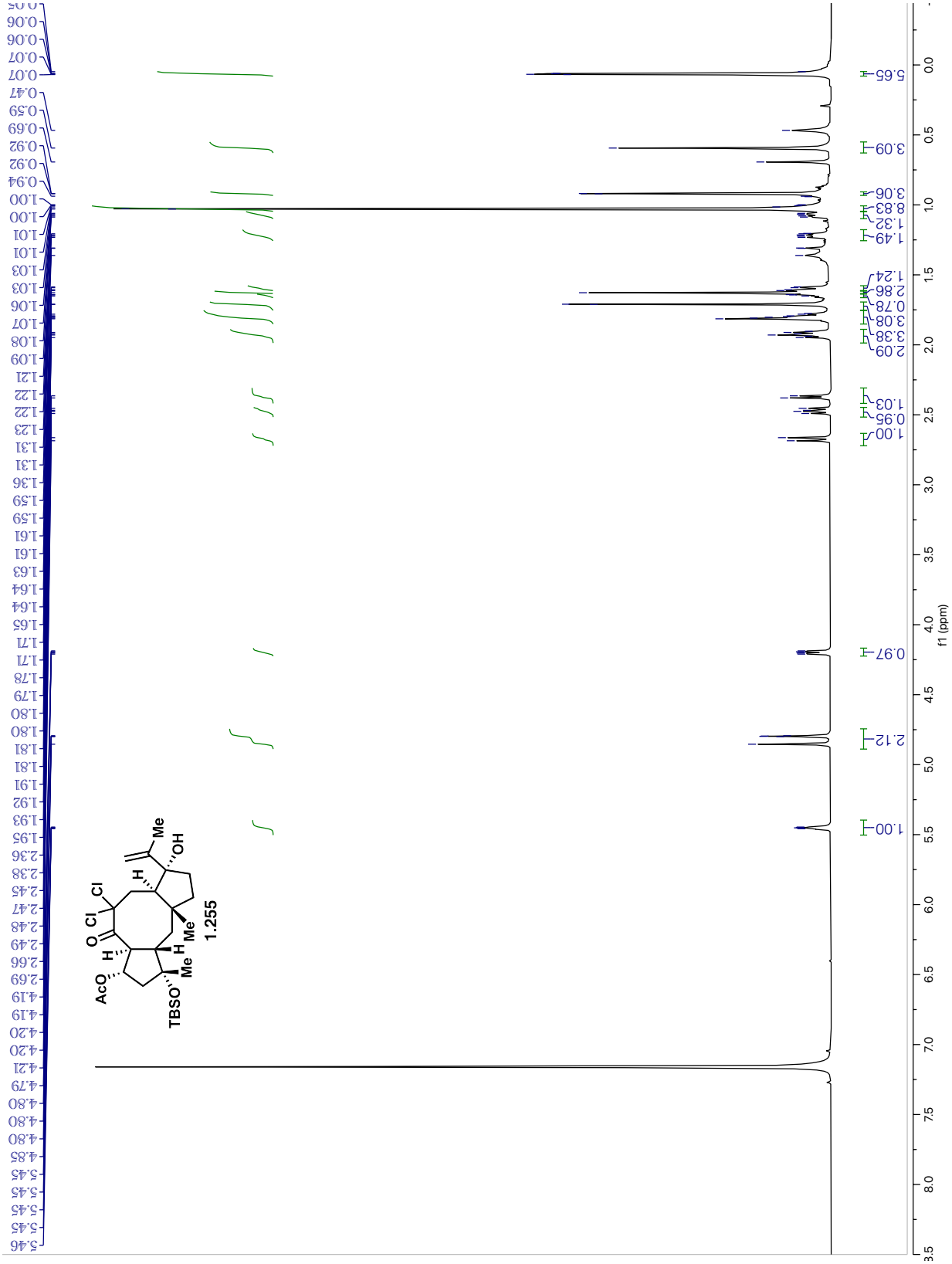

205.35
194.03
131.61
124.52
88.93
77.40
61.49
57.15
55.81
50.78
48.14
41.28
38.83
36.73
25.98
23.24
22.84
22.44
17.99
17.93
-2.41
-2.64
O
O
Cl
Cl
H
H
Me
Me
TBSO
Me
H
Me
1.253
210
200
190
180
170
160
150
140
130
120
110
100
90
80
70
60
50
40
30
20
10
0
-10
f1 (ppm)


Me
Me
H
Cl
Cl
HO
H
HO
TBSO
Me
H
Me
SI-1
5.02
2.48
8.19
2.46
1.02
1.18
3.17
2.47
3.09
0.96
1.10
1.05
0.89
0.94
1.88
0.87
0.99
0.96
1.00
f1 (ppm)

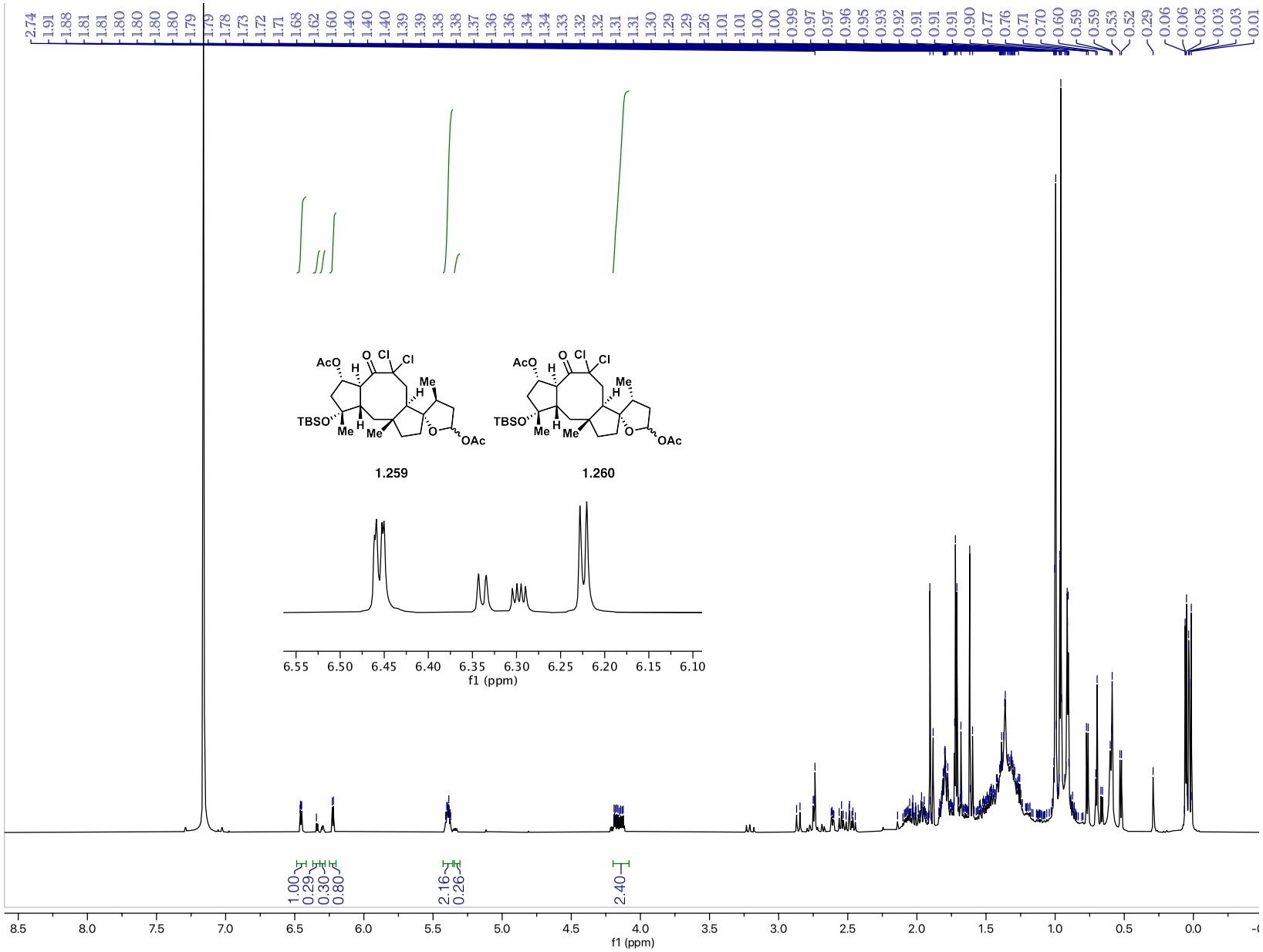

HO
HO
Cl
Cl
H
H
Me
Me
TBSO
Me
H
Me
SI-1
140.54
123.87
104.25
84.32
80.20
73.47
55.05
51.59
47.52
47.26
46.87
46.31
43.83
43.47
31.78
29.17
26.21
23.20
21.99
21.24
18.58
1.85
-2.13
210
200
190
180
170
160
150
140
130
120
110
100
90
80
70
60
50
40
30
20
10
0
-10
f1 (ppm)

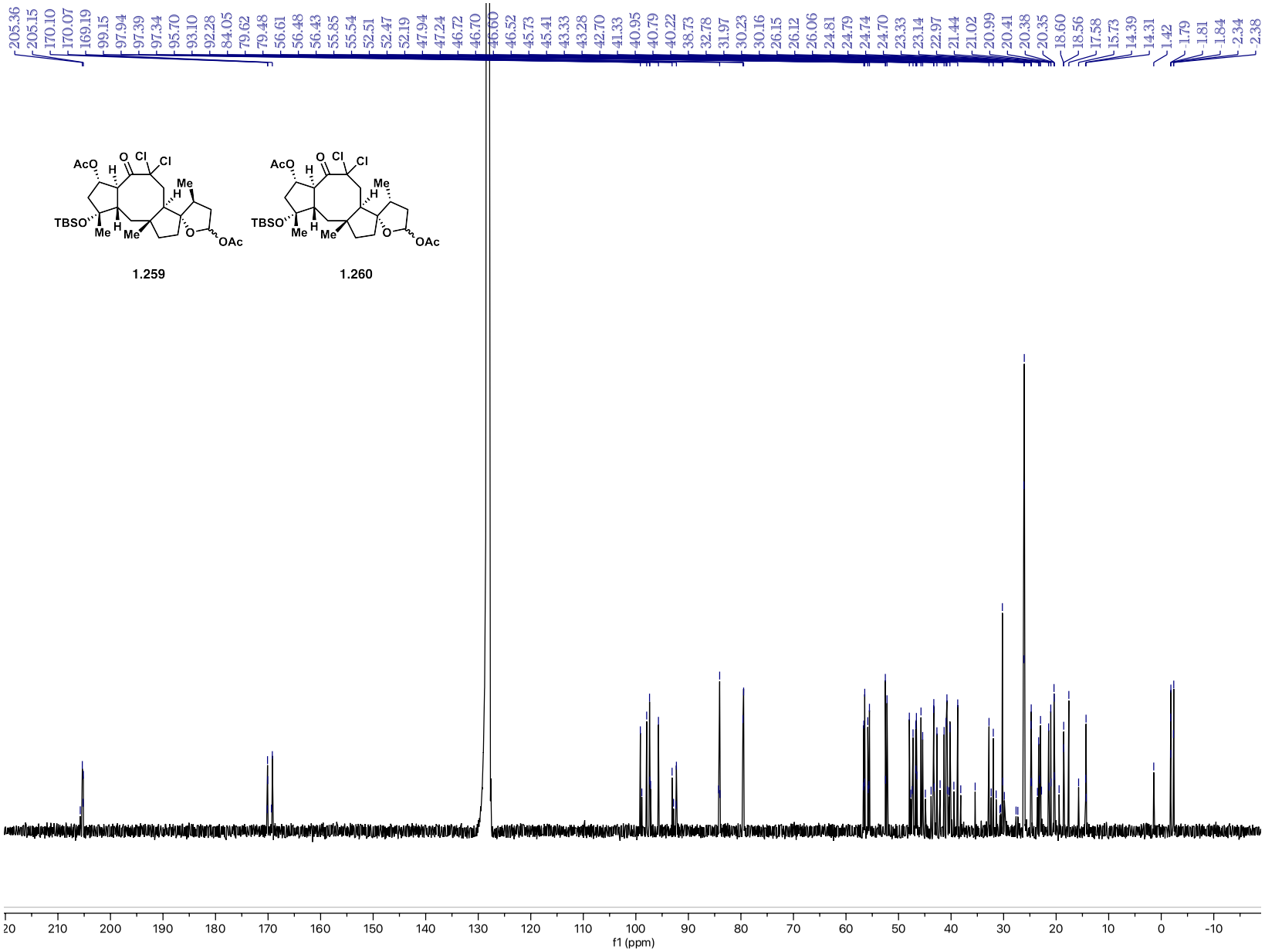

f1 (ppm)
6.03
2.75
3.07
9.03
1.13
1.09
3.07
1.13
4.38
3.23
3.15
1.10
0.91
1.05
1.99
0.99
1.00
AcO
TBSO
Cl
Cl
O
Me
Me
Me
Me
H
H
H
1.254

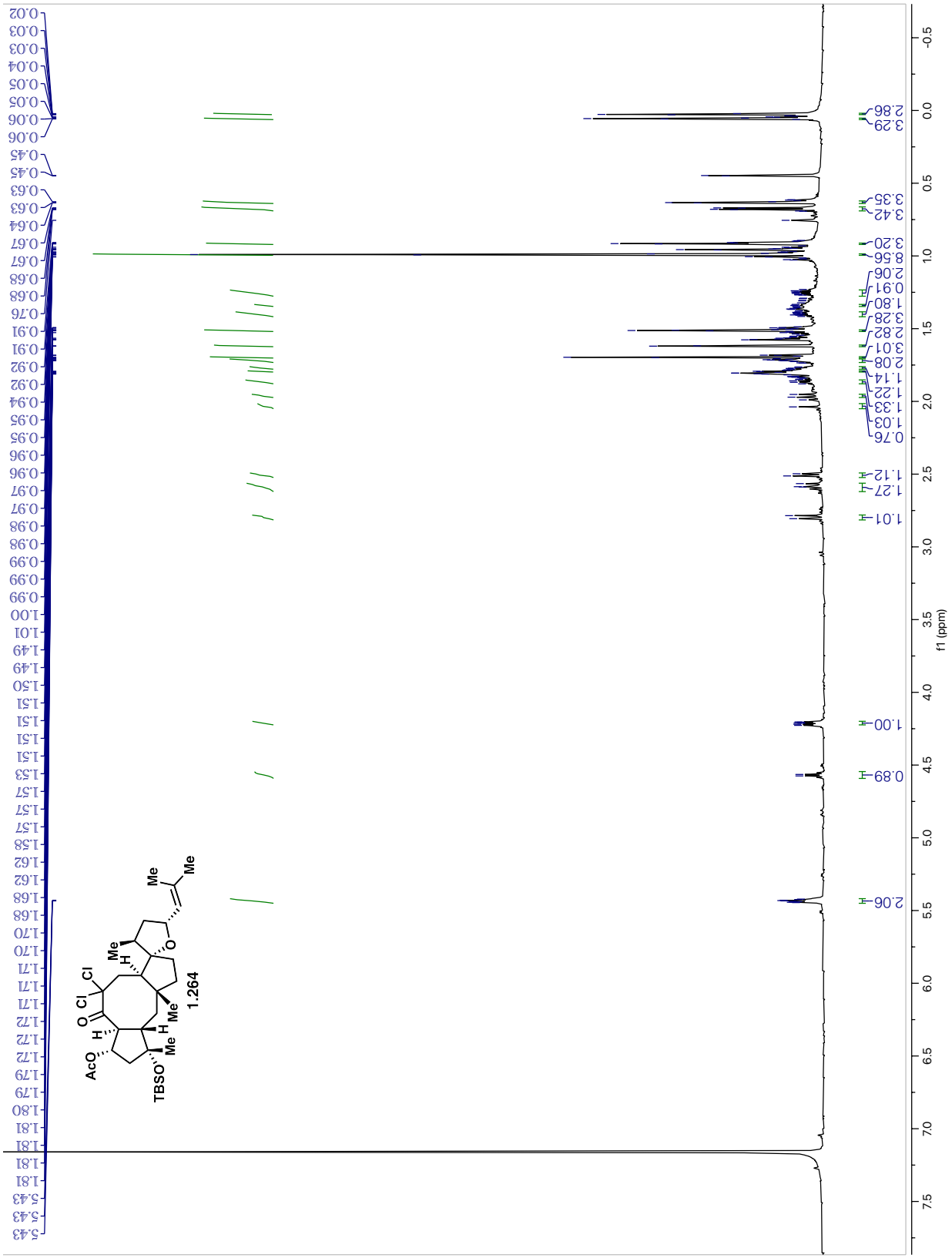

205.07
169.89
141.15
123.04
93.63
84.00
79.44
56.78
55.89
51.79
47.06
46.81
45.69
43.73
42.75
28.56
26.15
24.70
22.31
21.58
20.78
20.46
18.59
1.83
-2.35
AcO
O
Cl
Cl
H
H
Me
Me
TBSO
Me
H
Me
1.254
f1 (ppm)

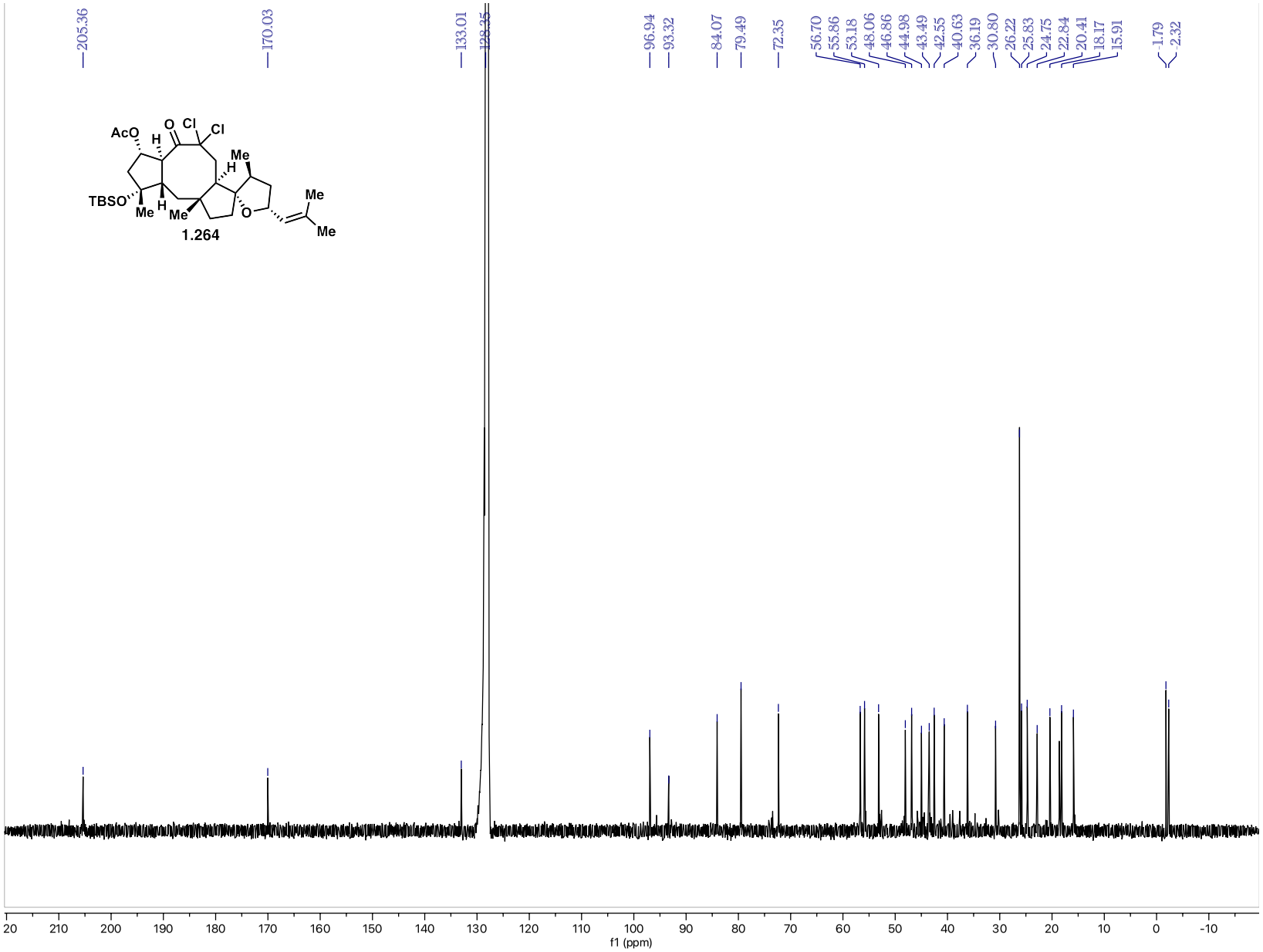

1.255
f1 (ppm)

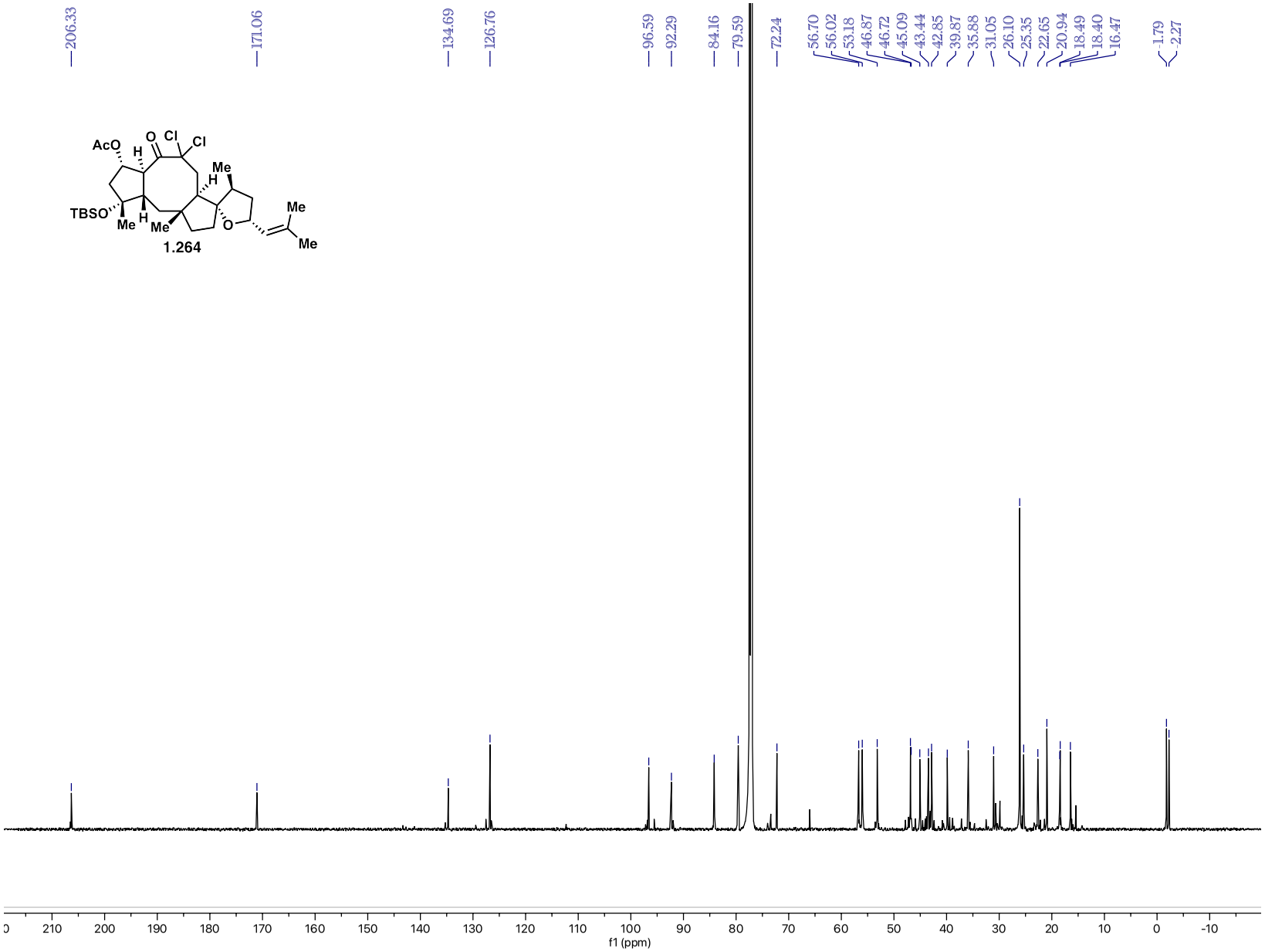
204.97
169.97
147.87
113.20
93.53
89.71
83.96
79.53
56.86
55.75
54.23
49.20
46.92
44.40
42.81
42.27
35.72
26.23
24.74
22.56
20.43
20.30
18.65
-1.77
-2.32
1.255
f1 (ppm)

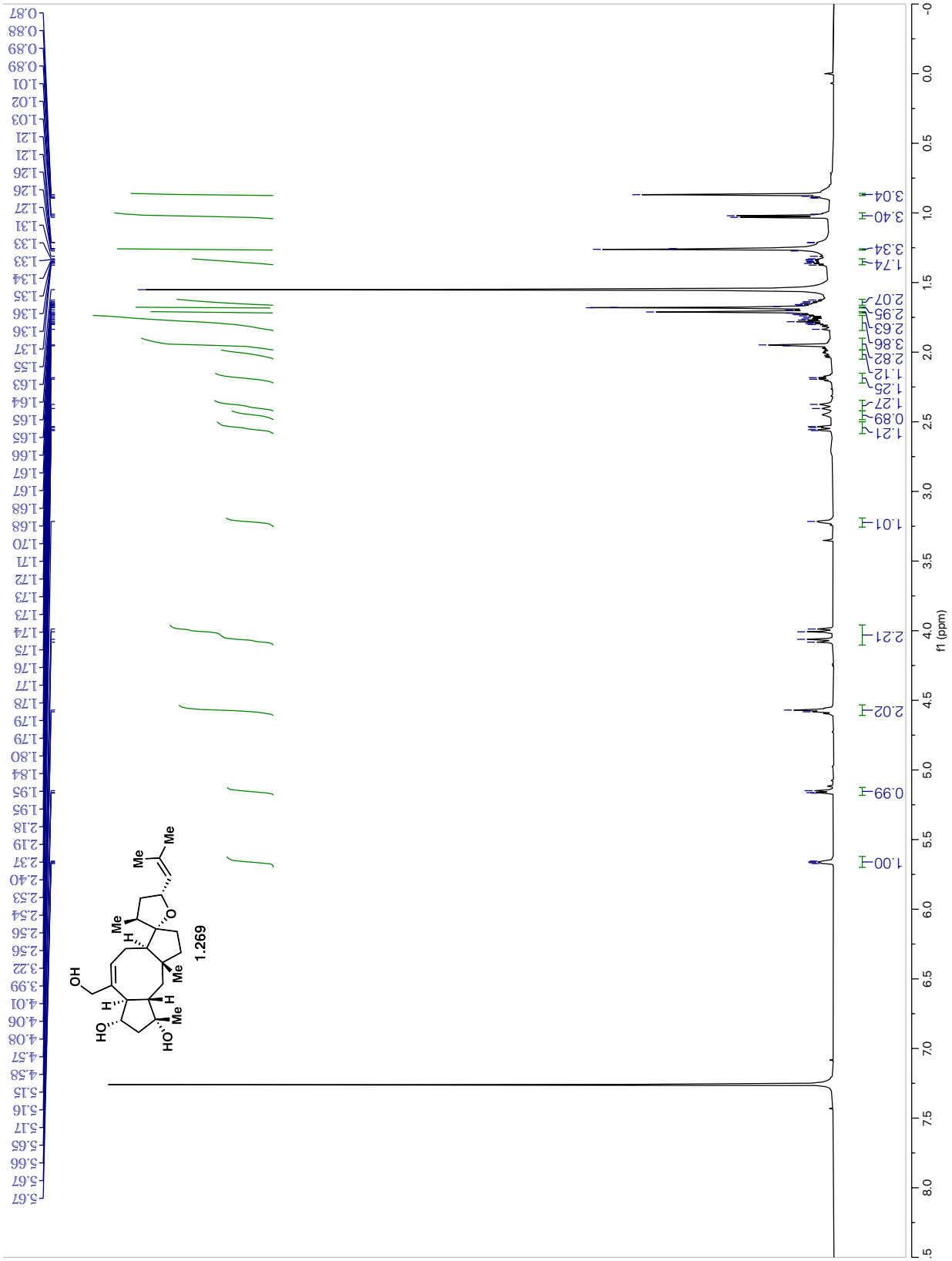

1.259
1.260
f1 (ppm)
f1 (ppm)

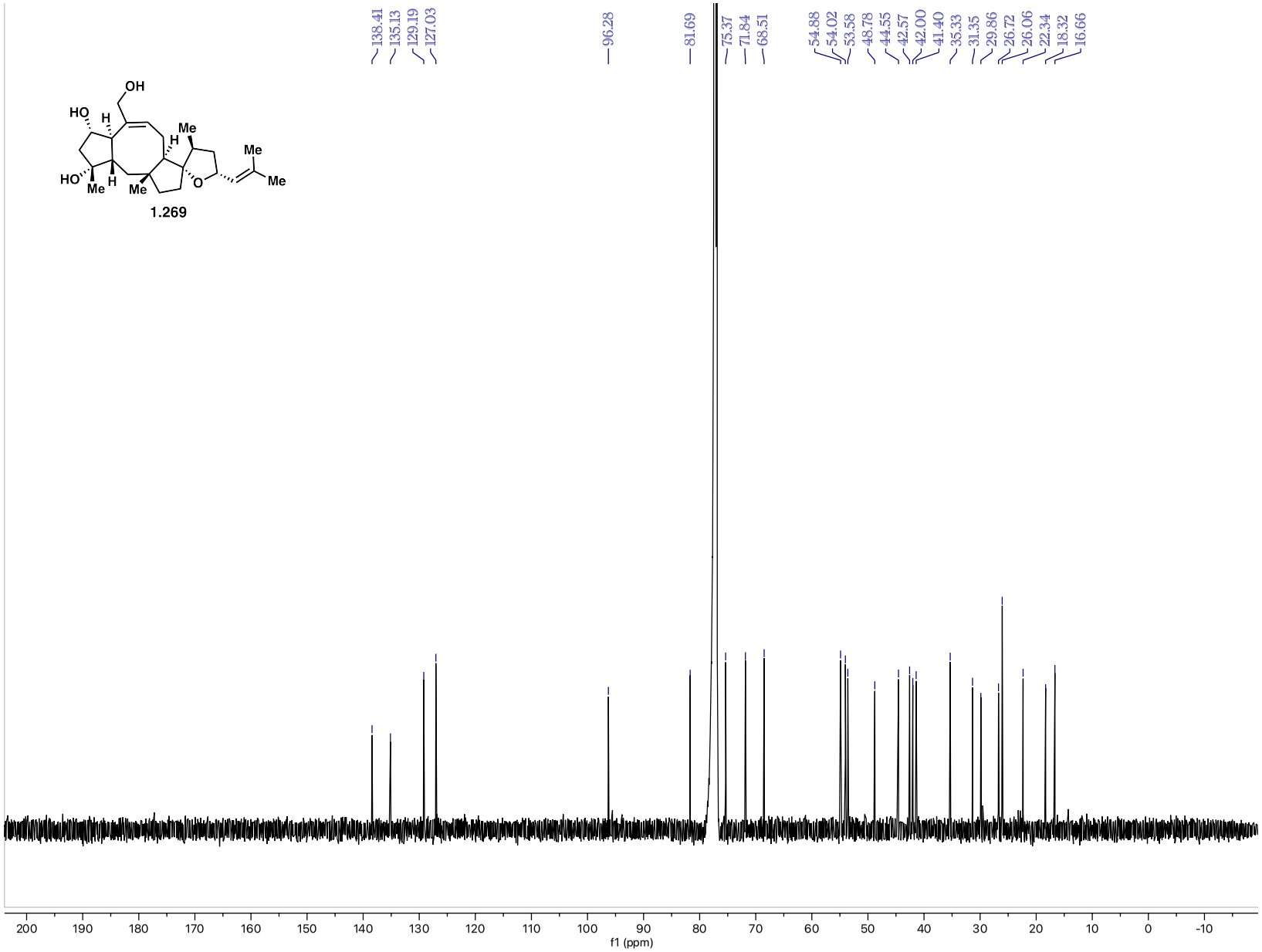

205.36
205.15
170.10
170.07
169.19
99.15
97.94
97.39
97.34
95.70
93.10
92.28
84.05
79.62
79.48
56.61
56.48
56.43
55.85
55.54
52.51
52.47
52.19
47.94
47.24
46.72
46.70
46.60
46.52
45.73
45.41
43.33
43.28
42.70
41.33
40.95
40.79
40.22
38.73
32.78
31.97
30.23
30.16
26.15
26.12
26.06
24.81
24.79
24.74
24.70
23.33
23.14
22.97
21.44
21.02
20.99
20.41
20.38
20.35
18.60
18.56
17.58
15.73
14.39
14.31
1.42
-1.79
-1.81
-1.84
-2.34
-2.38
AcO
H
O
Cl
Cl
Me
H
TBSO
Me
H
Me
O
OAc
1.259
1.260
f1 (ppm)

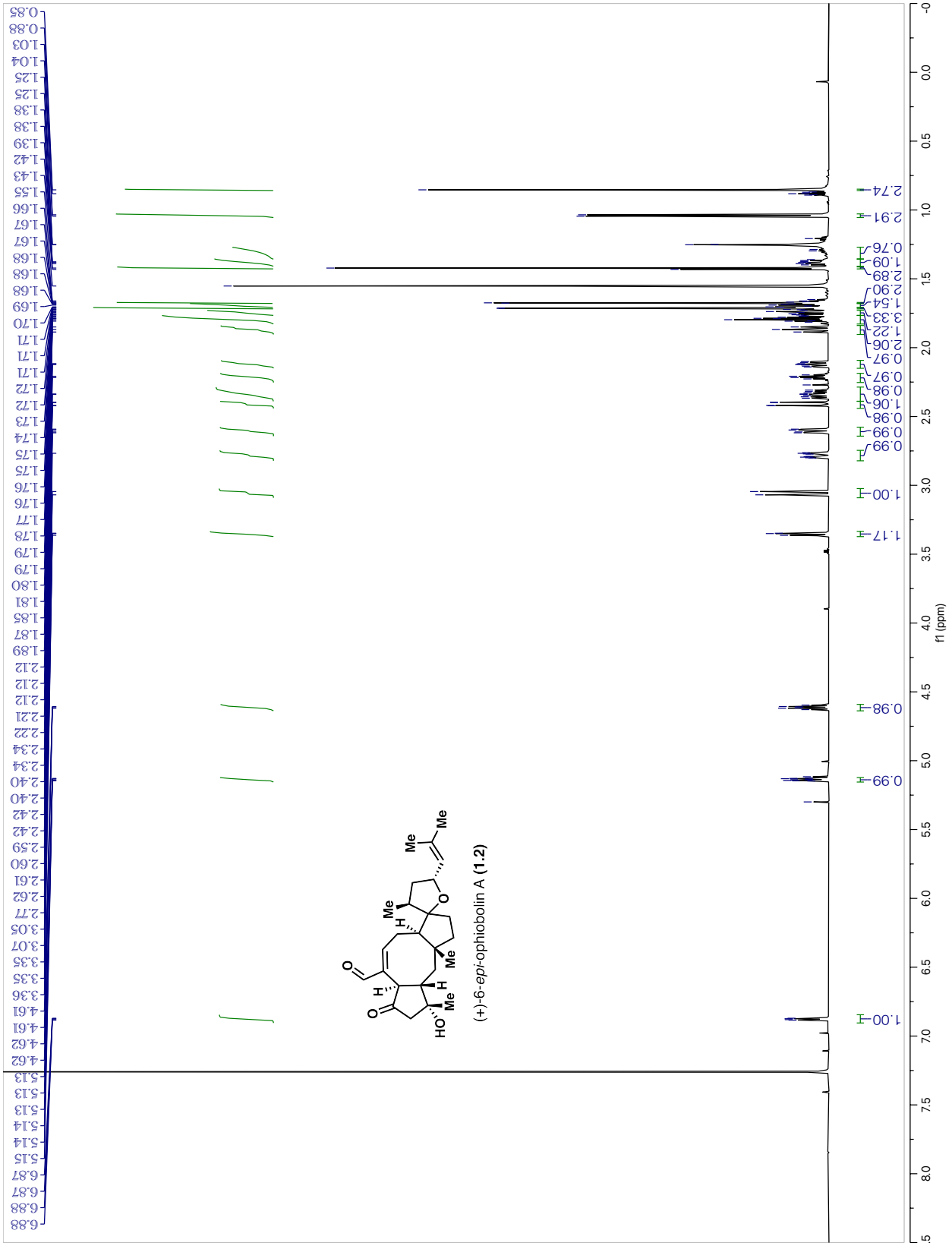

1.264
f1 (ppm)

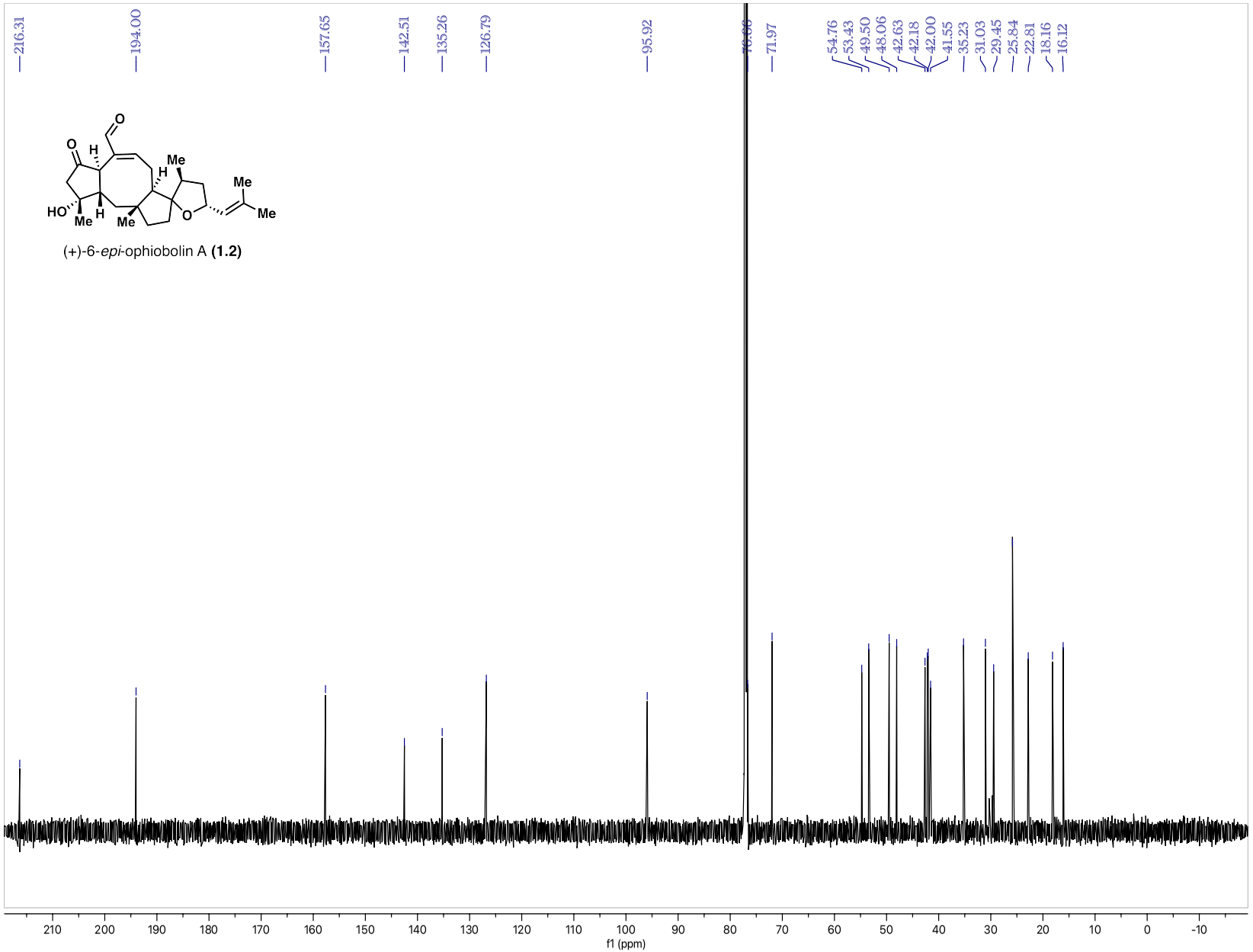

205.36
170.03
133.01
128.35
96.94
93.32
84.07
79.49
72.35
56.70
55.86
53.18
48.06
46.86
44.98
43.49
42.55
40.63
36.19
30.80
26.22
25.83
24.75
22.84
20.41
18.17
15.91
1.79
2.32
AcO
H
O
Cl
Cl
Me
H
TBSO
Me
H
Me
O
Me
Me
1.264
f1 (ppm)


206.33
171.06
134.69
126.76
96.59
92.29
84.16
79.59
72.24
56.70
56.02
53.18
46.87
46.72
45.09
43.44
42.85
39.87
35.88
31.05
26.10
25.35
22.65
20.94
18.49
18.40
16.47
1.79
-2.27
AcO
H
O
Cl
Cl
Me
H
TBSO
Me
H
Me
O
Me
Me
1.264
f1 (ppm)


1.269
f1 (ppm)


138.41
135.13
129.19
127.03
96.28
81.69
75.37
71.84
68.51
54.88
54.02
53.58
48.78
44.55
42.57
42.00
41.40
35.33
31.35
29.86
26.72
26.06
22.34
18.32
16.66
OH
HO
H
Me
H
Me
HO
Me
H
Me
O
Me
1.269
200
190
180
170
160
150
140
130
120
110
100
90
80
70
60
50
40
30
20
10
0
-10
f1 (ppm)


(+)-6-epi-ophiobolin A (1.2)
f1 (ppm)



(+)-6-*epi*-ophiobolin A **(1.2)**

X-ray Crystal Structure Report

X-ray Crystallography. Crystals were coated with Paratone-N oil, attached to a Kapton loop, and mounted onto an Rigaku XtaLAB P200 equipped with a MicroMax 007HF rotating anode and Pilatus3 R 200K-A hybrid pixel array detector. Data were collected using Cu Kα radiation (λ = 1.5418 Å). Crystals were kept at 100(2) K throughout the collection. Data collection was performed with CrysAlisPro (ref. 1). Data processing was done with CrysAlisPro and included a multi-scan absorption correction applied using the SCALE3 ABSPACK scaling algorithm within CrysAlisPro.

Reference #1 - Rigaku Oxford Diffraction, (2015), CrysAlisPro Software system, version 1.171.40.54a, Rigaku Corporation, Oxford, UK.

Compound 1.255:

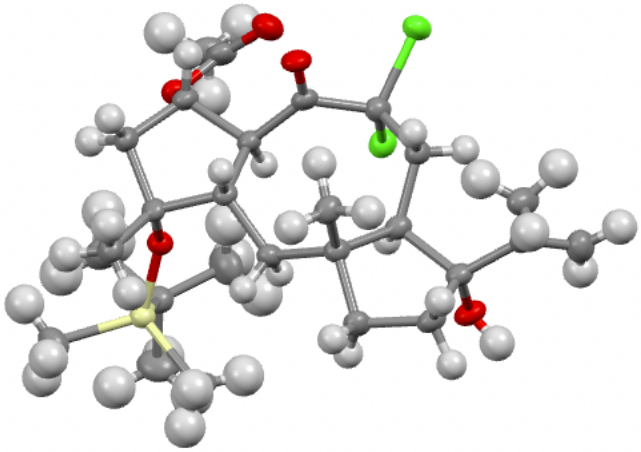


Table 1 Crystal data and structure refinement for DQT_SO2_3.

Identification code	DQT_SO2_3
Empirical formula	$C_{27}H_{41}Cl_2O_5Si$
Formula weight	544.59
Temperature/K	100(2)
Crystal system	orthorhombic
Space group	$P2_12_12_1$
a/Å	8.77930(10)
b/Å	14.87570(10)
c/Å	22.7728(2)
α/°	90
β/°	90

γ/°	90
Volume/Å^3	2974.09(5)
Z	4
ρ_{calc}g/cm^3	1.216
μ/mm^{-1}	2.612
F(000)	1164.0
Crystal size/mm^3	0.237 × 0.143 × 0.047
Radiation	CuKα (λ = 1.54184)
2Θ range for data collection/°	7.098 to 158.322
Index ranges	-10 ≤ h ≤ 11, -18 ≤ k ≤ 18, -28 ≤ l ≤ 28
Reflections collected	129933
Independent reflections	6332 [R_{int} = 0.1042, R_{sigma} = 0.0247]
Data/restraints/parameters	6332/0/326
Goodness-of-fit on F^2	1.078
Final R indexes [I>=2σ (I)]	R_1 = 0.0476, wR_2 = 0.1216
Final R indexes [all data]	R_1 = 0.0497, wR_2 = 0.1243
Largest diff. peak/hole / e Å^{-3}	0.58/-0.43
Flack parameter	0.000(4)

Table 2 Fractional Atomic Coordinates (×10^4) and Equivalent Isotropic Displacement Parameters (Å^2×10^3) for DQT_SO2_3. U_{eq} is defined as 1/3 of the trace of the orthogonalised U_{IJ} tensor.

Atom	*x*	*y*	*z*	U(eq)
Cl2	6635.1(11)	7388.7(6)	7110.9(4)	33.9(2)
Cl1	8787.1(11)	7229.4(8)	6159.8(4)	38.8(2)
Si1	5560.7(12)	4968.0(7)	9120.4(4)	28.0(2)
O5	6930(3)	5021.7(18)	8628.4(11)	27.2(5)
O4	9730(3)	6313(2)	8364.4(12)	34.0(6)
O1	2513(3)	6187(2)	6512.0(13)	35.1(6)
O2	9459(3)	5492(2)	6672.1(12)	33.0(6)
O3	10125(4)	7236(2)	7598.2(13)	42.3(7)

Table 2 Fractional Atomic Coordinates ($\times 10^4$) and Equivalent Isotropic Displacement Parameters ($Å^2 \times 10^3$) for DQT_SO2_3. U_{eq} is defined as 1/3 of the trace of the orthogonalised U_{IJ} tensor.

Atom	*x*	*y*	*z*	U(eq)
C14	7442(4)	4691(2)	7617.2(16)	25.0(7)
C13	8163(4)	5636(3)	7574.7(16)	25.6(7)
C9	6302(5)	4085(3)	6415.2(18)	33.4(8)
C16	7784(4)	4428(3)	8256.9(16)	27.2(8)
C15	5765(4)	4627(3)	7448.3(16)	27.2(7)
C12	8506(4)	5886(3)	6956.2(16)	28.1(8)
C7	5270(4)	4675(3)	6796.1(16)	27.7(8)
C8	5039(4)	5649(3)	6549.8(17)	28.4(8)
C18	9628(4)	5564(3)	7957.7(17)	30.6(8)
C4	3509(4)	5624(3)	6171.6(17)	28.7(8)
C19	9984(5)	7129(3)	8119.3(19)	36.2(9)
C10	6349(4)	6138(3)	6235.8(16)	29.9(8)
C6	3623(5)	4307(3)	6776.7(17)	31.9(8)
C17	9457(5)	4702(3)	8314.1(18)	32.8(8)
C5	2970(4)	4651(3)	6203.1(18)	32.3(8)
C2	3614(5)	5955(3)	5543.4(18)	34.4(9)
C21	7508(5)	3445(3)	8404.0(18)	33.7(9)
C11	7529(5)	6602(3)	6631.5(16)	31.2(8)
C25	5564(5)	6140(3)	9432.3(19)	36.2(9)
C23	5950(6)	4124(3)	9708(2)	44.0(11)
C20	10023(6)	7848(4)	8575(2)	48.5(11)
C3	2852(6)	6681(3)	5364(2)	44.3(11)
C1	4521(5)	5407(4)	5111.7(19)	44.0(11)
C22	3666(5)	4696(4)	8789(2)	47.8(12)
C27	4168(6)	6280(4)	9826(2)	51.4(12)
C24	5553(7)	6840(3)	8946(2)	53.1(12)
C26	7012(6)	6282(4)	9800(3)	52.9(13)

Table 3 Anisotropic Displacement Parameters ($Å^2×10^3$) for DQT_SO2_3. The Anisotropic displacement factor exponent takes the form: $-2\pi^2[h^2a^{*2}U_{11}+2hka^*b^*U_{12}+\ldots]$.

Atom	U_{11}	U_{22}	U_{33}	U_{23}	U_{13}	U_{12}
Cl2	32.1(5)	35.0(5)	34.6(4)	-3.4(4)	-3.1(4)	1.3(4)
Cl1	32.6(5)	50.0(6)	33.8(5)	8.7(4)	-0.3(4)	-11.4(4)
Si1	25.5(5)	33.2(5)	25.5(5)	0.4(4)	3.0(4)	-1.1(4)
O5	26.4(13)	30.4(13)	24.9(12)	-1.4(11)	2.8(10)	-0.5(11)
O4	30.4(15)	43.0(16)	28.7(13)	-1.2(12)	-1.8(11)	-8.2(12)
O1	22.2(13)	43.3(16)	39.7(16)	-8.7(13)	2.0(11)	2.3(12)
O2	22.3(13)	43.0(16)	33.8(14)	-2.5(12)	7.0(11)	-0.6(12)
O3	40.5(16)	49.4(18)	36.8(16)	5.6(14)	5.7(12)	-8.5(15)
C14	22.1(17)	29.3(18)	23.7(17)	-3.5(14)	2.7(14)	1.9(14)
C13	19.4(16)	31.6(18)	25.9(17)	0.1(14)	-0.4(13)	-0.1(14)
C9	31(2)	38(2)	30.8(19)	-6.8(16)	-3.0(16)	1.7(17)
C16	21.8(17)	33.0(19)	26.7(17)	1.4(15)	2.8(13)	5.0(15)
C15	24.5(18)	33.1(18)	24.1(17)	-0.7(14)	0.9(14)	-4.1(15)
C12	19.1(17)	35.7(19)	29.4(18)	-2.4(15)	-0.3(14)	-4.5(15)
C7	24.4(18)	34.3(19)	24.5(17)	-3.8(14)	0.9(14)	-1.5(15)
C8	24.3(17)	32.5(19)	28.4(18)	-5.1(15)	0.2(14)	-0.8(15)
C18	19.8(17)	43(2)	28.6(18)	0.5(16)	0.0(14)	-3.3(15)
C4	21.6(17)	36.2(19)	28.3(18)	-3.6(15)	2.2(14)	-0.4(15)
C19	24.3(18)	45(2)	39(2)	1.1(18)	-1.6(16)	-9.5(17)
C10	24.7(18)	38(2)	26.6(17)	-0.3(15)	0.1(15)	-1.1(15)
C6	30(2)	35(2)	30.6(19)	-0.3(16)	-2.0(16)	-6.1(16)
C17	24.6(18)	45(2)	28.5(18)	5.6(16)	-2.1(15)	0.5(17)
C5	22.7(18)	41(2)	33(2)	-5.6(17)	-2.0(15)	-1.8(15)
C2	27(2)	45(2)	31.2(19)	-0.2(17)	-5.2(15)	-6.6(17)
C21	30(2)	37(2)	34(2)	3.7(16)	1.3(16)	3.4(16)
C11	29(2)	39(2)	26.2(18)	0.8(15)	-1.6(15)	-4.8(16)
C25	34(2)	37(2)	38(2)	-1.0(17)	4.3(18)	0.7(18)
C23	48(3)	44(2)	40(2)	8.6(19)	9(2)	1(2)
C20	44(2)	53(3)	49(3)	-11(2)	2(2)	-15(2)
C3	45(3)	47(3)	41(2)	5(2)	-8(2)	-3(2)
C1	35(2)	66(3)	31(2)	-3(2)	-0.3(18)	-7(2)

Table 3 Anisotropic Displacement Parameters ($Å^2×10^3$) for DQT_SO2_3. The Anisotropic displacement factor exponent takes the form: $-2\pi^2[h^2a^{*2}U_{11}+2hka^*b^*U_{12}+\ldots]$.

Atom	U_{11}	U_{22}	U_{33}	U_{23}	U_{13}	U_{12}
C22	29(2)	67(3)	47(2)	-13(2)	6(2)	-7(2)
C27	51(3)	50(3)	54(3)	-10(2)	19(2)	4(2)
C24	67(3)	36(2)	56(3)	5(2)	7(3)	10(2)
C26	44(3)	56(3)	60(3)	-17(3)	-7(2)	-6(2)

Table 4 Bond Lengths for DQT_SO2_3.

Atom	Atom	Length/Å	Atom	Atom	Length/Å
Cl2	C11	1.783(4)	C16	C21	1.520(6)
Cl1	C11	1.801(4)	C15	C7	1.549(5)
Si1	O5	1.645(3)	C12	C11	1.555(6)
Si1	C25	1.883(4)	C7	C8	1.567(5)
Si1	C23	1.867(5)	C7	C6	1.546(5)
Si1	C22	1.871(5)	C8	C4	1.596(5)
O5	C16	1.435(4)	C8	C10	1.538(5)
O4	C18	1.452(5)	C18	C17	1.525(6)
O4	C19	1.354(5)	C4	C5	1.525(6)
O1	C4	1.438(5)	C4	C2	1.516(5)
O2	C12	1.209(5)	C19	C20	1.490(6)
O3	C19	1.204(5)	C10	C11	1.537(5)
C14	C13	1.545(5)	C6	C5	1.516(5)
C14	C16	1.538(5)	C2	C3	1.334(6)
C14	C15	1.525(5)	C2	C1	1.505(6)
C13	C12	1.487(5)	C25	C27	1.534(6)
C13	C18	1.558(5)	C25	C24	1.519(6)
C9	C7	1.531(5)	C25	C26	1.536(6)
C16	C17	1.530(5)			

Table 5 Bond Angles for DQT_SO2_3.

Atom	Atom	Atom	Angle/°	Atom	Atom	Atom	Angle/°
O5	Si1	C25	102.16(17)	C10	C8	C4	112.9(3)
O5	Si1	C23	112.77(19)	O4	C18	C13	110.8(3)
O5	Si1	C22	112.66(18)	O4	C18	C17	108.2(3)
C23	Si1	C25	110.6(2)	C17	C18	C13	106.0(3)
C23	Si1	C22	107.8(2)	O1	C4	C8	101.9(3)
C22	Si1	C25	110.7(2)	O1	C4	C5	109.8(3)
C16	O5	Si1	138.9(2)	O1	C4	C2	110.8(3)
C19	O4	C18	115.8(3)	C5	C4	C8	105.0(3)
C16	C14	C13	102.2(3)	C2	C4	C8	116.8(3)
C15	C14	C13	115.9(3)	C2	C4	C5	111.9(3)
C15	C14	C16	114.3(3)	O4	C19	C20	111.1(4)
C14	C13	C18	103.9(3)	O3	C19	O4	122.8(4)
C12	C13	C14	111.7(3)	O3	C19	C20	126.0(4)
C12	C13	C18	112.4(3)	C11	C10	C8	116.4(3)
O5	C16	C14	107.4(3)	C5	C6	C7	105.0(3)
O5	C16	C17	106.7(3)	C18	C17	C16	105.9(3)
O5	C16	C21	112.3(3)	C6	C5	C4	104.1(3)
C17	C16	C14	101.5(3)	C3	C2	C4	121.5(4)
C21	C16	C14	115.0(3)	C3	C2	C1	120.3(4)
C21	C16	C17	113.0(3)	C1	C2	C4	118.2(4)
C14	C15	C7	120.7(3)	Cl2	C11	Cl1	107.2(2)
O2	C12	C13	121.7(4)	C12	C11	Cl2	113.7(3)
O2	C12	C11	117.3(3)	C12	C11	Cl1	107.5(3)
C13	C12	C11	120.7(3)	C10	C11	Cl2	110.9(3)
C9	C7	C15	110.5(3)	C10	C11	Cl1	107.2(3)
C9	C7	C8	113.8(3)	C10	C11	C12	110.1(3)
C9	C7	C6	109.5(3)	C27	C25	Si1	110.1(3)
C15	C7	C8	115.0(3)	C27	C25	C26	108.9(4)
C6	C7	C15	105.9(3)	C24	C25	Si1	111.1(3)
C6	C7	C8	101.3(3)	C24	C25	C27	109.2(4)
C7	C8	C4	106.3(3)	C24	C25	C26	108.0(4)
C10	C8	C7	120.5(3)	C26	C25	Si1	109.5(3)

Table 6 Hydrogen Atom Coordinates (Å×10^4) and Isotropic Displacement Parameters (Å^2×10^3) for DQT_SO2_3.

Atom	*x*	*y*	*z*	U(eq)
H1	1646.28	6155.41	6379.77	53
H14	8018.37	4286.72	7359.98	30
H13	7470.9	6080.61	7746.68	31
H9A	7304.06	4342.18	6400.89	50
H9B	5892.1	4050.48	6025.01	50
H9C	6356.6	3492.45	6580.84	50
H15A	5235.47	5104.47	7654.25	33
H15B	5383.12	4063.71	7604.77	33
H8	4800.14	6020.75	6893.01	34
H18	10537.51	5535.41	7708.85	37
H10A	6878.43	5705.71	5990.73	36
H10B	5912.12	6587.95	5977.59	36
H6A	3623.03	3654.63	6785.04	38
H6B	3036.77	4527.14	7107.64	38
H17A	9718.22	4807.04	8722.3	39
H17B	10116.8	4234.79	8160.2	39
H5A	1866.07	4618.34	6205.19	39
H5B	3353.63	4305.94	5873.21	39
H21A	7811.82	3331.09	8802.08	51
H21B	8091.62	3072.59	8143.48	51
H21C	6444.5	3309.73	8359.54	51
H23A	5753.79	3530.62	9559.99	66
H23B	5301.05	4238.95	10038.89	66
H23C	6996.24	4166.95	9827.74	66
H20A	9065.96	7862.75	8778.49	73
H20B	10200	8418.22	8389.77	73
H20C	10826.98	7725.42	8848.75	73
H3A	2880	6850.09	4971.17	53
H3B	2292.44	7017.94	5632.23	53

Table 6 Hydrogen Atom Coordinates (Å×10^4) and Isotropic Displacement Parameters (Å^2×10^3) for DQT_SO2_3.

Atom	*x*	*y*	*z*	U(eq)
H1A	5404.18	5165.46	5303.58	66
H1B	4834	5783	4790.89	66
H1C	3903.48	4924.16	4965.45	66
H22A	3390.18	5156.13	8513.42	72
H22B	2911.06	4663.44	9093.24	72
H22C	3724.35	4127.59	8590.18	72
H27A	3257.19	6217.71	9596.37	77
H27B	4202.14	6870.29	9995.7	77
H27C	4168.9	5838.06	10133.82	77
H24A	6440.25	6766.1	8704.88	80
H24B	5555.68	7430.58	9116.21	80
H24C	4654.67	6765.32	8710.76	80
H26A	7006.61	5876.33	10127.46	79
H26B	7042.46	6890.07	9939.86	79
H26C	7892.19	6167.41	9560.73	79

Experimental

Single crystals of $C_{27}H_{41}Cl_2O_5Si$ **[DQT_SO2_3]** were **[]**. A suitable crystal was selected and **[]** on a **ROD, Synergy Custom DW system, Pilatus 200K** diffractometer. The crystal was kept at 100(2) K during data collection. Using Olex2 [1], the structure was solved with the SHELXT [2] structure solution program using Intrinsic Phasing and refined with the SHELXL [3] refinement package using Least Squares minimisation.

1. Dolomanov, O.V., Bourhis, L.J., Gildea, R.J, Howard, J.A.K. & Puschmann, H. (2009), J. Appl. Cryst. 42, 339-341.
2.
3.

Crystal structure determination of [DQT_SO2_3]

Crystal Data for $C_{27}H_{41}Cl_2O_5Si$ (M =544.59 g/mol): orthorhombic, space group $P2_12_12_1$ (no. 19), a = 8.77930(10) Å, b = 14.87570(10) Å, c = 22.7728(2) Å, V = 2974.09(5) Å^3, Z = 4, T = 100(2) K, μ(CuKα) = 2.612 mm^{-1}, *Dcalc* = 1.216 g/cm^3, 129933 reflections measured (7.098° ≤ 2Θ ≤ 158.322°), 6332 unique (R_{int} = 0.1042, R_{sigma} = 0.0247) which were used in all calculations. The final R_1 was 0.0476 (I > 2σ(I)) and wR_2 was 0.1243 (all data).

Refinement model description

Number of restraints - 0, number of constraints - unknown.

Details:

1.a Ternary CH refined with riding coordinates:
C14(H14), C13(H13), C8(H8), C18(H18)
1.b Secondary CH2 refined with riding coordinates:
C15(H15A,H15B), C10(H10A,H10B), C6(H6A,H6B), C17(H17A,H17B), C5(H5A,H5B)

1.c X=CH2 refined with riding coordinates:
C3(H3A,H3B)
1.d Idealised Me refined as rotating group:
C9(H9A,H9B,H9C), C21(H21A,H21B,H21C), C23(H23A,H23B,H23C), C20(H20A,H20B, H20C), C1(H1A,H1B,H1C), C22(H22A,H22B,H22C), C27(H27A,H27B,H27C), C24(H24A, H24B,H24C), C26(H26A,H26B,H26C)
1.e Idealised tetrahedral OH refined as rotating group:
O1(H1)

This report has been created with Olex2, compiled on 2022.04.07 svn.rca3783a0 for OlexSys. Please let us know if there are any errors or if you would like to have additional features.

2.9 Experimental Procedures and Characterization Data

General Procedures:

All reactions were performed in flame- or oven-dried glassware under a positive pressure of nitrogen or argon, unless otherwise noted. Air-and moisture-sensitive liquids were transferred via syringe. When indicated, solvents or reagents were degassed by sparging with argon for 10 minutes in an ultrasound bath at 25 °C. Volatile solvents were removed under reduced pressure rotary evaporation below 35 °C. Analytical and preparative thin-layer chromatography (TLC) were performed using glass plates pre-coated with silica gel (0.25-mm, 60-Å pore size, Merck TLC Silicagel 60 F254) impregnated with a fluorescent indicator (254 nm). TLC plates were visualized by exposure to ultraviolet light (UV) and then were stained by submersion in an ethanolic anisaldehyde solution or ceric ammonium molybdate solution, followed by brief heating on a hot plate. Flash column chromatography was performed with silica gel purchased from Silicycle (SiliaFlash ® , 60 Å, 230-400 mesh, 40-63 μm). Ethyl vinyl ether and *tert*-Butyl vinyl ether, diisopropylamine, hexamethylphosphoramide (HMPA), thionyl chloride ($SOCl_2$), methanesulfonyl chloride (MsCl), and acetyl chloride were distilled over calcium hydride prior to use. KHMDS solutions were purchased from Sigma. Tributyl tin hydride was distilled over hydroquinone. All other reagents were used as received from commercial sources, unless stated otherwise. Anhydrous tetrahydrofuran (THF), dichloromethane (DCM), methanol (MeOH), dimethylformamide (DMF), and toluene (PhMe) were obtained by passing these previously degassed solvents through activated alumina columns. Proton nuclear magnetic resonance (^{1}H NMR) spectra and carbon nuclear magnetic resonance (^{13}C NMR) spectra were recorded on Bruker AV-600 spectrometer at 23 °C. Proton chemical shifts are expressed as parts per million (ppm, δ scale) and are referenced to residual solvent ($CDCl_3$: δ 7.26, C_6D_6 : δ 7.16), unless stated otherwise. Carbon chemical shifts are expressed as parts per million (ppm, δ scale) and are referenced to the solvent ($CDCl_3$: δ 77.16, C_6D_6 : δ 128.06), unless stated otherwise. Data is represented as follows: chemical shift, multiplicity (s = singlet, d = doublet, dd = doublet of doublets, ddd, doublet of doublet of doublet, dt = triplet of doublets, t = triplet, q = quartet, m = multiplet, br = broad), coupling constant (J) in Hertz (Hz), and integration. Infrared (IR) spectra were recorded on a Bruker Alpha FT- IR spectrometer as thin films and are reported in frequency of absorption (cm^{-1}). Only selected resonances are reported. High-resolution mass spectra (HRMS) were obtained by the mass spectrometry facility at the University of California, Berkeley using a Finnigan LTQFT mass spectrometer (Thermo Electron Corporation). X-ray diffraction data was collected at the Small Molecule X-ray Crystallography Facility (CheXray) at University of California, Berkeley using a Rigaku XtaLAB P200 equipped with a MicroMax 007HF rotating anode and Pilatus3 R 200K-A hybrid pixel array detector. Data were collected using CuKα radiation (λ = 1.5418 Å).

Chapter 2

Synthetic Studies Toward Ineleganolide

Chapter 2

Synthetic Studies Toward Ineleganolide

2.1 Background and Introduction

2.1.1 A Brief Overview of Furanocembranoid Natural Products

The cembranoid natural products are a vast family of highly oxygenated C_{20}-diterpenoids isolated from marine and terrestrial organisms.[1] Despite the vast number of cembranoid diterpenes originating from marine invertebrates (octocorals and soft corals),[2-6] these metabolites are also found in plants (tobacco),[7, 8] insects (termites),[9-11] and in rare occasions, even the glands of vertebrates (*Alligator sinensis*).[12] Cembranoids produced by marine invertebrates are in frequently isolated from soft corals of the genera *Sinularia, Lobophytum, Eunicea, Clavularia* and from the gorgonian octocorals of the genera *Pseudopterogorgia, Leptogorgia and Lophogorgia*.[5, 13] In nature, these structurally diverse metabolites are hypothesized to act as a chemical defense against predatory fish and/or competing organisms. Unsurprisingly, this family of natural products, which boasts potent cytotoxicity amongst its myriad of biological properties such as anti-inflammatory, anti-tumor, anti-bacterial, anti-viral, neuroprotective, and antiarthritic, has garnered significant interest from the scientific community.[1, 3, 5]

The most biologically active members of the cembranoid natural products are found in a subclass of furanobutenolide C_{20}-diterpenes and C_{19}-norditerpenes (Figure 1.), classically typified by their distinctive 14-membered carbocyclic skeleton containing C3–C6 furan and C10–C20 butenolide-moieties. The distinguishing feature between the C_{20}-diterpenes and C_{19}-norditerpenes is the absence of the C18 carbon unit, believed to be lost through an oxidative C–C scission process.[14] Alongside the furanobutenolide norcembranoids there exists several congeners possessing rearranged carbocyclic skeletons, such as the pseudopteranes and gersolanes. The rearrangement of the classical 14-membered macrocyclic furanobutenolide skeleton to the pseudopterane and gersolane cores is believed to involve photochemistry in nature, furnishing 12-membered macrocycle and bicyclo[11.1.0]tetradecane ring systems, respectively.[15] Additionally, macrocyclic cembranolides which lack the furan heterocyclic moiety but possessing 5- through 8-membered lactones within the macrocyclic skeleton are also common. Less common though are the biscembranoids, secocembranes, and 13-membered macrocyclic cembranoids.[1]

As one of the most notable members of the polycylic furanobutenolide cembranoids, bielschowskysin (**2.19**) is highly active against EKVX nonsmall cell lung cancer,[16] while ineleganolide[17] (**2.1**) and sinulochmodin C[18] (**2.23**) possess anti-leukemia activity. Additionally, intricarene (**2.22**),[19] and rameswaralide[20] (**2.21**) are mildly active against lung cancer (Figure 1.). While macrocyclic furanobutenolide cembranoids and norcembranoids such as lophotoxin[21] (**2.11**, neurotoxin), bipinnatin D[22] (**2.12**, anti-leukemic), bipinnatin I (**2.13**), sinuleptolide, and 5-episinuleptolide (**2.18**) all exhibit marked biological profiles,[23, 24] from a synthetic perspective the polycyclic furanobutenolide cembranoids and norcembranoids are of particular interest due to their structural complexity. These intricate molecular architectures are believed to be biosynthetically related and are derived from various transannular cyclizations of macrocyclic C_{20}- and C_{19}-furanobutenolide scaffolds.

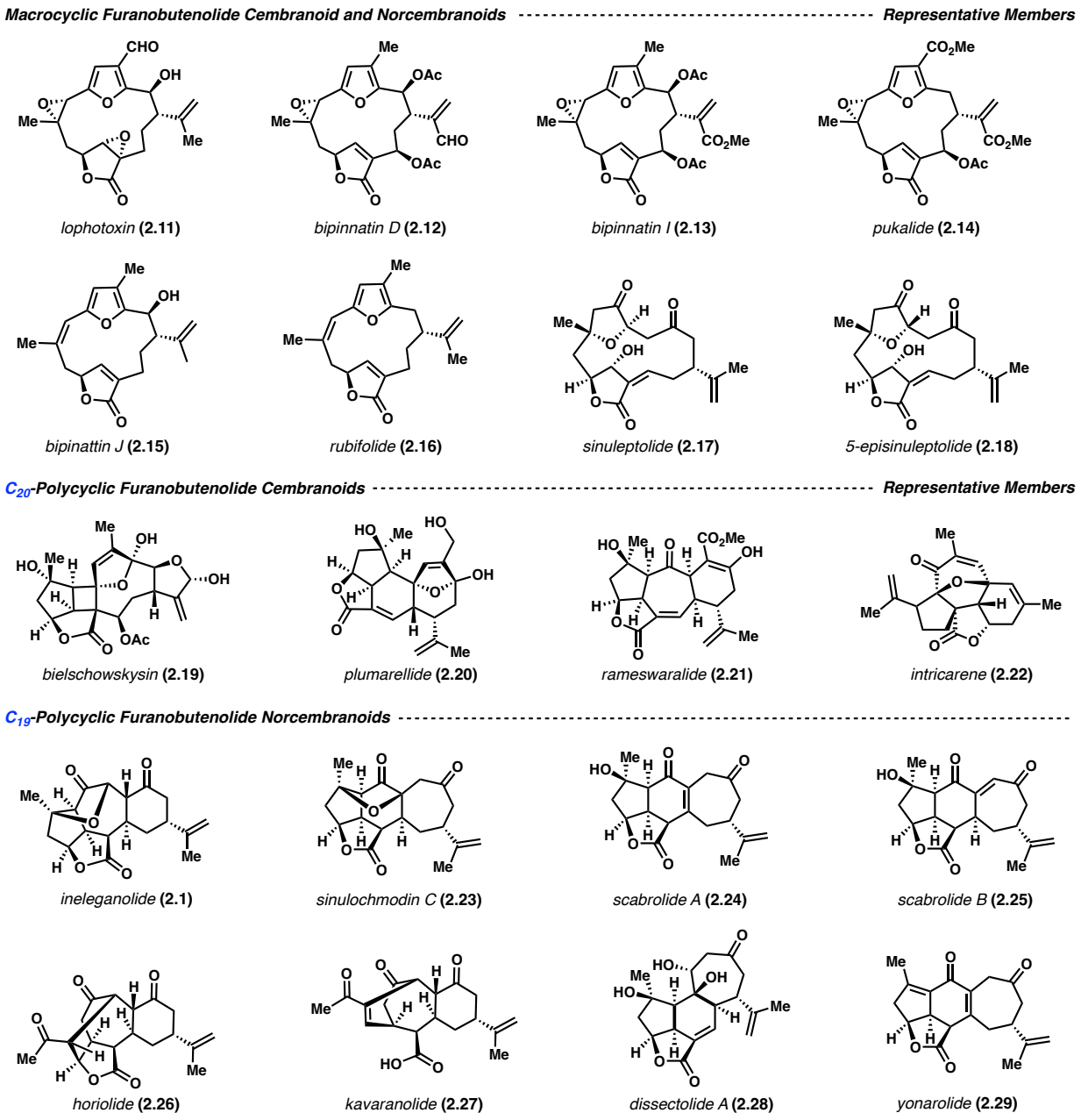


Figure 1. Overview of Furanobutenolide C_{20}-Cembranoids and C_{19}-Norcembranoids.

2.1.2 Isolation and Biological Activity of Ineleganolide

Ineleganolide (**2.1**) is a polycyclic, C_{19}-norditerpene furanobutenolide natural product isolated from the Formosan soft coral *Sinularia inelegans* in 1999 by Duh and co-workers.[17] The Sheu group also subsequently identified the presence of **2.1** in a variety of other coral species such as *S. leptoclados, S. lochmodes, S. parva,* and *S. scabra*.[18, 25, 26] Ineleganolide belongs to a privileged subclass of furanobutenolide norcembranoid natural products which, to date, consists of ten other congeners with varying oxidation states and structural features: horiolide (**2.26**),[27] kavaranolide (**2.27**),[28] sinulochmodin C (**2.23**),[18] yonarolide (**2.29**),[29] dissectolide (**2.28**),[30] and scabrolides A and B (**2.24** and **2.25**, respectively)[31] (Figure 1). Recently, two new polycyclic furanobutenolide natural products have been isolated, adding to this class of natural products.[32]

The highly oxidized and cage-like structure of 2.1 was determined unambiguously by nuclear magnetic resonance spectroscopy and X-ray crystallographic analysis. Initial biological evaluation revealed that **1** exhibits potent cytotoxicity against murine leukemia P-388 cell line (ED_{50} = 3.82 μg/mL); however, more recent studies have shown that **1** exhibits limited cytotoxicity against human oral epidermoid (KB) and liver (Hepa59T/VGH) carcinoma cells (ED50 > 20μg/mL). To date, **1** has not been subject to intensive biological evaluation and the biological mechanism of action remains nebulous, likely as a result of its prohibitively low natural abundance.

2.2 Biosynthesis

2.2.1 Biosynthesis of Furanocembranoid Diterpenes and Norditerpenes

The vast chemical space occupied by terpene natural products is the result of the enzymatic machinery evolved over countless generations to catalyze the construction and subsequent oxidation of polycyclic architectures from oligomeric polyprenyl chains, itself iteratively derived from simple 5-carbon units.

In the case of the cembranoid diterpene natural products, the enzymatically-assisted intramolecular cyclization of geranylgeranyl pyrophosphate (GGPP) provides cembrene A (also known as neocembrene),[14] the common biosynthetic intermediate possessing a 14-membered macrocyclic tetraene core from which all cembranoids are derived. Several enzymatic oxidations of this biosynthetic progenitor at the C3, C6, C10, and C20 positions, presumably mediated by P450 monooxygenases, would then provide the highly oxidized macrocyclic furanocembranoid scaffolds such as rubifolide (**2.16**), the least oxidized member of the furanobutenolide cembranoid family of natural products.

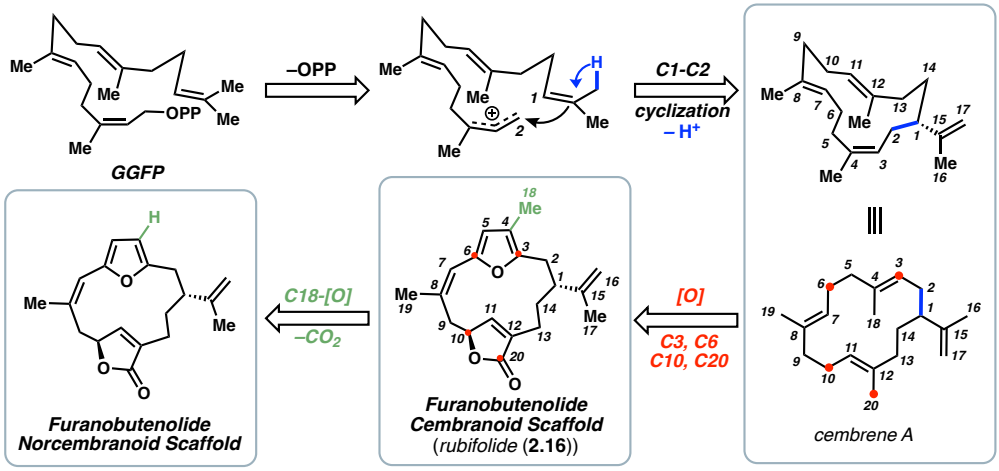


Figure 2. Biosynthesis of furanobutenolide cembranoid and norcembranoid cores from GGPP.

The macrocyclic and polycyclic furanobutenolide C_{19}-norcembranoids architectures found in nature are proposed to arise via the oxidative loss of the C18 carbon unit and subsequent oxidation of the cembrene core. To this end, Pattenden has proposed that the biosynthetic precursor of **2.1**, the furanobutenolide C_{19}-norcembranoid 5-episinuleptolide (**2.18**), is accessed through several oxidative transformations of the furanobutenolide C_{20}-cembranoid rubifolide.[14] The

deletion of the C18 carbon unit is believed to proceed via two sequential oxidations; the first being conversion of the C18 methyl group to a methyl ester followed by oxidative ring opening of the furan moiety to arrive at bisenone **2.161**. Intermediate **2.161** is then believed to undergo hydration at the C8 position to an intermediate bearing a tertiary alcohol (**2.162**) which is then poised to undergo a transannular oxa-Michael reaction to close the bridging ether found in several members (see **2.163**). The resulting β-ketoester can then undergoes decarboxylation to excise the C18 carbon unit and arrive at the macrocyclic furanobutenolide C_{19}-norcembranoid core. Enzyme-mediated C–H oxidation of the C11 position on the butenolide moiety completes the biosynthesis of the epimeric sinuleptolides (**2.17** and **2.18**). The macrocyclic sinuleptolides may then undergo further transannular cyclizations to complete the biosynthesis of the various polycyclic furanobutenolide norcembranoid natural products.

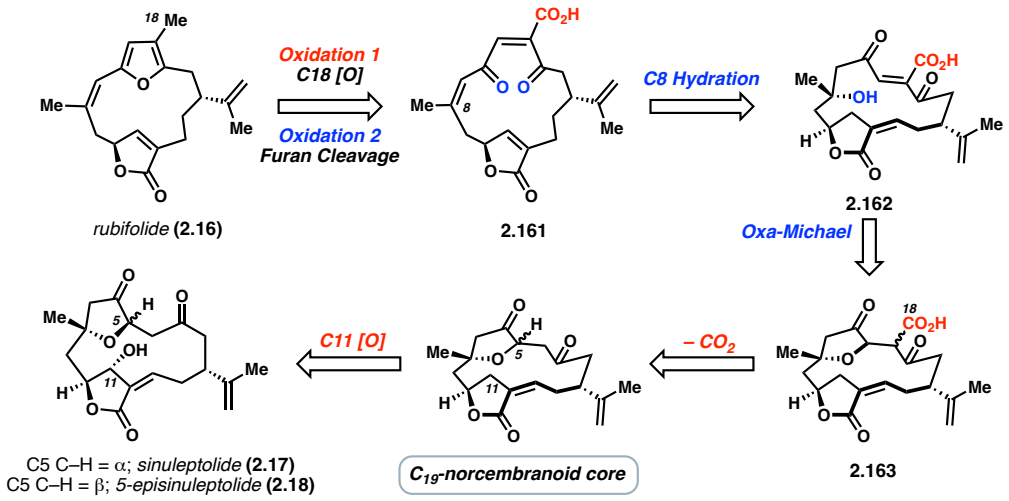


Figure 3. Proposed biosynthetic pathway leading to norcembranoid cores

2.2.2 Biosynthesis of polycyclic furanobutenolide cembranoids and norcembranoids

Within the subclass of furanobutenolide cembranoids and norcembranoids, there exists a limited number of highly oxygenated polycyclic furanobutenolide natural products. To date, there are 10 known polycyclic furanobutenolide cembranoids and 10 furanobutenolide norcembranoids. The intricate molecular architecture of these cyclized cembranoids and norcembranoids arises from the various transannular cyclization that may occur in subsequent steps of the biosynthesis.

As mentioned above, the biosynthesis of the C19-norcembranoids proceeds through the decarboxylation of the C18 methyl group commonly appended to the furan moiety of the furanobutenolide cembranoids. Given that the polycyclic furanobutenolide norcembranoids are exclusively isolated from the soft corals of the genus *Sinularia*, it is speculated that these natural products arise from the same biosynthetic progenitor, the epimeric sinuleptolides. In contrast to the biosynthesis of the gorgonian polycyclic furanocembranoids, sinuleptolides are, by virtue of the oxidative deletion of the C18 methyl, are relatively oxidized and are therefore poised to undergo transannular cyclization events.

Ineleganolide, which boasts antileukemic properties, is believed to arise from a intramolecular 6-*exo*-trig Michael addition (C4–C13) to arrive at intermediate **2.181** with concomitant dehydration of the C11-β-alcohol. The resultant butenolide can then undergo a second 5-*exo*-trig Michael addition (C7-C11) to forge the pentacyclic core of **1**. The related cyclized furanobutenolide norcembranoids horiolide (**2.26**) and kavaranolide (**2.27**), are therefore

speculated to be downstream products originating from ineleganolide. The formation of **2.26** and **2.27** likely arises from the cleavage of the ether linkage at C5 and subsequent retro-Aldol cleavage, ablating the five membered A-ring (**2.182**). Tautomerization to the corresponding C6-C7 enol, followed by an intramolecular Michael addition then leads to horiolide (**2.26**). The structurally peculiar natural product horiolide then undergoes an additional dehydration to provide the carboxylic acid containing natural product kavaranolide (**2.27**).

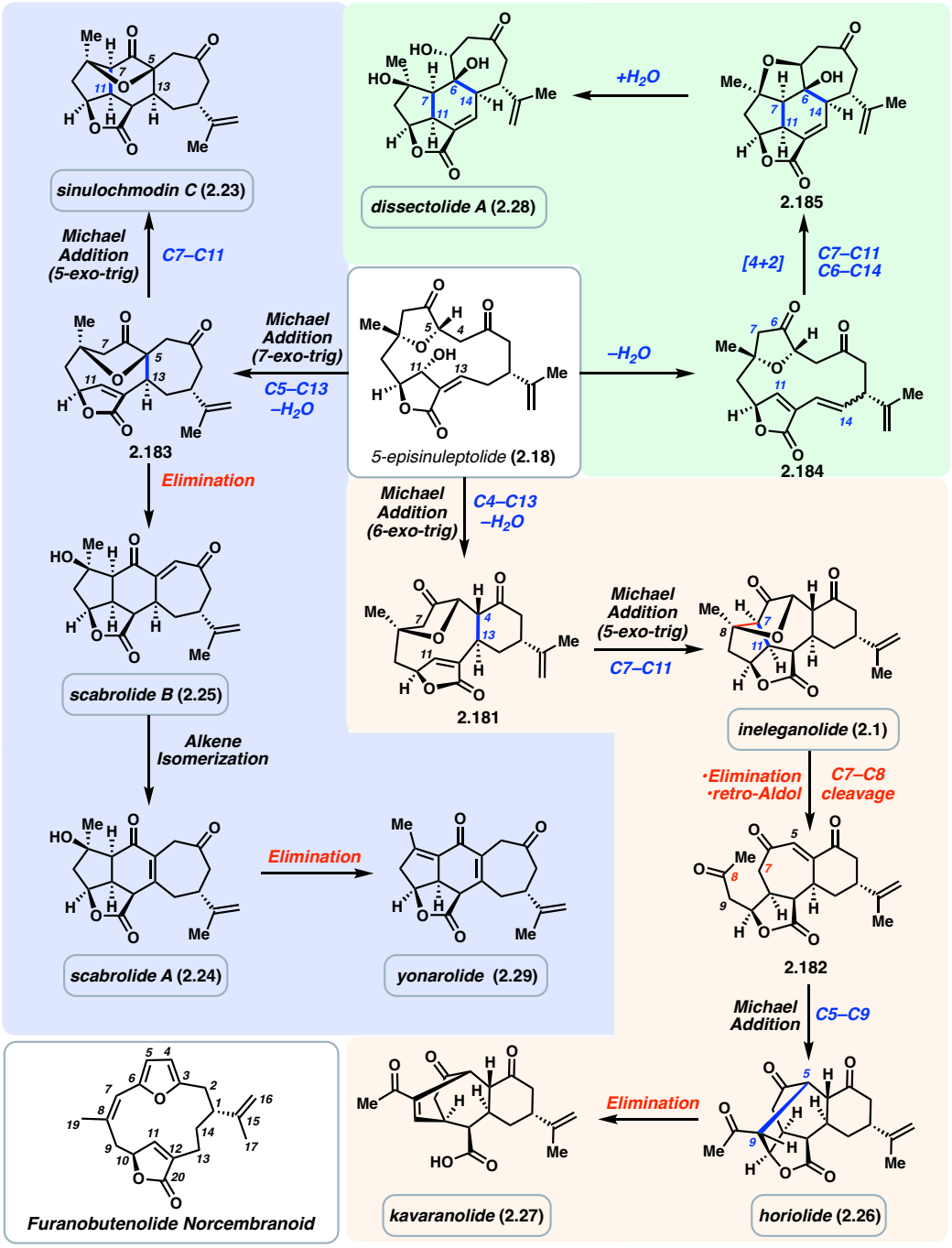


Figure 4. Overview of biosynthetic pathways leading to various polycyclic furanobutenolide norcembranoids.

In contrast to the biosynthesis of ineleganolide, horiolide and kavaranolide which begin with formation of the C4-C13 bond thus constructing the 6-membered carbocycle (E-ring), an alternative pathway exists where the C5–C13 bond is forged to form a 7-membered E-ring (**2.183**). In similar fashion to the proposed biosynthesis of ineleganolide, the C7–C11 bond can be constructed via a Michael-type addition, arriving at sinulochmodin C (**2.23**), an isomeric form of ineleganolide. This same intermediate (**2.183**) can then access scabrolide B (**2.25**) and ultimately scabrolide A (**2.24**) through a retro-oxa-Michael/Michael addition sequence to install the C4–C5 alkene and construct the C7–C11 bond. Isomerization of the alkene to the internal position leads to **2.24** and dehydration of the hydroxy-ketone accesses yonarolide (**2.29**). Of note, recent synthetic studies have cast doubt on the purported structure of scabrolide B.[33] Although the structure of **2.25** has not been corroborated at this time, for the purposes of this thesis we will continue forward with the shown depiction of **2.25**. The last member of the furanobutenolide norcembranoids is dissectolide A (**2.28**), which bears structural resemblance to the plumarellide (**2.20**) furanobutenolide cembranoids.[34] Although little is known about the biosynthesis of dissectolide A, an analogy can be drawn to the proposed biosynthesis of the plumarellides which are proposed to arise via an intramolecular [4+2] cycloaddition to construct the 6,7 fused ring system. As such, it is believed that from sinuleptolide, vinylogous enolization and elimination affords the C11-C12, C13-C14 conjugated system. Enolization at C7 can then undergo either a concerted cycloaddition or a stepwise sequence involving Michael addition and vinylogous aldol to the ether-bridged core of dissectolide A. Subsequent hydrolysis of the C5 position, likely through elimination and hydration, completes the biosynthesis of dissectolide A.

One of the most prominent examples of a polycyclic furanobutenolide cembranoid is bielschowskysin (BSK, **2.19**) which notably features a densely decorated cyclobutane ring within its complex hexacyclic skeleton. As the flagship furanobutenolide C_{20}-cembranoid, the biogenesis of this beautiful molecular architecture remains a topic of interest among the chemical community and warrants discussion.

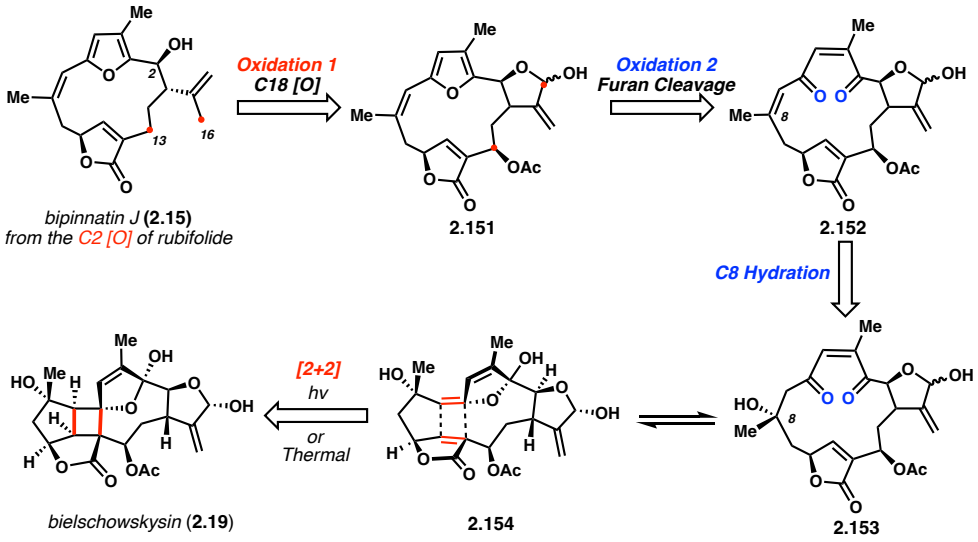


Figure 5. Proposed biosynthesis of BSK **(2.19)**

The biosynthesis of **2.19** is postulated to arise from either photochemical cycloaddition or stepwise anionic cyclizations of a highly oxidized derivative of bipinnatin J (**2.15**).[35] Bipinnatin J itself, is either biosynthetically derived from direct oxidation of neocembrene at the C2 position in addition to the C3, C6, C10, and C20 positions, or is the result of oxidative tailoring of rubifolide. Hydroxylation of the C13 and C16 positions of **2.15** provides the cyclic allylic alcohol moiety

found in **2.151**. In analogy to the oxidative fragmentation invoked in biosynthesis of the norcembranoids (*vide supra*), cleavage of the furan moiety to the bisenone (**2.152**) followed by hydration at C8 provides a putative hydroxylated bisenone intermediate **2.153**. This likely undergoes tautomerization and hemiketalization to provide the exocyclic enol-ether intermediate that can undergo either thermal or photochemical cyclization (see **2.154**).

At this juncture it is not clear whether the closure of the densely functionalized cyclobutane moiety, the structural hallmark of **2.19**, proceeds through a photochemical [2+2] cycloaddition or via an anionic Michael/Aldol bond-forming sequence. To complicate the matter, the discrete nature of the intermediates which engage in either the photochemical or anionic pathways is also poorly understood.

In 2015, the Paton group computed the energetics of the photochemical and thermal formation of the strained cyclobutane ring in **2.19**.[36] Their studies suggest that the formation of the cyclobutane of **2.19** can arise from a nonenzyme-mediated, concerted, but asynchronous, thermal [2+2] cyclization in aqueous media ($\Delta G^{\ddagger}_{(aq)}$ = 21.6 kcal/mol). However, their calculations revealed that the radical pathway (photochemical) is also plausible via the triplet sensitization of the closed exocyclic enol-ether ($\Delta G^{\ddagger}_{(aq)}$ = 7.3 kcal/mol). Although these studies do not concretely delineate the plausible modes of cyclizations, it was revealed in the same study that the open-form 1,4 diketone intermediate is 4.6 kcal/mol favored over the closed hemi-ketal state and that the transition state barrier for the thermal cyclization is predicted to be 26.2 kcal/mol and thus may be prohibitively slow under biological conditions.

It is worth noting that although the photochemical [2+2] is widely invoked in the biosynthesis of BSK, the existence of the closely related congener verrillin which is epimeric at C8 and lacks the central cyclobutane ring, lends credence to the possibility of a stepwise mechanism for the cyclobutane formation of BSK.[37]

2.3 Previous Synthetic Efforts Toward Ineleganolide and Related Norcembranoids

The antileukemic furanobutenolide norcembranoid ineleganolide has captivated the synthetic community since its isolation in 1999. The winding array of contiguous stereogenic centers which ornately decorate the caged-like pentacyclic core of **2.1**, makes this natural product a formidable synthetic target. As such, many groups have pursued the total synthesis of **2.1**; however, its total chemical synthesis remains elusive. The groups of Pattenden,[38] Moeller,[39] Vanderwal,[40] and Stoltz[41-43] have disclosed synthetic studies toward **2.1**. These studies highlight many of the challenges in the assembly and manipulation of this highly oxygenated and stereochemically dense pentacyclic core.

2.3.1 Pattenden's Biomimetic Semisynthesis of Ineleganolide and Sinulochmodin C

The polycyclic furanobutenolide norcembranoids are all exclusively isolated from the soft corals of the genus *Sinularia*. The co-occurrence of ineleganolide, sinulochmodin C and the epimeric sinuleptoplides led scientists to speculate whether the biosynthetic origins of **2.1** and **2.23** arise from various cyclizations of a common macrocyclic progenitor. These speculative biosynthetic interconnections were borne out by the studies disclosed by Pattenden in 2011.[38] From these semi-synthetic studies, we now know that ineleganolide and sinulochmodin C likely arise from a series of Michael additions from the common biosynthetic progenitor 5-episinuleptolide.

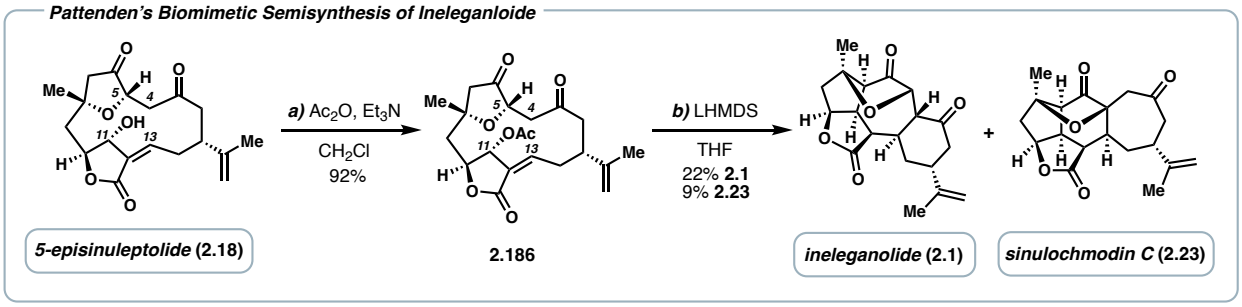


Figure 6. Conversion of 5-episinuleptolide to **2.1** and **2.23**

In their study, the Pattenden group sought to confirm whether **2.1** and **2.23** indeed could arise from the transannular cyclizations of the macrocyclic norcembranoid 5-episinuleptolide. Starting from natural **2.18** isolated from *Sinularia* sp. and donated by the Sheu group,[38] the authors report that acetylation of the C11 alcohol cleanly provided acetoxy-5-episinuleptolide **2.186**, whereas attempts to mesylate the C11 alcohol led to direct elimination. Upon treatment of **X** with LHMDS, and followed by prolonged stirring and slowly warming, the authors were able to directly observe the formation of ineleganolide and trace quantities of sinulochmodin C, thus providing evidence in support of the role of 5-episinuleptolide in the biogenesis of these polycyclic furanobutenolide norcembranoids.

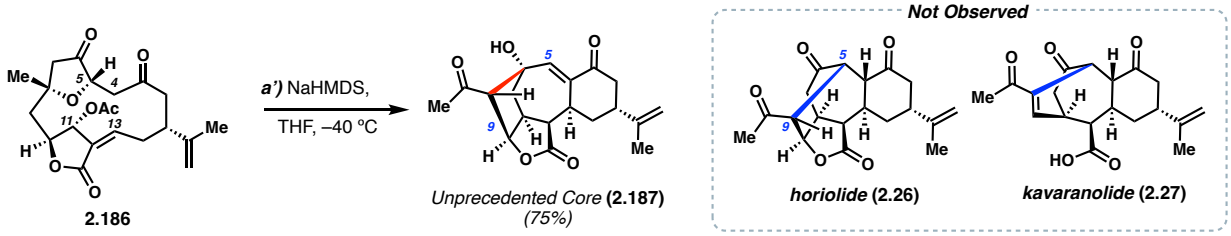


Figure 7. Pattenden's unsuccessful conversion of 5-episinuleptolide to **X** and **X**

These studies also included attempts to directly access the natural products horiolide and kavaranolide which were believed to biosynthetically arise from the elimination of the ether-bridge followed by retro-Aldol and Michael closure. However, exposure of **2.186** to KHMDS for extended times led to an isomeric structure which has not been observed in nature (**2.187**) and that arises from a retro-Aldol/Aldol closure. Although unsuccessful in accessing the hypothetical downstream congeners **2.26** and **2.27**, these studies confirm the likelihood of the retro-Aldol process and led the author to speculate about the role of enzymes in this cyclization event.

The studies by Pattenden have shed light on the biosynthetic interconnections of the structurally diverse subclass of polycyclic furanobutenolide norcembranoids and it is now widely speculated that the remaining members likely arise from the same biosynthetic progenitor (see section 2.2.2).

2.3.2 Vanderwal's Synthetic Studies Toward Ineleganolide.

In 2016, the Vanderwal group disclosed their studies towards an asymmetric total synthesis of ineleganolide.[40] Retrosynthetically, they postulated that the central 7-membered ring of **2.1** could be constructed through an intramolecular cyclization of a tetracyclic intermediate containing a "latent oxocarbenium" (see **2.270b**) which in turn could arise from the union of 5,5,5-fused tricycle (**2.270a**) and norcarvone via a Mukaiyama Michael addition. The tricyclic intermediate

could, in turn be accessed via a radical cyclization cascade of the propargylic bis-allylic alcohol **2.270**.

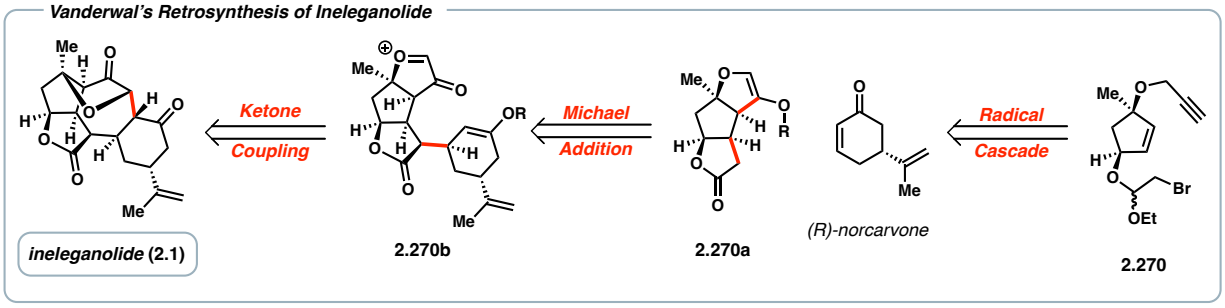


Figure 8. Vanderwal's synthetic strategy toward **2.1**

Their efforts began with the synthesis of enantiomerically pure propargyl acetal **2.270**, which was accomplished in 6 steps from furfuryl alcohol. This was accomplished via the propargylation of a diol intermediate and haloacetalization with ethyl vinyl-ether in the presence of NBS to provide **2.270** as a mixture inconsequential epimers at C19. Reductive radical bicyclization followed by ozonolysis of the resultant exocyclic alkene provided tricyclic ketone **2.271**.

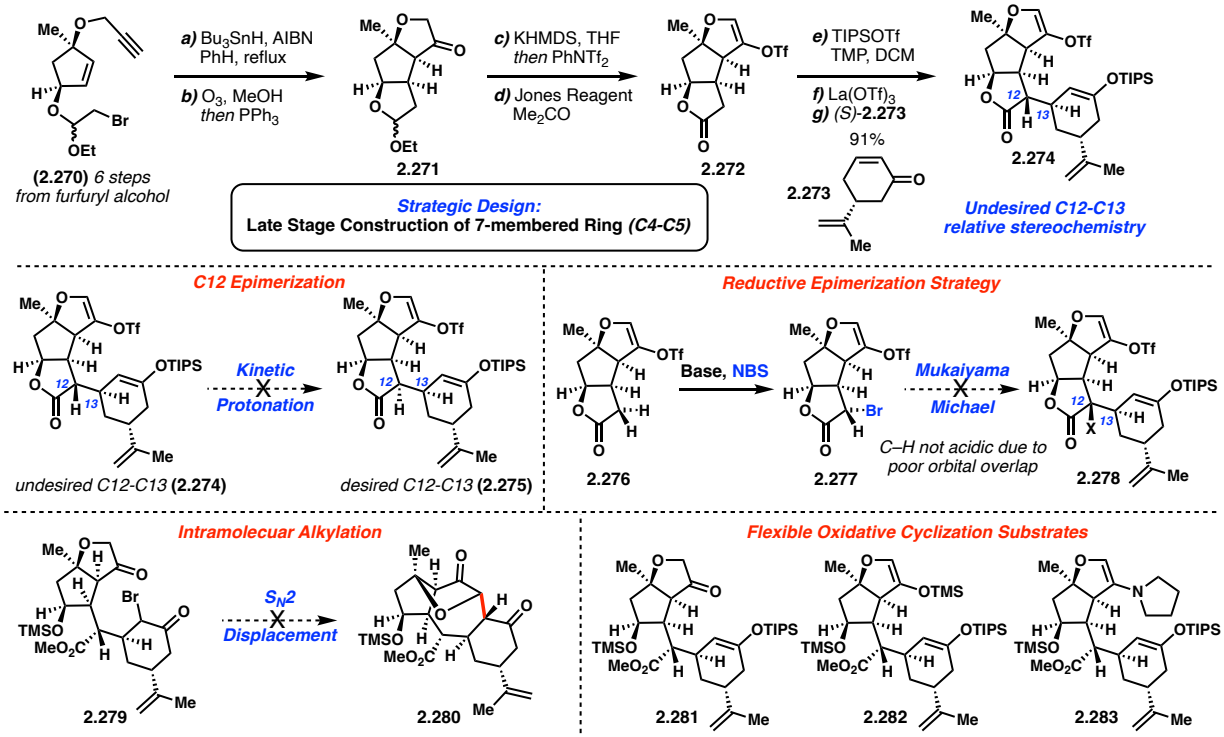


Figure 9. Summary of Vanderwal's synthetic studies

Vanderwal's overarching synthetic strategy hinged on the formation of a cyclic oxocarbenium intermediate (see **2.270b**, Figure 8.) which could undergo intramolecular cyclization to construct the pentacyclic core of 2.1. This strategy necessitated the prefunctionalization of the E-ring carbonyl which the authors envisioned could be accomplished by employing a vinyl-triflate as a masked oxocarbenium handle to complete the pentacyclic core

of **2.1**. As such, with the tricyclic ketone **2.271** in hand, the vinyl triflate **2.272** was synthesized and proved to be robust enough for further elaboration.

This vinyl-triflate intermediate was then converted to the silyl-enol ether **2.274** in two steps via Jones oxidation and soft enolization in the presence of a silylating reagent. The Mukaiyama Michael addition of tricyclic intermediate **2.272** and norcarvone **2.273**, itself prepared enantioselectively in 6 steps, proceeded efficiently (91% yield), forming the product as a single diastereomer. Despite possessing the correct C13 stereochemistry, the C12 stereocenter of **2.1** was formed with the incorrect configuration compared to the natural product.

Given the conformation of the undesired C12-epimer, which places the cyclohexene ring prohibitively far from the electrophilic vinyl-triflate moiety, significant experimentation was done to epimerize the C12 position to provide the desired diastereomer (*cis*-fused) of the tetracyclic intermediate. These efforts were met with little success, and cleavage of the vinyl-triflate was observed. The authors noted that deuteration studies revealed the unusual acidity of the vinylic C–H proton at C6 and deuterium incorporation at the C12 position was not observed. This, in conjunction with the positioning of the C12 C–H bond within the cavity of the 5,5,5-fused tricycle, suggests that the deprotonation of the C12 position may not be feasible. Alternative strategies to affect the C12 epimerization, such as preinstallation of a halide, selenide, or sulfonyl group which could be readily removed under reductive radical generating conditions were unsuccessful. Surprisingly, the Mukaiyama-Michael addition on substrates possessing a reductive handle at C12 were unsuccessful. Rationalized by a crystal structure of bromo-lactone **2.277**, the authors attribute this phenomenon to the poor orbital overlap between the C12 C–H and the lactone carbonyl leading to a diminished acidity of the proton.

Importantly, and most relevant to our own synthetic studies, the Vanderwal group surmised that the substrates bearing the incorrect configuration at C12 may still be synthetically viable intermediates for forging the central cycloheptanone if the geometric constraints of the system were relieved by alcoholysis of the 5-membered lactone. As such, silyl-enol ether **2.283**, enamine **2.282**, and ketone **2.281** and subjected to oxidative radical cyclization conditions. Unfortunately, the cyclization to construct the central 7-membered ring through a 7-*exo*-trig predominantly led to decomposition of the starting materials or undesired oxidation reactions.

This study highlights the key stereochemical challenges associated with the construction of the highly oxidized and cage-like pentacyclic core of **2.1**. Of particular importance is the realization that the formation of the A, B and E tricyclic system at an early stage enforces geometric constraints which preclude *endo*-selective functionalization due to the latent concavity of the substrate. These studies therefore have been an integral part in our own synthetic design and will be revisited in future sections (see section 2.4).

2.3.3 Stoltz's Synthetic Studies Toward Ineleganolide

The most recent approach towards **2.1** was reported in 2017 by the Stoltz group.[42] The strategy revolved around the oxidation of tetracyclic intermediate **2.287** which, in contrast to the efforts by the Vanderwal group, already possessed the core 7-membered carbocycle (Figure 10). The corresponding 5,5,7,6-fused ring system could ultimately arise from a tandem cyclopropanation–[3,3]-sigmatropic rearrangement of a bicyclic diazo intermediate **2.286**. This key intermediate could be constructed through the union of enantiomerically pure cyclopentenol (**2.284**) and norcarvone derived fragments (**2.285**).

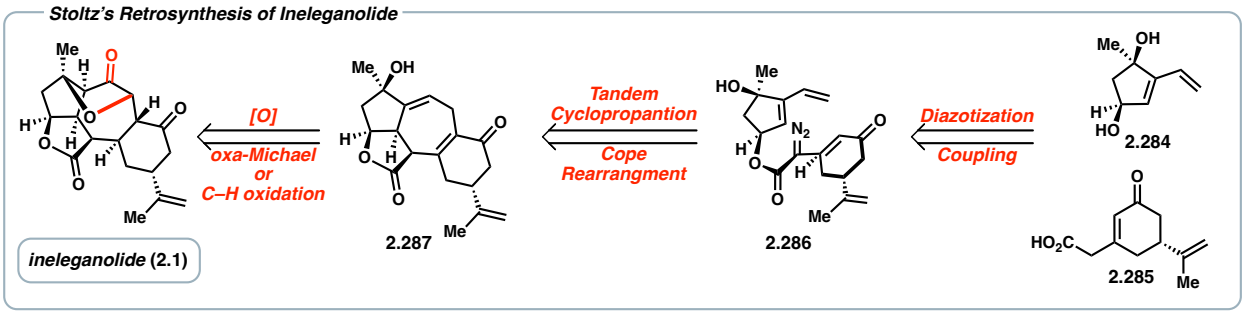


Figure 10. Stoltz's synthetic strategy toward **2.1**

In the forward sense, the Stoltz group began their studies with the synthesis of enantiomerically pure cyclopentene **2.284**, which was accomplished in 15 steps from commercially available starting materials. The cyclohexenone fragment **2.285** was synthesized from norcarvone, prepared in 9 steps from (*R*)-carvone, in an additional two steps. The union of these two chiral fragments provides the key intermediate **2.286** in a total of 20 steps (LLS). Subjecting **2.286** to rhodium-catalyzed carbene insertion then triggered the intramolecular cyclopropanation reaction, which readily underwent a Cope-rearrangement to access tetracycle **2.287** in 53% yield.

From this intermediate, the authors were able to access the core of ineleganolide as its C7 epimer and without the bridging ether ring. The conversion of **2.287** to **2.292** begins with a vanadium- catalyzed directed epoxidation of the allylic alkene (Figure 11A). After several attempts to convert **2.289** directly to **2.292** via a two-step sequence consisting of reductive epoxide opening and oxidation with DMP, the authors deemed this strategy unproductive. Ultimately, the authors then developed a 4-step sequence which included opening of epoxide **2.289** followed by Kornblum oxidation. Reductive cleavage of the ether bond by Sm(II) promoted spin-center shift leading to lactol intermediate **2.291**. Acidic cleavage of the lactol with concomitant dehydration provides the ineleganolide core, coined "isoineleganolide" (**2.292**) by the authors. From this intermediate, the authors attempted to affect the isomerization of the C3–C4 olefin and subsequent oxa-Michael addition to complete the synthesis of **2.1**, however, after extensive efforts they were unable to observe any isomerization of the olefin to natural product **2.1** (Figure 11C).

Additionally, the authors sought to perform a direct C–H etherification of the 5,5,7,6 tetracyclic core of **2.295**, lacking the C3–C4 alkene, to access **2.1**. As mentioned above, although the reductive epoxide opening-oxidation sequence did not proceed efficiently from **2.289**, the authors found this synthetic maneuver could be accomplished if the C3–C4 alkene was saturated (Figure 11B). To this end, starting from tetracycle **2.287** a SmI_2 mediated reduction of the alkene provided intermediate **2.293** possessing the correct relative stereochemistry at the C4 and C13. Vanadium-catalyzed allylic epoxidation provided epoxide **2.294** which was then subjected to Ti(III)-mediated reductive epoxide opening conditions. Subsequent DMP oxidation then provided the 5,5,7,6 core of ineleganolide (**2.295**) again without the bridging ether ring. Stoltz and coworkers then surveyed a variety of oxidation conditions to affect a direct C5-C–H etherification of the C8 hydroxyl group of **2.295**, however these attempts were again met with little success. Additionally, X-ray crystallographic analysis **2.295** suggests that due to the conformation of the tetracyclic intermediate, which places the C8–OH group prohibitively far from the C5 position, strategies which rely on the late-stage formation of the bridging ether ring may be ineffective.

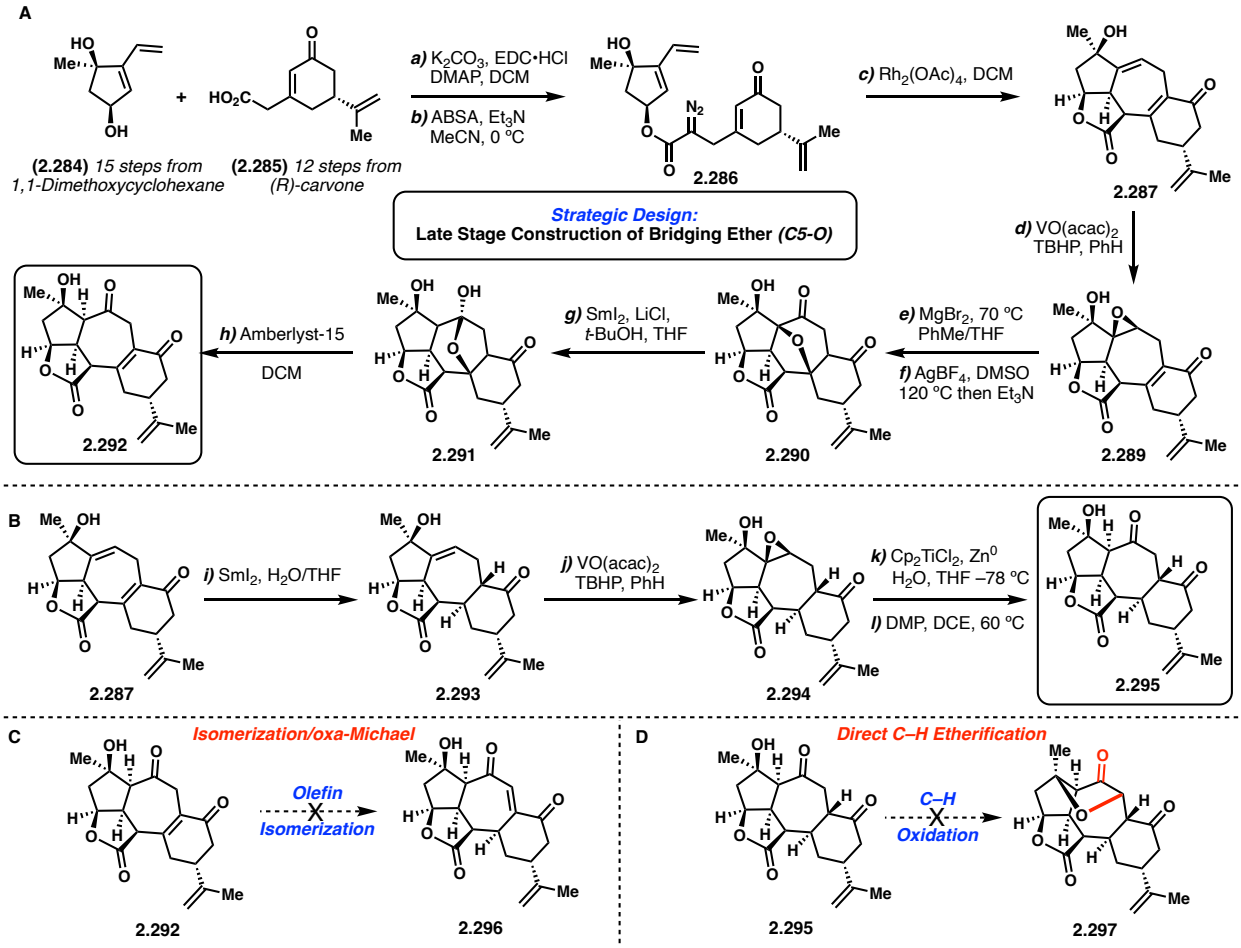


Figure 11. Summary of Stoltz's synthetic studies

To better understand the nature of the alkene isomerization/oxa-Michael addition, calculations by the Stoltz and Houk groups suggest that, in contrast to their key assumptions, the alkene isomerization into conjugation between both carbonyls was thermodynamically unfavorable and that the oxa-Michael addition to form the bridging ether may not be feasible due to the conformation of the tetracycle.[44]

Overall, the synthetic and computational studies by the Stoltz and Houk groups, respectively, have greatly informed our own synthetic design. Specifically, these studies suggest that synthetic strategies which rely on the late-stage construction of the bridging ether ring from a 5-5-7-6 tetracyclic intermediate, although provocative at first glance, may ultimately be doomed due to the conformation constraints of the system. Considering the studies by Vanderwal and Stoltz, we therefore have devised our own synthetic strategy which seeks to avoid the synthetic challenges faced in both strategies toward **2.1**.

2.4 Strategic Considerations and Retrosynthesis

2.4.1 Strategic Design Principles

At the outset of our synthetic planning, we sought to devise a strategy which could circumvent the seemingly insurmountable challenges which arose during the Vanderwal and Stoltz synthetic campaigns. Although a more detailed discussion of the previous strategies toward **2.1** has already been provided (see section 2.3), the central pitfalls of the Vanderwal and Stoltz strategies are summarized below (Figure 12).

Briefly, in the Vanderwal studies, the authors sought to construct the tricyclic 5,5,5 ring system (A/B/E-rings) at an early stage (Figure 12A). They hypothesized that the remainder of the pentacyclic core could be assembled through the stereochemically controlled construction of the C12–C13 and C4–C5 bonds in sequential fashion. However, the construction of the *cis*-fused-5,5,5 tricyclic ring system at an early stage in the synthesis introduced a substrate-controlled bias for *exo*-functionalization of the tricycle which could not be overwritten. As a result, the Vanderwal group notes that the functionalization of the C12 position, although proceeding with excellent selectivity at C13, provides exclusively the undesired C12 stereochemical configuration. Ultimately this proved to be intractable as all attempts to construct the pentacyclic framework (C4–C5 bond) from the tetracyclic intermediate possessing the incorrect C12 stereoconfiguration were unsuccessful.

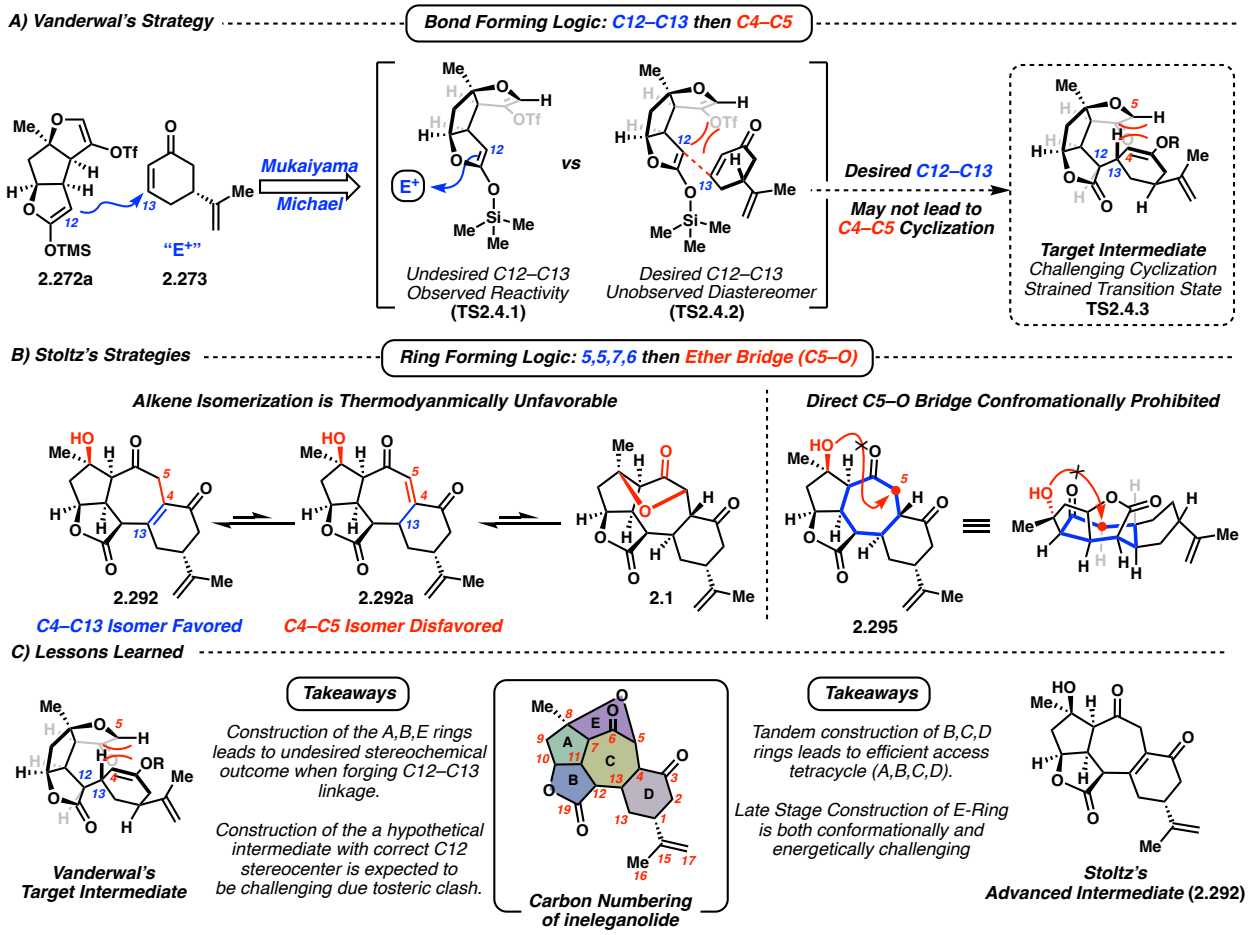


Figure 12. Overview and analysis of failed strategies toward **2.1**

In the Stoltz strategy, the authors develop a tandem cyclopropanation-Cope rearrangement strategy to access the 5,5,7,6 tetracyclic core (A/B/C/D-rings) of ineleganolide with the hopes to construct the final bridging ether (E-ring) at a late-stage through either an intramolecular oxa-Michael addition or direct C–H etherification (Figure 12B). However, upon securing the tetracyclic intermediates **2.292** or **2.295**, differing in oxidation at the C4–C13 junction, the authors were unable to construct the final bridging ether ring. As mentioned in the previous section, computational studies have revealed that the isomerization/oxa-Michael Addition was thermodynamically unfavorable and that the oxa-Michael addition to form the bridging ether may be kinetically inaccessible.

With these considerations in mind, at the outset of our strategic planning stage it was clear that 1) the ether bridge (E-ring) will be challenging to construct at a late stage with the rest of the carbon skeleton assembled due to the unfavorable energetics alongside conformational limitations and 2) the construction of the ether bridge at early stage in the synthesis may lead to stereochemical challenges due to the concave nature of the 5,5,5 (A/B/E) tricyclic core; which suggests that the introduction of the D-ring prior to the formation of the E-ring may be a fruitful approach. Additionally, rudimentary modeling and ground-state calculations suggest that the tetracyclic intermediate possessing the correct relative C12–C13 stereochemistry targeted by Vanderwal, may be resistant to the cyclization to forge the C4–C5 bond due to the congested transition state leading to the formation of the pentacyclic core (see Figure 12A), further suggesting that the formation of the E-ring at an early stage of the synthesis should be avoided.

2.4.2 Retrosynthesis

Taken together, the unsuccessful attempts towards ineleganolide by Vanderwal and Stoltz underscore several formidable challenges associated with the stereochemically controlled construction of the highly oxidized framework of **2.1**. To this end, we have devised a synthetic strategy which seeks to construct the pentacyclic core of **2.1** in a manner which avoids the pitfalls of the previous attempts towards ineleganolide.

Retrosynthetically, we envisioned that **2.1** may be constructed from the late-stage introduction of the C3 carbonyl group from a pentacyclic intermediate bearing the C3–C4 alkene via an *exo*-face epoxidation-Meinwald rearrangement sequence. This alkene intermediate could in turn arise from the construction of the cycloheptane ring through an oxidative radical cyclization to forge the C12–C13 linkage of a tetracyclic intermediate **2.299** possessing the A/B/D/E rings. Importantly, we believe that the intramolecular 7-*endo*-trig cyclization to forge the C-ring should provide the desired C12–C13 relative stereochemistry due to the steric-influence of the C1-isopropenyl group on the conformation of the tetracycle (see Figure 14). The corresponding tetracyclic **2.299** intermediate would be constructed via an intramolecular oxidative etherification of suitably functionalized tricyclic intermediate which could arise from the union of a two-carbon fragment and two monoterpene derived fragments.

To contextualize the differences in synthetic strategies, a summary of the ring forming logic of our synthetic strategy compared to the Vanderwal and Stoltz strategy is presented in Figure 13. Briefly, the Vanderwal first relies on the tandem construction of the A, B, and E-rings. This is followed by the union of the A/B/E tricycle with a D-ring containing fragment. With the final C4–C5 bond remaining to construct the C-ring and complete the pentacyclic core of **2.1**. In the Stoltz strategy, the A- and D-ring fragments are first united. A tandem process enables the construction of the B and C rings to provide tetracyclic intermediate containing the A/B/C/D rings. The formation of the final C5–O bond would then complete the E-ring and the ineleganolide core. In

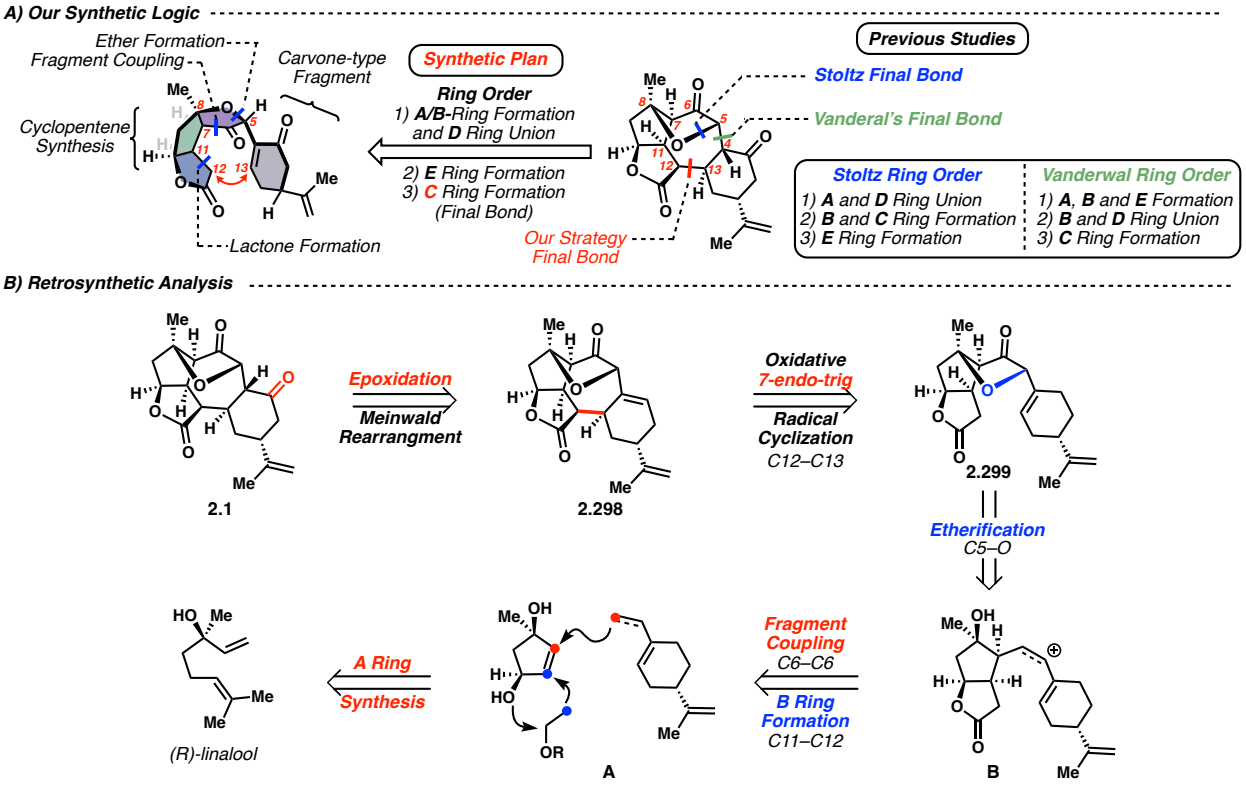


Figure 13. Our Synthetic Design; A) Strategy-Level Design and B) Retrosynthetic Analysis of **2.1**

contrast to these previous strategies, our strategy seeks to construct the E-ring from an intermediate containing the A/B/D ring preassembled. Although we seek to construct the central C-ring at a late-stage, in analogy to the Vanderwal strategy, we believe the formation of the intramolecular formation of C12–C13 bond to be a viable strategy which precludes the stereochemical pitfalls in the previous strategy.

2.5 Synthetic Studies Toward Ineleganolide

2.5.1 Application of the Oshima-Utimoto Reaction Toward the Synthesis of Ineleganolide

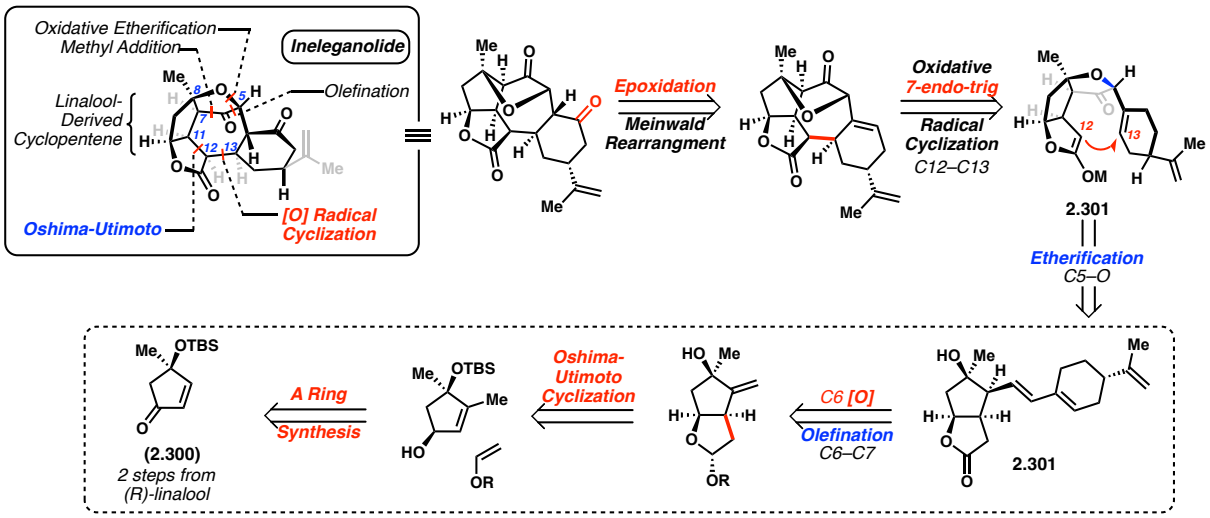
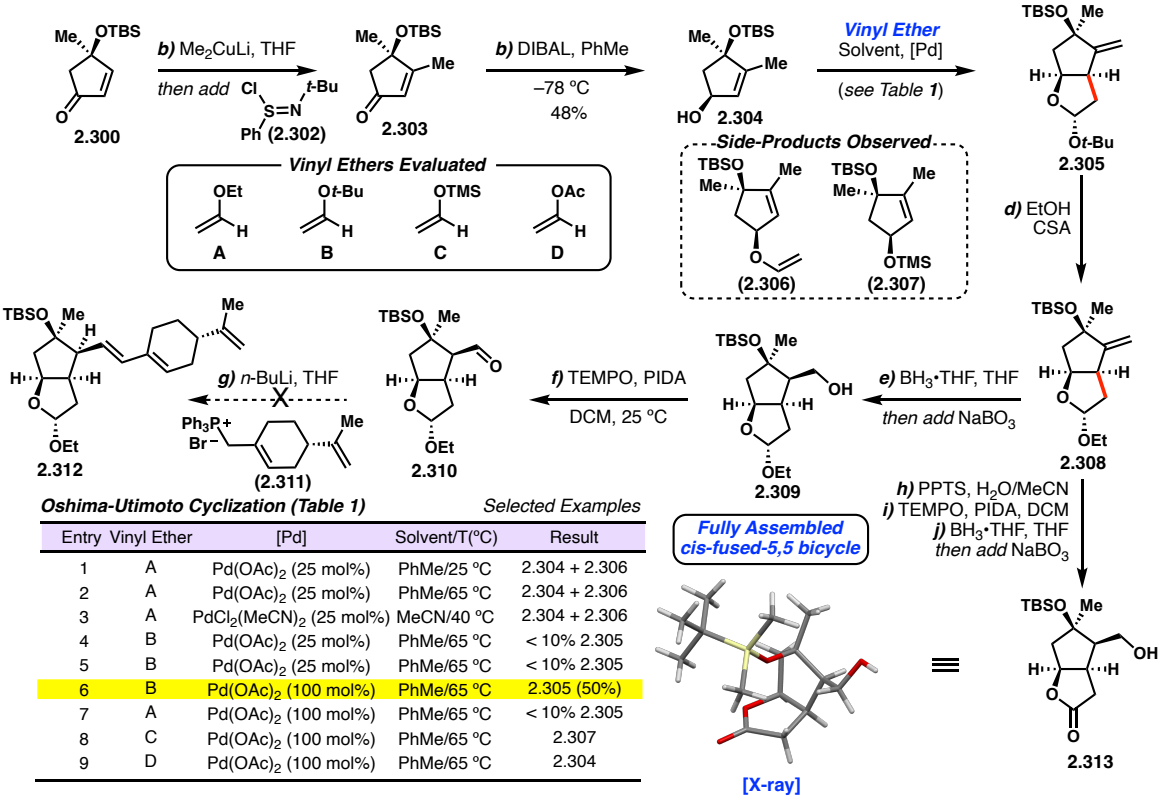


Figure 14. An Oshima-Utimoto-based strategy toward **2.1.**

At the outset of our synthetic studies, we identified that the A-ring of **2.1** could arise from the linalool derived cyclopentenone (**2.300**) used in the synthesis of 6-*epi*-ophiobolin A (see Chapter 1). We sought to leverage the inherent chirality of **2.300** to construct the *cis*-fused tricyclic 5,5-bicyclic core (A/B) in a stereocontrolled fashion through the strategic application of the Oshima-Utimoto reaction and subsequent elaboration to a tricyclic diene **2.301**.[45-48] We postulated that the oxidative etherification of the dienyl moiety could provide the tetracyclic intermediate such as **2.302**. The 7-*endo*-trig radical cyclization of this tetracyclic intermediate would then provide the fully assembled pentacyclic core *en*-route to ineleganolide following several redox manipulations.

Our initial synthetic efforts focused on the elaboration of **2.300** to a 5,5 bicyclic aldehyde (**2.313**, Figure 17.) which we believed could be leveraged to construct the C6–C5 bond and introduce the D-ring of the scaffold. In analogy to the dehydrogenative coupling strategy presented in the previous Chapter, we were able to access methylated cyclopentenone **2.303** via the conjugate addition of methyl-cuprate followed by *in situ* dehydrogenation with Mukaiyama's reagent (**2.302**).[49, 50] This one carbon homologated substrate was then reduced to provide cyclopentene **2.304** in high diastereoselectivity and set the C10 stereocenter of **2.1.**

At this stage, we sought to construct the B-ring in a manner which would enable us to install oxidation to the newly introduced methyl group at the C6 position. Inspired by the seminal work from the Oshima and Utimoto groups, we envisioned that the lactone moiety could be introduced through the palladium-mediated coupling of allylic alcohol **2.304** and a commercially available vinyl ether. Notably, this process would introduce, by way of β-hydride elimination of the corresponding alkyl-palladium complex, an *exo*-cyclic alkene which could serve as a handle to introduce the remaining carbons of the core.



Entry	Vinyl Ether	[Pd]	Solvent/T(°C)	Result
1	A	$Pd(OAc)_2$ (25 mol%)	PhMe/25 °C	2.304 + 2.306
2	A	$Pd(OAc)_2$ (25 mol%)	PhMe/65 °C	2.304 + 2.306
3	A	$PdCl_2(MeCN)_2$ (25 mol%)	MeCN/40 °C	2.304 + 2.306
4	B	$Pd(OAc)_2$ (25 mol%)	PhMe/65 °C	< 10% 2.305
5	B	$Pd(OAc)_2$ (25 mol%)	PhMe/65 °C	< 10% 2.305
6	B	$Pd(OAc)_2$ (100 mol%)	PhMe/65 °C	2.305 (50%)
7	A	$Pd(OAc)_2$ (100 mol%)	PhMe/65 °C	< 10% 2.305
8	C	$Pd(OAc)_2$ (100 mol%)	PhMe/65 °C	2.307
9	D	$Pd(OAc)_2$ (100 mol%)	PhMe/65 °C	2.304

Figure 15. Application of the Oshima-Utimoto Reaction the Synthesis of 5,5-bicycle **2.313.**

Our initial attempts to affect this transformation using catalytic palladium with ethyl vinyl-ether as the two-carbon synthon led to either no reaction or β-alkoxide elimination to the vinyl ether product **2.306**. We presumed that the β-alkoxide elimination of the alkyl palladium species formed after intermolecular attack outcompeted a slow migratory insertion to construct the bicyclic intermediate **2.305**, owing to the steric congestion imparted by the large TBS group (C8–O). To test this hypothesis, the silyl ether was deprotected and subjected to the same reaction conditions leading to little improvement. We ultimately found that the use of stoichiometric amounts of palladium acetate and replacing ethyl vinyl-ether with *tert*-Butyl vinyl ether (effectively slowing β-alkoxide elimination) at elevated temperatures, this transformation proceeded in 50% yield of **2.305** from allylic alcohol **2.304**. Downstream studies suggested that although the *tert*-Butyl acetal of **2.305** may be difficult to remove once the core has been elaborated, we were able to deprotect substrates possessing the ethyl-acetal moiety. Accordingly, we were able to convert **2.305** to **2.308** in near quantitative yields at this early stage.

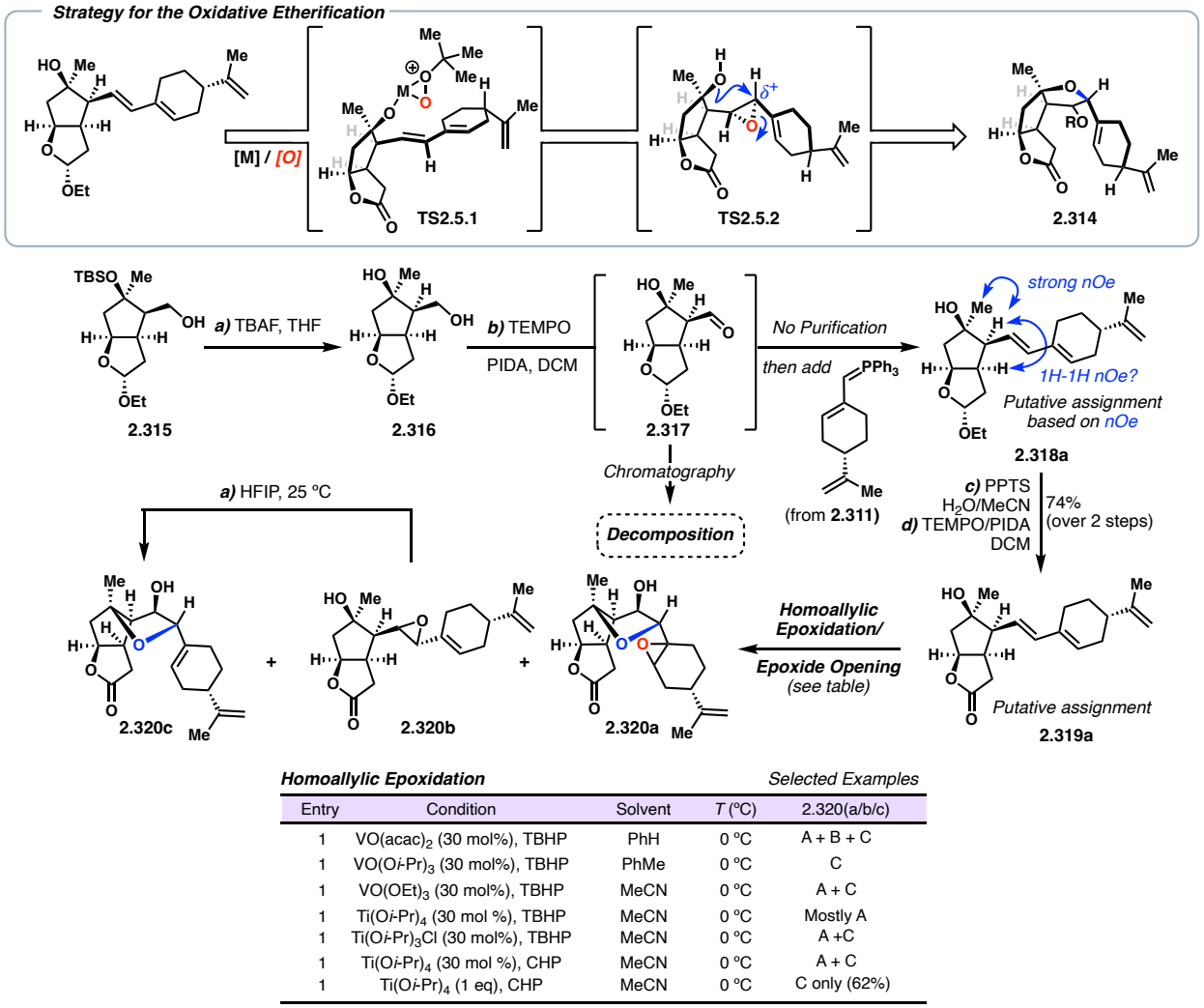
With the 5,5-bicyclic intermediate **2.308** in hand, we were able to introduce oxidation at the C6 position through a hydroboration-oxidation sequence. As expected, hydroboration occurred from the *exo*-face of the 1,1 disubstituted alkene and set the C7 stereogenic center to complete the stereochemically dense, *cis*-fused bicyclic intermediate (**2.309**). We also carried out the hydroboration sequence on the 5,5-bicycle possessing the lactone oxidation state at C19 (**2.313**). This allowed us to unambiguously assign the relative stereoconfiguration of the hydroboration product by X-ray analysis (see Figure 17).

We next sought to introduce the remaining carbon units required for the core of ineleganolide through a Wittig olefination reaction of the corresponding aldehyde with phosphonium ylide (**2.311**), prepared in two steps from perillyl alcohol.[51] We envisioned that the formation of the tetracyclic intermediate possessing the cyclic ether (E-ring, see **2.314**, Figure 16) could be accomplished via a regioselective homoallylic epoxidation of the Wittig product followed by an intramolecular opening of the allylic epoxide to give a tetracycle intermediate via a formal oxidative etherification (Figure 16.).

To evaluate the olefination reaction, we oxidized the primary alcohol **2.309** to aldehyde **2.310**. Our attempts to perform the olefination reaction with the silylated intermediate **2.310** led exclusively to elimination of the C8–siloxy group (Figure 15). We were, however, able to deprotect the silyl-ether prior to oxidation of the C7 alcohol thus providing diol intermediate **2.316** (Figure 16). This material is readily oxidized in the presence of a variety of oxidants; however, the isolated aldehyde proved exceptionally prone to decomposition during chromatography. We found that by using oxoammonium-based oxidation conditions (TEMPO/PIDA) the intermediate could be carried on crude to the Wittig olefination reaction, avoiding the superfluous purification step altogether.[52]

Subjecting crude aldehyde intermediate **2.317** to the previous olefination conditions provided the diene **2.318a** (62%). Given the propensity for the tertiary alcohol at C8 to undergo E_1Cb elimination, we initially believed that any deprotonation of the C7 position would induce this process. Additionally, we observed through space correlations (NOESY) between the C8 methyl group and the C7 C–H. We also observed correlation signals between the C7–C11 vicinal protons. Taken together our observations signaled to us that the relative stereochemical relationship was intact.

As such, we then evaluated the oxidative etherification of diene intermediate **2.318a** to construct the ether bridge (E-Ring, C5–O), a pivotal bond-forming step of our synthetic strategy. As mentioned above, we were inspired by reports by Hartung and sought to use the homoallylic



Homoallylic Epoxidation *Selected Examples*

Entry	Condition	Solvent	*T* (ºC)	2.320(a/b/c)
1	$VO(acac)_2$ (30 mol%), TBHP	PhH	0 ºC	A + B + C
1	$VO(O\textit{i}\text{-}Pr)_3$ (30 mol%), TBHP	PhMe	0 ºC	C
1	$VO(OEt)_3$ (30 mol%), TBHP	MeCN	0 ºC	A + C
1	$Ti(O\textit{i}\text{-}Pr)_4$ (30 mol %), TBHP	MeCN	0 ºC	Mostly A
1	$Ti(O\textit{i}\text{-}Pr)_3Cl$ (30 mol%), TBHP	MeCN	0 ºC	A +C
1	$Ti(O\textit{i}\text{-}Pr)_4$ (30 mol %), CHP	MeCN	0 ºC	A + C
1	$Ti(O\textit{i}\text{-}Pr)_4$ (1 eq), CHP	MeCN	0 ºC	C only (62%)

Figure 16. Synthesis of the putative diene (**2.319a**) and evaluation of the oxidative etherification reaction.

C8 alcohol to direct the regioselective epoxidation of the internal alkene which could then undergo an intramolecular opening of the allylic epoxide to give the E-ring of **2.1**.[53-57] Our downstream studies revealed that deprotection of the ethyl acetal following the oxidative etherification may be challenging due to the introduction of additional oxidation on C6. Although we were unable to deprotect the *tert*-butyl variant of 2.318a (not shown), hydrolysis of the ethyl acetal proceeded smoothly and following oxidation (TEMPO/PIDA) provided the putative tricyclic diene intermediate **2.319a**.

With lactone **2.319a** in hand, we began our investigation of the oxidative etherification with stoichiometric epoxidation reagents such as *m*-CPBA and DMDO which provided a mixture epoxides. Switching to a vanadium-catalyzed homoallylic epoxidation yielded epoxidation product **2.320b** as a single diastereomer, as well as the *in-situ* epoxide opening product **2.320c** and an over-epoxidation product **2.320a**. We rationalized that epoxy-ether **2.320a** arises from the opening of the epoxide **2.320b** to the hydroxy-THF ring (**2.320c**) which can then undergo a second directed epoxidation. An extensive optimization campaign to suppress the formation of the over epoxidation product is summarized in Figure **16**, during which we found that by switching to stoichiometric titanium-catalyzed epoxidation conditions we could affect the desired mono-epoxidation-ring opening reaction in 62% yield without any observed double-epoxidation product.

We rationalized that the use of stoichiometric Ti(O*i*-Pr)$_4$ in the presence of cumene hydroperoxide as oxidant leads to a mixture of epoxide and ether products, the latter of which is presumed to open during quenching of the reaction. The lack of ether products present in the crude reaction mixture suggests that the ether does not form readily and may be triggered either by activation or hydrolysis of the titanium adduct, thus preventing any secondary epoxidation. We also noted that after quenching the reaction mixture with citric acid, the crude reaction mixture which contained mostly epoxide **2.320b**, could be converted to the ether product by stirring in hexafluoroisopropanol at room temperature.[58-63] This could ultimately be done in a one-pot process without any formation of the epoxy-ether product, albeit in slightly diminished yields. Notably, the use of stoichiometric vanadium to affect the same results were unsuccessful likely due to the difference in oxophilicity and bond length of the vanadium–O vs titanium–O bond. Whereas vanadium could readily undergo epoxide opening *in situ*, titanium was unable to do so until the titanium complex was dissociated in a second, discrete event.

At this stage, the putative tetracyclic intermediate **2.320c** containing the A/B/C and E rings could be accessed in substantial quantities, which enabled the evaluation of the 7-*endo*-trig radical cyclization. After screening various base and oxidant combinations and only observing trace oxidation and decomposition of **2.319a**, we were suspicious of the stereochemistry of the C5 position which we had assigned as the correct stereocenter based on NOESY correlations. We then sought to confirm our assigned stereochemistry of tetracycle **2.320c**, however, we were unable to obtain suitable single crystals. After extensive efforts, we were able obtain X-ray diffraction data on the olefination product **2.319a**. To our surprise, this revealed that the Wittig olefination product, which we had originally assigned to possess the correct relative stereochemical configuration at C7 and C8, had undergone a double inversion to provide a product which is epimeric at both C7 and C8 (**2.322**) (Figure 17).

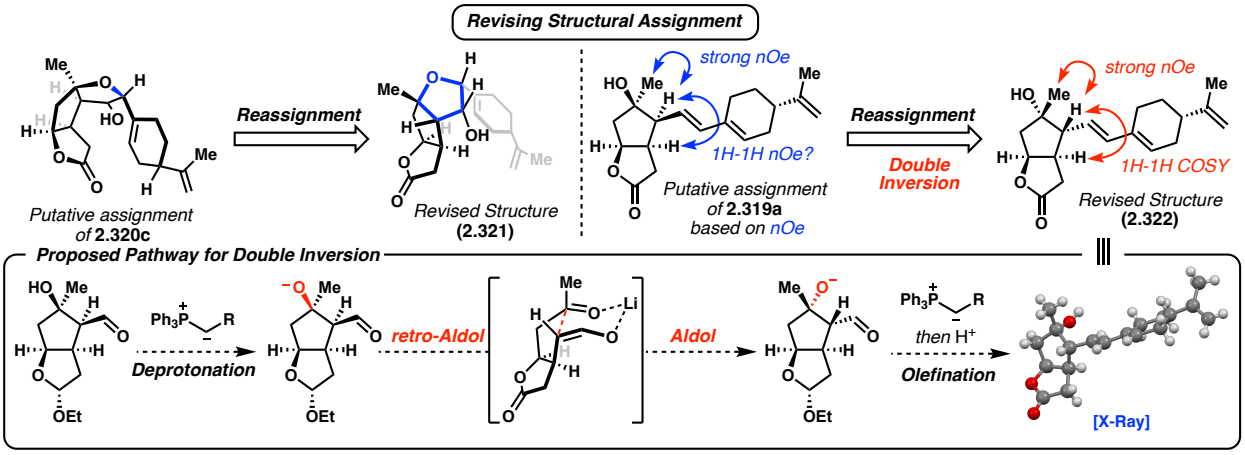
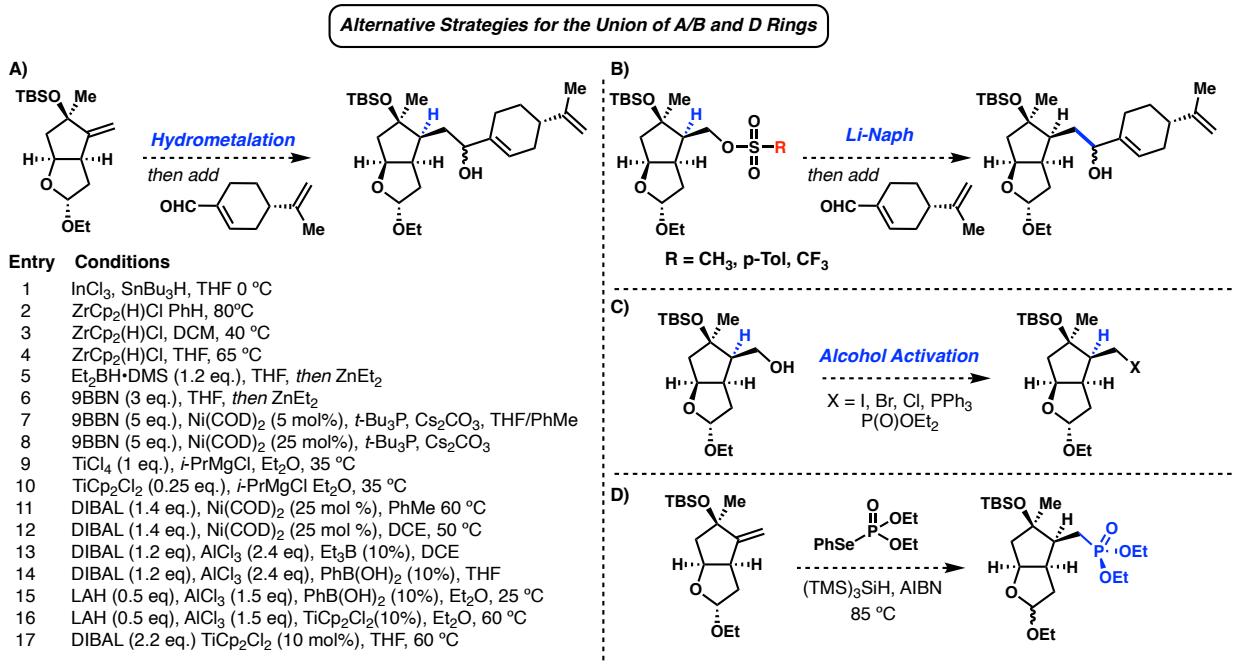


Figure 17. Structural revision of **2.320c** and **2.319a.**

We postulated that this double inversion could arise from the deprotonation of the C8 hydroxyl group which then undergoes a retro-Aldol opening of the A-ring followed by intramolecular Aldol closure from a 6-membered transition state which favors the formation of the double inversion product. The revised structure of the olefination product **2.322** then leads to the revised structure of the oxidative etherification product **2.321**. Attempts to circumvent this deleterious pathway by using other olefination methodologies or modification of the existing conditions and substrates were unsuccessful.

With robust and scalable access to 5,5-fused bicyclic alkene **2.308**, we hoped to be able to leverage this strategy to access synthetically relevant intermediates which may converge to the desired oxidative etherification substrate. We have tried extensively to functionalize the 1,1 disubstituted alkene of **2.308** but have found little success (see Figure 18). Briefly, we have investigated hydrometallation of the *exo*-cyclic olefin of **2.308** to generate carbanion equivalents which may alkylate perillaldehyde to construct the C5–C7 bond, and in turn set the C7 stereogenic center. However, well documented methodologies, which can generate alkyl-metal species such as hydrozirconation,[64] hydromagnesiation,[65, 66]hydrotitanation,[67]hydroboration-transmetallation,[68] and hydroalumination,[69-72] all failed to provide any alkylation products upon treatment with an aldehyde electrophile. Notably, in many cases the reduction product is observed alongside recovered starting material.



Entry	Conditions
1	$InCl_3$, $SnBu_3H$, THF 0 °C
2	$ZrCp_2(H)Cl$ PhH, 80°C
3	$ZrCp_2(H)Cl$, DCM, 40 °C
4	$ZrCp_2(H)Cl$, THF, 65 °C
5	Et_2BH•DMS (1.2 eq.), THF, *then* $ZnEt_2$
6	9BBN (3 eq.), THF, *then* $ZnEt_2$
7	9BBN (5 eq.), $Ni(COD)_2$ (5 mol%), *t*-Bu_3P, Cs_2CO_3, THF/PhMe
8	9BBN (5 eq.), $Ni(COD)_2$ (25 mol%), *t*-Bu_3P, Cs_2CO_3
9	$TiCl_4$ (1 eq.), *i*-PrMgCl, Et_2O, 35 °C
10	$TiCp_2Cl_2$ (0.25 eq.), *i*-PrMgCl Et_2O, 35 °C
11	DIBAL (1.4 eq.), $Ni(COD)_2$ (25 mol %), PhMe 60 °C
12	DIBAL (1.4 eq.), $Ni(COD)_2$ (25 mol %), DCE, 50 °C
13	DIBAL (1.2 eq), $AlCl_3$ (2.4 eq), Et_3B (10%), DCE
14	DIBAL (1.2 eq), $AlCl_3$ (2.4 eq), $PhB(OH)_2$ (10%), THF
15	LAH (0.5 eq), $AlCl_3$ (1.5 eq), $PhB(OH)_2$ (10%), Et_2O, 25 °C
16	LAH (0.5 eq), $AlCl_3$ (1.5 eq), $TiCp_2Cl_2$(10%), Et_2O, 60 °C
17	DIBAL (2.2 eq.) $TiCp_2Cl_2$ (10 mol%), THF, 60 °C

Figure 18. Alternative strategies to functionalize bicyclic intermediate **2.308**

Reductive lithiation of the mesylates, tosylates or triflates derived from alcohol **2.309**,[73, 74] was also unsuccessful and instead led to decomposition or reduction of the carbon–oxygen bond. We also note that subjecting alcohol **2.309** to Appel conditions did not provide the halogenation product, and in many cases, strangely resulted in elimination of the primary alcohol to regenerate the *exo*-cyclic olefin. Taken together, these studies suggest that the primary alcohol and alkene of bicycle are indeed too hindered to undergo any productive radical addition or displacement or addition. This phenomenon likely also explains the retro-Aldol/Aldol double inversion pathway – that the addition to the aldehyde is too slow and the undesired inversion supersedes any productive olefination.

Although the synthetic route to access diene **2.301** proved to be intractable, we were still hopeful that the homoallylic epoxidation-epoxide opening strategy would enable the construction the tetracyclic core of the ineleganolide in an efficient manner, and thus prompted us to devise an alternative strategy to access intermediate **2.301**.

2.5.2 Alternative Strategy to Access Diene Intermediate 2.301

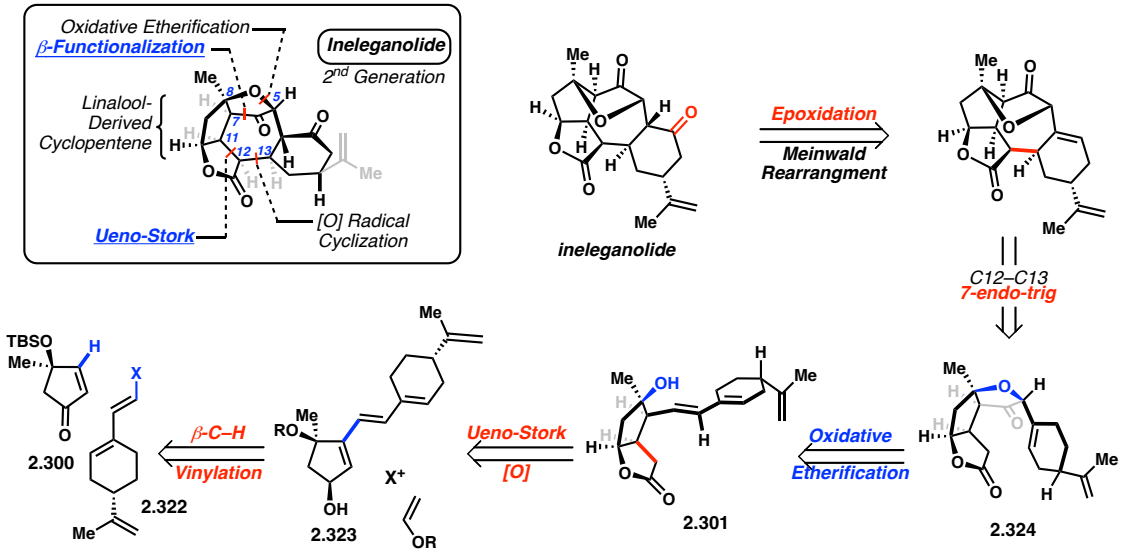
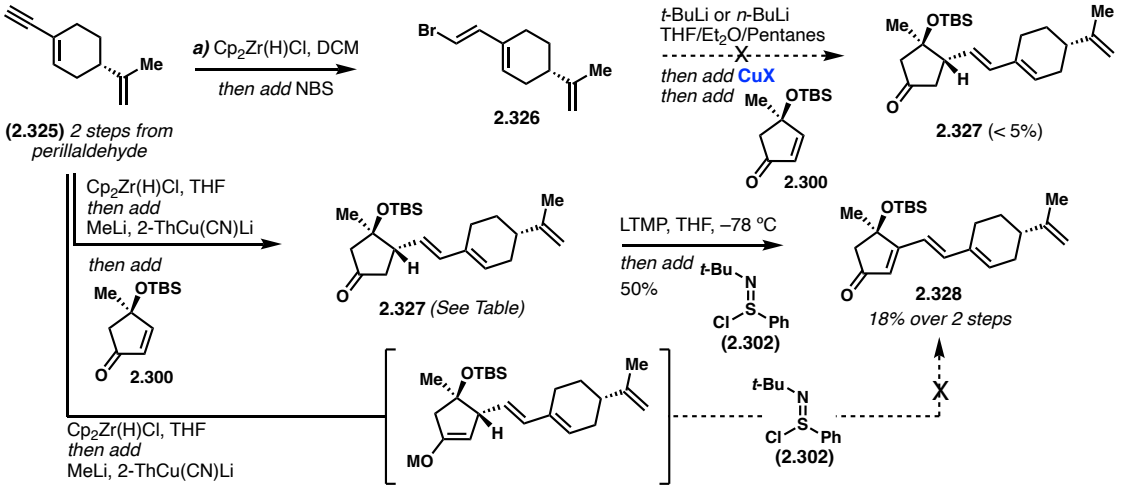


Figure 19. Revised Retrosynthesis to Key Diene Intermediate **2.301**.

Given the difficulties in the functionalization of the bicyclic intermediate **2.309**, we sought to devise an alternative synthetic strategy to access diene **2.301** and avoid potential pitfalls of the Oshima-Utimoto route. Retrosynthetically, we maintained our confidence that the tetracyclic intermediate could arise from the oxidative etherification of diene **2.301**. In contrast to the previous strategy, this bicyclic diene intermediate could arise from the radical 5-*exo*-trig radical cyclization of a triene intermediate **2.323**. This triene intermediate could ultimately be constructed from a conjugate addition of a vinyl nucleophile derived from perillaldehyde followed by oxidation of the resultant enolate to formally provide the β-C–H vinylation intermediate **2.323**.

Our initial efforts to affect this transformation focused on the copper-mediated conjugate addition of vinyl bromide **2.326**, which could be synthesized in a single step from the perillaldehyde derived alkyne (**2.325**, Figure 21). To our surprise, cuprate formation via lithiation and transmetallation with a variety of copper salts led to only trace formation of the conjugate addition product **2.327**. We suspected this may be the result of the instability of the vinyl lithium species formed prior to cuprate formation and turned to strategies involving hydrometallation of alkyne **2.325**. Although hydroalumination followed by transmetallation did not provide conjugate addition product, the use of a stabilized copper salt and mixed solvent system provided the desired conjugate addition product in 38%. Our attempts to elicit a one-pot addition/desaturation process by the addition of Mukaiyama's reagent (**2.302**) following the conjugate addition led to complex reaction mixtures devoid of any triene **2.328**. We found that although the *in-situ* oxidation of the enolate was intractable, diene **2.327** could be oxidized to triene **2.328** in a separate step in moderate yields (50%). Ultimately, after extensive efforts to improve the conjugate addition reaction, we were unable to improve the efficiency of this step and were thus constrained to a sequence that yields triene **2.328** in 16% over two steps which led us to devise a more robust strategy to access this intermediate.



Conjugate Addition Optimization *Selected Entries*

Entry	Conditions	Solvent/T(°C)	Result
1	DIBAL *then* CuI or CuBr	THF, –78 °C	2.300
2	DIBAL *then* 2-ThCu(CN)Li	THF, –78 °C	2.300
3	DIBAL *then* CuTC	THF, –78 °C	2.300
4	Cp_2ZrCl_2, DIBAL; *then*, CuI or CuBr	THF, –78 °C	2.300
5	Cp_2ZrCl_2, DIBAL; *then* 2-ThCu(CN)Li or CuTc	THF, –78 °C	2.300
6	$Cp_2Zr(H)Cl$; *then* Cu(OTf)	THF, –78 °C	2.327 (< 5%)
7	$Cp_2Zr(H)Cl$; *then* $Cu(MeCN)_4PF_6$	THF, –78 °C	2.300
8	$Cp_2Zr(H)Cl$; *then* $[Rh(COD)Cl]_2$	THF, –78 °C	2.327 (< 5%)
9	$Cp_2Zr(H)Cl$; *then* $Ni(acac)_2$	THF, –78 °C	2.327 (12%)
10	$Cp_2Zr(H)Cl$; *then* MeLi, CuTc	THF, –78 °C	2.300
11	$Cp_2Zr(H)Cl$; *then* MeLi, 2-ThCu(CN)Li	THF, –78 °C	2.327 (11%)
12	$Cp_2Zr(H)Cl$; *then* MeLi, 2-ThCu(CN)Li	THF/Et_2O, –78 °C	2.327 (38%)

Figure 20. Efforts to Access Triene **2.328** via Conjugate Addition.

Inspired by recent reports from Newhouse and coworkers on the dehydrogenative stannylation of α,β-unsaturated cyclic ketones,[75] we hoped that the formal β-C–H stannylation would enable facile access to vinyl stannane **2.329**. Stille coupling of the vinyl stannane derived from the linalool cyclopentenone **2.300** with vinyl bromide **2.326** which could be prepared in 3 steps from perillaldehyde could provide the desired triene **2.328**. Notably, this strategy could enable rapid construction of tetracyclic core owing to the convergent nature of the cross-coupling based synthetic approach.

Our synthetic efforts on this revised strategy begin with the synthesis of the vinyl-stannane **2.329**. We were inspired by Newhouse's recently reported dehydrogenative stannylation methodology, which formally provides the *β*-C–H stannylation product through sequential conjugate addition/enolate dehydrogenation steps, in analogy to our efforts toward a one-pot dehydrogenative coupling of cuprate derived from **2.326** (Figure 21). Subjecting enone **2.300** to the standard procedure reported by Newhouse and coworkers provided an appreciable amount of the stannylation product **2.329** (26%). Control experiments revealed that the major products of this reaction were the 1,2-addition of the stannyl-lithiate and a *β*-stannylated product which did not undergo subsequent dehydrogenation. After a short optimization campaign, we found that the addition of HMPA to the stannyl-lithiate greatly reduced the formation of the 1,2 adduct, and that the addition of solid $ZnCl_2$ prior to the palladium dehydrogenation step could improve the

efficiency of the dehydrogenation event and provide the desired vinyl stannane **2.329** in 76% yield in near-decagram quantities.

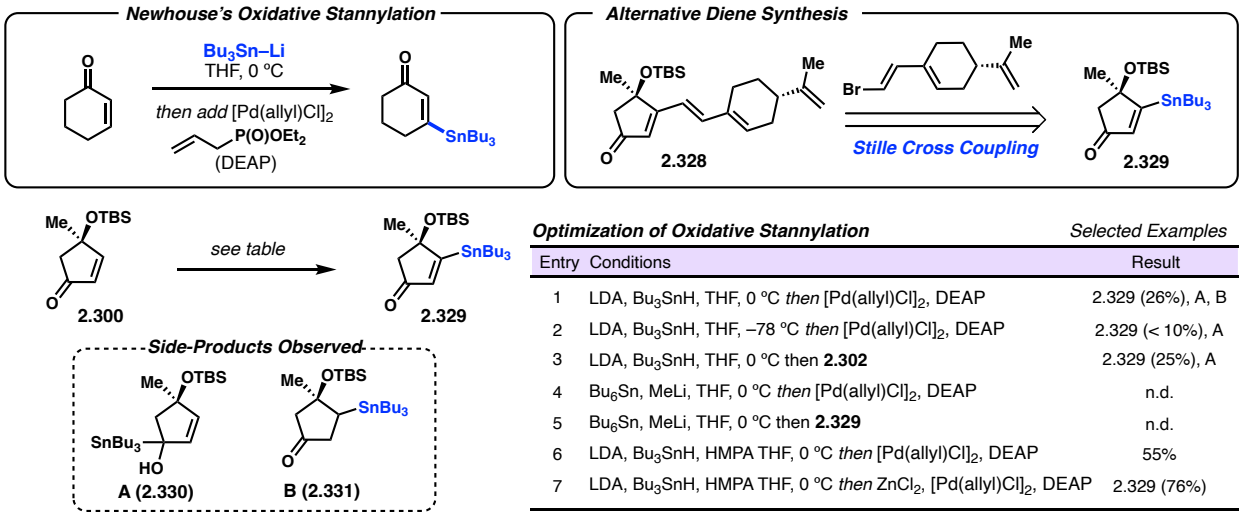


Figure 21. Synthesis of Stille-Coupling Partner **2.329** via Oxidative Stannylation.

With both coupling fragments in hand, canonical Pd-catalyzed Stille cross-coupling conditions ($Pd(PPh_3)_4$, CuI, DMF) provided conjugated triene intermediate **2.328** in 74% yield. From this intermediate, a highly diastereoselective reduction of the C10 carbonyl (>10:1 *dr*) provided allylic alcohol **2.329** in 83% yield. Iodoacetalization of allylic alcohol **2.329** with ethyl vinyl-ether in the presence of *N*-iodo-succinimide (NIS) provided the radical cyclization precursor **2.330** in 74% yield.

At this stage we set out to construct the B-ring of the natural product through a 5-*exo*-trig radical cyclization of iodide **2.330**. After numerous attempts to cyclize this intermediate, we were unable to observe any formation of the biyclic diene (**2.301**). Notably, we found that the use of samarium(II)-based conditions often led to an unproductive cyclization with concomitant loss of the C8 siloxy group. We suspected that the large, TBS-protected C8 hydroxyl group of **2.330** may be detrimental to the radical cyclization, however, all attempts to cyclize the desilylated intermediate **2.330** were also unsuccessful.

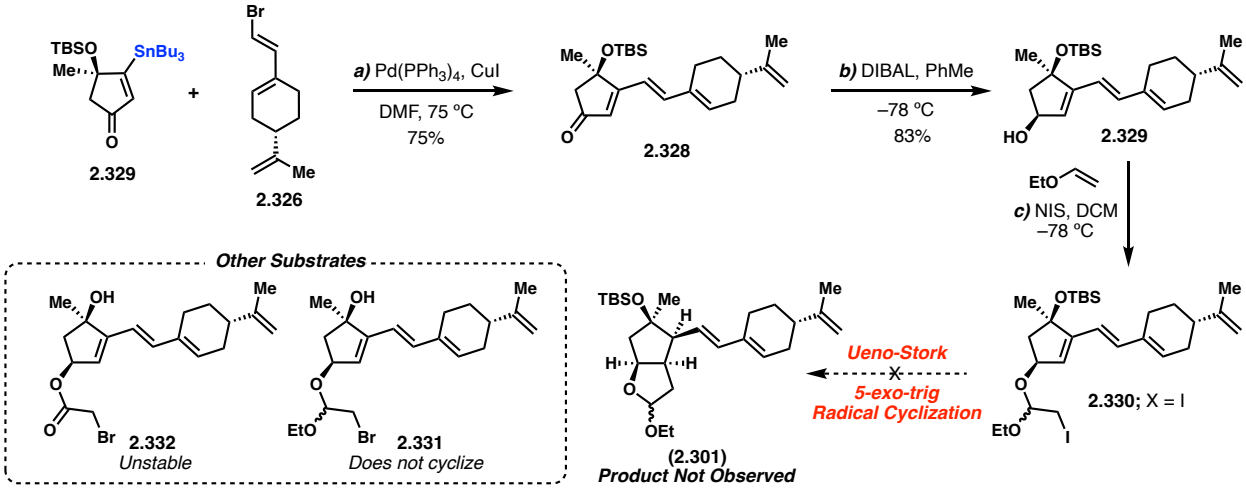


Figure 22. Stille Coupling Strategy to Triene **2.328** and Attempts to Construct Bicyclic Diene **2.301.**

Although Ueno-Stork type radical cyclizations have been shown to proceed efficiently with either activated or unactivated alkenes,[76, 77] the radical cyclization of **2.330** is understood to be kinetically unfavorable due to polar effects.[78] As such, we sought to synthesize iodo- or bromo-ester derivatives of **2.330** with hopes of improving the kinetics of the radical cyclization, however, under a slew of esterification conditions, the corresponding acylation product proved to be unstable and indiscriminately led to decomposition among trace amounts of recovered saponification products. Simple esters such as the C11-acetoxy group proved to be unstable even at cryogenic temperatures.

These failed attempts to construct the B-ring from the conjugated triene intermediate led us to reexamine our synthetic strategy. Our retrosynthesis hinged on the construction of the pentacyclic core of ineleganolide through a radical cyclization of tetracyclic intermediate **2.324** bearing the A, B, D and E rings. The studies on the doubly inverted substrate **2.322** in the previous section gave credence to the formation of the E-ring through a formal oxidative etherification of an intermediate possessing a bicyclic intermediate with a pendant dienyl moiety. Although we had devised a strategy to rapidly unite the linalool and perillaldehyde derived fragments, by way of a dehydrogenative stannylation-cross coupling sequence, we were unable to construct the B-ring through an intramolecular radical cyclization which we attribute to the poor kinetics of a polarity mismatched radical cyclization. Importantly, stannyl-enone **2.329** may serve as a useful synthetic linchpin for the union of A- and D-ring fragments and enable efficient identification of suitable substrates which will allow for the evaluation of our synthetic strategy.

2.5.3 Evaluation of a Liebeskind-Srogl Coupling Strategy

Strategically, we have identified that the installation of oxidation at the C7 position might sufficiently polarize the A-ring alkene and improve the facility of the radical cyclization to construct the B-ring of **2.1**. We envisioned that the incorporation of the C7 oxidation may be accomplished through the coupling of vinyl stannane **2.329** and a D-ring fragment. Although the formation of such an intermediate may also provide opportunities for the formation of the B-ring through polar mechanisms, we note that preliminary studies not included in this thesis highlight the propensity for E1Cb type elimination of the C8 alcohol following anionic Michael additions into conjugated alkenes such as intermediate **2.334**. With these considerations in mind, we proposed a third synthetic strategy to access the key oxidative etherification substrate with the goal of introducing a carbonyl group at C7 to polarize the alkene and improve the facility of the radical cyclization (B-Ring) but also provide a functional handle which may be converted to diene intermediate **2.301**.

In this third generation synthetic strategy, we identified that the coupling of thioesters with vinyl stannanes developed by Liebeskind and coworkers would be a suitable alternative to our previous Stille-based strategy.[79-81] The application of the Liebeskind-Srogl coupling would enable union of stannane **2.333** with the thioester derived from perillyl alcohol to provide radical cyclization precursor containing C7 carbonyl function that may then be converted to the diene intermediate **2.301** (Figure 23).

As an aside, we also identified that the bicyclic intermediate (**2.335**), which arises from the Liebeskind-Srogl coupling (**2.334**) and subsequent radical cyclization, has the potential to undergo direct C–H oxidative etherification to provide tetracyclic intermediate **2.324** (see, Figure 23), likely though the intermediacy of α-iodonoium ketone displacement. We were hopeful that this strategy would provide multiple avenues to forget the E-ring.

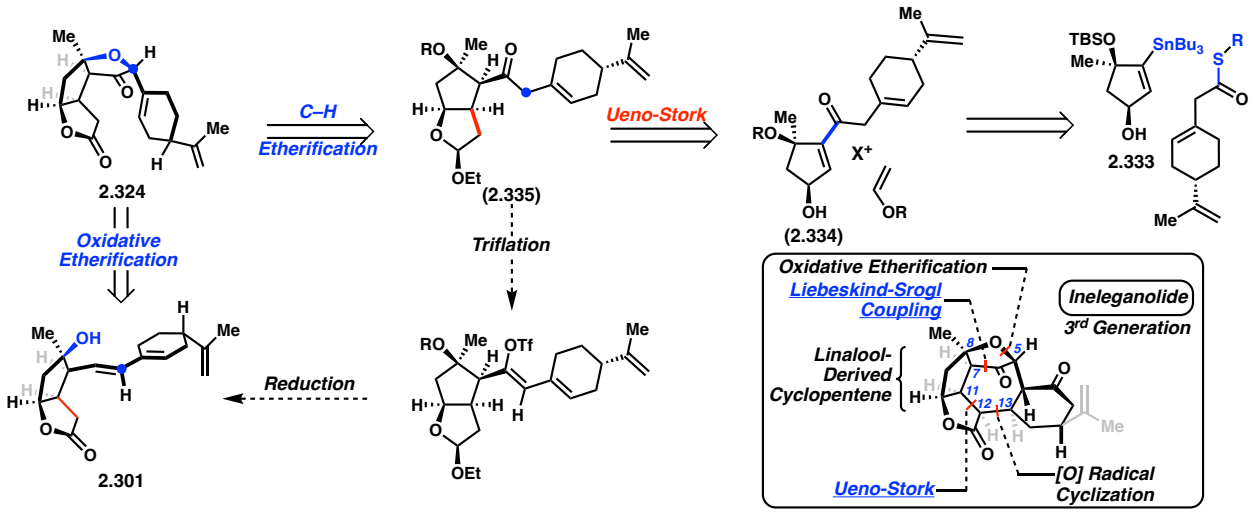


Figure 23. 3rd-Generation Retrosynthesis of Diene **2.301** via a Liebeskind-Srogl Coupling

With this new strategy, we began our studies with the synthesis of the perillyl alcohol-derived thioester which was accomplished through a four-step sequence (Figure 24A). Briefly, dithiane displacement of the allylic bromide formed from the Appel reaction of perillyl alcohol (**2.337**), and subsequent two-step dithiane cleavage and pinnick oxidation provides carboxylic acid (**2.338**). Thioester formation was then accomplished via DCC coupling with *p*-thiocresol to provide the D-ring thioester (**2.339**).

We reasoned that reduction of the cyclopentenone would proceed with poor regioselectivity after the Liebeskind coupling, which led us to reduce the C10 carbonyl to the first**.** (Figure 24B). To prepare the A-ring coupling partner, we began with the carbonyl reduction of

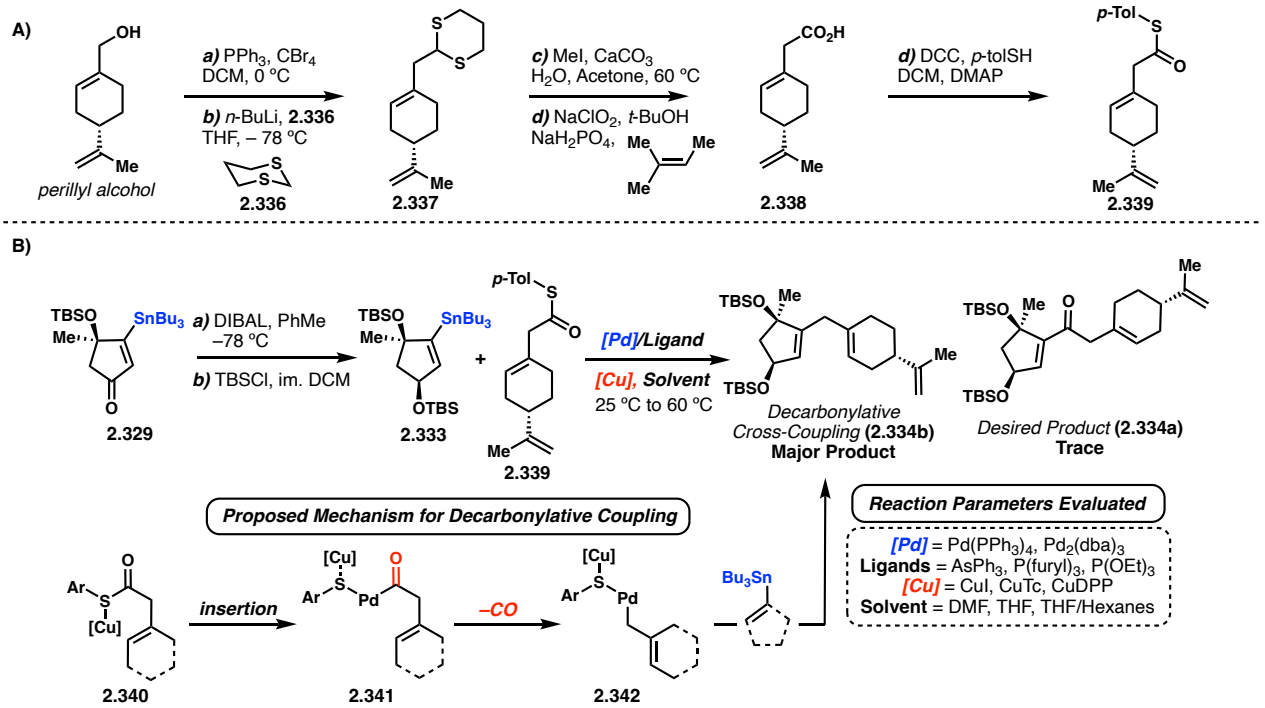


Figure 24. Evaluation of the Liebeskind Cross Coupling Strategy.

vinyl stannane **2.329** give an allylic alcohol which was then TBS-protected to avoid any aberrant reactivity in the Liebeskind coupling and provide the remaining coupling partner (**2.333a)**.

We then evaluated conditions to promote the Liebeskind-Srogl coupling of thioester **2.339** and stannane **2.333a**. Under a variety of conditions, little to no formation of the desired coupling product was observed. Rather, the major product in these reactions arose from a decarbonylative coupling thus producing skipped diene intermediate **2.334b**. A proposed mechanism for this undesired transformation is presented in Figure 27B. All attempts to suppress the formation of this undesired product were met with little success. It has been documented in the literature that the decarbonylation of thioesters to stabilized palladium intermediates is a facile process. [82] In the case of **2.341** (which arises from the C–S insertion of **2.340**), decarbonylation would provide a stabilized palladium-allyl species (2.342) which then undergoes coupling at the least hindered position (Figure 24B). [83, 84]

Common strategies to suppress this decarbonylative pathway are the use of phosphite ligands or the inclusion of ancillary groups, such as *N*-Boc or hydroxyl groups, to stabilize the palladium intermediate following thioester insertion.[82, 85] Given that the use of phosphite ligands were unable to suppress the decarbonylative pathway in our system, we considered the introduction of a stabilizing group on the thioester fragment. We were hesitant to introduce an unprotected alcohol at the α-position of the thioester fragment as it introduces additional selectivity concerns in future steps. Although it was unclear at the outset of these studies whether the inclusion of the OAc group in α-acetoxy thioester **2.346** could sufficiently prevent the decarbonylative pathway, our preliminary efforts revealed that the Liebeskind coupling of the unprotected alcohol (**2.333**) and **2.346** eliminated the decarbonylative pathway present in the previous system (Figure 25B). The α-acetoxy thioester **2.346** could be prepared in four-steps from perillaldehyde through a similar sequence involving dithiane addition to perillaldehyde followed by *in-situ* acetylation. The remaining three steps are identical to the synthesis of **2.339** (Figure 25A).

After examining various ligands, solvents, and copper additives, we found that CuDPP was uniquely capable of facilitating the desired coupling of vinyl stannane **2.333** and acetoxy thioester **2.346**.[79] Liebeskind and coworkers have proposed a rationale for this phenomenon, namely that CuDPP serves as both an activator for the S–C bond and a scavenger of tin by products.

Nonetheless, with the optimized conditions in hand, we were able to procure gram quantities of the coupled product as a 1:1 mixture of inconsequential diastereomers at C5 in a combined 89% yield. It is worth noting that in this reaction the free hydroxyl group at C11 in **2.333** led to slightly improved yields of the reaction when compared to silyl protected stannane **2.333a**. Subsequent installation of the two-carbon unit using ethyl vinyl-ether and NIS provided the third generation of the radical cyclization, **2.348** and **2.349**, intermediate bearing an activated olefin due to the incorporation of the C7 oxidation. In this revised system, subjecting the epimeric iodides **2.348** and **2.349** to canonical radical generating conditions led to the construction of the 5,5-fused bicyclic intermediate **2.350** and **2.351**, respectively. Although 4 diastereomers were formed in the iodoacetalation, distinct diastereomers at C5 (but epimeric at C20) could be separated and advanced individually (Figure 25B).

With bicycles **2.350** and **2.351** in hand, which we believed possessed correct C7 and C8 stereochemistry, we were poised to evaluate the oxidative etherification reaction. Before we could study the E-ring formation on this **2.350** and **2.351** we first needed to identify a route to access diene intermediate **2.301**.

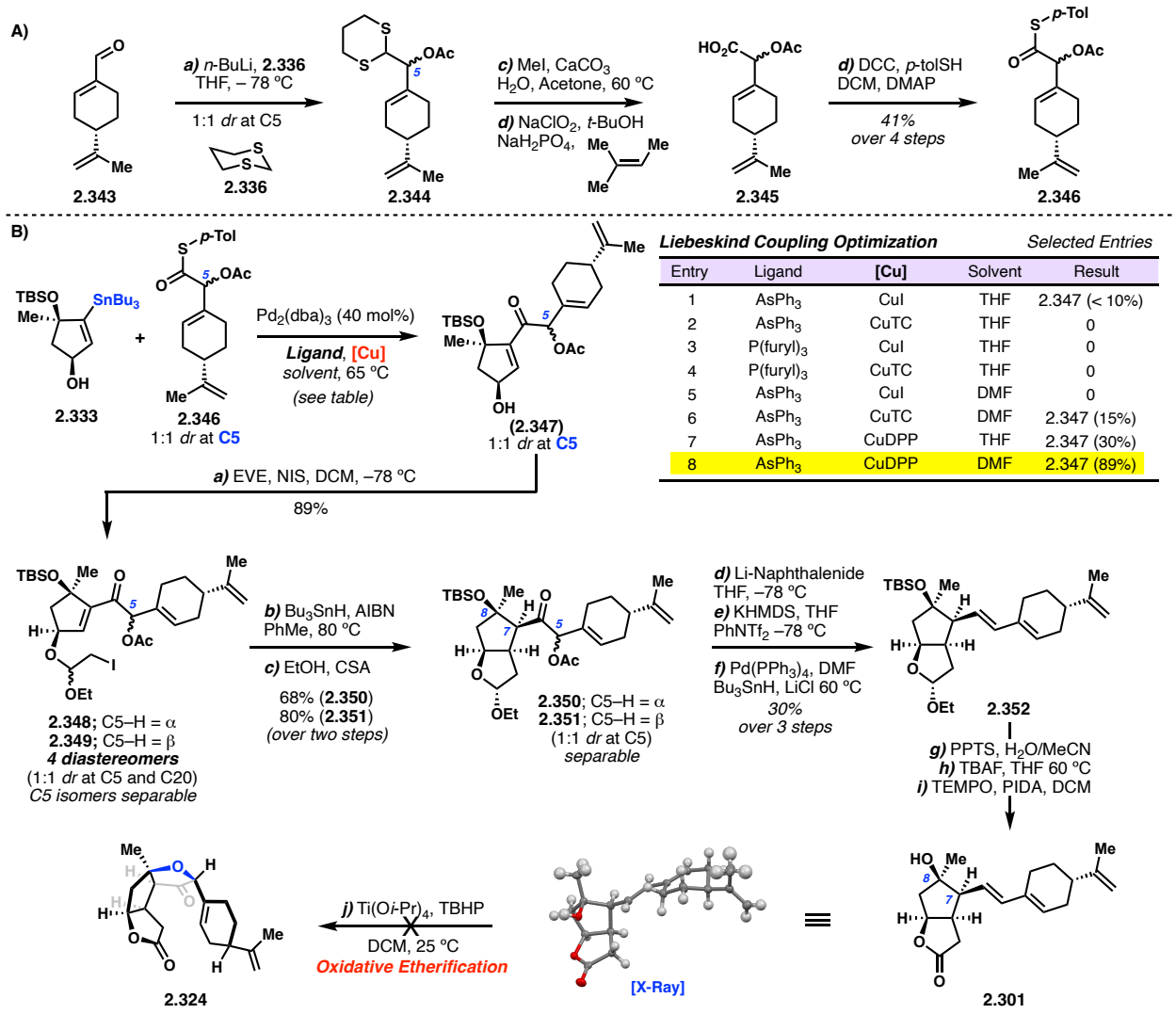


Figure 25. Alternative Liebeskind Cross Coupling to Diene **2.301** and Unsuccessful Oxidative Etherification.

Ultimately, we found that the mixture of C5 diastereomers could converge to a single product by removal of the α-acetoxy group mediated by single electron reduction with lithium naphthalenide. Kinetic deprotonation followed by *in-situ* triflation with *N*-phenyl-bistriflamide provided the conjugated enol triflate which was then subsequently reduced under palladium-catalyzed conditions to provide diene **2.352**. It is worth noting that replacing KHMDS with LHMDS or LDA leads to poor efficiency in the triflation step and a reversal in the regiochemistry of the reprotonation, respectively. Importantly, diene **2.352** is spectroscopically distinct from the double inversion product from the previous strategies. We were then able to unambiguously assign the relative stereochemistry of the C7 and C8 positions through X-ray crystallographic analysis of **2.301** via routine conversion (3 steps) of **2.352** to the lactone-diene **2.301** (see Figure 25 for X-ray). We subjected this newly acquired lactone intermediate (**2.301**) to our previously identified Sharpless homoallylic epoxidation conditions which led to only trace amounts of the epoxide and no tetracycle (**2.324**) was observed.

We hypothesize that this discrepancy in reactivity may be attributed to the cage-like structure of the desired diene **2.301**. In the previously double inverted diene **2.322**, the C8 alcohol and pendant diene were on the convex face of the bicyclic ring system allowing for easy complexation to the epoxidation catalyst. Whereas in the lactone intermediate **2.301** with the correct stereoconfiguration, the positioning of the C8 alcohol on the concave face of the bicycle precluded any complexation and leading to poor ability to direct homoallylic epoxidation.

In retrospect, the discrepancy between epoxidation/etherification sequence for double inverted diene **2.322** and desired diene **2.301** underscores the challenges associated with the construction of the E-ring of ineleganolide and are reminiscent of the challenges faced in the synthetic studies by the Stoltz group. Although ultimately unsuccessful, these studies to access the tetracyclic core of ineleganolide through olefin oxidative etherification have provided invaluable insight to guide future generations of synthetic design. Namely, given the poor efficiency of the metal-mediated homoallylic epoxidation reaction, strategies to close the E-ring C5–O bond should be devised with special consideration to avoid the requirement of complexation of the C8 hydroxyl to metal species within the concavity of the bicycle. Rather, the natural solution is likely through the discrete formation of the C8 alkoxide. Additionally, we were hopeful that the etherification could proceed if the pendant side chain were appropriately activated and positioned.

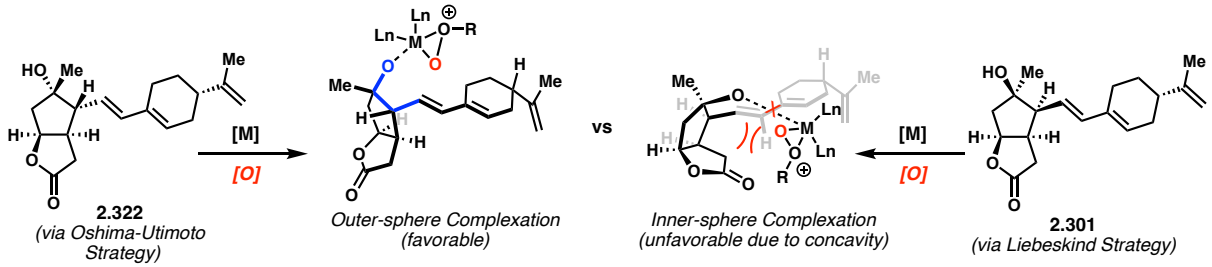


Figure 28. Rationalizing the Difference in Reactivity Between **2.322** and **2.301** in the Oxidative Etherification

With these considerations in mind, we re-evaluated our synthetic strategy which relies on the Liebeskind-Srogl union of terpene derived fragments to unite the A and D rings of **2.1**. Although we initially viewed the keto-acetate moiety as a functional handle for the elaboration into the diene intermediate, we recognized that the C5-acetate group could serve as an electrophile for the formation of the C5–O bond in the E-ring. We sought to leverage this acetate to construct the E-ring either by direct displacement or to access the C5-hydroxyl which could be converted to a potent leaving group in a subsequent step. The successful implementation of this strategy would lead to the construction of the tetracyclic intermediate **2.324** for our studies on the oxidative radical cyclization.

At the outset of these studies, we were hopeful that the two diastereomers of bicycles **2.350** and **2.351** could be elaborated into a pair epimeric tetracycles, which could be interconverted by epimerization of the C5 stereocenter (see Figure 27).

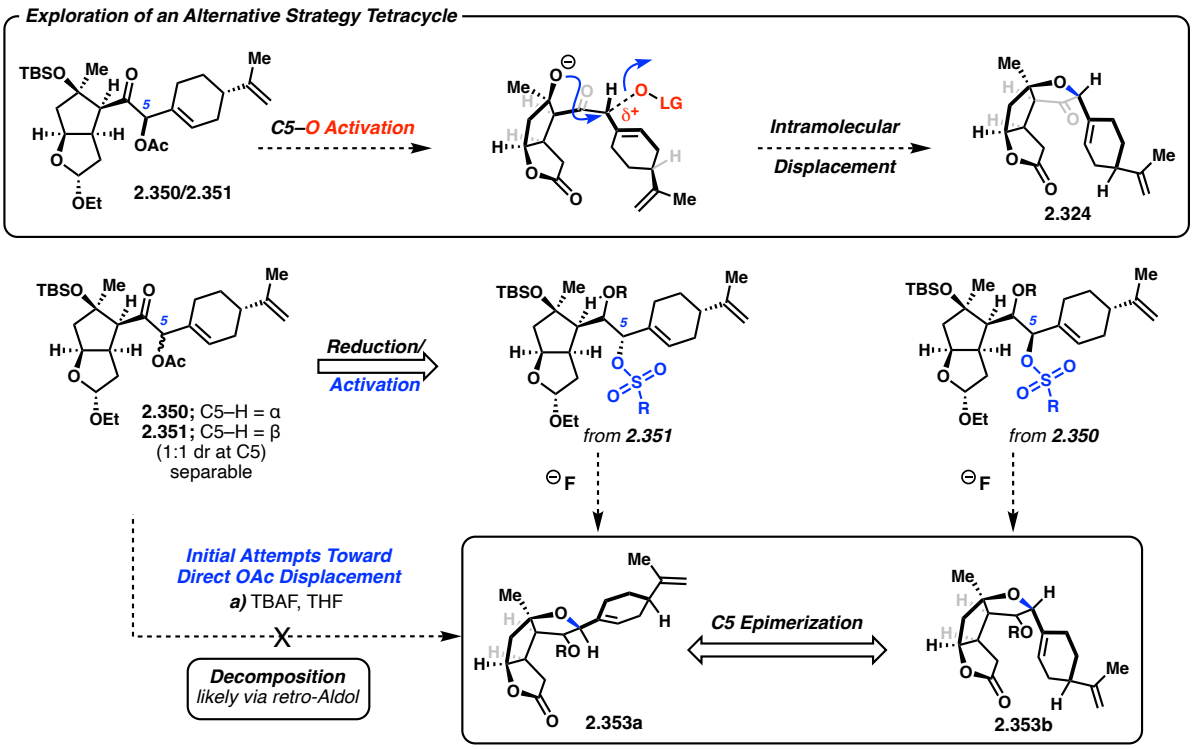
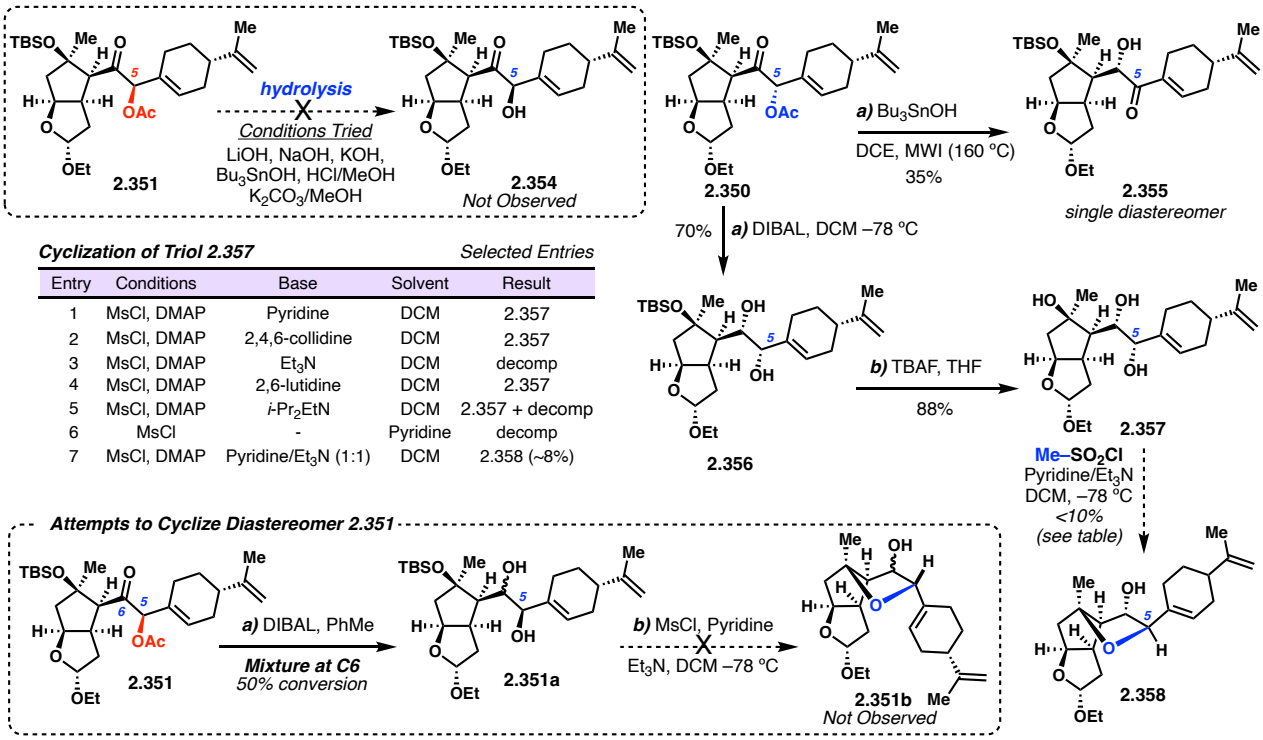


Figure 27. Alternative Strategy for the Construction of Tetracycle **2.324**.

Our initial efforts focused on the direct displacement of the C5-acetoxy group of **2.350** and **2.351** by the C8-alkoxide. We found that subjecting the keto-acetate substrates to silyl ether deprotection conditions (TBAF) led to decomposition. We presume that the decomposition pathway is also due to deleterious retro-Aldol events. Additionally, we attempted to deprotect the C5-acetoxy group to provide the bare C5–OH intermediate which we could subsequently displace following the conversion to a suitable leaving group. However, evaluating a variety of deprotection conditions revealed that acetate deprotection of either diastereomer **2.350** or **2.351** was largely ineffective, often leading to intractable mixtures of products (Figure 28). Notably, the keto-acetate diastereomer **2.350** provided the redox isomer **2.355** in 35% yield upon treatment with Me_3SnOH under microwave irradiation conditions.[86] The 1,2 hydride shift proceeded with high diastereoselectivity and attempts to advance this intermediate to the tetracycle were met with little success

Given our inability to affect the deprotection of the acetate group, we sought to reduce the keto-acetate moiety to a diol and then access a triol intermediate following desilylation. We hypothesized that subjection of the triol intermediate to mesylation conditions could selectively mesylate the less hindered C5 hydroxyl, and in the presence of base, lead to *in situ* displacement to construct the ether bridge.[87] We first reduced the keto acetate **2.350** by treatment with 2 equivalents of DIBAL at cryogenic conditions to provide a single diastereomer of diol **2.356**. In contrast to the deprotection of **2.350** or **2.351**, exposure of diol **2.356** to TBAF at elevated temperatures cleanly provided the triol intermediate **2.357** and lends support to the likelihood of retro-Aldol processes when the C7 position is at the ketone oxidation state.

We then subjected the triol intermediate **2.357** to mesylation conditions and observed that generally, the use of pyridine and tertiary amine bases led to decomposition of the reaction mixture and on some occasions, recovered starting material. However, we found that although the mesylation reaction did not occur in the presence of pyridine as base at –78 ºC and led to decomposition at higher temperatures, the addition of triethylamine following the introduction of mesyl chloride led to the trace formation of the tetracycle **2.358** (*ca.* 8%). In all cases, the inclusion of catalytic or stoichiometric amounts of DMAP and/or replacement of MsCl with TsCl lead to no improvement of the reaction outcome. Despite this initial success, the reaction condition which provided **2.358**, was challenging to reproduce and efforts to optimize the yield of this transformation were unsuccessful. Additionally, we found that the reduction of the other keto-acetate diastereomer **2.351** proceeded with low conversion and was resistant to etherification using the mesylate strategy. We postulate that the presence of three hydroxyl groups in intermediate **2.357** may have complicated the regioselective formation of the mesylate and subsequent cyclization. It is also likely that the cyclization of the triol intermediate proceeds through epoxide formation then displacement, which could be detrimental to the efficiency of the E-ring closure as we observed in the cyclization of diene **2.301**.



Entry	Conditions	Base	Solvent	Result
1	MsCl, DMAP	Pyridine	DCM	2.357
2	MsCl, DMAP	2,4,6-collidine	DCM	2.357
3	MsCl, DMAP	Et_3N	DCM	decomp
4	MsCl, DMAP	2,6-lutidine	DCM	2.357
5	MsCl, DMAP	*i*-Pr_2EtN	DCM	2.357 + decomp
6	MsCl	-	Pyridine	decomp
7	MsCl, DMAP	Pyridine/Et_3N (1:1)	DCM	2.358 (~8%)

Figure 28. Initial Attempts to Advance Keto-Acetates **2.351** and **2.350** via Mesylate Displacement.

For these reasons, we sought to employ differentially activated systems which preclude such complications. To this end, we sought to tether the diol with a group which can suitably activate the C5 position but also prevent any unwanted side reactions involving the neighboring hydroxyl group. We initially attempted to form the cyclic carbonate through reaction with CDI, this 1,2-carbonate proved unusually unreactive.[88, 89] Attempts to access the thiocarbonate were also unsuccessful.

We were cognizant of the high reactivity of 1,2-cyclic sulfites and sulfates which can undergo a slew of displacement reactions and rearrangements.[90] We rationalized that the cyclic sulfite or sulfone could serve as a mesylate equivalent while preventing epoxide formation and upon formation of the C8–alkoxide, could directly construct the E-ring of **2.1**.

To validate these hypotheses, we were able to form an isomeric mixture of cyclic sulfites **2.360a** and **2.360b** through treatment of the diol **2.356** with thionyl chloride and an amine base. Our attempts to access the 1,2-cyclic sulfate variant were unsuccessful likely due to the marked ring strain of the product. To our surprise, treatment of the mixture of sulfites (chiral at S) with TBAF led to tetracycle **2.361** with the incorrect stereochemistry at C5 in 84% yield. Oxidation of the C6 alcohol to the ketone (**2.362**) proceeded smoothly and following deprotection of the ethyl acetal and oxidation to the lactone, the structure of **2.363a** was confirmed unambiguously by X-ray diffraction experiments (Figure 29).

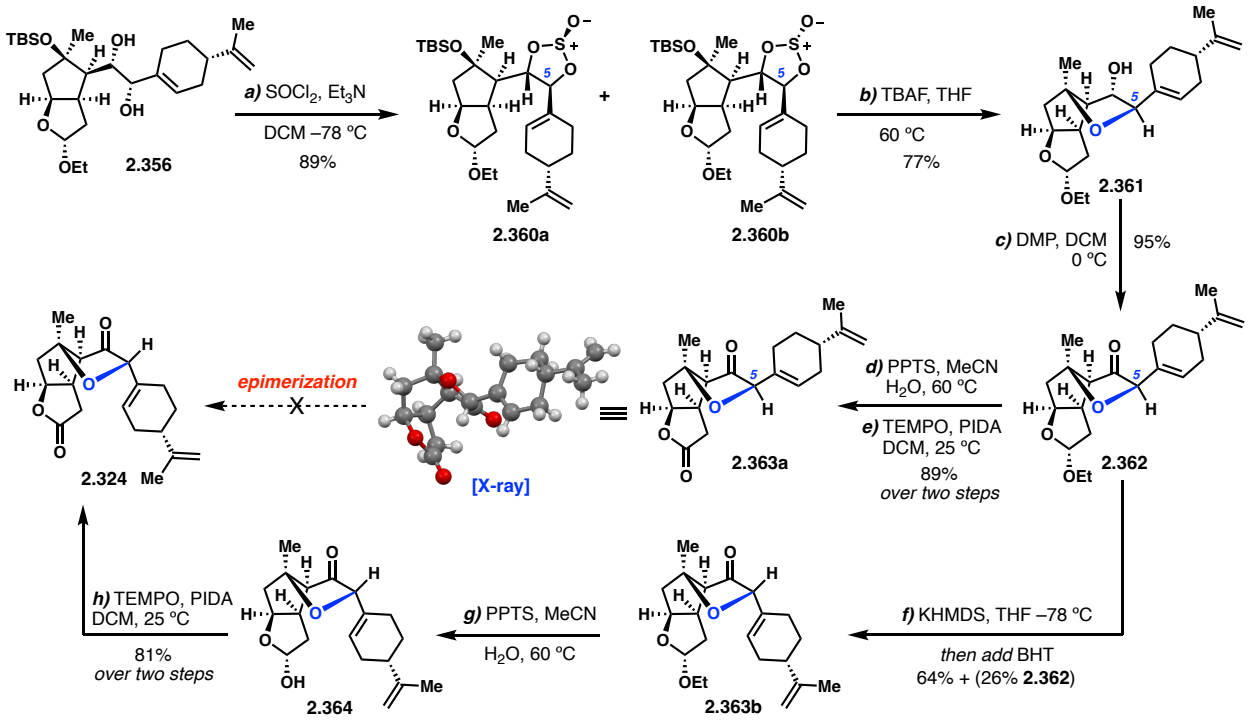


Figure 29. Synthesis of the Tetracyclic Intermediate via Intramolecular Cyclizations of Cyclic Sulfites.

With the successful construction of the tetrahydrofuran ring, we next sought to epimerize the C5 stereocenter. Although many groups have reported the use of ethyl salicylate[91, 92] and the trityl anion[93] for the epimerization of acidic protons, these conditions led to the isolation of the starting epimer. We found that the epimerization of tetracycle **2.362** could be accomplished via deprotonation of the C5 position with KHMDS, followed by kinetic quenching with BHT, as reported by Trauner and coworkers, to provide an enriched mixture of C5 epimers (**2.363b** + **2.362**) which could be recycled to obtain the tetracycle **2.363b** possessing the correct C5 configuration.[94] Notably, our studies revealed that the use of LDA and LHMDS, led to the selective deprotonation of the C7 position (confirmed by bromine incorporation) and no epimerization, respectively, and KHMDS was uniquely capable of facilitating this deprotonation even when replaced with LTMP. We also note that quenching the reaction at higher temperature provides products which resemble protonation at the γ-position as opposed to the α-position resulting in a conjugated system.

Importantly, a modified synthetic route to access the tetracyclic intermediate from the keto-acetate diastereomer **2.351**, which was previously resistant to elaboration, was developed. In this sequence, the biyclic intermediate could be diastereoselectively reduced using DIBAL-ate complex formed *in situ* from the addition of *tert*-Butyl lithium to DIBAL, affording diol intermediate **2.365**.[95, 96] Conversion of this intermediate to the sulfite provide a mixture of 1,2-cyclic sulfites **2.366**. In contrast to the intramolecular etherification of **2.360a/b** which proceeds smoothly with TBAF as the fluoride source, only hydrolysis of the cyclic sulfite and subsequent deprotection of the alcohol was observed. As a result, the cyclization of this sulfite required the use of TASF at elevated temperatures in DMF. Importantly, the inclusion of HMPA and molecular sieves in the solvent mixture led to improved yields and diminished hydrolysis. Notably, the cyclization of diastereomer **2.367** provides a tetracyclic intermediate which possesses the desired C5 relative stereochemistry which was confirmed by DMP oxidation.

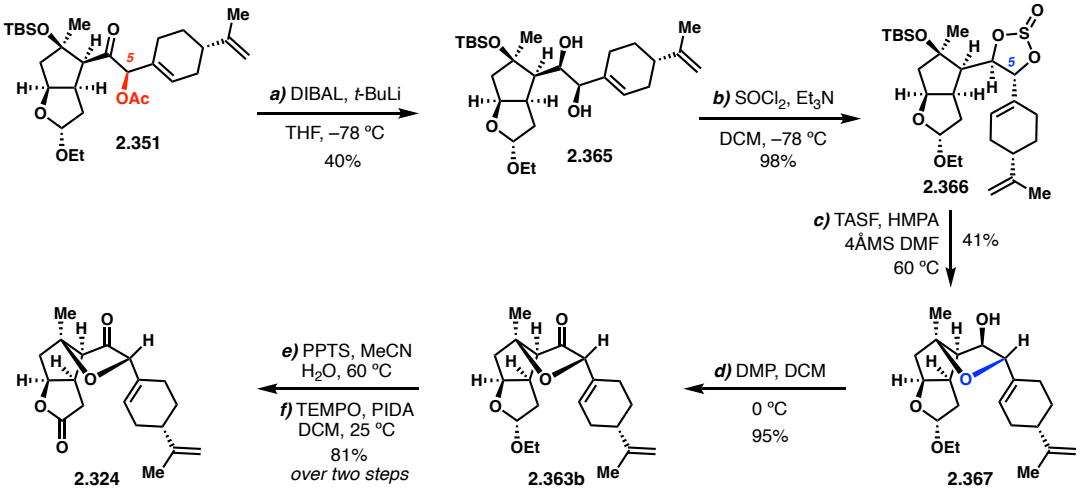


Figure 30. Converging Diastereomeric Keto-Acetates to Tetracycle **2.324.**

With access to the tetracyclic intermediate from both diastereomers of the keto-acetate, we were poised to begin our studies on the construction of the C12–C13 bond and ultimately the completion of the pentacyclic core of ineleganolide. In contrast to the synthetic efforts by the Vanderwal and Stoltz groups, our advanced synthetic intermediate possesses the correct configuration at every position in the ineleganolide core and has the E ring installed prior to the formation of the cycloheptane ring, respectively.

Although our synthetic strategy aimed to directly oxidize the B-ring enolate to perform the radical cyclization, we were hesitant due to the presence of the C6 carbonyl group. To circumvent these challenges of regiochemical deprotonation between the C12 position and C6 and C7 positions, we began our efforts to forge the pentacyclic core by converting the B-ring to the dihydrofuran **2.369**. As previously mentioned, the epimerization of the C5 position in tetracycle **2.362** provided an enriched ratio of **2.363b** (~2.5:1). We found that the epimerization of dihydrofuran **2.369 to 2.370** proceeded in improved yields with only minor amounts of the un-epimerized intermediate. Given the facility of this epimerization, we opted to proceed with the un-epimerized C5 tetracycle **2.369** which was readily converted to the dihydrofuran via deprotection of the ethyl acetal followed by elimination of the lactol (**2.368)** mediated by MsCl and Et_3N at elevated temperature. Applying the same conditions, **2.369** was epimerized to afford the tetracyclic intermediate **2.370.** It is worth noting that both **2.369** and **2.370** dihydrofurans are generally stable to purification on preparative scale, however upon increasing to larger scale these intermediates proved to be unstable to purification and storage even under inert and anaerobic conditions.

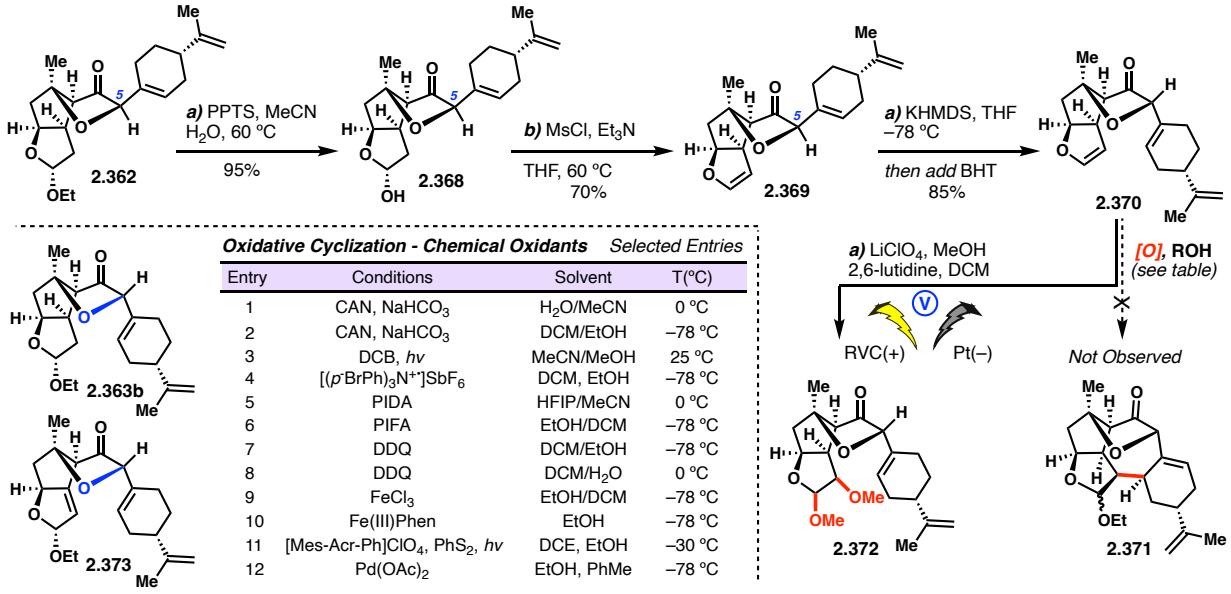


Figure 31. Oxidative 7-*endo*-trig Radical Cyclization of Dihydrofuran **2.370**

We then surveyed a variety of oxidative conditions to promote the desired 7-*endo*-trig oxidative radical cyclization which could proceed via single electron oxidation of the electron rich vinyl ether to a radical cation that could undergo trapping with protic nucleophiles and radical cyclization. Subjecting **2.370** to Ce(IV) buffered with sodium bicarbonate in either ethanolic or aqueous mixed solvent systems led to a mixture of unidentifiable products lacking the B-ring. The use of DDQ or a triarylamine radical cation salt led to the formation product **2.362** which likely arises due to either protonation of the vinyl ether and quenching with solvent alcohol nucleophile, or radical cation trapping with alcohol followed by hydrogen-atom transfer from the solvent. The former is believed to be the operative mechanism for the formation of **2.363b** in the case of $FeCl_3$ as the oxidant due to the presumed release of HCl by ethanolysis of the Fe–Cl bond. The use of hypervalent iodonium reagents, PIDA and PIFA led to intermediates that are tentatively assigned as fragmentation products. Attempts to promote a redox neutral radical cyclization using photochemical methods also led to no observable products. Interestingly, treatment of **2.370** with $Pd(OAc)_2$ and EtOH in toluene to promote an Oshima-Utimoto-like cyclization led to the formation of the **2.373**. This is believed to arise from nucleophillic palladation preferentially from the *exo*-face with concomitant with trapping of the oxocarbenium followed by a *syn* β-hydride elimination.

In the face of the failed attempts to cyclize intermediate **2.370**, we then turned to electrochemical methods to facilitate this transformation. Inspired by Trauner's synthesis of guanacastepene and Moeller's studies on anodic cyclizations, we employed similar conditions in a batch chemical reactor using RVC anode and Pt cathode in the presence of methanol and 2,6-lutidine as a base.[97-102] We found that under these conditions, the major product formed was the dimethoxylation of the dihydrofuran moiety (**2.372**). We postulate that the mechanism of this transformation is the anodic oxidation of the cyclic vinyl ether to provide a radical cation which gets attacked by methanol to provide a β-methoxy radical that undergoes a second oxidation to provide a second cation which is trapped by a second equivalent of methanol. Given the general instability of these compounds and the propensity for hydroetherification back to intermediate

2.363b, owing to the acidic nature of the reaction medium, we wanted to explore alternative strategies for the construction of the cycloheptane ring.

We considered the possibility that the tetracyclic intermediate possessing the carbonyl group at C6 may be affected conformationally by the sp^2-hybridized C6 carbon effectively lengthening the distance between the C12 and C13 positions. With the goal of obtaining a tetracyclic substrate possessing a C6 sp^3-hybridized center, and hopefully enforcing a conformation change to promote the cyclization, intermediate **2.363b** was reduced with DIBAL to provide secondary alcohol **2.374** (Figure 32). It is noteworthy that under a variety of reducing reagents tried, the reduction occurs with complete diastereoselectivity due to the cage-like structure of intermediate **2.374**. Our downstream studies revealed that the free hydroxyl group at C6 is operationally incompatible with the C19 lactone oxidation state due to its tendency for intramolecular trans-lactonizations. As such, exhaustive efforts to protect the secondary alcohol of **2.374a** resulted were unsuccessful. Unsurprisingly nucleophilic displacement of this secondary alcohol was also ineffective due to inability to activate the C6-hydroxyl.

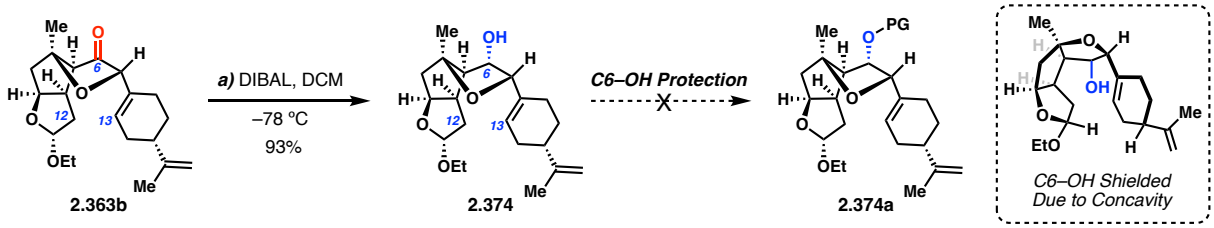


Figure 32. Attempts to Access Protected C6-(sp^3)–Hydroxy Substrate.

Given the inability to functionalize the reduction product **2.374**, due to the shielding of the C6-hydroxyl group, we turned to alternative strategies to construct the C12–C13 bond. Inspired by the MacMillan group's organocatalytic enamine oxidative radical additions,[103-107] we envisioned that the tetracyclic intermediate bearing sp^3-hybridized C6 carbon and a lactol oxidation state could be a suitable substrate for an enamine catalyzed oxidative radical cyclization.

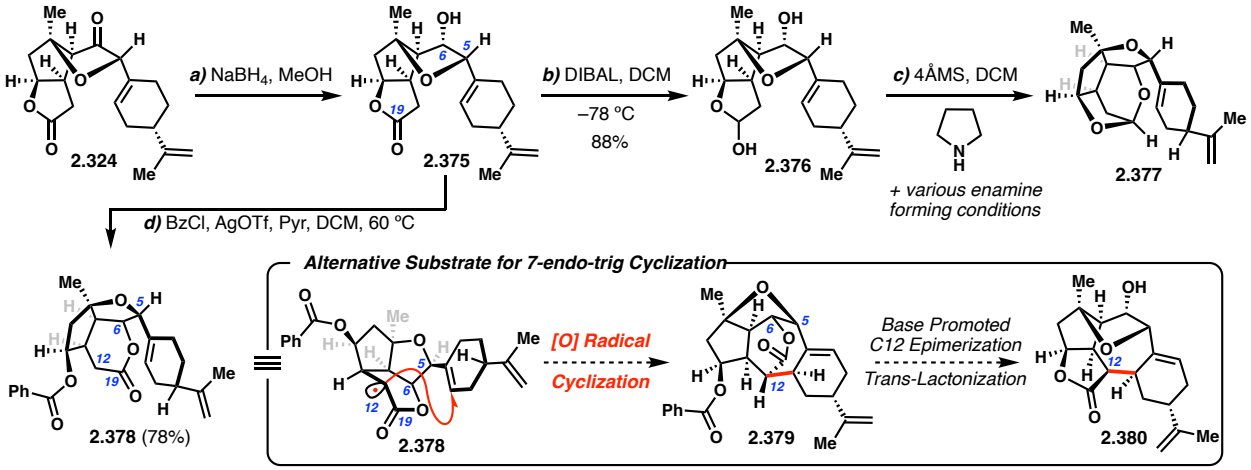


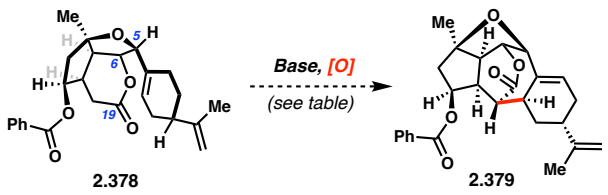
Figure 33. Unsuccessul Oxidative Enamine Cyclizations and Identification of a New Cyclization Substrate.

We found that the deprotection of the ethyl acetal moiety under acidic conditions leads directly to the formation of pentacyclic acetal **2.377** (see Figure 33). To circumvent this pathway, ketolactone intermediate **2.324** was reduced chemoselectively at C6 and subsequent reduction of

the C19 lactone was accomplished through the use of DIBAL. It is worth mentioning that the use of excess DIBAL to reduce both the C6 and C19 carbonyls led to complex mixtures consisting of reduction and/or translactonization. Given the propensity of the C6 hydroxyl group to form a transannular acetal, we were cautiously hopeful that the use of catalytic quantities of secondary amines may lead to the preferential formation of the tricyclic enamine which may then be oxidized to forge the final bond. Subjecting intermediate **2.376** to catalytic or stoichiometric amounts of pyrrolidine or proline with or without chemical oxidants led the near quantitative conversion to pentacyclic acetal **2.377**, the product we observed previously.

During these studies, we found that treatment of tetracycle **2.375** with benzoyl triflate led to the rearranged tetracyclic intermediate **2.378** possessing a 6-membered lactone and benzoyl group at C11–O. We surmised that this intermediate may also undergo the proposed oxidative radical cyclization to construct pentacycle **2.379** which upon treatment with alkoxide conditions could undergo epimerization at C12 with concomitant translactonization to provide the pentacycle **2.380**.

Tetracycle **2.378** was then treated with a variety of bases and oxidants in an attempt to promote the desired transformation (Figure 34). We found that subjecting **2.378** to LDA followed by $Fe(acac)_3$ or Cu(II)ethylhexanoate (Cu(II)EtH) resulted in mostly recovered starting material and some intramolecular Claisen condensation product **2.379b** (Figure 35), respectively. Switching to LHMDS in the presence of Cu(II)EtH led to predominantly α-hydroxylation (**2.379a**) of the C12 position upon quenching likely due to the introduction of molecular oxygen during the addition of the solid oxidant. Whereas the use of $FeCl_3$ provided some of the Claisen condensation product, the use of $[Fe(Phen)_3](PF_6)_3$ or cupric chloride led to intractable reaction mixtures.



Direct Oxidative Radical Cyclization *Selected Entries*

Entry	Base	Oxidant	Solvent/*T*(°C)	Result
1	LDA	Cu(II)EtH	THF	rsm + 2.379b
2	LDA	$Fe(III)(acac)_3$	THF	rsm
3	LHMDS	Cu(II)EtH	THF	2.379a
4	LHMDS	$FeCl_3$	THF	rsm + 2.379b
5	LHMDS	$Fe(Phen)_3PF_6$	THF	2.379b
6	LHMDS	$CuCl_2$	THF	decomp

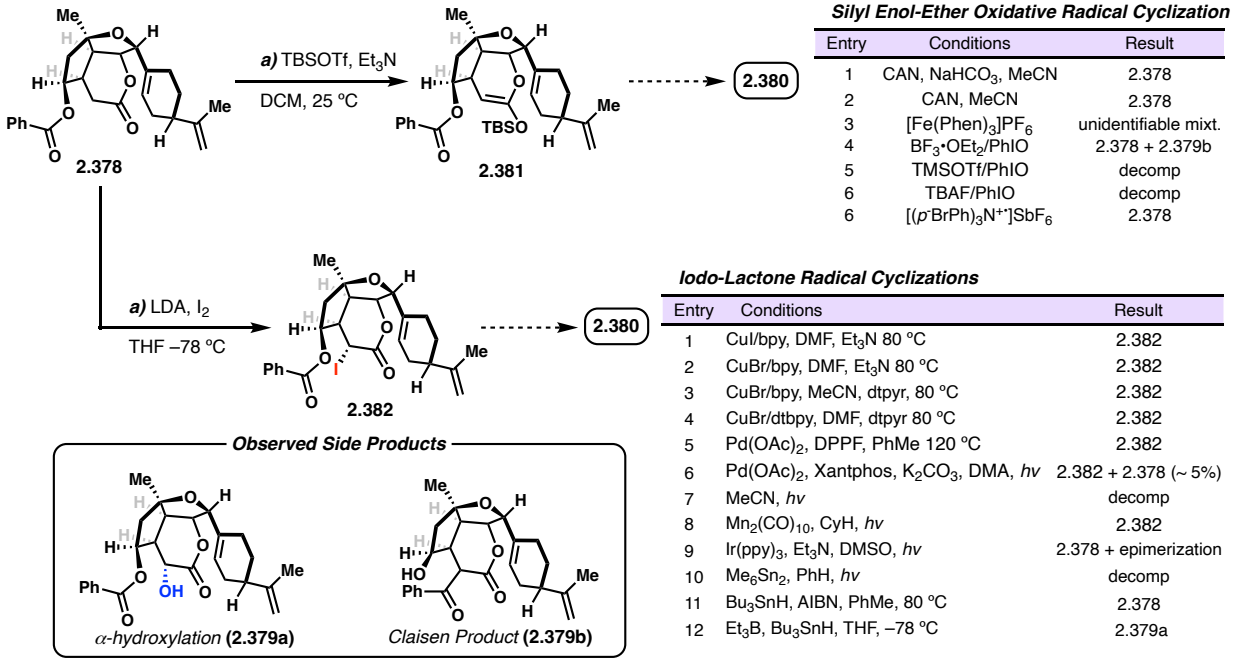
Figure 34. Efforts Toward the Oxidative Enolate Cyclization of Lactone **2.378**.

Given the observance of products arising from intermolecular Claisen condensation, we opted to study the oxidative radical cyclization in the absence of strong base by using activated systems such as the silyl enol-ether **2.381** and the α-iodolactone **2.382** individually prepared in a single step from **2.378** (see Figure 35).

First, we evaluated the cyclization of the *tert*-butylsilyl enol ether **2.381**. Again, we found that treating this intermediate with Ce(IV) and Fe(III) oxidants led to no observable cyclization product. Following precedence by Moriarty and coworkers,[108-110] we sought to generate the α–hypervalent iodonium which could undergo nucleophilic displacement by the 6-membered alkene and elimination to provide the desired product. However, we found that treatment of **2.381** with BF_3•OEt_2/PhIO results in deprotection of the silyl-ketene acetal, which was also observed when using radical cation salt oxidants. The use of other iodosobenzene-activator complex led to immediate decomposition of the starting material.

We also explored a variety of conditions to facilitate oxidative, reductive, or atom-transfer radical cyclization of iodolactone **2.382**. We first evaluated copper-mediated atom transfer cyclizations and found that under all conditions, there was no consumption of **2.382**. We believe the lack of reactivity in these systems may be due to a mismatch in reduction potentials of iodolactone or the shielded nature of the iodide preventing outer-sphere electron transfer from the

Cu/bpy complex. Additionally, the use of thermal or photochemical palladium-mediated Heck cyclizations led to only recovered starting material and small quantities of protodeiodination (**2.387**). Irradiating the iodide at 254 nm light in acetonitrile led to decomposition and the use Mn-mediated atom transfer led to recovered starting material.[111] Interestingly, attempts to use $Ir(ppy)_3$ as a photoredox catalyst to promote the radical cyclization led to complete protodeiodination with concomitant epimerization of the C11 position. Lastly, our attempts to promote a reductive radical cyclization led to protodeiodination product and alpha hydroxylation (entries 11-12, Figure 38).



Silyl Enol-Ether Oxidative Radical Cyclization

Entry	Conditions	Result
1	CAN, $NaHCO_3$, MeCN	2.378
2	CAN, MeCN	2.378
3	$[Fe(Phen)_3]PF_6$	unidentifiable mixt.
4	$BF_3{\cdot}OEt_2$/PhIO	2.378 + 2.379b
5	TMSOTf/PhIO	decomp
6	TBAF/PhIO	decomp
6	$[(p\text{-}BrPh)_3N^{+\cdot}]SbF_6$	2.378

Iodo-Lactone Radical Cyclizations

Entry	Conditions	Result
1	CuI/bpy, DMF, Et_3N 80 °C	2.382
2	CuBr/bpy, DMF, Et_3N 80 °C	2.382
3	CuBr/bpy, MeCN, dtpyr, 80 °C	2.382
4	CuBr/dtbpy, DMF, dtpyr 80 °C	2.382
5	$Pd(OAc)_2$, DPPF, PhMe 120 °C	2.382
6	$Pd(OAc)_2$, Xantphos, K_2CO_3, DMA, *hv*	2.382 + 2.378 (~ 5%)
7	MeCN, *hv*	decomp
8	$Mn_2(CO)_{10}$, CyH, *hv*	2.382
9	$Ir(ppy)_3$, Et_3N, DMSO, *hv*	2.378 + epimerization
10	Me_6Sn_2, PhH, *hv*	decomp
11	Bu_3SnH, AIBN, PhMe, 80 °C	2.378
12	Et_3B, Bu_3SnH, THF, –78 °C	2.379a

Figure 35. Alternative Radical Cyclizations to Construct the 7-membered Ring.

Concomitant to our studies on the oxidative 7-*endo*-trig radical cyclization, we explored the strategies to introduce additional oxidation on the 6-membered ring of tetracycle **2.362** or **2.363b** (D-ring). Preliminary efforts to perform allylic oxidations on **2.362** resulted in no reaction or poor regioselectivity. This prompted us to consider methods for transpositive-allylic oxidation, such as the Schenck-ene reaction. Extensive efforts to realize this transformation on tetracycle **2.363b**, which possesses the correct C5 configuration, were undertaken, but unsuccessful. Notably, we found that the tetracyclic intermediate **2.362** with the incorrect C5 configuration provided trace amounts of the desired allylic alcohol product (**2.383**) when TPP was used as the photosensitizer. We observed poor mass recover of the reaction which we attribute to photochemical decomposition (via Hock-type fragmentation of hydroperoxide intermediates) of the starting material and/or products. Witzel has noted that the rates of Schenck-ene reaction of cyclohexenyl alkenes are unfavorable and, importantly, the use of TPP as the photosensitizer can lead to the decomposition of hydroperoxides formed in the reaction.[112] For these reasons, we turned to the one-pot oxidative Schenck-ene reaction which provided α,β-unsaturated ketone **2.384** in 37% yield after 30 hours of irradiation. Unfortunately, neither **2.384** or its derivatives **2.386** and **2.387**, accessed in an additional one and two steps, respectively, could be epimerized to provide the

tetracyclic intermediates with the correct C5 stereoconfiguration (**2.388** and **2.389**) thus thwarting our attempts to study the anionic cyclization modes.

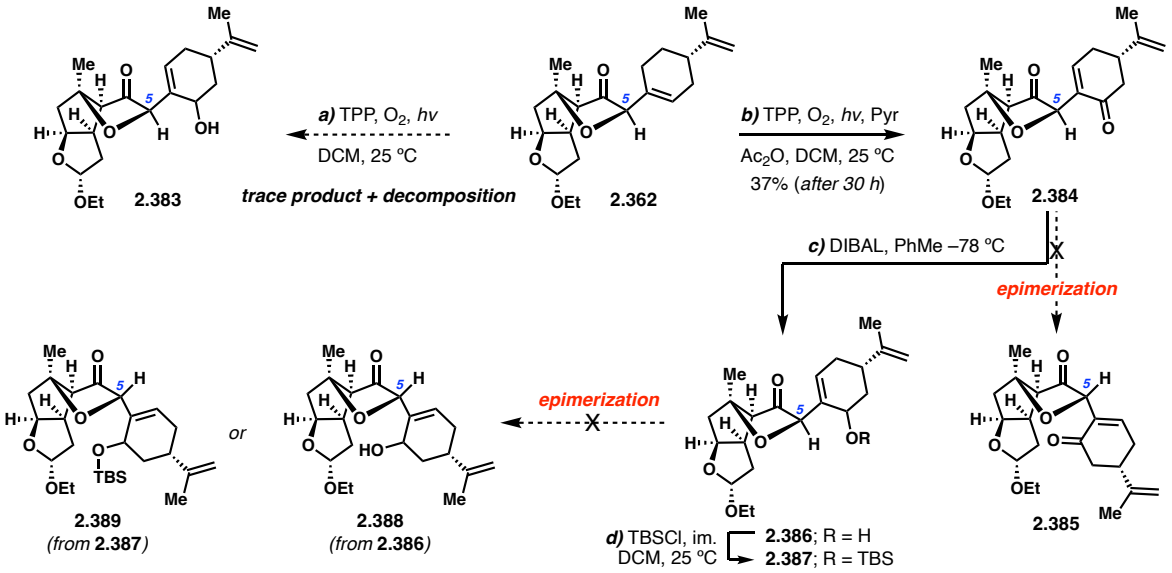


Figure 36. D-Ring Functionalization via Schenck-Ene Reaction.

Our current efforts are now focused on the investigation of **2.391** and **2.393** as 7-*endo* radical cyclization substrates. Specifically, we hope that cyanohydrin intermediate **2.391**, which possesses an sp^3-hybridized C7 carbon will be a competent cyclization substrate due to its conformational flexibility compared to intermediates possessing the C7 carbonyl. Additionally, we believed that intermediate **2.393** which possesses the opposite stereochemistry at the C7-hydroxyl has the potential to provide the pentacyclic core of **2.1**. These current efforts are being pursued by myself and Mr. Danny Huang; and future synthetic studies will be executed mainly by Mr. Huang.

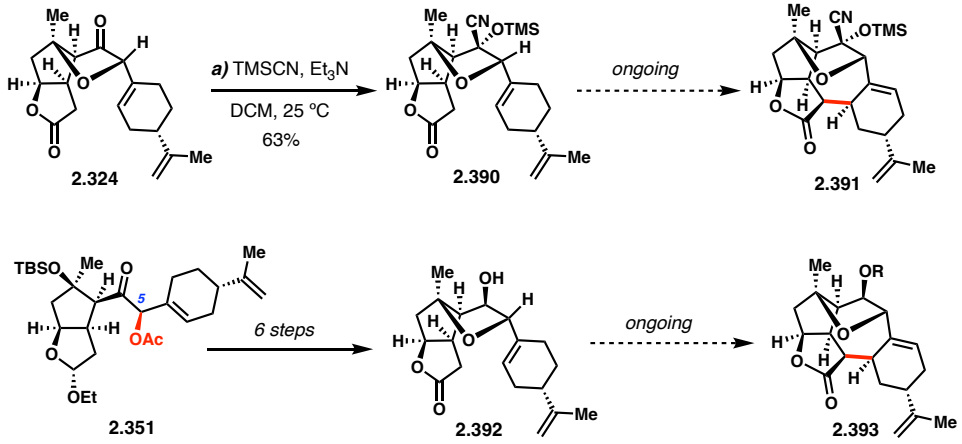


Figure 37. Current Efforts Toward the Pentacyclic Core of **2.1**.

2.6 Conclusion

What began as a post-quarantine project has resulted in, what this author believes is, a winning strategy toward ineleganolide. Although significant work is still required to successfully achieve the total synthesis of ineleganolide, these studies stand as a strong foundation for current and future studies toward this architecturally exquisite natural product.

In summary, we have devised a synthetic strategy which seeks to construct the pentacyclic core of ineleganolide in a disparate manner to the previous attempts by Stoltz and Vanderwal. Our initial efforts, which sought to employ the Oshima-Utimoto reaction to construct the stereochemically dense A/B rings of **2.1**, were met with an unexpected stereochemical issues. Those studies, however, led us to a cross coupling strategy with the hopes of obtaining a tetracyclic intermediate **2.324** which we believed could be elaborated to the pentacyclic core of **2.1**. Ultimately, we found that the application of the Liebeskind-Srogl coupling reaction enabled the rapid assembly of nearly all the carbons and rings of ineleganolide. We then developed a synthetic sequence to construct the tetracyclic core of **2.1** through a series of radical and polar intramolecular cyclizations. We are now currently investigating the construction of the final C–C bond toward **2.1**.

For the sake of brevity, the work described in this chapter is by no means a comprehensive overview of our synthetic campaign towards **2.1** and **2.21**. We are hopeful that the final bond of the pentacyclic core and ultimately the total synthesis of **2.1** can be realized in the near future.

2.7 Distribution of Credit

The synthetic strategies outlined in this chapter were a result of a collaborative process between Professor Thomas Maimone, Mr. Danny Huang, and myself. The conjugate addition of **2.352** and conversion **2.351** to **2.367** and **2.301** were predominantly explored by Danny Huang. The remainder of the experimental work in this chapter was performed by me under the guidance of Professor Maimone. All X-ray crystal structures were obtained by Dr. Nick Settineri and Dr. Jeffery S. Derrick, following my submission of suitable crystalline samples. In the future, efforts to complete the synthesis of ineleganolide will be pursued primarily by Mr. Huang.

2.8 References

1. Yang, B.; Zhou, X. F.; Lin, X. P.; Liu, J.; Peng, Y.; Yang, X. W.; Liu, Y. H., *Curr. Org. Chem.* **2012,** *16,* 1512-1539.
2. Abdel-Lateff, A.; Alarif, W. M.; Alburae, N. A.; Algandaby, M. M., *Molecules* **2019,** *24,* 20.
3. Rodrigues, I. G.; Miguel, M. G.; Mnif, W., *Molecules* **2019,** *24,* 33.
4. Hu, L. C.; Yen, W. H.; Su, J. H.; Chiang, M. Y. N.; Wen, Z. H.; Chen, W. F.; Lu, T. J.; Chang, Y. W.; Chen, Y. H.; Wang, W. H.; Wu, Y. C.; Sung, P. J., *Mar. Drugs* **2013,** *11,* 2154-2167.
5. Nurrachma, M. Y.; Sakaraga, D.; Nugraha, A. Y.; Rahmawati, S. I.; Bayu, A.; Sukmarini, L.; Atikana, A.; Prasetyoputri, A.; Izzati, F.; Warsito, M. F.; Putra, M. Y., *Nat. Product. Bioprospecting* **2021,** *11,* 243-306.
6. Sang, V. T.; Dat, T. T. H.; Vinh, L. B.; Cuong, L. C. V.; Oanh, P. T. T.; Ha, H.; Kim, Y. H.; Anh, H. L. T.; Yang, S. Y., *Mar. Drugs* **2019,** *17,* 46.
7. Baraka, H. N.; Khanfar, M. A.; Williams, J. C.; El-Giar, E. M.; El Sayed, K. A., *Planta Med.* **2011,** *77,* 467-476.
8. Yan, N.; Du, Y. M.; Liu, X. M.; Zhang, H. B.; Liu, Y. H.; Zhang, Z. F., *Biomolecules* **2019,** *9,* 9.
9. Leclercq, S.; de Biseau, J. C.; Braekman, J. C.; Daloze, D.; Quinet, Y.; Luhmer, M.; Sundin, A.; Pasteels, J. M., *Tetrahedron* **2000,** *56,* 2037-2042.
10. Laurent, P.; Daloze, D.; Pasteels, J. M.; Braekman, J. C., *J. Nat. Prod.* **2005,** *68,* 532-536.
11. Wiemer, D. F.; Meinwald, J.; Prestwich, G. D.; Miura, I., *J. Org. Chem.* **1979,** *44,* 3950-3952.
12. Mattern, D. L.; Scott, W. D.; McDaniel, C. A.; Weldon, P. J.; Graves, D. E., *J. Nat. Prod.* **1997,** *60,* 828-831.
13. Lei, H., *Chem. Biodivers.* **2016,** *13,* 345-365.
14. Palframan, M. J.; Pattenden, G., *Eur. J. Org. Chem.* **2020,** *2020,* 2330-2349.
15. Roethle, P. A.; Trauner, D., *Nat. Prod. Rep.* **2008,** *25,* 298-317.
16. Marrero, J.; Rodriguez, A. D.; Baran, P.; Raptis, R. G.; Sanchez, J. A.; Ortega-Barria, E.; Capson, T. L., *Org. Lett.* **2004,** *6,* 1661-1664.
17. Duh, C. Y.; Wang, S. K.; Chia, M. C.; Chiang, M. Y., *Tetrahedron Lett.* **1999,** *40,* 6033-6035.
18. Tseng, Y. J.; Ahmed, A. F.; Dai, C. F.; Chiang, M. Y.; Sheu, J. H., *Org. Lett.* **2005,** *7,* 3813-3816.
19. Marrero, J.; Rodriguez, A. D.; Barnes, C. L., *Org. Lett.* **2005,** *7,* 1877-1880.
20. Ramesh, P.; Reddy, N. S.; Venkateswarlu, Y.; Reddy, M. V. R.; Faulkner, D. J., *Tetrahedron Lett.* **1998,** *39,* 8217-8220.
21. Fenical, W.; Okuda, R. K.; Bandurraga, M. M.; Culver, P.; Jacobs, R. S., *Science* **1981,** *212,* 1512-1514.
22. Rodriguez, A. D.; Shi, J. G.; Huang, S. D., *J. Nat. Prod.* **1999,** *62,* 1228-1237.
23. Kamel, H. N.; Ferreira, D.; Garcia-Fernandez, L. F.; Slattery, M., *J. Nat. Prod.* **2007,** *70,* 1223-1227.
24. Shoji, N.; Umeyama, A.; Arihara, S., *J. Nat. Prod.* **1993,** *56,* 1651-1653.
25. Sheu, J. H.; Ahmed, A. F.; Shiue, R. T.; Dai, C. F.; Kuo, Y. H., *J. Nat. Prod.* **2002,** *65,* 1904-1908.

26. Ahmed, A. F.; Shiue, R. T.; Wang, G. H.; Dai, C. F.; Kuo, Y. H.; Sheu, J. H., *Tetrahedron* **2003,** *59,* 7337-7344.
27. Radhika, P.; Rao, P. V. S.; Anjaneyulu, V.; Asolkar, R. N.; Laatsch, H., *J. Nat. Prod.* **2002,** *65,* 737-739.
28. Lillsunde, K. E.; Festa, C.; Adel, H.; De Marino, S.; Lombardi, V.; Tilvi, S.; Nawrot, D. A.; Zampella, A.; D'Souza, L.; D'Auria, M. V.; Tammela, P., *Mar. Drugs* **2014,** *12,* 4045-4068.
29. Iguchi, K.; Kajiyama, K.; Yamada, Y., *Tetrahedron Lett.* **1995,** *36,* 8807-8808.
30. Kobayashi, M.; Rao, K.; Krishna, M. M.; Anjaneyulu, V., *J. Chem. Res.-S* **1995,** 188-189.
31. Thao, N. P.; Nam, N. H.; Cuong, N. X.; Quang, T. H.; Tung, P. T.; Dat, L. D.; Chae, D.; Kim, S.; Koh, Y. S.; Kiem, P. V.; Minh, C. V.; Kim, Y. H., *Bioorg. Med. Chem. Lett.* **2013,** *23,* 228-231.
32. Yen, W. H.; Su, Y. D.; Chang, Y. C.; Chen, Y. H.; Dai, C. F.; Wen, Z. H.; Su, J. H.; Sung, P. J., *Tetrahedron Lett.* **2013,** *54,* 2267-2270.
33. Meng, Z. C.; Furstner, A., *J. Am. Chem. Soc.* **2022,** *144,* 1528-1533.
34. Stonik, V. A.; Kapustina, II; Kalinovsky, A. I.; Dmitrenok, P. S.; Grebnev, B. B., *Tetrahedron Lett.* **2002,** *43,* 315-317.
35. Williams, D.; Andersen, R. J.; Vanduyne, G. D.; Clardy, J., *J. Org. Chem.* **1987,** *52,* 332-335.
36. Tang, B. C.; Simion, R.; Paton, R. S., *Synlett* **2015,** *26,* 501-507.
37. Rodriguez, A. D.; Shi, Y. P., *J. Org. Chem.* **2000,** *65,* 5839-5842.
38. Li, Y.; Pattenden, G., *Tetrahedron* **2011,** *67,* 10045-10052.
39. Moeller, K. D., *Tetrahedron* **2000,** *56,* 9527-9554.
40. Horn, E. J.; Silverston, J. S.; Vanderwal, C. D., *J. Org. Chem.* **2016,** *81,* 1819-1838.
41. Craig, R. A.; Smith, R. C.; Roizen, J. L.; Jones, A. C.; Virgil, S. C.; Stoltz, B. M., *J. Org. Chem.* **2018,** *83,* 3467-3485.
42. Craig, R. A.; Roizen, J. L.; Smith, R. C.; Jones, A. C.; Virgil, S. C.; Stoltz, B. M., *Chem. Sci.* **2017,** *8,* 507-514.
43. Roizen, J. L.; Jones, A. C.; Smith, R. C.; Virgil, S. C.; Stoltz, B. M., *J. Org. Chem.* **2017,** *82,* 13051-13067.
44. Cusumano, A. Q.; Houk, K. N.; Stoltz, B. M., *Tetrahedron* **2021,** *93,* 6.
45. Jordheim, L. P.; Durantel, D.; Zoulim, F.; Dumontet, C., *Nat. Rev. Drug Discov.* **2013,** *12,* 447-464.
46. Fugami, K.; Oshima, K.; Utimoto, K., *Tetrahedron Lett.* **1987,** *28,* 809-812.
47. Fugami, K.; Oshima, K.; Utimoto, K., *Bull. Chem. Soc. Jpn.* **1989,** *62,* 2050-2054.
48. Evans, M. A.; Morken, J. P., *Org. Lett.* **2005,** *7,* 3367-3370.
49. Mukaiyama, T.; Matsuo, J.; Yanagisawa, M., *Chem. Lett.* **2000,** 1072-1073.
50. Mukaiyama, T.; Matsuo, J.; Kitagawa, H., *Chem. Lett.* **2000,** 1250-1251.
51. Buchecker, R.; Marti, U.; Eugster, C. H., *Helv. Chim. Acta* **1982,** *65,* 896-912.
52. Tohma, H.; Kita, Y., *Adv. Synth. Catal.* **2004,** *346,* 111-124.
53. Magano, J.; Dunetz, J. R., *Chem. Rev.* **2011,** *111,* 2177-2250.
54. Hartung, J.; Drees, S.; Greb, M.; Schmidt, P.; Svoboda, I.; Fuess, H.; Murso, A.; Stalke, D., *Eur. J. Org. Chem.* **2003,** *2003,* 2388-2408.
55. Hartung, J., *Pure Appl. Chem.* **2005,** *77,* 1559-1574.
56. Hartung, J.; Schmidt, P., *Synlett* **2000,** 367-370.
57. Hartung, J.; Greb, M., *J. Organomet. Chem.* **2002,** *661,* 67-84.

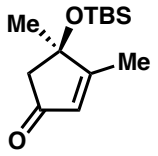
58. Pozhydaiev, V.; Power, M.; Gandon, V.; Moran, J.; Leboeuf, D., *Chem. Commun.* **2020,** *56,* 11548-11564.
59. Trillo, P.; Baeza, A.; Najera, C., *J. Org. Chem.* **2012,** *77,* 7344-7354.
60. An, X. D.; Xiao, J., *Chem. Rec.* **2020,** *20,* 142-161.
61. Colomer, I.; Chamberlain, A. E. R.; Haughey, M. B.; Donohoe, T. J., *Nat. Rev. Chem.* **2017,** *1,* 12.
62. Qi, C. X.; Force, G.; Gandon, V.; Leboeuf, D., *Angew. Chem.-Int. Edit.* **2021,** *60,* 946-953.
63. Llopis, N.; Baeza, A., *Molecules* **2020,** *25,* 12.
64. Wieclaw, M. M.; Stecko, S., *Eur. J. Org. Chem.* **2018,** *2018,* 6601-6623.
65. Dzhemilev, U. M.; Ibragimov, A. G., *Uspekhi Khimii* **2005,** *74,* 886-904.
66. Greenhalgh, M. D.; Jones, A. S.; Thomas, S. P., *ChemCatChem* **2015,** *7,* 190-222.
67. Sato, F.; Urabe, H.; Okamoto, S., *Chem. Rev.* **2000,** *100,* 2835-2886.
68. Langer, F.; Schwink, L.; Devasagayaraj, A.; Chavant, P. Y.; Knochel, P., *J. Org. Chem.* **1996,** *61,* 8229-8243.
69. Lautens, M.; Chiu, P.; Ma, S. H.; Rovis, T., *J. Am. Chem. Soc.* **1995,** *117,* 532-533.
70. Lautens, M.; Rovis, T., *Tetrahedron* **1998,** *54,* 1107-1116.
71. Dzhemilev, U. M.; Ibragimov, A. G., *Uspekhi Khimii* **2000,** *69,* 134-149.
72. Negishi, E.; Yoshida, T., *Tetrahedron Lett.* **1980,** *21,* 1501-1504.
73. Wolleb, H.; Carreira, E. M., *Angew. Chem.-Int. Edit.* **2017,** *56,* 10890-10893.
74. Alonso, E.; Ramon, D. J.; Yus, M., *Tetrahedron* **1996,** *52,* 14341-14348.
75. Schuppe, A. W.; Huang, D.; Chen, Y. F.; Newhouse, T. R., *J. Am. Chem. Soc.* **2018,** *140,* 2062-2066.
76. Salom-Roig, X. J.; Denes, F.; Renaud, P., *Synthesis* **2004,** 1903-1928.
77. Stork, G.; Sher, P. M.; Chen, H. L., *J. Am. Chem. Soc.* **1986,** *108,* 6384-6385.
78. Tedder, J. M.; Walton, J. C., *Tetrahedron* **1980,** *36,* 701-707.
79. Wittenberg, R.; Srogl, J.; Egi, M.; Liebeskind, L. S., *Org. Lett.* **2003,** *5,* 3033-3035.
80. Cheng, H. G.; Chen, H.; Liu, Y.; Zhou, Q. H., *Asian J. Org. Chem.* **2018,** *7,* 490-508.
81. Li, H.; Yang, H.; Liebeskind, L. S., *Org. Lett.* **2008,** *10,* 4375-4378.
82. Yang, H.; Li, H.; Wittenberg, R.; Egi, M.; Huang, W. W.; Liebeskind, L. S., *J. Am. Chem. Soc.* **2007,** *129,* 1132-1140.
83. Osakada, K.; Yamamoto, T.; Yamamoto, A., *Tetrahedron Lett.* **1987,** *28,* 6321-6324.
84. Cao, H.; Liu, X. J.; Bie, F. S.; Shi, Y. J.; Han, Y.; Yan, P.; Szostak, M.; Liu, C. W., *Org. Chem. Front.* **2021,** *8,* 1587-1592.
85. Thottumkara, A. P.; Kurokawa, T.; Du Bois, J., *Chem. Sci.* **2013,** *4,* 2686-2689.
86. Nicolaou, K. C.; Estrada, A. A.; Zak, M.; Lee, S. H.; Safina, B. S., *Angew. Chem.-Int. Edit.* **2005,** *44,* 1378-1382.
87. O'Donnell, C. J.; Burke, S. D., *J. Org. Chem.* **1998,** *63,* 8614-8616.
88. Rollin, P.; Soares, L. K.; Barcellos, A. M.; Araujo, D. R.; Lenardao, E. J.; Jacob, R. G.; Perin, G., *Appl. Sci.-Basel* **2021,** *11,* 56.
89. Olsson, J. V.; Hult, D.; Cai, Y. L.; Garcia-Gallego, S.; Malkoch, M., *Polym. Chem.* **2014,** *5,* 6651-6655.
90. Hardacre, C.; Messina, I.; Migaud, M. E.; Ness, K. A.; Norman, S. E., *Tetrahedron* **2009,** *65,* 6341-6347.
91. Krause, N.; Ebert, S.; Haubrich, A., *Liebigs Ann.-Recl.* **1997,** 2409-2418.
92. Krause, N., *Angew. Chem.-Int. Edit. Engl.* **1994,** *33,* 1764-1765.
93. Gensler, W. J.; Gatsonis, C. D., *J. Am. Chem. Soc.* **1962,** *84,* 1748-&.

94. Carson, M. W.; Kim, G.; Hentemann, M. F.; Trauner, D.; Danishefsky, S. J., *Angew. Chem.-Int. Edit.* **2001,** *40,* 4450-+.
95. Bian, J. W.; Van Wingerden, M.; Ready, J. M., *J. Am. Chem. Soc.* **2006,** *128,* 7428-7429.
96. Liu, G.; Romo, D., *Angew. Chem.-Int. Edit.* **2011,** *50,* 7537-7540.
97. Hughes, C. C.; Miller, A. K.; Trauner, D., *Org. Lett.* **2005,** *7,* 3425-3428.
98. Liu, B.; Moeller, K. D., *Tetrahedron Lett.* **2001,** *42,* 7163-7165.
99. Reddy, S. H. K.; Chiba, K.; Sun, Y. M.; Moeller, K. D., *Tetrahedron* **2001,** *57,* 5183-5197.
100. Moeller, K. D. In *Intramolecular anodic olefin coupling reactions*, Symposium on Fundamentals and Potential Applications of Electrochemical Synthesis, Montreal, Canada, May 04-09; Electrochemical Society Inc: Montreal, Canada, 1997; pp 13-24.
101. Tesfai, Z.; Moeller, K. D., *Denki Kagaku* **1994,** *62,* 1115-1118.
102. Frey, D. A.; Marx, J. A.; Moeller, K. D., *Electrochim. Acta* **1997,** *42,* 1967-1970.
103. Comito, R. J.; Finelli, F. G.; MacMillan, D. W. C., *J. Am. Chem. Soc.* **2013,** *135,* 9358-9361.
104. Mastracchio, A.; Warkentin, A. A.; Walji, A. M.; MacMillan, D. W. C., *Proc. Natl. Acad. Sci. U. S. A.* **2010,** *107,* 20648-20651.
105. Capacci, A. G.; Malinowski, J. T.; McAlpine, N. J.; Kuhne, J.; MacMillan, D. W. C., *Nat. Chem.* **2017,** *9,* 1073-1077.
106. Conrad, J. C.; Kong, J.; Laforteza, B. N.; MacMillan, D. W. C., *J. Am. Chem. Soc.* **2009,** *131,* 11640-+.
107. Beeson, T. D.; Mastracchio, A.; Hong, J. B.; Ashton, K.; MacMillan, D. W. C., *Science* **2007,** *316,* 582-585.
108. Moriarty, R. M.; Vaid, R. K., *Synthesis* **1990,** 431-447.
109. Moriarty, R. M.; Prakash, O., *Accounts Chem. Res.* **1986,** *19,* 244-250.
110. Moriarty, R. M., *J. Org. Chem.* **2005,** *70,* 2893-2903.
111. Weng, W. Z.; Liang, H.; Liu, R. Z.; Ji, Y. X.; Zhang, B., *Org. Lett.* **2019,** *21,* 5586-5590.
112. Quast, H.; Dietz, T.; Witzel, A., *Liebigs Ann.-Recl.* **1995,** 1495-1501.

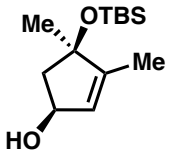
2.9 Experimental Procedures and Characterization Data

General Procedures:

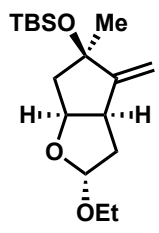
All reactions were performed in flame- or oven-dried glassware under a positive pressure of nitrogen or argon, unless otherwise noted. Air-and moisture-sensitive liquids were transferred via syringe. When indicated, solvents or reagents were degassed by sparging with argon for 10 minutes in an ultrasound bath at 25 °C. Volatile solvents were removed under reduced pressure rotary evaporation below 35 °C. Analytical and preparative thin-layer chromatography (TLC) were performed using glass plates pre-coated with silica gel (0.25-mm, 60-Å pore size, Merck TLC Silicagel 60 F254) impregnated with a fluorescent indicator (254 nm). TLC plates were visualized by exposure to ultraviolet light (UV) and then were stained by submersion in an ethanolic anisaldehyde solution or ceric ammonium molybdate solution, followed by brief heating on a hot plate. Flash column chromatography was performed with silica gel purchased from Silicycle (SiliaFlash ® , 60 Å, 230-400 mesh, 40-63 μm). Ethyl vinyl ether and *tert*-Butyl vinyl ether, diisopropylamine, hexamethylphosphoramide (HMPA), thionyl chloride ($SOCl_2$), methanesulfonyl chloride (MsCl), and acetyl chloride were distilled over calcium hydride prior to use. KHMDS solutions were purchased from Sigma. Tributyl tin hydride was distilled over hydroquinone. All other reagents were used as received from commercial sources, unless stated otherwise. Anhydrous tetrahydrofuran (THF), dichloromethane (DCM), methanol (MeOH), dimethylformamide (DMF), and toluene (PhMe) were obtained by passing these previously degassed solvents through activated alumina columns. Proton nuclear magnetic resonance (^{1}H NMR) spectra and carbon nuclear magnetic resonance (^{13}C NMR) spectra were recorded on Bruker AV-600 spectrometer at 23 °C. Proton chemical shifts are expressed as parts per million (ppm, δ scale) and are referenced to residual solvent ($CDCl_3$: δ 7.26, C_6D_6 : δ 7.16), unless stated otherwise. Carbon chemical shifts are expressed as parts per million (ppm, δ scale) and are referenced to the solvent ($CDCl_3$: δ 77.16, C_6D_6 : δ 128.06), unless stated otherwise. Data is represented as follows: chemical shift, multiplicity (s = singlet, d = doublet, dd = doublet of doublets, ddd, doublet of doublet of doublet, dt = triplet of doublets, t = triplet, q = quartet, m = multiplet, br = broad), coupling constant (J) in Hertz (Hz), and integration. Infrared (IR) spectra were recorded on a Bruker Alpha FT- IR spectrometer as thin films and are reported in frequency of absorption (cm^{-1}). Only selected resonances are reported. High-resolution mass spectra (HRMS) were obtained by the mass spectrometry facility at the University of California, Berkeley using a Finnigan LTQFT mass spectrometer (Thermo Electron Corporation). X-ray diffraction data was collected at the Small Molecule X-ray Crystallography Facility (CheXray) at University of California, Berkeley using a Rigaku XtaLAB P200 equipped with a MicroMax 007HF rotating anode and Pilatus3 R 200K-A hybrid pixel array detector. Data were collected using CuKα radiation (λ = 1.5418 Å).



2.303: To a stirring suspension of CuI (463 mg, 2.43 mmol, 1.1 equiv) in THF was added MeLi (1.6 M in Et_2O, 3.0 mL, 4.86 mmol, 2.2 equiv) at –78 ºC. The resulting suspension was stirred at –78 ºC for 15 minutes then placed in a 0 ºC ice bath until a clear solution was formed and stirred for an additional 15 minutes then cooled to –78 C. A solution of enone **2.300** (azeotropically dried, three times with benzene) (500 mg, 2.21 mmol, 1.0 equiv) in THF (2 mL) was then added dropwise to the suspension containing the Gilman cuprate. The resulting orange suspension was warmed to 0 ºC over the course of 1 hour or until consumption of the starting enone **2.300**, as indicated by TLC, the reaction mixture was then cooled to –78 ºC, followed by dropwise addition of a solution of Mukaiyama's reagent (**2.302**) (713 mg, 3.32 mmol, 1.5 equiv) in THF (2 mL). The resulting brown suspension was stirred for 1 hour, slowly warming to 0 °C. Upon completion of the reaction as indicated by TLC, the reaction was quenched with saturated aqueous $NaHCO_3$ (3 mL). The organic layer was then separated and the aqueous phase was extracted with Et_2O (3 x 6 mL), the combined organic extracts were then washed with brine (3 mL), dried over Na_2SO_4 and concentrated under reduced pressure. The resulting slurry was filtered over a pad of celite and washed with Et_2O, (3 x 5 mL) and reconcentrated. The crude oil was then purified by column chromatography (2% Et_2O in hexanes → 15% Et_2O) to provide 255 mg (1.06 mmol, 48%) of **2.303** as a yellow oil. ^{1}H NMR (700 MHz, C_6D_6) δ 5.24 (p, J = 1.6 Hz, 1H), 4.33 (s, 1H), 2.25 (dd, J = 12.7, 6.8 Hz, 1H), 1.89 (dd, J = 12.7, 5.4 Hz, 1H), 1.63 (t, J = 1.7 Hz, 3H), 1.08 (d, J = 0.8 Hz, 3H), 0.97 (s, 10H), 0.11 (d, J = 4.8 Hz, 6H). ^{13}C NMR (126 MHz, C_6D_6) δ 148.97, 82.78, 73.05, 52.03, 27.44, 25.69, 17.95, 11.18, -2.62 (d, J = 53.2 Hz). HRMS (ESI) calcd for $C_{13}H_{24}NaO_2Si$ [M + Na^+] m/z 263.1443, found 263.1439.



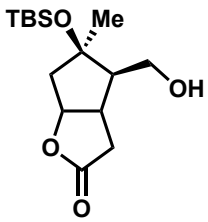
2.304: To a stirring solution of **2.303** (450 mg, 1.87 mmol, 1.0 equiv) in PhMe (9.4 mL) was added dropwise DIBAL (1M in PhMe, 2.43 mL, 2.43 mmol, 1.3 equiv) at –78 ºC. The resulting suspension was stirred at –78 ºC for 1 hour then warmed gradually to 0 ºC over the course of 1 hour. Upon completion of the reaction as indicated by TLC, the reaction was quenched with saturated aqueous $NaHCO_3$ (5 mL) and then saturated aqueous solution of Rochelle's salt (5 mL) and stirred for 3 hours. The organic phases were separated and the aqueous phase was extracted with Et_2O (3 x 6 mL). The combined organic extracts were then washed with brine (3 mL), dried over Na_2SO_4 and concentrated under reduced pressure. The resulting crude oil was then purified by column chromatography (5% Et_2O in hexanes → 40% Et_2O) to provide 390.7 mg (1.62 mmol, 87%) of **2.304** as a clear colorless oil. ^{1}H NMR (600 MHz, $CDCl_3$) δ 4.56 (d, J = 6.6 Hz, 1H), 2.47 (dd, J = 13.0, 6.7 Hz, 1H), 1.87 (dd, J = 13.0, 5.0 Hz, 1H), 1.73 (t, J = 1.6 Hz, 3H), 1.58 (s, 3H), 1.52 – 1.43 (m, 1H), 0.89 (s, 9H), 0.13 (d, J = 5.3 Hz, 6H). ^{13}C NMR (151 MHz, $CDCl_3$) δ 150.70, 127.15, 83.03, 73.90, 52.19, 27.66, 25.91, 18.16, 11.60, -2.25 (d, J = 48.3 Hz). HRMS (EI+) calcd for $C_{13}H_{26}O_2Si$ *m/z* 242.1702, found 242.1694.



2.308: *Step 1*. A solution of $Pd(OAc)_2$ (3.46 g, 15.44 mmol, 1.1 equiv) in PhMe (150 mL) was stirred vigorously at 65 ºC. In a separate flask containing **2.304** (3.4 g, 14.03 mmol, 1.0 equiv), was added *tert*-Butyl vinyl ether (9.22 mL, 77.21mmol, 5.0 equiv). The solution containing **2.304** was then added to the solution containing $Pd(OAc)_2$ in one shot washing with small amounts of PhMe (3 x 1 mL) to ensure quantitative transfer. The reaction mixture was stirred for 5 minutes at 65 ºC and then removed from the heat and cooled to room-temperature. The resulting crude

reaction mixture was filtered over a plug of celite and washed with Et_2O. This mixture was then successively washed with saturated aqueous $NaHCO_3$ (15 mL), brine (10 mL), dried over Na_2SO_4, and concentrated under reduced pressure. The resulting crude mixture was then advanced to the next step without any further purification. **2.305:** ^{1}H NMR (600 MHz, $CDCl_3$) δ 5.50 (d, *J* = 4.8 Hz, 1H), 5.44 (dd, *J* = 5.7, 3.1 Hz, 1H), 5.14 (dd, *J* = 12.8, 2.7 Hz, 2H), 4.82 – 4.76 (m, 2H), 4.60 (q, *J* = 7.1 Hz, 1H), 4.50 (q, *J* = 7.8 Hz, 1H), 3.33 (q, *J* = 8.4 Hz, 1H), 3.17 – 3.10 (m, 1H), 2.36 (ddd, *J* = 12.8, 10.9, 5.7 Hz, 1H), 2.25 – 2.14 (m, 4H), 1.91 (ddt, *J* = 16.8, 8.4, 4.5 Hz, 2H), 1.85 – 1.71 (m, 2H), 1.26 (d, *J* = 0.8 Hz, 9H), 1.23 (d, *J* = 0.9 Hz, 9H), 0.92 (d, *J* = 0.8 Hz, 9H), 0.91 (d, *J* = 0.8 Hz, 9H), 0.14 – 0.08 (m, 12H).

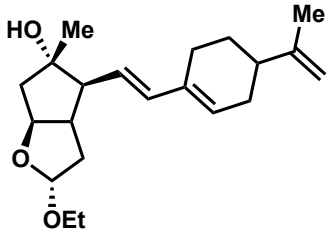
Step 2. CSA (325 mg, 1.403 mmol, 0.1 equiv) was added to a stirring solution of **2.305** in anhydrous EtOH (14 mL). The resulting reaction mixture was then stirred at 60 ºC for 10 hours. Upon completion of the reaction as indicated by TLC, the reaction was quenched with saturated aqueous $NaHCO_3$ (3 mL). The aqueous phase was extracted with Et_2O (3 x **X** mL) and the combined organic extracts were then washed with brine (5 mL), dried over Na_2SO_4 and concentrated under reduced pressure. The crude oil was then purified by column chromatography (4% Et_2O in hexanes → 10% Et_2O) to provide 2.19 g (7.02 mmol, 50%) of **2.308** as a yellow oil. ^{1}H NMR (600 MHz, $CDCl_3$) δ 5.18 (dd, *J* = 5.5, 1.4 Hz, 1H), 5.14 (dd, *J* = 3.0, 0.9 Hz, 1H), 4.80 (d, *J* = 2.5 Hz, 1H), 4.59 (q, *J* = 7.7 Hz, 1H), 3.69 (dq, *J* = 9.8, 7.1 Hz, 1H), 3.39 (dq, *J* = 9.7, 7.0 Hz, 1H), 3.15 (tt, *J* = 8.6, 2.8 Hz, 1H), 2.34 – 2.27 (m, 1H), 2.22 (dd, *J* = 11.8, 7.4 Hz, 1H), 2.07 – 1.98 (m, 2H), 1.22 (d, *J* = 1.0 Hz, 3H), 1.14 (t, *J* = 7.1 Hz, 3H), 0.89 (s, 8H), 0.09 (d, *J* = 12.3 Hz, 6H). ^{13}C NMR (151 MHz, $CDCl_3$) δ 160.08, 106.25, 104.52, 81.39, 62.78, 47.89, 42.76, 39.09, 30.68, 25.95, 18.22, 15.13, -2.13, -2.37. HRMS (ESI) calcd for $C_{17}H_{32}NaO_3Si$ [M + Na^+] *m/z* 335.2018, found 335.2014.



2.313: *Step 1*. To a stirring solution of **2.308** (100 mg, 0.320 mmol, 1.0 equiv) in MeCN (2 mL) and H_2O (2 mL) was added PPTS (24.1 mg, 0.096 mmol, 0.3 equiv). The resulting reaction mixture was then stirred at 60 ºC for 10 hours. Upon completion of the reaction as indicated by TLC, the reaction was quenched with saturated aqueous $NaHCO_3$ (3 mL). The organic layer was then separated and the aqueous phase was extracted with Et_2O (3 x 4 mL) and the combined organic extracts were washed with brine (6 mL), dried over Na_2SO_4 and concentrated under reduced pressure. The crude material filtered through a plug of silica (eluting witg Et_2O) and concentrated This material (**Lactol SI-1**) was carried on to the next step without any further purification.

Step 2. To a reaction tube containing the **Lactol SI-1** prepared in the previous step, was added successively added TEMPO (20.0 mg, 0.0128 mmol, 0.4 equiv), $PhI(OAc)_2$ (164.9 mg, 0.512 mmol, 1.6 equiv) and DCM (4 mL). The solution was stirred for 3 hours at 25 ºC until completion of the reaction, as judged by TLC. The reaction was quenched with saturated aqueous solutions of $NaHCO_3$ (2 mL) and $Na_2S_2O_3$ (2 mL). The organic layer was then separated and the aqueous phase was extracted with DCM (3 x 4 mL) and the combined organic extracts were washed with brine (5 mL), dried over Na_2SO_4 and concentrated under reduced pressure. The crude oil was then purified by column chromatography (1% Et_2O in DCM → 6% Et_2O in DCM) to provide 69.4 mg (0.246 mmol, 77%) of **Lactone SI-2** as a clear colorless oil. **Lactone SI-2:** ^{1}H NMR (700 MHz, $CDCl_3$) δ 5.22 (d, *J* = 2.3 Hz, 1H), 5.00 – 4.92 (m, 2H), 3.43 (ddt, *J* = 10.7, 8.2, 2.8 Hz, 1H), 2.92 (dd, *J* = 18.3, 11.1 Hz, 1H), 2.60 (dd, *J* = 18.3, 3.7 Hz, 1H), 2.24 – 2.07 (m, 2H), 1.37 (s, 3H), 0.87 (d, *J* = 0.8 Hz, 9H), 0.10 (d, *J* = 9.7 Hz, 6H).

Step 3. To a stirring solution of lactone **Lactone SI-2** (69.4 mg, 0.246 mmol, 1.0 equiv) in THF (2.5 mL) at 25 ºC was added a BH_3•THF (1M in THF, 1.23 mL, 1.23 mmol, 5 equiv). Upon completion of the reaction as indicated by TLC, the reaction mixture was cooled to –78 ºC and solid $NaBO_3$•$4H_2O$ (0.185 mg, 1.84 mmol, 7.5 equiv) is added. The suspension was removed from the dry-ice bath and H_2O (2 mL) was added dropwise and stirred gradually warming to room temperature. The crude reaction mixture was then filtered over cotton to remove excess oxidant, then quenched with saturated aqueous $NaHCO_3$ (3 mL). The organic layer was then separated and the aqueous phase was extracted with Et_2O (3 x 4 mL), washed with brine (8 mL), dried over Na_2SO_4 and concentrated under reduced pressure. The crude oil was then purified by column chromatography (1% Et_2O in DCM → 15% Et_2O in DCM) to provide 39.6 mg (0.132 mmol, 54%) of **2.313** as a white solid. ^{1}H NMR (700 MHz, $CDCl_3$) δ 5.04 (t, *J* = 7.7 Hz, 1H), 3.98 (dd, *J* = 10.8, 5.3 Hz, 1H), 3.86 (dd, *J* = 10.8, 8.4 Hz, 1H), 3.25 – 3.17 (m, 1H), 2.87 (dd, *J* = 18.6, 5.5 Hz, 1H), 2.56 (dd, *J* = 18.6, 11.7 Hz, 1H), 1.96 (td, *J* = 8.6, 5.2 Hz, 1H), 1.91 (dd, *J* = 15.3, 7.3 Hz, 1H), 1.41 (s, 3H), 0.86 (s, 10H), 0.12 (d, *J* = 2.9 Hz, 6H).



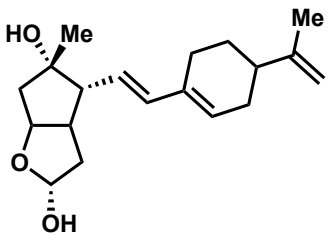
2.318a: *Step 1*. To a stirring solution of bicycle **2.308** (250 mg, 0.800 mmol, 1.0 equiv) in THF (4 mL) at 25 ºC was added a BH_3•THF (1M in THF, 4 mL, 4 mmol, 5 equiv). Upon completion of the reaction as indicated by TLC, the reaction mixture was cooled to –78 ºC and solid $NaBO_3$•$4H_2O$ is added. The suspension was removed from the dry-ice bath and H_2O (4 mL) was added dropwise and stirred gradually warming to room temperature. The crude reaction mixture was then filtered over cotton to remove excess oxidant, then quenched with saturated aqueous $NaHCO_3$ (3 mL). The organic layer was separated and the aqueous phase was extracted with Et_2O (3 x 5 mL), washed with brine (15 mL), dried over Na_2SO_4 and concentrated under reduced pressure. The crude oil was then quickly purified by column chromatography (10% Et_2O in hexanes → 50% Et_2O) to remove boric acid impurities. Following concentration under reduced pressure to provide 214 mg (0.648 mmol, 81%) of primary alcohol **2.315**.

Step 2. To a stirring solution of **2.315** (214 mg, 0.648 mmol, 1.0 equiv) in THF (1.6 mL) was added TBAF (1M in THF, 0.78 mL, 0.777 mmol, 1.2 equiv). The resulting reaction mixture was then stirred at 60 ºC for 1 hours. Upon completion of the reaction as indicated by TLC, the reaction was quenched with saturated aqueous $NaHCO_3$ (3 mL) and extracted with Et_2O (3 x 3 mL), washed with brine (10 mL), dried over Na_2SO_4 and concentrated under reduced pressure. The crude material was purified by column chromatography (10% Et_2O in hexanes → 100% Et_2O) to yield 102 mg (0.473 mmol, 73%) of **2.316**.

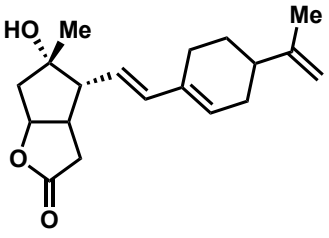
Step 3. To a reaction tube containing the **2.316** (102 mg, 0.473 mmol, 1.0 equiv), prepared in the previous step, was added successively added TEMPO (29.5 mg, 0.189 mmol, 0.4 equiv), $PhI(OAc)_2$ (213.2 mg, 0.662 mmol, 1.4 equiv) and DCM (1 mL). The solution was stirred for 3 hours at 25 ºC or until completion of the reaction, as judged by TLC. The reaction was quenched with saturated aqueous solutions of $NaHCO_3$ (1 mL) and $Na_2S_2O_3$ (1 mL). This mixture was then extracted with DCM (3 x 1 mL), washed with brine (3 mL), dried over Na_2SO_4 and concentrated under reduced pressure to give *ca.* 140 mg of a crude orange oil. Given the general lability of this intermediate, it was subjected to the olefination reaction immediately after concentration.

Step 4. To a solution containing phosphonium salt **2.311** (676 mg, 1.42 mmol, 3.0 equiv) in THF (3 mL) at 0 ºC was added *n*-BuLi (2.5 M in THF, 0.53 mL, 1.32 mmol, 2.8 equiv). The

resulting deep red solution containing the ylide of **2.311** was then added dropwise to a solution of crude aldehyde obtained in the previous step in THF (1 mL) at 40 ºC. Upon completion of the reaction as indicated by TLC (typically 5 minutes), the reaction was quenched with saturated aqueous $NaHCO_3$ (3 mL). The organic layer was then separated and the aqueous phase was and extracted with Et_2O (3 x 3 mL), washed with brine (10 mL), dried over Na_2SO_4 and concentrated under reduced pressure. The crude material was purified by column chromatography (10% Et_2O in hexanes → 100% Et_2O) to yield 100 mg (0.302 mmol, 64%) of **2.318a** over two steps. **2.318a:** ^{1}H NMR (600 MHz, $CDCl_3$) δ 6.16 (d, *J* = 15.8 Hz, 1H), 5.75 (d, *J* = 4.6 Hz, 1H), 5.49 (dd, *J* = 15.8, 8.0 Hz, 1H), 5.23 (d, *J* = 5.3 Hz, 1H), 4.76 – 4.71 (m, 2H), 4.67 (td, *J* = 7.1, 4.1 Hz, 1H), 3.72 (dtd, *J* = 10.1, 7.6, 6.6 Hz, 1H), 3.42 (dtd, *J* = 10.1, 7.6, 6.6 Hz, 1H), 2.87 (q, *J* = 10.7 Hz, 1H), 2.37 – 2.22 (m, 3H), 2.19 (d, *J* = 11.8 Hz, 1H), 2.12 – 2.01 (m, 3H), 1.96 – 1.87 (m, 1H), 1.80 (ddd, *J* = 14.8, 10.4, 4.7 Hz, 2H), 1.75 (s, 3H), 1.27 – 1.24 (s, 3H). ^{13}C NMR (151 MHz, $CDCl_3$) δ 149.7, 136.7, 135.1, 128.6, 122.3, 108.7, 106.0, 83.7, 81.7, 62.5, 59.7, 46.9, 46.5, 41.2, 38.0, 31.3, 27.4, 26.5, 25.1, 20.8, 15.2. HRMS (ESI) calcd for $C_{21}H_{32}NaO_3$ [M + Na^+] *m/z* 355.2249, found 355.2247.

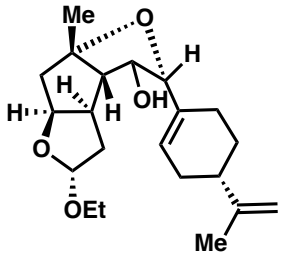


SI-3: To a stirring solution of **2.318a** (30 mg, 0.090 mmol, 1.0 equiv) in MeCN (1 mL) and H_2O (1 mL) was added PPTS (6.8 mg, 0.027 mmol, 0.3 equiv). The resulting reaction mixture was then stirred at 60 ºC for 10 hours. Upon completion of the reaction as indicated by TLC, the reaction was quenched with saturated aqueous $NaHCO_3$ (0.5 mL). The organic layer was then separated and the aqueous phase was extracted with Et_2O (3 x 2 mL) and the combined organic extracts were washed with brine (**X** mL), dried over Na_2SO_4 and concentrated under reduced pressure. The crude material was purified by column chromatography (10% Et_2O in hexanes → 100% Et_2O) to yield 26.5 mg (0.0873 mmol, 97%) of a mixture of lactol isomers (**SI-3). Lactol SI-3:** ^{1}H NMR (600 MHz, $CDCl_3$) δ 6.2 (dd, *J* = 37.4, 15.8 Hz, 1H), 5.8 (s, 1H), 5.7 – 5.6 (m, 1H), 5.5 (dt, *J* = 15.5, 7.5 Hz, 1H), 4.9 – 4.8 (m, 1H), 4.8 – 4.7 (m, 2H), 3.0 – 2.9 (m, 1H), 2.8 (q, *J* = 9.2 Hz, 0H), 2.8 – 2.7 (m, 0H), 2.4 – 2.3 (m, 2H), 2.3 – 2.2 (m, 1H), 2.2 (s, 1H), 2.2 – 2.0 (m, 3H), 2.0 – 1.9 (m, 2H), 1.8 (s, 3H), 1.5 (dd, *J* = 12.3, 5.4 Hz, 1H), 1.3 (s, 5H).^{13}C NMR (151 MHz, $CDCl_3$) δ 149.8, 149.7, 136.8, 136.6, 135.2, 135.1, 123.1, 122.2, 108.8, 108.7, 84.8, 83.6, 83.2, 82.2, 59.6, 58.6, 49.8, 47.0, 46.9, 46.6, 41.3, 41.2, 38.8, 37.6, 31.3, 27.4, 27.4, 26.5, 26.2, 25.1, 20.8. HRMS (ESI) calcd for $C_{19}H_{28}NaO_3$ [M + Na^+] *m/z* 327.1936, found 327.1928.

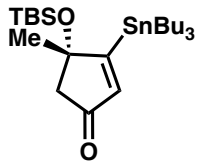


2.319a: To a reaction tube containing the lactol **SI-3** (400 mg, 1.31 mmol, 1.0 equiv) prepared in the previous step, was added successively added TEMPO (102.2 mg, 0..655 mmol, 0.5 equiv), $PhI(OAc)_2$ (632.7 mg, 1.96 mmol, 1.5 equiv) and DCM (13 mL). The solution was stirred for 3 hours at 25 ºC until completion of the reaction, as judged by TLC. The reaction was quenched with saturated aqueous solutions of $NaHCO_3$ (2 mL) and $Na_2S_2O_3$ (2 mL). The organic layer was then separated and the aqueous phase was extracted with DCM (3 x 4 mL). The combined organic layers were washed with brine (10 mL), dried over Na_2SO_4 and concentrated under reduced pressure. The crude oil was then purified by column chromatography (1% Et_2O in DCM → 20% Et_2O in DCM) to provide 325 mg (1.07 mmol, 82%) of **2.319a** as a clear colorless oil. **2.319a:** ^{1}H NMR (600 MHz, $CDCl_3$) δ 6.18 (d, *J* = 15.8 Hz, 1H), 5.79 (t, *J* =

3.8 Hz, 1H), 5.45 (dd, *J* = 15.8, 8.3 Hz, 1H), 5.03 (td, *J* = 7.3, 4.1 Hz, 1H), 4.79 – 4.67 (m, 2H), 3.05 – 2.91 (m, 1H), 2.73 (ddd, *J* = 18.3, 9.2, 1.6 Hz, 1H), 2.45 (ddd, *J* = 15.1, 7.5, 1.6 Hz, 1H), 2.34 (dd, *J* = 18.3, 1.8 Hz, 2H), 2.27 (dd, *J* = 24.8, 7.8 Hz, 1H), 2.23 – 2.03 (m, 5H), 2.01 – 1.87 (m, 2H), 1.75 (s, 3H), 1.55 – 1.46 (m, 1H), 1.29 (d, *J* = 1.6 Hz, 3H). ^{13}C NMR (151 MHz, $CDCl_3$) δ 177.1, 149.5, 138.0, 134.8, 129.6, 120.3, 108.9, 83.7, 81.6, 58.5, 47.4, 43.3, 41.1, 33.6, 31.3, 27.3, 26.0, 25.1, 20.8. HRMS (ESI) calcd for $C_{19}H_{28}NaO_3$ [M + Na^+] *m/z* 325.1780, found 325.1776

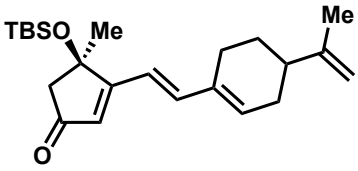


2.320c: To a stirring solution of Diene **2.319a** (20 mg, 0.066 mmol, 1.0 equiv) in DCM (2.7 mL) at 0 ºC was added Ti(O*i*-Pr)$_4$ (0.022 mL, 00.0727 mmol, 1.1 equiv) and stirred for 1 minute. Cumene hydroperoxide (0.0148 mL, 0.099 mmol, 1.5 equiv) was then added and stirred at 0 ºC until completion of the reaction as indicated by TLC. The reaction was then quenched with an aqueous solution of citric acid (5% w/w) and stirred for 10 minutes. The organic layer was then separated and the aqueous phase was extracted with Et_2O (3 x 2 mL). The combined organic layers were washed with brine (6 mL), dried over Na_2SO_4 and concentrated under reduced pressure to provide a mixture of an intermediate epoxide and ether **2.320c**. The crude mixture was then stirred in HFIP (3 mL) for 3 hours at 25 ºC. The solvent was directly removed under reduced pressure. The crude material was purified by column chromatography (5% EtOAc in DCM → 30% EtOAc in DCM) to yield 14.2 mg (0.041 mmol, 62%) of **2.320c**. **2.320c:** ^{1}H NMR (700 MHz, $CDCl_3$) δ 5.84 – 5.78 (m, 1H), 5.04 (td, *J* = 6.4, 3.4 Hz, 1H), 4.72 (dp, *J* = 24.2, 1.3 Hz, 2H), 4.17 (d, *J* = 6.1 Hz, 1H), 3.95 (dd, *J* = 6.1, 4.1 Hz, 1H), 2.89 – 2.81 (m, 2H), 2.50 – 2.41 (m, 2H), 2.23 – 2.11 (m, 5H), 1.98 (t, *J* = 15.0 Hz, 3H), 1.89 – 1.85 (m, 2H), 1.73 (t, *J* = 1.1 Hz, 3H), 1.50 (s, 3H). ^{13}C NMR (151 MHz, $CDCl_3$) δ 176.4, 149.4, 134.5, 124.1, 108.8, 91.1, 89.7, 86.2, 81.4, 64.0, 46.2, 44.4, 40.9, 35.9, 30.3, 27.2, 25.4, 24.4, 20.8. HRMS (ESI) calcd for $C_{21}H_{32}NaO_4$ [M + Na^+] *m/z* 371.2198, found 371.2191.

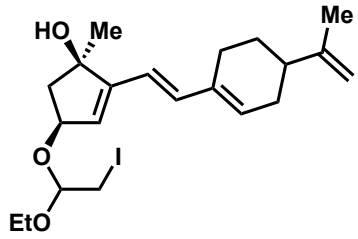


2.329: To a 250 mL round bottom flask was added diisopropylamine (4.0 mL, 28.3 mmol, 1.3 equiv) and THF (20 mL). The stirring solution was then cooled to 0 ºC for 10 minutes and then *n*-BuLi (2.5 M in hexanes, 10.6 mL, 26.5 mmol, 1.2 equiv) was added dropwise to the reaction. After stirring for 15 minutes at 0 ºC, Bu_3SnH (7.5 mL, 27.8 mmol 1.25 equiv) was added to the mixture and the reaction mixture was stirred at 0 ºC for an additional 30 minutes, resulting in a pale yellow solution. To the reaction mixture was added a HMPA (4 mL, 23.0 mmol, 1.05 equiv) at 0 ºC, resulting in a bright yellow solution. The solution was then added cooled to –78 ºC and stirred for 5 minutes resulting in a pale yellow solution. A solution of enone **2.300** (azeotropically dried, three times with benzene) (5 g, 22.1 mmol, 1.0 equiv) in THF (5 mL) was then added dropwise to the solution containing the stannyl-lithiate at –78 ºC, resulting in a dark yellow solution. The reaction mixture was stirred at –78 ºC for one hour and slowly warmed to –40 ºC over the course of 1 hour. Upon full consumption of the starting **2.300**, as judged by TLC, the acetone-dry ice cooling bath was replaced with a water-ice (0 ºC) bath. Rapidly, the septum of the reaction flask was removed and solid (anhydrous) $ZnCl_2$ (5.5 g, 40.3 mmol, 1.82 equiv) was added and the flask was quickly resealed. The reaction flask was then removed from the ice bath and warmed to room temperature and stirred for 5 minutes, before a solution of [Pd(allyl)Cl]$_2$

(200 mg, 0.55 mmol, 2.5 mol %) and diethyl allyl phosphate (4 mL, 22.4 mmol, 1.01 equiv) in THF (5 mL) was added. The resulting in a light red-orange solution. was then heated to 60 ºC for 1 hour. Upon completion of the reaction as indicated by TLC, the reaction vessel was removed from the heating apparatus and immediately quenched (while hot) with a solution of saturated aqueous NH_4Cl (30 mL). After cooling the reaction mixture to 25 ºC, the organic layer was then separated and the aqueous phase was extracted with with Et_2O (3 x 30 mL), washed with brine (100 mL), dried over Na_2SO_4 and concentrated under reduced pressure. The crude oil was then purified by column chromatography (2% Et_2O in hexanes → 18% Et_2O) to provide 8.67 g (16.8 mmol, 76%) of **2.329** as a light yellow oil. **2.329**: ^{1}H NMR (600 MHz, $CDCl_3$) δ 6.14 (s, 1H), 2.55 – 2.45 (m, 2H), 1.53 – 1.47 (m, 6H), 1.41 (s, 3H), 1.36 – 1.28 (m, 6H), 1.09 – 1.03 (m, 6H), 0.89 (t, *J* = 7.3 Hz, 9H), 0.86 (s, 9H), 0.13 (d, *J* = 17.2 Hz, 6H).^{13}C NMR (151 MHz, $CDCl_3$) δ 206.5, 196.1, 140.1, 83.5, 60.5, 52.8, 30.4, 29.2, 27.4, 25.9, 18.1, 13.8, 10.5, -2.0, -2.4. HRMS (EI+) calcd for $C_{27}H_{46}NaO_6SSi$ [M + H^+] *m/z* 517.2524, found 517.2527.



2.328: A round bottom flask equipped with a magnetic stir bar was transferred to a nitrogen-filled glove-box. To this flask was added CuI (37 mg, 0.194 mmol, 2.0 equiv) and $Pd(PPh_3)_4$ (22.4 mg, 0.0194 mmol, 0.2 equiv). The reaction vessel was then removed from the glove-box, placed under argon, and charged with freshly distilled and degassed DMF (2 mL). In a separate flask, stannane **2.329** (50 mg, 0.097 mmol, 1.0 equiv) and vinyl bromide **2.326** (27.3 mg, 0.116 mmol, 1.2 equiv) was dissolved in freshly distilled and degassed DMF (X mL). This solution was then transferred, washing with DMF to ensure quantitative transfer, to the solution of palladium and copper at 75 ºC, give a dark gray-black solution. Upon completion of the reaction as indicated by TLC, the reaction was quenched with saturated aqueous $NaHCO_3$ (3 mL). The organic layer was then separated and the aqueous phase was extracted with EtOAc (3 x 3 mL). The combined organic layers were washed with H_2O (5 x 5 mL), dried over Na_2SO_4 and concentrated under reduced pressure. The resulting slurry was filtered over a pad of celite and washed with EtOAc, (3 times, 10 mL) and reconcentrated. The crude oil was then purified by column chromatography (4% Et_2O in hexanes → 20% Et_2O in hexanes) to provide 26.7 mg (0.0718 mmol, 74%) of **2.328** as a clear oil. **2.328:** ^{1}H NMR (600 MHz, $CDCl_3$) δ 7.09 (d, *J* = 16.2 Hz, 1H), 6.27 (d, *J* = 16.2 Hz, 1H), 6.17 – 6.06 (m, 1H), 6.01 (s, 1H), 4.79 – 4.72 (m, 2H), 2.71 (d, *J* = 17.7 Hz, 1H), 2.57 (d, *J* = 17.7 Hz, 1H), 2.45 – 2.32 (m, 2H), 2.25 – 2.13 (m, 3H), 2.00 – 1.92 (m, 1H), 1.76 (s, 2H), 1.55 (s, 5H), 0.88 (s, 9H), 0.14 (s, 3H), 0.06 (s, 3H). ^{13}C NMR (151 MHz, $CDCl_3$) δ 135.3, 123.9, 117.5, 109.1, 51.2, 29.3, 28.6, 24.1, 19.6, 13.8.

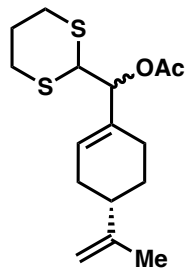


2.331: *Step 1:* To a stirring solution of **2.238** (1.3 g, 3.5 mmol, 1.0 equiv) in PhMe (35 mL) was added dropwise DIBAL (1M in PhMe, 4.2 mL, 4.2 mmol, 1.2 equiv) at –78 ºC. The resulting solution was stirred at –78 ºC for 1 hour then warmed gradually to 0 ºC over the course of 1 hour. Upon completion of the reaction as indicated by TLC, the reaction was quenched with saturated aqueous $NaHCO_3$ (15 mL) and saturated aqueous solution of Rochelle's salt (20 mL) and stirred for 3 hours. This mixture was then extracted with Et_2O (3 x 6 mL), washed with brine (3 mL), dried over Na_2SO_4 and concentrated under reduced pressure. The crude oil was quickly purified through a short silica plug eluting with Et_2O and concentrated. The resulting colorless oil **2.329** (1.1 g, 2.91 mmol, 83%) of was used in the next step without further purification. **2.329:**

^{1}H NMR (700 MHz, $CDCl_3$) δ 6.84 (d, *J* = 16.3 Hz, 1H), 6.06 (d, *J* = 16.3 Hz, 1H), 5.86 (s, 1H), 5.72 (d, *J* = 2.2 Hz, 1H), 4.76 (d, *J* = 9.7 Hz, 2H), 4.65 (d, *J* = 7.3 Hz, 1H), 2.57 (dd, *J* = 12.6, 6.8 Hz, 1H), 2.39 (d, *J* = 17.1 Hz, 1H), 2.31 (d, *J* = 13.8 Hz, 1H), 2.25 – 2.06 (m, 4H), 1.95 (dd, *J* = 12.6, 6.2 Hz, 2H), 1.78 (d, *J* = 1.3 Hz, 3H), 1.56 – 1.48 (m, 1H), 1.42 – 1.37 (m, 3H), 0.91 (s, 9H), 0.15 (d, *J* = 35.1 Hz, 6H).

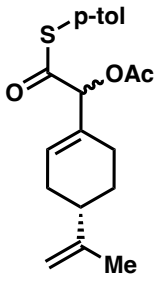
Step 2. To a stirring solution of **2.329** (1.1 g, 2.91 mmol, 1.0 equiv) in THF (20 mL) was added TBAF (1M in THF, 3.5 mL, 3.5 mmol, 1.2 equiv). The resulting reaction mixture was then stirred at 60 ºC for 1 hours. Upon completion of the reaction as indicated by TLC, the reaction was quenched with saturated aqueous $NaHCO_3$ (5 mL) and extracted with Et_2O (3 x 5 mL), dried over Na_2SO_4 and concentrated under reduced pressure. The crude oil was quickly purified through a short silica plug eluting with EtOAc and concentrated to yield 589 mg (2.26 mmol, 78%) of **SI-4.** as a colorless oil which was advanced without any further purification.

Step 3. Diol **SI-4** (589 mg, 2.26 mmol, 1.0 equiv) was dissolved in DCM (10 mL) and cooled to – 78 ºC. To the cooled solution was added freshly distilled ethyl vinyl ether (1.1 mL, 11.3 mmol, 5.0 equiv) followed by NIS (610 mg, 2.71 mmol, 1.2 equiv), resulting in a yellow-orange solution. The reaction mixture was stirred for 2 hours at –78 ºC and then slowly warmed to 0 ºC over the course of 1 hour. Upon completion of the reaction as indicated by TLC, the reaction was quenched with saturated aqueous solutions of $NaHCO_3$ (3 mL) and $Na_2S_2O_3$ (8 mL). The organic layer was then separated and the aqueous phase was extracted with Et_2O (3 x 6 mL). The combined organic extracts dried over Na_2SO_4 and concentrated under reduced pressure. The resulting crude oil was then purified by column chromatography (3% EtOAc in hexanes → 15% EtOAc in hexanes) to provide 880 mg (1.92 mmol, 85%) a mixture of iodides **2.331** as a yellow oil. **2.331**: ^{1}H NMR (600 MHz, $CDCl_3$) δ 6.74 (dd, *J* = 50.0, 16.3 Hz, 1H), 6.09 (dt, *J* = 8.8, 4.4 Hz, 2H), 5.91 (d, *J* = 6.5 Hz, 2H), 4.86 (ddd, *J* = 70.8, 6.3, 4.7 Hz, 1H), 4.79 – 4.74 (m, 2H), 4.64 (dt, *J* = 40.6, 7.8 Hz, 1H), 3.71 – 3.17 (m, 4H), 2.42 – 2.09 (m, 4H), 1.78 (dd, *J* = 2.6, 1.3 Hz, 3H), 1.59 (s, 3H), 1.46 (d, *J* = 6.9 Hz, 4H), 1.27 – 1.15 (m, 3H). ^{13}C NMR (151 MHz, $CDCl_3$) δ 137.0 134.2, 132.3, 117.5, 109.1, 96. 9, 96.3, 72.7, 60.2, 57.6, 48.0, 47.3, 40.9, 29.3, 27.9, 27.5, 27.35, 26.7, 26.1, 20.3, 14.1, 4.8.



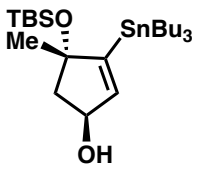
2.344: To a solution of 1,3-dithiane (6.0 g, 50.0 mmol, 1.01 equiv) in THF (300 mL) at – 78 ºC was added *t*-BuLi (1.6 M in THF, 31.3 mL, 50.1 mmol, 1.01 equiv). The resulting yellow solution was stirred at –78 ºC for 30 minutes followed by the dropwise addition of perillaldehyde (neat, 7.78 mL, 49.3 mmol, 1.0 equiv). This reaction mixture was stirred an additional 15 minutes at –78 ºC before slowly warming to –30 ºC. Upon consumption of the aldehyde starting material, as judged by TLC, the reaction mixture was cooled to –78 ºC. Freshly distilled acetyl chloride was then added dropwise and stirred at –78 ºC for an additional 15 minutes before warming to 0 ºC. Upon completion of the reaction as indicated by TLC, the reaction was quenched with saturated aqueous $NaHCO_3$ (150 mL). The organic layer was then separated and the aqueous phase was extracted with Et_2O (3 x 100 mL). The combined organic extracts were washed with brine (200 mL), dried over Na_2SO_4 and concentrated under reduced pressure to yield 15.6 g (50.0 mmol) of the crude **2.344**. This material was carried on to the next step without any further purification. ^{1}H NMR (700 MHz, $CDCl_3$) δ 5.89 (d, *J* = 27.0 Hz, 1H), 5.52 (t, *J* = 9.8 Hz, 1H), 4.75 – 4.69 (m, 2H), 4.13 (dd, *J* = 46.6, 9.0 Hz, 1H), 2.94 (ddtd, *J* = 34.6, 13.3, 7.2, 2.8 Hz, 2H), 2.81 – 2.70 (m, 2H), 2.25 – 2.16 (m, 4H), 2.12 (dd, *J* = 9.9, 0.8 Hz, 4H), 2.08 (dp, *J* = 10.6, 3.5 Hz, 1H), 2.04 – 1.92 (m, 1H), 1.87 (t, *J* = 15.2 Hz, 1H), 1.75 (d,

J = 1.4 Hz, 3H), 1.57 – 1.45 (m, 1H). ^{13}C NMR (151 MHz, $CDCl_3$) δ 170.0, 169.9, 149.6, 149.5, 133.0, 132.8, 128.6, 127.8, 108.9, 108.8, 77.7, 47.7, 46.9, 40.8, 30.6, 30.5, 28.7, 28.6, 28.5, 28.2, 27.3, 27.2, 25.6, 25.6, 24.5, 23.9, 21.1, 21.1, 20.7, 20.7. HRMS (ESI) calcd for $C_{16}H_{24}NaO_2S_2$ [M + Na^+] *m/z* 335.1115, found 335.1112.

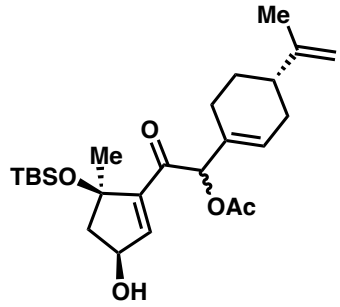


2.346: *Step 1.* To a 2 L round-bottomed flask containing the crude acetates (15.6 g, 50.0 mmol, 1.01 equiv) was added $CaCO_3$ (40 g, 0.4 mol, 8 equiv), H_2O (150 mL), MeCN (500 mL), and acetone (500 mL), and MeI (160 mL, 257 mmol, 5.14 equiv). This reaction mixture was heated at 40 ºC overnight or until complete consumption of the starting material, as indicated by TLC. The suspension was then filtered over a pad of celite and washed with Et_2O (3 x 150 mL). The organic layer was then separated and the aqueous phase was extracted with Et_2O (3 x 100 mL). The combined organic extracts were washed with brine (500 mL), dried over Na_2SO_4 and concentrated under reduced pressure to yield 10 g of the crude aldehyde **SI-5**. This material was subjected to the following reaction without any further purification. *Step 2.* To a round bottom flask containing intermediate **SI-5** was added *t*-BuOH (340 mL), H_2O (100 mL) and 2-methyl-2-butene (340 mL). The resulting reaction mixture was then cooled to 0 ºC followed by the addition of NaH_2PO_4 (48 g, 400 mmol, 8.0 equiv) and NaClO (17.6 g, 194 mmol, 3.9 equiv; in two portions). Upon completion of the reaction, as indicated by TLC, the reaction was quenched with saturated aqueous $Na_2S_2O_3$ (250 mL). The organic layer was then separated and the aqueous phase was extracted with Et_2O (3 x 200 mL) and the combined organic extracts were washed with brine (2 x 200 mL), dried over Na_2SO_4 and concentrated under reduced pressure to yield 8.8 g of the crude **2.345.**

Step 3. To a round bottom flask containing stirring a solution of acid **2.345** (8.8 g, 36.9 mmol, 1.0 equiv) in DCM (370 mL) at 0 ºC was added successively DCC (9.14 g, 44.3 mmol, 1.2 equiv) and *p*-thiocresol (6.87 g, 55.35 mmol, 1.5 equiv). The reaction mixture was then stirred for an additional 3 hours. Upon completion of the reaction, as indicated by TLC, the reaction was diluted with Et_2O and filtered over a pad of celite washing with Et_2O. The resulting mixture was then washed with saturated aqueous $NaHCO_3$ (200 mL). The organic layer was then separated and the aqueous phase was extracted with Et_2O (3 x 6 mL), the combined organic extracts were then washed with brine (150 mL), dried over Na_2SO_4 and concentrated under reduced pressure. The crude oil was then purified by column chromatography (5% DCM in hexanes → 80% DCM in hexanes) to provide a thioester 7.36 g (20.4 mmol, 41% over 4 steps) as a yellow oil. **2.346:** ^{1}H NMR (700 MHz, $CDCl_3$) δ 7.28 (dd, J = 8.3, 2.3 Hz, 2H), 7.22 (d, J = 7.8 Hz, 2H), 6.06 – 6.02 (m, 1H), 5.68 (d, J = 7.2 Hz, 1H), 4.78 – 4.69 (m, 2H), 2.37 (s, 3H), 2.32 – 2.22 (m, 2H), 2.20 (m, J = 1.2 Hz, 4H), 2.14 – 2.00 (m, 2H), 1.87 (tq, J = 10.8, 3.7 Hz, 1H), 1.55 – 1.46 (m, 2H), 1.33 – 1.27 (m, 2H). ^{13}C NMR (151 MHz, $CDCl_3$) δ 195.497, 195.463, 169.716, 149.204, 149.098, 139.861, 134.673, 131.327, 131.082, 130.632, 130.439, 130.092, 109.097, 109.024, 82.177, 81.951, 40.507, 40.383, 30.789, 30.730, 27.177, 24.880, 24.595, 21.334, 20.862, 20.819, 20.737. HRMS (ESI) calcd for $C_{20}H_{24}NaO_3S$ [M + Na^+] *m/z* 367.1344, found 367.1340.

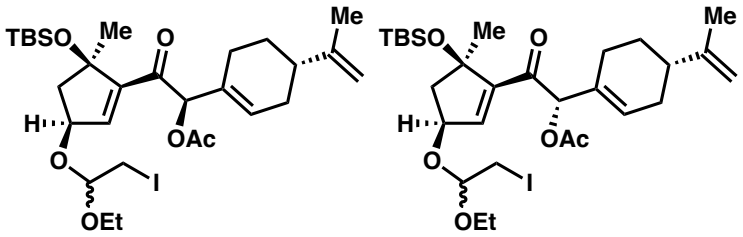


2.333: To a stirring solution of **2.329** (1 g, 1.94 mmol, 1.0 equiv) in PhMe (20 mL) was added dropwise DIBAL (1M in PhMe, 2.52 mL, 2.52 mmol, 1.3 equiv) at –78 ºC. The resulting suspension was stirred at –78 ºC for 1 hour then warmed gradually to 0 ºC over the course of 1 hour. Upon completion of the reaction as indicated by TLC, the reaction was quenched with saturated aqueous $NaHCO_3$ (10 mL) and saturated aqueous solution of Rochelle's salt (15 mL) and stirred for 3 hours. Once the emulsion has dissipated, the biphasic mixture was diluted with Et_2O (10 mL) and the organic layer was separated and the aqueous was extracted with Et_2O (3 x 6 mL). The combined organic layers were then washed with brine (3 mL), dried over Na_2SO_4 and concentrated under reduced pressure. The resulting crude oil was then purified by column chromatography (10% Et_2O in hexanes → 50% Et_2O) to provide 86 mg (1.73 mmol, 89%) of **2.333** as a clear colorless oil. **2.333:** ^{1}H NMR (700 MHz, $CDCl_3$) δ 5.78 (d, *J* = 1.6 Hz, 1H), 4.69 (q, *J* = 7.2 Hz, 1H), 2.48 (dd, *J* = 12.2, 6.5 Hz, 1H), 1.74 (dd, *J* = 12.2, 6.2 Hz, 1H), 1.56 (s, 3H), 1.52 – 1.47 (m, 6H), 1.31 (h, *J* = 7.3 Hz, 6H), 1.24 (s, 3H), 0.95 (ddd, *J* = 10.2, 6.9, 3.4 Hz, 6H), 0.89 (t, *J* = 7.3 Hz, 9H), 0.87 (s, 9H), 0.11 (s, 6H). ^{13}C NMR (151 MHz, $CDCl_3$) δ 159.5, 141.7, 87.7, 77.8, 52.8, 30.1, 29.3, 27.5, 26.1, 18.1, 13.8, 10.0, -1.8, -2.0. HRMS (ESI) calcd for $C_{24}H_{50}NaO_2SiSn$ [M + Na^+] *m/z* 541.2500, found 541.2499.

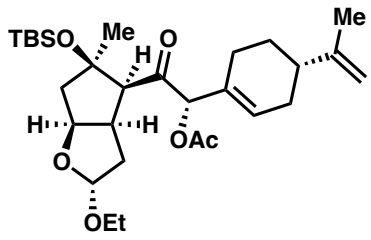


2.347a and **2.347b:** A 250 mL round-bottomed flask equipped with a magnetic stir bar was transferred to a nitrogen-filled glove-box. To this flask was added freshly prepared CuDPP (10.2 g, 36.3 mmol, 1.3 equiv) $AsPh_3$ (10.3 g, 33.5 mmol, 1.2 equiv)and $Pd_2(dba)_3$ (10.2 g, 11.2 mmol, 0.4 equiv). The reaction vessel was then removed from the glove-box, placed under argon, and charged with freshly distilled and degassed DMF (220 mL). In a separate 50 mL round-bottomed flask, stannane **2.333** (14.4 g, 27.9, 1.0 equiv) and thioester **2.346** (12.1 g, 33.5 mmol, 1.2 equiv) were azeotropically dried (3 x benzene) and dissolved in freshly distilled and degassed DMF (10 mL). This solution was then cannulated to suspension containing palladium, washing with DMF (2 x 5 mL) to ensure quantitative transfer, at 25 ºC to give a gray suspension. The reaction mixture was then placed in an preheated oil bath at 60 ºC. Upon completion of the reaction (typically 1.5 hours), as indicated by TLC, the reaction was cooled to 25 ºC and quenched with saturated aqueous $NaHCO_3$ (3 mL). The reaction mixture was then diluted with EtOAc (200 mL) and filtered over a thick pad of celite eluting with EtOAc and then H_2O (200 mL) was added. The emulsion (typically observed) is then filtered again over another thick pad of celite and rinsed EtOAc. The resulting biphasic mixture was then separated the aqueous phase was extracted with EtOAc (3 x 200 mL). The combined organic layers were then washed with H_2O (5 x 200 mL), dried over Na_2SO_4 and concentrated under reduced pressure. The resulting slurry was filtered over a pad of celite and washed with EtOAc, (3 x 100 mL) and reconcentrated. The crude oil was then purified by column chromatography (100% DCM (2 column lengths) then 100% hexanes (2 column lengths) then 1% Et_2O in DCM to 8% Et_2O in DCM) to provide a 11.13 g (24.83 mmol, 89%) of a mixture of ketoacetates **2.347a** and **2.347b** (1:1 *dr* at C5) as a colorless oil. **2.347a:** ^{1}H NMR (600 MHz, $CDCl_3$) δ 6.68 (d, *J* = 2.3 Hz, 1H), 5.91 (s, 1H), 5.85 (s, 1H), 4.72 (t, *J* = 2.0 Hz, 1H), 4.69 – 4.61 (m, 2H), 2.34 – 2.28 (m, 1H), 2.26 – 2.15 (m, 3H), 2.14 (s, 3H), 2.11 (s, 1H), 1.98 (dd, *J* = 13.3, 3.9 Hz, 1H), 1.84 (t, *J* = 12.0 Hz, 2H), 1.72 (d, *J* = 2.7 Hz, 4H), 1.48 (s, 3H), 0.84 (s, 9H), 0.12 (d, *J* = 22.1 Hz, 6H).^{13}C NMR (151 MHz, $CDCl_3$) δ 192.9, 170.1, 149.0, 147.6, 142.9, 132.0, 130.4,

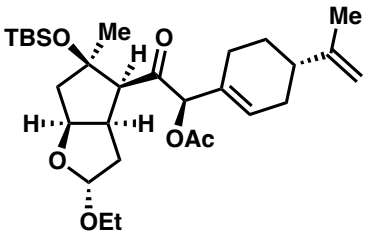
109.2, 83.7, 80.6, 73.8, 52.1, 40.2, 30.8, 27.1, 26.9, 25.9, 25.8, 24.9, 21.0, 20.9, 18.1, -2.3, -2.5. **2.347b:** ^{1}H NMR (600 MHz, $CDCl_3$) δ 6.68 (d, *J* = 2.1 Hz, 1H), 5.95 (d, *J* = 4.8 Hz, 1H), 5.83 (s, 1H), 4.73 (d, *J* = 1.7 Hz, 1H), 4.69 (s, 2H), 2.43 (dd, *J* = 12.7, 6.9 Hz, 1H), 2.19 (d, *J* = 19.5 Hz, 2H), 2.14 (s, 3H), 2.11 – 1.97 (m, 3H), 1.96 – 1.87 (m, 1H), 1.86 – 1.76 (m, 2H), 1.72 (d, *J* = 1.3 Hz, 3H), 1.38 (s, 3H), 0.83 (s, 9H), 0.12 (d, *J* = 12.7 Hz, 6H).^{13}C NMR (151 MHz, $CDCl_3$) δ 192.1, 170.5, 149.2, 147.5, 142.5, 131.6, 130.7, 109.0, 82.8, 79.8, 73.2, 52.7, 40.4, 30.8, 30.0, 29.7, 27.6, 27.2, 25.7, 25.3, 20.8, 20.7, 17.9, -2.3, -2.4. HRMS (ESI) calcd for $C_{25}H_{41}O_5Si$ [M + H^+] *m/z* 449.2723, found 449.2722.



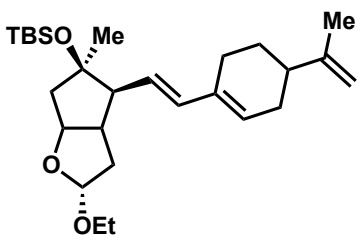
2.348 and 2.349: The mixture of ketoacetates **2.347a** and **2.347b** (9.75 g, 21.75 mmol, 1 equiv) was dissolved in DCM (200 mL) and cooled to – 78 ºC. To the cooled solution was added freshly distilled ethyl vinyl ether (10.5 mL, 108.75 mmol, 5.0 equiv) followed by NIS (8.8 g, 39.2 mmol, 1.8 equiv), resulting in a yellow-orange solution. The reaction mixture was stirred for 2 hours at –78 ºC and then slowly warmed to 0 ºC over the course of 1 hour. Upon completion of the reaction as indicated by TLC, the reaction was quenched with saturated aqueous solutions of $NaHCO_3$ (3 mL) and $Na_2S_2O_3$. The organic layer was then separated and the aqueous phase was extracted with Et_2O (**3** x 40 mL). The combined organic extracts were washed with brine (100 mL), dried over Na_2SO_4 and concentrated under reduced pressure to yield a crude mixture of 4 diastereomers of iodides **2.347a** and **2.347b**. The mixture was then purified by column chromatography (4% Et_2O in hexanes → 30% Et_2O) to provide 11.97 g (18.53 mmol, 85%) of the mixture of iodoacetals as a yellow oil (5.97 g of **2.348** (C5–H = α) + 6.0 g of **2.349** (C5–H = β). **2.348:** ^{1}H NMR (700 MHz, $CDCl_3$) δ 6.55 (dd, *J* = 3.8, 1.9 Hz, 1H), 5.92 (d, *J* = 4.5 Hz, 1H), 5.86 (s, 1H), 3.71 – 3.53 (m, 2H), 3.29 – 3.20 (m, 2H), 2.44 (dt, *J* = 12.8, 6.4 Hz, 1H), 2.28 – 2.20 (m, 1H), 2.20 – 2.06 (m, 6H), 2.05 – 1.92 (m, 2H), 1.83 (d, *J* = 13.1 Hz, 1H), 1.72 (s, 4H), 1.58 (s, 2H), 1.50 – 1.41 (m, 4H), 1.28 – 1.23 (m, 4H), 0.84 (t, *J* = 1.1 Hz, 9H), 0.10 (d, *J* = 8.7 Hz, 7H).^{13}C NMR (151 MHz, $CDCl_3$) δ 192.6, 192.5, 169.8, 149.0, 147.9, 147.8, 132.1, 132.0, 130.2 – 130.2 (m), 109.0, 109.0, 101.6, 101.4, 82.5, 82.3, 80.5, 80.4, 61.7, 61.6, 50.6, 49.9, 40.2 (d, *J* = 2.1 Hz), 30.7, 30.7, 28.4, 28.4, 27.1, 25.8, 24.9, 24.9, 20.8, 20.8, 20.7, 18.1, 15.2, 15.1, 5.2, 5.1, -2.5, -2.6. HRMS (ESI) calcd for $C_{29}H_{47}O_6INaSi$ [M + Na^+] *m/z* 669.2079, found 669.2081. **2.349:** ^{1}H NMR (700 MHz, $CDCl_3$) δ 6.66 (dd, *J* = 12.2, 1.9 Hz, 1H), 5.98 (t, *J* = 6.4 Hz, 1H), 5.86 (d, *J* = 9.8 Hz, 1H), 4.83 – 4.74 (m, 2H), 4.74 – 4.57 (m, 2H), 3.81 – 3.55 (m, 2H), 3.33 – 3.22 (m, 2H), 2.49 (dd, *J* = 12.2, 7.2 Hz, 1H), 2.25 – 2.15 (m, 5H), 2.15 – 1.96 (m, 4H), 1.83 (t, *J* = 8.9 Hz, 1H), 1.74 (s, 3H), 1.58 (s, 3H), 1.49 (qd, *J* = 11.2, 4.6 Hz, 1H), 1.28 (tdd, *J* = 7.0, 5.0, 1.0 Hz, 3H), 0.90 – 0.83 (m, 9H), 0.13 (dd, *J* = 28.6, 2.2 Hz, 6H). ^{13}C NMR (151 MHz, $CDCl_3$) δ 191.90, 191.87, 170.58, 170.55, 149.30, 147.91, 147.87, 140.51, 139.80, 131.39, 131.32, 130.73, 130.64, 108.94, 102.00, 101.63, 81.99, 81.85, 79.91, 76.75, 76.69, 62.00, 61.88, 51.20, 50.55, 40.45, 40.44, 30.80, 30.75, 28.32, 27.27, 25.74, 25.27, 20.82, 20.72, 17.93, 15.19, 15.15, 5.34, 5.30, -2.30 (d, *J* = 2.8 Hz), -2.38. HRMS (ESI) calcd for $C_{29}H_{47}O_6INaSi$ [M + Na^+] *m/z* 669.2079, found 669.2083.



2.351: To a reaction vessel containing **2.349** (6 g, 9.28 mmol, 1 equiv) was added AIBN (305 mg, 1.86 mmol, 0.2 equiv) and distilled PhMe (100 mL). This mixture sparged with argon for 10 minutes in an ultrasound bath. To the degassed solution containing **2.349** was added Bu_3SnH (2.5 mL, 9.28 mmol, 1 equiv). The reaction mixture was stirred at 80 ºC for 1 hour before a second portion of AIBN (305 mg, 1.86 mmol, 0.2 equiv; 0.4 equiv total) and Bu_3SnH (1.25 mL, 4.6 mmol, 0.5 equiv; 1.5 equiv total) was added at 80 ºC. Upon completion of the reaction as indicated by TLC, the reaction was quenched with saturated aqueous $NaHCO_3$ (75 mL) and stirred for 30 min. The organic layer was then separated and the aqueous phase was extracted with Et_2O (3 x 6 mL). The combined organic extracts were then washed with brine (3 mL), dried over Na_2SO_4 and concentrated under reduced pressure***. Epimerization of the Ethyl Acetal:*** In a separate step, CSA (325 mg, 1.403 mmol, 0.1 equiv) was added to a stirring solution of the crude mixture of **2.351** in anhydrous EtOH (14 mL). The resulting reaction mixture was then stirred at 25 ºC for 3 hours. Upon completion of the reaction as indicated by TLC, the reaction was quenched with saturated aqueous $NaHCO_3$ (3 mL). The aqueous phase was extracted with Et_2O (3 x 5 mL) and the combined organic extracts were then washed with brine (5 mL), dried over Na_2SO_4 and concentrated under reduced pressure. The crude oil was then purified by column chromatography (4% Et_2O in hexanes → 25% Et_2O in hexanes) to provide a bicycle 1.93 g (3.71 mmol, 80%) of **2.351** as a clear oil. ^{1}H NMR (700 MHz, $CDCl_3$) δ 6.0 (s, 1H), 5.5 (s, 1H), 5.1 (d, *J* = 4.8 Hz, 1H), 4.7 (t, *J* = 1.8 Hz, 1H), 4.7 – 4.6 (m, 2H), 3.7 (dq, *J* = 9.8, 7.1 Hz, 1H), 3.4 (dq, *J* = 9.8, 7.0 Hz, 1H), 3.3 (p, *J* = 8.8 Hz, 1H), 2.7 (d, *J* = 8.5 Hz, 1H), 2.3 (ddd, *J* = 13.3, 8.9, 4.8 Hz, 1H), 2.1 (s, 3H), 2.1 – 2.0 (m, 2H), 1.8 (d, *J* = 11.2 Hz, 2H), 1.7 (s, 3H), 1.7 (dd, *J* = 14.3, 7.1 Hz, 1H), 1.6 (s, 3H), 1.3 (s, 2H), 1.2 (t, *J* = 7.1 Hz, 3H), 0.8 (s, 8H), 0.1 (s, 5H). ^{13}C NMR (151 MHz, $CDCl_3$) δ 201.1, 169.6, 148.9, 131.4, 130.5, 109.0, 105.5, 83.0, 82.9, 81.9, 62.2, 58.0, 47.8, 44.0, 40.0, 36.3, 30.5, 28.1, 26.8, 25.8, 24.1, 20.9, 20.8, 18.3, 15.3, -2.2, -2.5. HRMS (ESI) calcd for $C_{29}H_{48}NaO_6Si$ [M + Na^+] *m/z* 543.3112, found 543.3117.



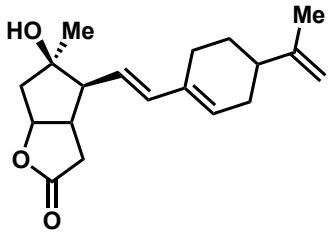
2.350: The cyclization and epimerization procedure of **2.349** is identical to that of iodide **2.348** (see above); 68% yield. **2.350**: ^{1}H NMR (700 MHz, $CDCl_3$) δ 5.99 (d, *J* = 5.0 Hz, 1H), 5.44 (s, 1H), 5.14 (d, *J* = 4.8 Hz, 1H), 4.80 – 4.69 (m, 2H), 4.61 (t, *J* = 7.7 Hz, 1H), 3.66 (dq, *J* = 10.1, 7.0 Hz, 1H), 3.40 (dq, *J* = 10.0, 7.0 Hz, 1H), 2.98 (q, *J* = 8.5 Hz, 1H), 2.93 (d, *J* = 8.0 Hz, 1H), 2.79 (ddd, *J* = 13.4, 8.9, 4.9 Hz, 1H), 2.28 – 2.16 (m, 2H), 2.13 (d, *J* = 3.2 Hz, 4H), 2.11 – 1.98 (m, 2H), 1.83 (dd, *J* = 14.4, 7.2 Hz, 2H), 1.74 (s, 4H), 1.50 (s, 2H), 1.17 (dd, *J* = 7.9, 6.3 Hz, 3H), 0.85 (d, *J* = 3.0 Hz, 9H), 0.07 (d, *J* = 2.5 Hz, 6H). ^{13}C NMR (151 MHz, $CDCl_3$) δ 201.5, 169.9, 149.0, 131.6, 130.8, 109.2, 105.7, 84.5, 84.4, 82.2, 62.2, 57.1, 47.7, 45.0, 40.7, 35.1, 30.9, 28.7, 27.2, 25.7, 25.1, 20.8, 20.7, 18.2, 15.3, -2.2, -2.6. HRMS (ESI) calcd for $C_{29}H_{48}NaO_6Si$ [M + Na^+] *m/z* 543.3112, found 543.3118



2.352: *Step 1.* To a solution of ketoacetate **2.348** (140 mg, 0.268 mmol, 1 equiv) in THF was added Lithium Naphthalenide (0.5 M in THF, 8 mL, 4.0 mmol, 15 equiv) at –78 ºC. Upon completion of the reaction (typically 5 minutes) as indicated by TLC, the reaction was warmed to room temperture and poured into a solution of saturated aqueous $NaHCO_3$ (10 mL) and stirred for 5 min. The organic layer was then separated and the aqueous phase was extracted with Et_2O (3 x 10 mL). The combined organic extracts were then washed with brine (3 mL), dried over Na_2SO_4 and concentrated under reduced pressure. The crude oil was then purified by column chromatography (0% Et_2O in hexanes → 24% Et_2O in hexanes) to obtain 83 mg (0.180 mmol, 67%) of ketone **SI-6** (83 mg, 67%).

Step 2. A reaction tube containing a solution of Comin's reagent (25 mg, 0.064 mmol, 2 equiv) in THF (0.6 mL) was cooled to –78 ºC. After stirring this mixture at –78 ºC for 5 minutes, KHMDS (0.5M in PhMe, 0.13 mL, 0.064 mmol, 2 equiv) was added resulting in a dark yellow solution. To this mixture was added a solution of ketone **SI-6** (15 mg, 0.032 mmol, 1 equiv) in THF (0.4 mL). After stirring for 15 minutes at –78 ºC, the reaction mixture was warmed to room temperature resulting in a red/orange solution. After 10 minutes of continued stirring at room temperature, the reaction mixture was quenched with a saturated aqueous solution of $NaHCO_3$ (1 mL). The organic layer was then separated and the aqueous phase was extracted with Et_2O (3 x 1 mL). The combined organic extracts were washed with brine (3 mL), dried over Na_2SO_4 and concentrated under reduced pressure. The crude oil was then purified by column chromatography (0% Et_2O in hexanes → 24% Et_2O in hexanes) to obtain 14 mg (0.0467 mmol, 73%) of vinyl triflate **SI-7**.

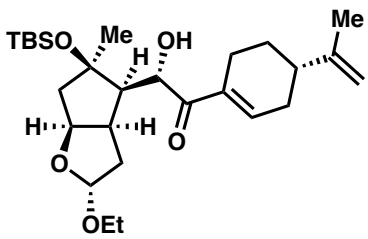
Step 3. To a round-bottomed flask containing triflate **SI-7** (12 mg, 0.212 mmol, 1.0) was sequentially added solutions of triethylamine (8.2 mg, 0.08 mmol, 4.0 equiv), $Pd(PPh_3)_4$ (4.6 mg, 4 μmol, 0.2 equiv), and HCO_2H (2.8 mg, 0.06 mmol, 3.0 equiv) in DMF (0.2 mL each). This mixture was then heated to 55 ºC for 12 hours. Upon completion of the reaction as indicated by TLC, the reaction was quenched with a saturated aqueous solution of $NaHCO_3$ (3 mL), filtered through celite eluting with Et_2O. The organic layer was then separated and the aqueous phase was extracted with Et_2O (3 x 0.5 mL). The combined organic extracts were washed with a solution of LiCl (5%, 2 mL), dried over Na_2SO_4 and concentrated under reduced pressure. The crude oil was then purified by preparative thin layer chromatography to yield 7 mg (0.168 mmol, 79%) of **2.352:** ^{1}H NMR (700 MHz, C_6D_6) δ 6.16 (d, *J* = 15.8 Hz, 1H), 5.91 (dd, *J* = 15.8, 9.1 Hz, 1H), 5.74 – 5.67 (m, 1H), 5.27 (d, *J* = 4.7 Hz, 1H), 4.85 – 4.76 (m, 2H), 4.65 (t, *J* = 7.4 Hz, 1H), 3.81 (dq, *J* = 9.6, 7.1 Hz, 1H), 3.36 (dq, *J* = 9.6, 7.0 Hz, 1H), 3.04 (p, *J* = 8.8 Hz, 1H), 2.60 – 2.56 (m, 1H), 2.51 – 2.43 (m, 1H), 2.17 (dd, *J* = 16.1, 10.8 Hz, 3H), 2.12 – 1.96 (m, 4H), 1.80 (ddq, *J* = 12.7, 4.7, 2.3 Hz, 1H), 1.62 (d, *J* = 1.2 Hz, 3H), 1.50 – 1.43 (m, 2H), 1.16 (t, *J* = 7.1 Hz, 3H), 1.10 (s, 3H), 1.03 (s, 9H), 0.21 (s, 3H), 0.11 (s, 3H). ^{1}H NMR (600 MHz, $CDCl_3$) δ 6.07 (d, *J* = 15.8 Hz, 1H), 5.72 – 5.65 (m, 2H), 5.09 (d, *J* = 4.7 Hz, 1H), 4.73 (dt, *J* = 2.6, 1.3 Hz, 2H), 4.61 (t, *J* = 7.5 Hz, 1H), 3.66 (dq, *J* = 9.7, 7.1 Hz, 1H), 3.40 (dq, *J* = 9.7, 7.0 Hz, 1H), 2.99 (p, *J* = 8.8 Hz, 1H), 2.37 (ddd, *J* = 12.5, 9.1, 4.8 Hz, 1H), 2.34 – 2.28 (m, 1H), 2.28 – 2.21 (m, 1H), 2.21 – 2.14 (m, 1H), 2.11 (d, *J* = 14.9 Hz, 1H), 2.09 – 2.01 (m, 1H), 1.91 (ddd, *J* = 10.4, 5.6, 2.9 Hz, 0H), 1.80 – 1.77 (m, 1H), 1.75 (q, *J* = 1.5 Hz, 3H), 1.17 (t, *J* = 7.1 Hz, 3H), 0.87 (s, 9H), 0.08 (d, *J* = 8.9 Hz, 6H).^{13}C NMR (151 MHz, $CDCl_3$) δ 135.53, 127.15, 108.80, 105.26, 82.40, 65.98, 62.12, 61.80, 56.32. 47.63, 47.31, 46.66, 41.51, 34.7, 31.2, 31.21, 30.24, 27.67, 25.74, 25.09, 20.59, 15.11. HRMS (ESI) calcd for $C_{27}H_{46}NaO_3Si$ [M + Na^+] *m/z* 469.3114, found 469.3120.



2.301: *Step 1.* To a stirring solution of **2.352** (25 mg, 0.056 mmol, 1.0 equiv) in MeCN (1 mL) and H_2O (1 mL) was added PPTS (15.6 mg, 0.062 mmol, 1.1 equiv). The resulting reaction mixture was then stirred at 60 ºC for 10 hours. Upon completion of the reaction as indicated by TLC, the reaction was quenched with saturated aqueous $NaHCO_3$ (1 mL). The organic layer was then separated and the aqueous phase was extracted with Et_2O (3 x 1 mL) and the combined organic extracts were dried over Na_2SO_4 and concentrated under reduced pressure. The crude oil was purified over a short silica plug to yield 23 mg (0.055 mmol) of the crude lactol **SI-8** which was processed without any further purification.

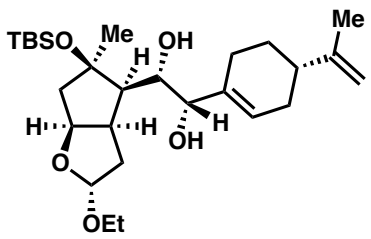
Step 2. To a stirring solution of **SI-9** (23 mg, 0.055 mmol, 1.0 equiv) in THF (0.5 mL) was added TBAF (1M in THF, 0.072 mL, 0.072 mmol, 1.3 equiv). The resulting reaction mixture was then stirred at 60 ºC for 1 hours. Upon completion of the reaction as indicated by TLC, the reaction was quenched with saturated aqueous $NaHCO_3$ (0.5 mL) and extracted with Et_2O (3 x 1 mL), dried over Na_2SO_4 and concentrated under reduced pressure. The crude oil was purified over a short silica plug to yield 15 mg (0.0495 mmol) of the crude **SI-10** which was advanced without any further purification.

Step 3. To a reaction tube containing the lactol **SI-10** (15 mg, 0.0495, 1.0 equiv) prepared in the previous step, was added successively added TEMPO (3.1 mg, 0.0198 mmol, 0.4 equiv), $PhI(OAc)_2$ (25 mg, 0.0743 mmol, 1.5 equiv) and DCM (0.5 mL). The solution was stirred for 3 hours at 25 ºC until completion of the reaction, as judged by TLC. The reaction was quenched with saturated aqueous solutions of $NaHCO_3$ (0.3 mL) and $Na_2S_2O_3$ (0.3 mL). The organic layer was then separated and the aqueous phase was extracted with DCM (3 x 0.5 mL) and the combined organic extracts were dried over Na_2SO_4 and concentrated under reduced pressure. The crude oil was then purified by column chromatography (3% Et_2O in DCM → 20% Et_2O in DCM) to provide 12 mg (0.0396 mmol, 80%) of **2.301** as a clear colorless oil. ^{1}H NMR (700 MHz, $CDCl_3$) δ 6.17 (d, *J* = 15.7 Hz, 1H), 5.77 – 5.73 (m, 1H), 5.64 (dd, *J* = 15.7, 9.2 Hz, 1H), 5.06 (t, *J* = 7.1 Hz, 1H), 4.76 – 4.73 (m, 2H), 3.12 (dtd, *J* = 12.1, 8.3, 4.1 Hz, 1H), 2.86 (dd, *J* = 18.6, 4.2 Hz, 1H), 2.51 (dd, *J* = 18.6, 11.9 Hz, 1H), 2.40 (t, *J* = 8.9 Hz, 1H), 2.37 – 2.34 (m, 1H), 2.28 – 2.13 (m, 5H), 2.07 (dd, *J* = 18.3, 12.1 Hz, 1H), 1.91 (dd, *J* = 15.2, 6.6 Hz, 1H), 1.75 (d, *J* = 1.3 Hz, 3H), 1.24 (s, 2H). HRMS (ESI) calcd for $C_{19}H_{26}NaO_3$ [M + Na^+] *m/z* 325.1780, found 325.1779.

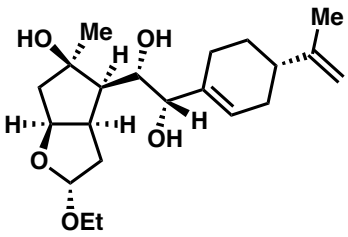


2.356: To a microwave reaction tube was added ketoacetate **2.350** (30 mg, 0.0576 mmol, 1.0 equiv), Me_3SnOH (100 mg, 0.576 mmol, 10.0 equiv), and dichloroethane (2 mL). The reaction vessel was then placed in a microwave reactor and irradiated at 160 ºC for 6 hours. The reaction mixture was cooled to room temperature at which point it opened and quenched with a solution of saturated aqueous NH_4Cl (2 mL). The organic layer was then separated and the aqueous phase was extracted with DCM (3 x 2 mL) and the combined organic extracts were washed with brine (5 mL), dried over Na_2SO_4 and concentrated under reduced pressure. The crude oil was then purified by column chromatography (5% Et_2O in hexanes → 30% Et_2O in hexanes) to provide 8.2 mg (0.0202 mmol, 35%) of **2.356** as a clear colorless oil. **2.356**: ^{1}H NMR (600 MHz, $CDCl_3$) δ 7.07 – 7.05 (m, 1H), 5.18 (t, *J* = 6.2 Hz, 1H), 5.09 (d, *J* = 4.7 Hz, 1H), 4.77 (q, *J* = 1.5 Hz, 1H), 4.75 – 4.71 (m, 1H), 4.57 (t, *J* = 7.7 Hz, 1H),

3.65 (dd, *J* = 9.7, 7.1 Hz, 1H), 3.39 (dd, *J* = 9.7, 7.0 Hz, 1H), 3.19 (d, *J* = 6.3 Hz, 1H), 3.04 (p, *J* = 8.7 Hz, 1H), 2.71 – 2.63 (m, 1H), 2.52 (ddd, *J* = 12.7, 9.7, 4.7 Hz, 1H), 2.39 (d, *J* = 18.1 Hz, 1H), 2.26 – 2.15 (m, 4H), 2.12 – 2.05 (m, 2H), 2.05 – 1.97 (m, 1H), 1.96 – 1.87 (m, 1H), 1.82 – 1.72 (m, 5H), 1.51 – 1.43 (m, 1H), 1.26 (d, *J* = 3.5 Hz, 4H), 0.88 (s, 9H), 0.13 (d, *J* = 33.7 Hz, 6H).^{13}C NMR (151 MHz, $CDCl_3$) δ 142.6, 110.41, 105.91, 81.44, 70.4, 62.1, 55.0, 48.0, 44.1, 40.9, 35.1, 35.0, 32.5, 30.6, 29.4, 28.6, 27.4, 26.1, 24.1, 21.0, 15.8, -2.3. ^{13}C NMR (151 MHz, $CDCl_3$) δ 201.4, 148.7, 141.2, 137.8, 109.6, 105.5, 84.3, 81.1, 70.0, 62.2, 54.2, 47.7, 43.9, 40.3, 35.3, 31.7, 28.7, 27.0, 26.0, 23.8, 20.8, 18.3, 15.4, -1.7, -2.4.

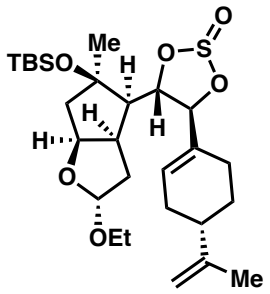


2.356: To a stirring solution of **2.350** (3.8 g, 7.3 mmol, 1.0 equiv) in DCM (150 mL) was added dropwise (over 1 hour) DIBAL (1M in PhMe, 18.25 mL g, 18.25 mmol, 2.5 equiv) at –78 ºC. The resulting solution was stirred at –78 ºC for 1 hour then warmed gradually to 0 ºC over the course of 1 hour. Upon completion of the reaction as indicated by TLC, the reaction was quenched with saturated aqueous $NaHCO_3$ (30 mL) and saturated aqueous solution of Rochelle's salt (60 mL) and stirred for 3 hours. The organic layer was then separated and the aqueous phase was extracted with DCM (3 x 100 mL) and the combined organic extracts were washed with brine (X mL), dried over Na_2SO_4 and concentrated under reduced pressure. The crude oil was then purified by column chromatography (10% Et_2O in hexanes → 70% Et_2O in hexanes) to provide 2.7 g (5.6 mmol, 77%) of **2.356** as a clear colorless oil. **2.356**: ^{1}H NMR (600 MHz, $CDCl_3$) δ 5.90 (s, 1H), 5.11 (d, *J* = 4.6 Hz, 1H), 4.76 – 4.68 (m, 2H), 4.64 (t, *J* = 7.9 Hz, 1H), 4.27 (dd, *J* = 7.2, 2.4 Hz, 1H), 4.16 (d, *J* = 7.3 Hz, 1H), 3.74 – 3.64 (m, 1H), 3.43 (dt, *J* = 9.5, 7.1 Hz, 1H), 3.29 – 3.19 (m, 1H), 2.62 (td, *J* = 12.4, 4.6 Hz, 1H), 2.30 – 2.13 (m, 6H), 2.13 – 2.04 (m, 1H), 2.02 (d, *J* = 14.1 Hz, 1H), 1.94 – 1.86 (m, 1H), 1.86 – 1.79 (m, 1H), 1.76 (d, *J* = 7.2 Hz, 3H), 1.45 (d, *J* = 3.2 Hz, 3H), 1.21 (t, *J* = 7.1 Hz, 3H), 0.90 (s, 9H), 0.21 (d, *J* = 12.7 Hz, 6H). ^{13}C NMR (151 MHz, $CDCl_3$) δ 151.7, 139.1, 126.4, 110.3, 107.3, 88.8, 83.3, 72.8, 63.9, 51.5, 49.2, 44.5, 42.6, 38.5, 36.0, 32.3, 30.0, 29.3, 27.8, 26.0, 24.2, 22.7, 19.9, 17.2, 15.9, 0.0, -0.8. HRMS (ESI) calcd for $C_{27}H_{48}NaO_5Si$ [M+H$^+$] m/z 503.3163, found 503.3168.

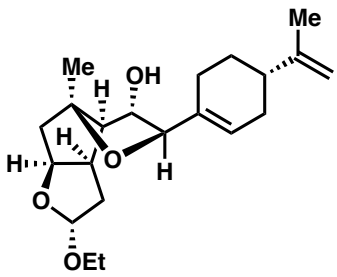


2.357: To a stirring solution of **2.356** (100 mg, 0.208 mmol, 1.0 equiv) in THF (2 mL) was added TBAF (1M in THF, 0.312 mL, 0.312 mmol, 1.5 equiv). The resulting reaction mixture was then stirred at 60 ºC for 3 hours. Upon completion of the reaction as indicated by TLC, the reaction was cooled to room temperature and quenched with saturated aqueous $NaHCO_3$ (3 mL). The organic layer was then separated and the aqueous phase was extracted with Et_2O (3 x 3 mL). The combined organic extracts were washed with brine (5 mL), dried over Na_2SO_4 and concentrated under reduced pressure. The crude oil was then purified by column chromatography (3% Et_2O in DCM → 15% Et_2O in DCM) to provide 57.8 mg (0.158 mmol, 76%) of **2.357** as a clear colorless oil. **2.357:** ^{1}H NMR (600 MHz, $CDCl_3$) δ 5.88 (s, 1H), 5.19 (d, *J* = 5.1 Hz, 1H), 4.74 (dt, *J* = 12.7, 1.4 Hz, 2H), 4.70 – 4.62 (m, 1H), 4.38 (s, 1H), 4.25 (dd, *J* = 8.4, 3.1 Hz, 1H), 4.14 (dd, *J* = 12.2, 7.7 Hz, 1H), 3.78 – 3.66 (m, 1H), 3.45 (dq, *J* = 9.7, 7.1 Hz, 1H), 3.26 – 3.17 (m, 1H), 3.13 (s, 1H), 2.97 (ddd, *J* = 13.6, 7.3, 5.2 Hz, 1H), 2.28 (t, *J* = 17.0 Hz, 4H), 2.21 – 2.11 (m, 2H), 2.07 (s, 2H), 2.06 – 1.98 (m, 1H), 1.92 (ddd, *J* = 9.2, 6.5, 3.4 Hz, 2H), 1.82 (dd, *J* = 14.8, 5.9 Hz, 1H), 1.76 (q, *J* = 1.4 Hz, 3H), 1.40 (d, *J* = 0.8 Hz, 3H), 1.22 (t, *J* = 7.1

Hz, 3H). ^{13}C NMR (151 MHz, $CDCl_3$) δ 149.8, 137.8, 125.6, 108.6, 104.6, 83.8, 82.0, 77.3, 71.3, 62.4, 48.6, 46.4, 41.8, 41.0, 36.7, 30.6, 27.5, 25.2, 23.8, 20.8, 15.2. HRMS (ESI) calcd for $C_{21}H_{34}NaO_5$ [M + Na^+] *m/z* 389.2304, found 389.2295.

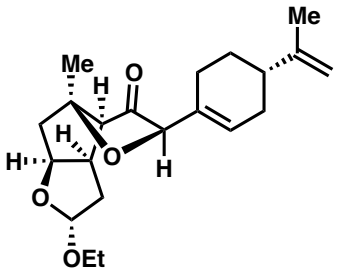


2.360(a/b): To a stirring solution of **2.356** (2.68 g, 5.58 mmol, 1 equiv) in DCM (25 mL) at –78 ºC was added triethylamine (7.77 mL, 55.8 mmol, 10 equiv) followed by thionyl chloride (0.465 mL, 0.417 mmol, 1.15 equiv). The resulting reaction mixture was then stirred at –78 ºC for 15 minutes. Upon completion of the reaction as indicated by TLC, the reaction was warmed to –50 ºC and quenched with saturated aqueous $NaHCO_3$ (10 mL). The organic layer was then separated and the aqueous phase was extracted with DCM (3 x 10 mL). The combined organic extracts were washed with brine (20 mL), dried over Na_2SO_4 and concentrated under reduced pressure. The crude oil was then purified by column chromatography (5% Et_2O in hexanes → 30% Et_2O in hexanes) to provide 2.59 g (4.91 mmol, 88%) mixture of sulfite isomers **2.360a and 2.360b** as an orange-yellow oil. **2.360a and 2.360b:** ^{1}H NMR (600 MHz, $CDCl_3$) δ 5.88 (dd, *J* = 54.3, 4.5 Hz, 2H), 5.32 (dd, *J* = 9.8, 5.4 Hz, 1H), 5.17 (d, *J* = 5.4 Hz, 1H), 5.08 (d, *J* = 4.6 Hz, 2H), 4.85 (dd, *J* = 9.8, 5.6 Hz, 1H), 4.81 (d, *J* = 5.6 Hz, 1H), 4.75 (s, 2H), 4.62 (q, *J* = 7.6 Hz, 2H), 3.65 (ddd, *J* = 10.5, 6.9, 3.6 Hz, 2H), 3.40 (dq, *J* = 9.5, 7.0 Hz, 2H), 3.21 (dq, *J* = 26.2, 8.8 Hz, 2H), 2.80 – 2.73 (m, 1H), 2.42 (ddd, *J* = 13.9, 9.8, 4.7 Hz, 1H), 2.34 (ddd, *J* = 13.8, 9.8, 4.6 Hz, 1H), 2.25 (s, 1H), 2.23 – 1.97 (m, 12H), 1.97 – 1.91 (m, 2H), 1.88 – 1.78 (m, 4H), 1.73 (d, *J* = 2.8 Hz, 6H), 1.30 – 1.14 (m, 14H), 0.88 (d, *J* = 8.8 Hz, 18H), 0.17 – 0.11 (m, 12H). ^{13}C NMR (151 MHz, $CDCl_3$) δ 149.0, 148.8, 133.6, 132.4, 131.8, 109.3, 109.2, 105.0, 104.8, 89.4, 87.4, 82.7, 82.6, 81.9, 81.3, 81.2, 78.3, 62.1, 62.0, 50.3, 49.7, 48.1, 48.0, 45.9, 45.9, 41.1, 40.9, 35.8, 35.7, 31.0, 30.7, 30.0, 29.7, 27.4, 27.2, 26.0, 25.9, 25.6, 24.8, 20.6, 20.6, 18.3, 18.3, 15.3, 15.3, -1.8, -1.8, -2.7, -2.7. HRMS (ESI) calcd for $C_{27}H_{46}NaO_6SSi$ [M + Na^+] *m/z* 549.2683, found 549.2677.

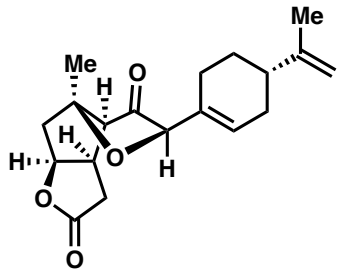


2.361: To a stirring solution of **2.360a and 2.360b** (2.59 g, 4.91 mmol, 1.0 equiv) in THF (45 mL) was added TBAF (1M in THF, 6.3 mL, 6.38 mmol, 1.3 equiv). The resulting reaction mixture was then stirred at 60 ºC for 1 hour. Upon completion of the reaction as indicated by TLC, the reaction was cooled to room temperature and quenched with saturated aqueous $NaHCO_3$ (10 mL). The organic layer was then separated and the aqueous phase was extracted with Et_2O (3 x 10 mL) and the combined organic extracts were washed with brine (100 mL), dried over Na_2SO_4 and concentrated under reduced pressure. The crude oil was then purified by column chromatography (5% Et_2O in hexanes → 45% Et_2O) to provide 1.36 g (3.78 mmol, 77%) of **2.361** as a clear colorless oil. **2.361**: ^{1}H NMR (700 MHz, $CDCl_3$) δ 5.96 (s, 1H), 5.15 (dd, *J* = 5.7, 2.2 Hz, 1H), 4.77 – 4.68 (m, 3H), 4.47 (td, *J* = 6.1, 2.8 Hz, 1H), 4.39 (s, 1H), 3.91 (d, *J* = 4.3 Hz, 1H), 3.72 (dq, *J* = 9.5, 7.1 Hz, 1H), 3.42 (dq, *J* = 9.6, 7.0 Hz, 1H), 2.99 – 2.92 (m, 1H), 2.31 (d, *J* = 10.2 Hz, 1H), 2.27 – 2.16 (m, 2H), 2.08 (dd, *J* = 15.4, 2.9 Hz, 1H), 2.05 – 1.96 (m, 6H), 1.74 (s, 3H), 1.53 (ddt, *J* = 16.3, 11.0, 5.7 Hz, 1H), 1.46 (s, 3H), 1.19 (t, *J* = 7.1 Hz, 3H). ^{13}C NMR (151 MHz, $CDCl_3$) δ 149.6, 132.8, 124.1, 108.8, 105.2, 92.8, 84.3,

83.8, 74.8, 63.0, 60.0, 44.3, 44.2, 41.4, 35.5, 30.3, 28.4, 27.2, 26.9, 20.8, 15.2. HRMS (ESI) calcd for $C_{21}H_{32}NaO_4$ [M + Na^+] *m/z* 371.2198, found 371.2192.



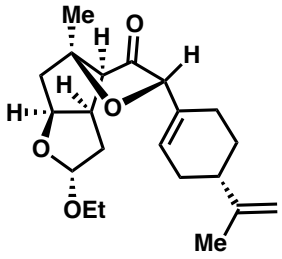
2.362: To a stirring solution of **2.361** (100 mg, 0.287 mmol, 1.0 equiv) in DCM (3 mL) was added *t*-BuOH (0.3 mL) and DMP (182.6 g, 0.431mmol, 1.5 equiv). The resulting reaction mixture was then stirred at 25 ºC for 3 hours or until the completion of the reaction as indicated by TLC. The reaction is then quenched with saturated aqueous solutions of $NaHCO_3$ (2 mL) and $Na_2S_2O_3$ (2 mL) and the biphasic mixture is stirred for 30 minutes. The organic layer was then separated and the aqueous phase was extracted with DCM (3 x 3 mL) and the combined organic extracts were washed with brine (5 mL), dried over Na_2SO_4 and concentrated under reduced pressure. The crude oil was then purified by column chromatography (4% Et_2O in hexanes → 30% Et_2O) to provide 92.4 mg (0.267 mmol, 93%) of **2.362** as a clear colorless oil. **2.362:** ^{1}H NMR (700 MHz, $CDCl_3$) δ 5.85 (d, *J* = 3.9 Hz, 1H), 4.92 (dd, *J* = 5.9, 3.0 Hz, 1H), 4.73 (dd, *J* = 12.0, 1.7 Hz, 2H), 4.50 (s, 1H), 4.45 (t, *J* = 4.7 Hz, 1H), 3.72 (dq, *J* = 9.7, 7.1 Hz, 1H), 3.43 (dq, *J* = 9.7, 7.1 Hz, 1H), 3.01 – 2.91 (m, 2H), 2.33 (d, *J* = 15.9 Hz, 1H), 2.27 – 2.17 (m, 3H), 2.17 – 2.13 (m, 1H), 2.12 (d, *J* = 9.9 Hz, 1H), 2.09 – 2.01 (m, 1H), 1.88 (ddd, *J* = 14.2, 7.8, 3.0 Hz, 1H), 1.82 (ddt, *J* = 11.4, 3.9, 2.0 Hz, 1H), 1.74 (s, 4H), 1.55 (s, 3H), 1.54 – 1.45 (m, 1H), 1.19 (t, *J* = 7.1 Hz, 3H). ^{13}C NMR (151 MHz, $CDCl_3$) δ 216.8, 149.6, 133.2, 127.7, 108.8, 105.1, 90.7, 84.6, 82.8, 63.4, 56.5, 48.8, 44.0, 40.7, 33.7, 30.6, 28.3, 27.3, 25.2, 20.7, 15.2. HRMS (EI+) calcd for $C_{21}H_{30}O_4$ *m/z* 346.2144, found 346.2142.



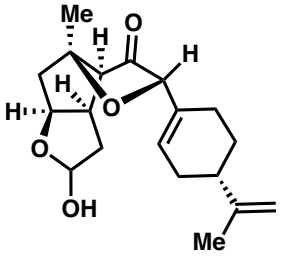
2.363a: *Step 1*. To a stirring solution of **2.362** (100 mg, 0.288 mmol, 1.0 equiv) in MeCN (2 mL) and H_2O (2 mL) was added PPTS (21.6 mg, 0.086 mmol, 0.3 equiv). The resulting reaction mixture was then stirred at 60 ºC for 8 hours. Upon completion of the reaction as indicated by TLC, the reaction was quenched with saturated aqueous $NaHCO_3$ (3 mL). The organic layer was then separated and the aqueous phase was extracted with Et_2O (3 x 4 mL) and the combined organic extracts were washed with brine (6 mL), dried over Na_2SO_4 and concentrated under reduced pressure. The crude material filtered through a plug of silica (eluting witg Et_2O) and concentrated to provide **SI-11** This material was carried on to the next step without any further purification.

Step 2. To a reaction tube containing the lactol **SI-11** prepared in the previous step, was added successively added TEMPO (18 mg, 0.115 mmol, 0.4 equiv), $PhI(OAc)_2$ (120.4 mg, 0.374 mmol, 1.3 equiv) and DCM (4 mL). The solution was stirred for 3 hours at 25 ºC until completion of the reaction, as judged by TLC. The reaction was quenched with saturated aqueous solutions of $NaHCO_3$ (2 mL) and $Na_2S_2O_3$ (2 mL). The organic layer was then separated and the aqueous phase was extracted with DCM (3 x 4 mL) and the combined organic extracts were washed with brine (5 mL), dried over Na_2SO_4 and concentrated under reduced pressure. The crude oil was then purified by column chromatography (1% Et_2O in DCM → 6% Et_2O in DCM) to provide 70.1 mg (0.222 mmol, 77%) of **2.363a** as a clear colorless oil. **2.363a**: ^{1}H NMR (600 MHz, $CDCl_3$) δ 5.82 – 5.66 (m, 1H), 4.84 (td, *J* = 6.3, 2.2 Hz, 1H), 4.71 – 4.56 (m, 2H), 4.30 (s, 1H), 3.22 – 3.10 (m, 1H), 3.04 (d, *J* = 18.3 Hz, 1H), 2.60 (dd, *J* = 18.1, 8.9 Hz, 1H), 2.47 – 2.33 (m, 2H), 2.24 – 2.16 (m, 1H), 2.11 (dt, *J* = 20.0, 12.8 Hz, 2H), 1.93 (t, *J* = 14.5 Hz, 1H), 1.74 (dd, *J*

= 14.8, 5.1 Hz, 2H), 1.65 (d, *J* = 1.3 Hz, 3H), 1.50 (s, 3H), 1.46 – 1.35 (m, 2H). ^{13}C NMR (151 MHz, $CDCl_3$) δ 214.7, 175.4, 149.4, 132.3, 127.2, 108.9, 90.1, 85.5, 84.8, 56.5, 44.3, 43.1, 40.7, 30.7, 30.5, 27.6, 27.2, 25.3, 20.7. HRMS (ESI) calcd for $C_{19}H_{24}NaO_4$ [M + Na^+] *m/z* 339.1572, found 339.1570.

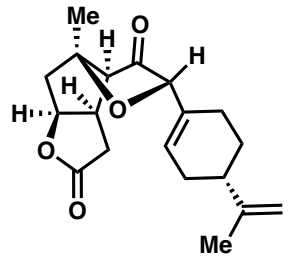


2.363b: To a stirring solution of **2.362** (109.5 mg, 0.316 mmol, 1.0 equiv) in THF (3 mL) at –78 ºC was added KHMDS (0.5 M in PhMe, 0.6 mL, 0.30 mmol, 0.95 equiv). The resulting reaction mixture was then stirred at –78 ºC for 30 minutes and then gradually warmed to –35 ºC over the course of 1 hour. This reaction mixture is stirred at –35 ºC for 5 minutes and then cooled to –78 ºC. In separate reaction tube, BHT (209 mg, 0.948 mmol, 3.0 equiv) is azeotropically dried (3x in benzene) and dissolved in freshly distilled and degassed THF (x mL). This solution of BHT is then transferred by syringe to the mixture containing the potassium enolate of **2.362** and stirred at –78 ºC for an additional 5 minutes. The reaction mixture is warmed to –35 ºC and quenched then with saturated aqueous $NaHCO_3$ (3 mL). The organic layer was then separated and the aqueous phase was extracted with Et_2O (3 x 3 mL). The combined organic extracts were washed with brine (5 mL) and dried over Na_2SO_4 and concentrated under reduced pressure. The crude oil was then purified by column chromatography (4% Et_2O in hexanes → 20% Et_2O) to provide 69.9 mg (0.202 mmol, 64%) of **2.363b** as a clear colorless oil and recovered **2.363b** (28.4 mg, %). **2.363b:** ^{1}H NMR (600 MHz, $CDCl_3$) δ 5.93 (s, 1H), 4.99 (dd, *J* = 5.6, 2.1 Hz, 1H), 4.77 – 4.71 (m, 3H), 4.66 (t, *J* = 5.6 Hz, 1H), 4.32 (s, 1H), 3.71 (dq, *J* = 9.6, 7.1 Hz, 1H), 3.41 (dq, *J* = 9.5, 7.1 Hz, 2H), 3.22 – 3.10 (m, 1H), 2.64 (d, *J* = 11.7 Hz, 1H), 2.55 (d, *J* = 15.6 Hz, 1H), 2.45 (d, *J* = 17.5 Hz, 1H), 2.36 (ddd, *J* = 14.1, 5.6, 3.8 Hz, 1H), 2.29 – 2.14 (m, 2H), 2.03 (dd, *J* = 15.5, 5.8 Hz, 1H), 2.01 – 1.83 (m, 3H), 1.75 (d, *J* = 1.4 Hz, 3H), 1.48 (s, 3H), 1.19 (t, *J* = 7.1 Hz, 3H). ^{13}C NMR (151 MHz, $CDCl_3$) δ 215.6, 149.8, 131.8, 125.7, 108.6, 104.9, 91.4, 84.4, 83.9, 62.9, 59.0, 46.6, 44.8, 40.9, 35.1, 30.6, 27.5, 25.2, 25.0, 20.8, 15.2. HRMS (ESI) calcd for $C_{21}H_{30}NaO_4$ [M + Na^+] *m/z* 369.2042, found 369.2038.

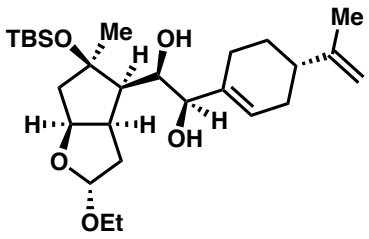


2.364 To a stirring solution of **2.363b** (150 mg, 0.433 mmol, 1.0 equiv) in MeCN (3 mL) and H_2O (4 mL) was added PPTS (32.4 mg, 0.144 mmol, 0.3 equiv). The resulting reaction mixture was then stirred at 60 ºC for 8 hours. Upon completion of the reaction as indicated by TLC, the reaction was quenched with saturated aqueous $NaHCO_3$ (4 mL). The organic layer was then separated and the aqueous phase was extracted with Et_2O (3 x 5 mL) and the combined organic extracts were washed with brine (10 mL), dried over Na_2SO_4 and concentrated under reduced pressure. The crude material filtered through a plug of silica (eluting witg Et_2O) and concentrated. This material was carried on to the next step without any further purification. **2.364:** ^{1}H NMR (700 MHz, $CDCl_3$) δ 5.94 – 5.89 (m, 1H), 5.42 (d, *J* = 5.5 Hz, 1H), 4.81 (t, *J* = 5.6 Hz, 1H), 4.77 – 4.69 (m, 3H), 4.33 (s, 1H), 3.23 – 3.13 (m, 1H), 2.65 (d, *J* = 11.6 Hz, 1H), 2.54 (d, *J* = 15.5 Hz, 1H), 2.49 – 2.38 (m, 3H), 2.27 – 2.12 (m, 3H), 2.05 (dd, *J* = 15.6, 5.8 Hz, 1H), 2.01 – 1.92 (m, 1H), 1.75 (s, 3H), 1.49 (s, 3H). ^{13}C NMR (151 MHz, $CDCl_3$) δ 215.3, 150.1, 149.7, 133.6, 131.8, 126.1, 125.9, 108.7, 108.5, 100.2, 99.6, 98.5, 91.2, 90.7, 87.6, 86.5, 84.7, 84.0, 59.2, 58.6, 47.6,

46.6, 44.8, 41.5, 40.9, 40.8, 35.7, 31.0, 31.0, 30.6, 27.7, 27.5, 27.1, 26.1, 25.1, 25.1, 20.8, 20.7. HRMS (ESI) calcd for $C_{19}H_{26}NaO_4$ [M + Na^+] *m/z* 341.1723, found 341.1726.

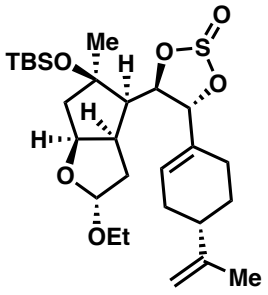


2.324: To a reaction tube containing the **2.364** (137 mg, 0.433 mmol, 1.0 equiv) was added successively added TEMPO (43.5 mg, 0.173 mmol, 0.4 equiv), $PhI(OAc)_2$ (223 mg, 0.693 mmol, 1.6 equiv) and DCM (8 mL). The solution was stirred for 3 hours at 25 ºC until completion of the reaction, as judged by TLC. The reaction was quenched with saturated aqueous solutions of $NaHCO_3$ (4 mL) and $Na_2S_2O_3$ (4 mL). The organic layer was then separated and the aqueous phase was extracted with DCM (3 x 6 mL) and the combined organic extracts were washed with brine (5 mL), dried over Na_2SO_4 and concentrated under reduced pressure. The crude oil was then purified by column chromatography (1% Et_2O in DCM → 6% Et_2O in DCM) to provide 111 mg (0.351 mmol, 81%) of **2.324** as a clear colorless oil. **2.324:** ^{1}H NMR (700 MHz, $CDCl_3$) δ 5.87 (t, *J* = 3.5 Hz, 1H), 5.07 (t, *J* = 6.3 Hz, 1H), 4.73 (dt, *J* = 2.1, 1.1 Hz, 2H), 4.35 (d, *J* = 1.8 Hz, 1H), 3.39 (dq, *J* = 12.3, 6.2 Hz, 1H), 2.82 (dd, *J* = 14.0, 9.4 Hz, 2H), 2.70 – 2.66 (m, 2H), 2.38 (d, *J* = 17.4 Hz, 1H), 2.22 – 2.11 (m, 3H), 2.07 – 1.98 (m, 1H), 1.95 – 1.83 (m, 2H), 1.77 – 1.72 (m, 3H), 1.53 (s, 3H), 1.51 – 1.44 (m, 1H). ^{13}C NMR (151 MHz, $CDCl_3$) δ 214.3, 175.5, 149.6, 130.1, 126.0, 108.7, 90.4, 86.6, 83.5, 59.3, 45.2, 42.7, 40.7, 31.8, 30.3, 27.3, 25.0, 23.7, 20.8. HRMS (ESI) calcd for $C_{19}H_{24}NaO_4$ [M + Na^+] *m/z* 339.1572, found 339.1567.

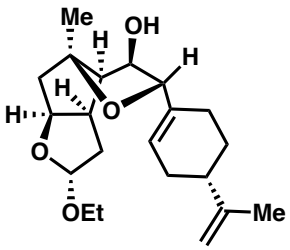


2.365: To a solution of DIBAL (1.0M in hexanes, 7.8 mL, 7.8 mmol, 10 equiv) in THF (8 mL) at 0 ºC was added *t*-BuLi (1.7M in pentane, 4.63mL, 7.8 mmol, 10 equiv) dropwise. The resulting yellow solution was stirred at 0 ºC for 5 minutes then cooled to –78 ºC. In a separate flask, **2.351** (410 mg, 0.787 mmol, 1.0 equiv) was dissolved in THF (8 mL). The solution containing X was then added dropwise to the solution containing the DIBAL/*t*-BuLi complex at –78 ºC. After allowing the reaction mixture to stir at –78°C for 30 minutes, the solution was warmed gradually to –10 °C and held at this temperature for 6 hours *(Special care is taken to ensure the reaction mixture does not warm above 0°C).* The reaction mixture was then quenched by careful addition of a saturated aqueous solution Rochelle's salt (20 mL). The biphasic mixture was stirred vigorously overnight, and the resulting well partitioned mixture was separated. The aqueous phase was extracted from with EtOAc (3 x 20 mL), and the combined organic phases were washed with brine (60 mL), dried over Na_2SO_4, and concentrated under reduced pressure. The resulting crude oil was purified by flash column chromatography (0% EtOAc in hexanes → 35% EtOAc in hexanes) to afford to provide 115 mg (0.315 mmol, 40%) of **2.365** as a clear colorless oil. ^{1}H NMR (700 MHz, $CDCl_3$) δ 5.89 – 5.85 (m, 1H), 5.11 (d, *J* = 4.6 Hz, 1H), 4.67 (d, *J* = 64.6 Hz, 2H), 4.60 (t, *J* = 7.8 Hz, 1H), 4.22 – 4.20 (m, 1H), 4.14 (s, 1H), 4.09 (d, *J* = 8.4 Hz, 1H), 3.73 – 3.64 (m, 1H), 3.43 (dq, *J* = 8.8, 6.9 Hz, 1H), 3.05 (p, *J* = 8.2 Hz, 1H), 2.84 – 2.76 (m, 1H), 2.62 (ddd, *J* = 13.9, 9.9, 4.8 Hz, 1H), 2.32 – 2.18 (m, 4H), 2.10 – 1.97 (m, 2H), 1.91 – 1.80 (m, 2H), 1.75 (s, 4H), 1.54 (tdd, *J* = 13.9, 8.3, 3.0 Hz, 1H), 1.41 (s, 4H), 1.21 (t, *J* = 7.1 Hz, 3H), 0.89 (s, 9H), 0.20 (s, 6H). ^{13}C NMR (151 MHz, $CDCl_3$) δ 151.0, 137.8,

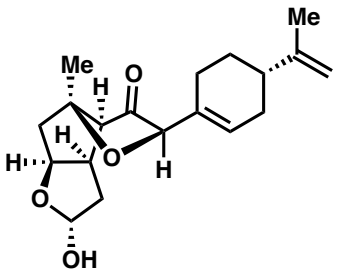
127.9, 110.3, 107.2, 88.3, 83.2, 80.5, 73.4, 64.0, 52.1, 49.0, 44.0, 41.8, 37.9, 31.9, 29.9, 28.6, 27.6, 24.6, 22.9, 19.8, 17.1, -0.0, -0.9. HRMS (ESI) calcd for $C_{27}H_{48}NaO_5Si$ [M + Na^+] *m/z* 503.3163, found 503.3164.



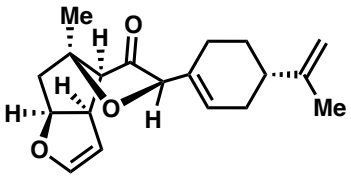
2.366: To a stirring solution of **2.365** (210 mg, 0.43 mmol, 1 equiv) in DCM (5 mL) at –78 ºC was added triethylamine (0.18 mL, 1.31 mmol, 3.0 equiv) followed by thionyl chloride (0.04 mL, 0.52 mmol, 1.2 equiv). The resulting reaction mixture was then stirred at –78 ºC for 15 minutes. Upon completion of the reaction as indicated by TLC, the reaction was warmed to –50 ºC and quenched with saturated aqueous $NaHCO_3$ (5 mL). The organic layer was then separated and the aqueous phase was extracted with DCM (3 x 5 mL) and the combined organic extracts were washed with brine (10 mL), dried over Na_2SO_4 and concentrated under reduced pressure. The crude oil was then purified by column chromatography (0% EtOAc in hexanes → 15% EtOAc in hexanes) to provide 225 mg (0.421 mmol, 98%) of **2.366** as a clear colorless oil. **2.366:** ^{1}H NMR (600 MHz, $CDCl_3$) δ 7.29 (s, 1H), 5.88 (d, *J* = 4.3 Hz, 1H), 5.11 (d, *J* = 4.7 Hz, 1H), 4.72 (t, *J* = 1.8 Hz, 1H), 4.63 (d, *J* = 2.1 Hz, 1H), 4.60 (t, *J* = 7.8 Hz, 1H), 4.21 (dd, *J* = 8.4, 2.9 Hz, 1H), 4.14 – 4.08 (m, 2H), 3.68 (dq, *J* = 9.7, 7.0 Hz, 1H), 3.43 (dq, *J* = 9.8, 7.0 Hz, 1H), 3.05 (p, *J* = 8.7 Hz, 1H), 2.62 (ddd, *J* = 12.9, 9.9, 4.8 Hz, 1H), 2.34 – 2.18 (m, 1H), 2.08 – 1.97 (m, 1H), 1.90 – 1.81 (m, 3H), 1.81 – 1.73 (m, 4H), 1.53 (ddt, *J* = 17.2, 12.8, 5.9 Hz, 2H), 1.46 – 1.38 (m, 4H), 1.21 (t, *J* = 7.0 Hz, 3H), 0.89 (s, 9H), 0.20 (s, 6H). ^{13}C NMR (151 MHz, $CDCl_3$) δ 151.0, 134.6, 131.5, 111.0, 106.7, 92.8, 85.3, 84.3, 82.3, 63.8, 59.0, 50.2, 48.1, 42.4, 37.4, 32.3, 31.1, 28.8 (d, *J* = 8.4 Hz), 27.7, 24.8, 22.5, 20.2, 17.2, -0.0, -0.9. HRMS (ESI) calcd for $C_{27}H_{46}NaO_6SSi$ [M + Na^+] *m/z* 549.2683, found 549.2677.



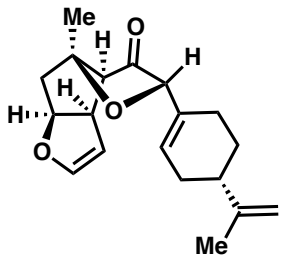
2.367: To a stirring solution of **2.366** (260 mg, 0.49 mmol, 1 equiv) in DMF (3 mL) was added 4Å molecular sieves (150 mg), and HMPA (0.5 mL). A solution of TASF (272 mg, 0.98 mmol, 2.0 equiv) in DMF (2 mL) was added dropwise to the solution containing the sulfite. The resulting reaction mixture was then stirred at 60 ºC for 3 hours. Upon completion of the reaction as indicated by TLC, the reaction was diluted with EtOAc (5 mL) and filtered through a pad of Celite eluting with EtOAc. The resulting solution was washed with water (5 mL), aqueous solution of LiCl (5%, 5 mL), brine (5 mL) and then dried over Na_2SO_4 and concentrated under reduced pressure. The crude oil was then purified by column chromatography (0% EtOAc in hexanes → 35% EtOAc in hexanes) to provide 63.3 mg (0.200 mmol, 41%) of **2.367** as a clear colorless oil. **2.367:** ^{1}H NMR (700 MHz, $CDCl_3$) δ 5.86 (d, *J* = 4.5 Hz, 1H), 5.25 (dd, *J* = 5.7, 1.9 Hz, 1H), 4.80 – 4.70 (m, 2H), 4.56 (td, *J* = 6.4, 2.5 Hz, 1H), 4.07 (d, *J* = 8.4 Hz, 1H), 3.93 (t, *J* = 8.2 Hz, 1H), 3.76 (dq, *J* = 9.7, 7.1 Hz, 1H), 3.46 (dq, *J* = 9.7, 7.0 Hz, 1H), 2.95 (tdd, *J* = 9.2, 6.1, 3.5 Hz, 1H), 2.45 (ddd, *J* = 14.1, 5.7, 3.5 Hz, 1H), 2.35 (d, *J* = 4.7 Hz, 1H), 2.27 (t, *J* = 8.5 Hz, 1H), 2.23 – 2.15 (m, 3H), 2.11 – 1.96 (m, 5H), 1.94 – 1.87 (m, 1H), 1.76 (q, *J* = 1.9 Hz, 3H), 1.51 (dt, *J* = 11.8, 5.7 Hz, 1H), 1.42 (d, *J* = 1.8 Hz, 3H), 1.22 (t, *J* = 7.1 Hz, 3H). ^{13}C NMR (151 MHz, $CDCl_3$) δ 149.8, 134.5, 126.6, 108.7, 105.8, 92.2, 88.9, 84.4, 76.4, 62.8, 59.4, 45.2, 43.1, 41.5, 35.1, 30.8, 27.6, 27.4, 23.4, 20.7, 15.2. HRMS (ESI) calcd for $C_{21}H_{32}NaO_4$ [M + Na^+] *m/z* 371.2198, found 371.2191.



2.368: To a stirring solution of **2.362** (100 mg, 0.290 mmol, 1.0 equiv) in MeCN (3 mL) and H_2O (3 mL) was added PPTS (80.2 mg, 0.319 mmol, 1.1 equiv). The resulting reaction mixture was then stirred at 60 ºC for 10 hours. Upon completion of the reaction as indicated by TLC, the reaction was quenched with saturated aqueous $NaHCO_3$ (3 mL). The organic layer was then separated and the aqueous phase was extracted with Et_2O (3 x 4 mL) and the combined organic extracts were washed with brine (3 mL), dried over Na_2SO_4 and concentrated under reduced pressure. The crude material was purified by column chromatography (10% Et_2O in hexanes → 100% Et_2O) to yield 90.4 mg (0.284 mmol, 98%). **2.368**: ^{1}H NMR (700 MHz, $CDCl_3$) δ 5.85 (d, *J* = 4.2 Hz, 1H), 5.37 – 5.31 (m, 1H), 4.76 – 4.71 (m, 2H), 4.60 (t, *J* = 4.8 Hz, 1H), 4.49 (s, 1H), 3.08 – 2.95 (m, 2H), 2.52 (s, 1H), 2.32 (d, *J* = 15.9 Hz, 1H), 2.28 – 2.12 (m, 5H), 2.05 (d, *J* = 30.7 Hz, 1H), 1.91 (ddd, *J* = 14.2, 7.7, 3.0 Hz, 1H), 1.87 – 1.79 (m, 1H), 1.74 (s, 3H), 1.58 (d, *J* = 9.8 Hz, 3H), 1.56 (s, 2H). ^{13}C NMR (151 MHz, $CDCl_3$) δ 216.7, 149.5, 133.1, 127.7, 108.8, 99.7, 90.7, 84.7, 83.1, 56.4, 49.0, 44.0, 40.7, 34.6, 30.6, 28.3, 27.3, 25.2, 20.7. HRMS (ESI) calcd for $C_{19}H_{26}NaO_4$ [M + Na^+] *m/z* 341.1723, found 341.1722.

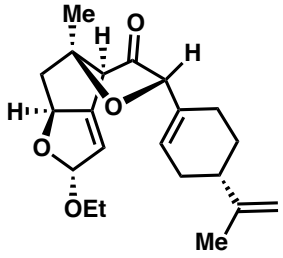


2.369: Lactol **2.368** (90 mg, 0.284 mmol, 1.0 equiv) was dissolved in THF (5 mL) and cooled to – 78 ºC. To this stirring solution was sequentially added triethylamine (0.4 mL, 2.82 mmol, 10.0 equiv) and MsCl (0.262 mL, 0.338 mmol, 1.2 equiv). The reaction mixture was stirred for 5 minutes at –78 ºC before it was transferred to a preheated oil bath at 60 ºC. After 10 minutes, or once the starting material has been consumed by TLC, the reaction was cooled to room temperature then quenched with saturated aqueous $NaHCO_3$ (3 mL). The organic layer was then separated and the aqueous phase was extracted with Et_2O (3 x 3 mL) and the combined organic extracts were washed with brine (10 mL), dried over Na_2SO_4 and concentrated under reduced pressure. The crude material was purified by column chromatography (10% Et_2O in hexanes → 100% Et_2O) to yield 59 mg (0.197 mmol, 70%). **2.369:** ^{1}H NMR (600 MHz, $CDCl_3$) δ 6.29 (t, *J* = 2.4 Hz, 1H), 5.88 – 5.79 (m, 1H), 5.06 (ddd, *J* = 9.2, 6.9, 4.1 Hz, 1H), 5.01 (t, *J* = 2.8 Hz, 1H), 4.79 – 4.70 (m, 2H), 4.33 (s, 1H), 3.77 (ddt, *J* = 11.4, 9.2, 2.4 Hz, 1H), 2.65 (d, *J* = 10.7 Hz, 1H), 2.46 (dd, *J* = 14.9, 4.1 Hz, 1H), 2.33 – 2.14 (m, 5H), 2.08 – 1.97 (m, 1H), 1.97 – 1.89 (m, 1H), 1.85 (ddt, *J* = 10.4, 5.9, 2.4 Hz, 1H), 1.74 (d, *J* = 1.2 Hz, 3H), 1.50 (s, 3H). ^{13}C NMR (151 MHz, $CDCl_3$) δ 215.0, 149.6, 145.7, 132.8, 125.7, 108.8, 100.6, 90.0, 87.2, 85.7, 61.5, 49.8, 45.9, 40.8, 30.5, 27.4, 26.6, 25.6, 20.7. HRMS (ESI) calcd for $C_{19}H_{24}NaO_3$ [M + Na^+] *m/z* 323.1623, found 323.1622.

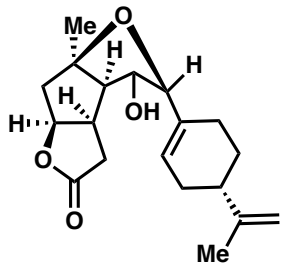


2.370: To a stirring solution of **2.369** (57 mg, 0.189 mmol, 1.0 equiv) in THF (2 mL) at –78 ºC was added KHMDS (0.5 M in PhMe, 0.36 mL, 0.180 mmol, 0.95 equiv). The resulting reaction mixture was then stirred at –78 ºC for 30 minutes and then gradually warmed to –35 ºC over the course of 1 hour. This reaction mixture is stirred at –35 ºC for 5 minutes and then cooled to –78 ºC. In separate reaction tube, BHT (125 mg, 0.567 mmol, 3 equiv) is azeotropically dried (3x in benzene) and dissolved in freshly distilled and degassed THF (1 mL). This solution of BHT is then transferred by syringe to the mixture containing the potassium enolate of **2.369** and stirred at –78

ºC for an additional 5 minutes. The reaction mixture is warmed to –35 ºC and quenched then with saturated aqueous $NaHCO_3$ (2 mL). The organic layer was then separated and the aqueous phase was extracted with Et_2O (3 x 2 mL) and the combined organic extracts were washed with brine (5 mL), dried over Na_2SO_4 and concentrated under reduced pressure. The crude oil was then purified by column chromatography (4% Et_2O in hexanes → 30% Et_2O) to provide 48 mg (0.160 mmol, 85%) of **2.370** as a clear colorless oil. **2.370**: ^{1}H NMR (600 MHz, $CDCl_3$) δ 6.20 (d, *J* = 15.8 Hz, 1H), 5.81 (t, *J* = 3.9 Hz, 1H), 5.47 (dd, *J* = 15.8, 8.3 Hz, 1H), 5.06 (td, *J* = 7.3, 4.0 Hz, 1H), 4.91 – 4.65 (m, 2H), 3.26 – 2.91 (m, 1H), 2.76 (ddd, *J* = 18.3, 9.2, 1.6 Hz, 1H), 2.47 (ddd, *J* = 15.0, 7.4, 1.6 Hz, 1H), 2.41 – 2.34 (m, 1H), 2.29 (dd, *J* = 24.9, 7.8 Hz, 1H), 2.25 – 2.04 (m, 4H), 2.01 – 1.89 (m, 2H), 1.78 (s, 3H), 1.54 (td, *J* = 11.9, 5.5 Hz, 1H), 1.32 (d, *J* = 1.6 Hz, 3H). ^{13}C NMR (151 MHz, $CDCl_3$) δ 177.1, 149.5, 138.0, 134.8, 129.6, 120.3, 108.9, 83.7, 81.6, 58.5, 47.4, 43.3, 41.1, 33.6, 31.3, 27.3, 26.0, 25.1, 20.8. HRMS (ESI) calcd for $C_{19}H_{24}NaO_3$ [M + Na^+] *m/z* 323.1623, found 323.1622.

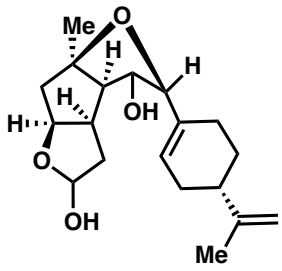


2.373: A solution of $Pd(OAc)_2$ (1.66 mg, 0.0074 mmol, 1.1 equiv) in PhMe (0.1 mL) was stirred vigorously at 65 ºC. In a separate flask containing **2.370** (2 mg, 0.0067 mmol, 1.0 equiv), was added PhMe (0.2 mL) and EtOH (1.95 µL g, 0.034 mmol, 5.0 equiv). The solution containing **2.370** was then added to the solution containing $Pd(OAc)_2$ in one shot washing with small amounts of PhMe (0.1 mL) to ensure quantitative transfer. The reaction mixture was stirred for 1 minutes at 65 ºC and then removed from the heat and cooled to room-temperature. The resulting crude reaction mixture was filtered over a plug of celite and washed with Et_2O. This mixture was then successively washed with saturated aqueous $NaHCO_3$ (0.5 mL), dried over Na_2SO_4, and concentrated under reduced pressure. The resulting crude oil was then purified by preparative thin layer chromatography to provide 1 mg (0.00302 mmol, 45%) of **2.373** as a clear colorless oil. **2.373:** ^{1}H NMR (700 MHz, $CDCl_3$) δ 5.9 (d, *J* = 3.5 Hz, 1H), 5.8 (s, 1H), 5.7 (s, 1H), 5.3 – 5.2 (m, 2H), 5.0 (s, 1H), 4.7 – 4.7 (m, 2H), 3.8 – 3.8 (m, 1H), 3.6 – 3.5 (m, 1H), 2.4 (dd, *J* = 13.2, 8.2 Hz, 1H), 2.3 (t, *J* = 7.5 Hz, 1H), 1.7 (s, 3H), 1.2 (t, *J* = 7.0 Hz, 19H). ^{13}C NMR (151 MHz, $CDCl_3$) δ128.6, 125.55 119.27 112.99 108.80 87.23 85.30 63.73 52.62 46.18 40.87 30.73 30.40 27.35 26.72 24.45 21.23 20.75 15.27 14.15.

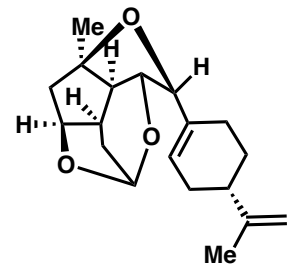


2.375: To a stirring solution of **2.324** (32.6 mg, 0.103 mmol, 1.0 equiv) in MeOH (1 mL) was added in one portion $NaBH_4$ (5.8 mg, 0.155 mmol, 1.5 equiv) at –78 ºC. The resulting solution was stirred at –78 ºC for 1 hour then warmed gradually to 0 ºC over the course of 2 hours. Upon completion of the reaction as indicated by TLC, the reaction was quenched with saturated aqueous H_2O (1 mL). This mixture was then extracted with Et_2O (3 x 2 mL), washed with brine (2 mL), dried over Na_2SO_4 and concentrated under reduced pressure. The resulting crude oil was then purified by column chromatography (10% Et_2O in hexanes → 40% Et_2O in hexanes) to provide 22.3 mg (0.070 mmol, 68%) of **2.375** as a clear colorless oil. ^{1}H NMR (600 MHz, $CDCl_3$) δ 5.95 (d, *J* = 5.2 Hz, 1H), 4.92 (dt, *J* = 8.7, 6.5 Hz, 1H), 4.70 – 4.60 (m, 2H), 4.46 (s, 1H), 4.01 (dd, *J* = 4.5, 2.3 Hz, 1H), 3.09 – 2.98 (m, 1H), 2.71 – 2.54 (m, 3H), 2.47 (dd, *J* = 9.4, 4.4 Hz, 1H),

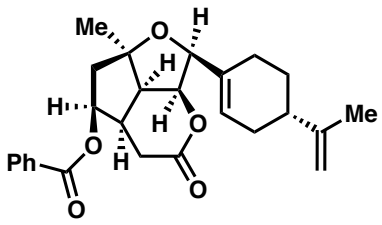
2.29 (d, J = 6.7 Hz, 2H), 2.09 (d, J = 10.1 Hz, 3H), 2.04 – 1.86 (m, 3H), 1.66 (q, J = 1.3 Hz, 3H), 1.30 (s, 3H). ^{13}C NMR (151 MHz, $CDCl_3$) δ 178.0, 149.4, 125.7, 109.2, 91.3, 87.5, 85.1, 71.9, 58.9, 47.7, 41.0, 37.3, 32.7, 30.2, 29.9, 27.9, 27.5, 27.0, 20.8. HRMS (ESI) calcd for $C_{19}H_{26}NaO_4$ [M + Na^+] *m/z* 341.1729, found 341.1721.



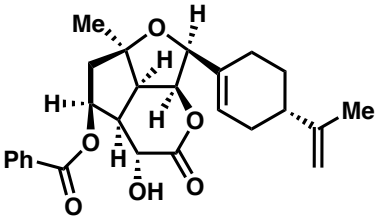
2.376: To a stirring solution of **2.375** (20 mg, 0.0628 mmol, 1.0 equiv) in DCM (3 mL) was added dropwise DIBAL (1M in PhMe, 0.0691 mL, 0.0691 mmol, 1.1 equiv) at –78 ºC. The resulting solution was stirred at –78 ºC for 1 hour then warmed gradually to 0 ºC over the course of 1 hour. Upon completion of the reaction as indicated by TLC, the reaction was quenched with saturated aqueous $NaHCO_3$ (1.5 mL) and saturated aqueous solution of Rochelle's salt (1.5 mL) and stirred for 3 hours. This mixture was then extracted with Et_2O (3 x 6 mL), washed with brine (2 mL), dried over Na_2SO_4 and concentrated under reduced pressure. The resulting crude oil was then purified by column chromatography (15% Et_2O in hexanes → 50% Et_2O in hexanes) to provide 14.3 mg (0.0446 mmol, 71%) of **2.376** as a clear colorless oil. **2.376:** ^{1}H NMR (700 MHz, $CDCl_3$) δ 5.81 (s, 1H), 5.50 (dd, J = 7.9, 5.2 Hz, 1H), 5.04 (s, 0H), 4.73 (d, J = 4.0 Hz, 2H), 4.37 (dd, J = 5.5, 3.3 Hz, 1H), 4.26 (d, J = 7.3 Hz, 1H), 4.07 – 4.02 (m, 1H), 3.42 (t, J = 11.7 Hz, 1H), 2.49 (d, J = 5.6 Hz, 1H), 2.37 – 2.30 (m, 1H), 2.25 (d, J = 14.9 Hz, 1H), 2.18 (dd, J = 12.7, 6.9 Hz, 2H), 2.10 (d, J = 6.9 Hz, 2H), 2.02 (t, J = 15.6 Hz, 1H), 1.84 (d, J = 12.8 Hz, 1H), 1.75 (d, J = 6.6 Hz, 4H), 1.61 (dt, J = 14.9, 5.4 Hz, 1H), 1.51 (ddd, J = 20.9, 11.5, 7.6 Hz, 1H), 1.38 (d, J = 3.7 Hz, 3H). ^{13}C NMR (151 MHz, $CDCl_3$) δ150.2, 121.7, 107.5, 88.7, 76.1, 68.3, 50.9, 47.0, 40.5, 39.2, 29.9, 29.4, 29.2, 28.8, 26.8, 25.97, 20.0, 19.9



2.377: Lactol **2.376** (5 mg, 0.0156 mmol, 1.0 equiv) was dissolved in THF (0.3 mL) and cooled to – 78 ºC. To this stirring solution was sequentially added 4ÅMS (*ca.* 0.5 mg) and freshly distilled pyrrolidine (1.28 μL, 1.1 μmol, 1.0). The reaction mixture was stirred for 5 minutes at 25 ºC. The reaction was then quenched with saturated aqueous $NaHCO_3$ (0.3 mL). The organic layer was then separated and the aqueous phase was extracted with Et_2O (3 x 0.5 mL) and the combined organic extracts were dried over Na_2SO_4 and concentrated under reduced pressure. The crude material was purified by preparative thin layer chromatography to yield 3.3 mg (0.011 mmol, 73%). **2.377**: ^{1}H NMR (600 MHz, $CDCl_3$) δ 5.77 – 5.72 (m, 1H), 5.35 (d, J = 3.7 Hz, 1H), 4.73 – 4.59 (m, 2H), 4.29 (t, J = 4.1 Hz, 1H), 3.96 (s, 1H), 3.83 (dd, J = 6.0, 2.4 Hz, 1H), 2.78 (dt, J = 8.7, 4.1 Hz, 1H), 2.67 (dd, J = 9.4, 6.0 Hz, 1H), 2.44 (d, J = 15.4 Hz, 1H), 2.14 – 2.04 (m, 5H), 2.00 – 1.92 (m, 1H), 1.85 (d, J = 11.8 Hz, 1H), 1.71 (ddt, J = 25.5, 11.8, 3.7 Hz, 3H), 1.65 (s, 3H), 1.28 (s, 3H). ^{13}C NMR (151 MHz, $CDCl_3$) δ 149.3, 132.0, 122.6, 107.4, 97.8, 91.0, 84.6, 84.4, 70.5, 56.7, 46.3, 40.4, 39.5, 31.0, 29.6, 26.7, 26.0, 25.8, 19.7. HRMS (ESI) calcd for $C_{19}H_{26}NaO_3$ [M + Na^+] *m/z* 325.1780, found 325.1781.

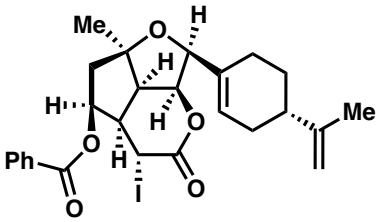


2.378: A reaction tube equipped with a magnetic stir bar was transferred to a nitrogen-filled glove-box. To this vessel was added AgOTf (40.4 mg, 0.157 mmol, 5.0 equiv). The sealed reaction vessel was then removed from the glove-box, placed under argon, and charged with DCM (0.7 mL). The resulting suspension was then cooled to –78 ºC. Freshly distilled benzoyl chloride (18.25 µL, 0.157 mmol, 5.0 equiv) was then added and the reaction mixture was then warmed to 0 ºC, resulting in a light pink solution. In a separate flask, lactone **2.375** (10 mg, 0.0314 mmol, 1.0 equiv) and pyridine (0.019 g, 0.236 mmol, 7.5 equiv) were dissolved in freshly distilled and degassed DCM (0.4 mL). The solution containing the benzoyl triflate was then transferred via syringe to the solution of **2.375** at – 78 ºC, washing with DCM (0.2 x 2) to ensure quantitative transfer. The reaction vessel was then removed from the acetone-dry ice bath and placed in a preheated oil bath at 60 ºC. Upon completion of the reaction as indicated by TLC, (typically 10 minutes) the reaction was cooled to room temperature and then quenched with saturated aqueous $NaHCO_3$ (1 mL). The organic layer was then separated and the aqueous phase was extracted with EtOAc (3 x 1 mL), washed with H_2O (3 mL), dried over Na_2SO_4 and concentrated under reduced pressure. The crude oil was then purified by column chromatography (8% Et_2O in hexanes → 30% Et_2O in hexanes) to provide 11.5 mg (0.0273 mmol, 87%) of **2.378** as a clear oil. **2.378:** ^{1}H NMR (600 MHz, $CDCl_3$) δ 8.06 – 7.90 (m, 2H), 7.53 – 7.46 (m, 1H), 7.38 – 7.33 (m, 2H), 5.75 (s, 1H), 5.43 (td, *J* = 6.5, 4.6 Hz, 1H), 4.87 (dd, *J* = 7.4, 4.0 Hz, 1H), 4.70 – 4.64 (m, 2H), 4.38 (s, 1H), 2.98 (dt, *J* = 10.8, 5.4 Hz, 1H), 2.77 (dd, *J* = 10.0, 7.4 Hz, 1H), 2.58 (dd, *J* = 16.6, 4.6 Hz, 1H), 2.50 – 2.34 (m, 2H), 2.13 (dd, *J* = 15.0, 6.4 Hz, 1H), 2.07 (d, *J* = 6.6 Hz, 2H), 1.97 – 1.84 (m, 1H), 1.74 (d, *J* = 12.3 Hz, 1H), 1.67 (d, *J* = 1.2 Hz, 3H), 1.37 (s, 3H), 1.19 (s, 3H).^{13}C NMR (151 MHz, $CDCl_3$) δ ^{13}C NMR (151 MHz, $CDCl_3$) δ 171.0, 166.3, 150.0, 133.2, 131.1, 130.1, 128.3, 123.9, 108.7, 89.6, 84.7, 81.7, 77.5, 50.8, 44.9, 41.2, 38.7, 30.4, 28.8, 25.0, 20.7, 17.5, 13.6. HRMS (ESI) calcd for $C_{26}H_{30}NaO_5$ [M + Na^+] *m/z* 445.1991, found 445.1988.

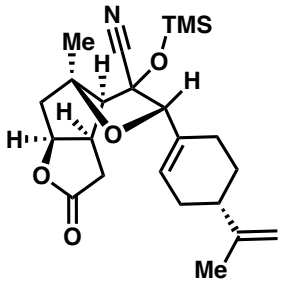


2.379a: To a stirring solution of **2.378** (2 mg, 3.46 µmol, 1.0 equiv) in THF (0.3 mL) was added Et_3B (1 M in THF, 3.46 µL, 3.46 µmol, 1.0 equiv) and Bu_3SnH (2.0 µL, 7.28 µmol, 2.0 equiv) at –78 ºC. A balloon of O_2 was bubbled through the stirring reaction mixture –78 ºC for 15 minutes then bubbling of O2 was ceased and the balloon was replaced with a balloon filled with argon. The reaction mixture was then warmed to 0 ºC at which point it was quenched with a with saturated aqueous solutions of $NaHCO_3$ (0.2 mL). The biphasic mixture was diluted with Et_2O (1 mL) and the organic layer was then separated. The aqueous phase was extracted with Et_2O (3 x 1 mL) and the combined organic extracts were washed with brine (1 mL), dried over Na_2SO_4 and concentrated under reduced pressure. The crude oil was then purified by preparative thin layer chromatography to provide to provide 0.8 mg (1.83 µmol,53%) of **2.379a** as a clear oil. **2.379a:** ^{1}H NMR (700 MHz, $CDCl_3$) δ 8.13 – 8.03 (m, 2H), 7.55 (t, *J* = 7.4 Hz, 1H), 7.43 (t, *J* = 7.7 Hz, 2H), 5.89 (s, 1H), 5.60 (q, *J* = 7.3 Hz, 1H), 5.22 (dd, *J* = 8.4, 5.5 Hz, 1H), 4.76 – 4.68 (m, 2H), 4.59 (d, *J* = 8.8 Hz, 1H), 4.52 (d, *J* = 5.5 Hz, 1H), 2.98 (dt, *J* = 8.9, 4.3 Hz, 2H), 2.89 (t, *J* = 8.7 Hz, 1H), 2.58 (dd, *J* = 14.7, 7.5 Hz, 1H), 2.37 (dd, *J* = 14.8, 7.7 Hz, 1H), 2.21 – 2.08 (m, 3H), 2.04 (d, *J* = 16.7 Hz, 1H), 1.94 (d, *J* = 16.8 Hz, 1H), 1.82 (d, *J* = 13.1 Hz, 1H), 1.73 (s, 3H), 1.42 (s, 3H). ^{13}C NMR (151 MHz, $CDCl_3$) δ 173.0, 166.5, 149.8, 133.2, 131.1,

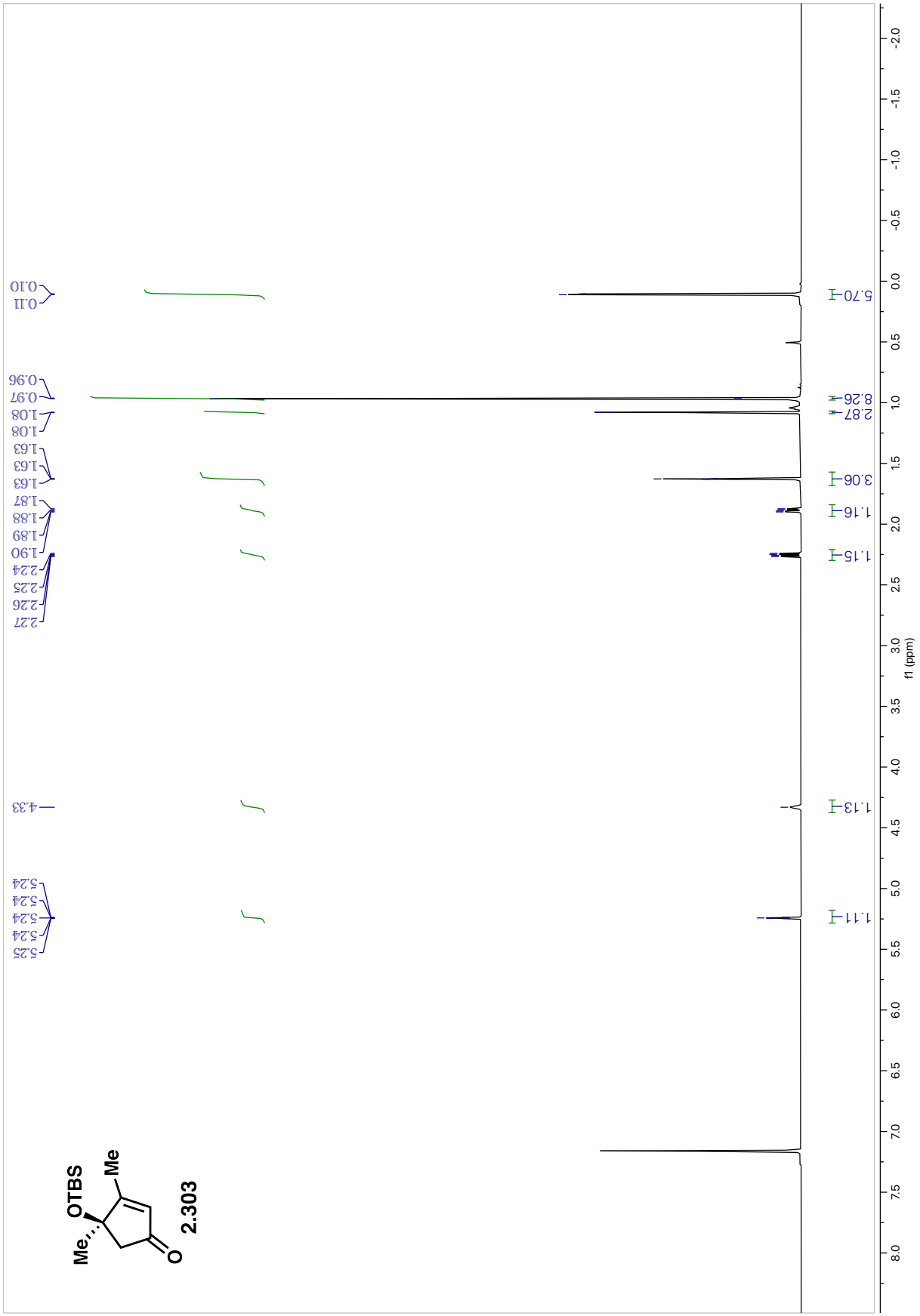
130.0 (d, J = 5.6 Hz), 128.5, 123.5, 109.0, 88.3, 83.8, 81.9, 75.9, 65.8, 48.9, 45.0, 43.6, 41.3, 30.4, 29.9, 27.5, 26.8, 24.5, 20.9. HRMS (ESI) calcd for $C_{26}H_{31}O_6$ [M + Na^+] *m/z* 439.2121, found 439.2114.



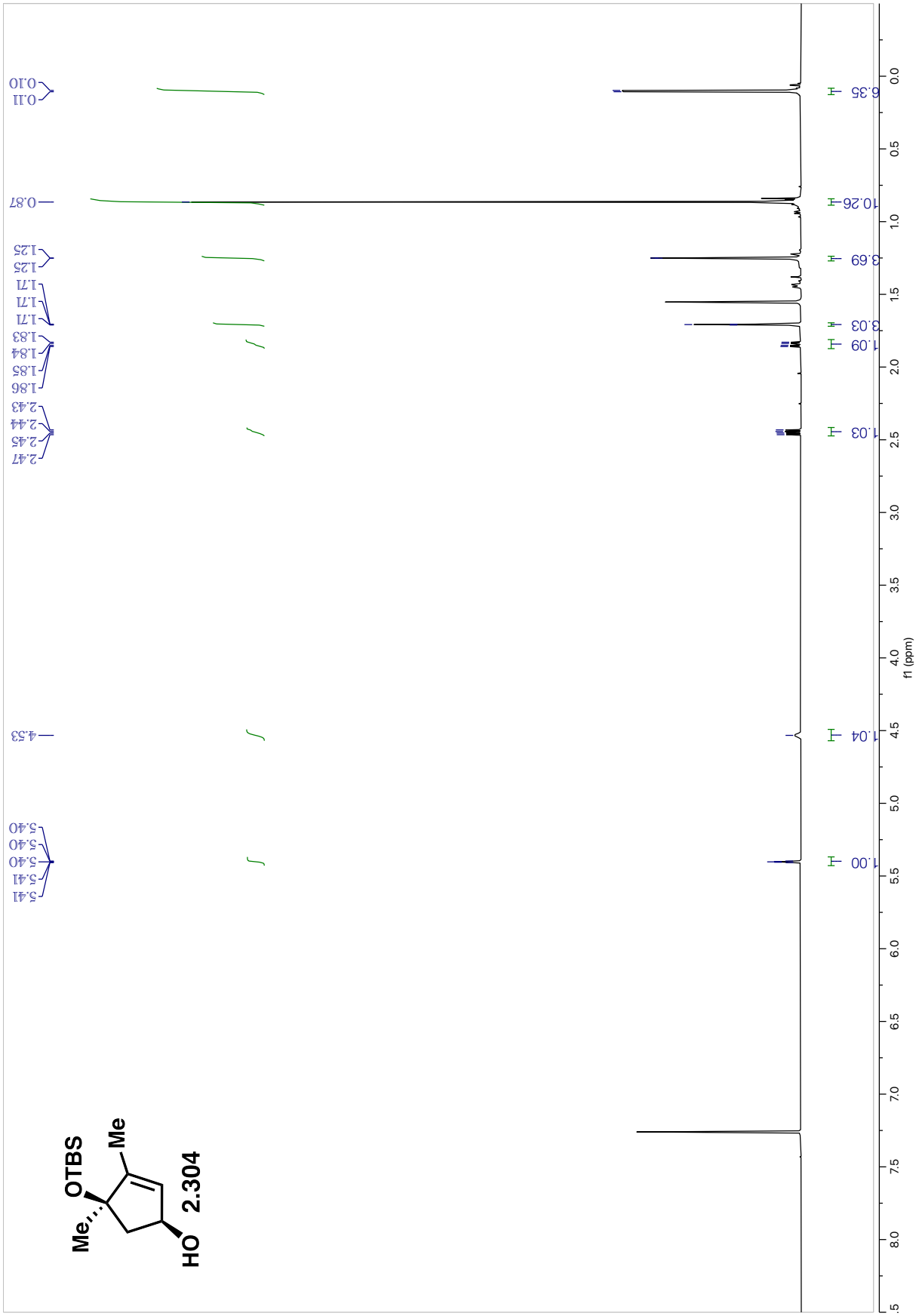
2.382: To a stirring solution of **2.378** (17.8 g, 0.0422 mmol, 1.0 equiv) in THF was added dropwise a freshly prepared solition of LHMDS (1 M in THF, 0.06 mL, 0.59 mmol, 1.0 equiv) at –78 ºC. The resulting solution was stirred at –78 ºC for 1 hour then warmed gradually to –30 ºC over the course of 30 minutes. The reaction mixture was then cooled to –78 ºC at which point a solution of I_2 (6.42 mg, 0.0506 mmol, 1.2 equiv) in THF (0.4 mL) was added dropwise. Upon completion of the reaction as indicated by TLC, the reaction was diluted with Et_2O (1 mL) quenched with saturated aqueous solutions of $NaHCO_3$ (0.5 mL) and $Na_2S_2O_3$ (0.5 mL). The organic layer was then separated and the aqueous phase was extracted with Et_2O (3 x 1 mL) and the combined organic extracts were washed with brine (1 mL), dried over Na_2SO_4 and concentrated under reduced pressure. The crude oil was then purified by column chromatography (5% Et_2O in hexanes → 25% Et_2O in hexanes) to provide 17.8 mg (0.0325 mmol, 77%) of **2.382** as a clear oil. **2.382:** ^{1}H NMR (600 MHz, $CDCl_3$) δ 7.98 – 7.91 (m, 2H), 7.49 – 7.45 (m, 1H), 7.33 (t, J = 7.8 Hz, 2H), 5.71 (d, J = 5.0 Hz, 1H), 5.46 (td, J = 5.7, 1.5 Hz, 1H), 5.07 (dd, J = 7.3, 3.5 Hz, 1H), 4.68 (s, 2H), 4.53 (d, J = 2.3 Hz, 1H), 4.36 (s, 1H), 3.15 (ddd, J = 10.5, 6.0, 2.3 Hz, 1H), 2.97 (dd, J = 10.5, 7.3 Hz, 1H), 2.48 (dd, J = 15.8, 1.5 Hz, 1H), 2.17 – 2.08 (m, 3H), 2.02 (dd, J = 15.7, 5.6 Hz, 2H), 1.95 – 1.81 (m, 2H), 1.75 (d, J = 13.0 Hz, 2H), 1.68 (d, J = 1.2 Hz, 3H), 1.38 (s, 3H). ^{13}C NMR (151 MHz, $CDCl_3$) δ 167.1, 166.3, 149.9, 133.3, 130.7, 130.2, 128.3, 124.2, 108.7, 89.6, 84.3, 82.7, 77.8, 50.3, 49.9, 46.0, 41.1, 30.4, 27.4, 26.7, 24.7, 20.8, 10.6. HRMS (ESI) calcd for $C_{26}H_{29}INaO_5$ [M + Na+] m/z 549.1139, found 549.1132.

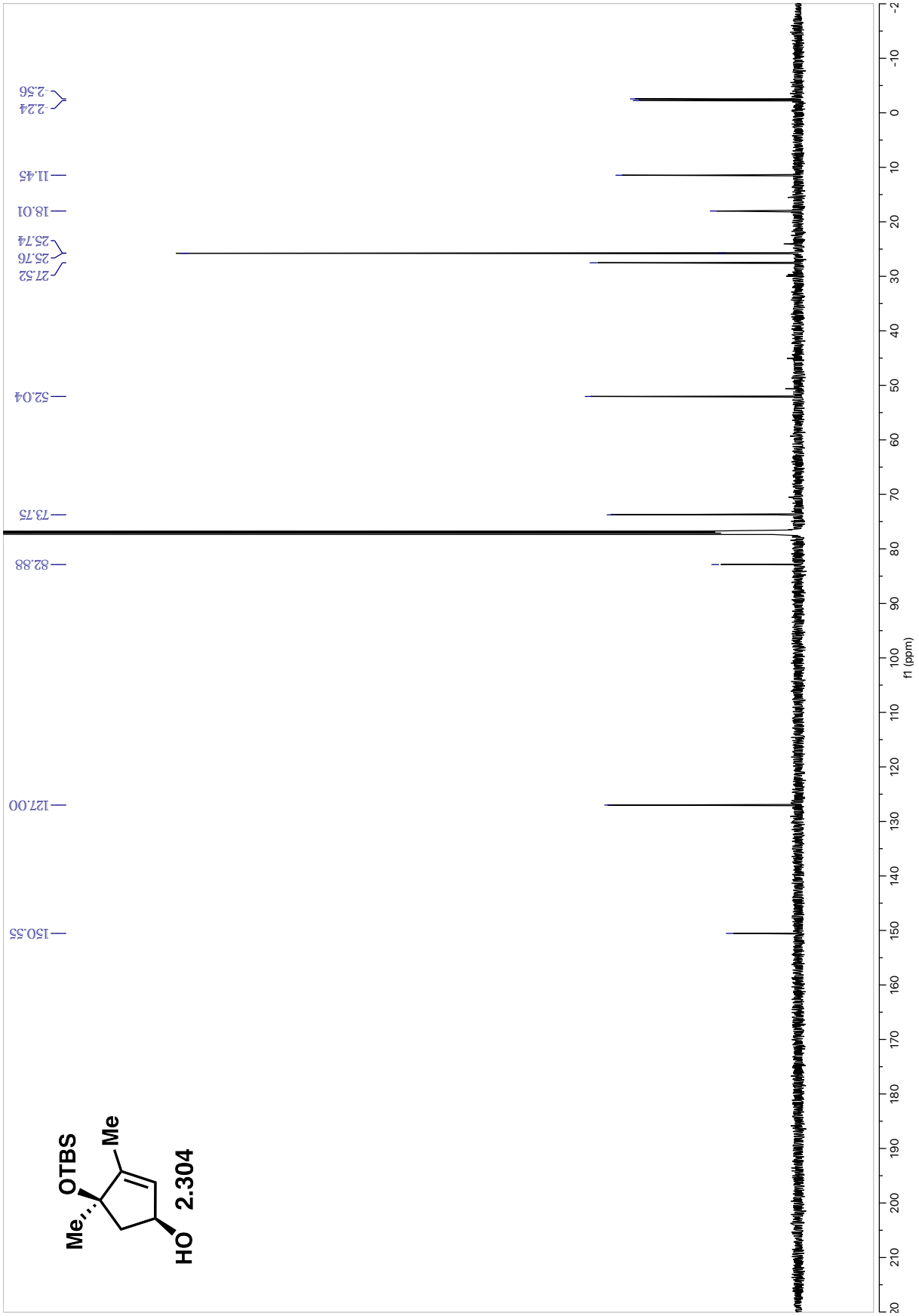


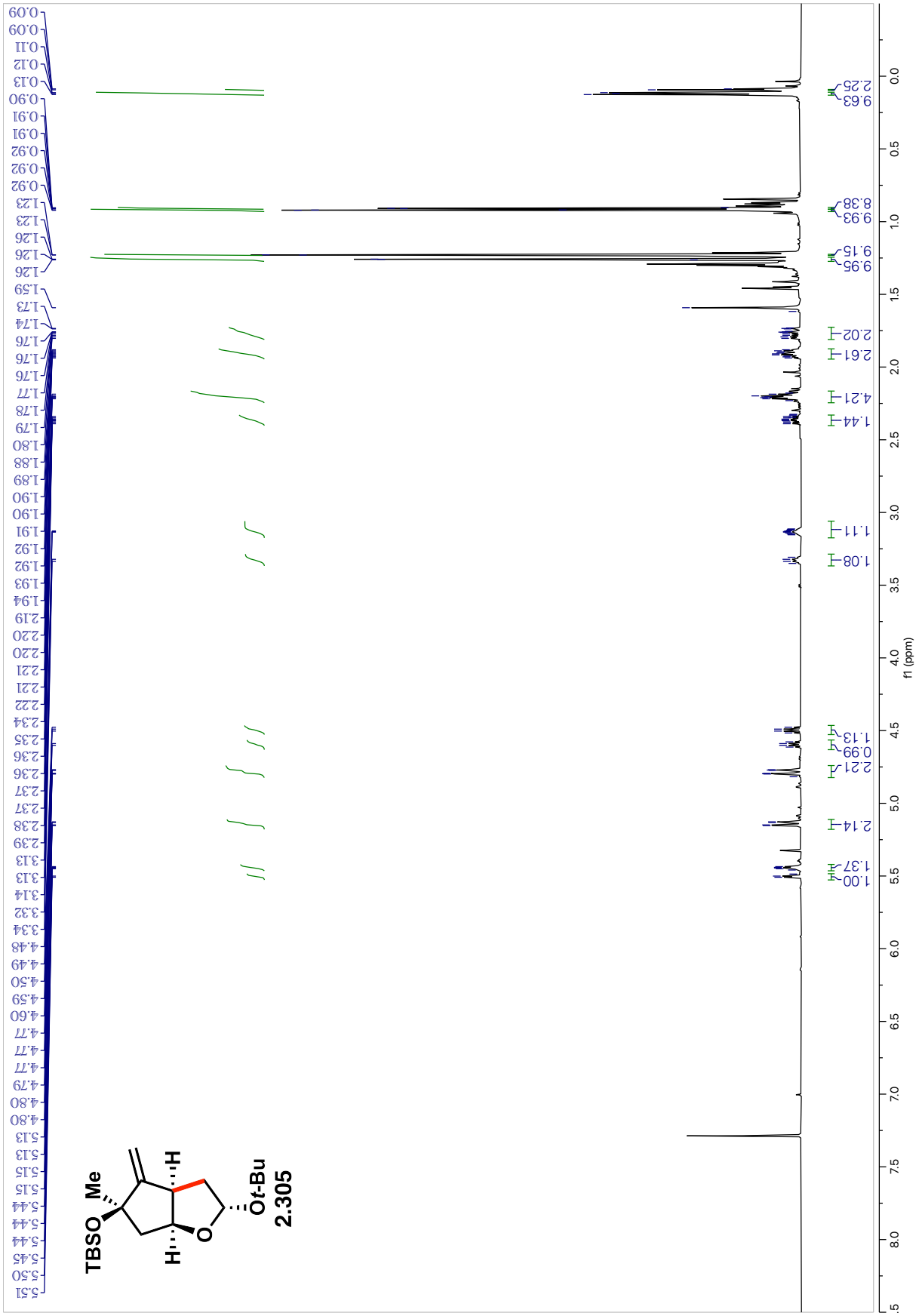
2.390: To a stirring solution of **2.324** (103 mg, 0.326 mmol, 1.0 equiv) in DCM (3 mL) was sequentially added Et_3N (0.045 mL, 0.326 mmol, 1.0 equiv) and TMSCN (0.045 mL, 0.359 mmol, 1.1 equiv) at 25 ºC. The reaction mixture was stirred at 25 ºC for 12 hours or upon completion of the reaction, as indicated by TLC. The reaction was then quenched with a with a saturated aqueous solution of $NaHCO_3$ (1.0 mL). The biphasic mixture was diluted with DCM (1 mL) and the organic layer was then separated. The aqueous phase was extracted with DCM (3 x 1 mL) and the combined organic extracts were washed with brine (1 mL), dried over Na_2SO_4 and concentrated under reduced pressure. The crude oil was then purified by column chromatography (5% Et_2O in hexanes → 50% Et_2O in hexanes) to provide 85.1 mg (0.205 mmol, 63%) of **2.390** as a light yellow oil. **2.390:** ^{1}H NMR (600 MHz, $CDCl_3$) δ 5.96 (s, 1H), 5.04 (qd, J = 7.2, 4.0 Hz, 1H), 4.76 (d, J = 16.0 Hz, 2H), 4.67 (s, 1H), 3.14 – 3.08 (m, 1H), 3.04 (ddd, J = 18.6, 7.3, 3.1 Hz, 1H), 2.97 (dd, J = 8.6, 3.1 Hz, 1H), 2.66 (ddd, J = 18.5, 10.7, 3.1 Hz, 1H), 2.43 – 2.38 (m, 2H), 2.30 – 2.17 (m, 3H), 2.07 (dd, J = 34.9, 19.4 Hz, 2H), 1.90 (d, J = 13.0 Hz, 1H), 1.77 (d, J = 3.7 Hz, 3H), 1.53 (dd, J = 12.0, 4.5 Hz, 1H), 1.45 (d, J = 3.2 Hz, 3H), 0.36 – 0.29 (m, 9H). ^{13}C NMR (151 MHz, $CDCl_3$) δ 177.3, 149.4, 130.7, 126.7, 121.0, 109.1, 90.1, 89.9, 83.7, 75.7, 63.1, 45.8, 40.8, 39.9, 32.3, 30.5, 27.3, 27.3, 24.6, 20.9, 1.2. HRMS (ESI) calcd for $C_{23}H_{33}NNaO_4Si$ [M + Na^+] *m/z* 438.2075, found 438.2071.

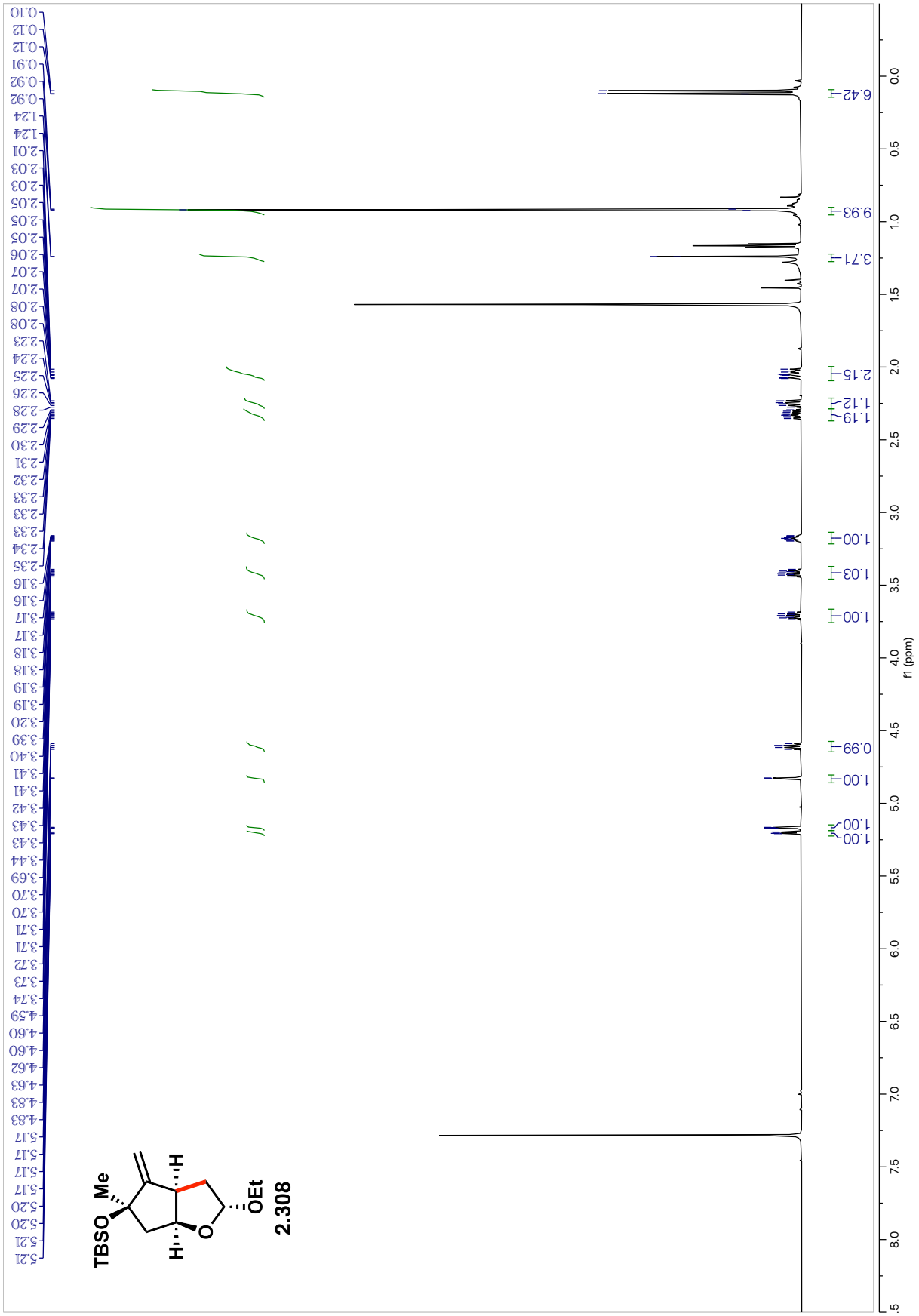

OTBS
Me
Me
O
2.303
0.11
0.10
0.97
0.96
1.08
1.08
1.63
1.63
1.63
1.87
1.88
1.89
1.90
2.24
2.25
2.26
2.27
4.33
5.24
5.24
5.24
5.24
5.25
5.70
8.26
2.87
3.06
1.16
1.15
1.13
1.11
f1 (ppm)

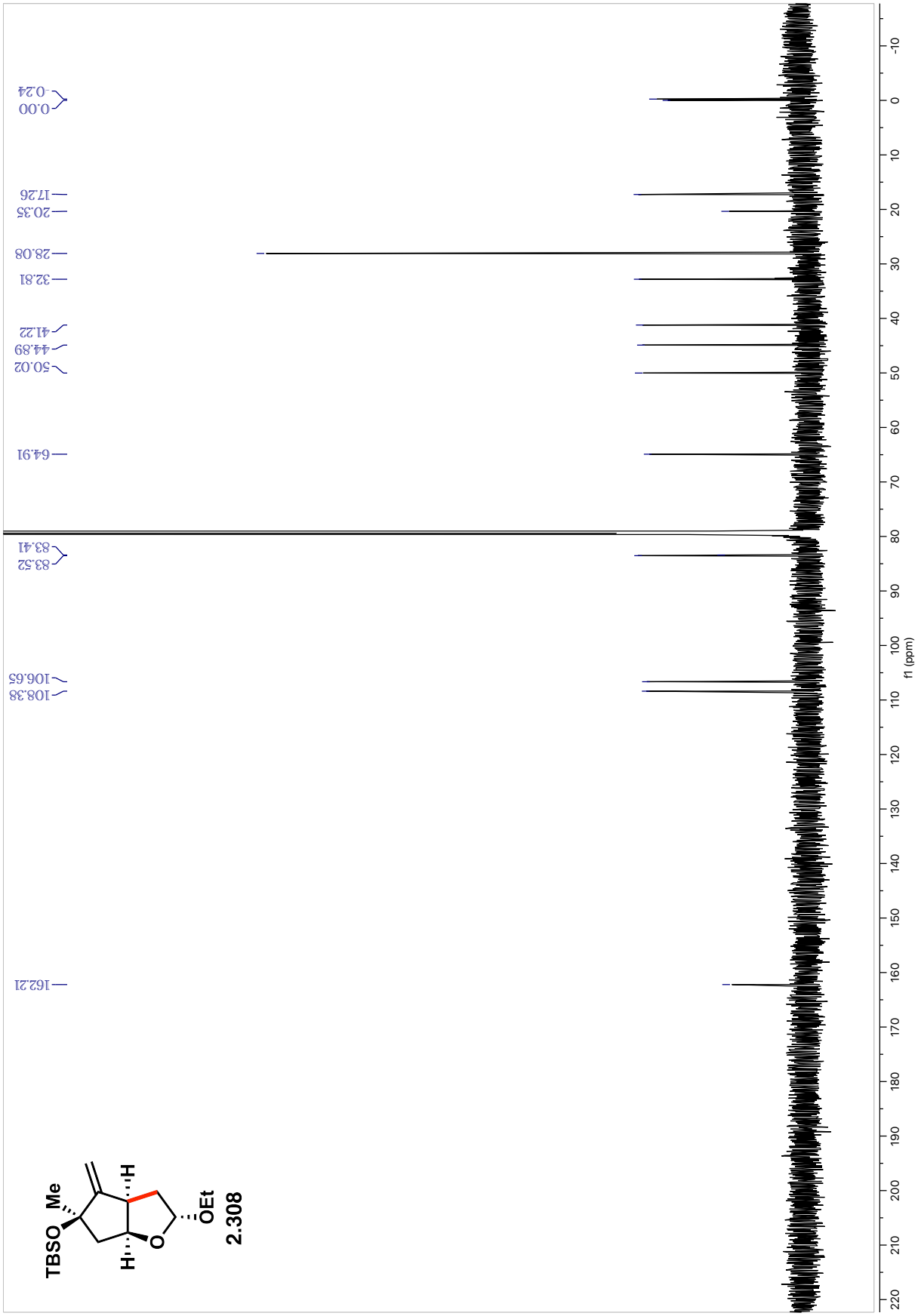

148.97
82.78
73.05
52.03
27.44
25.69
17.95
11.18
-2.41
-2.84
f1 (ppm)
OTBS
Me
Me
O
2.303

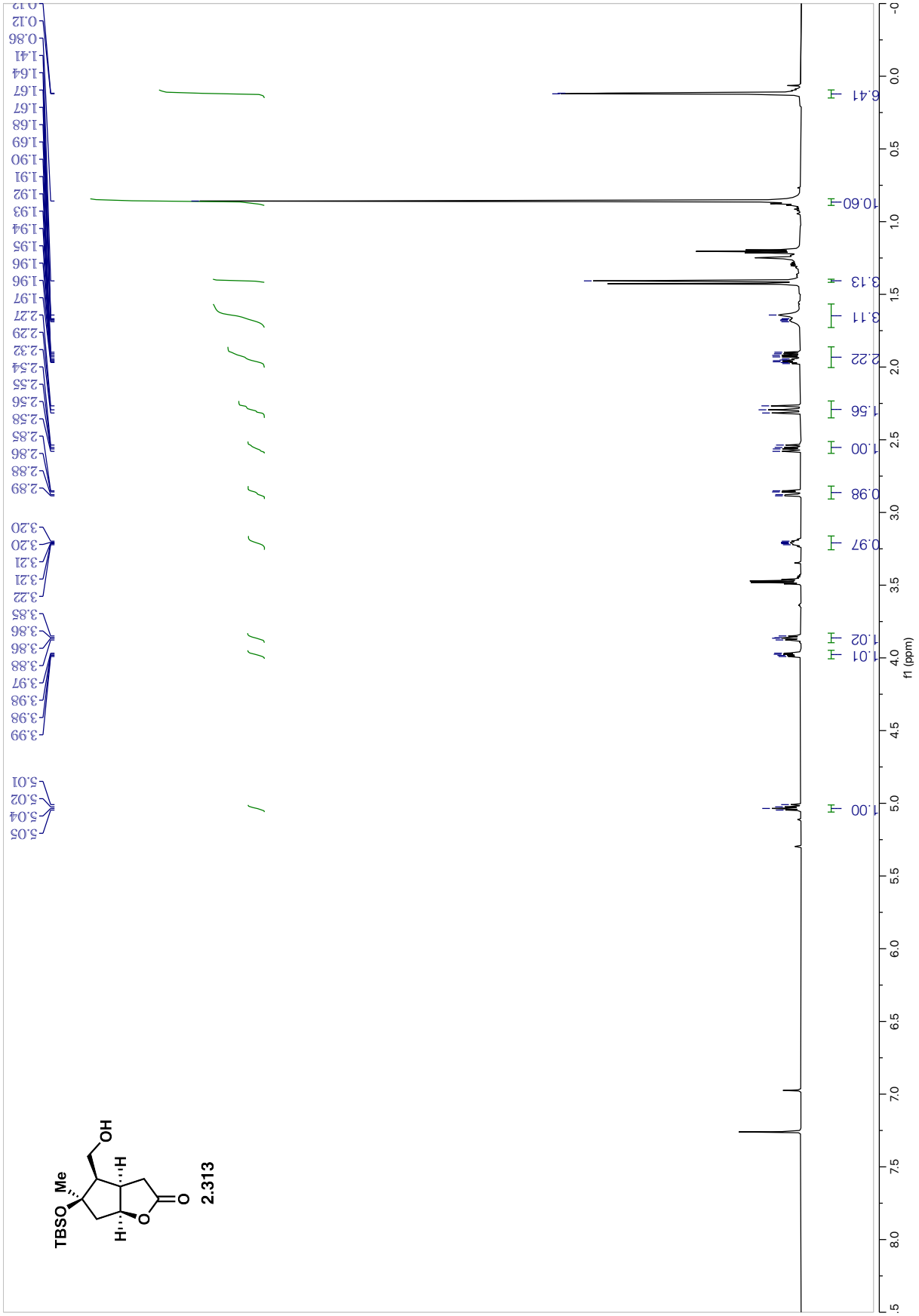

OTBS
Me
Me
HO
2.304
0.10
0.11
0.87
1.25
1.25
1.71
1.71
1.71
1.83
1.84
1.85
1.86
2.43
2.44
2.45
2.47
4.53
5.40
5.40
5.40
5.41
5.41
6.35
10.26
3.69
3.03
1.09
1.03
1.04
1.00
f1 (ppm)

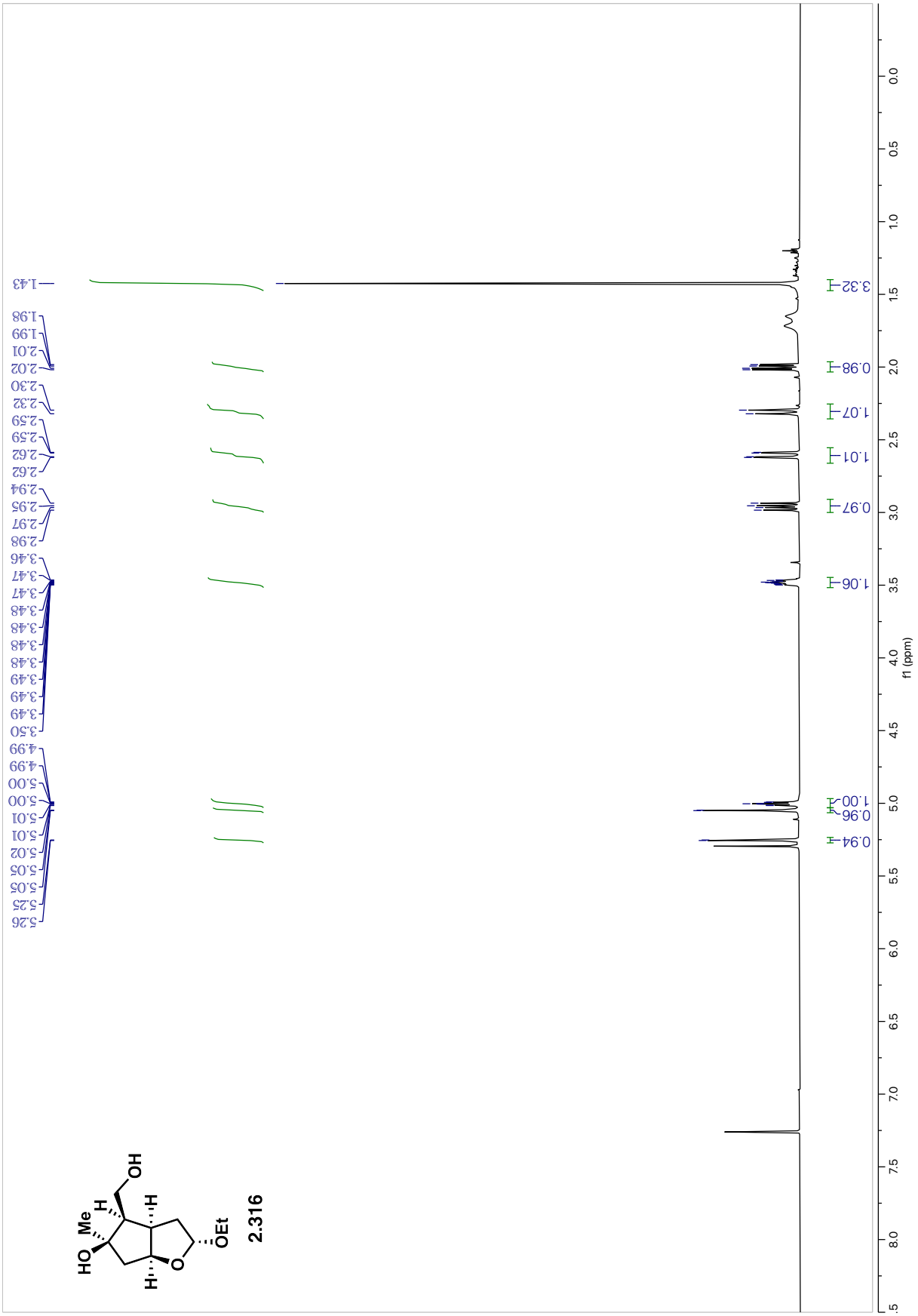

OTBS
Me
Me
HO
2.304
150.55
127.00
82.88
73.75
52.04
27.52
25.76
25.74
18.01
11.45
2.24
2.56
f1 (ppm)

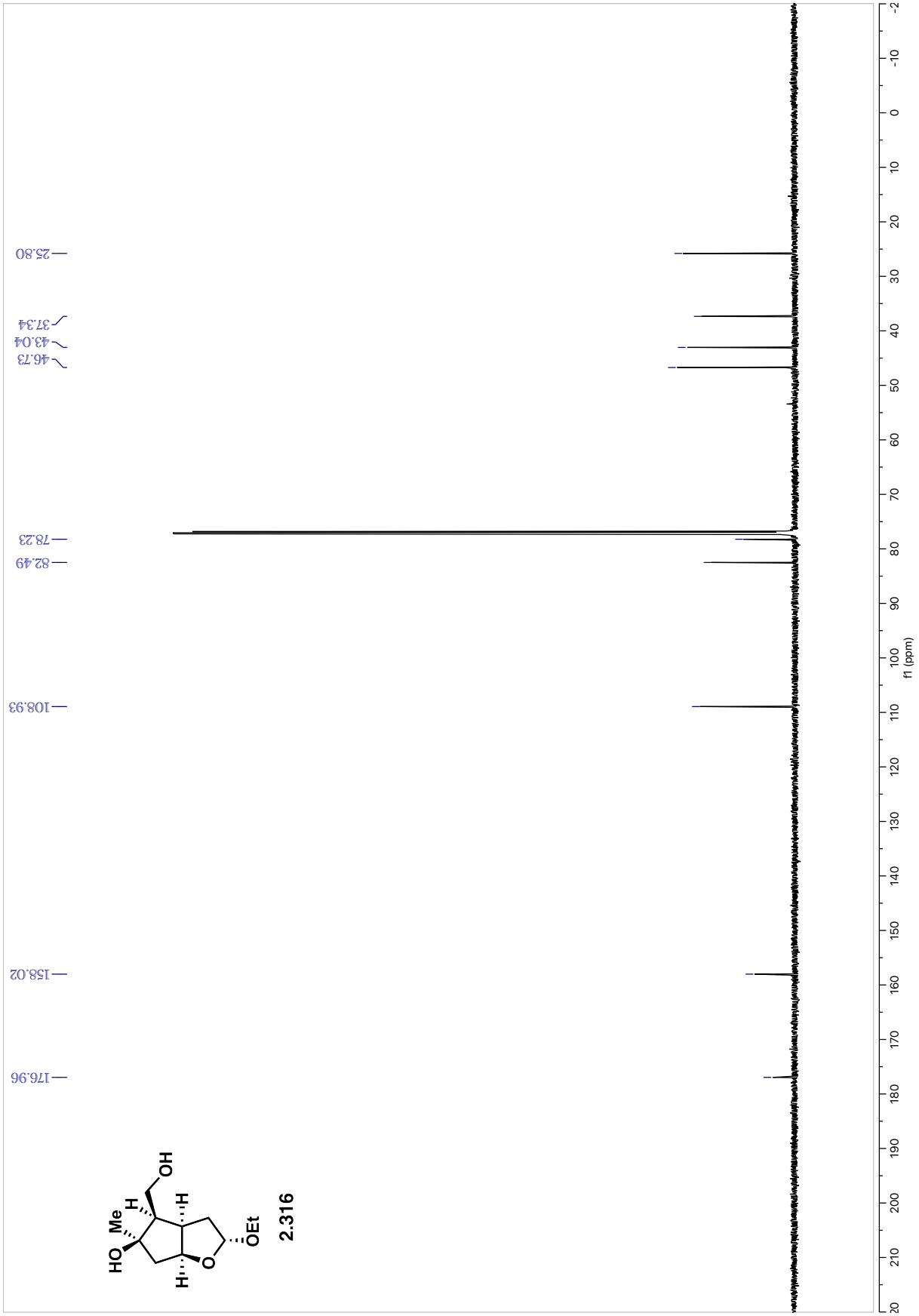

TBSO
Me
H
H
O
Ot-Bu
2.305
f1 (ppm)

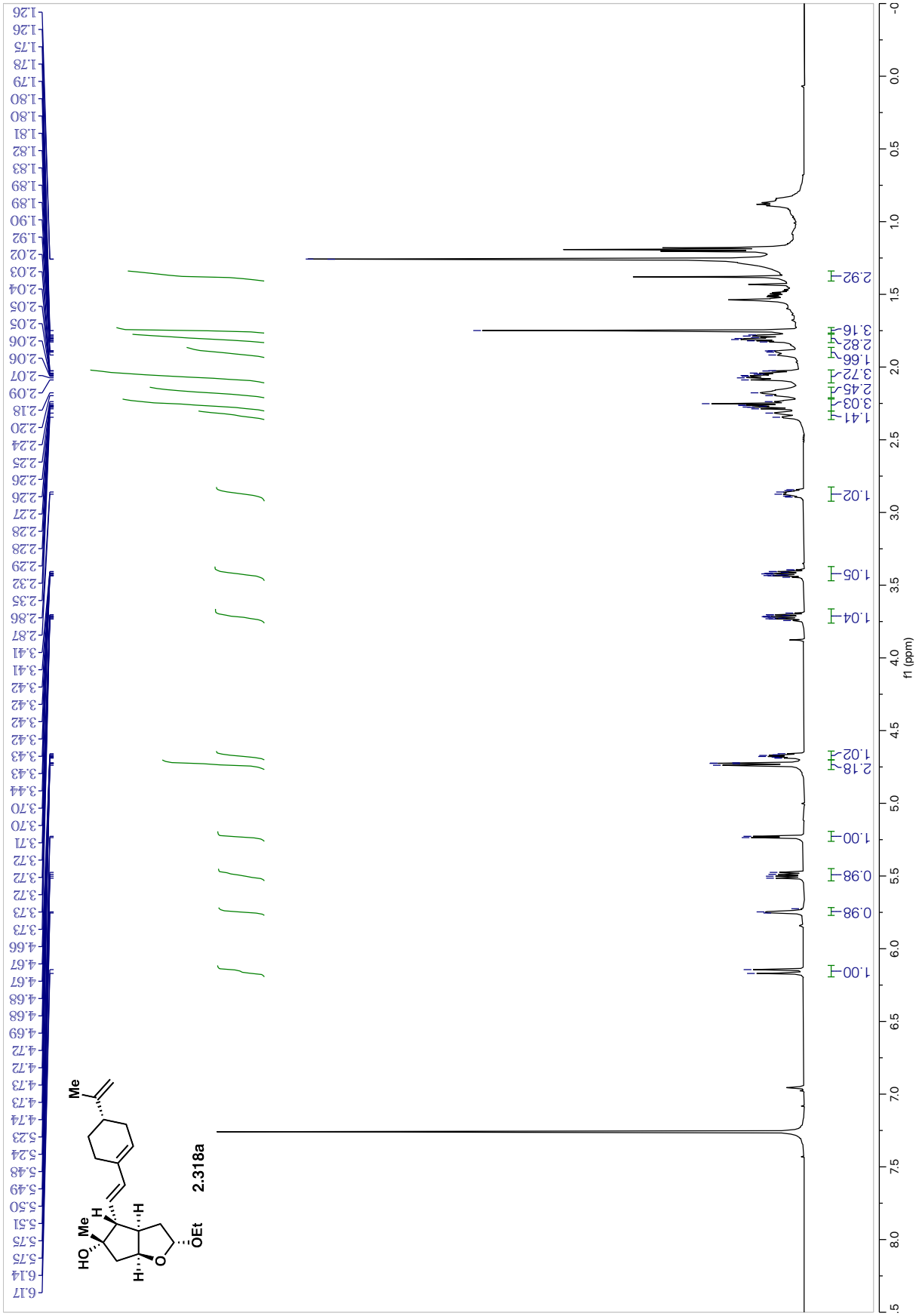

TBSO
Me
H
H
O
OEt
2.308
6.42
9.93
3.71
2.15
1.12
1.19
1.00
1.03
1.00
0.99
1.00
1.00
f1 (ppm)

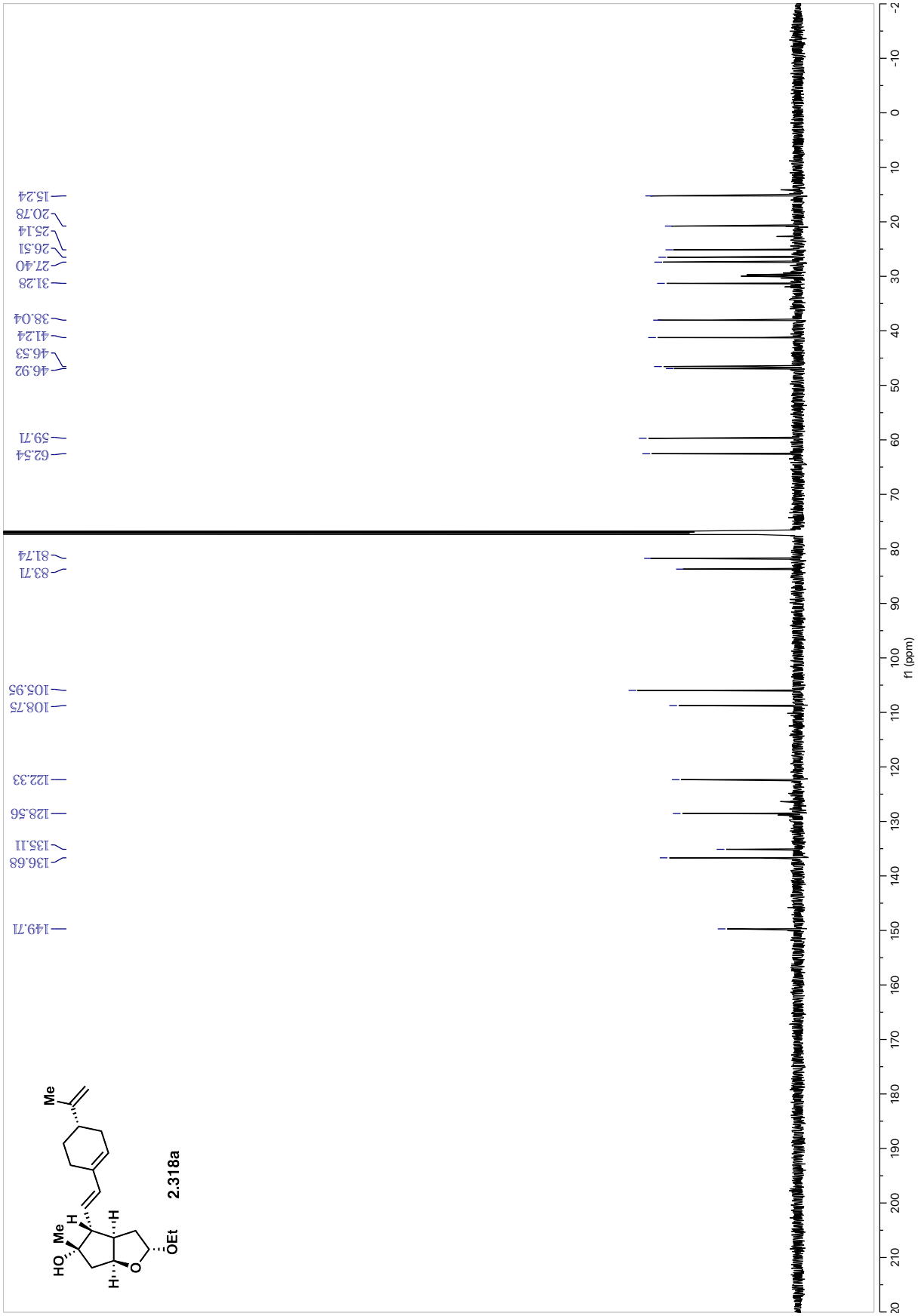

-0.24
0.00
17.26
20.35
28.08
32.81
41.22
44.89
50.02
64.91
83.41
83.52
106.65
108.38
162.21
f1 (ppm)
TBSO
Me
H
H
O
OEt
2.308

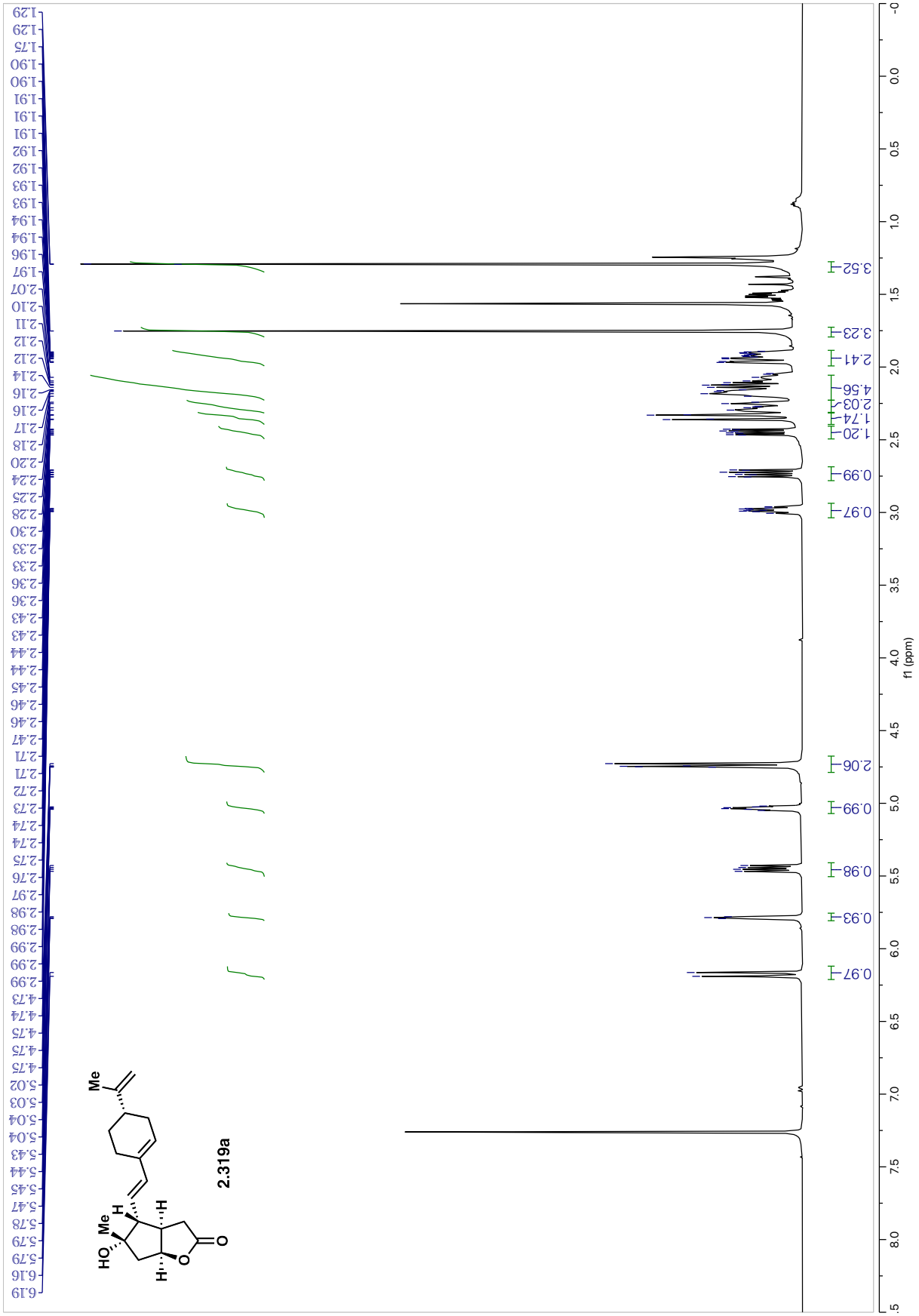

TBSO
Me
H
H
OH
O
O
2.313
f1 (ppm)

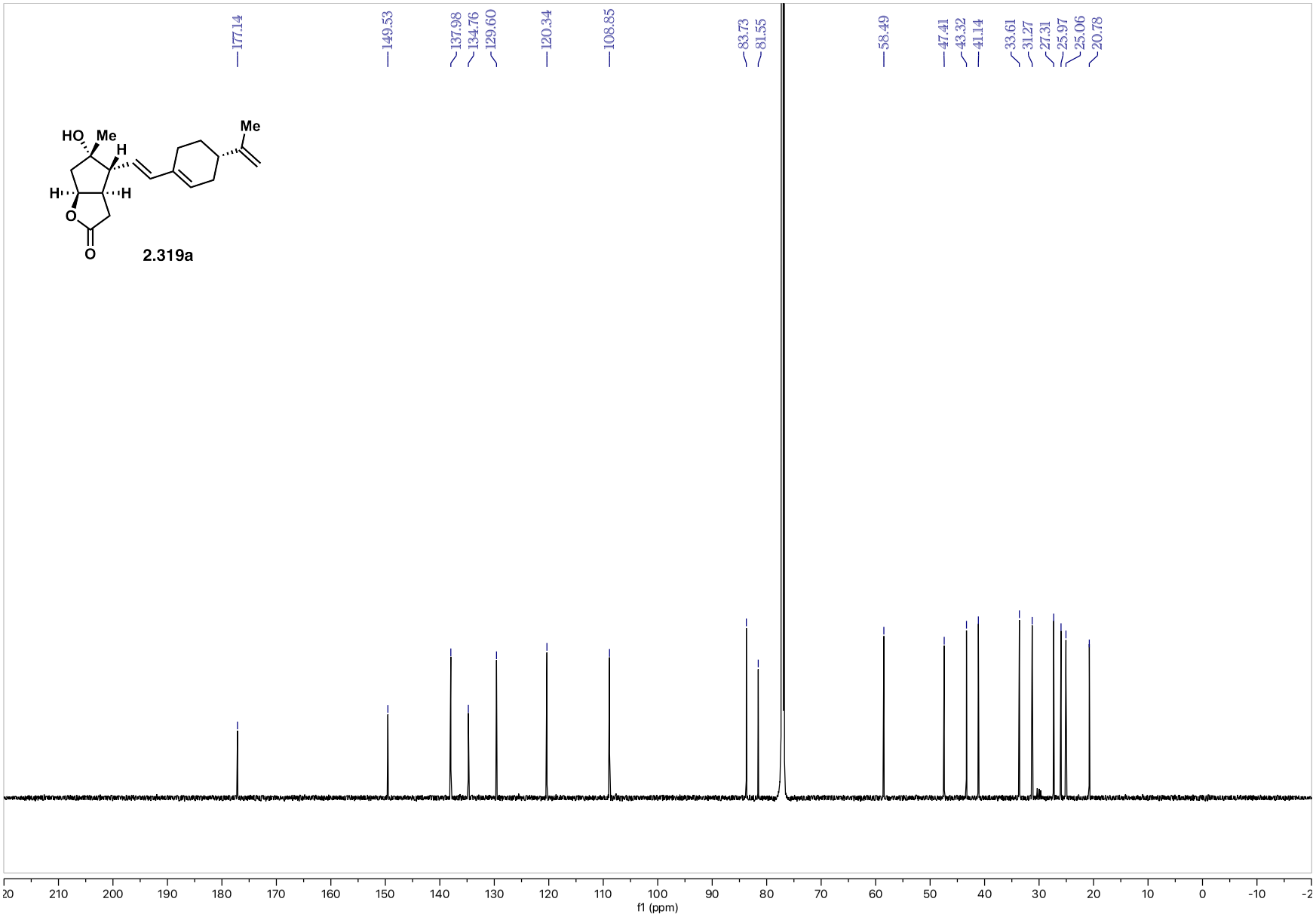

1.43
1.98
1.99
2.01
2.02
2.30
2.32
2.59
2.59
2.62
2.62
2.94
2.95
2.97
2.98
3.46
3.47
3.47
3.48
3.48
3.48
3.48
3.49
3.49
3.49
3.50
4.99
4.99
5.00
5.00
5.01
5.01
5.02
5.05
5.05
5.25
5.26
3.32
0.98
1.07
1.01
0.97
1.06
1.00
0.96
0.94
f1 (ppm)
HO
Me
H
OH
H
H
O
OEt
2.316

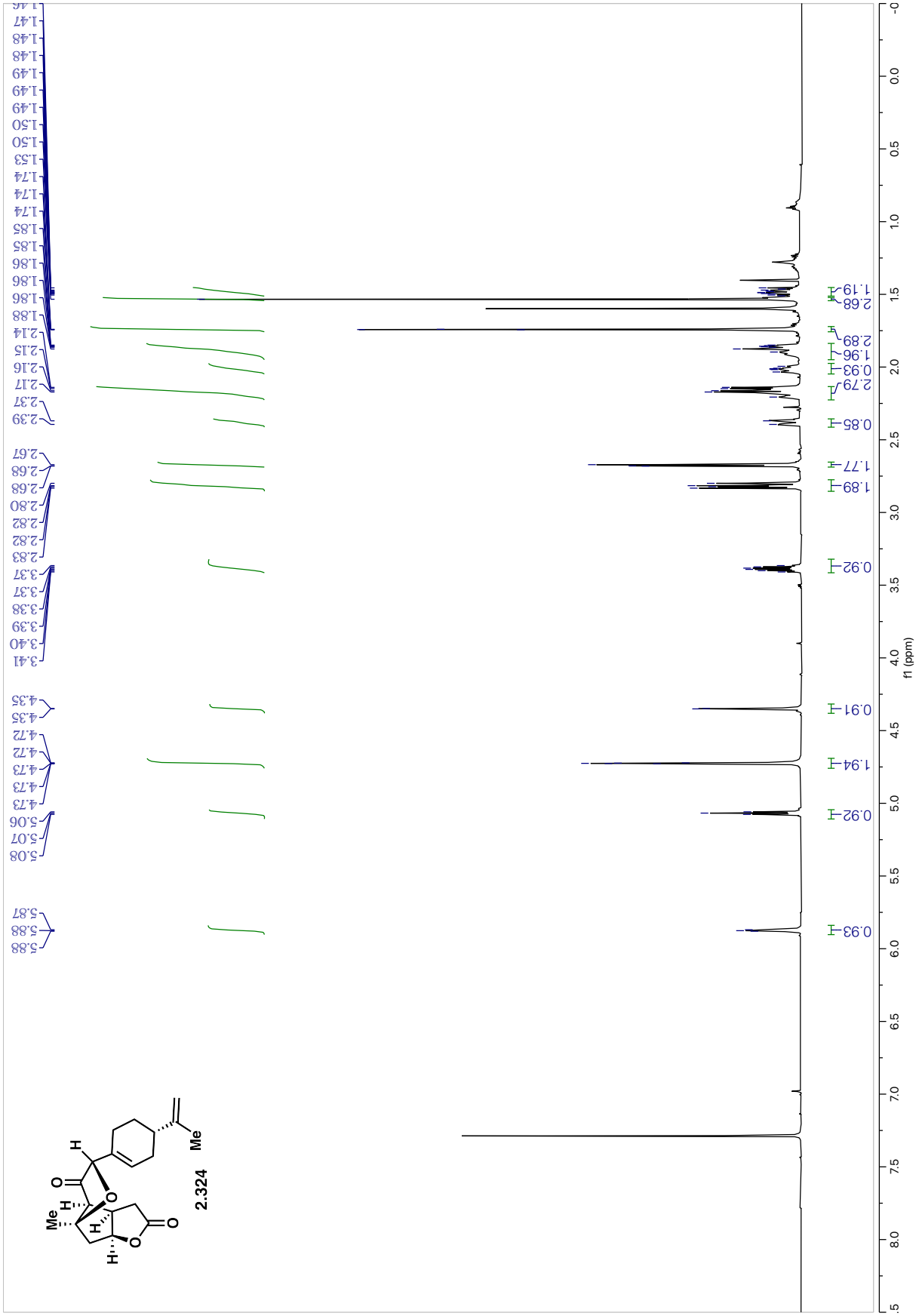

176.96
158.02
108.93
82.49
78.23
46.73
43.04
37.34
25.80
f1 (ppm)
HO
Me
H
OH
H
H
O
OEt
2.316

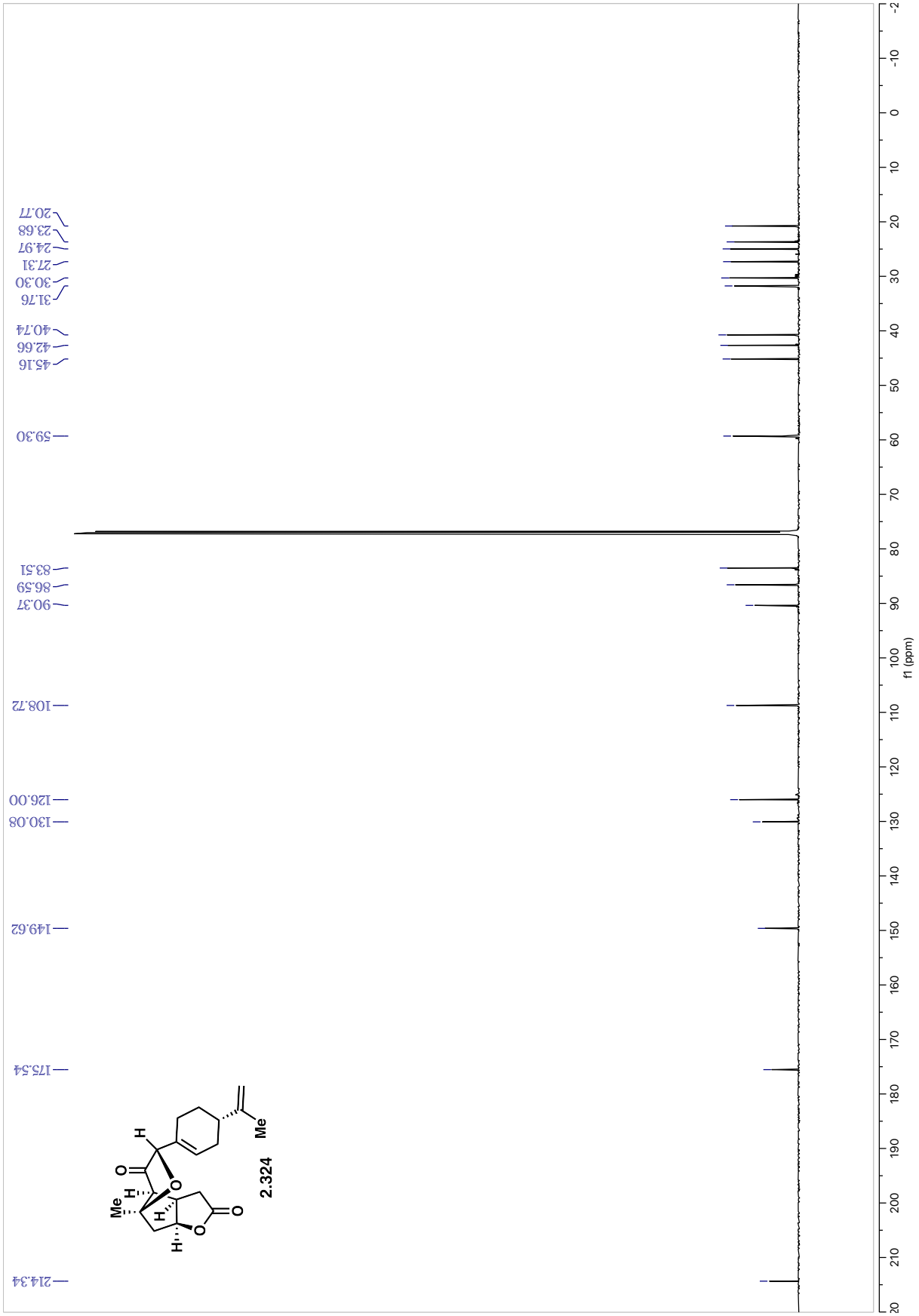

2.318a
Me
HO
Me
H
H
H
O
OEt
f1 (ppm)

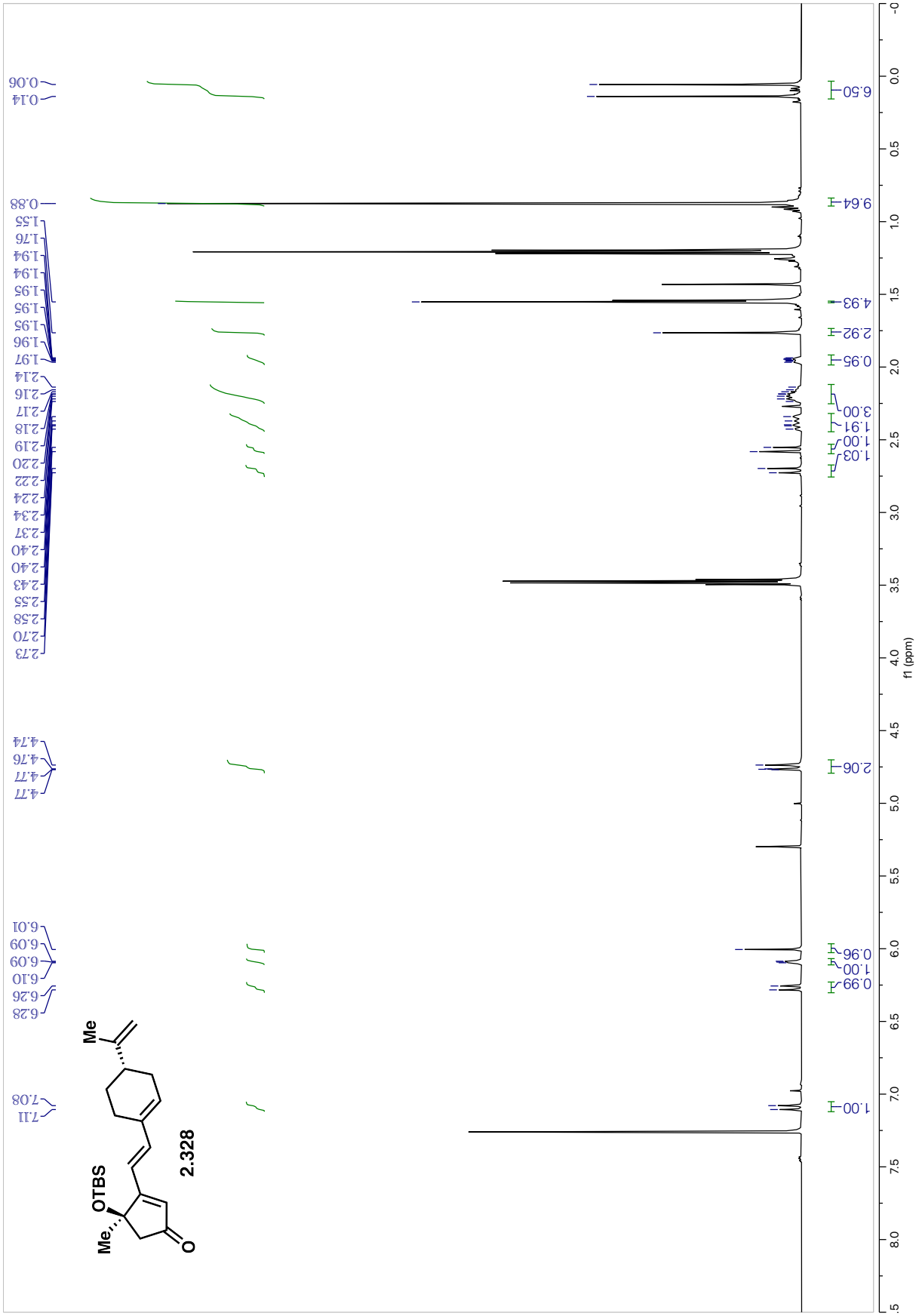

15.24
20.78
25.14
26.51
27.40
31.28
38.04
41.24
46.53
46.92
59.71
62.54
81.74
83.71
105.95
108.75
122.33
128.56
135.11
136.68
149.71
f1 (ppm)
Me
H
Me
HO
H
H
O
OEt
2.318a

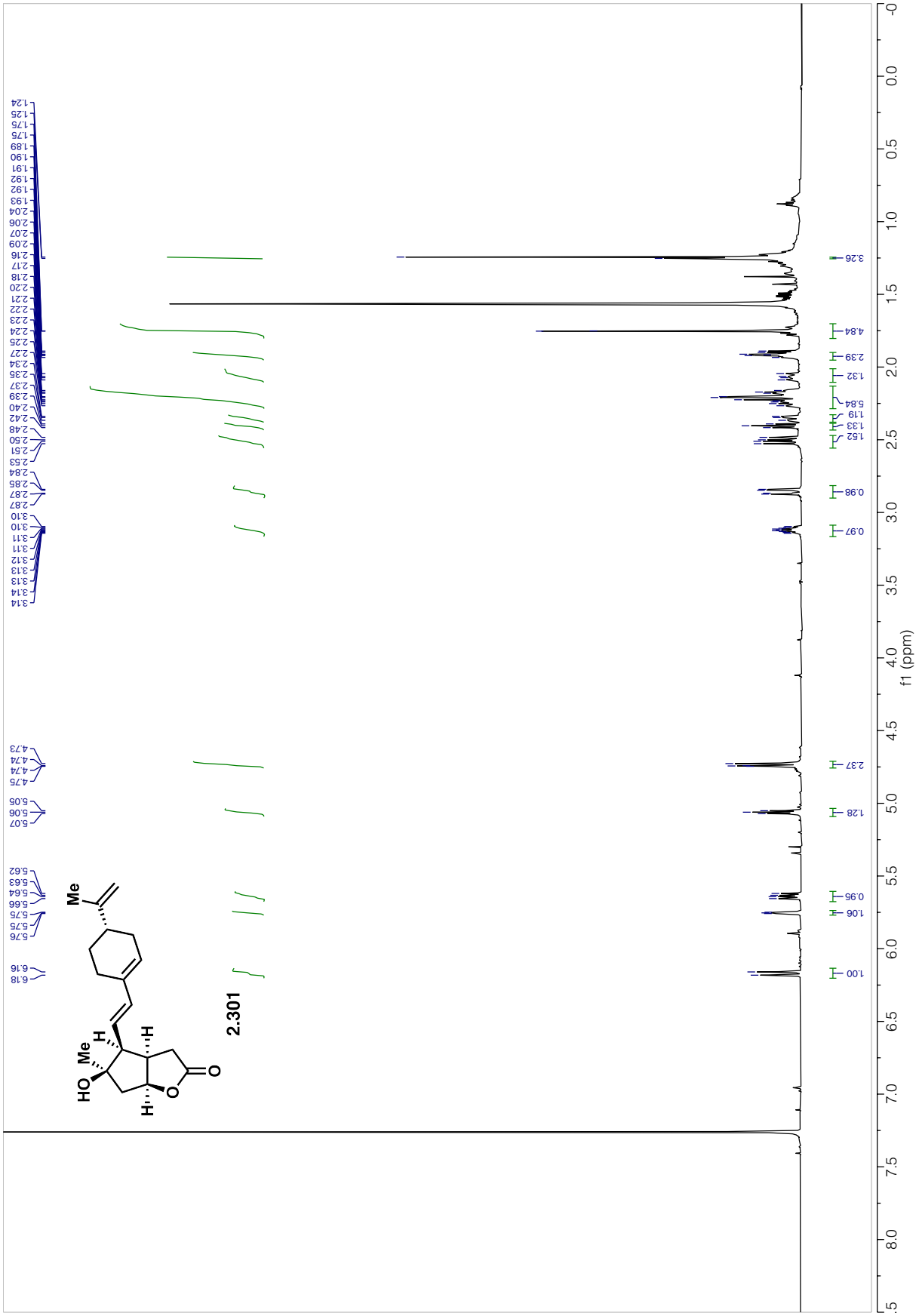

Me
H
Me
HO
H
H
O
O
2.319a
3.52
3.23
2.41
4.56
2.03
1.74
1.20
0.99
0.97
2.06
0.99
0.98
0.93
0.97
f1 (ppm)

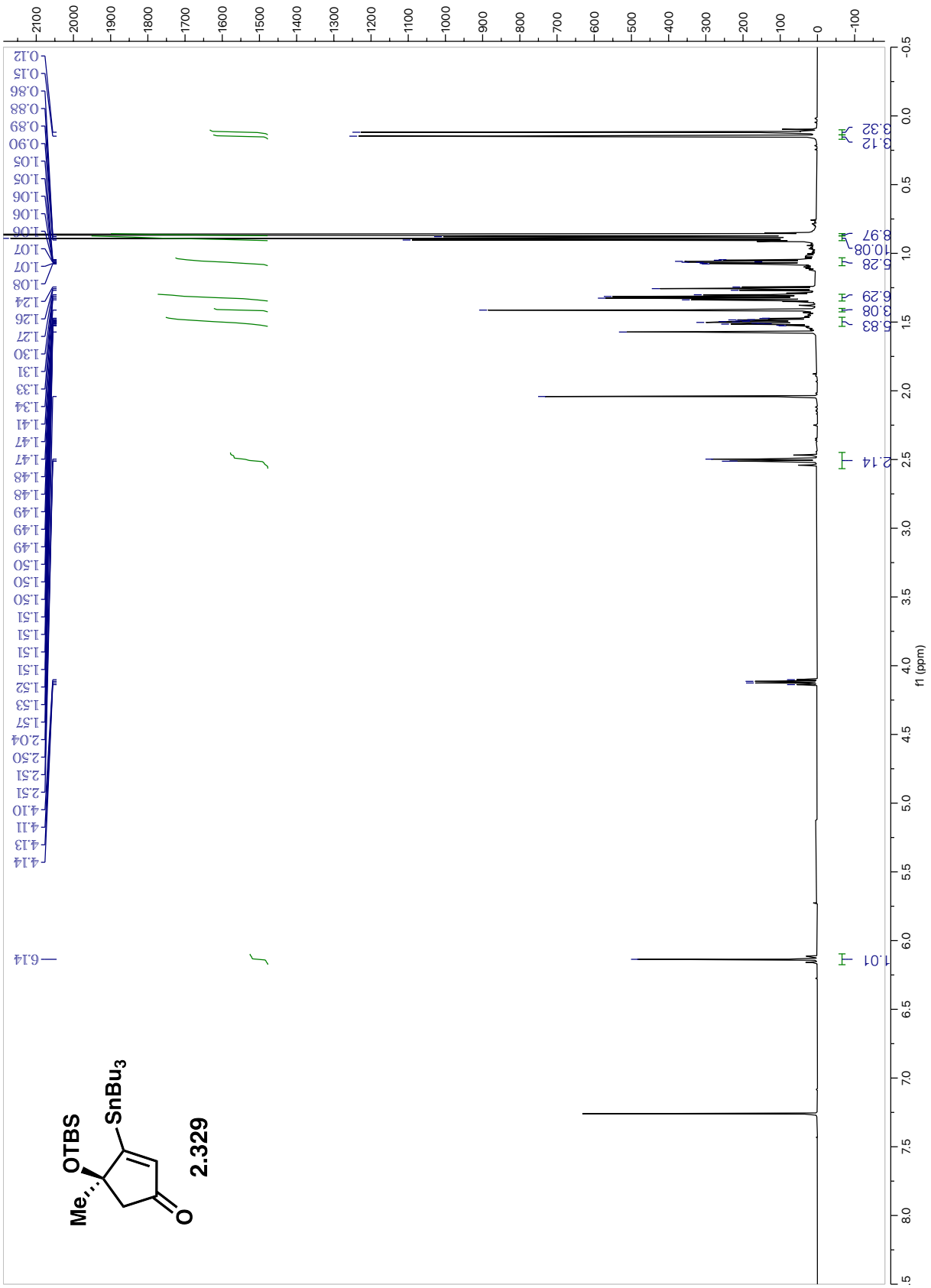

177.14
149.53
137.98
134.76
129.60
120.34
108.85
83.73
81.55
58.49
47.41
43.32
41.14
33.61
31.27
27.31
25.97
25.06
20.78
HO
Me
H
H
H
O
O
Me
2.319a
f1 (ppm)

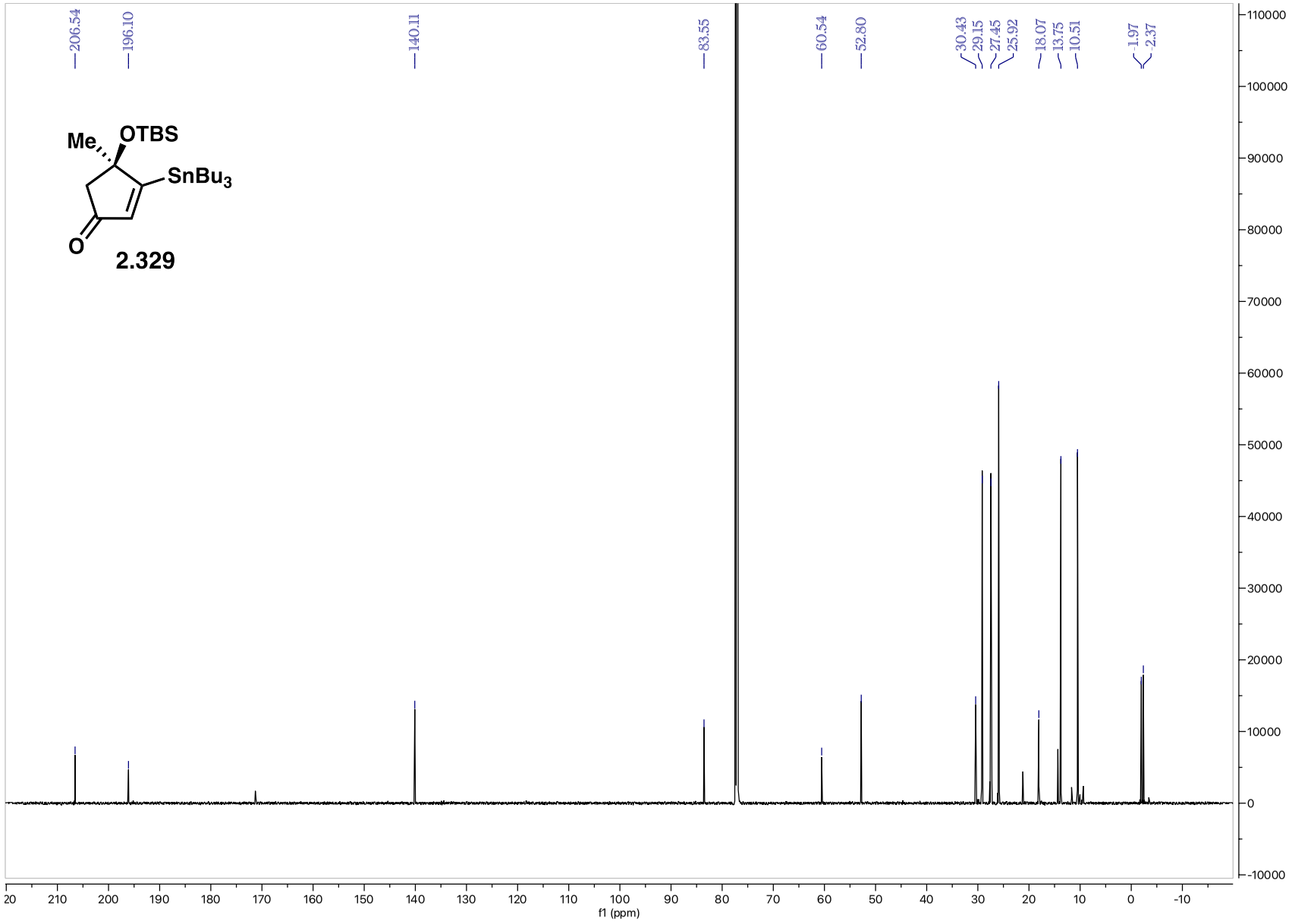

1.46
1.47
1.48
1.48
1.49
1.49
1.49
1.50
1.50
1.53
1.74
1.74
1.74
1.85
1.85
1.86
1.86
1.86
1.88
2.14
2.15
2.16
2.17
2.37
2.39
2.67
2.68
2.68
2.80
2.82
2.82
2.83
3.37
3.37
3.38
3.39
3.40
3.41
4.35
4.35
4.72
4.72
4.73
4.73
4.73
5.06
5.07
5.08
5.87
5.88
5.88
1.19
2.68
2.89
1.96
0.93
2.79
0.85
1.77
1.89
0.92
0.91
1.94
0.92
0.93
f1 (ppm)
2.324
Me
H
O
O
H
Me
H
O
O
O

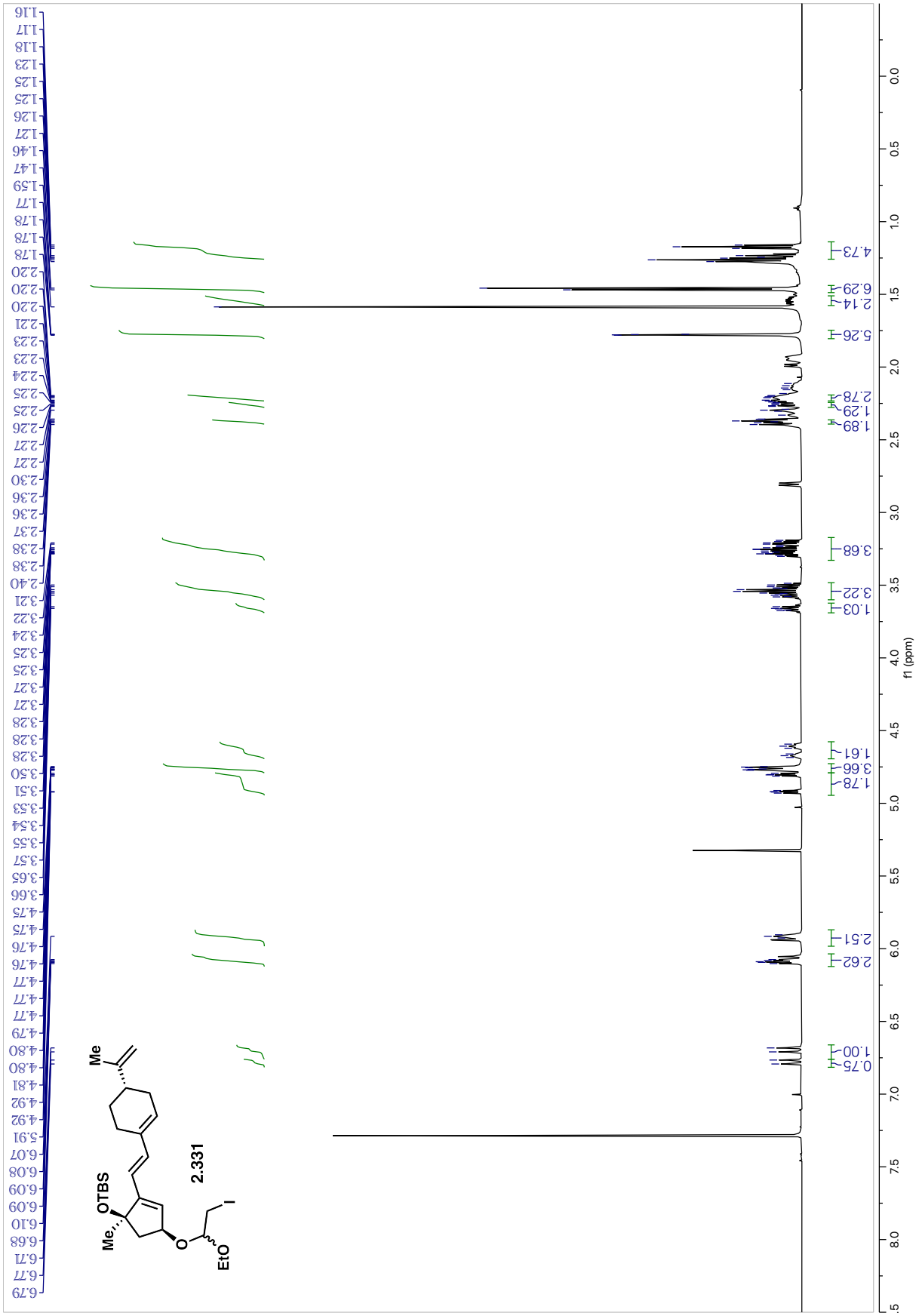

214.34
175.54
149.62
130.08
126.00
108.72
90.37
86.59
83.51
59.30
45.16
42.66
40.74
31.76
30.30
27.31
24.97
23.68
20.77
Me
H
O
O
H
O
H
O
O
Me
2.324
f1 (ppm)

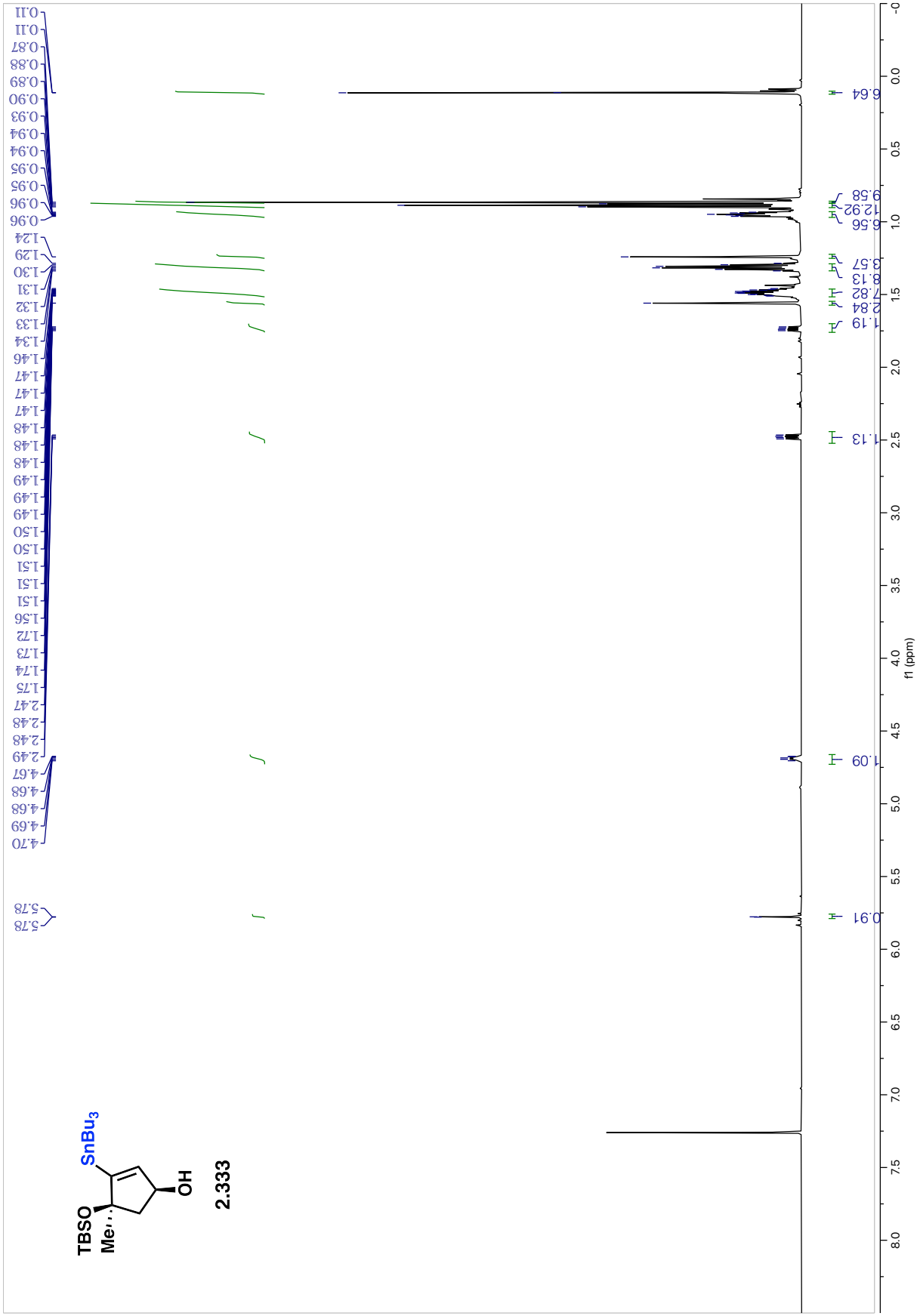

Me
OTBS
Me
O
2.328
f1 (ppm)

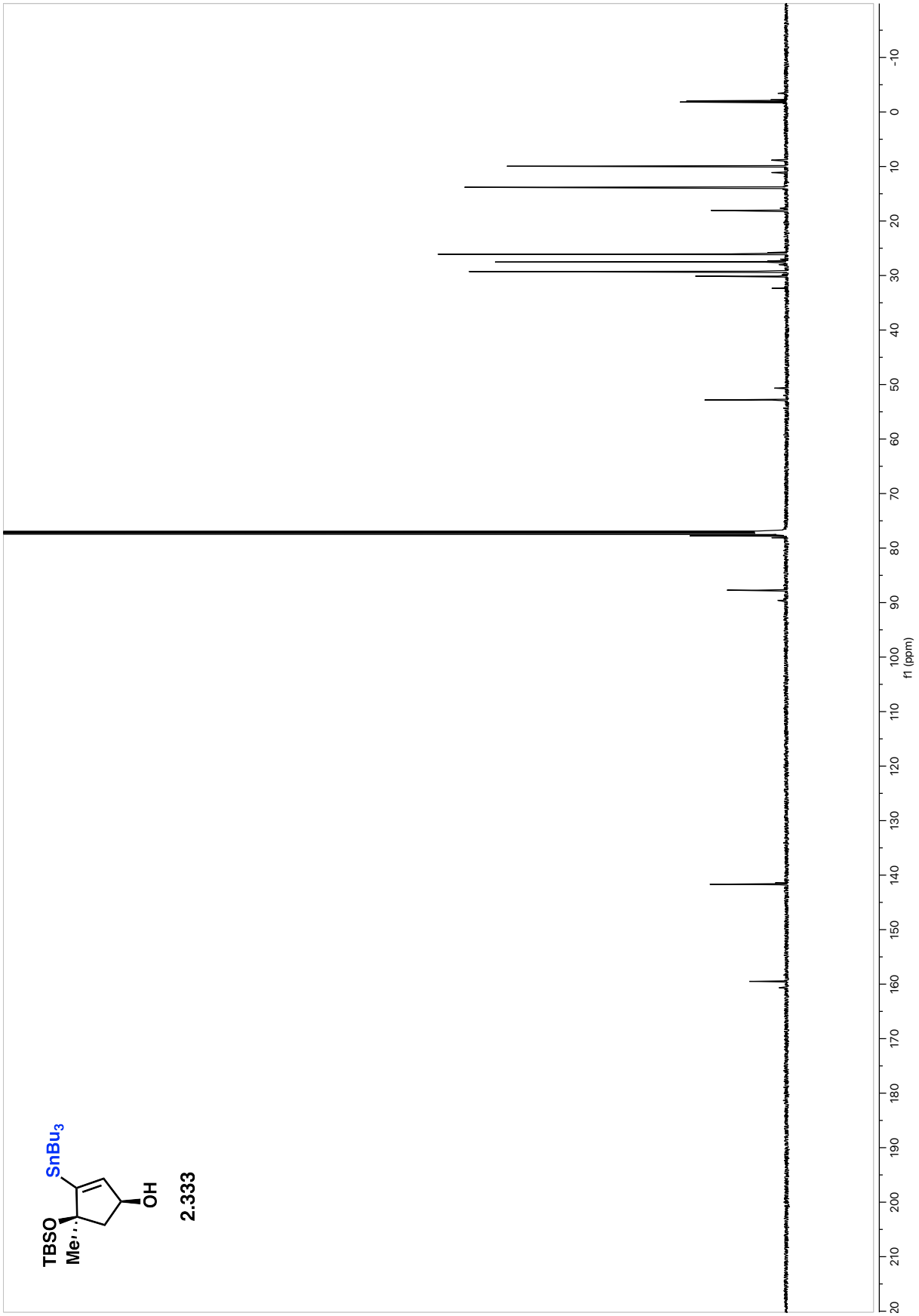

Me
HO
Me
H
H
H
O
O
2.301
f1 (ppm)

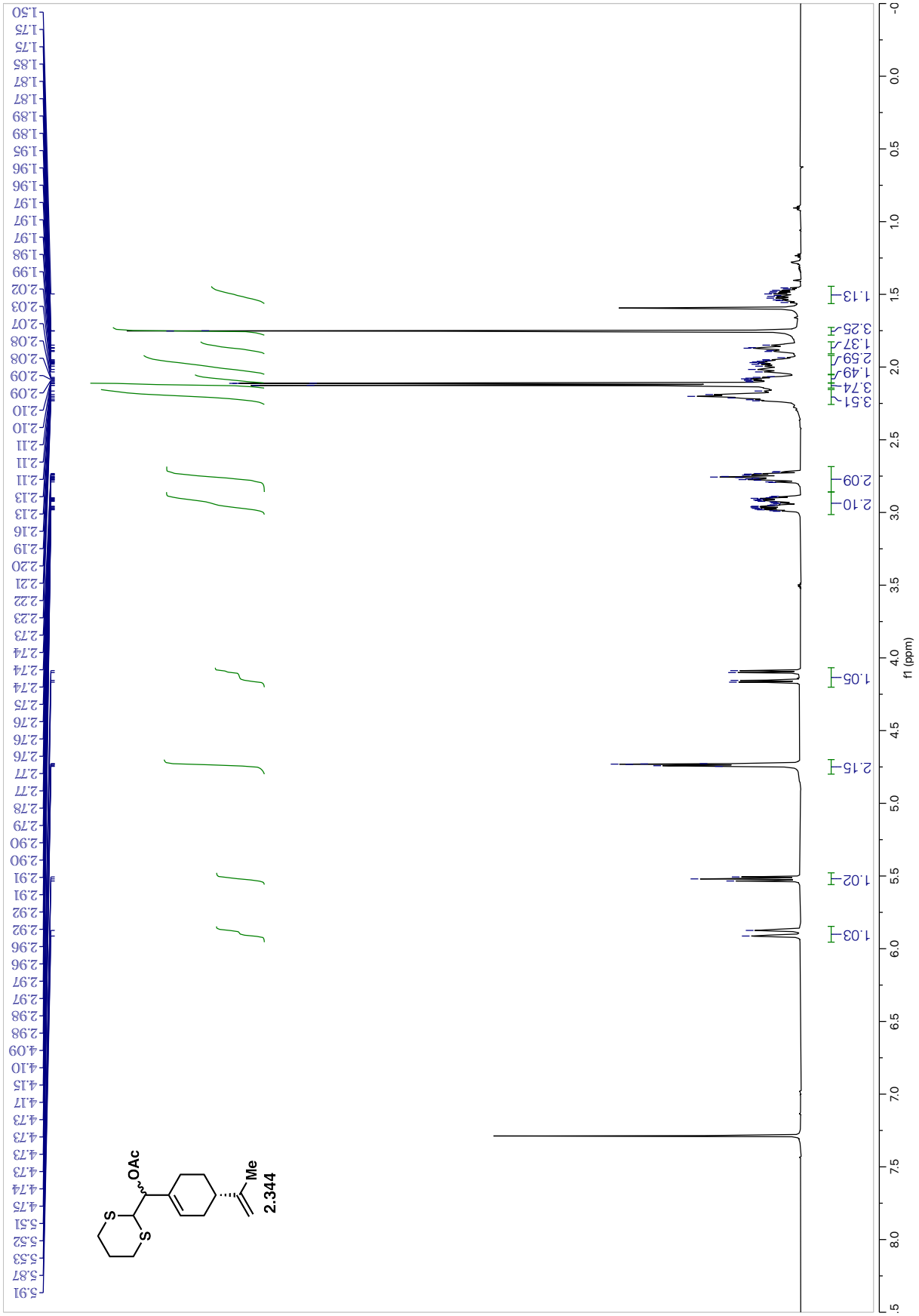

OTBS
SnBu3
Me
O
2.329
f1 (ppm)

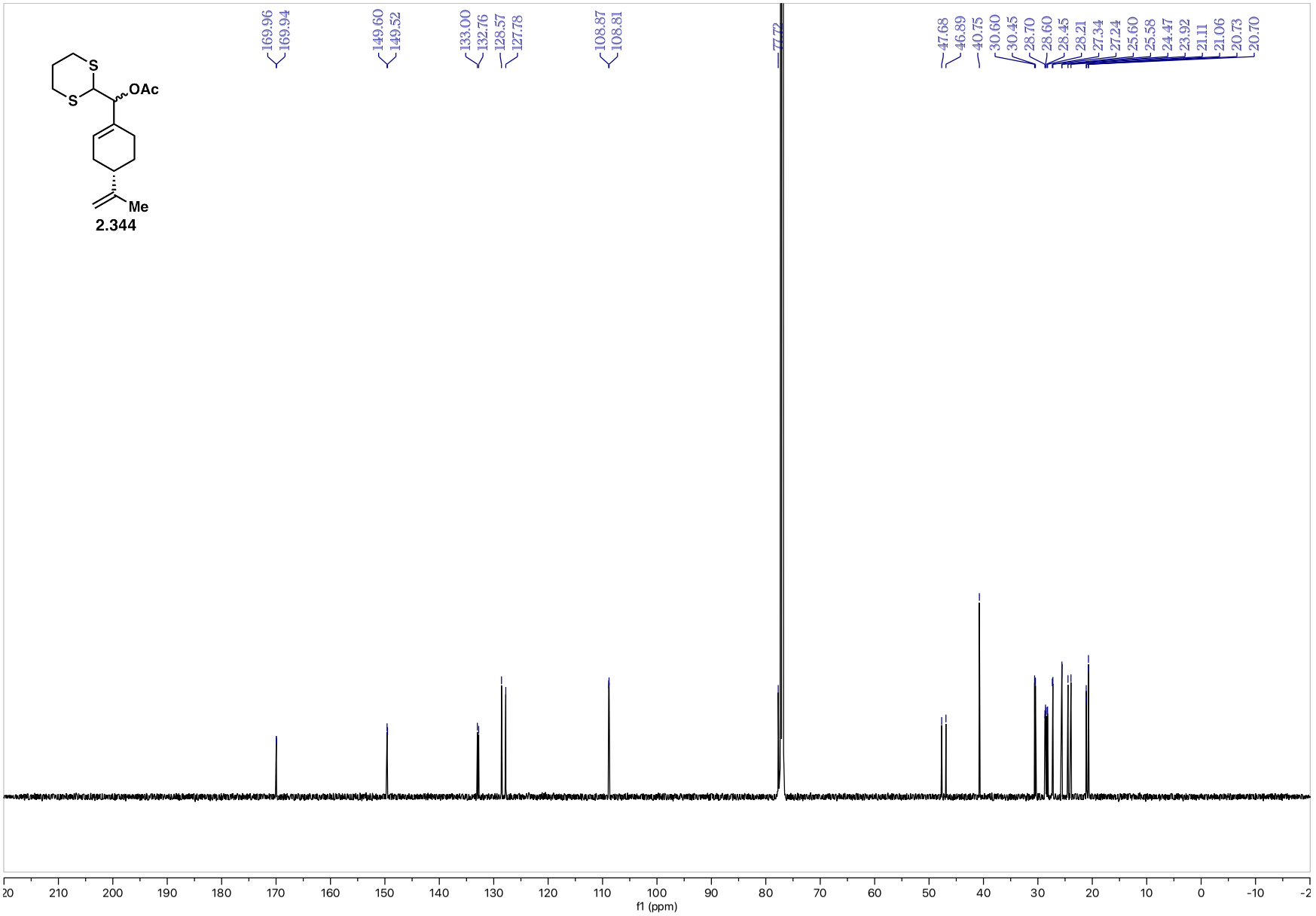

206.54
196.10
140.11
83.55
60.54
52.80
30.43
29.15
27.45
25.92
18.07
13.75
10.51
1.97
2.37
Me
OTBS
SnBu3
O
2.329
f1 (ppm)

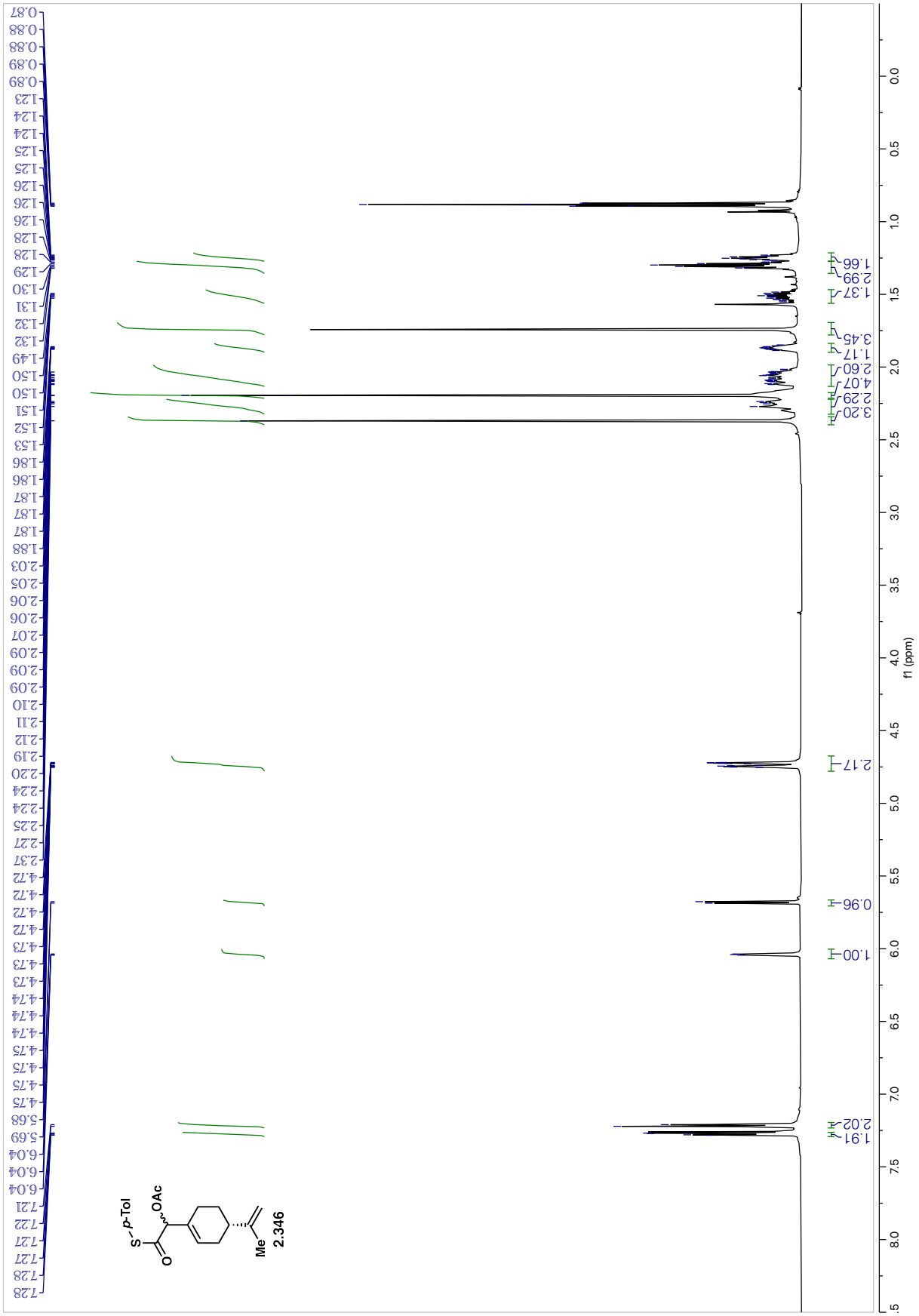

Me
OTBS
Me
O
EtO
I
2.331
4.73
6.29
2.14
5.26
2.78
1.29
1.89
3.68
3.22
1.03
1.61
3.66
1.78
2.51
2.62
1.00
0.75
f1 (ppm)

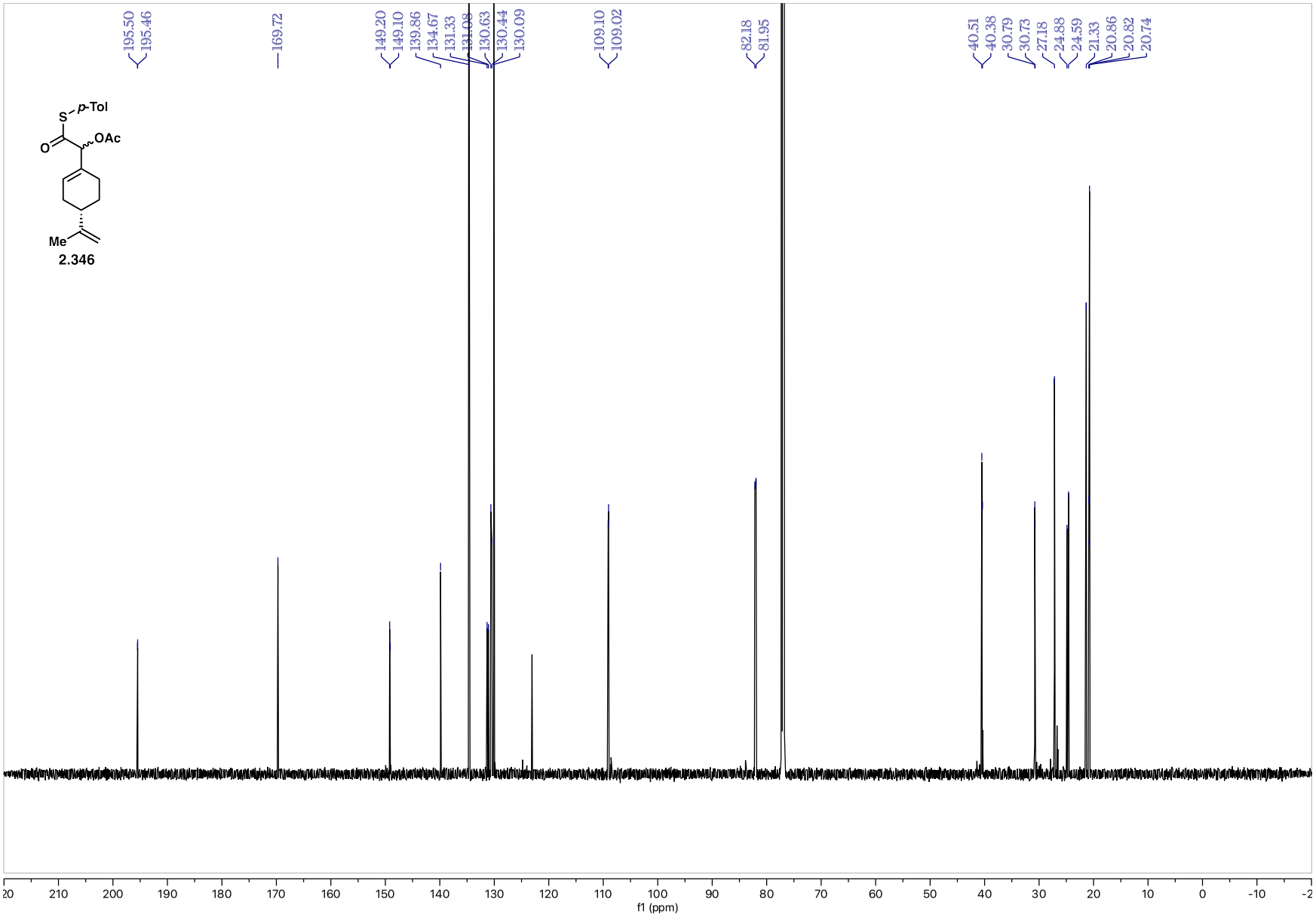

SnBu3
TBSO
OH
2.333
f1 (ppm)

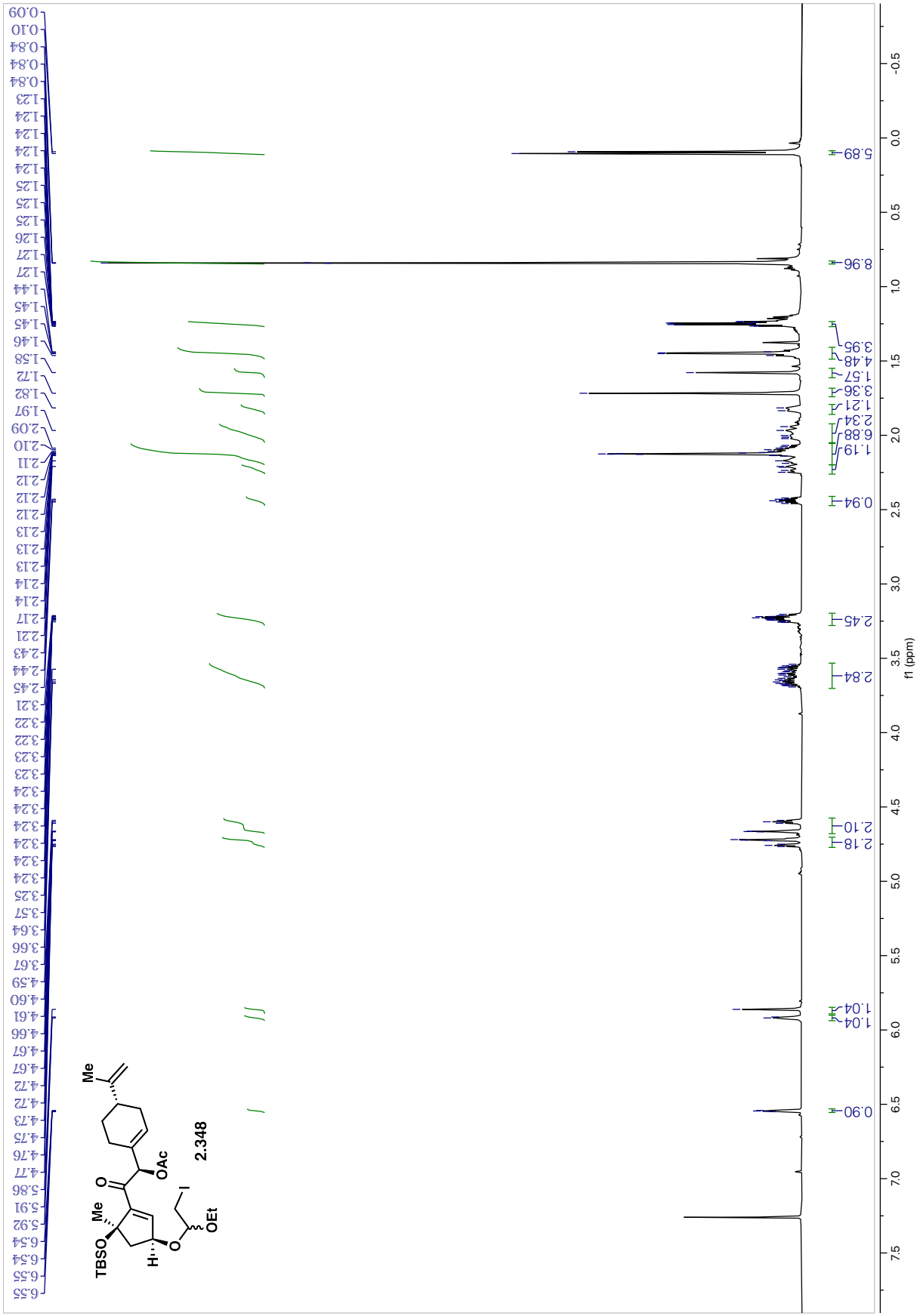

TBSO
Me
SnBu3
OH
2.333
f1 (ppm)

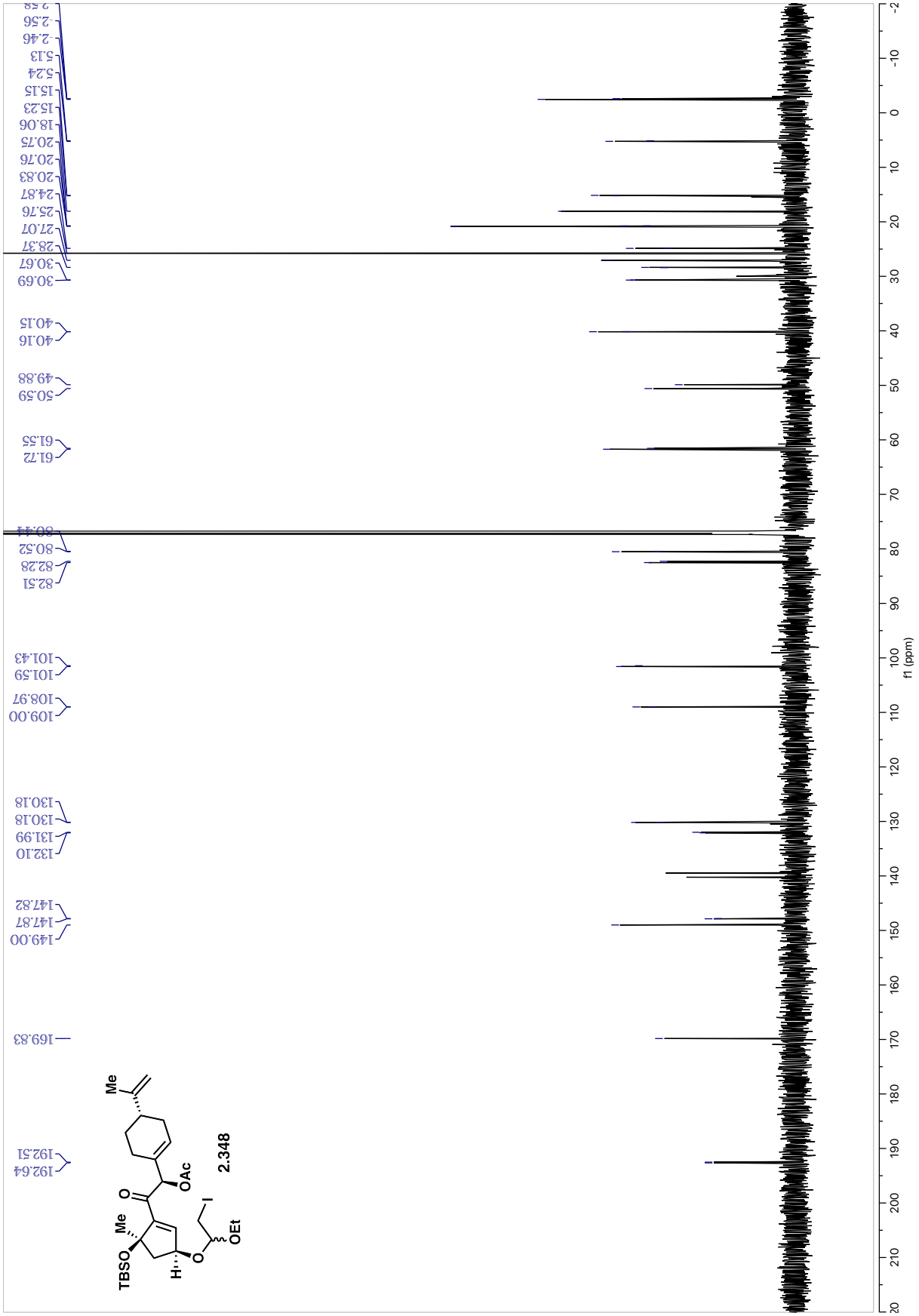

OAc
Me
S
S
2.344
f1 (ppm)

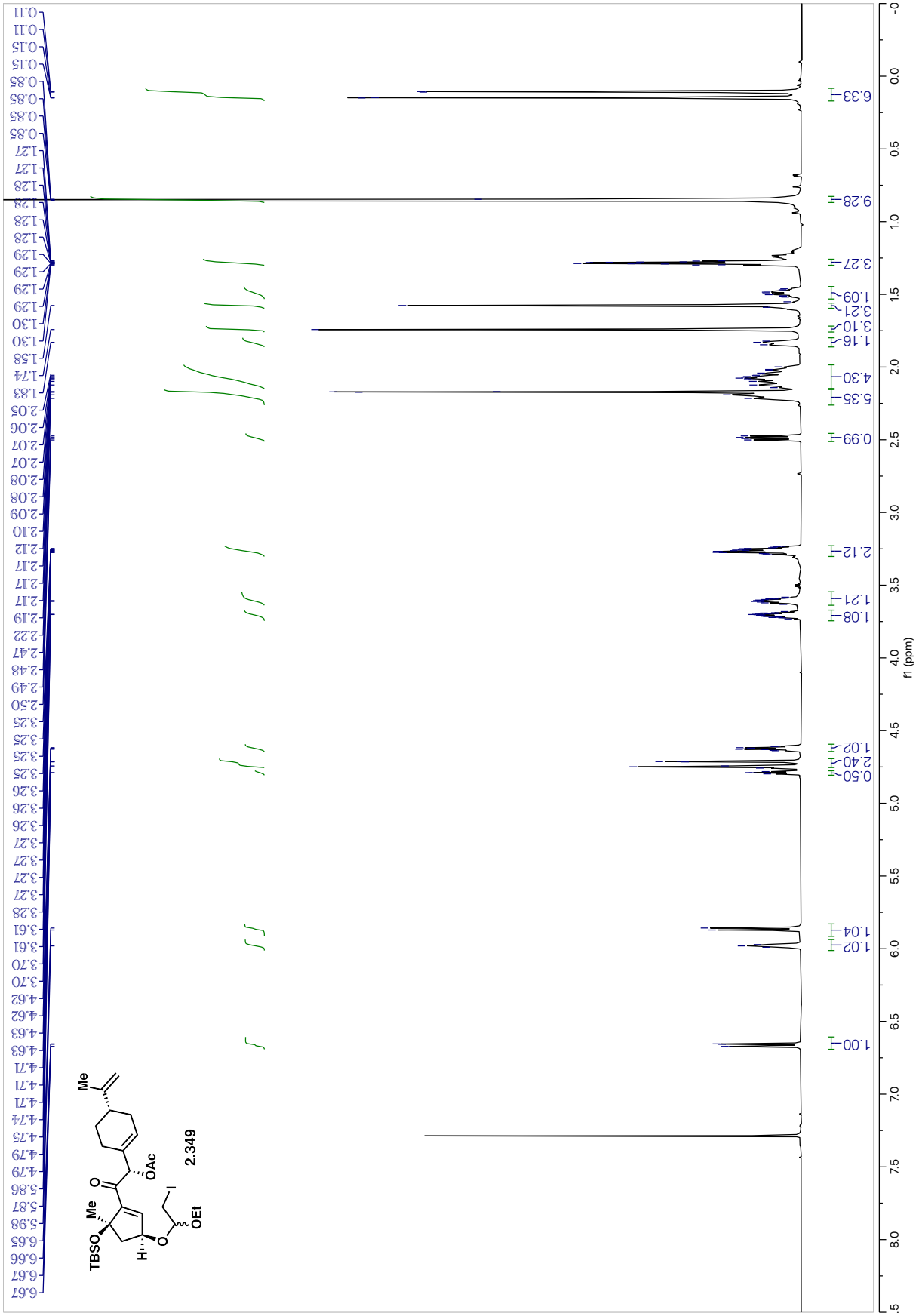

169.96
169.94
149.60
149.52
133.00
132.76
128.57
127.78
108.87
108.81
77.72
47.68
46.89
40.75
30.60
30.45
28.70
28.60
28.45
28.21
27.34
27.24
25.60
25.58
24.47
23.92
21.11
21.06
20.73
20.70
S
S
OAc
Me
2.344
f1 (ppm)

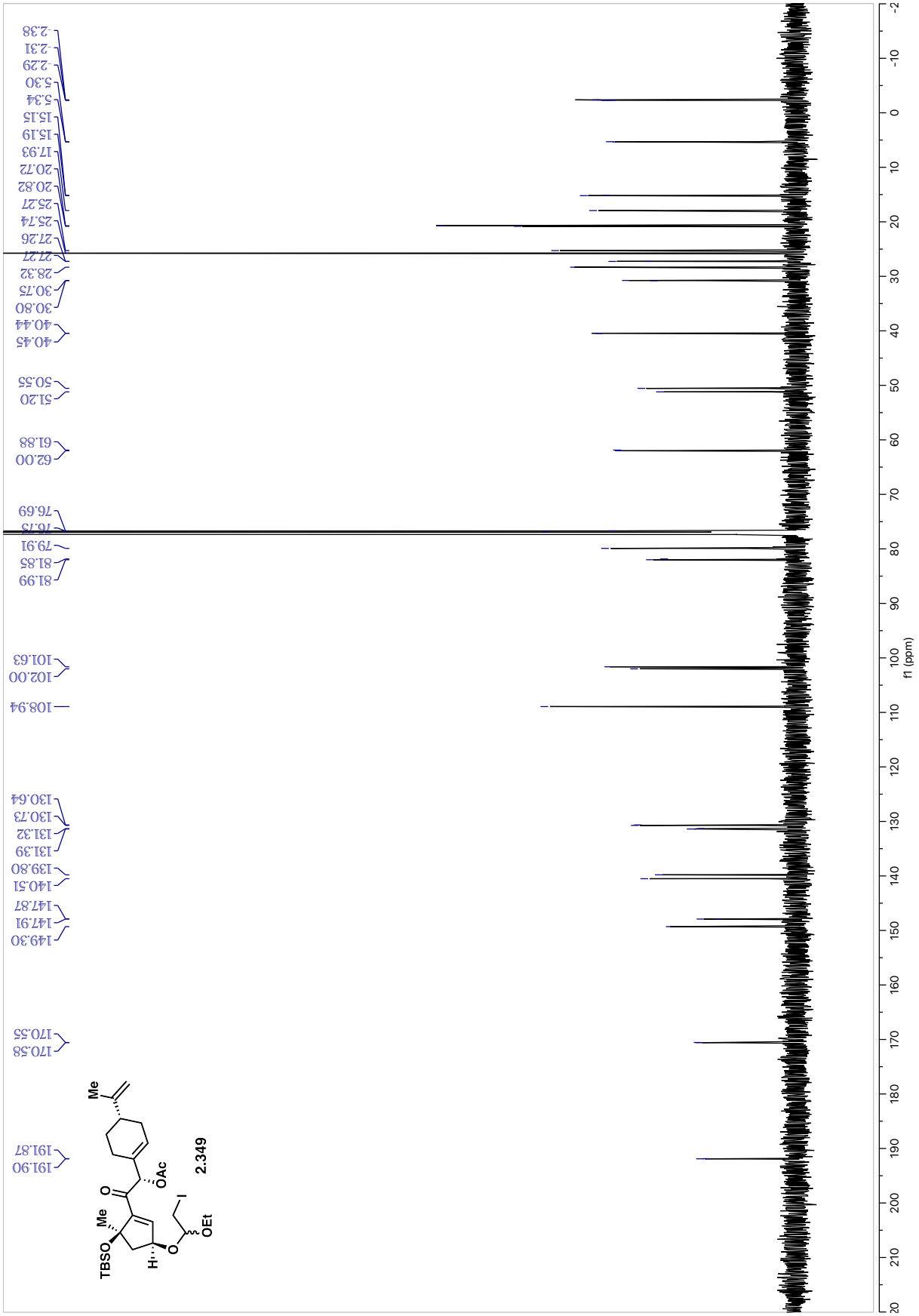

p-Tol
OAc
O
Me
2.346
f1 (ppm)

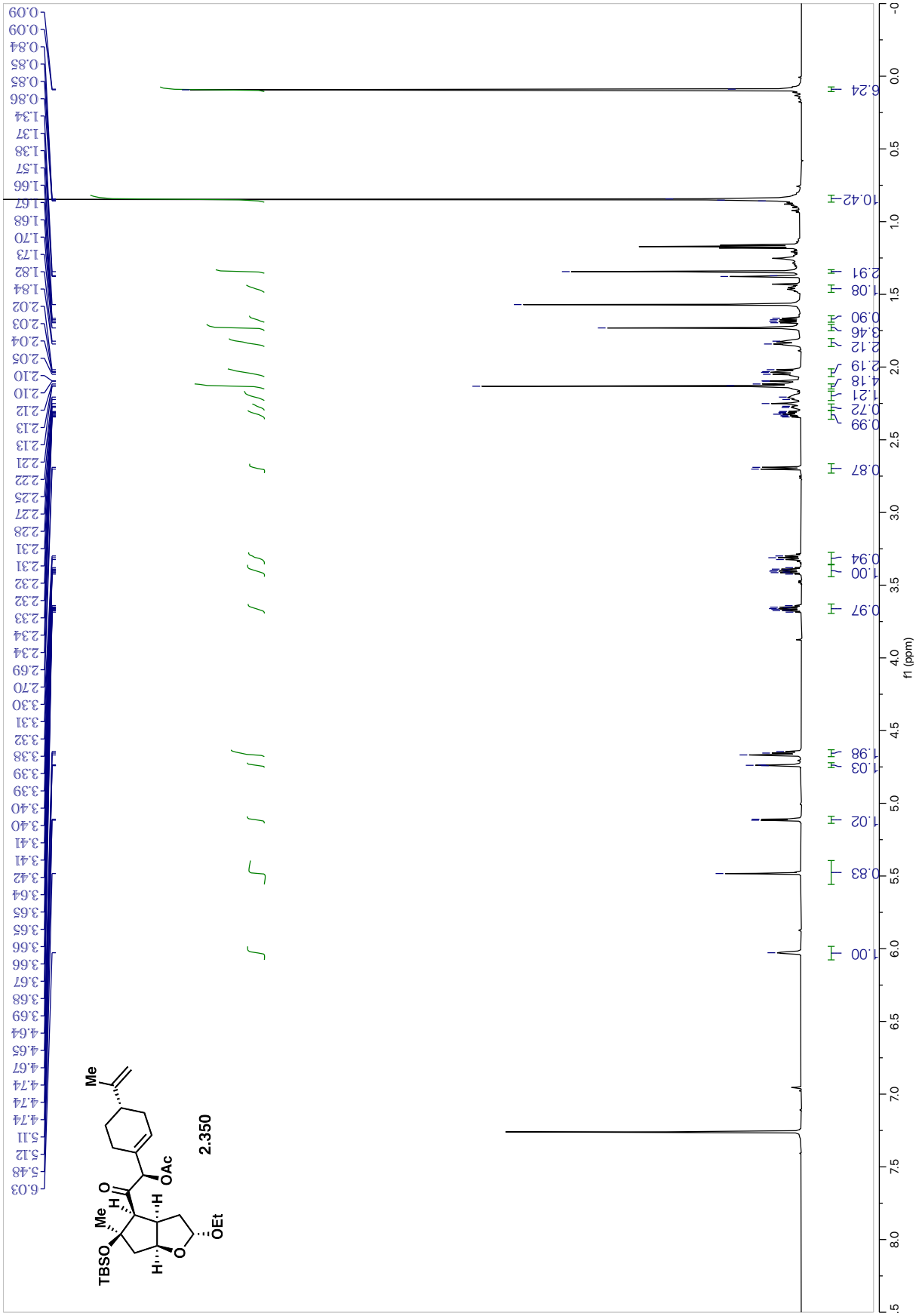

195.50
195.46
169.72
149.20
149.10
139.86
134.67
131.33
131.08
130.63
130.44
130.09
109.10
109.02
82.18
81.95
40.51
40.38
30.79
30.73
27.18
24.88
24.59
21.33
20.86
20.82
20.74
S
p-Tol
O
OAc
Me
2.346
f1 (ppm)

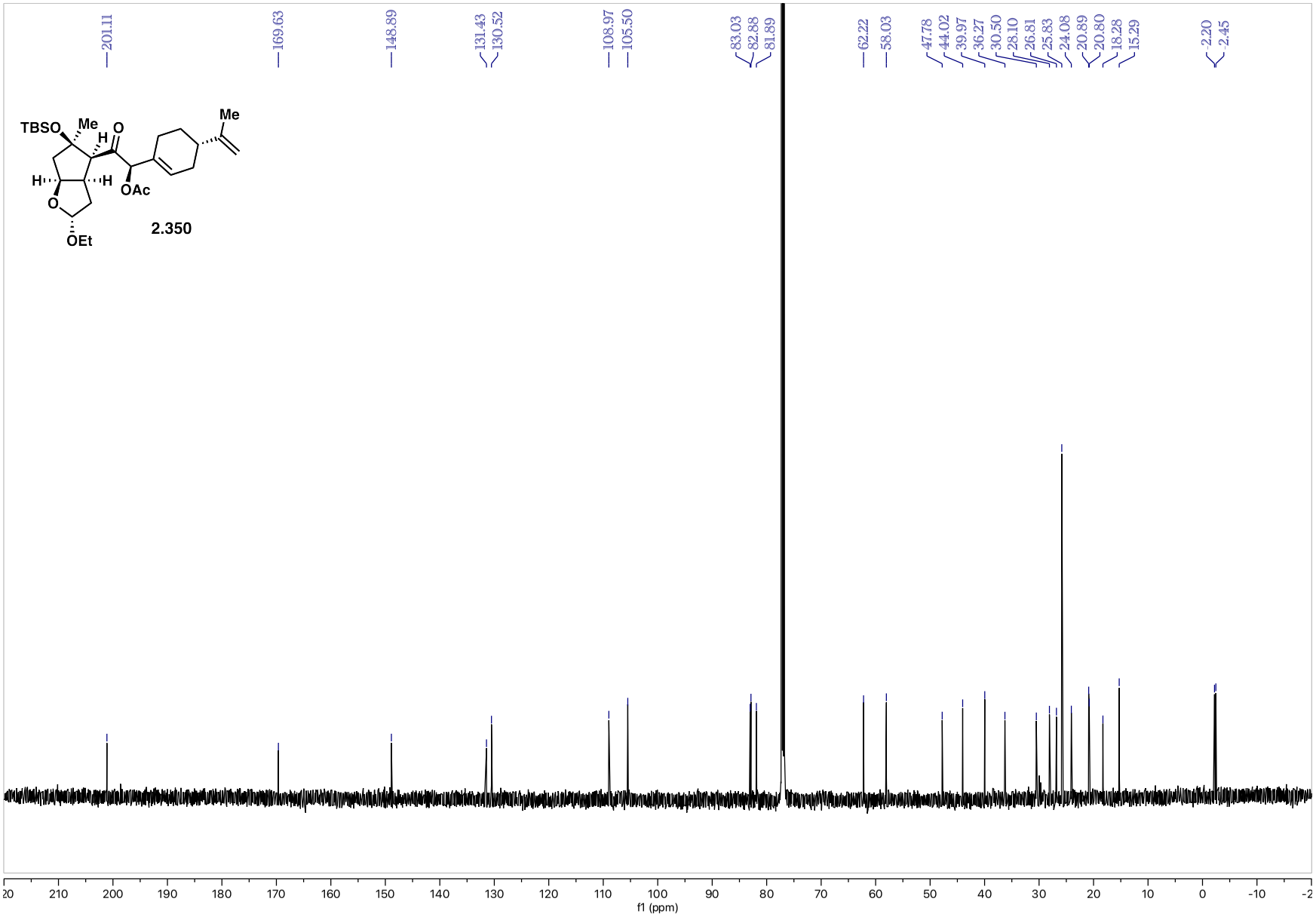

Me
OAc
O
Me
TBSO
H
O
I
OEt
2.348
f1 (ppm)

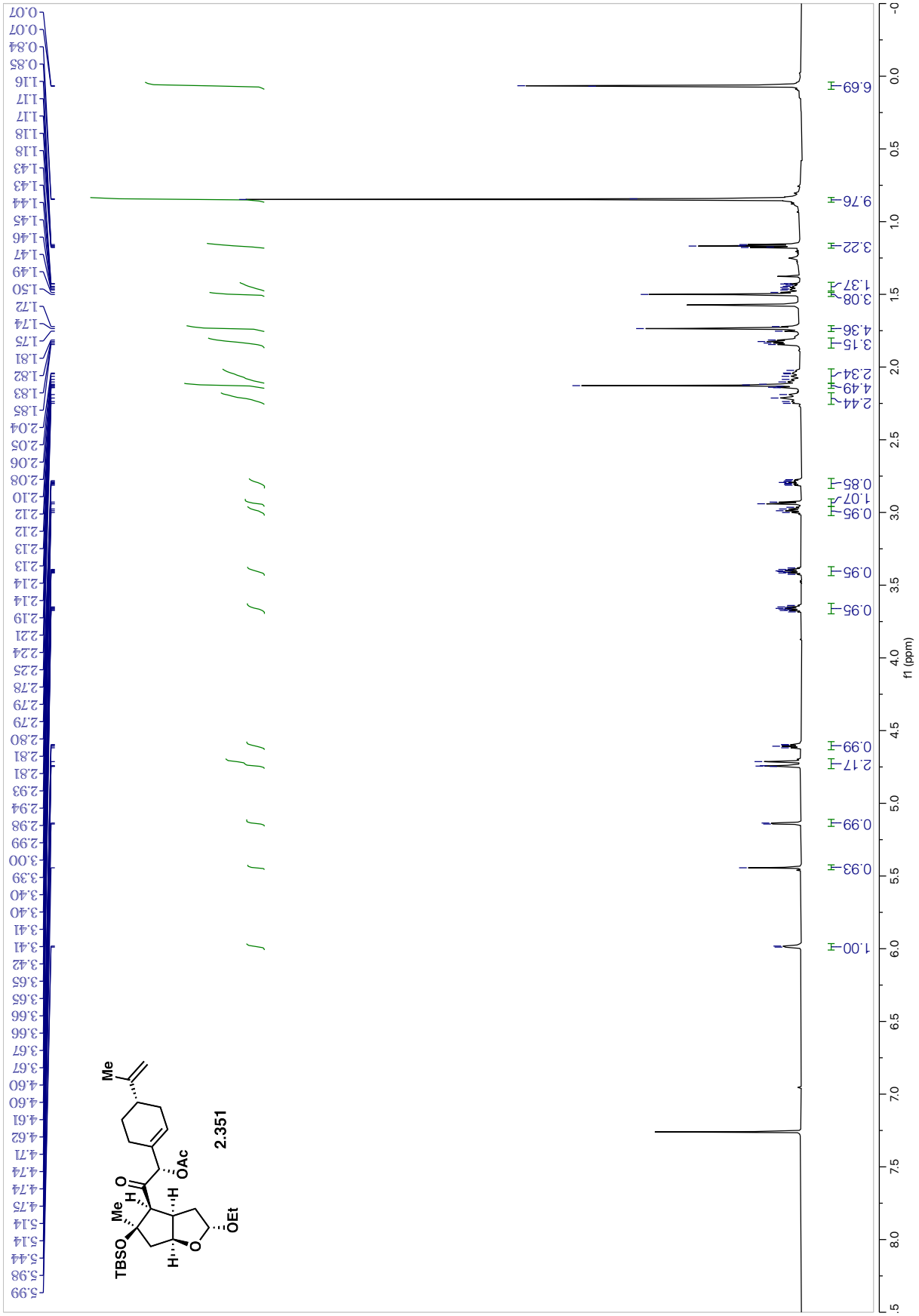

2.58
2.56
2.46
5.13
5.24
15.15
15.23
18.06
20.75
20.76
20.83
24.87
25.76
27.07
28.37
30.67
30.69
40.15
40.16
49.88
50.59
61.55
61.72
80.44
80.52
82.28
82.51
101.43
101.59
108.97
109.00
130.18
130.18
131.99
132.10
147.82
147.87
149.00
169.83
192.51
192.64
Me
OAc
O
Me
TBSO
H
O
I
OEt
2.348
f1 (ppm)

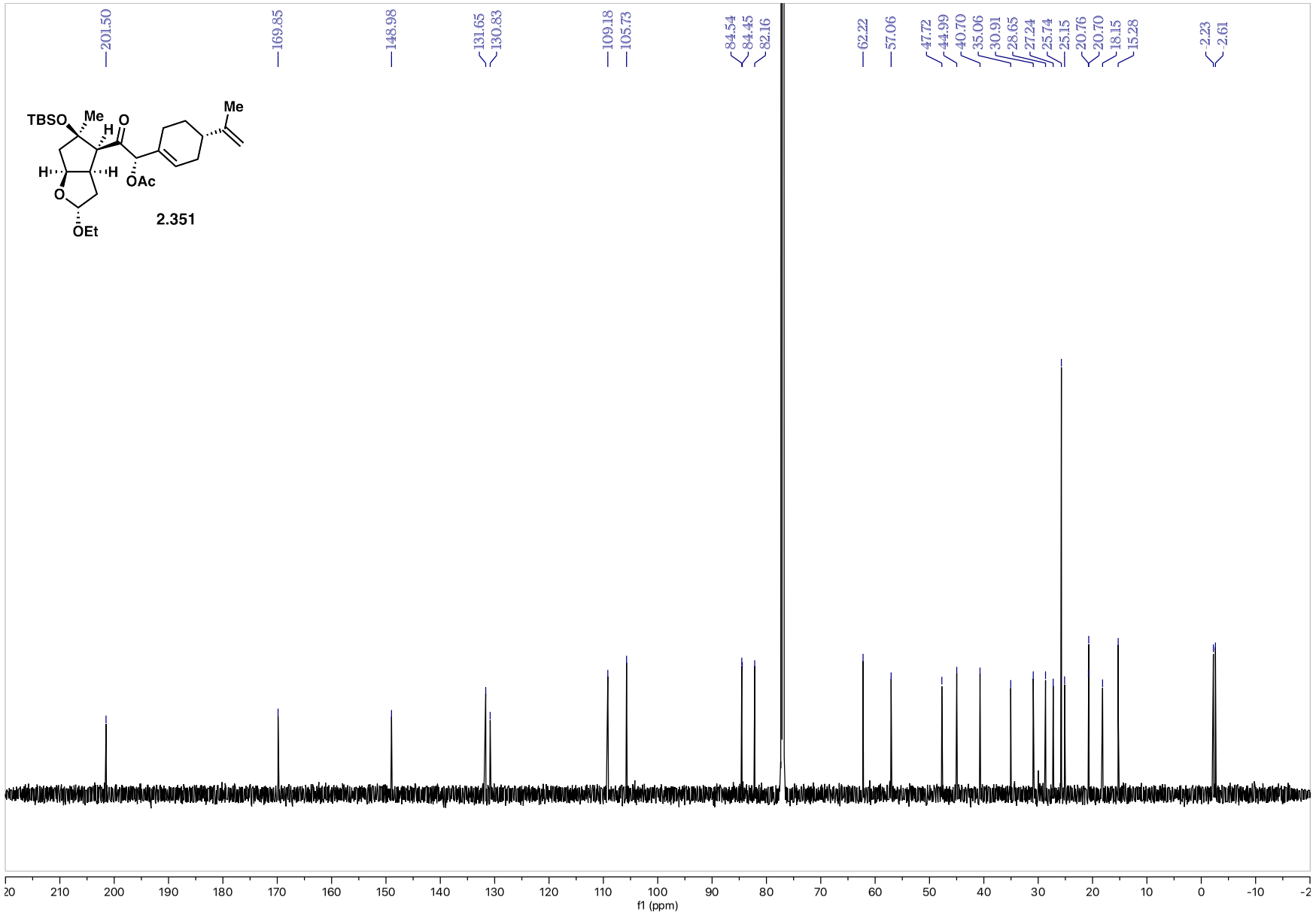

Me
OAc
O
Me
TBSO
H
O
I
OEt
2.349
f1 (ppm)

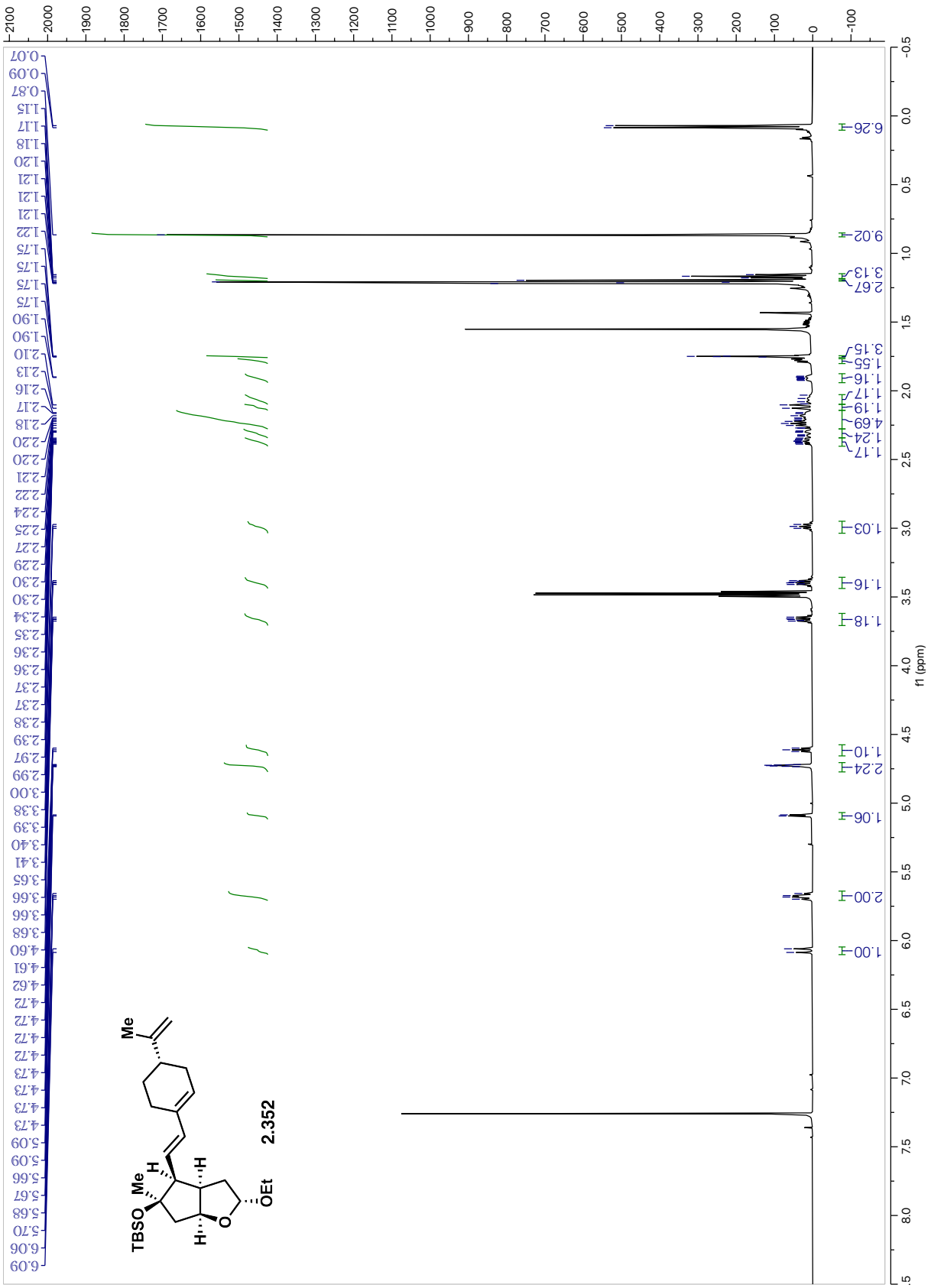

2.38
2.31
2.29
5.30
5.34
15.15
15.19
17.93
20.72
20.82
25.27
25.74
27.26
27.27
28.32
30.75
30.80
40.44
40.45
50.55
51.20
61.88
62.00
76.69
76.75
79.91
81.85
81.99
101.63
102.00
108.94
130.64
130.73
131.32
131.39
139.80
140.51
147.87
147.91
149.30
170.55
170.58
191.87
191.90
Me
O
OAc
I
OEt
2.349
Me
TBSO
H
O
f1 (ppm)

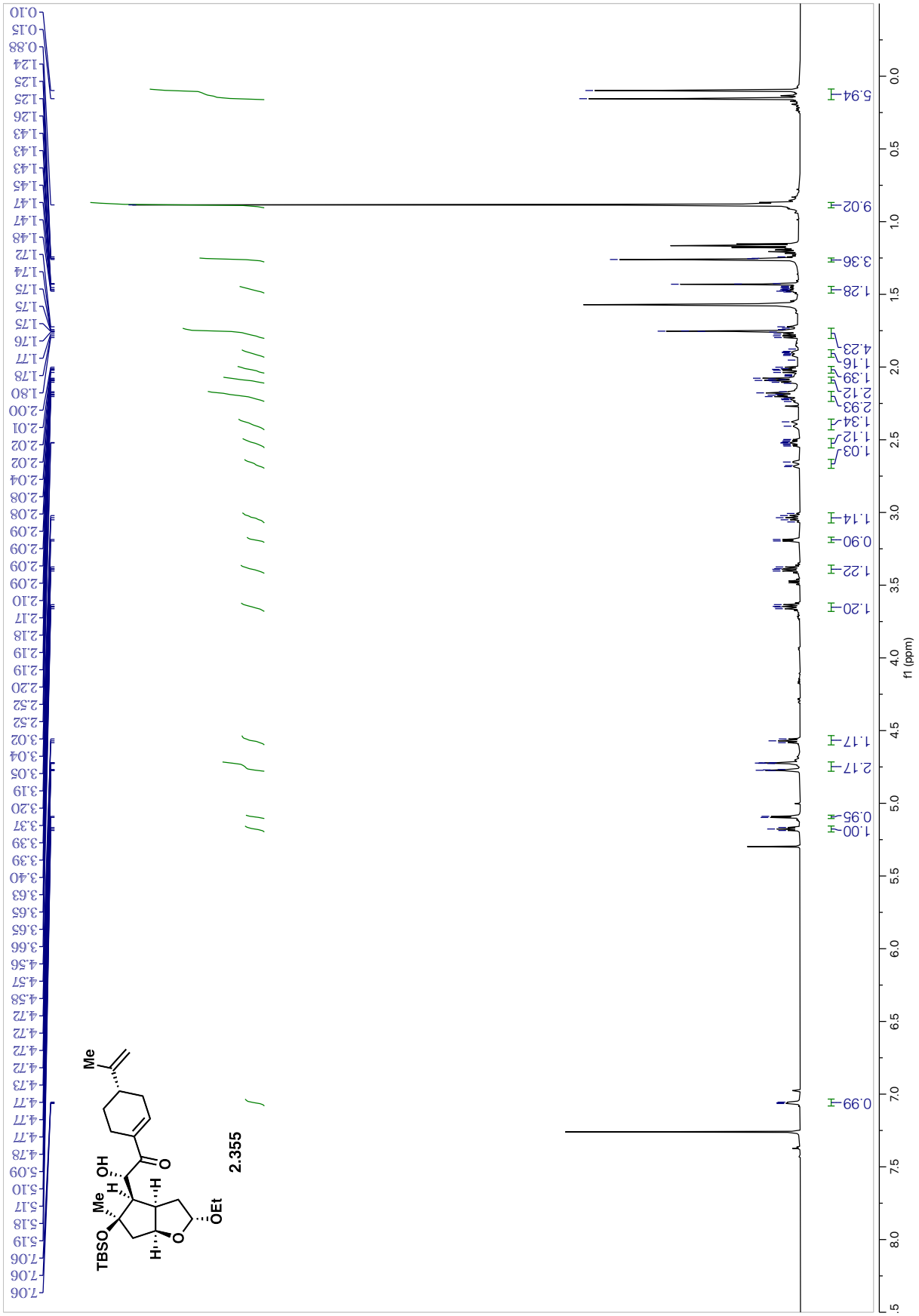

f1 (ppm)
2.350
TBSO
Me
H
O
OAc
OEt
H
H
O
Me

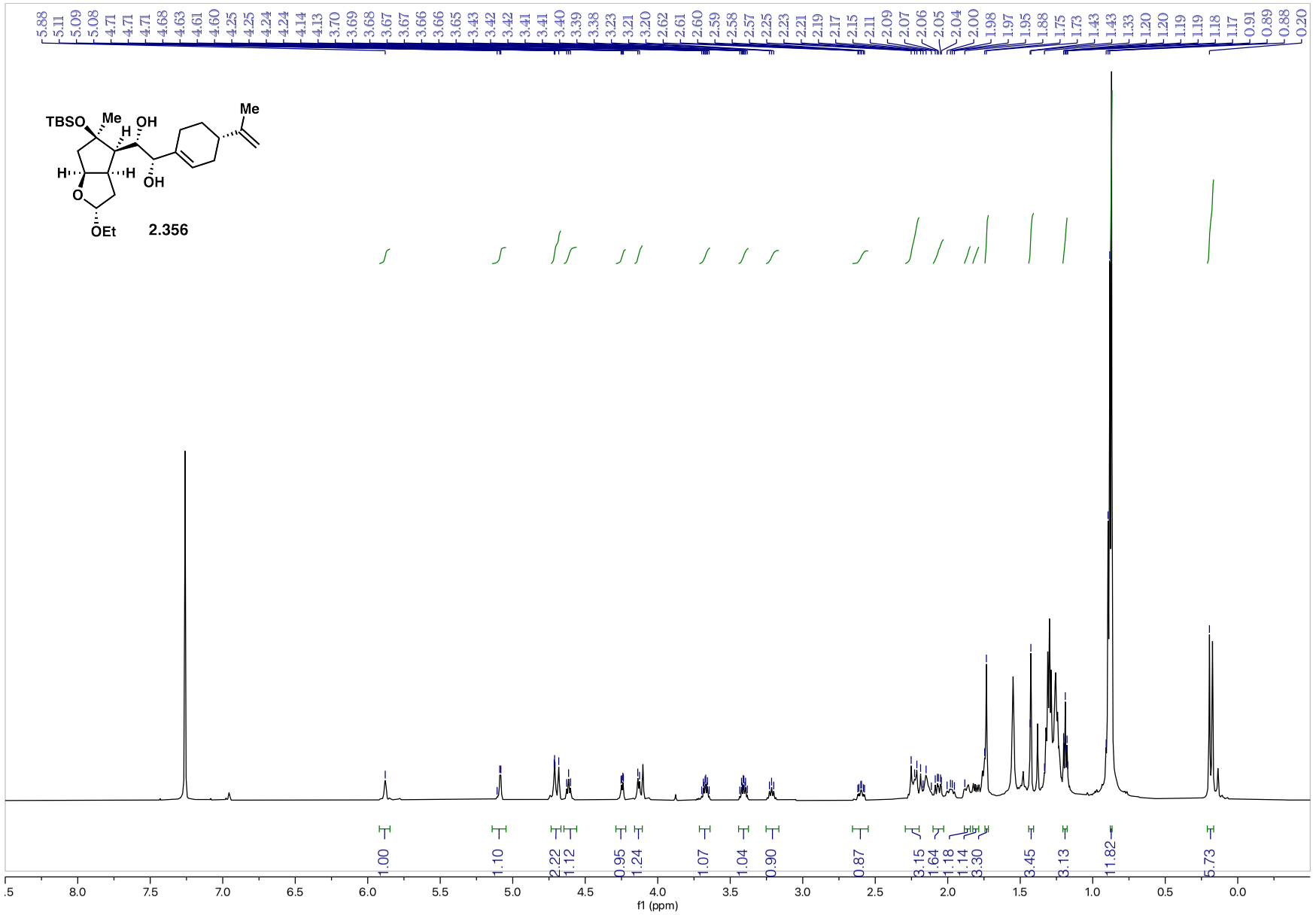

201.11
169.63
148.89
131.43
130.52
108.97
105.50
83.03
82.88
81.89
62.22
58.03
47.78
44.02
39.97
36.27
30.50
28.10
26.81
25.83
24.08
20.89
20.80
18.28
15.29
2.20
2.45
TBSO
Me
H
O
Me
H
H
O
OAc
OEt
2.350
f1 (ppm)

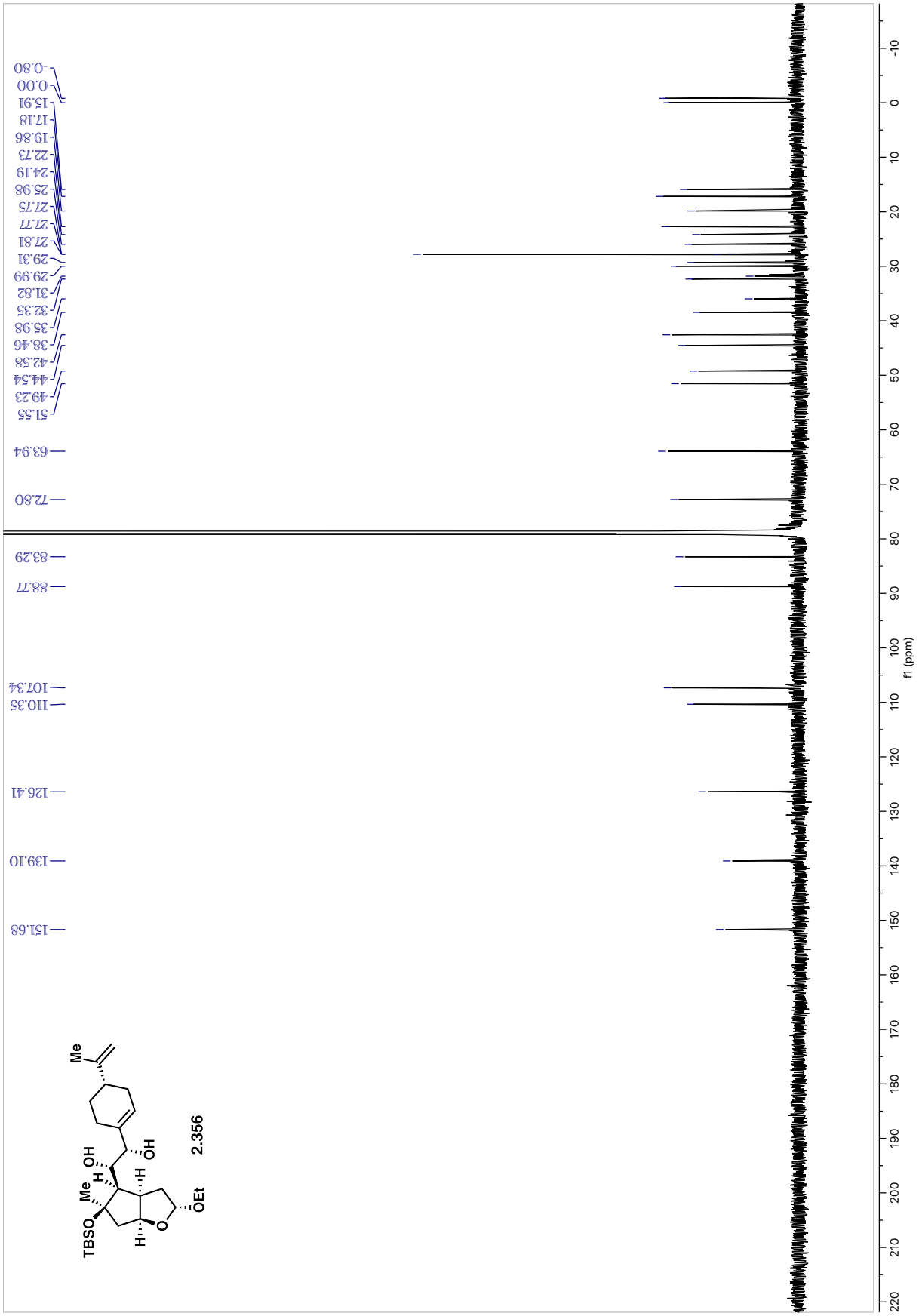

2.351
TBSO
Me
H
O
OAc
H
H
O
OEt
Me
f1 (ppm)

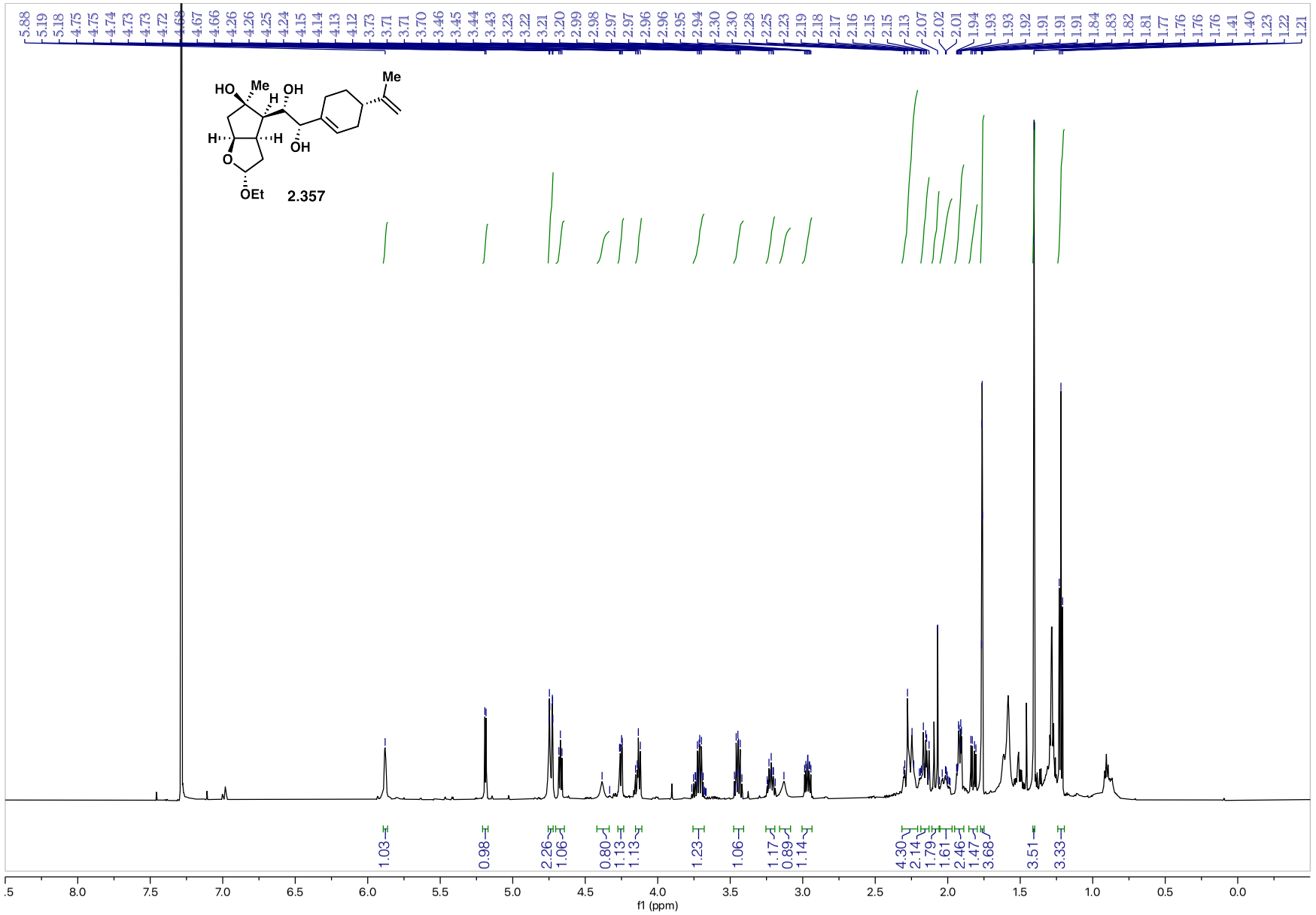

201.50
169.85
148.98
131.65
130.83
109.18
105.73
84.54
84.45
82.16
62.22
57.06
47.72
44.99
40.70
35.06
30.91
28.65
27.24
25.74
25.15
20.76
20.70
18.15
15.28
2.23
-2.61
TBSO
Me
H
O
Me
H
H
OAc
O
OEt
2.351
f1 (ppm)

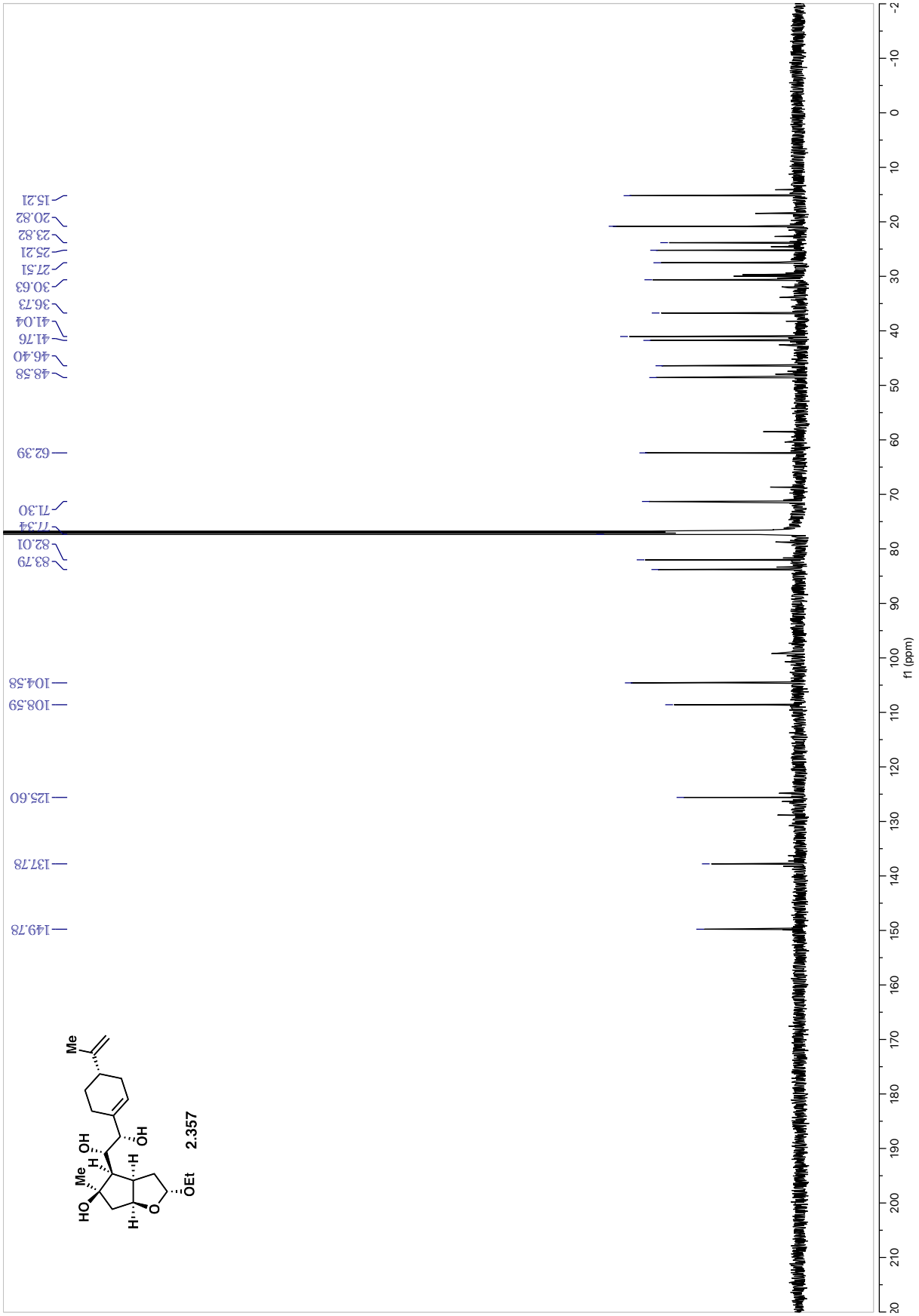

TBSO
Me
H
H
H
O
OEt
Me
2.352
f1 (ppm)

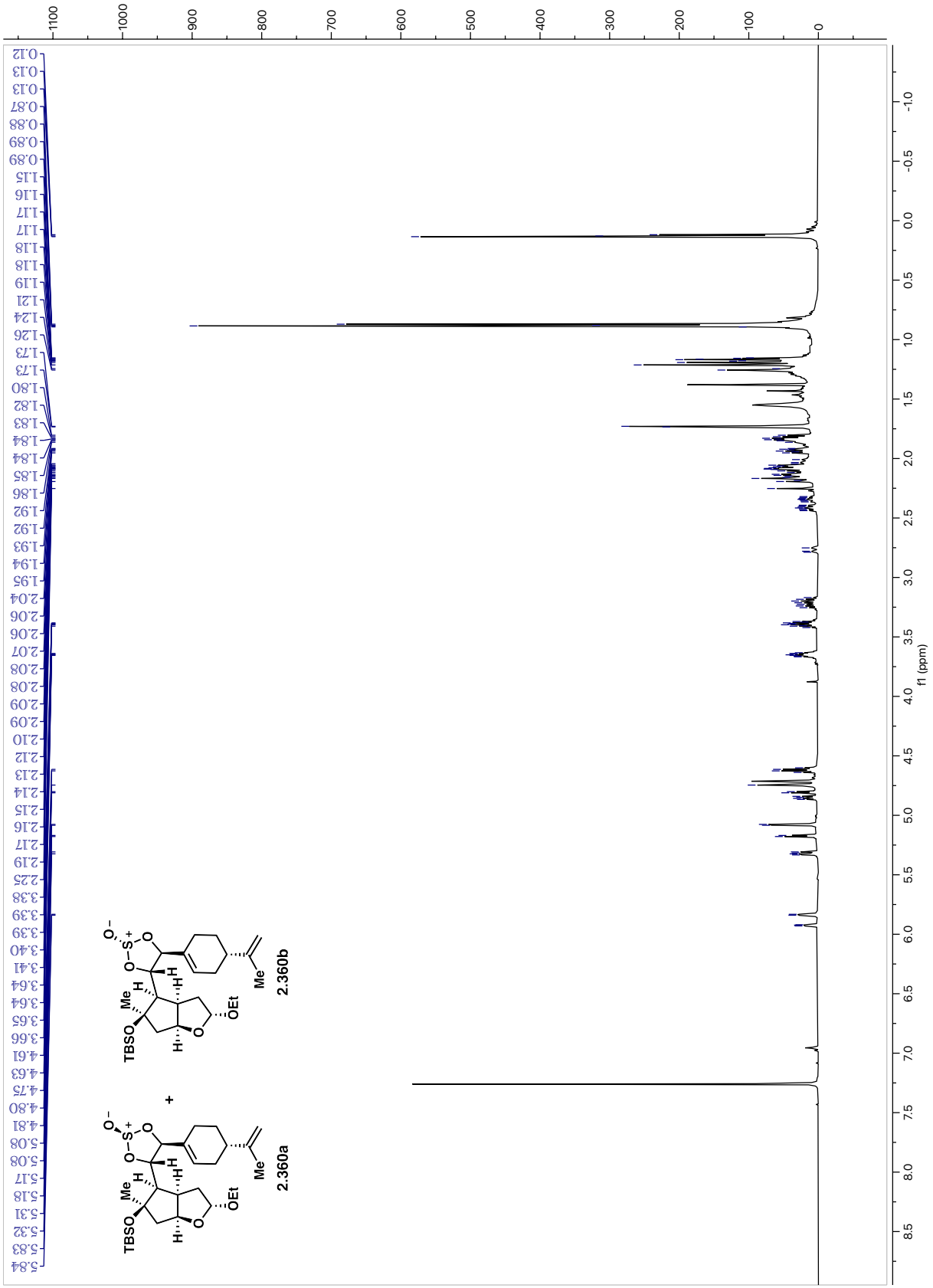

Me
OH
H
Me
TBSO
H
O
H
O
OEt
2.355
5.94
9.02
3.36
1.28
4.23
1.16
1.39
2.12
2.93
1.34
1.12
1.03
1.14
0.90
1.22
1.20
1.17
2.17
0.95
1.00
0.99
f1 (ppm)

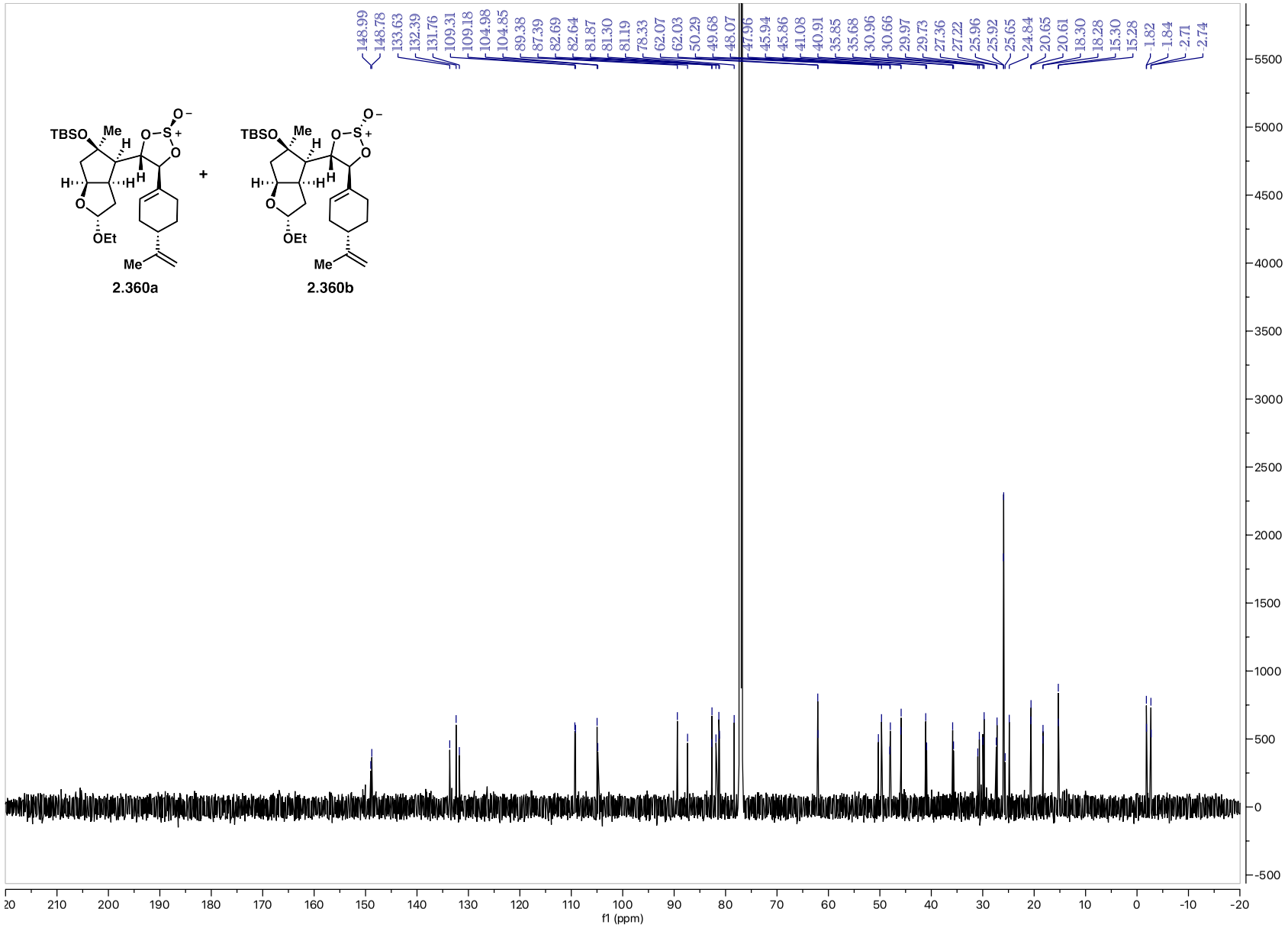

TBSO
Me
H
OH
Me
H
H
OH
O
OEt
2.356
f1 (ppm)

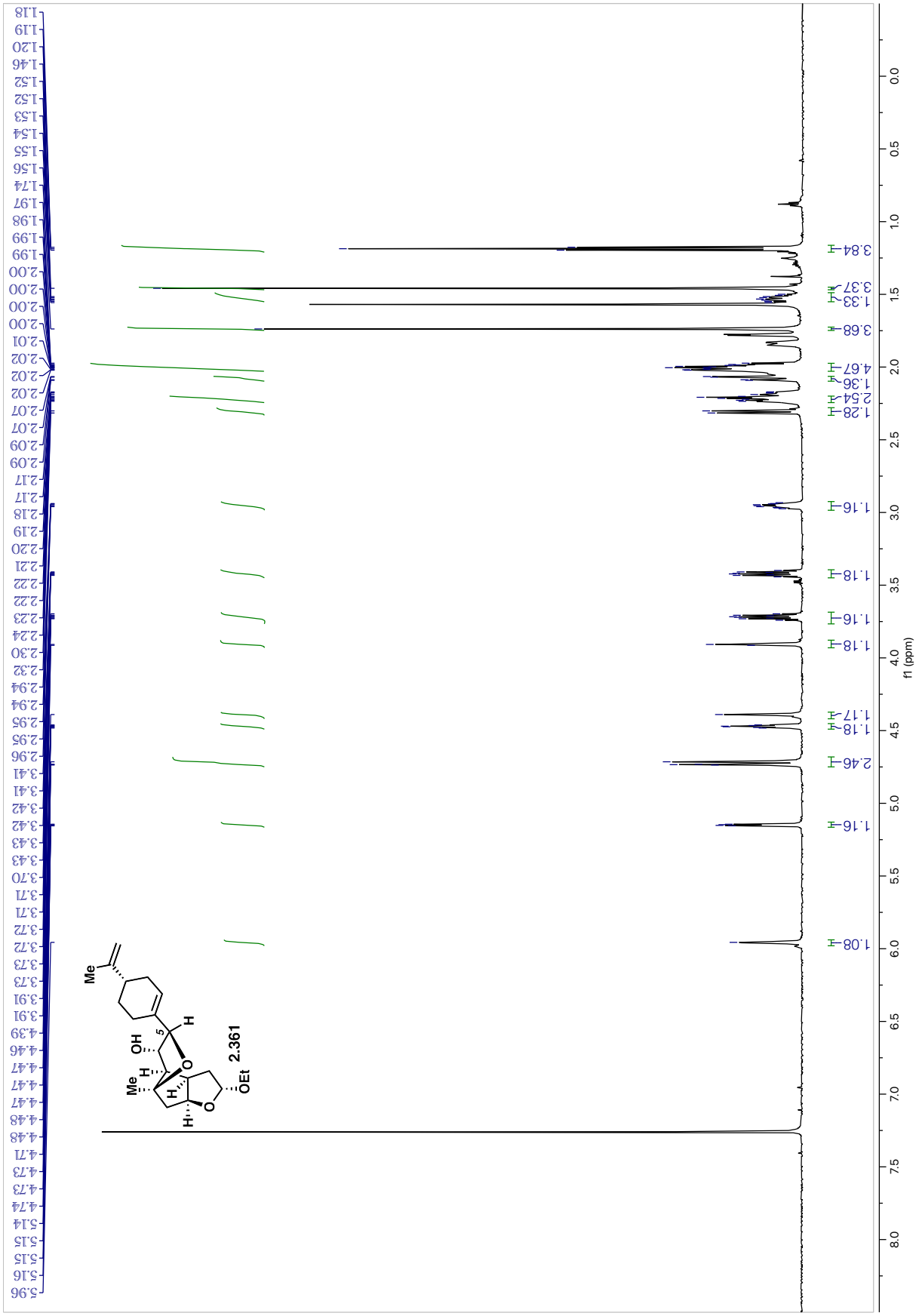

-0.80
0.00
15.91
17.18
19.86
22.73
24.19
25.98
27.75
27.77
27.81
29.31
29.99
31.82
32.35
35.98
38.46
42.58
44.54
49.23
51.55
63.94
72.80
83.29
88.77
107.34
110.35
126.41
139.10
151.68
Me
OH
Me
H
TBSO
H
H
O
OEt
2.356
f1 (ppm)

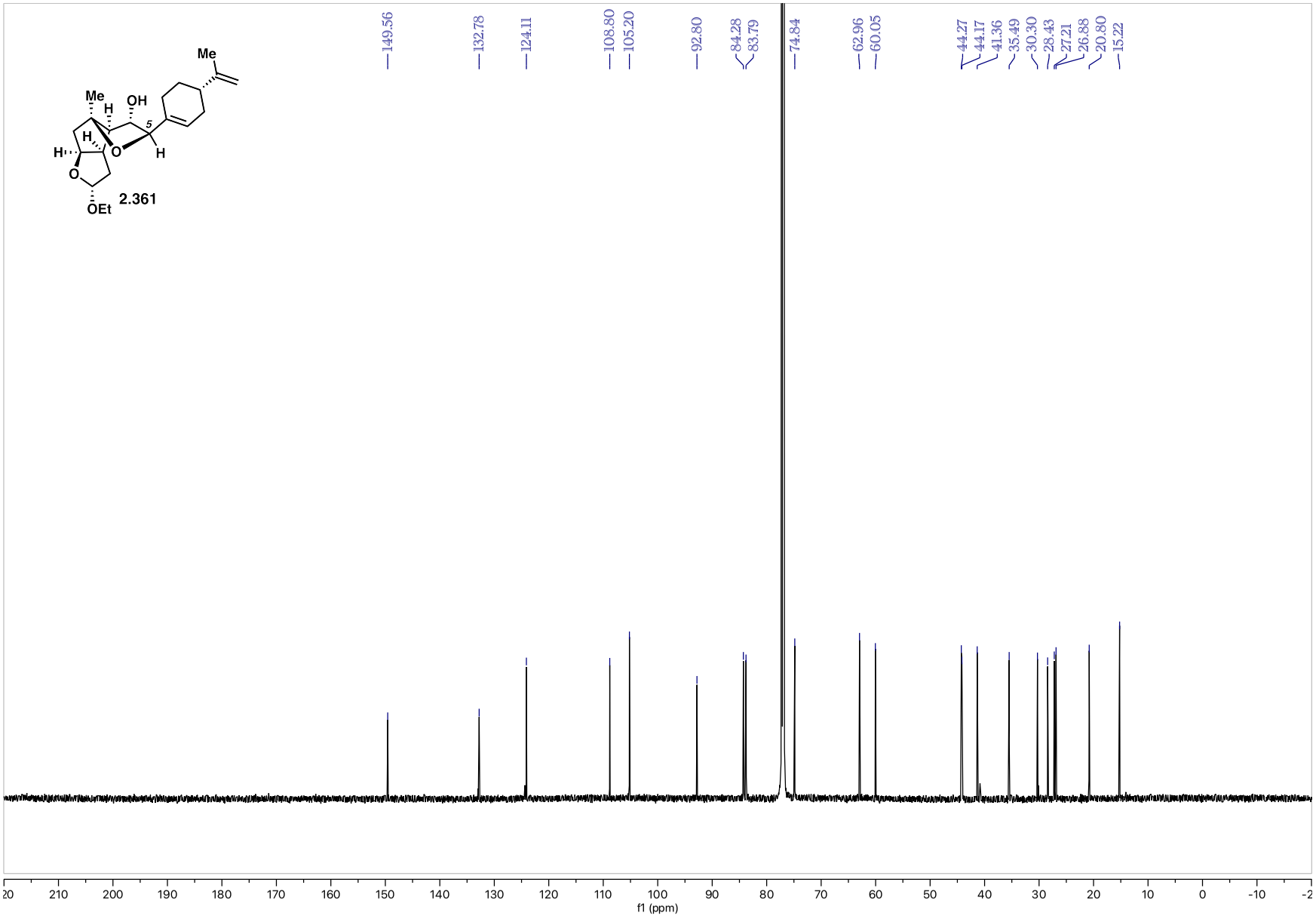

HO
Me
H
OH
Me
H
H
OH
O
OEt
2.357
f1 (ppm)

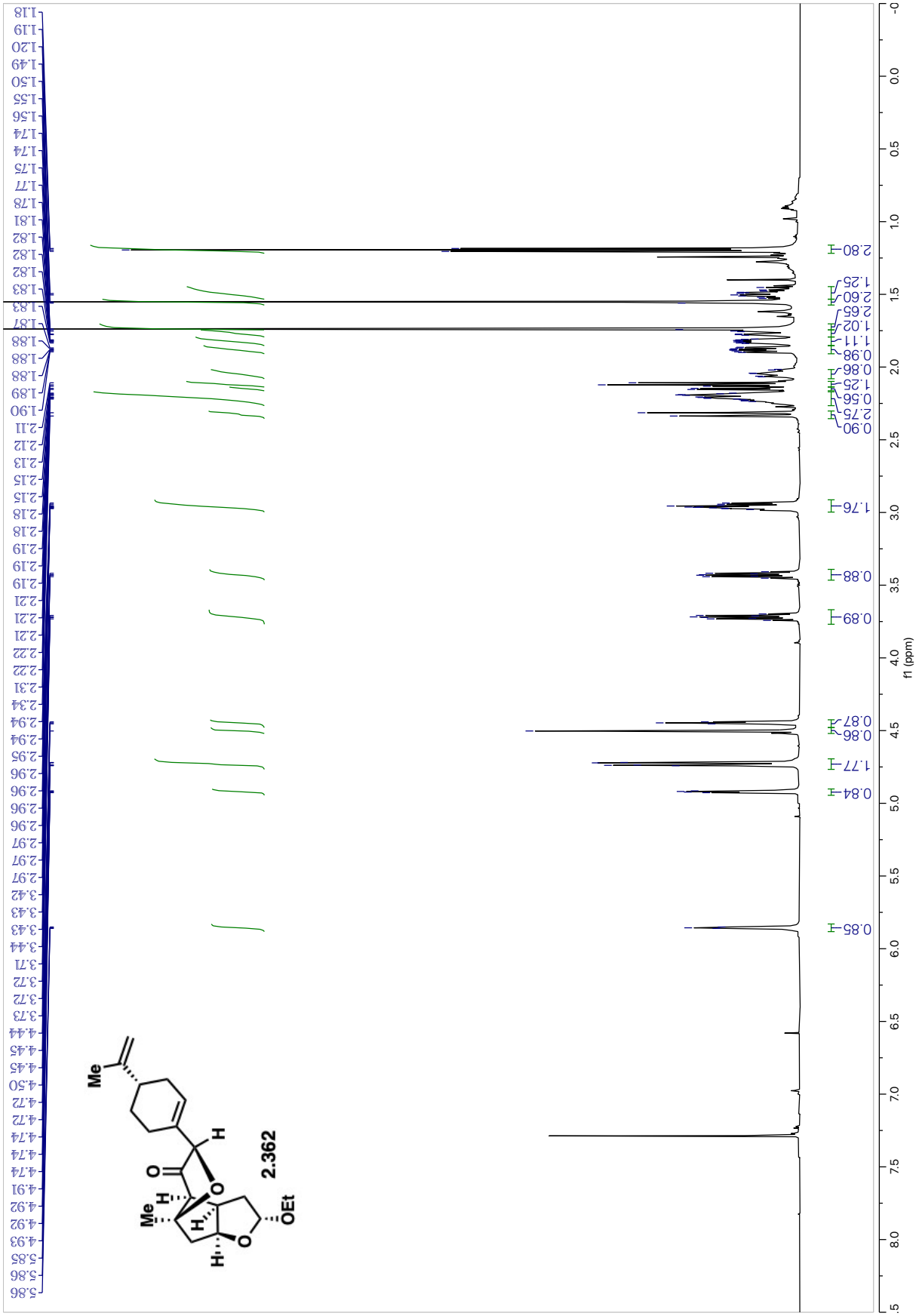

15.21
20.82
23.82
25.21
27.51
30.63
36.73
41.04
41.76
46.40
48.58
62.39
71.30
77.34
82.01
83.79
104.58
108.59
125.60
137.78
149.78
f1 (ppm)
Me
OH
H
Me
HO
H
O
H
OH
OEt
2.357

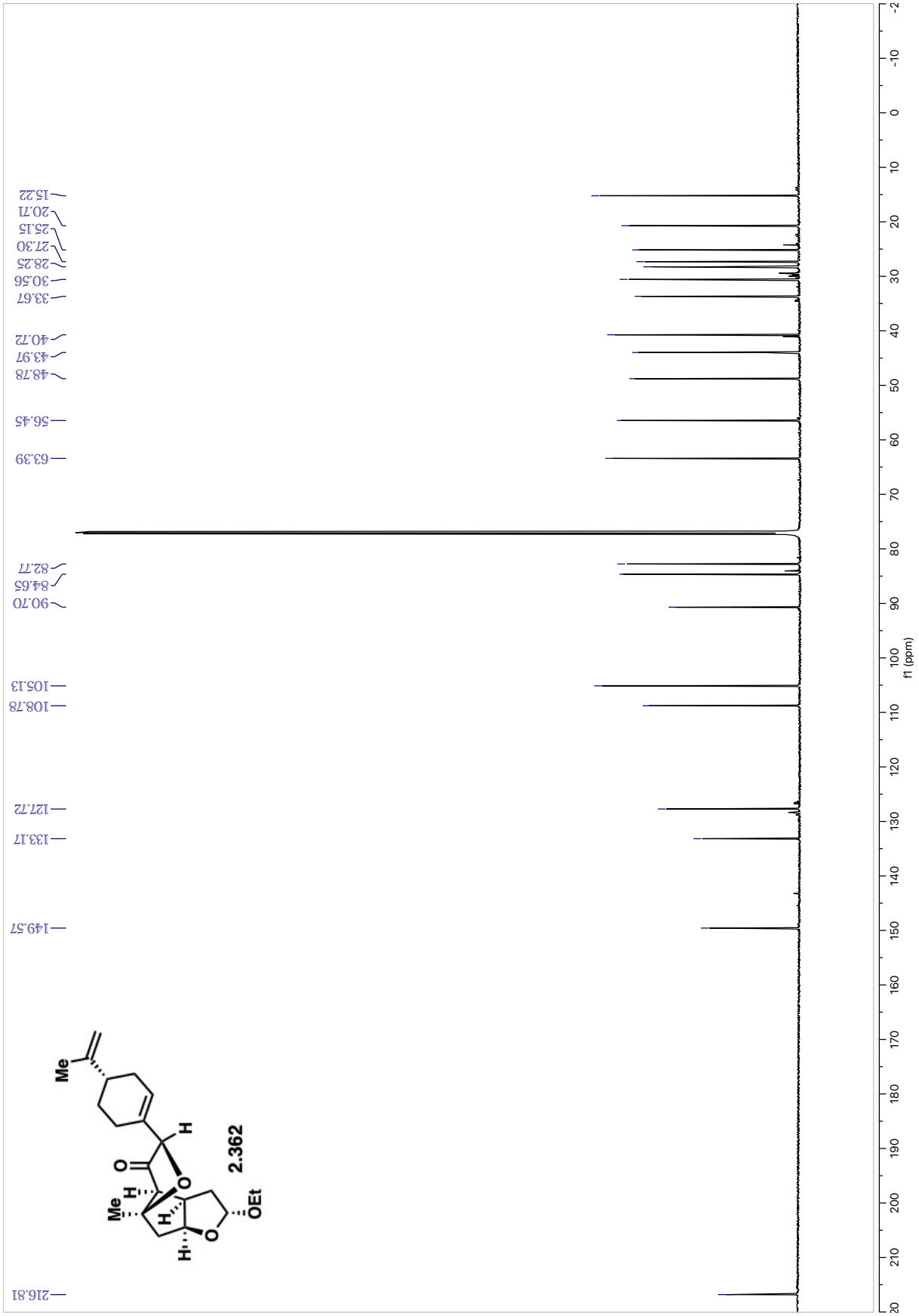

TBSO
Me
H
H
H
O
OEt
Me
2.360b
+
2.360a
f1 (ppm)

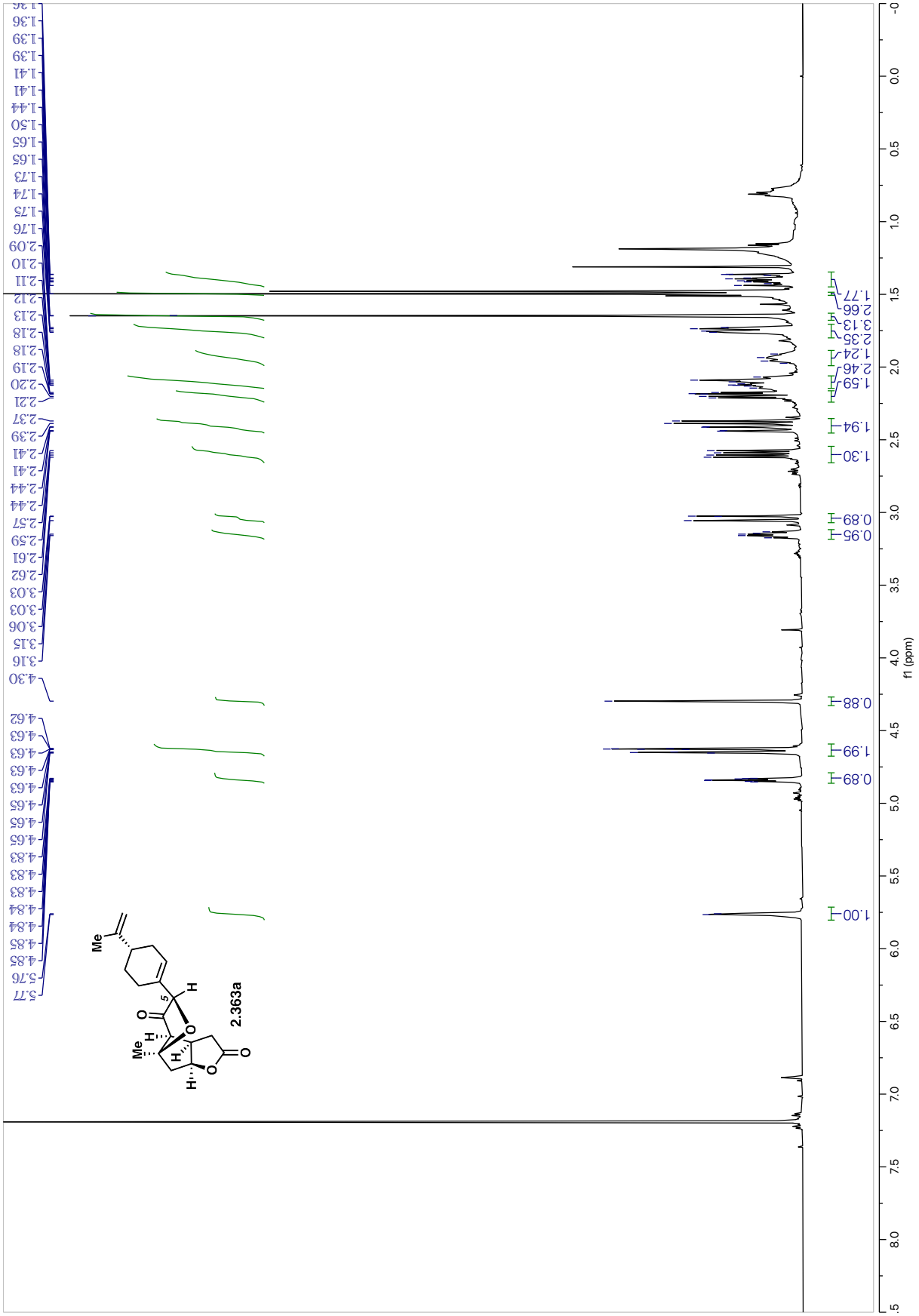

148.99
148.78
133.63
132.39
131.76
109.31
109.18
104.98
104.85
89.38
87.39
82.69
82.64
81.87
81.30
81.19
78.33
62.07
62.03
50.29
49.68
48.07
47.96
45.94
45.86
41.08
40.91
35.85
35.68
30.96
30.66
29.97
29.73
27.36
27.22
25.96
25.92
25.65
24.84
20.65
20.61
18.30
18.28
15.30
15.28
1.82
1.84
2.71
2.74
TBSO
Me
H
O
S
O
H
H
H
O
OEt
Me
2.360a
+
2.360b
f1 (ppm)

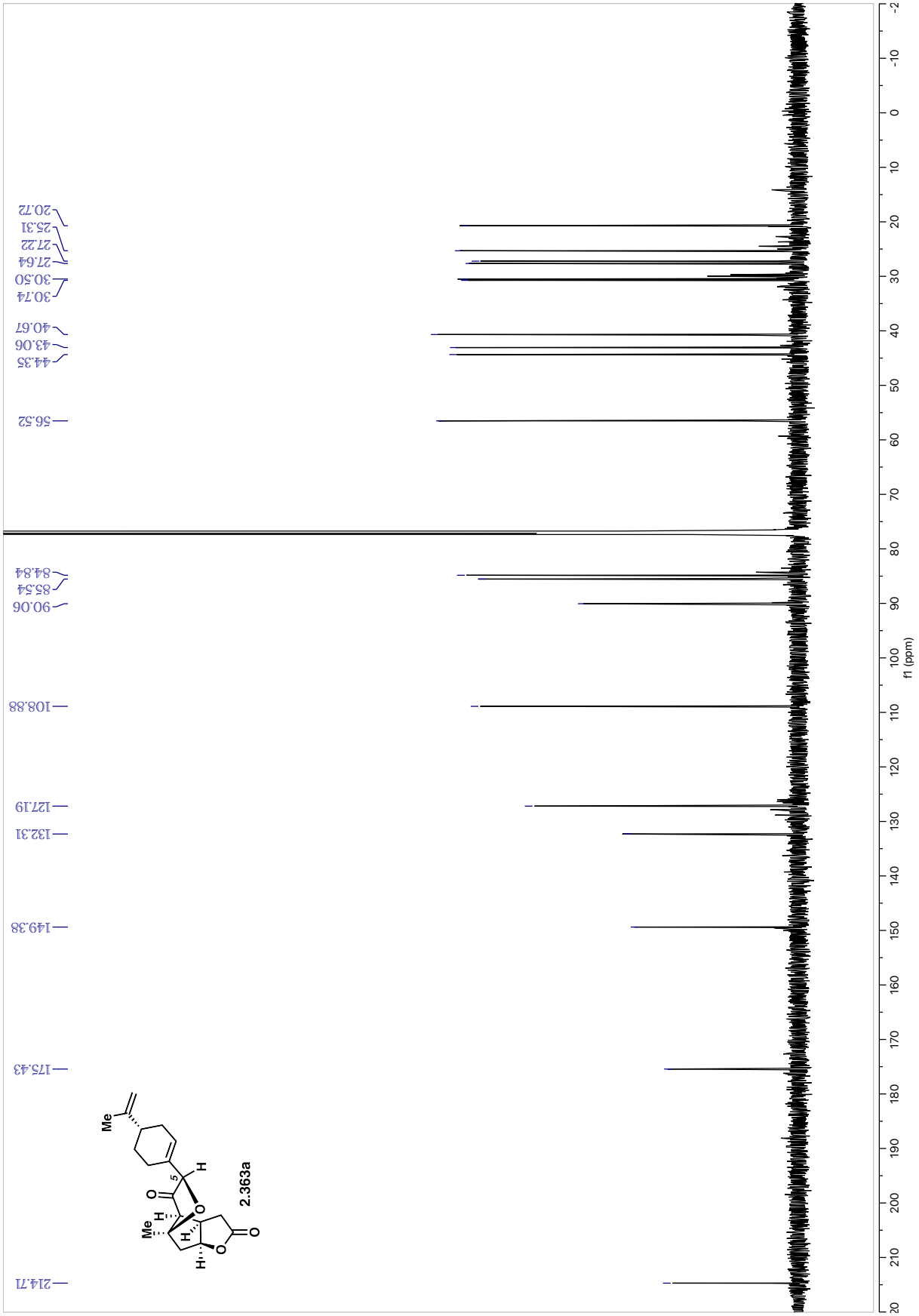

Me
OH
H
H
H
O
O
OEt
2.361
f1 (ppm)

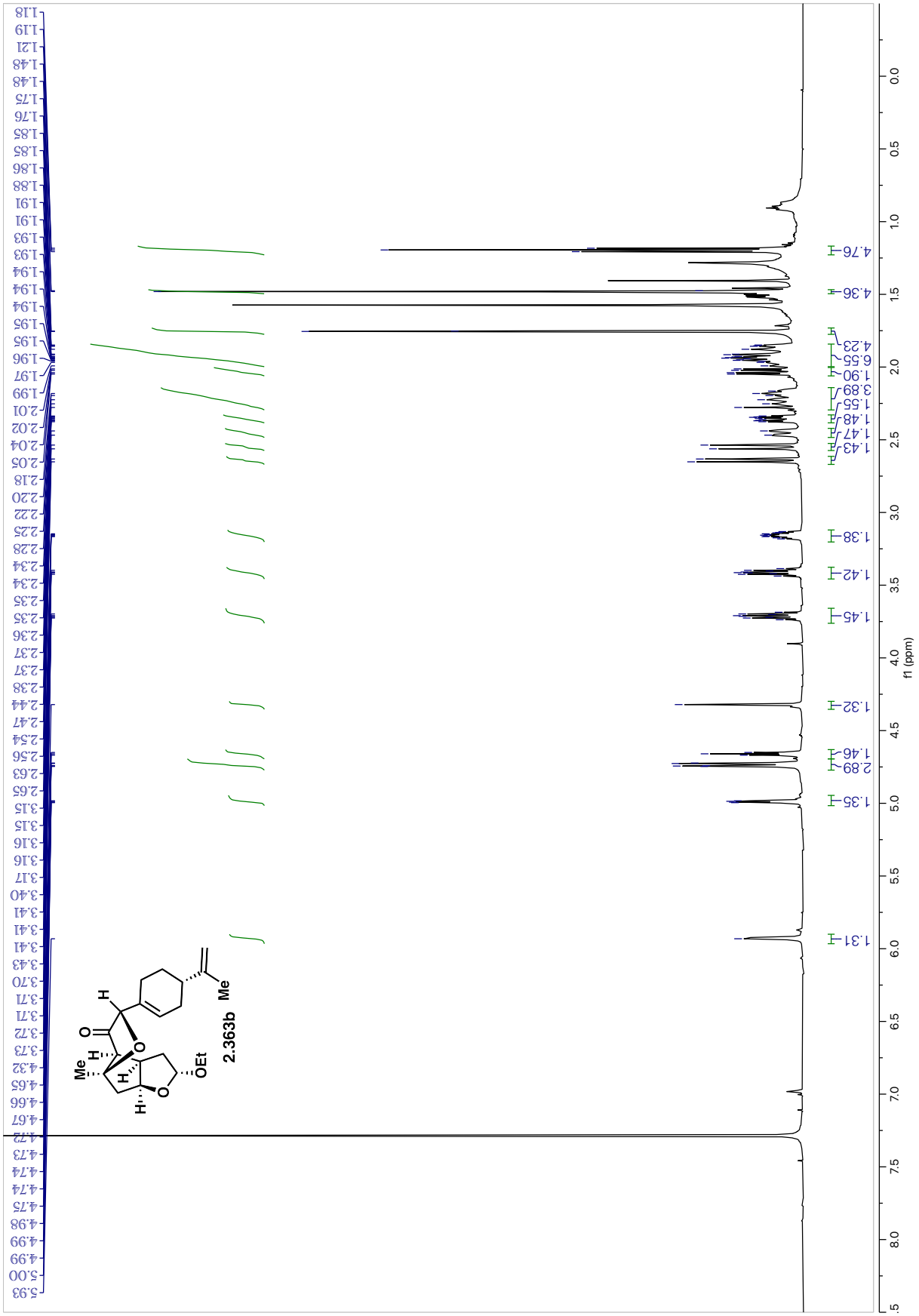

149.56
132.78
124.11
108.80
105.20
92.80
84.28
83.79
74.84
62.96
60.05
44.27
44.17
41.36
35.49
30.30
28.43
27.21
26.88
20.80
15.22
Me
Me
H
OH
5
H
H
O
O
H
OEt
2.361
f1 (ppm)

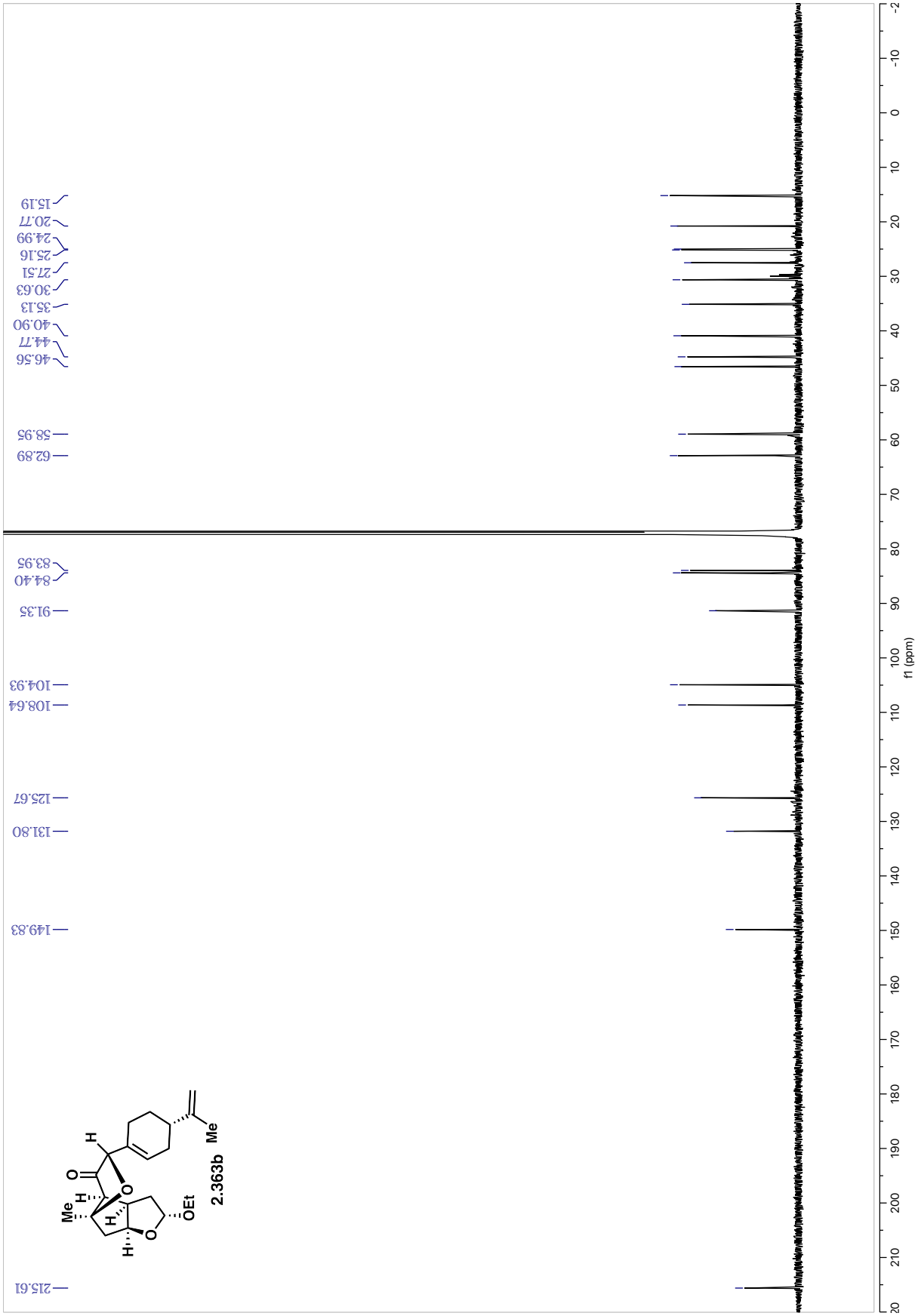

Me
H
O
Me
H
H
O
O
OEt
2.362
f1 (ppm)

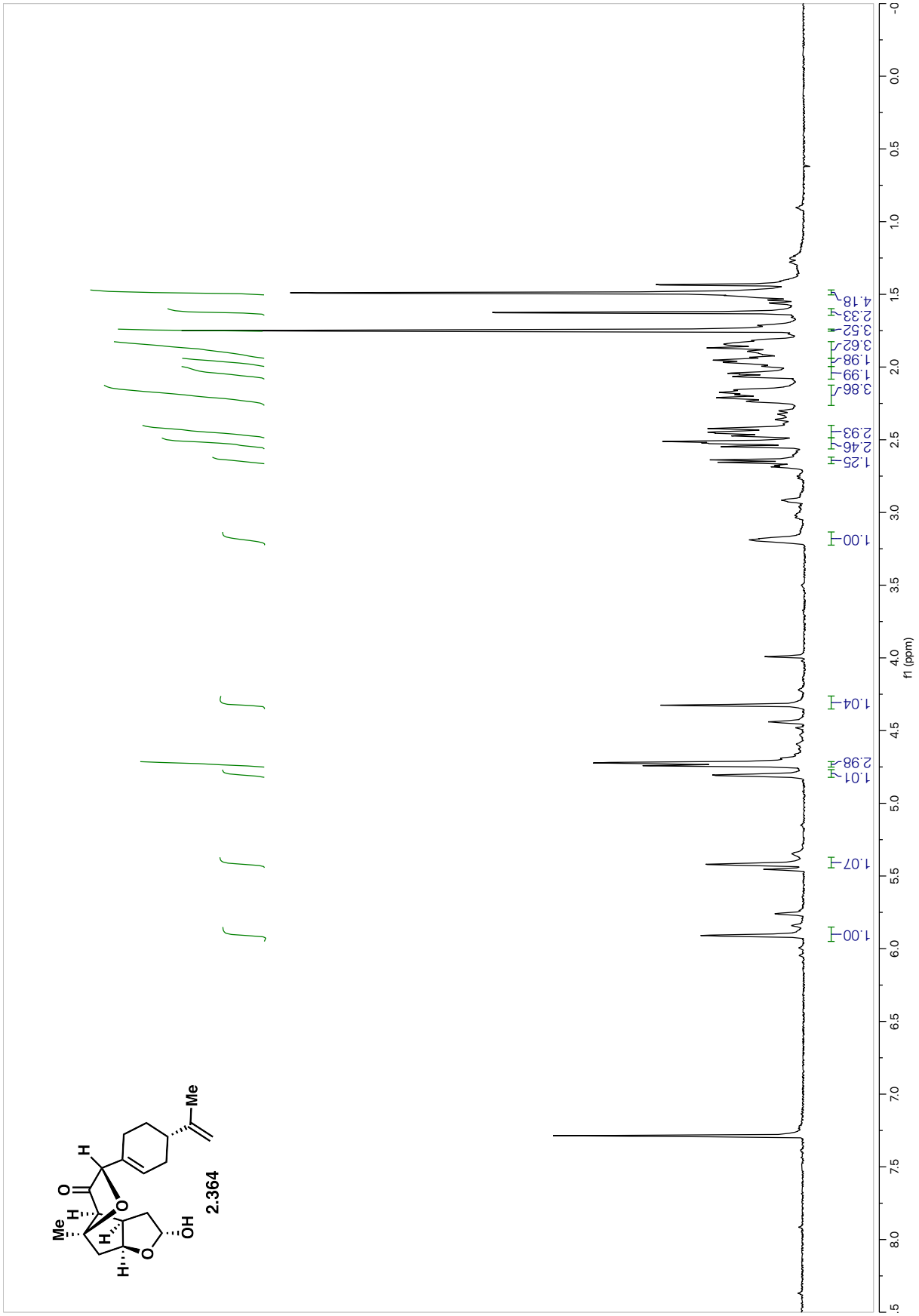

216.81
149.57
133.17
127.72
108.78
105.13
90.70
84.65
82.77
63.39
56.45
48.78
43.97
40.72
33.67
30.56
28.25
27.30
25.15
20.71
15.22
f1 (ppm)
Me
H
O
Me
H
H
O
O
OEt
2.362

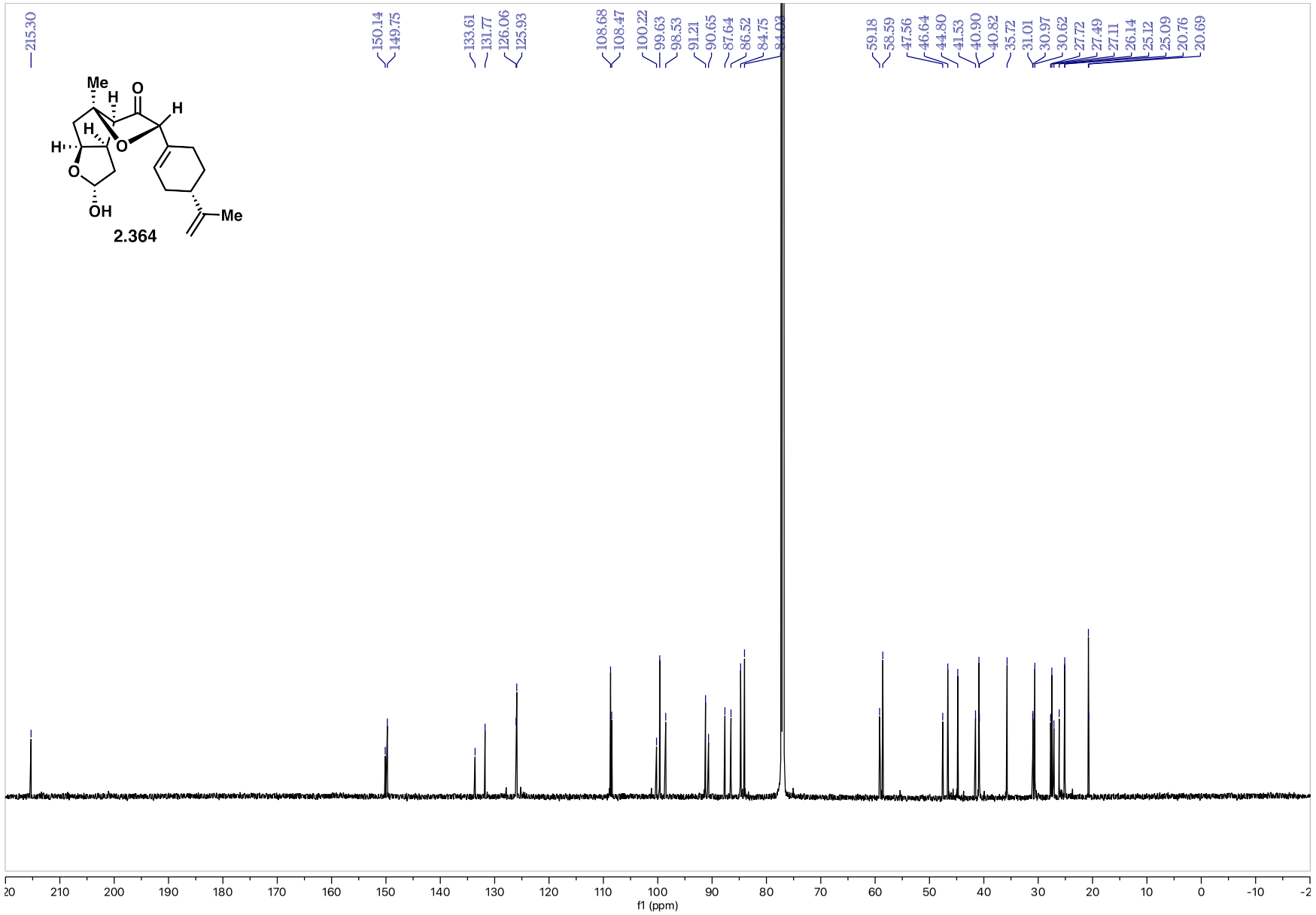

Me
H
O
O
H
Me
H
O
O
H
O
2.363a
1.00
0.89
1.99
0.88
0.95
0.89
1.30
1.94
1.59
2.46
1.24
2.35
3.13
2.66
1.77
f1 (ppm)

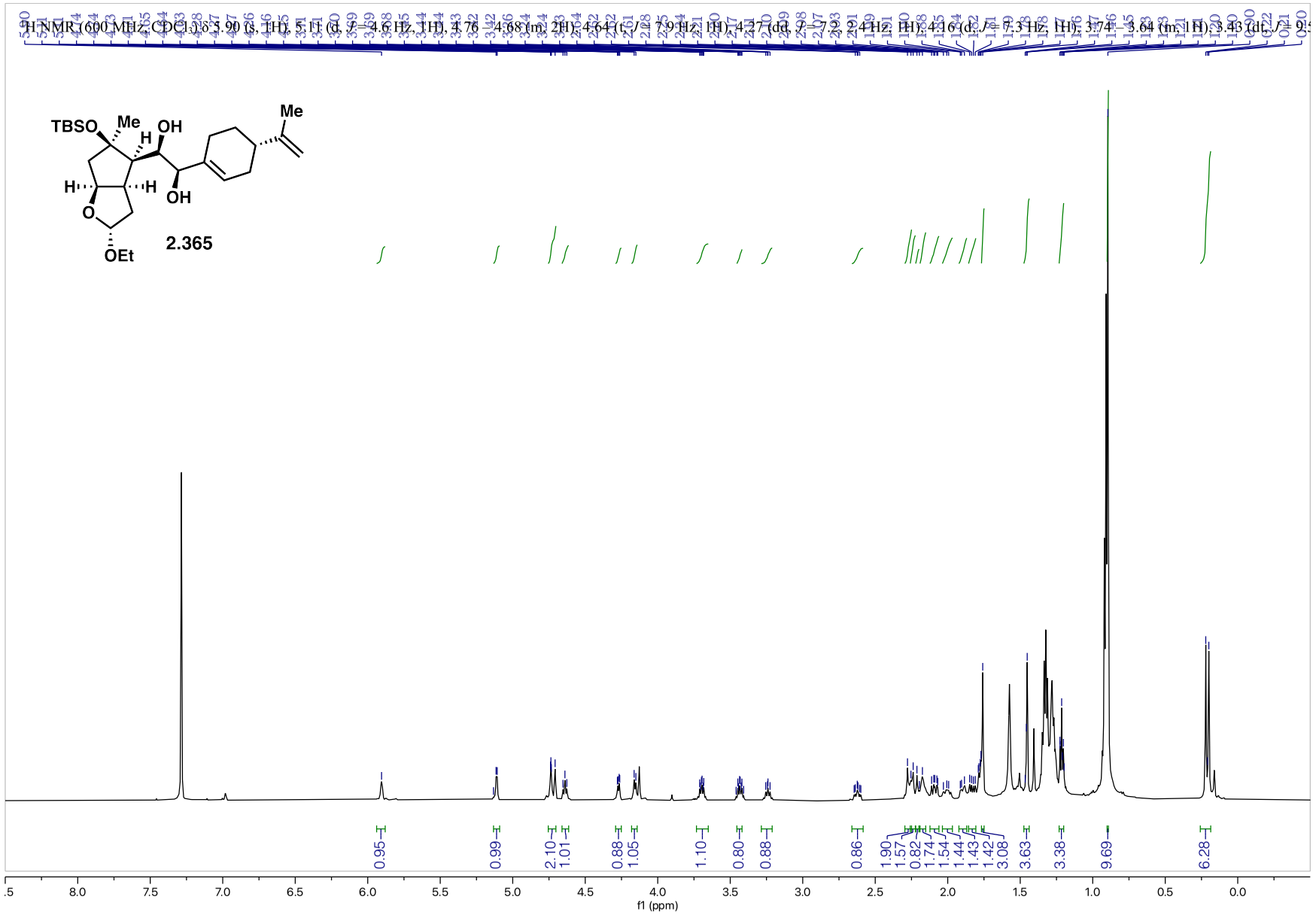

214.71
175.43
149.38
132.31
127.19
108.88
90.06
85.54
84.84
56.52
44.35
43.06
40.67
30.74
30.50
27.64
27.22
25.31
20.72
f1 (ppm)
2.363a

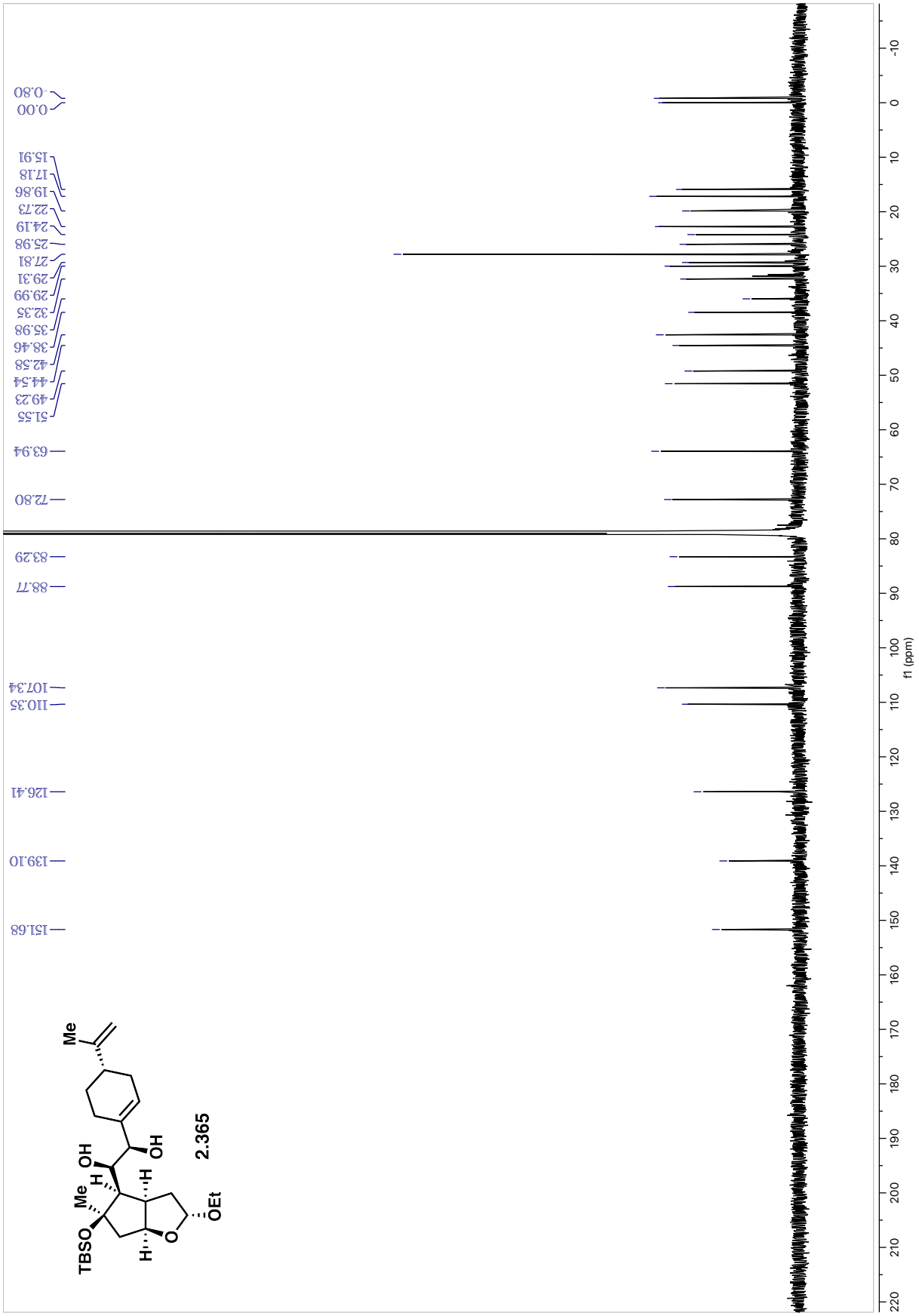

2.363b
Me
H
O
O
H
H
O
OEt
Me
4.76
4.36
4.23
6.55
1.90
3.89
1.55
1.48
1.47
1.43
1.38
1.42
1.45
1.32
1.46
2.89
1.35
1.31
f1 (ppm)

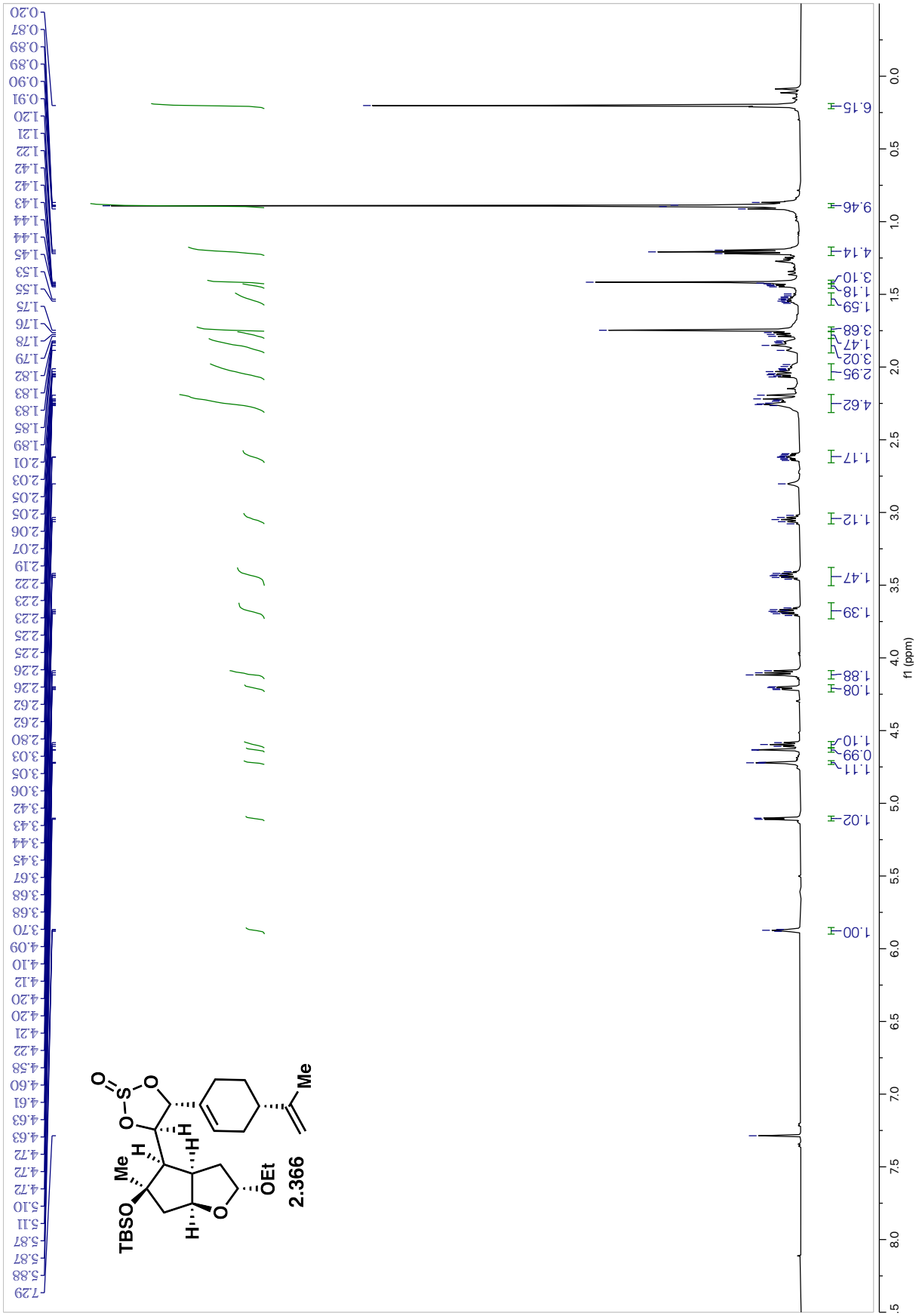

215.61
149.83
131.80
125.67
108.64
104.93
91.35
84.40
83.95
62.89
58.95
46.56
44.77
40.90
35.13
30.63
27.51
25.16
24.99
20.77
15.19
f1 (ppm)
2.363b
Me
H
O
H
Me
H
O
H
O
OEt

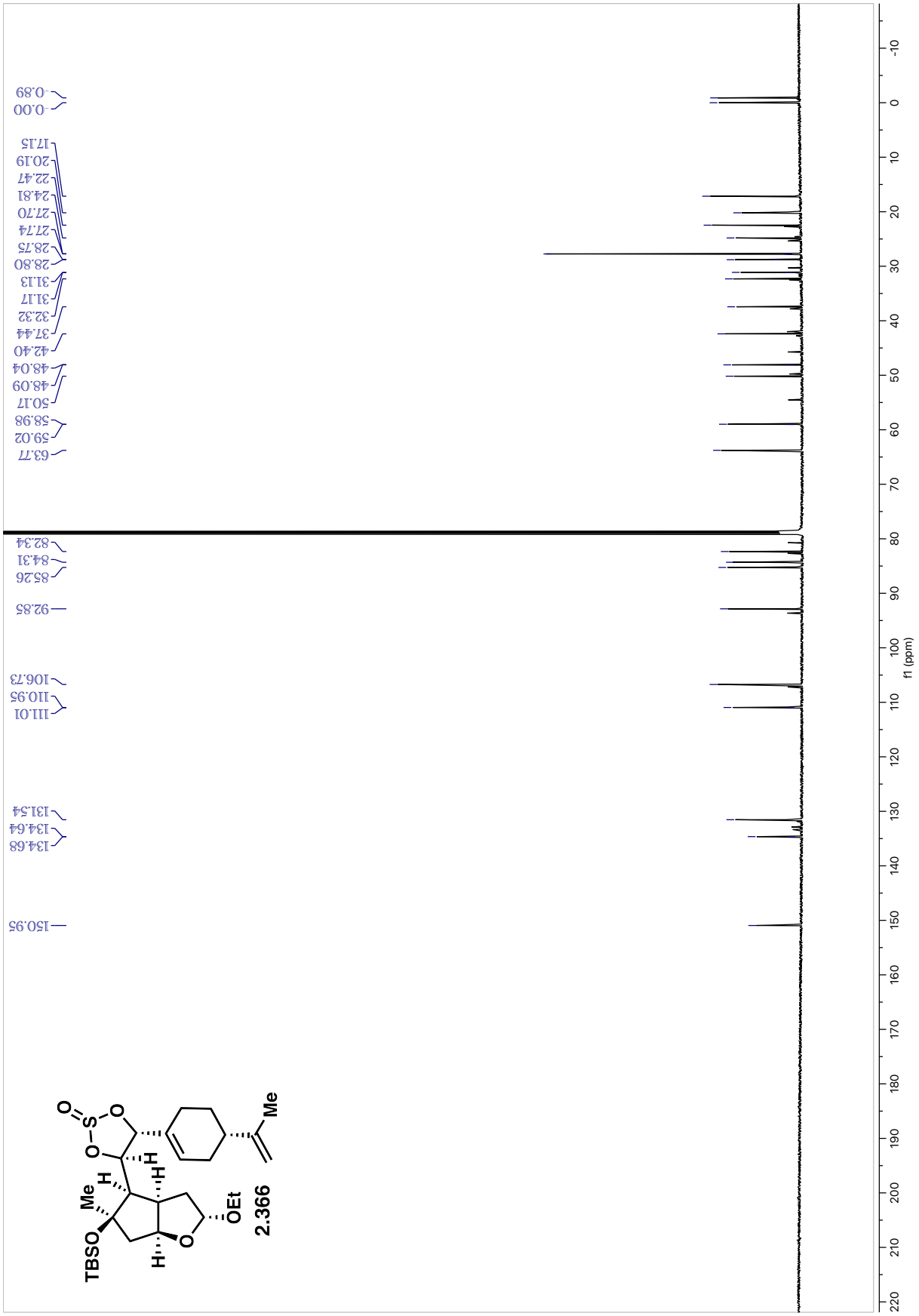

Me
H
O
Me
H
H
O
H
OH
O
2.364
4.18
2.33
3.52
3.62
1.98
1.99
3.86
2.93
2.46
1.25
1.00
1.04
2.98
1.01
1.07
1.00
f1 (ppm)

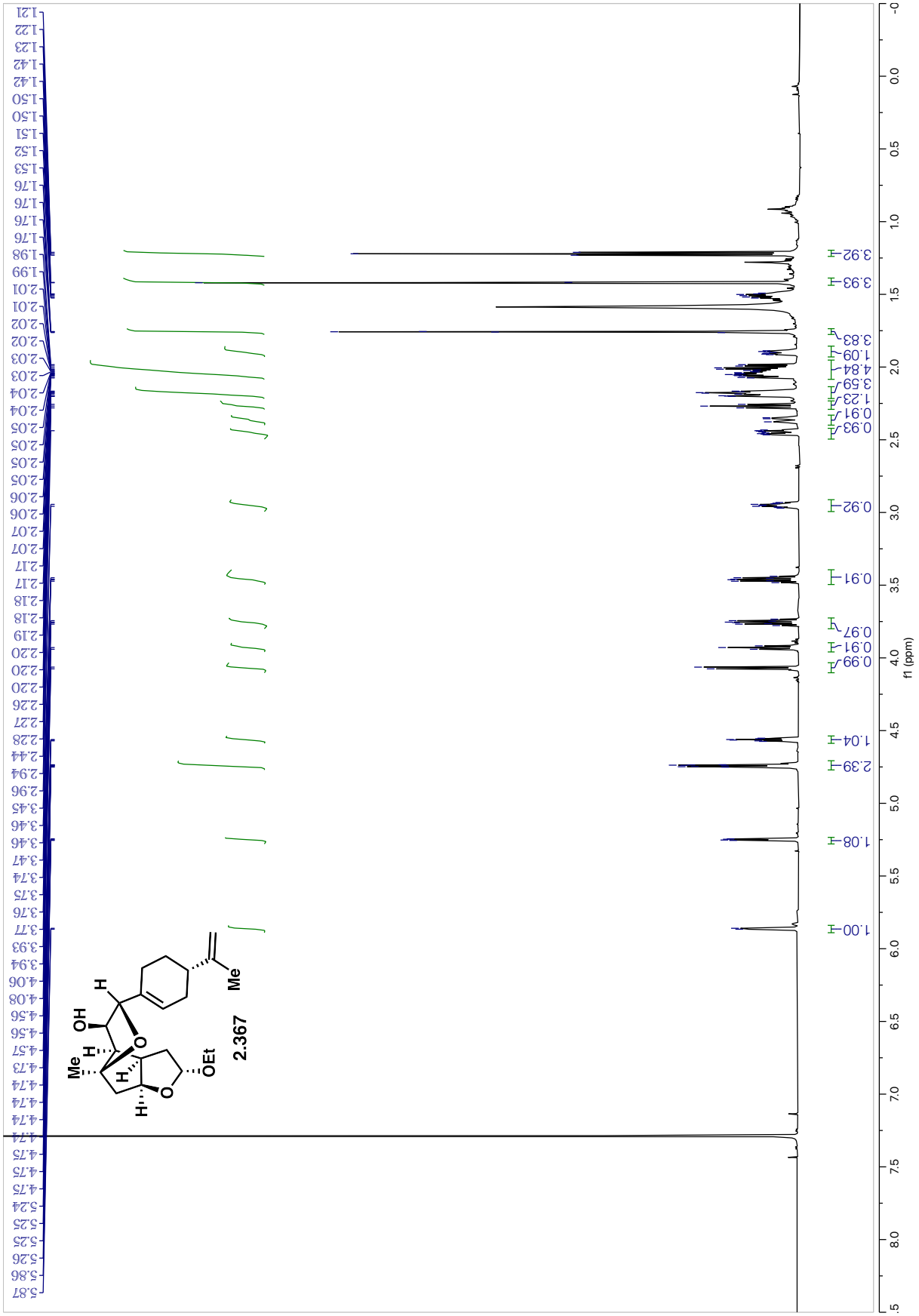

215.30
150.14
149.75
133.61
131.77
126.06
125.93
108.68
108.47
100.22
99.63
98.53
91.21
90.65
87.64
86.52
84.75
84.03
59.18
58.59
47.56
46.64
44.80
41.53
40.90
40.82
35.72
31.01
30.97
30.62
27.72
27.49
27.11
26.14
25.12
25.09
20.76
20.69
Me
H
O
H
H
H
O
O
OH
Me
2.364
f1 (ppm)

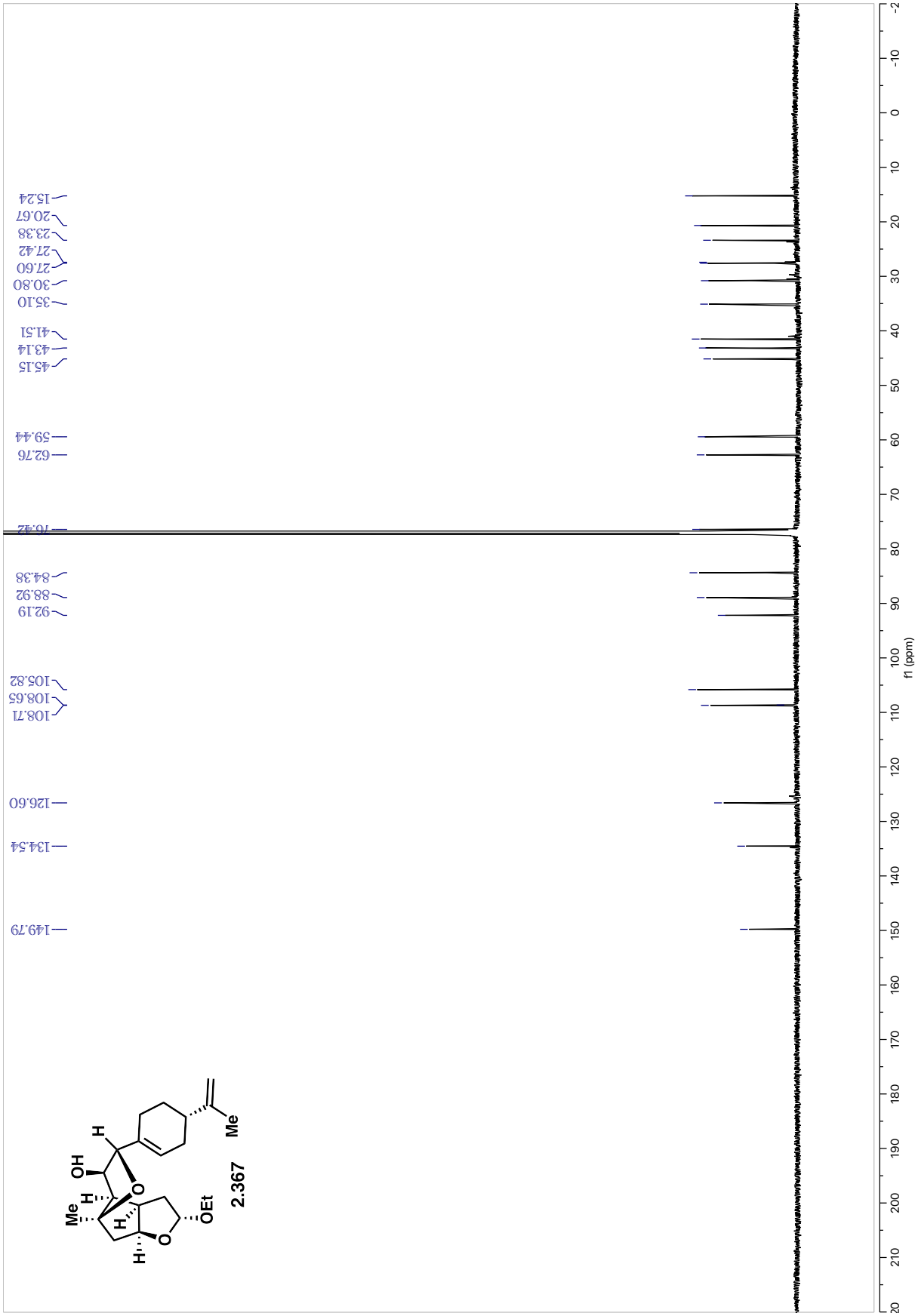

¹H NMR (600 MHz, CDCl3) δ 5.90 (s, 1H), 5.11 (d, J = 4.6 Hz, 1H), 4.76 – 4.68 (m, 2H), 4.64 (t, J = 7.9 Hz, 1H), 4.27 (dd, J = 7.2, 2.4 Hz, 1H), 4.16 (d, J = 7.3 Hz, 1H), 3.74 – 3.64 (m, 1H), 3.43 (dt, J = 9.5
TBSO
Me
H
OH
Me
H
H
O
OH
OEt
2.365
0.95
0.99
2.10
1.01
0.88
1.05
1.10
0.80
0.88
0.86
1.90
1.57
0.82
1.74
1.54
1.44
1.43
1.42
3.08
3.63
3.38
9.69
6.28
f1 (ppm)

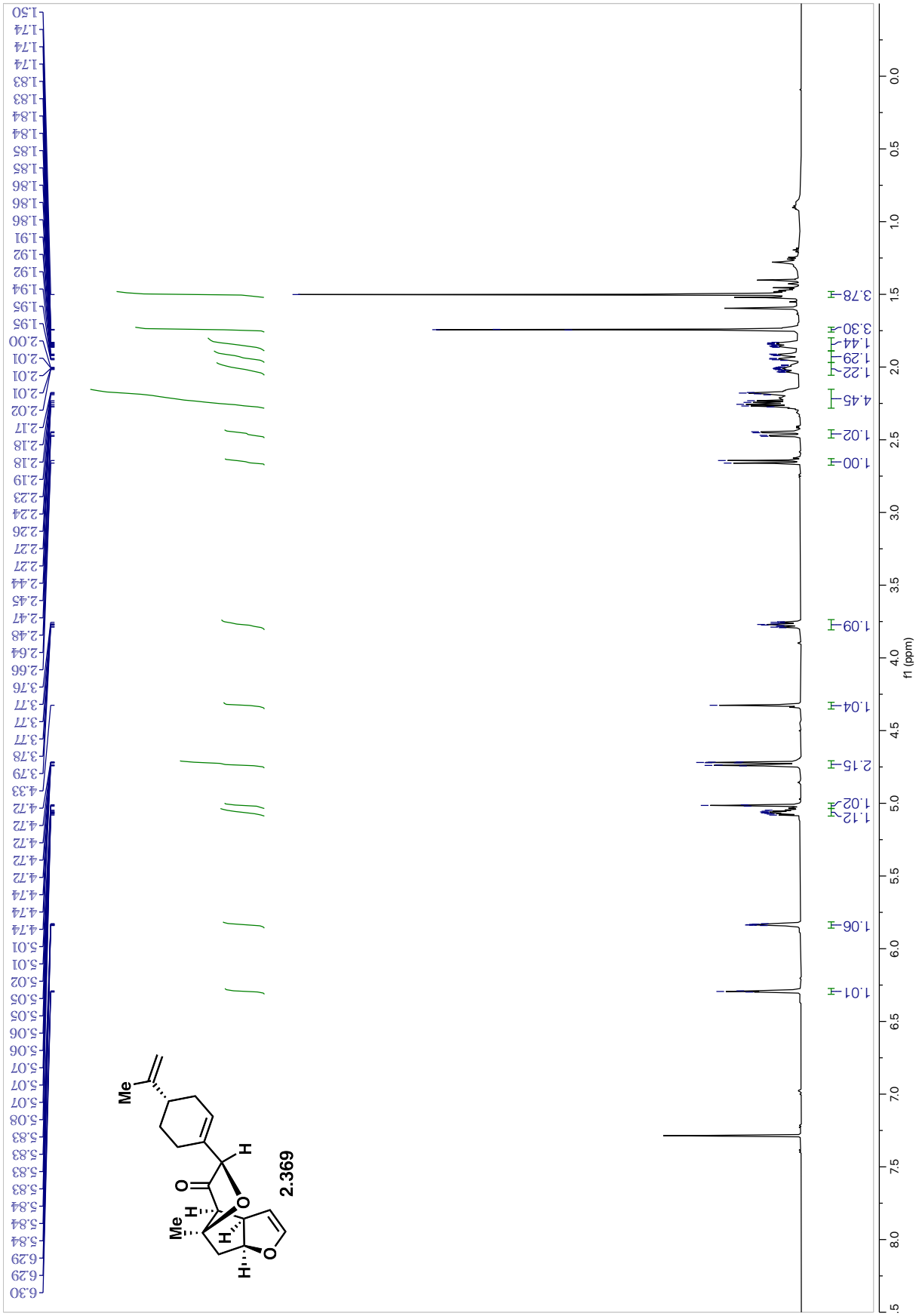

-0.80
0.00
15.91
17.18
19.86
22.73
24.19
25.98
27.81
29.31
29.99
32.35
35.98
38.46
42.58
44.54
49.23
51.55
63.94
72.80
83.29
88.77
107.34
110.35
126.41
139.10
151.68
f1 (ppm)
2.365
Me
OH
H
Me
TBSO
H
H
O
OH
OEt

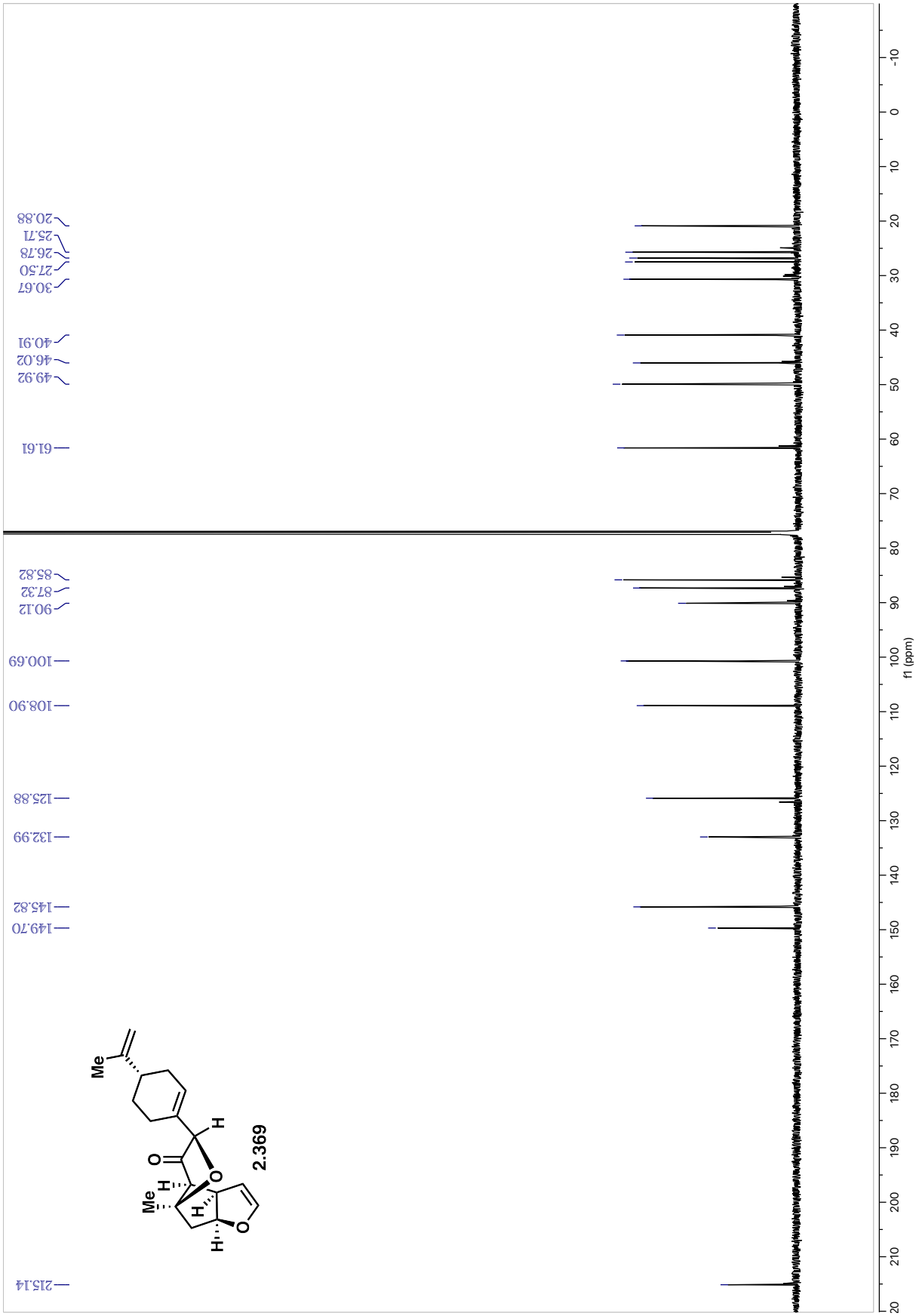

TBSO
Me
H
H
H
O
OEt
2.366
Me
f1 (ppm)

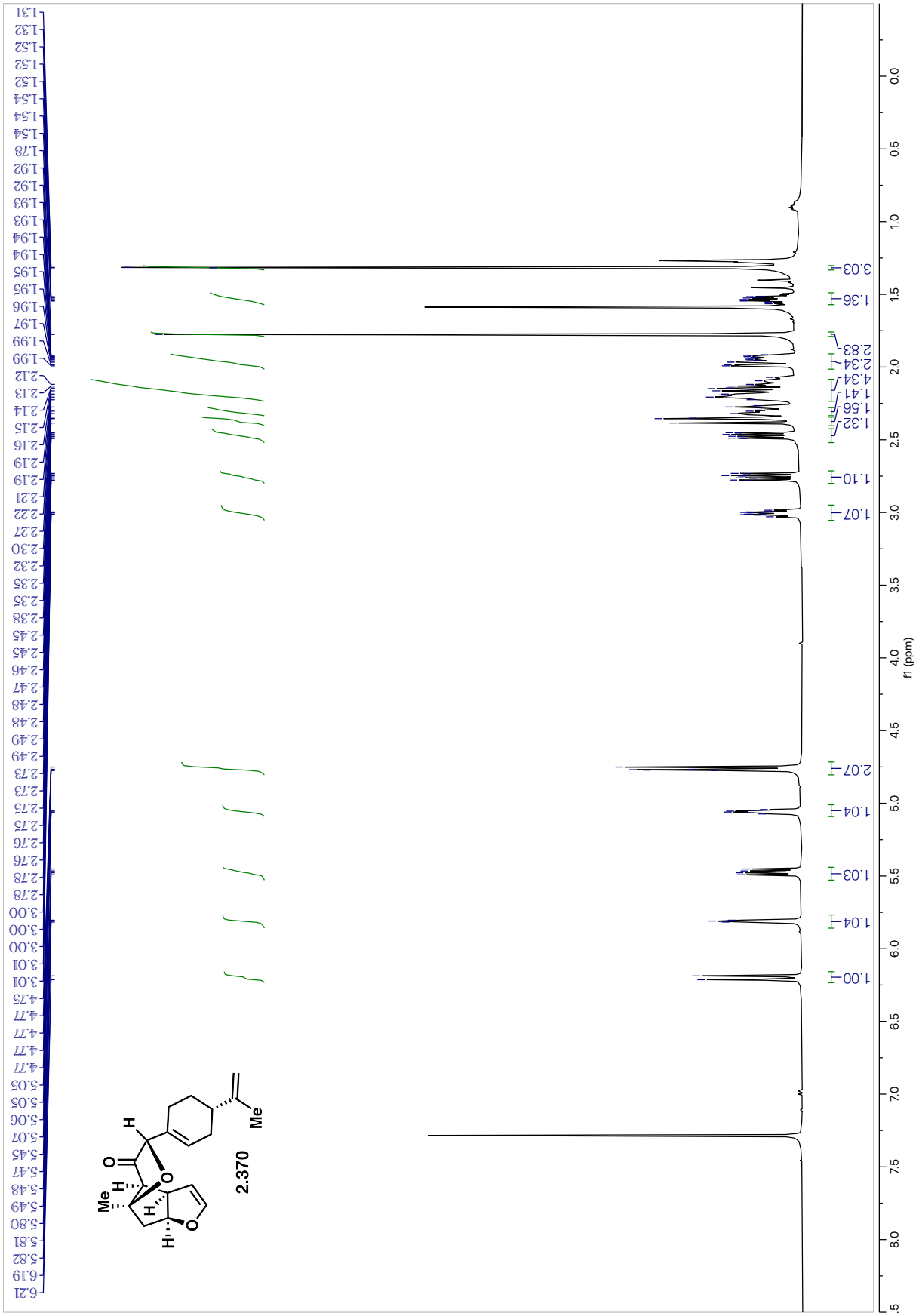

-0.89
-0.00
17.15
20.19
22.47
24.81
27.70
27.74
28.75
28.80
31.13
31.17
32.32
37.44
42.40
48.04
48.09
50.17
58.98
59.02
63.77
82.34
84.31
85.26
92.85
106.73
110.95
111.01
131.54
134.64
134.68
150.95
f1 (ppm)
TBSO
Me
H
H
H
O
OEt
2.366
Me

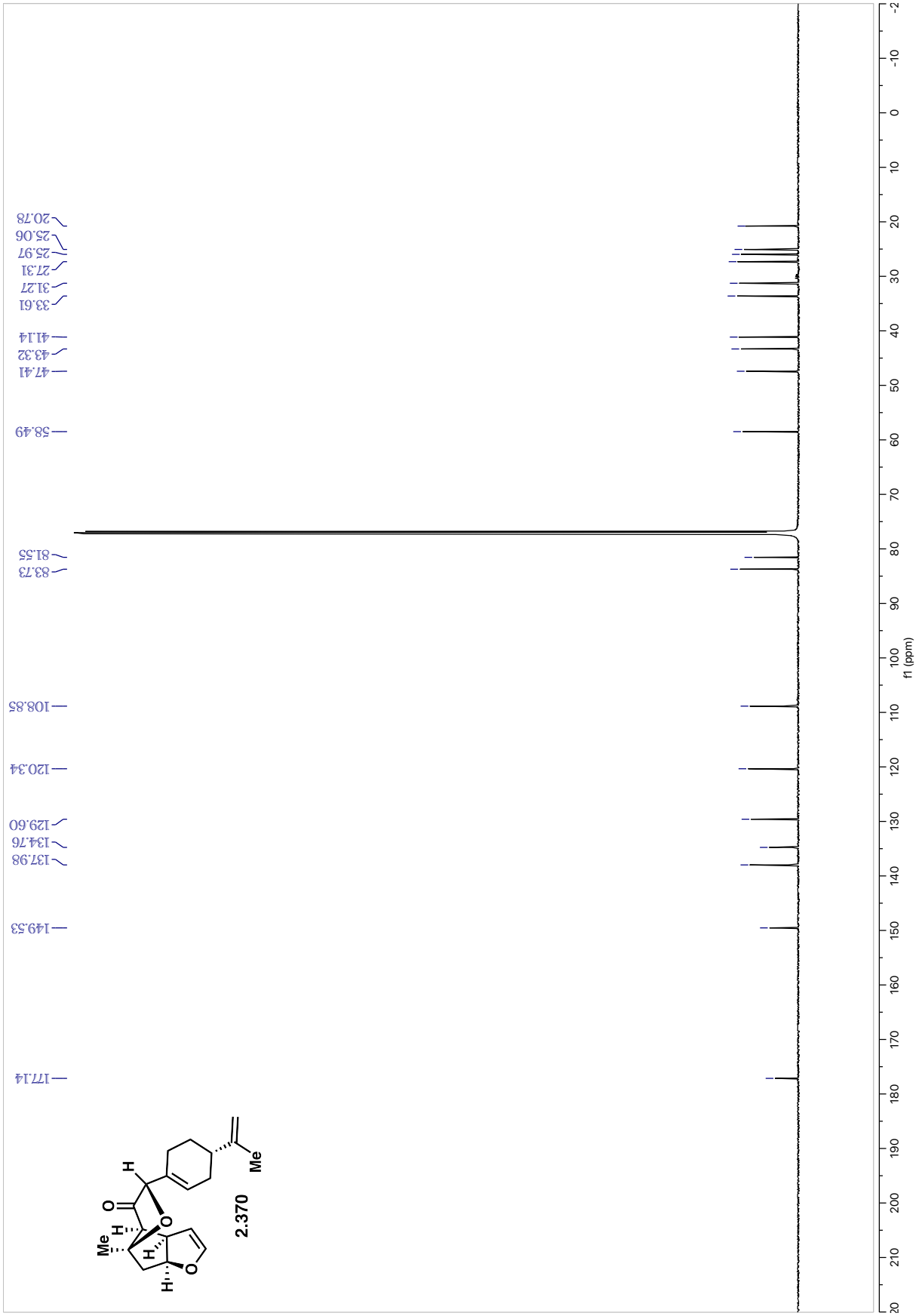

Me
H
OH
H
O
H
O
OEt
Me
2.367
3.92
3.93
3.83
1.09
4.84
3.59
1.23
0.91
0.93
0.92
0.91
0.97
0.91
0.99
1.04
2.39
1.08
1.00
f1 (ppm)

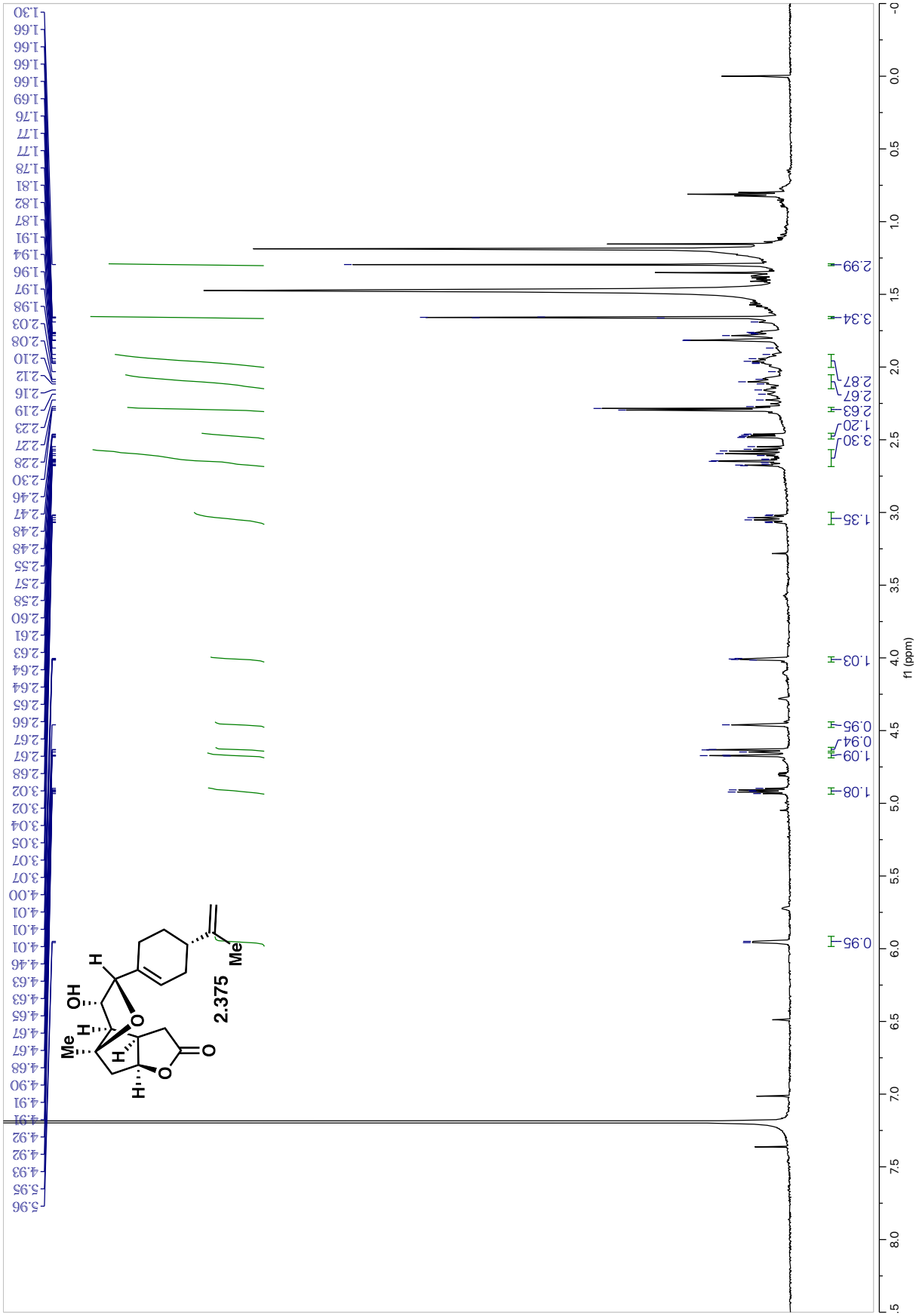

149.79
134.54
126.60
108.71
108.65
105.82
92.19
88.92
84.38
76.42
62.76
59.44
45.15
43.14
41.51
35.10
30.80
27.60
27.42
23.38
20.67
15.24
f1 (ppm)
2.367

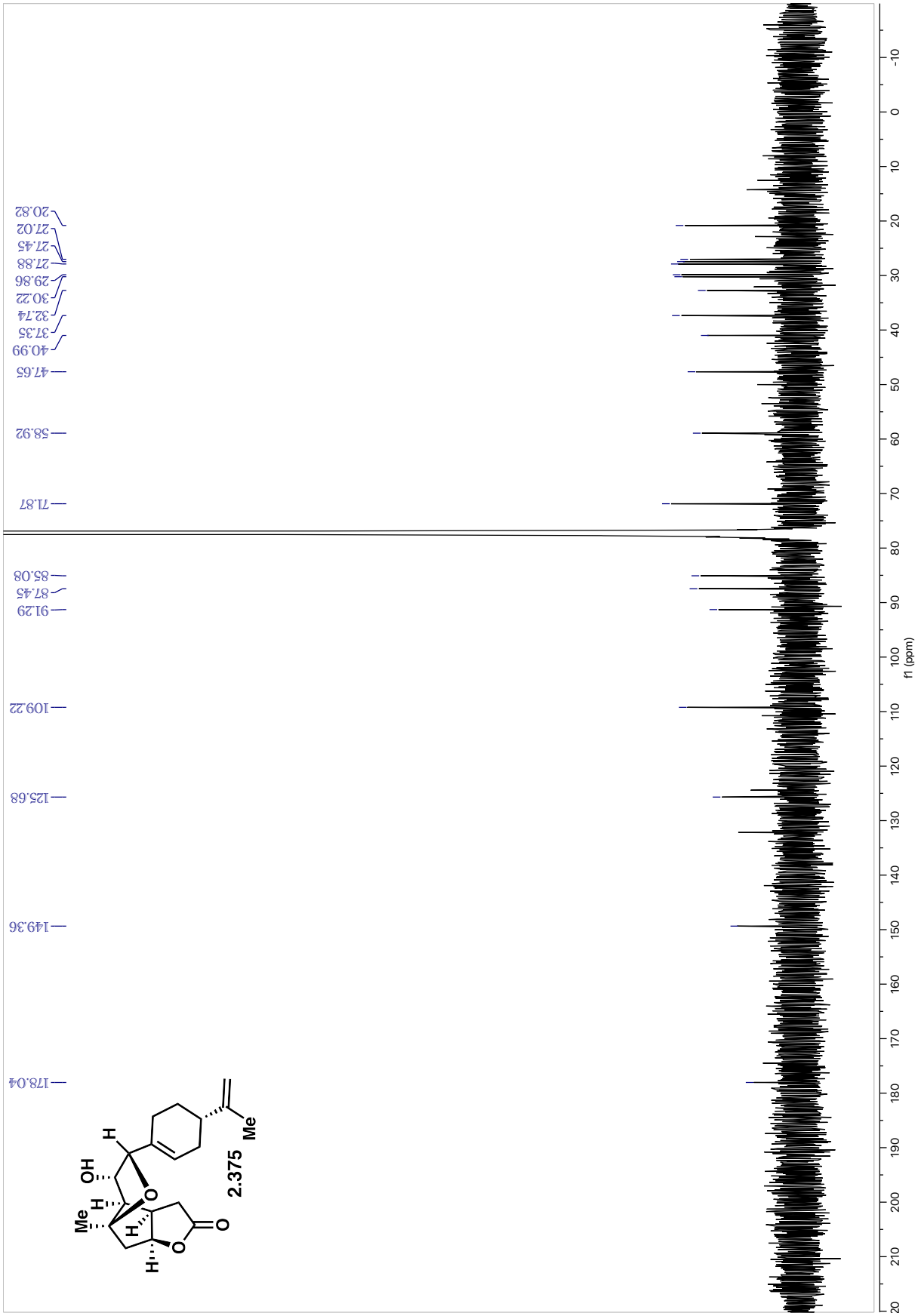

Me
H
O
H
Me
H
O
H
O
2.369
3.78
3.30
1.44
1.29
1.22
4.45
1.02
1.00
1.09
1.04
2.15
1.12
1.02
1.06
1.01
f1 (ppm)

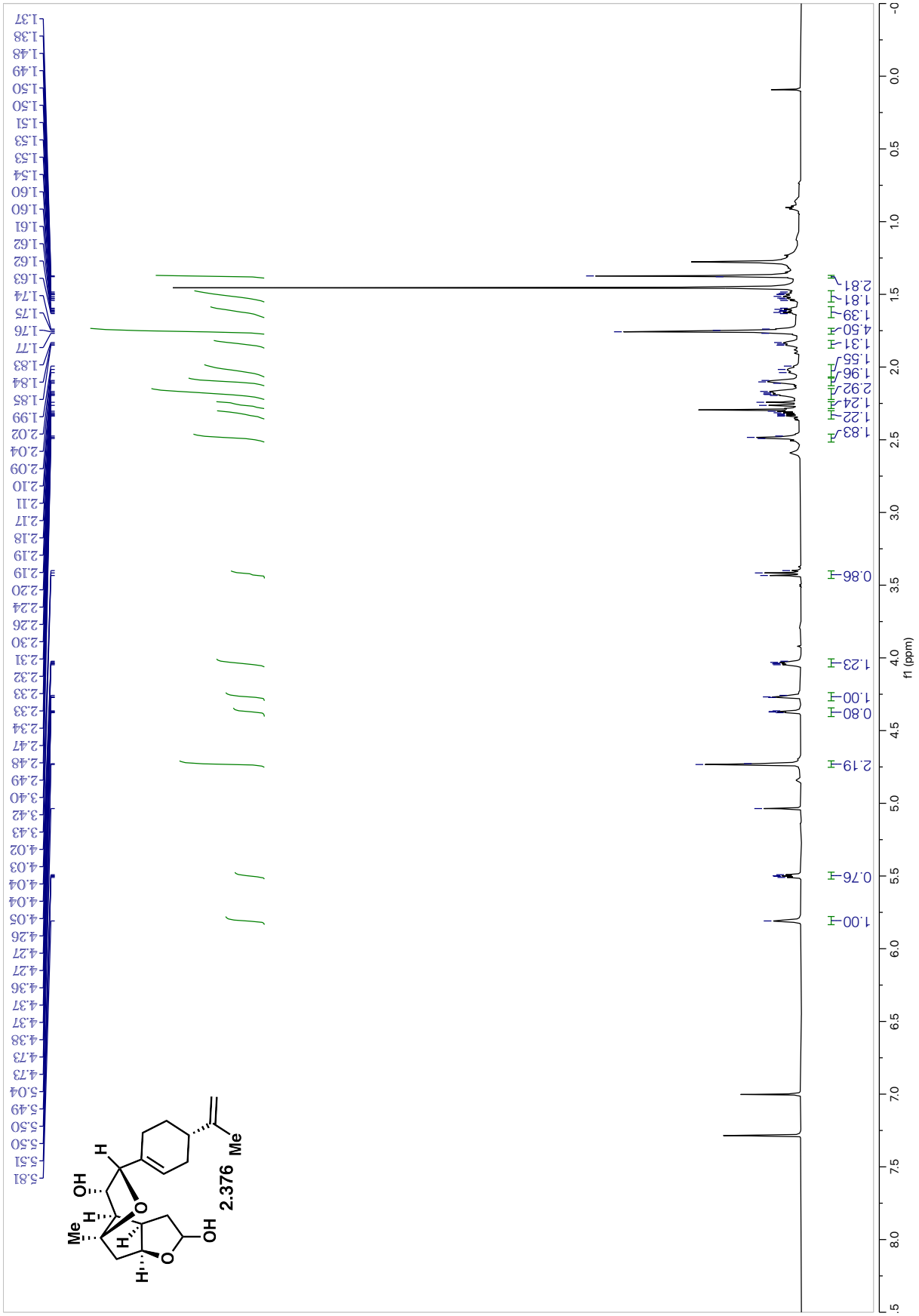

215.14
149.70
145.82
132.99
125.88
108.90
100.69
90.12
87.32
85.82
61.61
49.92
46.02
40.91
30.67
27.50
26.78
25.71
20.88
f1 (ppm)
2.369

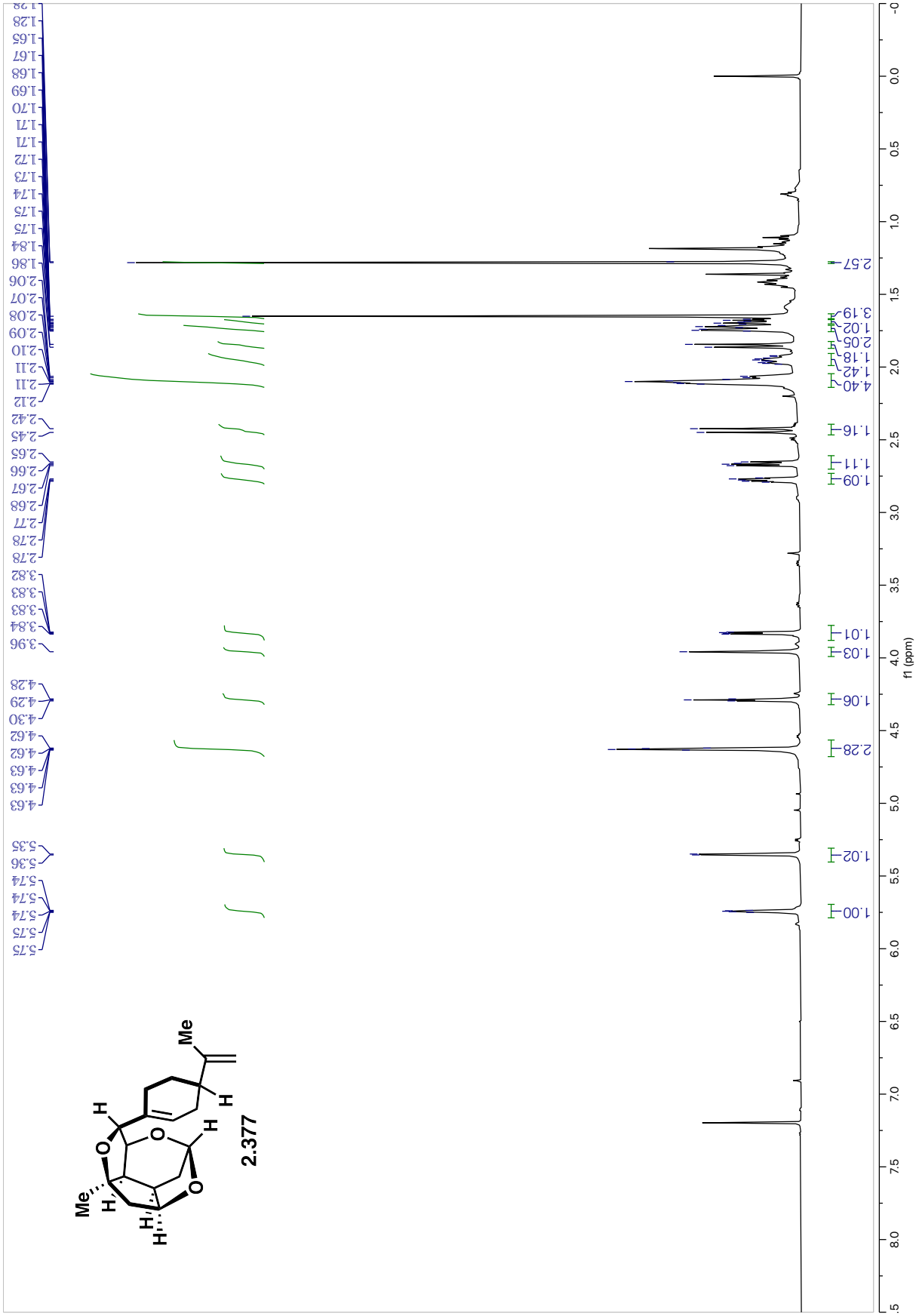

2.370
Me
Me
H
O
O
H
H
O
H
3.03
1.36
2.83
2.34
4.34
1.41
1.56
1.32
1.10
1.07
2.07
1.04
1.03
1.04
1.00
f1 (ppm)

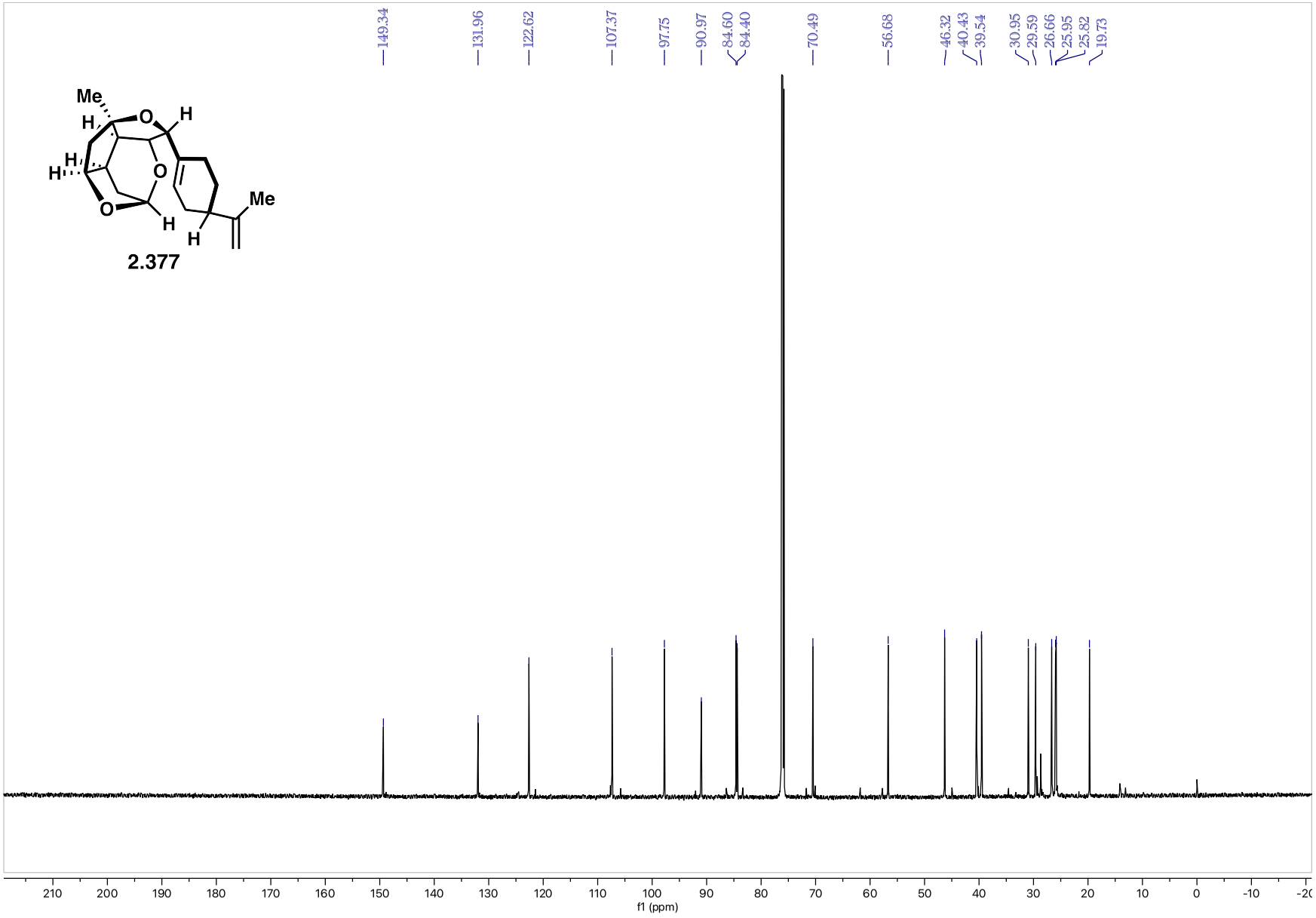

177.14
149.53
137.98
134.76
129.60
120.34
108.85
83.73
81.55
58.49
47.41
43.32
41.14
33.61
31.27
27.31
25.97
25.06
20.78
f1 (ppm)
2.370
Me
H
O
Me
H
H
O
O
H

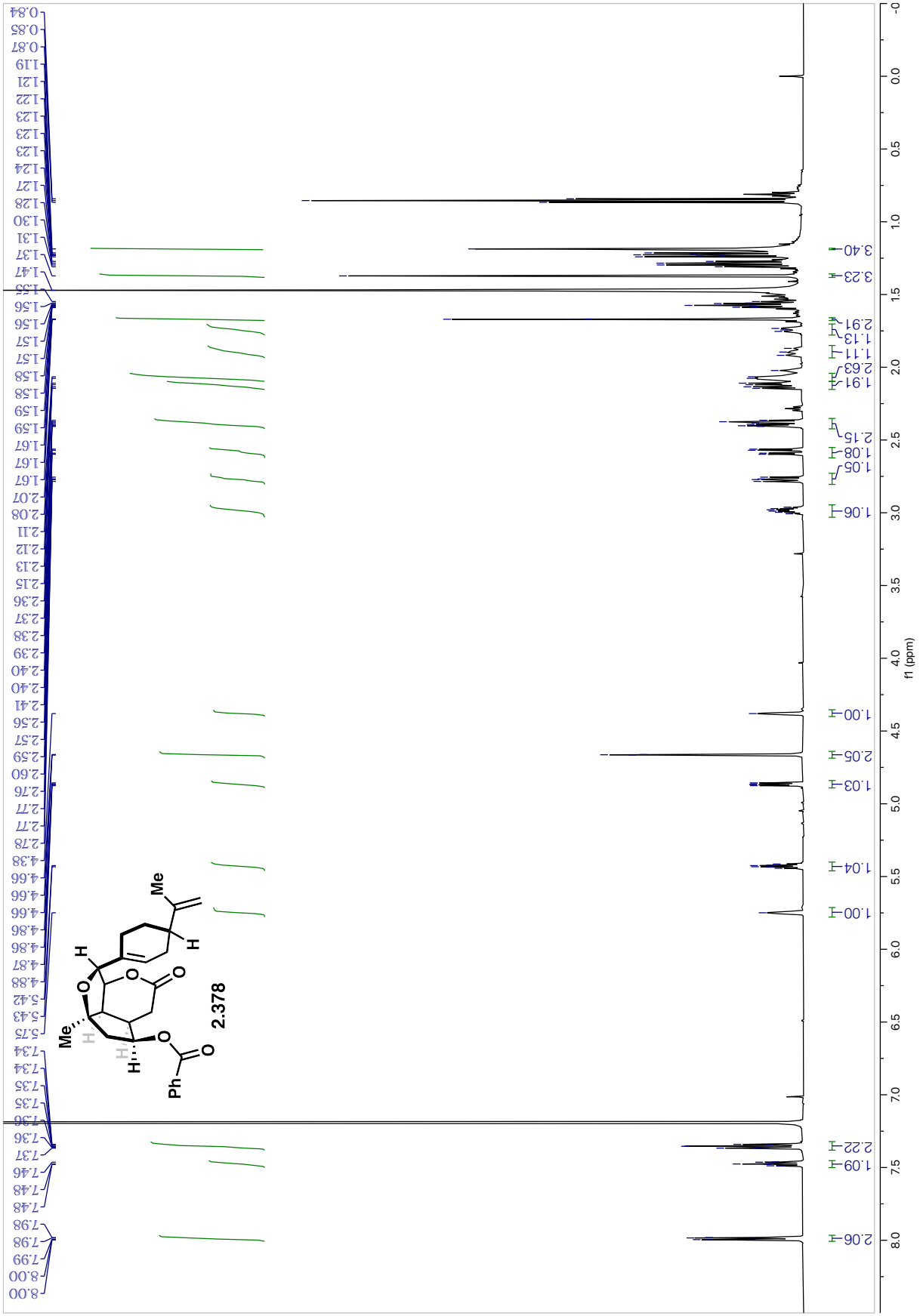

2.375
Me
OH
Me
H
H
H
O
O
O
f1 (ppm)

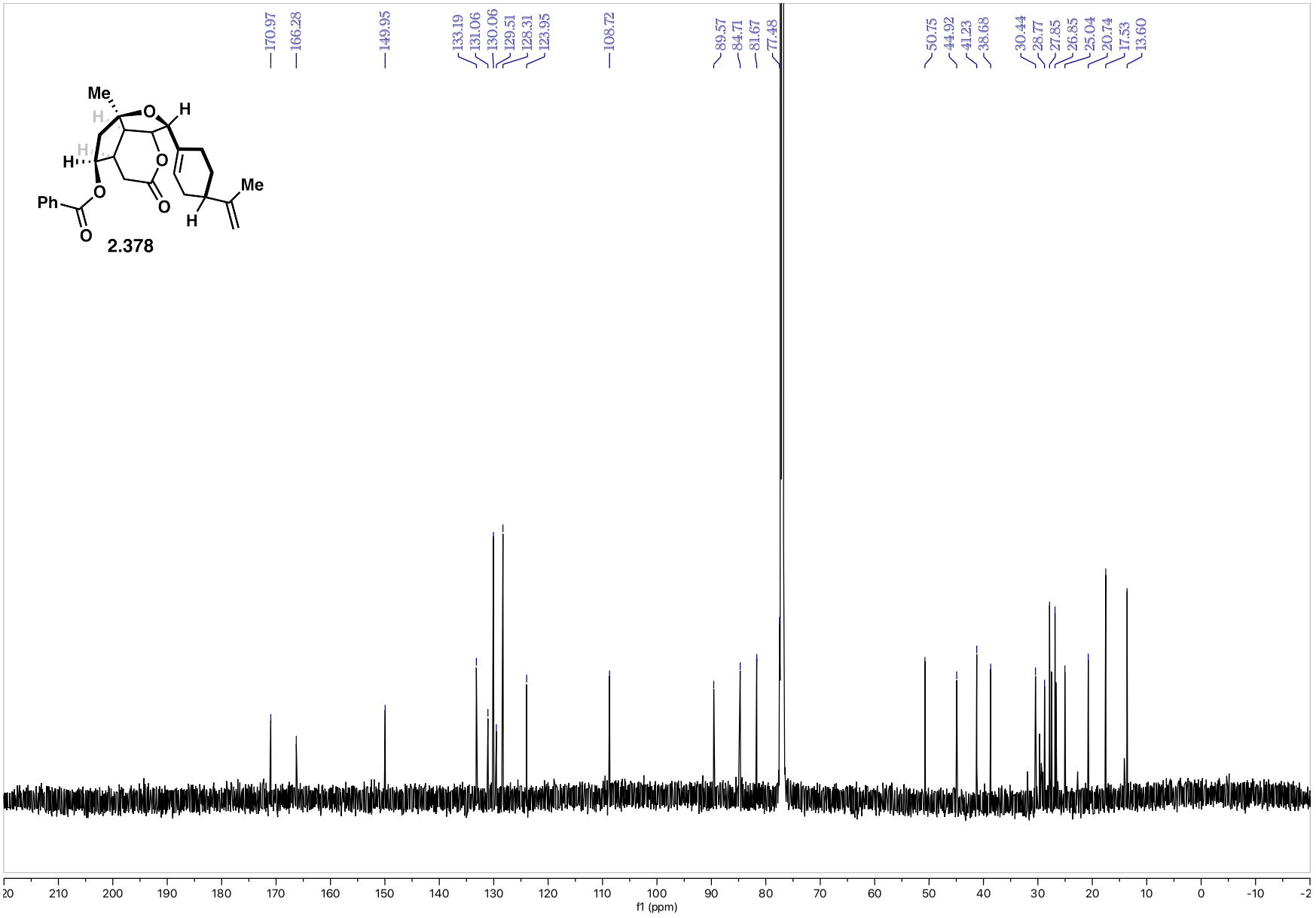

178.04
149.36
125.68
109.22
91.29
87.45
85.08
71.87
58.92
47.65
40.99
37.35
32.74
30.22
29.86
27.88
27.45
27.02
20.82
f1 (ppm)
2.375
Me
H
OH
Me
H
O
O
O
H

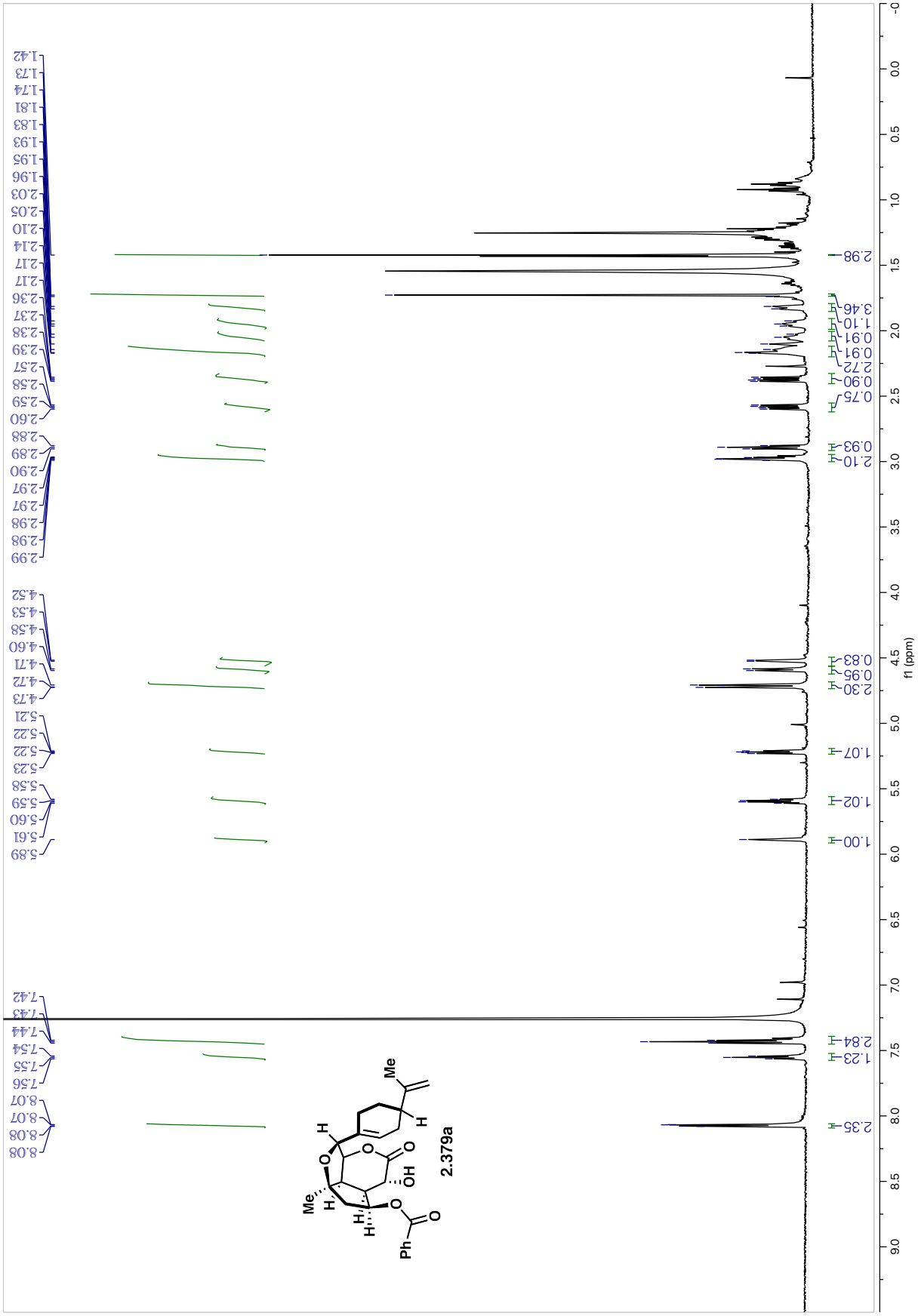

2.376
Me
OH
OH
Me
H
O
O
H
H
H
f1 (ppm)

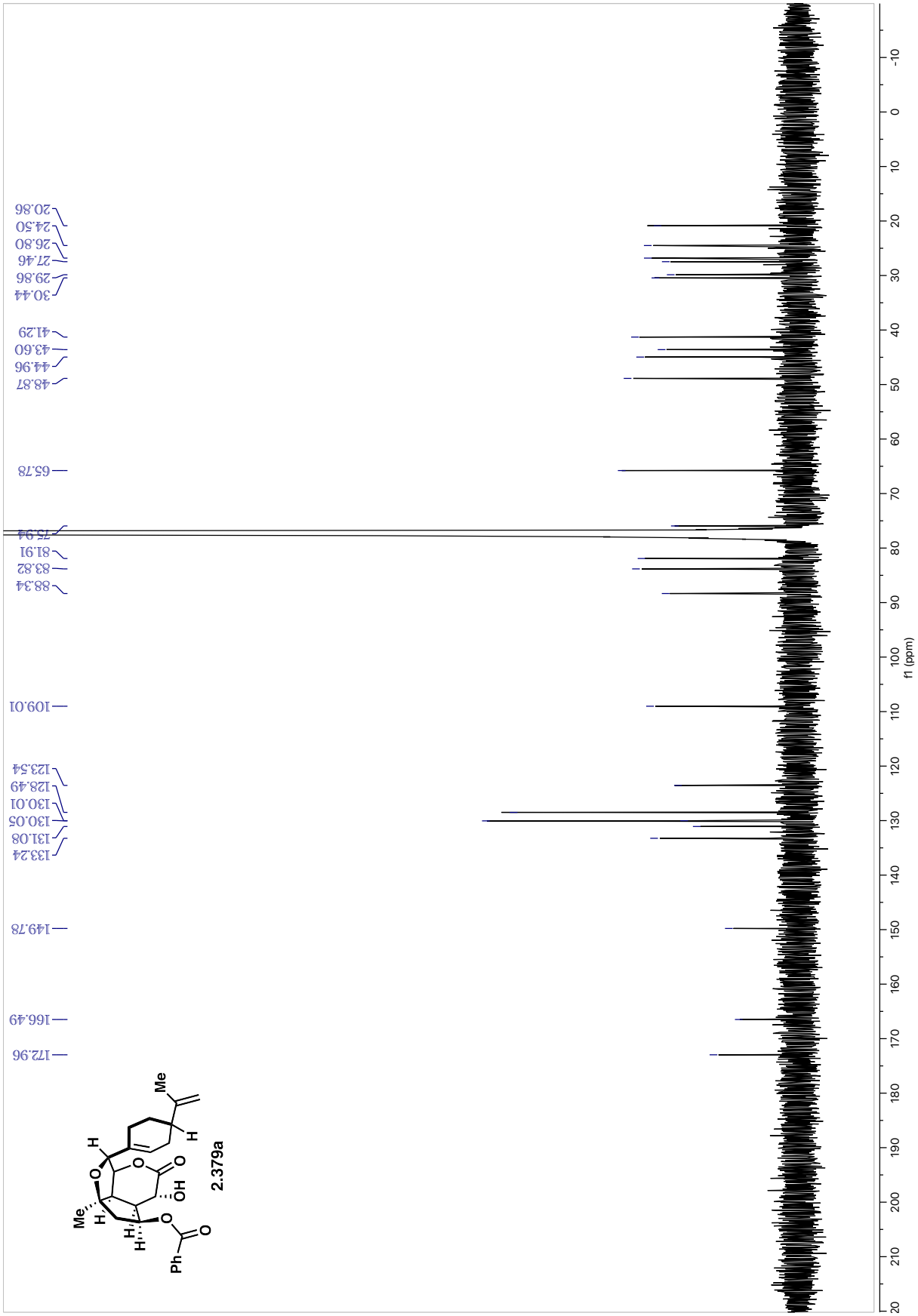

Me
H
O
O
H
H
O
Me
H
H
H
2.377
f1 (ppm)

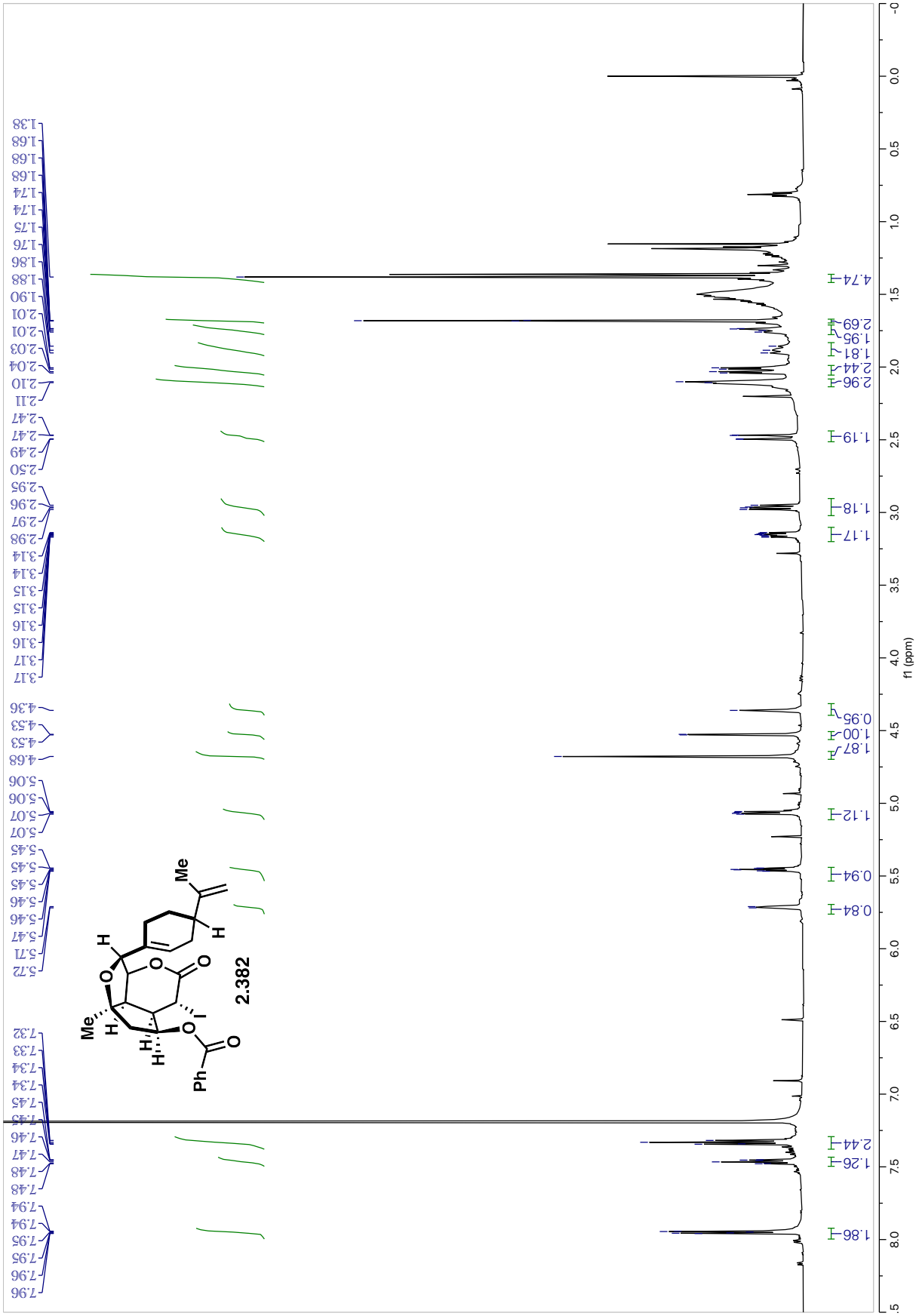

149.34
131.96
122.62
107.37
97.75
90.97
84.60
84.40
70.49
56.68
46.32
40.43
39.54
30.95
29.59
26.66
25.95
25.82
19.73
Me
H
O
H
H
O
O
H
H
Me
2.377
210
200
190
180
170
160
150
140
130
120
110
100
90
80
70
60
50
40
30
20
10
0
-10
f1 (ppm)

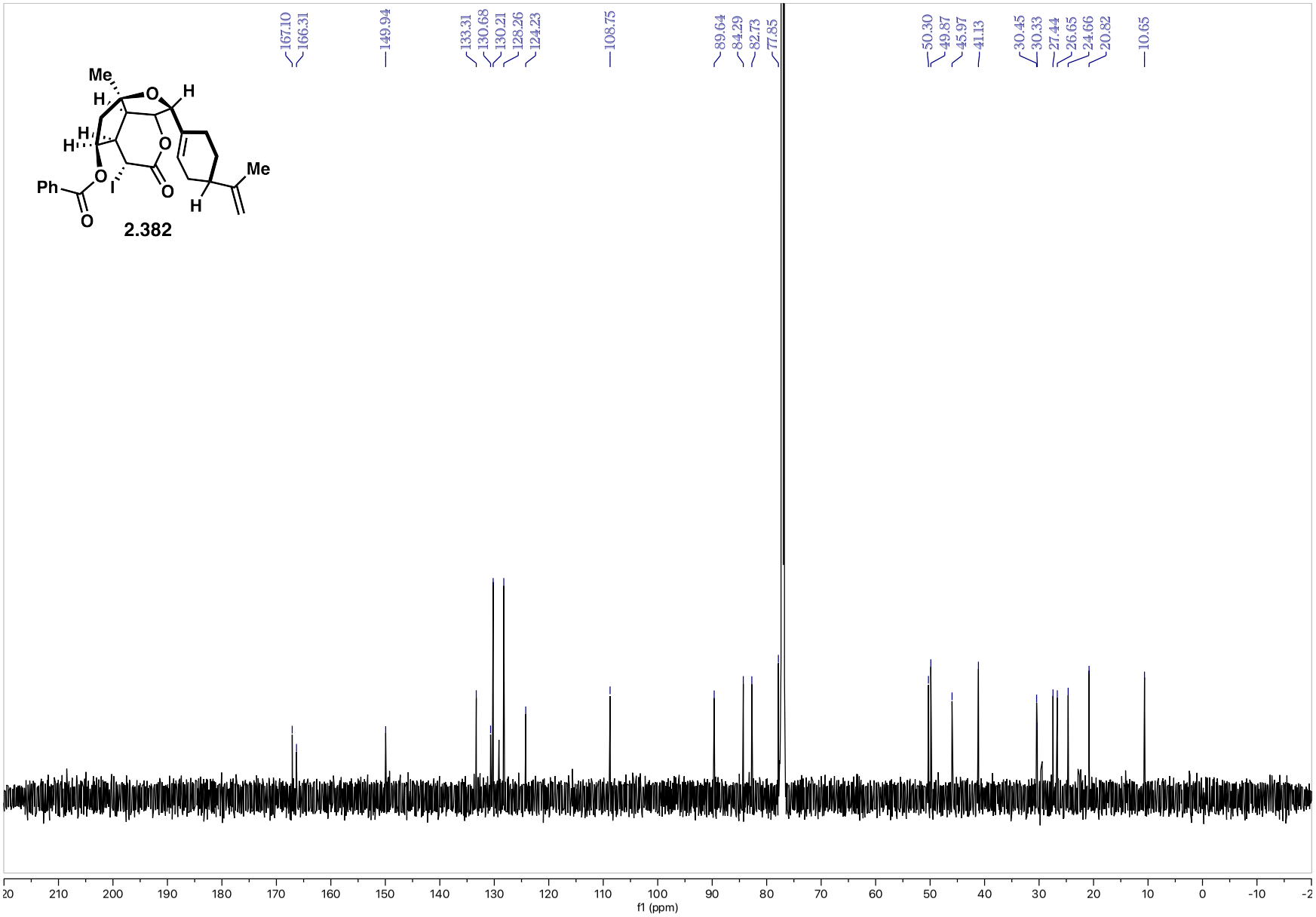

Me
H
H
O
O
O
O
H
Me
H
O
Ph
2.378
f1 (ppm)

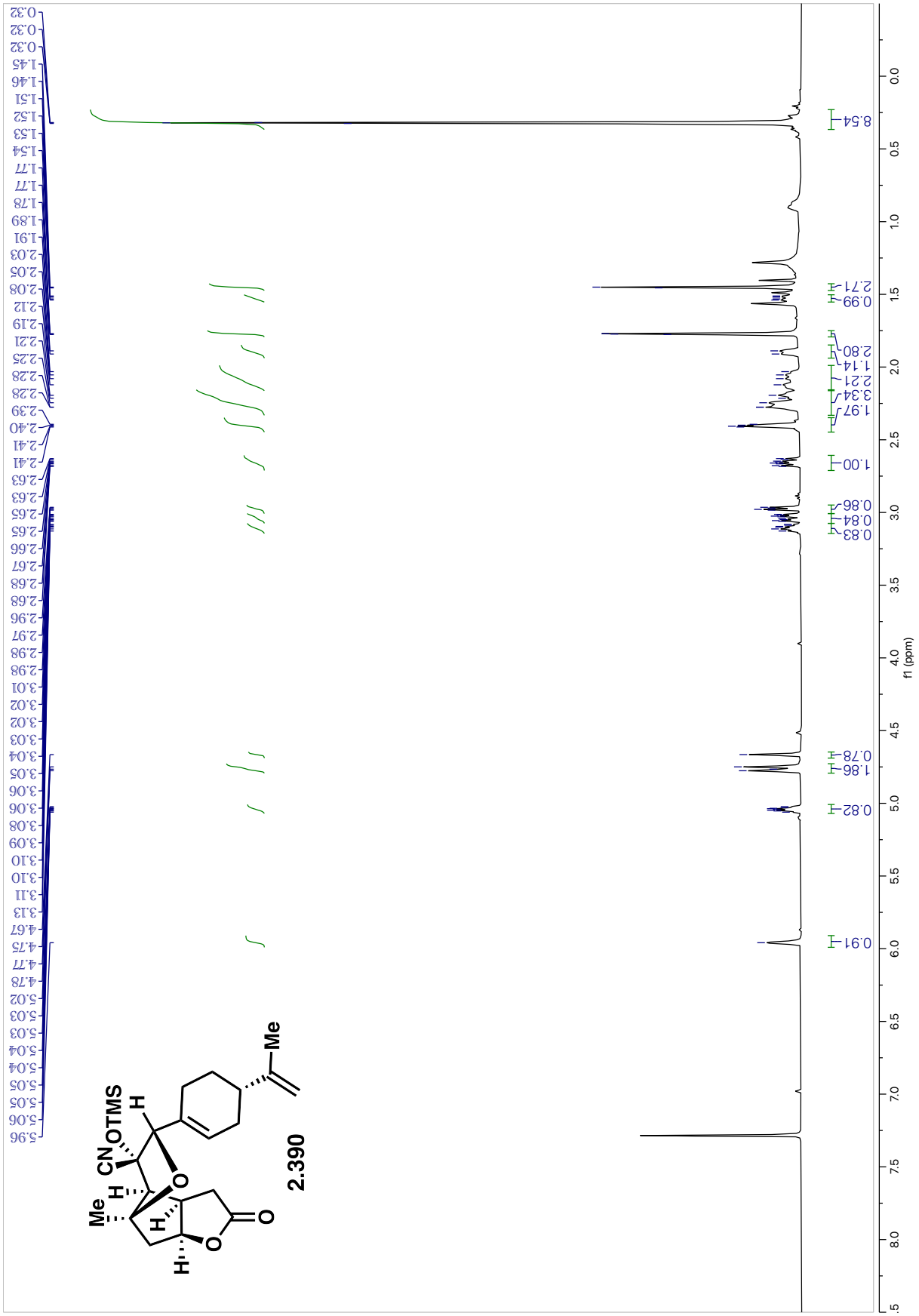

170.97
166.28
149.95
133.19
131.06
130.06
129.51
128.31
123.95
108.72
89.57
84.71
81.67
77.48
50.75
44.92
41.23
38.68
30.44
28.77
27.85
26.85
25.04
20.74
17.53
13.60
Me
H
O
H
H
O
Ph
O
O
O
Me
H
2.378
f1 (ppm)

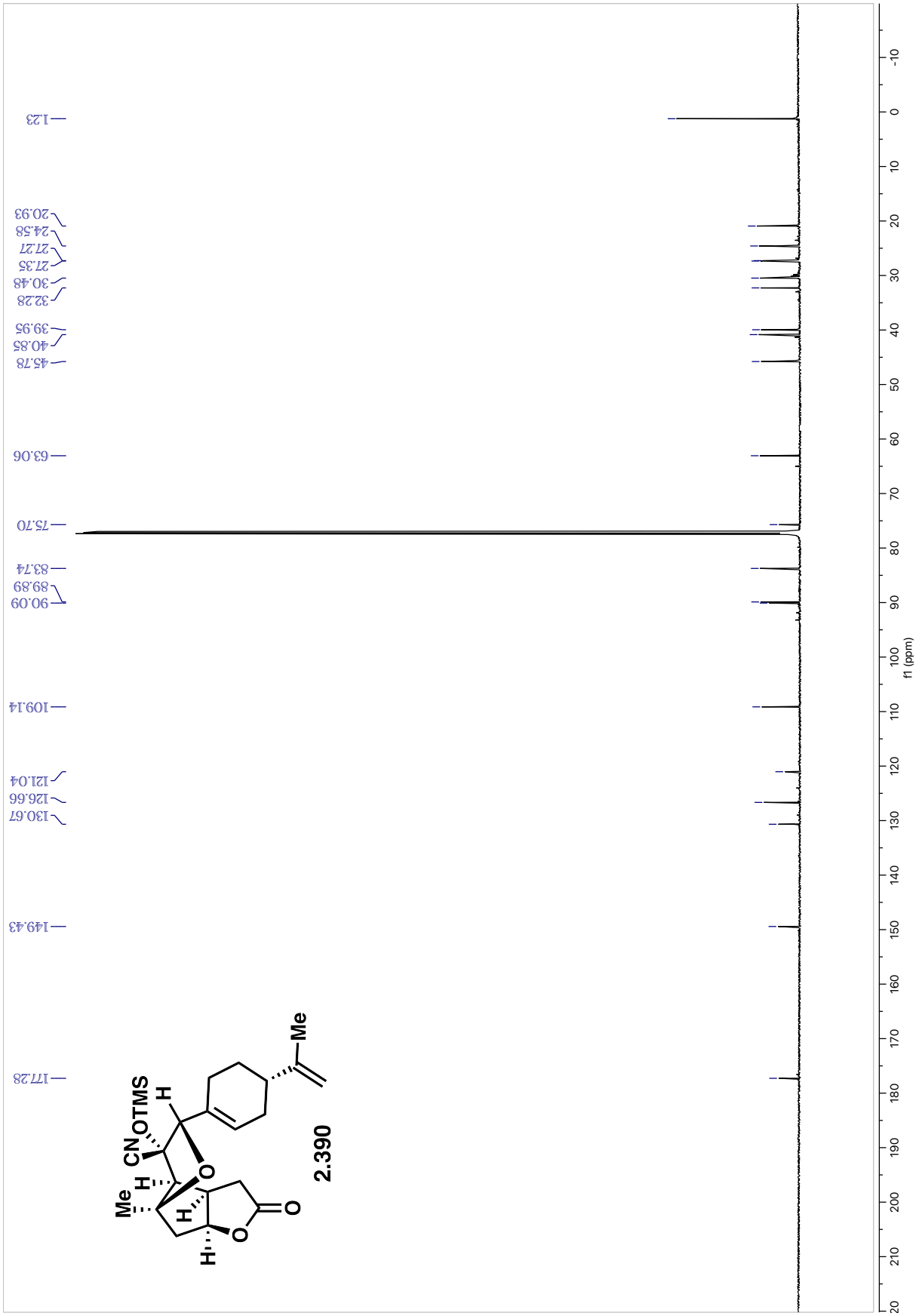

2.379a
f1 (ppm)

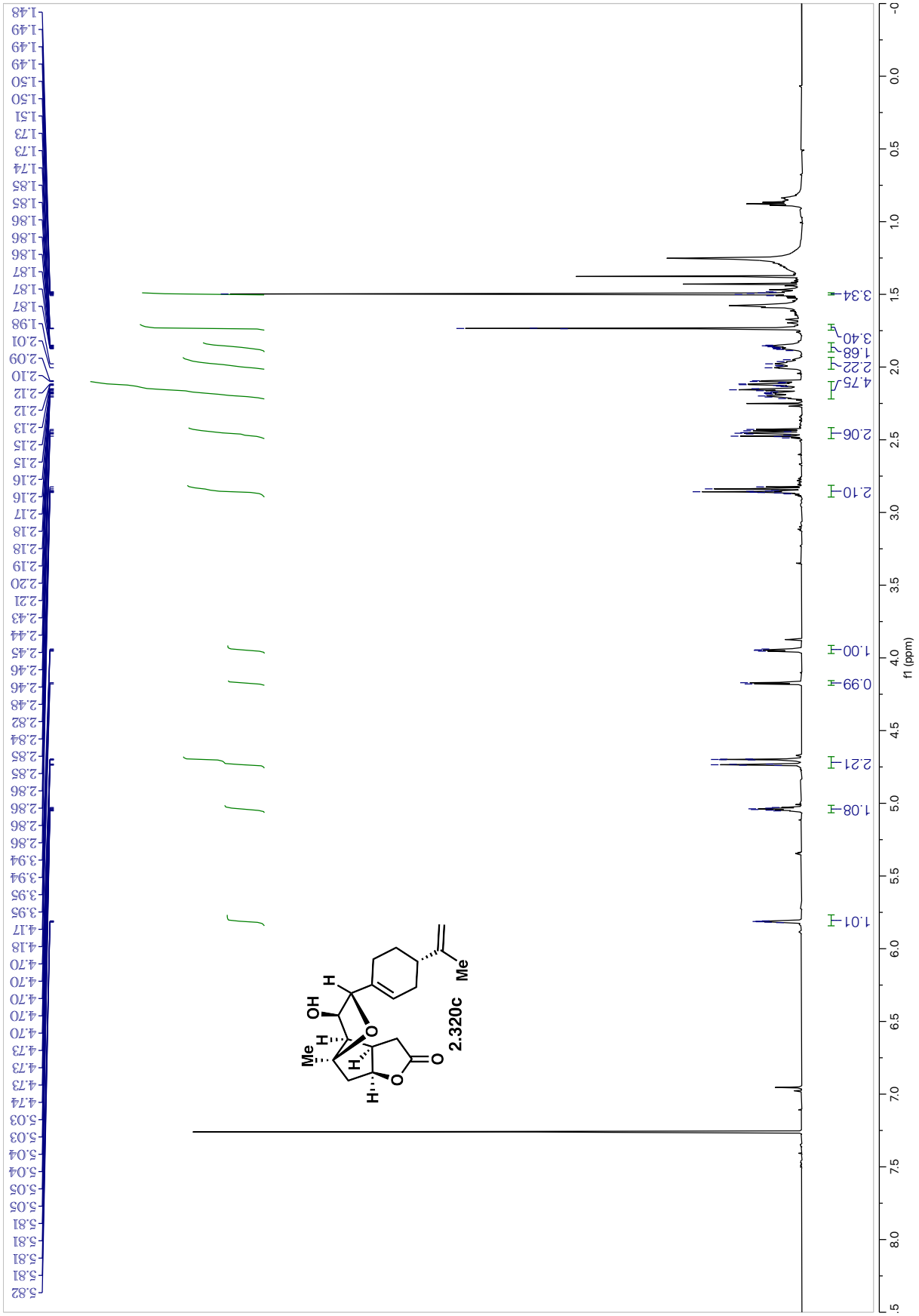

20.86
24.50
26.80
27.46
29.86
30.44
41.29
43.60
44.96
48.87
65.78
75.94
81.91
83.82
88.34
109.01
123.54
128.49
130.01
130.05
131.08
133.24
149.78
166.49
172.96
f1 (ppm)
2.379a


Me
H
O
O
O
O
H
H
Me
H
O
Ph
O
2.382
f1 (ppm)

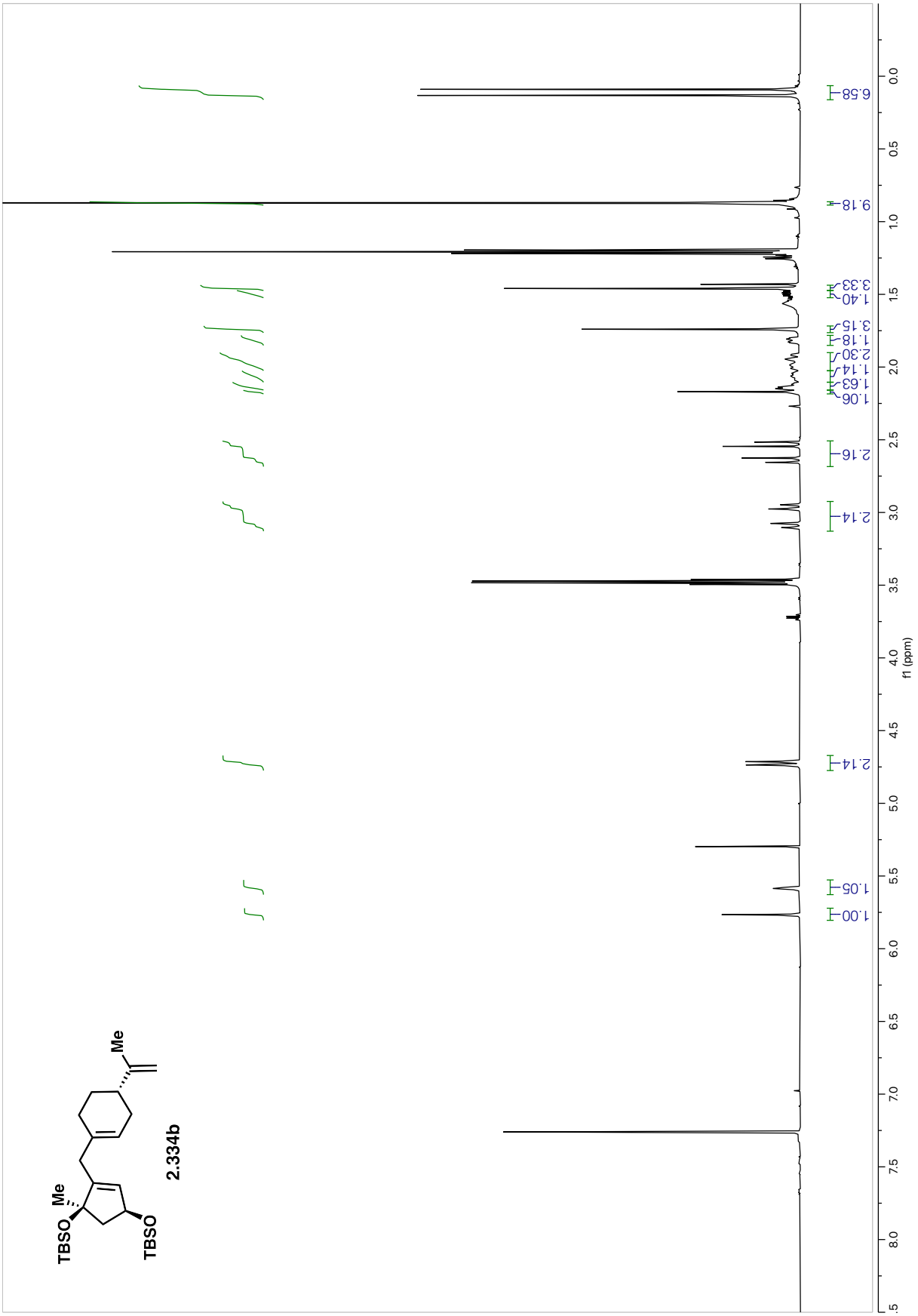

167.10
166.31
149.94
133.31
130.68
130.21
128.26
124.23
108.75
89.64
84.29
82.73
77.85
50.30
49.87
45.97
41.13
30.45
30.33
27.44
26.65
24.66
20.82
10.65
Me
H
O
H
H
H
O
O
Ph
O
O
O
Me
H
2.382
f1 (ppm)

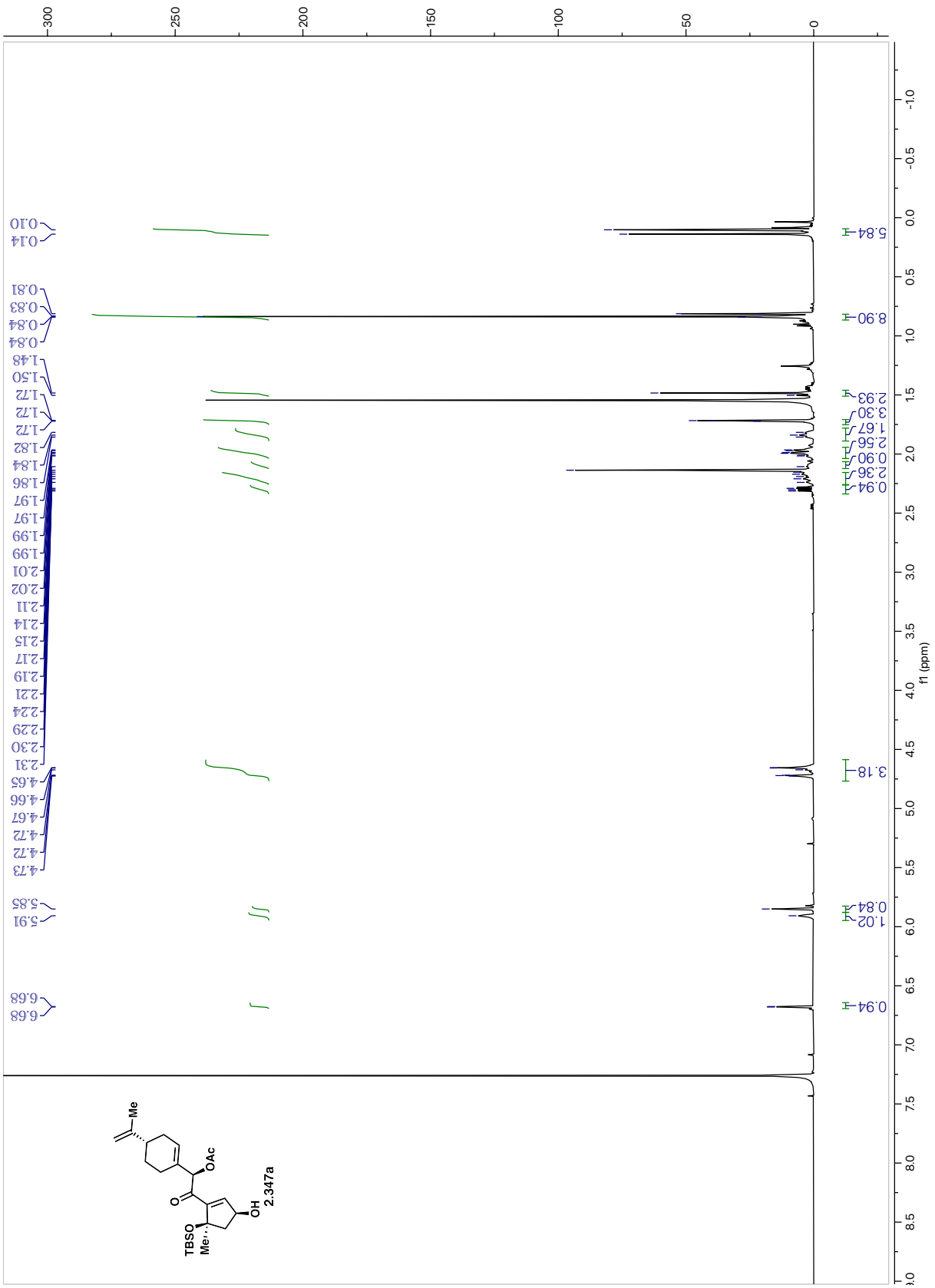

Me
H
CN
OTMS
H
O
H
O
O
Me
2.390
8.54
2.71
0.99
2.80
1.14
2.21
3.34
1.97
1.00
0.86
0.84
0.83
0.78
1.86
0.82
0.91
f1 (ppm)

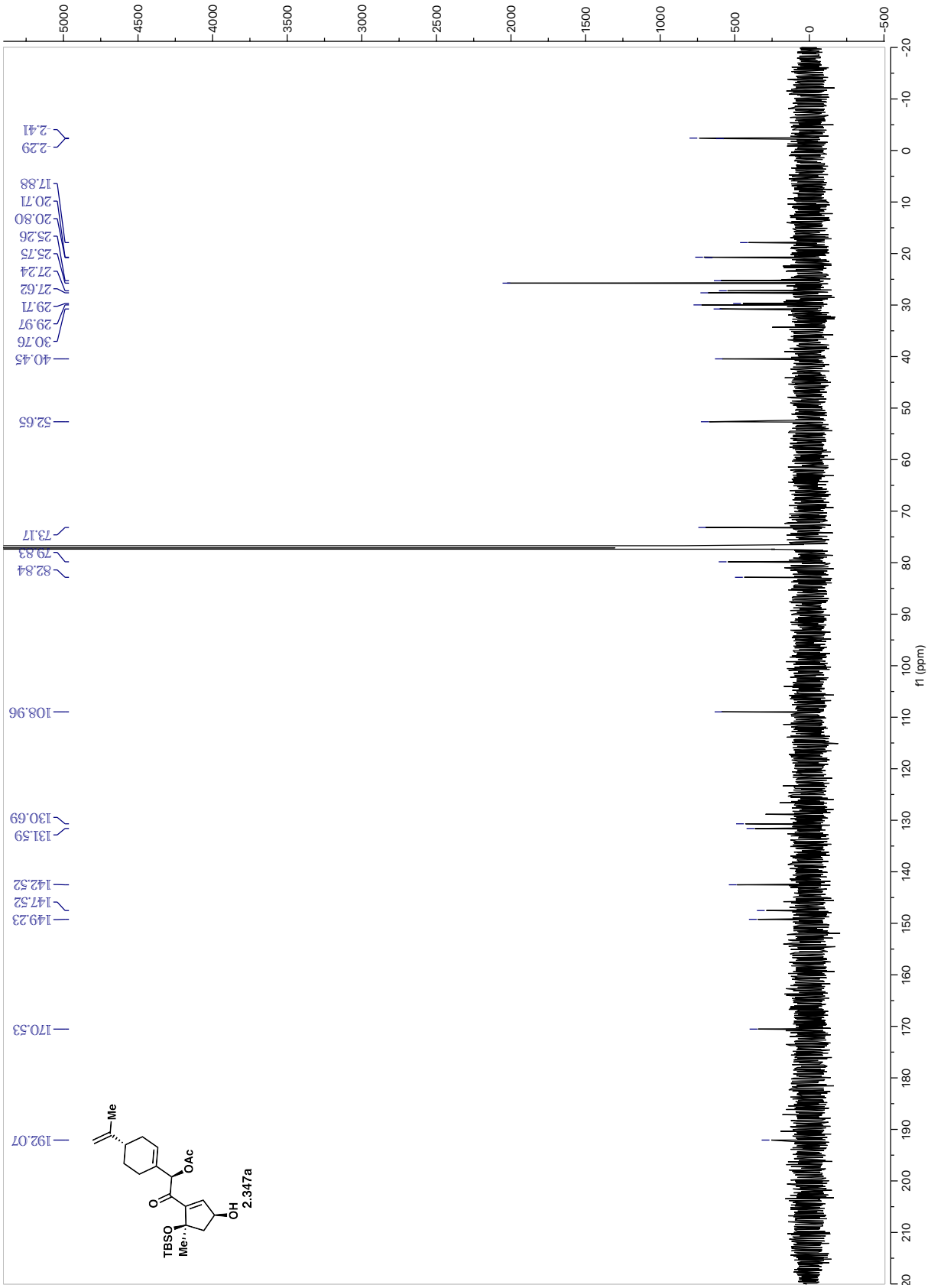

177.28
149.43
130.67
126.66
121.04
109.14
90.09
89.89
83.74
75.70
63.06
45.78
40.85
39.95
32.28
30.48
27.35
27.27
24.58
20.93
1.23
f1 (ppm)
Me
H
CN
OTMS
H
O
H
O
O
2.390

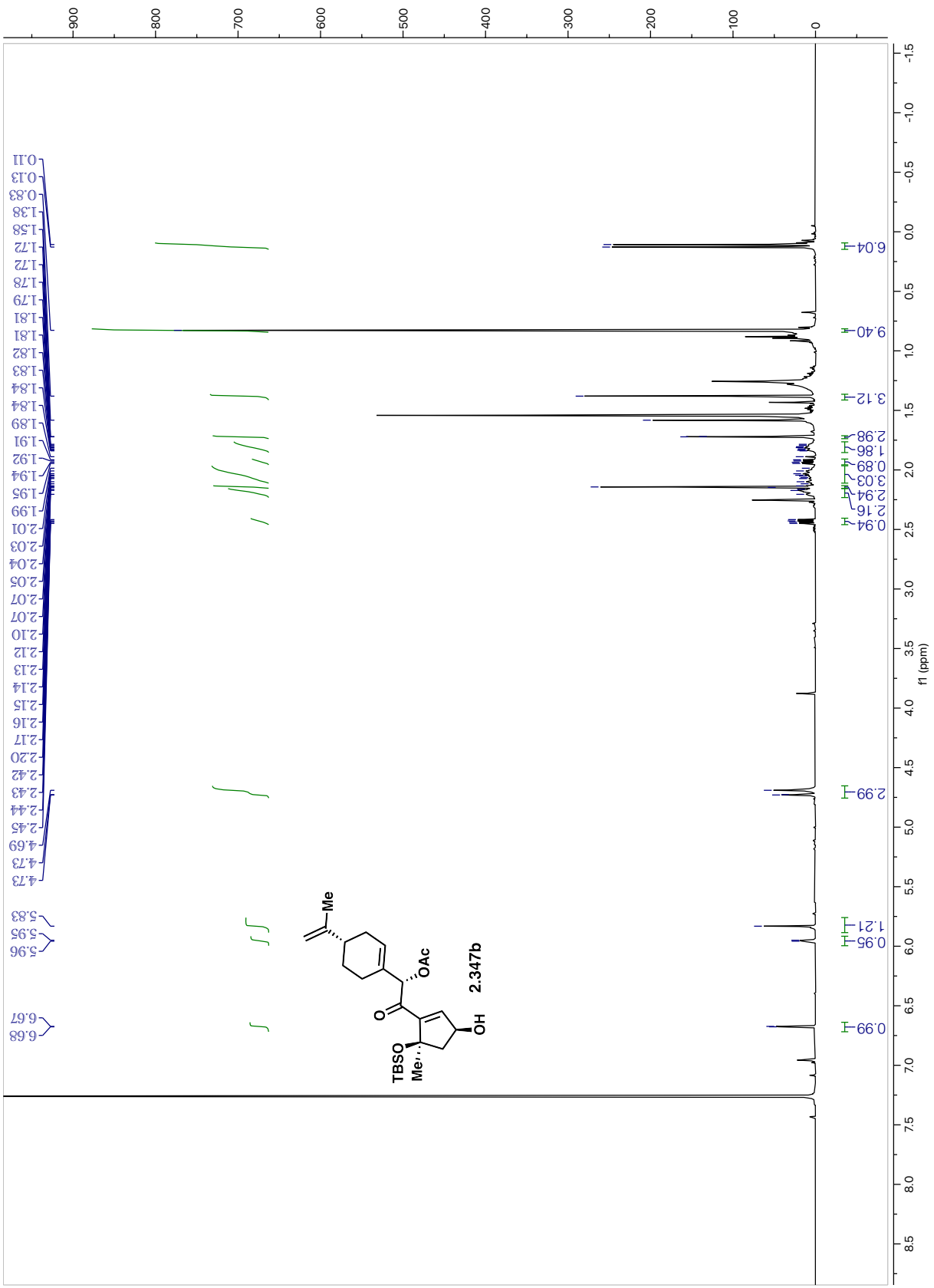

Me
H
OH
H
O
H
O
O
2.320c
Me
3.34
3.40
1.68
2.22
4.75
2.06
2.10
1.00
0.99
2.21
1.08
1.01
f1 (ppm)

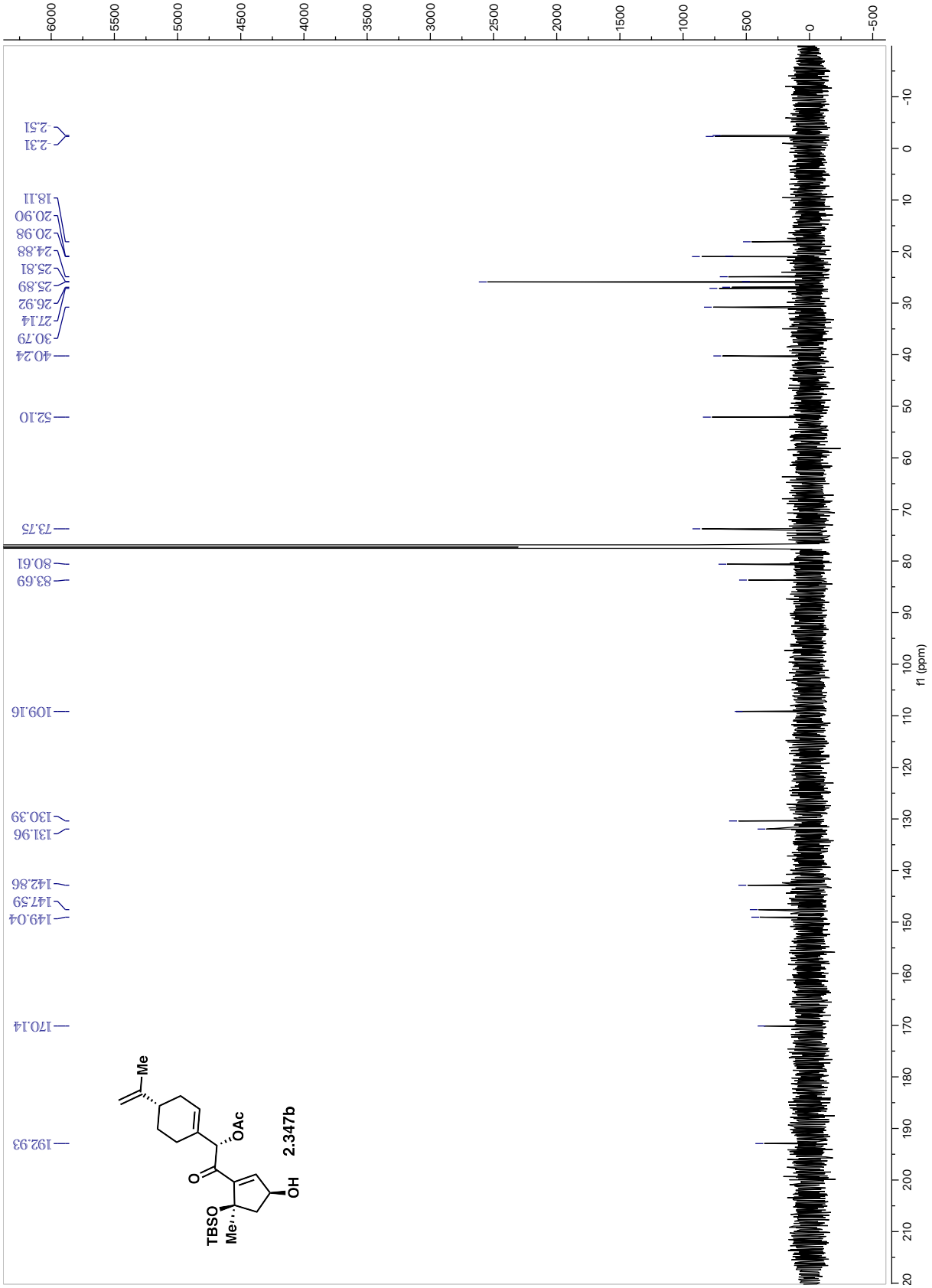
176.42
149.40
134.50
124.15
108.83
91.13
89.71
86.24
81.36
63.96
46.23
44.37
40.95
35.89
30.33
27.19
25.40
24.41
20.81
f1 (ppm)
2.320c

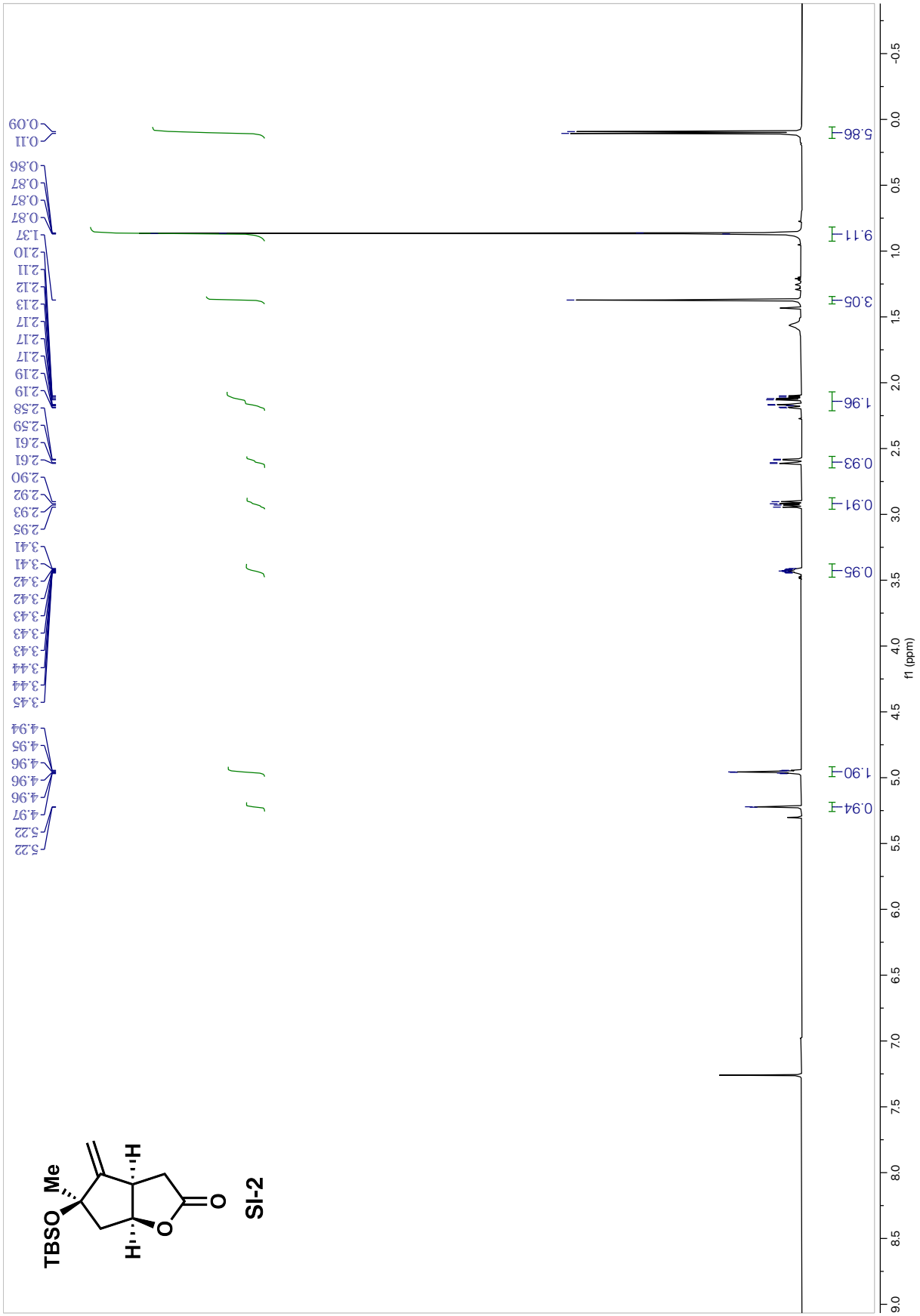

TBSO
Me
TBSO
Me
2.334b
6.58
9.18
3.33
1.40
3.15
1.18
2.30
1.14
1.63
1.06
2.16
2.14
2.14
1.05
1.00
f1 (ppm)

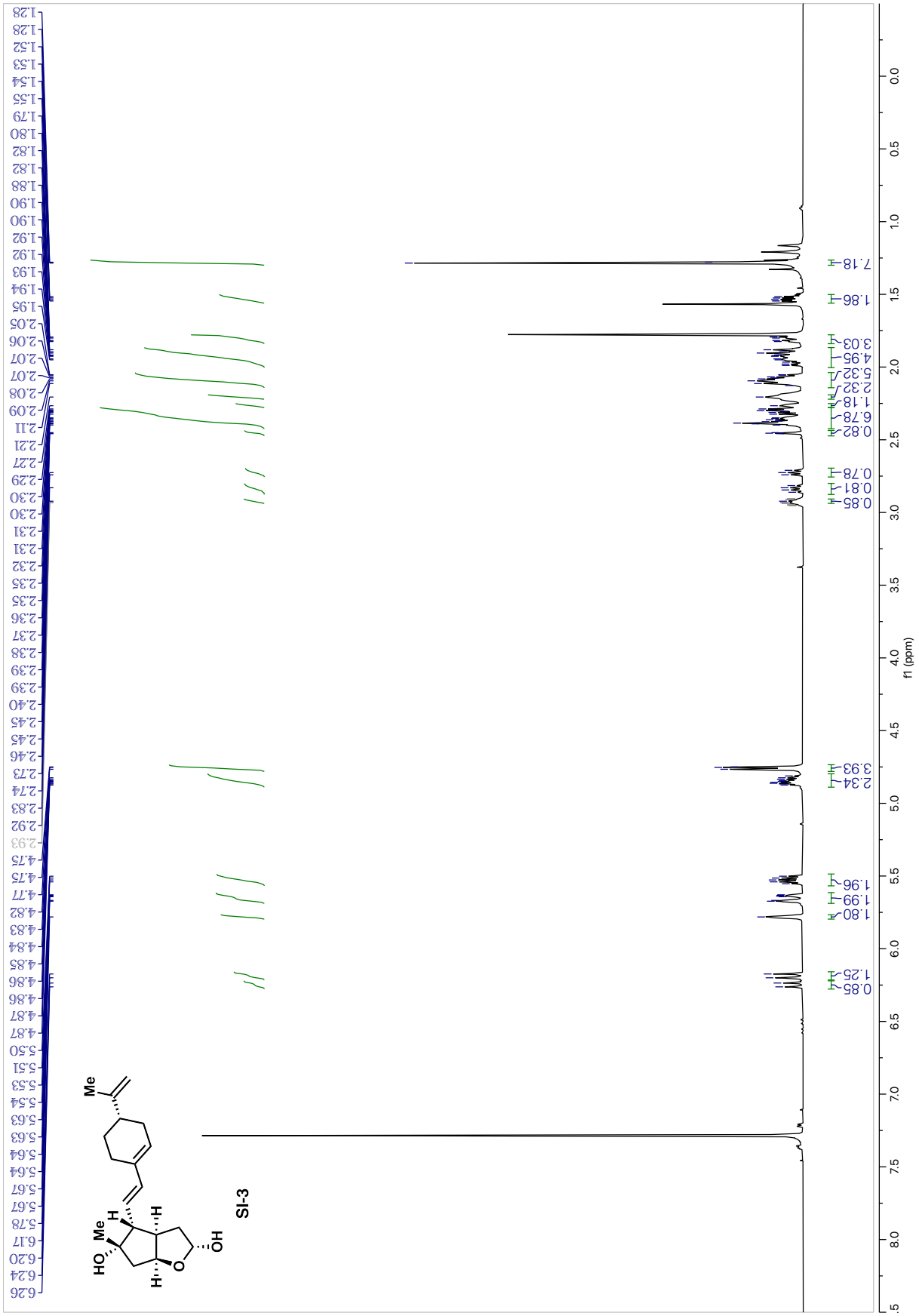

Me
OAc
O
OH
2.347a
TBSO
Me
f1 (ppm)


192.07
170.53
149.23
147.52
142.52
131.59
130.69
108.96
82.84
79.83
73.17
52.65
40.45
30.76
29.97
29.71
27.62
27.24
25.75
25.26
20.80
20.71
17.88
2.29
2.41
f1 (ppm)
2.347a
Me
OAc
O
OH
TBSO
Me

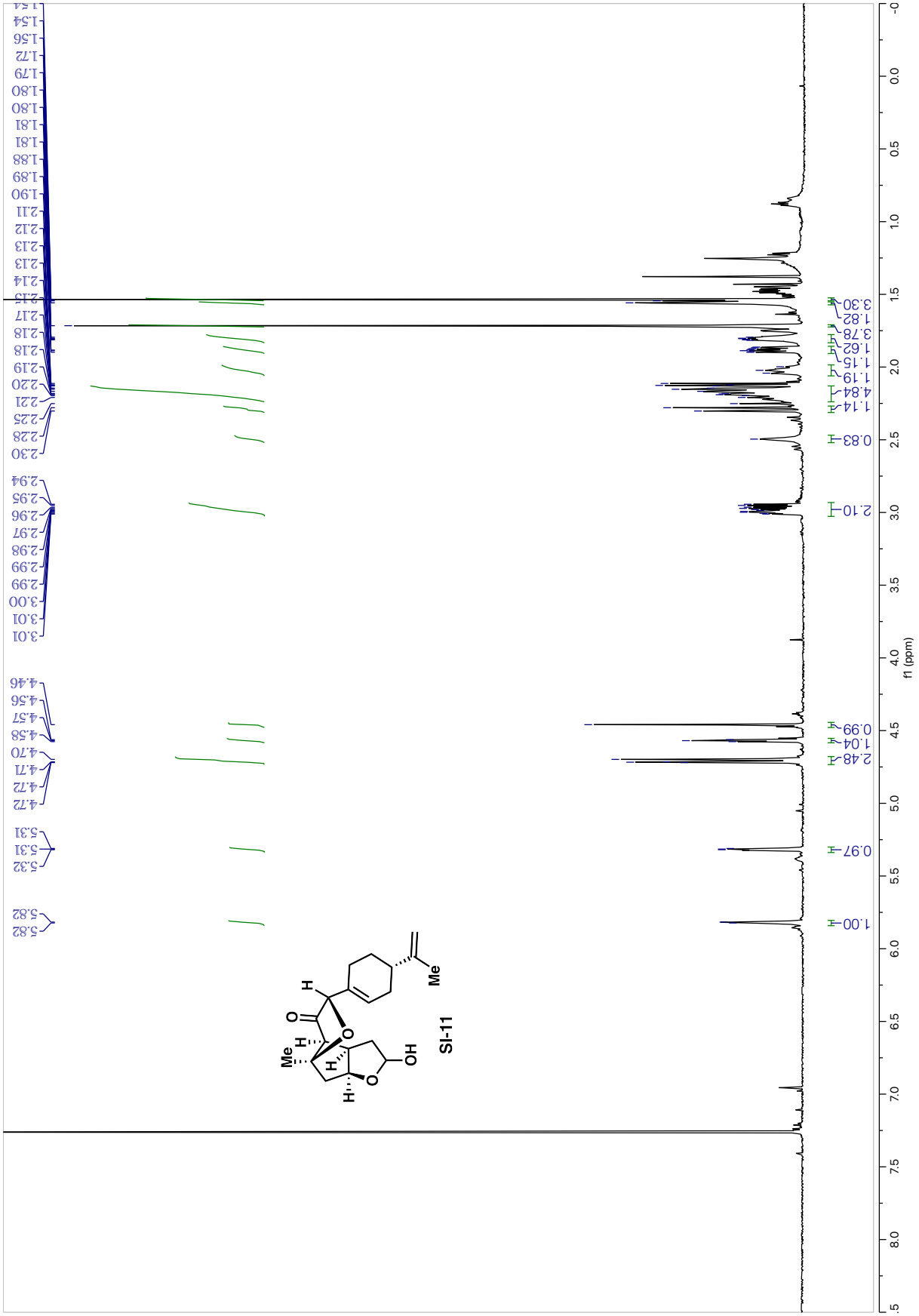

Me
OAc
O
OH
TBSO
Me
2.347b
f1 (ppm)

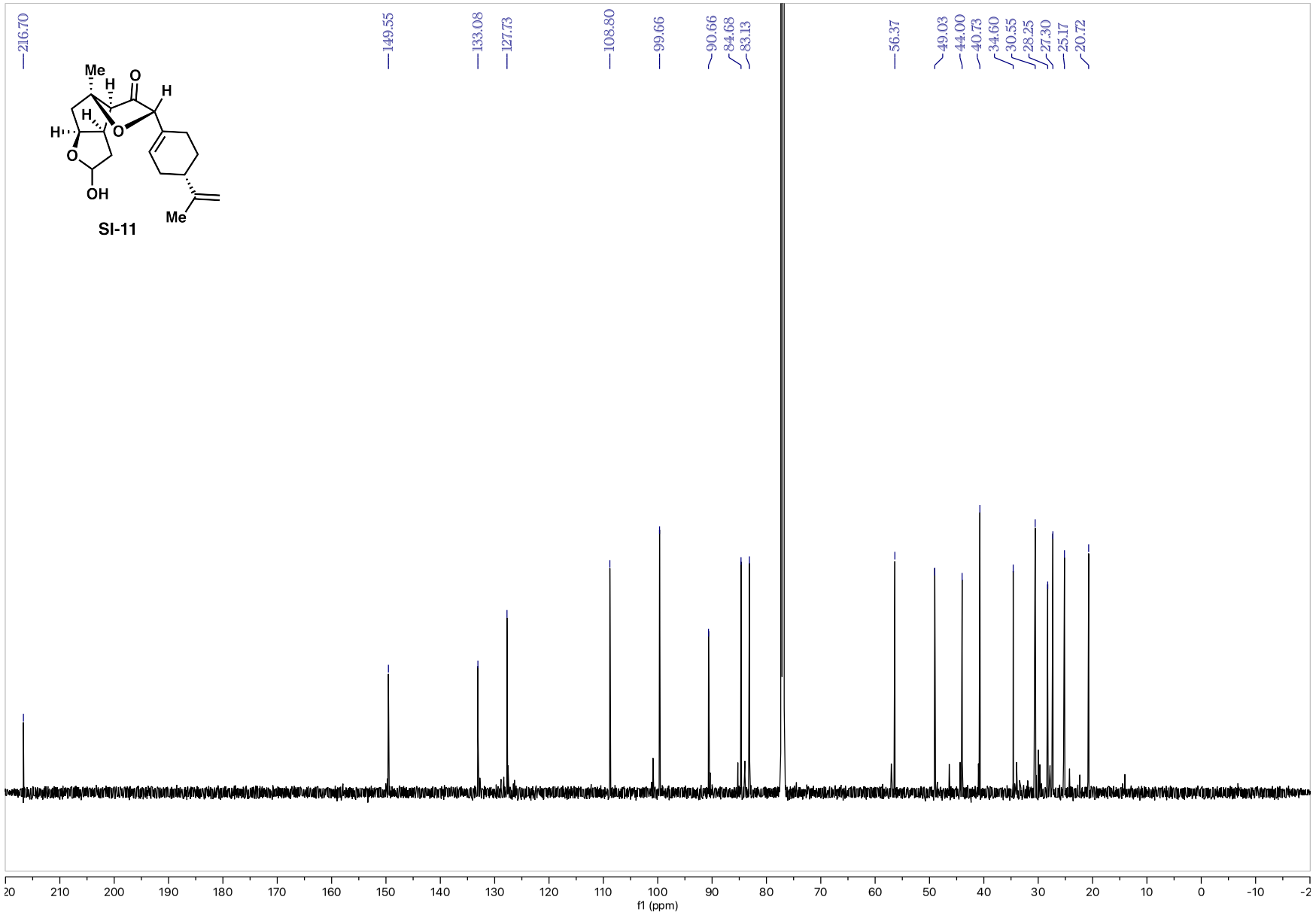

-2.31
-2.51
18.11
20.90
20.98
24.88
25.81
25.89
26.92
27.14
30.79
40.24
52.10
73.75
80.61
83.69
109.16
130.39
131.96
142.86
147.59
149.04
170.14
192.93
Me
OAc
O
OH
2.347b
TBSO
Me
f1 (ppm)


TBSO
Me
H
H
O
O
SI-2
0.09
0.11
0.86
0.87
0.87
0.87
1.37
2.10
2.11
2.12
2.13
2.17
2.17
2.17
2.19
2.19
2.58
2.59
2.61
2.61
2.90
2.92
2.93
2.95
3.41
3.41
3.42
3.42
3.43
3.43
3.43
3.44
3.44
3.45
4.94
4.95
4.96
4.96
4.96
4.97
5.22
5.22
5.86
9.11
3.05
1.96
0.93
0.91
0.95
1.90
0.94
f1 (ppm)


Me
H
Me
HO
H
H
O
OH
SI-3
7.18
1.86
3.03
4.95
5.32
2.32
1.18
6.78
0.82
0.78
0.81
0.85
3.93
2.34
1.80
1.99
1.96
0.85
1.25
f1 (ppm)

20.79
25.14
26.16
26.46
27.39
27.43
31.28
37.60
38.77
41.24
41.26
46.61
46.94
47.04
49.84
58.60
59.62
82.22
83.22
83.62
84.84
108.73
108.77
122.22
123.07
135.08
135.18
136.56
136.77
149.69
149.76
Me
HO
Me
H
H
H
O
OH
SI-3
f1 (ppm)


Me
H
O
Me
H
O
H
O
OH
SI-11
f1 (ppm)


216.70
149.55
133.08
127.73
108.80
99.66
90.66
84.68
83.13
56.37
49.03
44.00
40.73
34.60
30.55
28.25
27.30
25.17
20.72
Me
H
O
H
H
H
O
O
OH
Me
SI-11
f1 (ppm)

X-ray Crystal Structure Report

A colorless rod 0.37 x 0.16 x 0.07 mm in size was mounted on a Cryoloop with Paratone oil. Data were collected in a nitrogen gas stream at 100(2) K using omega scans. Crystal-to-detector distance was 33.00 mm and exposure time was 0.50 seconds per frame at low and high angles, using a scan width of 0.5°. Data collection was 100% complete to 74.000° in θ. A total of 34900 reflections were collected covering the indices -13<=h<=13, -13<=k<=13, -19<=l<=14. 6827 reflections were founded to be symmetry independent, with an R_{int} of 0.0348. Indexing and unit cell refinement indicated a primitive, monoclinic lattice. The space group was found to be P 21 (No. 4). The data were integrated using the CrysAlis^{Pro} 1.171.41.116a software program and scaled using the SCALE3 ABSPACK scaling algorithm. Solution by intrinsic phasing (SHELXT-2015) produced a heavy-atom phasing model consistent with the proposed structure. All non-hydrogen atoms were refined anisotropically by full-matrix least-squares (SHELXL-2014). All hydrogen atoms were placed using a riding model. Their positions were constrained relative to their parent atom using the appropriate HFIX command in SHELXL-2014.

Compound 2.363a:

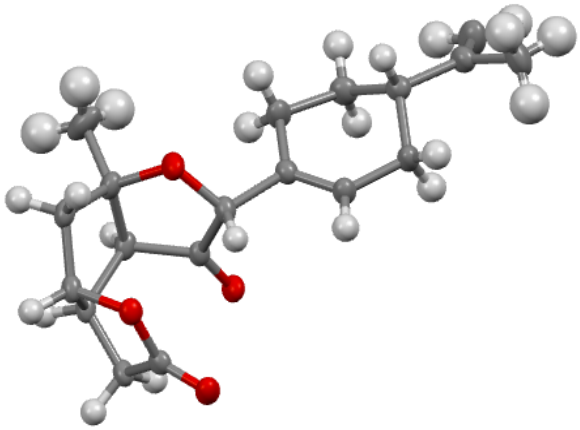


Table 1. Crystal data and structure refinement for DThach06_Maimone.

Identification code	DThach06_Maimone	
Empirical formula	C19 H24 O4	
Formula weight	316.38	
Temperature	100(2) K	
Wavelength	1.54184 Å	
Crystal system	Monoclinic	
Space group	P 21	
Unit cell dimensions	a = 10.69490(10) Å	α= 90°.
	b = 10.8534(2) Å	β= 109.487(2)°.
	c = 15.3030(2) Å	γ = 90°.
Volume	1674.56(5) $Å^3$	
Z	4	
Density (calculated)	1.255 Mg/m^3	
Absorption coefficient	0.702 mm^{-1}	
F(000)	680	
Crystal size	0.370 x 0.160 x 0.070 mm^3	
Theta range for data collection	3.063 to 74.504°.	
Index ranges	-13<=h<=13, -13<=k<=13, -19<=l<=14	
Reflections collected	34900	
Independent reflections	6827 [R(int) = 0.0348]	
Completeness to theta = 74.000°	99.9 %	
Absorption correction	Semi-empirical from equivalents	
Max. and min. transmission	1.00000 and 0.68879	
Refinement method	Full-matrix least-squares on F^2	
Data / restraints / parameters	6827 / 1 / 419	
Goodness-of-fit on F^2	1.078	
Final R indices [I>2sigma(I)]	R1 = 0.0446, wR2 = 0.1312	
R indices (all data)	R1 = 0.0461, wR2 = 0.1327	

Absolute structure parameter	0.04(5)
Extinction coefficient	n/a
Largest diff. peak and hole	0.468 and -0.202 e.Å^{-3}

Table 2. Atomic coordinates (x 10^4) and equivalent isotropic displacement parameters (Å^{2}x 10^3) for dthach06_maimone. U(eq) is defined as one third of the trace of the orthogonalized U^{ij} tensor.

	x	y	z	U(eq)
O(2A)	3097(1)	7987(2)	5299(1)	24(1)
O(2B)	8040(1)	8007(2)	5216(1)	25(1)
O(1A)	2781(2)	6465(2)	4268(1)	32(1)
O(1B)	7846(2)	6426(2)	4244(1)	31(1)
O(4A)	5873(2)	5477(2)	6064(1)	30(1)
O(4B)	10937(2)	5604(2)	6113(1)	29(1)
O(3B)	9330(2)	7278(2)	7369(1)	32(1)
O(3A)	4579(2)	7165(2)	7494(1)	38(1)
C(1B)	8494(2)	7274(2)	4665(1)	24(1)
C(1A)	3487(2)	7271(2)	4706(2)	24(1)
C(19B)	8900(2)	4054(2)	7179(2)	28(1)
C(11A)	4658(2)	4947(2)	7502(2)	24(1)
C(9B)	10459(2)	6400(2)	6452(1)	22(1)
C(9A)	5482(2)	6284(2)	6449(1)	23(1)
C(19A)	3758(2)	4049(2)	7254(2)	26(1)
C(10B)	9369(2)	6191(2)	6873(2)	24(1)
C(11B)	9607(2)	5064(2)	7478(2)	24(1)
C(3A)	5364(2)	8387(2)	5621(2)	22(1)
C(3B)	10305(2)	8471(2)	5585(2)	25(1)
C(4A)	4092(2)	8955(2)	5688(2)	23(1)
C(2A)	4853(2)	7654(2)	4724(2)	23(1)
C(8B)	10824(2)	7749(2)	6522(2)	24(1)

C(12A)	5904(2)	4841(2)	8330(2)	31(1)
C(15A)	5029(2)	1770(2)	9310(2)	29(1)
C(10A)	4461(2)	6108(2)	6936(2)	26(1)
C(2B)	9860(2)	7700(2)	4707(2)	25(1)
C(18A)	3872(2)	2851(2)	7770(2)	28(1)
C(8A)	5912(2)	7616(2)	6531(2)	22(1)
C(6A)	5309(2)	8160(2)	7237(2)	26(1)
C(14A)	4827(2)	2961(2)	8766(2)	25(1)
C(4B)	8989(2)	9012(2)	5598(2)	24(1)
C(14B)	9911(2)	3062(2)	8752(2)	28(1)
C(13A)	6125(2)	3534(3)	8733(2)	32(1)
C(5B)	9159(2)	9263(2)	6599(2)	27(1)
C(18B)	9119(2)	2871(2)	7718(2)	31(1)
C(12B)	10695(2)	5140(3)	8399(2)	34(1)
C(5A)	4332(2)	9155(2)	6711(2)	26(1)
C(6B)	10115(2)	8282(2)	7172(2)	27(1)
C(13B)	11105(2)	3879(3)	8844(2)	34(1)
C(15B)	10229(3)	1836(2)	9256(2)	33(1)
C(16A)	4352(3)	748(3)	8985(2)	40(1)
C(17B)	9090(3)	999(3)	9151(2)	46(1)
C(16B)	11466(3)	1490(3)	9738(2)	49(1)
C(7B)	11017(3)	8751(3)	8098(2)	48(1)
C(7A)	6337(3)	8607(3)	8123(2)	47(1)
C(17A)	5962(3)	1818(3)	10292(2)	50(1)

Table 3. Bond lengths [Å] and angles [°] for dthach06_maimone.

O(2A)-C(1A)	1.361(3)
O(2A)-C(4A)	1.472(2)
O(2B)-C(1B)	1.361(3)
O(2B)-C(4B)	1.472(3)
O(1A)-C(1A)	1.203(3)
O(1B)-C(1B)	1.202(3)
O(4A)-C(9A)	1.206(3)
O(4B)-C(9B)	1.206(3)
O(3B)-C(10B)	1.411(3)
O(3B)-C(6B)	1.467(3)
O(3A)-C(10A)	1.411(3)
O(3A)-C(6A)	1.462(3)
C(1B)-C(2B)	1.512(3)
C(1A)-C(2A)	1.511(3)
C(19B)-C(11B)	1.323(3)
C(19B)-C(18B)	1.501(3)
C(11A)-C(19A)	1.333(3)
C(11A)-C(10A)	1.504(3)
C(11A)-C(12A)	1.506(3)
C(9B)-C(8B)	1.510(3)
C(9B)-C(10B)	1.526(3)
C(9A)-C(8A)	1.510(3)
C(9A)-C(10A)	1.525(3)
C(19A)-C(18A)	1.504(3)
C(10B)-C(11B)	1.503(3)
C(11B)-C(12B)	1.502(3)
C(3A)-C(2A)	1.521(3)
C(3A)-C(4A)	1.528(3)

C(3A)-C(8A)	1.562(3)
C(3B)-C(2B)	1.518(3)
C(3B)-C(4B)	1.532(3)
C(3B)-C(8B)	1.564(3)
C(4A)-C(5A)	1.514(3)
C(8B)-C(6B)	1.550(3)
C(12A)-C(13A)	1.533(3)
C(15A)-C(16A)	1.326(4)
C(15A)-C(17A)	1.502(3)
C(15A)-C(14A)	1.513(3)
C(18A)-C(14A)	1.531(3)
C(8A)-C(6A)	1.547(3)
C(6A)-C(7A)	1.512(3)
C(6A)-C(5A)	1.531(3)
C(14A)-C(13A)	1.537(3)
C(4B)-C(5B)	1.507(3)
C(14B)-C(15B)	1.518(3)
C(14B)-C(13B)	1.523(3)
C(14B)-C(18B)	1.539(3)
C(5B)-C(6B)	1.532(3)
C(12B)-C(13B)	1.526(4)
C(6B)-C(7B)	1.511(3)
C(15B)-C(16B)	1.336(4)
C(15B)-C(17B)	1.485(4)

C(1A)-O(2A)-C(4A)	109.63(16)
C(1B)-O(2B)-C(4B)	109.72(16)
C(10B)-O(3B)-C(6B)	112.95(17)
C(10A)-O(3A)-C(6A)	112.69(17)
O(1B)-C(1B)-O(2B)	121.1(2)

O(1B)-C(1B)-C(2B)	129.3(2)
O(2B)-C(1B)-C(2B)	109.55(19)
O(1A)-C(1A)-O(2A)	120.8(2)
O(1A)-C(1A)-C(2A)	129.3(2)
O(2A)-C(1A)-C(2A)	109.93(18)
C(11B)-C(19B)-C(18B)	123.5(2)
C(19A)-C(11A)-C(10A)	120.0(2)
C(19A)-C(11A)-C(12A)	122.4(2)
C(10A)-C(11A)-C(12A)	117.6(2)
O(4B)-C(9B)-C(8B)	126.10(19)
O(4B)-C(9B)-C(10B)	124.6(2)
C(8B)-C(9B)-C(10B)	109.26(19)
O(4A)-C(9A)-C(8A)	126.2(2)
O(4A)-C(9A)-C(10A)	124.7(2)
C(8A)-C(9A)-C(10A)	109.09(19)
C(11A)-C(19A)-C(18A)	124.0(2)
O(3B)-C(10B)-C(11B)	112.29(18)
O(3B)-C(10B)-C(9B)	105.45(18)
C(11B)-C(10B)-C(9B)	112.65(17)
C(19B)-C(11B)-C(12B)	123.0(2)
C(19B)-C(11B)-C(10B)	120.1(2)
C(12B)-C(11B)-C(10B)	116.9(2)
C(2A)-C(3A)-C(4A)	102.26(16)
C(2A)-C(3A)-C(8A)	116.11(18)
C(4A)-C(3A)-C(8A)	103.49(16)
C(2B)-C(3B)-C(4B)	101.78(16)
C(2B)-C(3B)-C(8B)	116.50(19)
C(4B)-C(3B)-C(8B)	103.12(17)
O(2A)-C(4A)-C(5A)	111.76(17)
O(2A)-C(4A)-C(3A)	102.97(16)

C(5A)-C(4A)-C(3A)	106.27(16)
C(1A)-C(2A)-C(3A)	102.34(17)
C(9B)-C(8B)-C(6B)	103.76(18)
C(9B)-C(8B)-C(3B)	114.56(18)
C(6B)-C(8B)-C(3B)	107.55(17)
C(11A)-C(12A)-C(13A)	112.58(19)
C(16A)-C(15A)-C(17A)	120.0(2)
C(16A)-C(15A)-C(14A)	123.3(2)
C(17A)-C(15A)-C(14A)	116.5(2)
O(3A)-C(10A)-C(11A)	111.44(18)
O(3A)-C(10A)-C(9A)	105.04(18)
C(11A)-C(10A)-C(9A)	113.60(18)
C(1B)-C(2B)-C(3B)	102.68(17)
C(19A)-C(18A)-C(14A)	111.41(19)
C(9A)-C(8A)-C(6A)	103.72(17)
C(9A)-C(8A)-C(3A)	115.17(17)
C(6A)-C(8A)-C(3A)	107.38(16)
O(3A)-C(6A)-C(7A)	106.8(2)
O(3A)-C(6A)-C(5A)	109.27(17)
C(7A)-C(6A)-C(5A)	114.2(2)
O(3A)-C(6A)-C(8A)	106.89(17)
C(7A)-C(6A)-C(8A)	113.62(19)
C(5A)-C(6A)-C(8A)	105.82(17)
C(15A)-C(14A)-C(18A)	113.96(19)
C(15A)-C(14A)-C(13A)	113.54(18)
C(18A)-C(14A)-C(13A)	107.96(18)
O(2B)-C(4B)-C(5B)	111.77(18)
O(2B)-C(4B)-C(3B)	103.02(16)
C(5B)-C(4B)-C(3B)	106.41(17)
C(15B)-C(14B)-C(13B)	115.10(19)

C(15B)-C(14B)-C(18B)	110.9(2)
C(13B)-C(14B)-C(18B)	109.25(19)
C(12A)-C(13A)-C(14A)	111.57(18)
C(4B)-C(5B)-C(6B)	106.69(18)
C(19B)-C(18B)-C(14B)	112.4(2)
C(11B)-C(12B)-C(13B)	112.7(2)
C(4A)-C(5A)-C(6A)	107.00(17)
O(3B)-C(6B)-C(7B)	106.7(2)
O(3B)-C(6B)-C(5B)	108.41(17)
C(7B)-C(6B)-C(5B)	113.4(2)
O(3B)-C(6B)-C(8B)	106.86(17)
C(7B)-C(6B)-C(8B)	115.5(2)
C(5B)-C(6B)-C(8B)	105.57(18)
C(14B)-C(13B)-C(12B)	111.92(19)
C(16B)-C(15B)-C(17B)	120.9(3)
C(16B)-C(15B)-C(14B)	122.7(3)
C(17B)-C(15B)-C(14B)	116.4(2)

Symmetry transformations used to generate equivalent atoms:

Table 4. Anisotropic displacement parameters ($Å^2$x 10^3)for dthach06_maimone. The anisotropic displacement factor exponent takes the form: $-2\pi^2[h^2a^{*2}U^{11} + ... + 2 h k a^* b^* U^{12}]$

	U^{11}	U^{22}	U^{33}	U^{23}	U^{13}	U^{12}
O(2A)	16(1)	23(1)	31(1)	1(1)	5(1)	-1(1)
O(2B)	17(1)	25(1)	30(1)	1(1)	6(1)	0(1)
O(1A)	30(1)	28(1)	32(1)	-2(1)	1(1)	-8(1)
O(1B)	30(1)	28(1)	29(1)	0(1)	3(1)	-4(1)
O(4A)	40(1)	20(1)	31(1)	1(1)	13(1)	4(1)
O(4B)	35(1)	21(1)	34(1)	2(1)	14(1)	7(1)
O(3B)	41(1)	22(1)	38(1)	0(1)	20(1)	4(1)
O(3A)	58(1)	21(1)	47(1)	2(1)	33(1)	4(1)
C(1B)	22(1)	23(1)	25(1)	5(1)	5(1)	4(1)
C(1A)	22(1)	22(1)	26(1)	4(1)	3(1)	2(1)
C(19B)	24(1)	26(1)	28(1)	2(1)	2(1)	-2(1)
C(11A)	21(1)	23(1)	29(1)	3(1)	7(1)	3(1)
C(9B)	16(1)	21(1)	25(1)	2(1)	3(1)	0(1)
C(9A)	19(1)	22(1)	25(1)	2(1)	3(1)	2(1)
C(19A)	22(1)	25(1)	29(1)	0(1)	3(1)	0(1)
C(10B)	22(1)	21(1)	31(1)	3(1)	9(1)	1(1)
C(11B)	22(1)	23(1)	26(1)	2(1)	8(1)	2(1)
C(3A)	17(1)	17(1)	32(1)	1(1)	8(1)	1(1)
C(3B)	19(1)	19(1)	41(1)	2(1)	13(1)	1(1)
C(4A)	18(1)	17(1)	34(1)	1(1)	9(1)	0(1)
C(2A)	23(1)	19(1)	29(1)	0(1)	8(1)	-1(1)
C(8B)	16(1)	20(1)	35(1)	-2(1)	5(1)	0(1)
C(12A)	23(1)	29(1)	33(1)	6(1)	1(1)	-4(1)
C(15A)	28(1)	26(1)	34(1)	5(1)	12(1)	4(1)
C(10A)	23(1)	21(1)	35(1)	5(1)	9(1)	2(1)

C(2B)	24(1)	20(1)	33(1)	3(1)	13(1)	1(1)
C(18A)	29(1)	22(1)	29(1)	-1(1)	4(1)	-3(1)
C(8A)	14(1)	20(1)	32(1)	-2(1)	6(1)	0(1)
C(6A)	25(1)	22(1)	29(1)	-2(1)	6(1)	0(1)
C(14A)	24(1)	22(1)	29(1)	-1(1)	7(1)	1(1)
C(4B)	21(1)	18(1)	35(1)	2(1)	10(1)	1(1)
C(14B)	29(1)	27(1)	28(1)	1(1)	8(1)	5(1)
C(13A)	22(1)	35(1)	36(1)	9(1)	5(1)	1(1)
C(5B)	24(1)	20(1)	37(1)	-3(1)	10(1)	-1(1)
C(18B)	38(1)	24(1)	27(1)	1(1)	4(1)	-4(1)
C(12B)	32(1)	31(1)	30(1)	1(1)	0(1)	-7(1)
C(5A)	24(1)	18(1)	36(1)	-2(1)	12(1)	0(1)
C(6B)	25(1)	20(1)	32(1)	-3(1)	4(1)	0(1)
C(13B)	28(1)	37(1)	31(1)	3(1)	3(1)	2(1)
C(15B)	40(1)	28(1)	30(1)	4(1)	10(1)	6(1)
C(16A)	51(1)	27(1)	41(1)	5(1)	16(1)	-3(1)
C(17B)	45(1)	38(2)	54(2)	18(1)	15(1)	0(1)
C(16B)	48(1)	34(1)	50(1)	5(1)	-2(1)	6(1)
C(7B)	43(1)	42(2)	44(1)	-18(1)	-5(1)	7(1)
C(7A)	38(1)	53(2)	39(1)	-17(1)	-2(1)	9(1)
C(17A)	47(1)	51(2)	44(1)	15(1)	5(1)	-8(1)

Table 5. Hydrogen coordinates (x 10^4) and isotropic displacement parameters ($Å^2$x 10^3) for dthach06_maimone.

	x	y	z	U(eq)
H(19B)	8217	4079	6593	33
H(19A)	2999	4173	6721	32
H(10B)	8503	6097	6360	29
H(3A)	6009	9035	5585	26
H(3B)	10939	9131	5551	30
H(4A)	3859	9740	5329	28
H(2AA)	4806	8171	4181	28
H(2AB)	5420	6928	4738	28
H(8B)	11806	7850	6808	29
H(12A)	5851	5421	8816	37
H(12B)	6674	5081	8146	37
H(10A)	3554	6094	6459	32
H(2BA)	9818	8200	4157	30
H(2BB)	10461	6992	4751	30
H(18A)	4192	2202	7442	34
H(18B)	2985	2603	7779	34
H(8A)	6901	7672	6782	27
H(14A)	4427	3564	9091	30
H(4B)	8745	9776	5212	29
H(14B)	9324	3525	9027	34
H(13A)	6780	3561	9368	38
H(13B)	6494	3010	8349	38
H(5BA)	8294	9209	6702	32
H(5BB)	9529	10098	6779	32

H(18C)	9604	2288	7450	38
H(18D)	8249	2500	7658	38
H(12C)	10393	5658	8823	40
H(12D)	11476	5545	8316	40
H(5AA)	3489	9085	6842	31
H(5AB)	4708	9985	6902	31
H(13C)	11684	3468	8545	40
H(13D)	11623	3989	9509	40
H(16A)	4458	46	9374	48
H(16B)	3762	719	8364	48
H(17D)	8428	1423	9356	69
H(17E)	9400	260	9529	69
H(17F)	8691	762	8499	69
H(16C)	11626	699	10020	58
H(16D)	12186	2034	9800	58
H(7BA)	10483	9002	8477	71
H(7BB)	11523	9459	8000	71
H(7BC)	11630	8095	8416	71
H(7AA)	5898	8854	8564	71
H(7AB)	6812	9313	7987	71
H(7AC)	6968	7941	8392	71
H(17A)	6876	1891	10292	75
H(17B)	5873	1062	10616	75
H(17C)	5748	2532	10607	75

Table 6. Torsion angles [°] for dthach06_maimone.

C(4B)-O(2B)-C(1B)-O(1B)	-176.46(19)
C(4B)-O(2B)-C(1B)-C(2B)	4.5(2)
C(4A)-O(2A)-C(1A)-O(1A)	-175.71(19)
C(4A)-O(2A)-C(1A)-C(2A)	4.9(2)
C(10A)-C(11A)-C(19A)-C(18A)	179.4(2)
C(12A)-C(11A)-C(19A)-C(18A)	0.6(4)
C(6B)-O(3B)-C(10B)-C(11B)	134.06(18)
C(6B)-O(3B)-C(10B)-C(9B)	11.0(2)
O(4B)-C(9B)-C(10B)-O(3B)	166.70(19)
C(8B)-C(9B)-C(10B)-O(3B)	-13.7(2)
O(4B)-C(9B)-C(10B)-C(11B)	43.9(3)
C(8B)-C(9B)-C(10B)-C(11B)	-136.46(19)
C(18B)-C(19B)-C(11B)-C(12B)	-1.1(4)
C(18B)-C(19B)-C(11B)-C(10B)	176.8(2)
O(3B)-C(10B)-C(11B)-C(19B)	135.6(2)
C(9B)-C(10B)-C(11B)-C(19B)	-105.5(2)
O(3B)-C(10B)-C(11B)-C(12B)	-46.3(3)
C(9B)-C(10B)-C(11B)-C(12B)	72.6(3)
C(1A)-O(2A)-C(4A)-C(5A)	-139.17(17)
C(1A)-O(2A)-C(4A)-C(3A)	-25.5(2)
C(2A)-C(3A)-C(4A)-O(2A)	35.1(2)
C(8A)-C(3A)-C(4A)-O(2A)	-85.92(18)
C(2A)-C(3A)-C(4A)-C(5A)	152.72(18)
C(8A)-C(3A)-C(4A)-C(5A)	31.7(2)
O(1A)-C(1A)-C(2A)-C(3A)	-161.6(2)
O(2A)-C(1A)-C(2A)-C(3A)	17.7(2)
C(4A)-C(3A)-C(2A)-C(1A)	-31.9(2)
C(8A)-C(3A)-C(2A)-C(1A)	80.0(2)

O(4B)-C(9B)-C(8B)-C(6B)	-169.5(2)
C(10B)-C(9B)-C(8B)-C(6B)	10.9(2)
O(4B)-C(9B)-C(8B)-C(3B)	73.5(3)
C(10B)-C(9B)-C(8B)-C(3B)	-106.1(2)
C(2B)-C(3B)-C(8B)-C(9B)	-16.5(2)
C(4B)-C(3B)-C(8B)-C(9B)	94.0(2)
C(2B)-C(3B)-C(8B)-C(6B)	-131.26(18)
C(4B)-C(3B)-C(8B)-C(6B)	-20.8(2)
C(19A)-C(11A)-C(12A)-C(13A)	10.1(3)
C(10A)-C(11A)-C(12A)-C(13A)	-168.7(2)
C(6A)-O(3A)-C(10A)-C(11A)	139.04(19)
C(6A)-O(3A)-C(10A)-C(9A)	15.6(2)
C(19A)-C(11A)-C(10A)-O(3A)	127.8(2)
C(12A)-C(11A)-C(10A)-O(3A)	-53.3(3)
C(19A)-C(11A)-C(10A)-C(9A)	-113.8(2)
C(12A)-C(11A)-C(10A)-C(9A)	65.1(3)
O(4A)-C(9A)-C(10A)-O(3A)	164.1(2)
C(8A)-C(9A)-C(10A)-O(3A)	-16.0(2)
O(4A)-C(9A)-C(10A)-C(11A)	42.0(3)
C(8A)-C(9A)-C(10A)-C(11A)	-138.01(19)
O(1B)-C(1B)-C(2B)-C(3B)	-160.4(2)
O(2B)-C(1B)-C(2B)-C(3B)	18.5(2)
C(4B)-C(3B)-C(2B)-C(1B)	-32.5(2)
C(8B)-C(3B)-C(2B)-C(1B)	78.8(2)
C(11A)-C(19A)-C(18A)-C(14A)	20.7(3)
O(4A)-C(9A)-C(8A)-C(6A)	-169.7(2)
C(10A)-C(9A)-C(8A)-C(6A)	10.3(2)
O(4A)-C(9A)-C(8A)-C(3A)	73.2(3)
C(10A)-C(9A)-C(8A)-C(3A)	-106.7(2)
C(2A)-C(3A)-C(8A)-C(9A)	-18.5(2)

C(4A)-C(3A)-C(8A)-C(9A)	92.6(2)
C(2A)-C(3A)-C(8A)-C(6A)	-133.49(18)
C(4A)-C(3A)-C(8A)-C(6A)	-22.3(2)
C(10A)-O(3A)-C(6A)-C(7A)	-131.4(2)
C(10A)-O(3A)-C(6A)-C(5A)	104.6(2)
C(10A)-O(3A)-C(6A)-C(8A)	-9.4(2)
C(9A)-C(8A)-C(6A)-O(3A)	-1.1(2)
C(3A)-C(8A)-C(6A)-O(3A)	121.25(19)
C(9A)-C(8A)-C(6A)-C(7A)	116.4(2)
C(3A)-C(8A)-C(6A)-C(7A)	-121.2(2)
C(9A)-C(8A)-C(6A)-C(5A)	-117.50(18)
C(3A)-C(8A)-C(6A)-C(5A)	4.9(2)
C(16A)-C(15A)-C(14A)-C(18A)	-5.8(3)
C(17A)-C(15A)-C(14A)-C(18A)	179.7(2)
C(16A)-C(15A)-C(14A)-C(13A)	-130.0(3)
C(17A)-C(15A)-C(14A)-C(13A)	55.5(3)
C(19A)-C(18A)-C(14A)-C(15A)	-177.60(19)
C(19A)-C(18A)-C(14A)-C(13A)	-50.5(3)
C(1B)-O(2B)-C(4B)-C(5B)	-139.38(18)
C(1B)-O(2B)-C(4B)-C(3B)	-25.5(2)
C(2B)-C(3B)-C(4B)-O(2B)	35.4(2)
C(8B)-C(3B)-C(4B)-O(2B)	-85.67(18)
C(2B)-C(3B)-C(4B)-C(5B)	153.15(19)
C(8B)-C(3B)-C(4B)-C(5B)	32.0(2)
C(11A)-C(12A)-C(13A)-C(14A)	-42.1(3)
C(15A)-C(14A)-C(13A)-C(12A)	-169.8(2)
C(18A)-C(14A)-C(13A)-C(12A)	62.8(2)
O(2B)-C(4B)-C(5B)-C(6B)	80.0(2)
C(3B)-C(4B)-C(5B)-C(6B)	-31.8(2)
C(11B)-C(19B)-C(18B)-C(14B)	18.4(3)

C(15B)-C(14B)-C(18B)-C(19B)	-174.5(2)
C(13B)-C(14B)-C(18B)-C(19B)	-46.5(3)
C(19B)-C(11B)-C(12B)-C(13B)	13.3(3)
C(10B)-C(11B)-C(12B)-C(13B)	-164.8(2)
O(2A)-C(4A)-C(5A)-C(6A)	81.98(19)
C(3A)-C(4A)-C(5A)-C(6A)	-29.6(2)
O(3A)-C(6A)-C(5A)-C(4A)	-99.8(2)
C(7A)-C(6A)-C(5A)-C(4A)	140.6(2)
C(8A)-C(6A)-C(5A)-C(4A)	14.9(2)
C(10B)-O(3B)-C(6B)-C(7B)	-128.5(2)
C(10B)-O(3B)-C(6B)-C(5B)	109.0(2)
C(10B)-O(3B)-C(6B)-C(8B)	-4.4(2)
C(4B)-C(5B)-C(6B)-O(3B)	-96.4(2)
C(4B)-C(5B)-C(6B)-C(7B)	145.3(2)
C(4B)-C(5B)-C(6B)-C(8B)	17.8(2)
C(9B)-C(8B)-C(6B)-O(3B)	-4.3(2)
C(3B)-C(8B)-C(6B)-O(3B)	117.47(18)
C(9B)-C(8B)-C(6B)-C(7B)	114.2(2)
C(3B)-C(8B)-C(6B)-C(7B)	-124.0(2)
C(9B)-C(8B)-C(6B)-C(5B)	-119.56(18)
C(3B)-C(8B)-C(6B)-C(5B)	2.2(2)
C(15B)-C(14B)-C(13B)-C(12B)	-174.5(2)
C(18B)-C(14B)-C(13B)-C(12B)	59.9(3)
C(11B)-C(12B)-C(13B)-C(14B)	-42.9(3)
C(13B)-C(14B)-C(15B)-C(16B)	-0.6(3)
C(18B)-C(14B)-C(15B)-C(16B)	124.1(3)
C(13B)-C(14B)-C(15B)-C(17B)	-177.9(2)
C(18B)-C(14B)-C(15B)-C(17B)	-53.2(3)

Symmetry transformations used to generate equivalent atoms:

Compound 2.319a

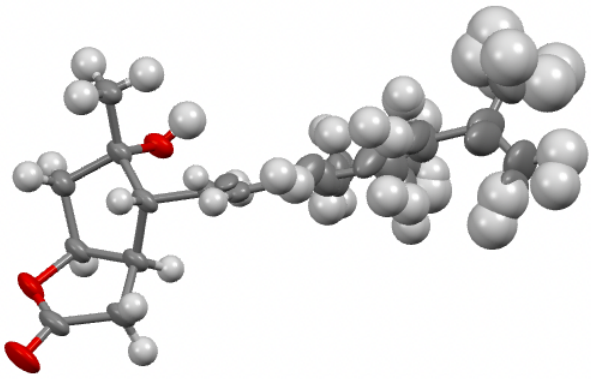


Table 1. Crystal data and structure refinement for DThach03_Maimone.

Identification code	DThach03_Maimone	
Empirical formula	C19 H26 O3	
Formula weight	302.40	
Temperature	100(2) K	
Wavelength	1.54184 Å	
Crystal system	Orthorhombic	
Space group	P 21 21 21	
Unit cell dimensions	a = 8.40730(10) Å	α= 90°.
	b = 23.0965(4) Å	β= 90°.
	c = 9.1183(2) Å	γ = 90°.
Volume	1770.58(5) $Å^3$	
Z	4	
Density (calculated)	1.134 Mg/m^3	
Absorption coefficient	0.596 mm^{-1}	
F(000)	656	
Crystal size	0.440 x 0.200 x 0.100 mm^3	
Theta range for data collection	3.828 to 74.498°.	

Index ranges	-9<=h<=10, -28<=k<=28, -10<=l<=11
Reflections collected	27615
Independent reflections	3615 [R(int) = 0.0427]
Completeness to theta = 74.000°	99.9 %
Absorption correction	Semi-empirical from equivalents
Max. and min. transmission	1.00000 and 0.84958
Refinement method	Full-matrix least-squares on F^2
Data / restraints / parameters	3615 / 105 / 286
Goodness-of-fit on F^2	1.074
Final R indices [I>2sigma(I)]	R1 = 0.0479, wR2 = 0.1266
R indices (all data)	R1 = 0.0509, wR2 = 0.1288
Absolute structure parameter	0.07(8)
Extinction coefficient	0.0030(6)
Largest diff. peak and hole	0.345 and -0.172 e.$Å^{-3}$

Table 2. Atomic coordinates (x 10^4) and equivalent isotropic displacement parameters ($Å^2$x 10^3) for dthatch03_maimone. U(eq) is defined as one third of the trace of the orthogonalized U^{ij} tensor.

	x	y	z	U(eq)
O(1)	10284(2)	7403(1)	7586(3)	63(1)
O(2)	8324(2)	7975(1)	8336(2)	47(1)
O(3)	3138(2)	7937(1)	8525(2)	39(1)
C(1)	6135(3)	7311(1)	8415(3)	32(1)
C(2)	7680(3)	6989(1)	8119(3)	39(1)
C(3)	8905(3)	7458(2)	7971(3)	45(1)
C(4)	6656(3)	7932(1)	8778(3)	38(1)
C(5)	5626(3)	8338(1)	7867(3)	42(1)
C(6)	4237(3)	7970(1)	7324(3)	35(1)
C(7)	3423(3)	8208(1)	5975(3)	44(1)
C(8)	5023(3)	7374(1)	7083(3)	33(1)

C(9)	3893(3)	6879(1)	6954(3)	37(1)
C(10A)	3770(20)	6461(8)	6023(16)	37(3)
C(10B)	3800(30)	6547(8)	5692(18)	29(2)
C(11A)	2502(19)	6013(7)	5973(15)	42(3)
C(11B)	2790(20)	6032(8)	5606(18)	39(3)
C(12A)	2482(15)	5635(6)	4934(14)	66(3)
C(12B)	2730(20)	5683(6)	4422(13)	60(3)
C(13A)	1234(15)	5146(5)	4859(16)	78(3)
C(13B)	1570(20)	5214(5)	4208(13)	76(4)
C(14A)	-60(20)	5247(8)	5791(17)	81(4)
C(14B)	90(30)	5218(7)	5302(18)	71(4)
C(15A)	-1353(15)	4794(5)	5680(30)	102(4)
C(15B)	-890(20)	4644(7)	5270(30)	102(4)
C(16A)	-1000(20)	4233(6)	5590(20)	116(5)
C(16B)	-330(20)	4126(7)	5600(30)	110(6)
C(17A)	-3039(13)	4985(6)	5844(18)	117(3)
C(17B)	-2510(20)	4795(7)	4970(20)	117(3)
C(18A)	100(13)	5540(5)	7045(13)	94(3)
C(18B)	843(14)	5311(4)	6845(12)	65(3)
C(19A)	1286(12)	6006(5)	7163(10)	50(2)
C(19B)	1666(18)	5907(6)	6784(17)	64(4)

Table 3. Bond lengths [Å] and angles [°] for dthatch03_maimone.

O(1)-C(3)	1.218(3)
O(2)-C(3)	1.332(4)
O(2)-C(4)	1.463(3)
O(3)-C(6)	1.435(3)
O(3)-H(3)	0.87(5)
C(1)-C(2)	1.521(3)
C(1)-C(4)	1.535(4)
C(1)-C(8)	1.540(3)
C(1)-H(1)	1.0000
C(2)-C(3)	1.500(4)
C(2)-H(2A)	0.9900
C(2)-H(2B)	0.9900
C(4)-C(5)	1.522(4)
C(4)-H(4)	1.0000
C(5)-C(6)	1.527(3)
C(5)-H(5A)	0.9900
C(5)-H(5B)	0.9900
C(6)-C(7)	1.512(4)
C(6)-C(8)	1.541(4)
C(7)-H(7A)	0.9800
C(7)-H(7B)	0.9800
C(7)-H(7C)	0.9800
C(8)-C(9)	1.492(3)
C(8)-H(8)	1.0000
C(9)-C(10A)	1.29(2)
C(9)-C(10B)	1.38(2)
C(9)-H(9A)	0.9500
C(9)-H(9B)	0.9500

C(10A)-C(11A)	1.483(19)
C(10A)-H(10A)	0.9500
C(10B)-C(11B)	1.46(2)
C(10B)-H(10B)	0.9500
C(11A)-C(12A)	1.289(16)
C(11A)-C(19A)	1.491(12)
C(11B)-C(12B)	1.347(18)
C(11B)-C(19B)	1.458(15)
C(12A)-C(13A)	1.543(16)
C(12A)-H(12A)	0.9500
C(12B)-C(13B)	1.472(17)
C(12B)-H(12B)	0.9500
C(13A)-C(14A)	1.399(18)
C(13A)-H(13A)	0.9900
C(13A)-H(13B)	0.9900
C(13B)-C(14B)	1.59(2)
C(13B)-H(13C)	0.9900
C(13B)-H(13D)	0.9900
C(14A)-C(18A)	1.334(16)
C(14A)-C(15A)	1.514(12)
C(14A)-H(14A)	1.0000
C(14B)-C(18B)	1.556(16)
C(14B)-C(15B)	1.566(17)
C(14B)-H(14B)	1.0000
C(15A)-C(16A)	1.333(10)
C(15A)-C(17A)	1.492(12)
C(15B)-C(16B)	1.320(17)
C(15B)-C(17B)	1.43(2)
C(16A)-H(16A)	0.9500
C(16A)-H(16B)	0.9500

C(16B)-H(16C)	0.9500
C(16B)-H(16D)	0.9500
C(17A)-H(17A)	0.9800
C(17A)-H(17B)	0.9800
C(17A)-H(17C)	0.9800
C(17B)-H(17D)	0.9800
C(17B)-H(17E)	0.9800
C(17B)-H(17F)	0.9800
C(18A)-C(19A)	1.472(13)
C(18A)-H(18A)	0.9900
C(18A)-H(18B)	0.9900
C(18B)-C(19B)	1.541(16)
C(18B)-H(18C)	0.9900
C(18B)-H(18D)	0.9900
C(19A)-H(19A)	0.9900
C(19A)-H(19B)	0.9900
C(19B)-H(19C)	0.9900
C(19B)-H(19D)	0.9900

C(3)-O(2)-C(4)	111.1(2)
C(6)-O(3)-H(3)	109(3)
C(2)-C(1)-C(4)	104.60(19)
C(2)-C(1)-C(8)	115.1(2)
C(4)-C(1)-C(8)	104.8(2)
C(2)-C(1)-H(1)	110.7
C(4)-C(1)-H(1)	110.7
C(8)-C(1)-H(1)	110.7
C(3)-C(2)-C(1)	104.4(2)
C(3)-C(2)-H(2A)	110.9
C(1)-C(2)-H(2A)	110.9

C(3)-C(2)-H(2B)	110.9
C(1)-C(2)-H(2B)	110.9
H(2A)-C(2)-H(2B)	108.9
O(1)-C(3)-O(2)	121.0(3)
O(1)-C(3)-C(2)	127.2(3)
O(2)-C(3)-C(2)	111.9(2)
O(2)-C(4)-C(5)	110.7(2)
O(2)-C(4)-C(1)	106.0(2)
C(5)-C(4)-C(1)	107.1(2)
O(2)-C(4)-H(4)	110.9
C(5)-C(4)-H(4)	110.9
C(1)-C(4)-H(4)	110.9
C(4)-C(5)-C(6)	105.6(2)
C(4)-C(5)-H(5A)	110.6
C(6)-C(5)-H(5A)	110.6
C(4)-C(5)-H(5B)	110.6
C(6)-C(5)-H(5B)	110.6
H(5A)-C(5)-H(5B)	108.7
O(3)-C(6)-C(7)	110.40(19)
O(3)-C(6)-C(5)	106.0(2)
C(7)-C(6)-C(5)	114.0(2)
O(3)-C(6)-C(8)	109.7(2)
C(7)-C(6)-C(8)	113.8(2)
C(5)-C(6)-C(8)	102.43(18)
C(6)-C(7)-H(7A)	109.5
C(6)-C(7)-H(7B)	109.5
H(7A)-C(7)-H(7B)	109.5
C(6)-C(7)-H(7C)	109.5
H(7A)-C(7)-H(7C)	109.5
H(7B)-C(7)-H(7C)	109.5

C(9)-C(8)-C(1)	112.1(2)
C(9)-C(8)-C(6)	115.04(18)
C(1)-C(8)-C(6)	103.40(19)
C(9)-C(8)-H(8)	108.7
C(1)-C(8)-H(8)	108.7
C(6)-C(8)-H(8)	108.7
C(10A)-C(9)-C(8)	132.7(8)
C(10B)-C(9)-C(8)	121.7(7)
C(10A)-C(9)-H(9A)	113.6
C(8)-C(9)-H(9A)	113.6
C(10B)-C(9)-H(9B)	119.1
C(8)-C(9)-H(9B)	119.1
C(9)-C(10A)-C(11A)	127.0(14)
C(9)-C(10A)-H(10A)	116.5
C(11A)-C(10A)-H(10A)	116.5
C(9)-C(10B)-C(11B)	121.8(12)
C(9)-C(10B)-H(10B)	119.1
C(11B)-C(10B)-H(10B)	119.1
C(12A)-C(11A)-C(10A)	120.4(12)
C(12A)-C(11A)-C(19A)	121.2(11)
C(10A)-C(11A)-C(19A)	118.5(12)
C(12B)-C(11B)-C(19B)	116.6(13)
C(12B)-C(11B)-C(10B)	123.4(13)
C(19B)-C(11B)-C(10B)	119.7(14)
C(11A)-C(12A)-C(13A)	122.6(10)
C(11A)-C(12A)-H(12A)	118.7
C(13A)-C(12A)-H(12A)	118.7
C(11B)-C(12B)-C(13B)	124.9(13)
C(11B)-C(12B)-H(12B)	117.6
C(13B)-C(12B)-H(12B)	117.6

C(14A)-C(13A)-C(12A)	112.2(10)
C(14A)-C(13A)-H(13A)	109.2
C(12A)-C(13A)-H(13A)	109.2
C(14A)-C(13A)-H(13B)	109.2
C(12A)-C(13A)-H(13B)	109.2
H(13A)-C(13A)-H(13B)	107.9
C(12B)-C(13B)-C(14B)	115.3(11)
C(12B)-C(13B)-H(13C)	108.4
C(14B)-C(13B)-H(13C)	108.4
C(12B)-C(13B)-H(13D)	108.4
C(14B)-C(13B)-H(13D)	108.4
H(13C)-C(13B)-H(13D)	107.5
C(18A)-C(14A)-C(13A)	121.9(12)
C(18A)-C(14A)-C(15A)	118.7(13)
C(13A)-C(14A)-C(15A)	113.7(13)
C(18A)-C(14A)-H(14A)	98.0
C(13A)-C(14A)-H(14A)	98.0
C(15A)-C(14A)-H(14A)	98.0
C(18B)-C(14B)-C(15B)	110.3(14)
C(18B)-C(14B)-C(13B)	104.6(12)
C(15B)-C(14B)-C(13B)	113.3(14)
C(18B)-C(14B)-H(14B)	109.5
C(15B)-C(14B)-H(14B)	109.5
C(13B)-C(14B)-H(14B)	109.5
C(16A)-C(15A)-C(17A)	120.5(12)
C(16A)-C(15A)-C(14A)	121.0(14)
C(17A)-C(15A)-C(14A)	118.2(11)
C(16B)-C(15B)-C(17B)	127.3(14)
C(16B)-C(15B)-C(14B)	125.0(15)
C(17B)-C(15B)-C(14B)	107.5(14)

C(15A)-C(16A)-H(16A)	120.0
C(15A)-C(16A)-H(16B)	120.0
H(16A)-C(16A)-H(16B)	120.0
C(15B)-C(16B)-H(16C)	120.0
C(15B)-C(16B)-H(16D)	120.0
H(16C)-C(16B)-H(16D)	120.0
C(15A)-C(17A)-H(17A)	109.5
C(15A)-C(17A)-H(17B)	109.5
H(17A)-C(17A)-H(17B)	109.5
C(15A)-C(17A)-H(17C)	109.5
H(17A)-C(17A)-H(17C)	109.5
H(17B)-C(17A)-H(17C)	109.5
C(15B)-C(17B)-H(17D)	109.5
C(15B)-C(17B)-H(17E)	109.5
H(17D)-C(17B)-H(17E)	109.5
C(15B)-C(17B)-H(17F)	109.5
H(17D)-C(17B)-H(17F)	109.5
H(17E)-C(17B)-H(17F)	109.5
C(14A)-C(18A)-C(19A)	120.0(10)
C(14A)-C(18A)-H(18A)	107.3
C(19A)-C(18A)-H(18A)	107.3
C(14A)-C(18A)-H(18B)	107.3
C(19A)-C(18A)-H(18B)	107.3
H(18A)-C(18A)-H(18B)	106.9
C(19B)-C(18B)-C(14B)	105.8(10)
C(19B)-C(18B)-H(18C)	110.6
C(14B)-C(18B)-H(18C)	110.6
C(19B)-C(18B)-H(18D)	110.6
C(14B)-C(18B)-H(18D)	110.6
H(18C)-C(18B)-H(18D)	108.7

C(18A)-C(19A)-C(11A)	114.8(9)
C(18A)-C(19A)-H(19A)	108.6
C(11A)-C(19A)-H(19A)	108.6
C(18A)-C(19A)-H(19B)	108.6
C(11A)-C(19A)-H(19B)	108.6
H(19A)-C(19A)-H(19B)	107.5
C(11B)-C(19B)-C(18B)	119.5(11)
C(11B)-C(19B)-H(19C)	107.4
C(18B)-C(19B)-H(19C)	107.4
C(11B)-C(19B)-H(19D)	107.4
C(18B)-C(19B)-H(19D)	107.4
H(19C)-C(19B)-H(19D)	107.0

Symmetry transformations used to generate equivalent atoms:

Table 4. Anisotropic displacement parameters ($Å^2$x 10^3)for dthatch03_maimone. The anisotropic displacement factor exponent takes the form: $-2\pi^2[h^2a^{*2}U^{11} + ... + 2 h k a^* b^* U^{12}]$

	U^{11}	U^{22}	U^{33}	U^{23}	U^{13}	U^{12}
O(1)	19(1)	103(2)	67(1)	-1(1)	2(1)	-3(1)
O(2)	21(1)	63(1)	56(1)	0(1)	-5(1)	-11(1)
O(3)	24(1)	55(1)	38(1)	-2(1)	2(1)	4(1)
C(1)	19(1)	45(1)	33(1)	-2(1)	1(1)	1(1)
C(2)	22(1)	57(2)	37(1)	-1(1)	-1(1)	3(1)
C(3)	20(1)	73(2)	41(1)	0(1)	-3(1)	-3(1)
C(4)	21(1)	50(2)	42(1)	-2(1)	-3(1)	-4(1)
C(5)	33(1)	45(1)	48(1)	2(1)	-6(1)	-6(1)
C(6)	22(1)	48(1)	36(1)	1(1)	1(1)	-3(1)
C(7)	31(1)	59(2)	40(1)	9(1)	-3(1)	-1(1)

C(8)	18(1)	50(1)	30(1)	-4(1)	0(1)	-2(1)
C(9)	24(1)	47(1)	41(1)	-1(1)	-4(1)	-3(1)
C(10A)	36(3)	43(6)	32(6)	12(4)	-5(4)	4(3)
C(10B)	34(4)	30(5)	23(6)	11(4)	-14(4)	-1(3)
C(11A)	39(5)	44(4)	44(6)	0(4)	-7(4)	-7(3)
C(11B)	45(7)	32(4)	41(6)	4(4)	-12(4)	-2(4)
C(12A)	53(4)	70(6)	75(7)	-25(6)	2(5)	-4(4)
C(12B)	97(9)	39(4)	42(5)	-7(4)	-16(5)	-9(4)
C(13A)	74(5)	64(6)	97(8)	-25(6)	-9(6)	-6(4)
C(13B)	127(10)	47(4)	55(6)	7(4)	-42(6)	-23(5)
C(14A)	83(6)	74(7)	87(8)	-9(6)	-3(6)	-16(5)
C(14B)	99(10)	41(6)	73(7)	13(5)	-49(7)	-25(6)
C(15A)	107(7)	38(5)	161(12)	-1(5)	-70(8)	-15(4)
C(15B)	107(7)	38(5)	161(12)	-1(5)	-70(8)	-15(4)
C(16A)	120(12)	43(6)	183(14)	11(6)	-27(12)	-21(6)
C(16B)	79(9)	40(5)	211(17)	20(6)	-38(10)	-16(5)
C(17A)	102(5)	117(5)	133(6)	-3(5)	-30(5)	-44(4)
C(17B)	102(5)	117(5)	133(6)	-3(5)	-30(5)	-44(4)
C(18A)	71(5)	94(7)	118(7)	-28(6)	1(5)	-33(5)
C(18B)	64(5)	56(5)	76(6)	12(4)	-17(5)	-25(4)
C(19A)	50(4)	60(5)	38(4)	-2(3)	-3(3)	-21(4)
C(19B)	71(8)	52(5)	70(8)	-13(5)	15(5)	-22(5)

Table 5. Hydrogen coordinates (x 10^4) and isotropic displacement parameters ($Å^2$x 10^3) for dthatch03_maimone.

	x	y	z	U(eq)

H(1)	5557	7135	9263	39
H(2A)	7944	6727	8943	46
H(2B)	7603	6759	7206	46
H(4)	6531	8014	9849	45
H(5A)	6238	8495	7029	50
H(5B)	5237	8664	8472	50
H(7A)	2530	7956	5707	65
H(7B)	4184	8224	5162	65
H(7C)	3026	8599	6181	65
H(8)	5685	7392	6173	39
H(9A)	3114	6869	7708	44
H(9B)	3221	6788	7760	44
H(10A)	4567	6438	5291	44
H(10B)	4407	6657	4859	35
H(12A)	3266	5657	4186	79
H(12B)	3487	5746	3669	72
H(13A)	844	5110	3838	94
H(13B)	1743	4775	5131	94
H(13C)	2126	4839	4313	92
H(13D)	1156	5235	3192	92
H(14A)	-587	5558	5204	97
H(14B)	-617	5553	5062	85
H(16A)	-1820	3951	5624	139
H(16B)	79	4114	5480	139
H(16C)	-1031	3804	5654	131
H(16D)	773	4076	5781	131
H(17A)	-3136	5233	6712	176
H(17B)	-3725	4645	5958	176
H(17C)	-3363	5202	4971	176
H(17D)	-2740	4720	3936	176

H(17E)	-2671	5206	5184	176
H(17F)	-3215	4562	5588	176
H(18A)	339	5254	7824	113
H(18B)	-950	5710	7279	113
H(18C)	11	5307	7613	78
H(18D)	1626	5003	7063	78
H(19A)	1839	5968	8116	60
H(19B)	723	6382	7163	60
H(19C)	821	6205	6745	77
H(19D)	2237	5962	7724	77
H(3)	2230(50)	7810(17)	8200(50)	76(13)

Table 6. Torsion angles [°] for dthatch03_maimone.

C(4)-C(1)-C(2)-C(3)	-13.1(3)
C(8)-C(1)-C(2)-C(3)	101.3(2)
C(4)-O(2)-C(3)-O(1)	-179.2(3)
C(4)-O(2)-C(3)-C(2)	0.1(3)
C(1)-C(2)-C(3)-O(1)	-172.1(3)
C(1)-C(2)-C(3)-O(2)	8.6(3)
C(3)-O(2)-C(4)-C(5)	-124.7(2)
C(3)-O(2)-C(4)-C(1)	-8.8(3)
C(2)-C(1)-C(4)-O(2)	13.5(3)
C(8)-C(1)-C(4)-O(2)	-108.0(2)
C(2)-C(1)-C(4)-C(5)	131.7(2)
C(8)-C(1)-C(4)-C(5)	10.2(3)
O(2)-C(4)-C(5)-C(6)	130.6(2)
C(1)-C(4)-C(5)-C(6)	15.4(3)
C(4)-C(5)-C(6)-O(3)	80.2(2)

C(4)-C(5)-C(6)-C(7)	-158.1(2)
C(4)-C(5)-C(6)-C(8)	-34.8(3)
C(2)-C(1)-C(8)-C(9)	89.6(3)
C(4)-C(1)-C(8)-C(9)	-156.1(2)
C(2)-C(1)-C(8)-C(6)	-145.9(2)
C(4)-C(1)-C(8)-C(6)	-31.6(2)
O(3)-C(6)-C(8)-C(9)	51.3(3)
C(7)-C(6)-C(8)-C(9)	-73.0(3)
C(5)-C(6)-C(8)-C(9)	163.5(2)
O(3)-C(6)-C(8)-C(1)	-71.3(2)
C(7)-C(6)-C(8)-C(1)	164.5(2)
C(5)-C(6)-C(8)-C(1)	41.0(2)
C(1)-C(8)-C(9)-C(10A)	-111.0(11)
C(6)-C(8)-C(9)-C(10A)	131.2(10)
C(1)-C(8)-C(9)-C(10B)	-124.0(10)
C(6)-C(8)-C(9)-C(10B)	118.3(10)
C(8)-C(9)-C(10A)-C(11A)	-175.6(11)
C(8)-C(9)-C(10B)-C(11B)	174.9(13)
C(9)-C(10A)-C(11A)-C(12A)	176.8(15)
C(9)-C(10A)-C(11A)-C(19A)	-4(2)
C(9)-C(10B)-C(11B)-C(12B)	-176.6(17)
C(9)-C(10B)-C(11B)-C(19B)	9(3)
C(10A)-C(11A)-C(12A)-C(13A)	177.7(14)
C(19A)-C(11A)-C(12A)-C(13A)	-1(2)
C(19B)-C(11B)-C(12B)-C(13B)	3(2)
C(10B)-C(11B)-C(12B)-C(13B)	-170.8(17)
C(11A)-C(12A)-C(13A)-C(14A)	15(2)
C(11B)-C(12B)-C(13B)-C(14B)	13(2)
C(12A)-C(13A)-C(14A)-C(18A)	-31(2)
C(12A)-C(13A)-C(14A)-C(15A)	176.6(14)

C(12B)-C(13B)-C(14B)-C(18B)	-46.9(15)
C(12B)-C(13B)-C(14B)-C(15B)	-167.1(14)
C(18A)-C(14A)-C(15A)-C(16A)	-112(2)
C(13A)-C(14A)-C(15A)-C(16A)	42(3)
C(18A)-C(14A)-C(15A)-C(17A)	62(3)
C(13A)-C(14A)-C(15A)-C(17A)	-144.7(18)
C(18B)-C(14B)-C(15B)-C(16B)	-57(3)
C(13B)-C(14B)-C(15B)-C(16B)	60(3)
C(18B)-C(14B)-C(15B)-C(17B)	118(2)
C(13B)-C(14B)-C(15B)-C(17B)	-125.0(17)
C(13A)-C(14A)-C(18A)-C(19A)	32(3)
C(15A)-C(14A)-C(18A)-C(19A)	-176.5(13)
C(15B)-C(14B)-C(18B)-C(19B)	-175.6(13)
C(13B)-C(14B)-C(18B)-C(19B)	62.2(13)
C(14A)-C(18A)-C(19A)-C(11A)	-15(2)
C(12A)-C(11A)-C(19A)-C(18A)	0(2)
C(10A)-C(11A)-C(19A)-C(18A)	-178.7(14)
C(12B)-C(11B)-C(19B)-C(18B)	17(2)
C(10B)-C(11B)-C(19B)-C(18B)	-168.2(16)
C(14B)-C(18B)-C(19B)-C(11B)	-52.3(18)

Symmetry transformations used to generate equivalent atoms:

X-ray Crystal Structure Report

A colorless block 0.20 x 0.14 x 0.07 mm in size was mounted on a Cryoloop with Paratone oil. Data were collected in a nitrogen gas stream at 100(2) K using omega scans. Crystal-to-detector distance was 33.00 mm and exposure time was 0.50 seconds per frame at low angles and 1.00 seconds at high angles, using a scan width of 0.5°. Data collection was 100% complete to 74.000° in θ. A total of 53852 reflections were collected covering the indices -23<=h<=23, -8<=k<=9, -43<=l<=43. 10146 reflections were founded to be symmetry independent, with an R_{int} of 0.0454. Indexing and unit cell refinement indicated a body-centered, monoclinic lattice. The space group was found to be I 2 (No. 5). The data were integrated using the CrysAlis^{Pro} 1.171.41.108a software program and scaled using the SCALE3 ABSPACK scaling algorithm. Solution by intrinsic phasing (SHELXT-2015) produced a heavy-atom phasing model consistent with the proposed structure. All non-hydrogen atoms were refined anisotropically by full-matrix least-squares (SHELXL-2014). All hydrogen atoms were placed using a riding model. Their positions were constrained relative to their parent atom using the appropriate HFIX command in SHELXL-2014.

Compound 2.313

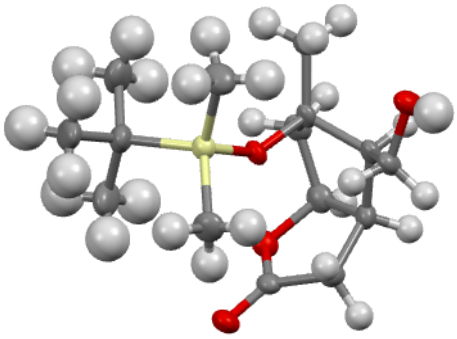


Table 1. Crystal data and structure refinement for DThach04_Maimone.

Identification code	DThach04_Maimone	
Empirical formula	C45 H86 O13 Si3	
Formula weight	919.40	
Temperature	100(2) K	
Wavelength	1.54184 Å	
Crystal system	Monoclinic	
Space group	I 2	
Unit cell dimensions	a = 19.0661(2) Å	α= 90°.
	b = 7.83340(10) Å	β= 91.4080(10)°.
	c = 34.7168(3) Å	γ = 90°.
Volume	5183.47(10) $Å^3$	
Z	4	
Density (calculated)	1.178 Mg/m^3	
Absorption coefficient	1.309 mm^{-1}	
F(000)	2008	
Crystal size	0.200 x 0.140 x 0.070 mm^3	
Theta range for data collection	2.672 to 74.501°.	
Index ranges	-23<=h<=23, -8<=k<=9, -43<=l<=43	
Reflections collected	53852	
Independent reflections	10146 [R(int) = 0.0454]	
Completeness to theta = 74.000°	99.6 %	
Absorption correction	Semi-empirical from equivalents	
Max. and min. transmission	1.00000 and 0.91805	
Refinement method	Full-matrix least-squares on F^2	
Data / restraints / parameters	10146 / 1 / 598	
Goodness-of-fit on F^2	1.071	
Final R indices [I>2sigma(I)]	R1 = 0.0390, wR2 = 0.1041	
R indices (all data)	R1 = 0.0412, wR2 = 0.1057	
Absolute structure parameter	-0.001(13)	

Extinction coefficient	n/a
Largest diff. peak and hole	0.795 and -0.399 e.Å^{-3}

Table 2. Atomic coordinates (x 10^4) and equivalent isotropic displacement parameters (Å^{2}x 10^3) for dthach04_maimone. U(eq) is defined as one third of the trace of the orthogonalized U^{ij} tensor.

	x	y	z	U(eq)
Si(2)	3311(1)	6356(1)	3327(1)	18(1)
Si(3A)	1658(1)	1294(3)	4964(1)	25(1)
Si(1)	9392(1)	8359(1)	3269(1)	29(1)
O(7)	4160(1)	6578(3)	3411(1)	20(1)
O(8)	5160(1)	4686(3)	3950(1)	21(1)
O(12)	3263(1)	2487(3)	5744(1)	24(1)
O(13)	2504(1)	1043(3)	4916(1)	21(1)
O(1)	8787(1)	6915(3)	3333(1)	26(1)
O(10)	4399(1)	1668(3)	4366(1)	23(1)
O(6)	5152(1)	11186(3)	3671(1)	27(1)
O(2)	8476(1)	3656(3)	2925(1)	32(1)
O(9)	4473(1)	5223(3)	4443(1)	32(1)
O(11)	3140(1)	5279(3)	5647(1)	33(1)
O(5)	3606(1)	1947(3)	6707(1)	33(1)
O(4)	7284(1)	9512(4)	3650(1)	38(1)
O(3)	8805(1)	4950(4)	2391(1)	37(1)
C(31)	3721(1)	1076(4)	4477(1)	20(1)
C(35)	3349(1)	3910(4)	5536(1)	22(1)
C(32)	3729(1)	415(4)	4889(1)	20(1)
C(27)	5589(1)	5597(4)	3672(1)	19(1)
C(28)	5534(1)	7514(4)	3773(1)	19(1)
C(7)	8290(1)	6333(4)	3611(1)	23(1)
C(16)	4741(2)	9908(4)	3480(1)	24(1)

C(26)	5282(1)	5379(4)	3265(1)	20(1)
C(38)	3010(1)	-258(4)	5016(1)	19(1)
C(17)	5187(1)	8342(4)	3410(1)	19(1)
C(18)	4788(1)	6901(4)	3200(1)	18(1)
C(29)	5109(2)	7544(4)	4143(1)	25(1)
C(13)	7474(2)	5346(5)	3106(1)	30(1)
C(36)	3618(1)	1032(4)	5575(1)	21(1)
C(30)	4868(1)	5760(4)	4200(1)	22(1)
C(37)	3107(2)	-380(4)	5457(1)	25(1)
C(19)	4639(2)	7292(4)	2776(1)	24(1)
C(33)	3967(1)	1683(4)	5204(1)	21(1)
C(14)	7553(1)	6668(4)	3438(1)	25(1)
C(23)	3305(2)	2964(4)	3575(1)	30(1)
C(25)	3455(2)	3386(5)	2866(1)	27(1)
C(21)	2918(2)	7052(5)	3788(1)	28(1)
C(34)	3716(2)	3527(4)	5168(1)	23(1)
C(11)	8397(2)	4841(5)	2652(1)	29(1)
C(20)	2954(2)	7748(5)	2932(1)	32(1)
C(39)	2808(2)	-1957(4)	4835(1)	28(1)
C(15)	7377(2)	8471(5)	3318(1)	30(1)
C(10)	7960(2)	3858(5)	3228(1)	33(1)
C(22)	3083(1)	4045(4)	3226(1)	21(1)
C(24)	2286(2)	3867(5)	3158(1)	31(1)
C(12)	7752(2)	5894(5)	2711(1)	31(1)
C(9)	8318(2)	4380(4)	3604(1)	31(1)
C(42)	1369(2)	2438(5)	4510(1)	38(1)
C(44)	1761(2)	4168(5)	4481(1)	44(1)
C(8)	8423(2)	7075(5)	4008(1)	32(1)
C(6)	9236(2)	9231(6)	2775(1)	42(1)
C(43)	1539(2)	1368(7)	4158(1)	51(1)

C(4)	10865(2)	8560(8)	3231(1)	60(1)
C(5)	9372(2)	10175(6)	3617(1)	48(1)
C(41)	1503(2)	2604(8)	5401(1)	58(1)
C(1)	10272(2)	7250(6)	3296(1)	42(1)
C(40)	1155(2)	-729(6)	5014(1)	50(1)
C(2)	10380(2)	6410(8)	3693(1)	57(1)
C(45)	572(2)	2829(7)	4518(1)	60(1)
C(3)	10304(2)	5868(7)	2983(1)	61(1)
Si(3B)	1632(4)	978(19)	4783(11)	14(6)

Table 3. Bond lengths [Å] and angles [°] for dthach04_maimone.

Si(2)-O(7)	1.6453(18)
Si(2)-C(21)	1.866(3)
Si(2)-C(20)	1.867(3)
Si(2)-C(22)	1.893(3)
Si(3A)-O(13)	1.638(2)
Si(3A)-C(41)	1.862(6)
Si(3A)-C(40)	1.862(5)
Si(3A)-C(42)	1.884(4)
Si(1)-O(1)	1.634(2)
Si(1)-C(6)	1.864(4)
Si(1)-C(5)	1.866(4)
Si(1)-C(1)	1.890(4)
O(7)-C(18)	1.441(3)
O(8)-C(30)	1.338(3)
O(8)-C(27)	1.465(3)
O(12)-C(35)	1.340(4)
O(12)-C(36)	1.456(3)
O(13)-C(38)	1.440(3)

O(13)-Si(3B)	1.717(14)
O(1)-C(7)	1.443(3)
O(10)-C(31)	1.435(3)
O(10)-H(10)	0.84(5)
O(6)-C(16)	1.423(4)
O(6)-H(6)	0.76(6)
O(2)-C(11)	1.333(4)
O(2)-C(10)	1.467(4)
O(9)-C(30)	1.222(4)
O(11)-C(35)	1.210(4)
O(5)-H(5D)	0.94(6)
O(5)-H(5E)	0.89(6)
O(4)-C(15)	1.425(4)
O(4)-H(4)	0.82(6)
O(3)-C(11)	1.211(4)
C(31)-C(32)	1.522(3)
C(31)-H(31A)	0.9900
C(31)-H(31B)	0.9900
C(35)-C(34)	1.502(4)
C(32)-C(33)	1.536(4)
C(32)-C(38)	1.543(4)
C(32)-H(32)	1.0000
C(27)-C(26)	1.527(4)
C(27)-C(28)	1.546(4)
C(27)-H(27)	1.0000
C(28)-C(29)	1.534(4)
C(28)-C(17)	1.553(4)
C(28)-H(28)	1.0000
C(7)-C(8)	1.513(4)
C(7)-C(9)	1.531(5)

C(7)-C(14)	1.538(4)
C(16)-C(17)	1.516(4)
C(16)-H(16A)	0.9900
C(16)-H(16B)	0.9900
C(26)-C(18)	1.531(4)
C(26)-H(26A)	0.9900
C(26)-H(26B)	0.9900
C(38)-C(39)	1.518(4)
C(38)-C(37)	1.540(4)
C(17)-C(18)	1.534(4)
C(17)-H(17)	1.0000
C(18)-C(19)	1.525(4)
C(29)-C(30)	1.486(4)
C(29)-H(29A)	0.9900
C(29)-H(29B)	0.9900
C(13)-C(10)	1.543(5)
C(13)-C(12)	1.544(4)
C(13)-C(14)	1.554(4)
C(13)-H(13)	1.0000
C(36)-C(37)	1.524(4)
C(36)-C(33)	1.552(4)
C(36)-H(36)	1.0000
C(37)-H(37A)	0.9900
C(37)-H(37B)	0.9900
C(19)-H(19A)	0.9800
C(19)-H(19B)	0.9800
C(19)-H(19C)	0.9800
C(33)-C(34)	1.526(4)
C(33)-H(33)	1.0000
C(14)-C(15)	1.508(5)

C(14)-H(14)	1.0000
C(23)-C(22)	1.530(4)
C(23)-H(23A)	0.9800
C(23)-H(23B)	0.9800
C(23)-H(23C)	0.9800
C(25)-C(22)	1.540(4)
C(25)-H(25A)	0.9800
C(25)-H(25B)	0.9800
C(25)-H(25C)	0.9800
C(21)-H(21A)	0.9800
C(21)-H(21B)	0.9800
C(21)-H(21C)	0.9800
C(34)-H(34A)	0.9900
C(34)-H(34B)	0.9900
C(11)-C(12)	1.498(5)
C(20)-H(20A)	0.9800
C(20)-H(20B)	0.9800
C(20)-H(20C)	0.9800
C(39)-H(39A)	0.9800
C(39)-H(39B)	0.9800
C(39)-H(39C)	0.9800
C(15)-H(15A)	0.9900
C(15)-H(15B)	0.9900
C(10)-C(9)	1.515(5)
C(10)-H(10A)	1.0000
C(22)-C(24)	1.538(4)
C(24)-H(24A)	0.9800
C(24)-H(24B)	0.9800
C(24)-H(24C)	0.9800
C(12)-H(12A)	0.9900

C(12)-H(12B)	0.9900
C(9)-H(9A)	0.9900
C(9)-H(9B)	0.9900
C(42)-C(43)	1.522(6)
C(42)-C(45)	1.552(5)
C(42)-C(44)	1.552(5)
C(44)-H(44A)	0.9800
C(44)-H(44B)	0.9800
C(44)-H(44C)	0.9800
C(8)-H(8A)	0.9800
C(8)-H(8B)	0.9800
C(8)-H(8C)	0.9800
C(6)-H(6A)	0.9800
C(6)-H(6B)	0.9800
C(6)-H(6C)	0.9800
C(43)-H(43A)	0.9800
C(43)-H(43B)	0.9800
C(43)-H(43C)	0.9800
C(4)-C(1)	1.547(6)
C(4)-H(4A)	0.9800
C(4)-H(4B)	0.9800
C(4)-H(4C)	0.9800
C(5)-H(5A)	0.9800
C(5)-H(5B)	0.9800
C(5)-H(5C)	0.9800
C(41)-H(41A)	0.9800
C(41)-H(41B)	0.9800
C(41)-H(41C)	0.9800
C(1)-C(3)	1.535(6)
C(1)-C(2)	1.537(6)

C(40)-H(40A)	0.9800
C(40)-H(40B)	0.9800
C(40)-H(40C)	0.9800
C(2)-H(2A)	0.9800
C(2)-H(2B)	0.9800
C(2)-H(2C)	0.9800
C(45)-H(45A)	0.9800
C(45)-H(45B)	0.9800
C(45)-H(45C)	0.9800
C(3)-H(3A)	0.9800
C(3)-H(3B)	0.9800
C(3)-H(3C)	0.9800

O(7)-Si(2)-C(21)	103.42(12)
O(7)-Si(2)-C(20)	114.06(13)
C(21)-Si(2)-C(20)	108.18(16)
O(7)-Si(2)-C(22)	110.75(12)
C(21)-Si(2)-C(22)	110.08(14)
C(20)-Si(2)-C(22)	110.10(14)
O(13)-Si(3A)-C(41)	108.9(2)
O(13)-Si(3A)-C(40)	114.73(19)
C(41)-Si(3A)-C(40)	107.5(3)
O(13)-Si(3A)-C(42)	103.93(17)
C(41)-Si(3A)-C(42)	111.8(2)
C(40)-Si(3A)-C(42)	110.0(2)
O(1)-Si(1)-C(6)	106.30(15)
O(1)-Si(1)-C(5)	114.52(16)
C(6)-Si(1)-C(5)	108.1(2)
O(1)-Si(1)-C(1)	107.67(17)
C(6)-Si(1)-C(1)	109.54(18)

C(5)-Si(1)-C(1)	110.59(19)
C(18)-O(7)-Si(2)	139.08(16)
C(30)-O(8)-C(27)	111.5(2)
C(35)-O(12)-C(36)	111.7(2)
C(38)-O(13)-Si(3A)	135.71(18)
C(38)-O(13)-Si(3B)	133.0(5)
C(7)-O(1)-Si(1)	141.8(2)
C(31)-O(10)-H(10)	110(3)
C(16)-O(6)-H(6)	107(4)
C(11)-O(2)-C(10)	111.6(3)
H(5D)-O(5)-H(5E)	109(5)
C(15)-O(4)-H(4)	107(4)
O(10)-C(31)-C(32)	111.9(2)
O(10)-C(31)-H(31A)	109.2
C(32)-C(31)-H(31A)	109.2
O(10)-C(31)-H(31B)	109.2
C(32)-C(31)-H(31B)	109.2
H(31A)-C(31)-H(31B)	107.9
O(11)-C(35)-O(12)	121.4(3)
O(11)-C(35)-C(34)	127.7(3)
O(12)-C(35)-C(34)	111.0(3)
C(31)-C(32)-C(33)	116.4(2)
C(31)-C(32)-C(38)	113.4(2)
C(33)-C(32)-C(38)	105.5(2)
C(31)-C(32)-H(32)	107.0
C(33)-C(32)-H(32)	107.0
C(38)-C(32)-H(32)	107.0
O(8)-C(27)-C(26)	110.3(2)
O(8)-C(27)-C(28)	106.4(2)
C(26)-C(27)-C(28)	107.0(2)

O(8)-C(27)-H(27)	111.0
C(26)-C(27)-H(27)	111.0
C(28)-C(27)-H(27)	111.0
C(29)-C(28)-C(27)	104.2(2)
C(29)-C(28)-C(17)	116.7(2)
C(27)-C(28)-C(17)	104.5(2)
C(29)-C(28)-H(28)	110.3
C(27)-C(28)-H(28)	110.3
C(17)-C(28)-H(28)	110.3
O(1)-C(7)-C(8)	113.1(2)
O(1)-C(7)-C(9)	106.4(2)
C(8)-C(7)-C(9)	113.1(3)
O(1)-C(7)-C(14)	107.1(2)
C(8)-C(7)-C(14)	114.9(2)
C(9)-C(7)-C(14)	101.3(3)
O(6)-C(16)-C(17)	109.8(2)
O(6)-C(16)-H(16A)	109.7
C(17)-C(16)-H(16A)	109.7
O(6)-C(16)-H(16B)	109.7
C(17)-C(16)-H(16B)	109.7
H(16A)-C(16)-H(16B)	108.2
C(27)-C(26)-C(18)	105.6(2)
C(27)-C(26)-H(26A)	110.6
C(18)-C(26)-H(26A)	110.6
C(27)-C(26)-H(26B)	110.6
C(18)-C(26)-H(26B)	110.6
H(26A)-C(26)-H(26B)	108.8
O(13)-C(38)-C(39)	111.1(2)
O(13)-C(38)-C(37)	110.3(2)
C(39)-C(38)-C(37)	112.4(2)

O(13)-C(38)-C(32)	106.5(2)
C(39)-C(38)-C(32)	113.5(2)
C(37)-C(38)-C(32)	102.6(2)
C(16)-C(17)-C(18)	113.5(2)
C(16)-C(17)-C(28)	115.9(2)
C(18)-C(17)-C(28)	105.9(2)
C(16)-C(17)-H(17)	107.0
C(18)-C(17)-H(17)	107.0
C(28)-C(17)-H(17)	107.0
O(7)-C(18)-C(19)	112.7(2)
O(7)-C(18)-C(26)	107.7(2)
C(19)-C(18)-C(26)	113.4(2)
O(7)-C(18)-C(17)	107.3(2)
C(19)-C(18)-C(17)	112.9(2)
C(26)-C(18)-C(17)	102.0(2)
C(30)-C(29)-C(28)	105.5(2)
C(30)-C(29)-H(29A)	110.6
C(28)-C(29)-H(29A)	110.6
C(30)-C(29)-H(29B)	110.6
C(28)-C(29)-H(29B)	110.6
H(29A)-C(29)-H(29B)	108.8
C(10)-C(13)-C(12)	103.7(3)
C(10)-C(13)-C(14)	104.6(3)
C(12)-C(13)-C(14)	116.4(3)
C(10)-C(13)-H(13)	110.5
C(12)-C(13)-H(13)	110.5
C(14)-C(13)-H(13)	110.5
O(12)-C(36)-C(37)	112.0(2)
O(12)-C(36)-C(33)	106.9(2)
C(37)-C(36)-C(33)	107.4(2)

O(12)-C(36)-H(36)	110.1
C(37)-C(36)-H(36)	110.1
C(33)-C(36)-H(36)	110.1
O(9)-C(30)-O(8)	120.4(3)
O(9)-C(30)-C(29)	127.8(3)
O(8)-C(30)-C(29)	111.8(2)
C(36)-C(37)-C(38)	106.5(2)
C(36)-C(37)-H(37A)	110.4
C(38)-C(37)-H(37A)	110.4
C(36)-C(37)-H(37B)	110.4
C(38)-C(37)-H(37B)	110.4
H(37A)-C(37)-H(37B)	108.6
C(18)-C(19)-H(19A)	109.5
C(18)-C(19)-H(19B)	109.5
H(19A)-C(19)-H(19B)	109.5
C(18)-C(19)-H(19C)	109.5
H(19A)-C(19)-H(19C)	109.5
H(19B)-C(19)-H(19C)	109.5
C(34)-C(33)-C(32)	117.9(2)
C(34)-C(33)-C(36)	103.8(2)
C(32)-C(33)-C(36)	104.6(2)
C(34)-C(33)-H(33)	110.0
C(32)-C(33)-H(33)	110.0
C(36)-C(33)-H(33)	110.0
C(15)-C(14)-C(7)	117.5(3)
C(15)-C(14)-C(13)	113.8(2)
C(7)-C(14)-C(13)	104.3(2)
C(15)-C(14)-H(14)	106.9
C(7)-C(14)-H(14)	106.9
C(13)-C(14)-H(14)	106.9

C(22)-C(23)-H(23A)	109.5
C(22)-C(23)-H(23B)	109.5
H(23A)-C(23)-H(23B)	109.5
C(22)-C(23)-H(23C)	109.5
H(23A)-C(23)-H(23C)	109.5
H(23B)-C(23)-H(23C)	109.5
C(22)-C(25)-H(25A)	109.5
C(22)-C(25)-H(25B)	109.5
H(25A)-C(25)-H(25B)	109.5
C(22)-C(25)-H(25C)	109.5
H(25A)-C(25)-H(25C)	109.5
H(25B)-C(25)-H(25C)	109.5
Si(2)-C(21)-H(21A)	109.5
Si(2)-C(21)-H(21B)	109.5
H(21A)-C(21)-H(21B)	109.5
Si(2)-C(21)-H(21C)	109.5
H(21A)-C(21)-H(21C)	109.5
H(21B)-C(21)-H(21C)	109.5
C(35)-C(34)-C(33)	105.8(2)
C(35)-C(34)-H(34A)	110.6
C(33)-C(34)-H(34A)	110.6
C(35)-C(34)-H(34B)	110.6
C(33)-C(34)-H(34B)	110.6
H(34A)-C(34)-H(34B)	108.7
O(3)-C(11)-O(2)	121.1(3)
O(3)-C(11)-C(12)	127.4(3)
O(2)-C(11)-C(12)	111.4(3)
Si(2)-C(20)-H(20A)	109.5
Si(2)-C(20)-H(20B)	109.5
H(20A)-C(20)-H(20B)	109.5

Si(2)-C(20)-H(20C)	109.5
H(20A)-C(20)-H(20C)	109.5
H(20B)-C(20)-H(20C)	109.5
C(38)-C(39)-H(39A)	109.5
C(38)-C(39)-H(39B)	109.5
H(39A)-C(39)-H(39B)	109.5
C(38)-C(39)-H(39C)	109.5
H(39A)-C(39)-H(39C)	109.5
H(39B)-C(39)-H(39C)	109.5
O(4)-C(15)-C(14)	110.2(2)
O(4)-C(15)-H(15A)	109.6
C(14)-C(15)-H(15A)	109.6
O(4)-C(15)-H(15B)	109.6
C(14)-C(15)-H(15B)	109.6
H(15A)-C(15)-H(15B)	108.1
O(2)-C(10)-C(9)	110.6(3)
O(2)-C(10)-C(13)	107.0(3)
C(9)-C(10)-C(13)	106.8(3)
O(2)-C(10)-H(10A)	110.8
C(9)-C(10)-H(10A)	110.8
C(13)-C(10)-H(10A)	110.8
C(23)-C(22)-C(24)	109.0(2)
C(23)-C(22)-C(25)	109.4(3)
C(24)-C(22)-C(25)	108.5(2)
C(23)-C(22)-Si(2)	108.9(2)
C(24)-C(22)-Si(2)	109.7(2)
C(25)-C(22)-Si(2)	111.3(2)
C(22)-C(24)-H(24A)	109.5
C(22)-C(24)-H(24B)	109.5
H(24A)-C(24)-H(24B)	109.5

C(22)-C(24)-H(24C)	109.5
H(24A)-C(24)-H(24C)	109.5
H(24B)-C(24)-H(24C)	109.5
C(11)-C(12)-C(13)	105.6(3)
C(11)-C(12)-H(12A)	110.6
C(13)-C(12)-H(12A)	110.6
C(11)-C(12)-H(12B)	110.6
C(13)-C(12)-H(12B)	110.6
H(12A)-C(12)-H(12B)	108.7
C(10)-C(9)-C(7)	105.5(3)
C(10)-C(9)-H(9A)	110.6
C(7)-C(9)-H(9A)	110.6
C(10)-C(9)-H(9B)	110.6
C(7)-C(9)-H(9B)	110.6
H(9A)-C(9)-H(9B)	108.8
C(43)-C(42)-C(45)	110.5(3)
C(43)-C(42)-C(44)	108.5(3)
C(45)-C(42)-C(44)	107.6(4)
C(43)-C(42)-Si(3A)	110.2(3)
C(45)-C(42)-Si(3A)	110.2(3)
C(44)-C(42)-Si(3A)	109.7(3)
C(42)-C(44)-H(44A)	109.5
C(42)-C(44)-H(44B)	109.5
H(44A)-C(44)-H(44B)	109.5
C(42)-C(44)-H(44C)	109.5
H(44A)-C(44)-H(44C)	109.5
H(44B)-C(44)-H(44C)	109.5
C(7)-C(8)-H(8A)	109.5
C(7)-C(8)-H(8B)	109.5
H(8A)-C(8)-H(8B)	109.5

C(7)-C(8)-H(8C)	109.5
H(8A)-C(8)-H(8C)	109.5
H(8B)-C(8)-H(8C)	109.5
Si(1)-C(6)-H(6A)	109.5
Si(1)-C(6)-H(6B)	109.5
H(6A)-C(6)-H(6B)	109.5
Si(1)-C(6)-H(6C)	109.5
H(6A)-C(6)-H(6C)	109.5
H(6B)-C(6)-H(6C)	109.5
C(42)-C(43)-H(43A)	109.5
C(42)-C(43)-H(43B)	109.5
H(43A)-C(43)-H(43B)	109.5
C(42)-C(43)-H(43C)	109.5
H(43A)-C(43)-H(43C)	109.5
H(43B)-C(43)-H(43C)	109.5
C(1)-C(4)-H(4A)	109.5
C(1)-C(4)-H(4B)	109.5
H(4A)-C(4)-H(4B)	109.5
C(1)-C(4)-H(4C)	109.5
H(4A)-C(4)-H(4C)	109.5
H(4B)-C(4)-H(4C)	109.5
Si(1)-C(5)-H(5A)	109.5
Si(1)-C(5)-H(5B)	109.5
H(5A)-C(5)-H(5B)	109.5
Si(1)-C(5)-H(5C)	109.5
H(5A)-C(5)-H(5C)	109.5
H(5B)-C(5)-H(5C)	109.5
Si(3A)-C(41)-H(41A)	109.5
Si(3A)-C(41)-H(41B)	109.5
H(41A)-C(41)-H(41B)	109.5

Si(3A)-C(41)-H(41C)	109.5
H(41A)-C(41)-H(41C)	109.5
H(41B)-C(41)-H(41C)	109.5
C(3)-C(1)-C(2)	109.0(4)
C(3)-C(1)-C(4)	108.9(4)
C(2)-C(1)-C(4)	109.4(3)
C(3)-C(1)-Si(1)	109.9(2)
C(2)-C(1)-Si(1)	109.8(2)
C(4)-C(1)-Si(1)	109.8(3)
Si(3A)-C(40)-H(40A)	109.5
Si(3A)-C(40)-H(40B)	109.5
H(40A)-C(40)-H(40B)	109.5
Si(3A)-C(40)-H(40C)	109.5
H(40A)-C(40)-H(40C)	109.5
H(40B)-C(40)-H(40C)	109.5
C(1)-C(2)-H(2A)	109.5
C(1)-C(2)-H(2B)	109.5
H(2A)-C(2)-H(2B)	109.5
C(1)-C(2)-H(2C)	109.5
H(2A)-C(2)-H(2C)	109.5
H(2B)-C(2)-H(2C)	109.5
C(42)-C(45)-H(45A)	109.5
C(42)-C(45)-H(45B)	109.5
H(45A)-C(45)-H(45B)	109.5
C(42)-C(45)-H(45C)	109.5
H(45A)-C(45)-H(45C)	109.5
H(45B)-C(45)-H(45C)	109.5
C(1)-C(3)-H(3A)	109.5
C(1)-C(3)-H(3B)	109.5
H(3A)-C(3)-H(3B)	109.5

C(1)-C(3)-H(3C)	109.5
H(3A)-C(3)-H(3C)	109.5
H(3B)-C(3)-H(3C)	109.5

Symmetry transformations used to generate equivalent atoms:

Table 4. Anisotropic displacement parameters ($Å^2 x\ 10^3$)for dthach04_maimone. The anisotropic displacement factor exponent takes the form: $-2\pi^2[\ h^2 a^{*2} U^{11} + ... + 2\ h\ k\ a^*\ b^*\ U^{12}\ ]$

	U^{11}	U^{22}	U^{33}	U^{23}	U^{13}	U^{12}
Si(2)	17(1)	22(1)	15(1)	0(1)	0(1)	2(1)
Si(3A)	18(1)	38(1)	19(1)	-1(1)	1(1)	-5(1)
Si(1)	26(1)	32(1)	27(1)	1(1)	2(1)	-2(1)
O(7)	18(1)	24(1)	17(1)	1(1)	1(1)	-1(1)
O(8)	28(1)	17(1)	19(1)	1(1)	4(1)	-1(1)
O(12)	31(1)	22(1)	18(1)	-1(1)	5(1)	1(1)
O(13)	20(1)	23(1)	20(1)	2(1)	1(1)	-1(1)
O(1)	24(1)	29(1)	25(1)	0(1)	9(1)	-2(1)
O(10)	20(1)	28(1)	22(1)	-1(1)	5(1)	-2(1)
O(6)	32(1)	20(1)	29(1)	-7(1)	6(1)	-2(1)
O(2)	35(1)	26(1)	34(1)	-3(1)	4(1)	3(1)
O(9)	40(1)	29(1)	27(1)	2(1)	14(1)	-6(1)
O(11)	47(1)	24(1)	28(1)	-3(1)	6(1)	5(1)
O(5)	29(1)	30(1)	39(1)	0(1)	4(1)	1(1)
O(4)	47(1)	41(2)	26(1)	-2(1)	4(1)	15(1)
O(3)	38(1)	48(2)	25(1)	-6(1)	5(1)	4(1)
C(31)	20(1)	24(2)	16(1)	-3(1)	1(1)	-1(1)
C(35)	24(1)	24(2)	19(1)	1(1)	-1(1)	-2(1)
C(32)	20(1)	22(2)	17(1)	-1(1)	0(1)	2(1)

C(27)	17(1)	22(2)	18(1)	1(1)	2(1)	-1(1)
C(28)	20(1)	19(2)	18(1)	0(1)	0(1)	-3(1)
C(7)	21(1)	28(2)	22(1)	6(1)	7(1)	-1(1)
C(16)	26(1)	20(2)	26(1)	-1(1)	2(1)	2(1)
C(26)	21(1)	19(2)	20(1)	-3(1)	1(1)	2(1)
C(38)	23(1)	18(2)	17(1)	1(1)	0(1)	1(1)
C(17)	20(1)	18(1)	18(1)	-1(1)	2(1)	1(1)
C(18)	17(1)	22(2)	16(1)	-1(1)	4(1)	-1(1)
C(29)	37(2)	20(2)	18(1)	-2(1)	6(1)	-4(1)
C(13)	20(1)	36(2)	32(2)	-3(1)	2(1)	-1(1)
C(36)	27(1)	20(2)	15(1)	1(1)	-2(1)	3(1)
C(30)	24(1)	23(2)	18(1)	0(1)	0(1)	-1(1)
C(37)	34(2)	23(2)	18(1)	3(1)	-2(1)	-5(1)
C(19)	27(1)	26(2)	18(1)	1(1)	1(1)	1(1)
C(33)	18(1)	27(2)	17(1)	-2(1)	-1(1)	-1(1)
C(14)	22(1)	31(2)	23(1)	4(1)	7(1)	1(1)
C(23)	33(2)	26(2)	30(2)	4(1)	-2(1)	1(1)
C(25)	28(1)	30(2)	24(1)	-9(1)	-1(1)	-1(1)
C(21)	24(1)	35(2)	25(1)	-7(1)	5(1)	-1(1)
C(34)	30(1)	23(2)	16(1)	0(1)	0(1)	-4(1)
C(11)	30(2)	34(2)	23(1)	-7(1)	-1(1)	-1(1)
C(20)	26(2)	38(2)	31(2)	9(1)	-3(1)	5(1)
C(39)	37(2)	22(2)	25(1)	-5(1)	0(1)	-7(1)
C(15)	31(1)	36(2)	23(1)	-1(1)	5(1)	9(1)
C(10)	34(2)	29(2)	37(2)	3(1)	6(1)	-6(1)
C(22)	20(1)	28(2)	17(1)	-4(1)	0(1)	0(1)
C(24)	24(1)	40(2)	28(1)	-6(1)	-1(1)	-6(1)
C(12)	29(1)	39(2)	25(1)	-4(1)	-3(1)	4(1)
C(9)	37(2)	27(2)	29(2)	8(1)	6(1)	2(1)
C(42)	25(2)	46(2)	42(2)	7(2)	-3(1)	-3(1)

C(44)	35(2)	37(2)	60(2)	13(2)	2(2)	-2(2)
C(8)	33(2)	38(2)	24(1)	1(1)	2(1)	5(1)
C(6)	46(2)	46(2)	35(2)	13(2)	4(1)	-10(2)
C(43)	57(2)	68(3)	26(2)	9(2)	-7(1)	-14(2)
C(4)	27(2)	106(4)	48(2)	-10(3)	3(2)	-16(2)
C(5)	55(2)	40(2)	48(2)	-10(2)	5(2)	-10(2)
C(41)	32(2)	97(4)	44(2)	-30(2)	3(2)	2(2)
C(1)	24(2)	65(3)	38(2)	-5(2)	0(1)	2(2)
C(40)	30(2)	64(3)	55(2)	26(2)	-4(2)	-15(2)
C(2)	37(2)	80(4)	54(2)	12(2)	-5(2)	16(2)
C(45)	23(2)	90(4)	68(3)	38(3)	-1(2)	7(2)
C(3)	36(2)	79(4)	67(3)	-24(2)	-4(2)	21(2)
Si(3B)	6(4)	15(6)	20(15)	0(5)	-3(4)	-4(3)

Table 5. Hydrogen coordinates (x 10^4) and isotropic displacement parameters ($Å^2$x 10^3) for dthach04_maimone.

	x	y	z	U(eq)
H(31A)	3565	150	4300	24
H(31B)	3379	2023	4452	24
H(32)	4062	-570	4901	23
H(27)	6087	5201	3688	23
H(28)	6012	8006	3823	23
H(16A)	4555	10357	3232	29
H(16B)	4338	9597	3641	29
H(26A)	5020	4291	3242	24
H(26B)	5658	5383	3074	24

H(17)	5575	8703	3239	22
H(29A)	5405	7925	4365	30
H(29B)	4704	8327	4114	30
H(13)	6977	4948	3079	35
H(36)	3983	577	5760	25
H(37A)	2652	-220	5584	30
H(37B)	3299	-1510	5531	30
H(19A)	4424	6292	2651	35
H(19B)	5079	7568	2650	35
H(19C)	4318	8266	2754	35
H(33)	4490	1651	5237	25
H(14)	7211	6336	3638	30
H(23A)	3810	3100	3625	44
H(23B)	3200	1761	3522	44
H(23C)	3048	3339	3801	44
H(25A)	3338	4125	2646	41
H(25B)	3299	2218	2809	41
H(25C)	3963	3395	2914	41
H(21A)	3130	6405	4002	42
H(21B)	2411	6844	3776	42
H(21C)	3006	8273	3827	42
H(34A)	4119	4307	5136	28
H(34B)	3390	3658	4944	28
H(20A)	3144	8904	2962	48
H(20B)	2441	7788	2944	48
H(20C)	3088	7284	2683	48
H(39A)	2414	-2451	4972	42
H(39B)	3210	-2737	4851	42
H(39C)	2671	-1781	4564	42
H(15A)	7761	8941	3163	36

H(15B)	6942	8475	3157	36
H(10A)	7685	2783	3261	40
H(24A)	2041	4340	3378	46
H(24B)	2165	2658	3127	46
H(24C)	2144	4489	2923	46
H(12A)	7397	5671	2504	37
H(12B)	7868	7126	2711	37
H(9A)	8810	3975	3615	37
H(9B)	8068	3898	3826	37
H(44A)	1615	4923	4690	66
H(44B)	1647	4703	4232	66
H(44C)	2268	3972	4504	66
H(8A)	8894	6755	4102	47
H(8B)	8074	6629	4185	47
H(8C)	8386	8322	3996	47
H(6A)	9146	8289	2595	63
H(6B)	9651	9867	2696	63
H(6C)	8829	9995	2775	63
H(43A)	2048	1247	4141	76
H(43B)	1352	1931	3926	76
H(43C)	1325	236	4182	76
H(4A)	10813	9047	2972	90
H(4B)	11321	7988	3257	90
H(4C)	10837	9473	3423	90
H(5A)	8892	10618	3630	72
H(5B)	9685	11083	3530	72
H(5C)	9528	9778	3872	72
H(41A)	1627	1938	5632	86
H(41B)	1007	2930	5408	86
H(41C)	1794	3635	5395	86

H(40A)	1202	-1418	4780	75
H(40B)	659	-465	5051	75
H(40C)	1339	-1370	5237	75
H(2A)	10306	7260	3895	86
H(2B)	10858	5960	3717	86
H(2C)	10043	5475	3720	86
H(45A)	313	1775	4569	90
H(45B)	416	3299	4268	90
H(45C)	481	3662	4721	90
H(3A)	9933	5025	3023	91
H(3B)	10762	5302	2997	91
H(3C)	10237	6396	2729	91
H(5D)	3650(30)	1370(80)	6943(16)	69(15)
H(5E)	4010(30)	1860(80)	6584(16)	67(16)
H(6)	4930(30)	11530(80)	3832(15)	68(17)
H(10)	4420(20)	2740(70)	4396(13)	47(14)
H(4)	7020(30)	10300(80)	3583(16)	74(18)

Table 6. Torsion angles [°] for dthach04_maimone.

C(21)-Si(2)-O(7)-C(18)	-152.4(3)
C(20)-Si(2)-O(7)-C(18)	-35.2(3)
C(22)-Si(2)-O(7)-C(18)	89.7(3)
C(41)-Si(3A)-O(13)-C(38)	97.0(3)
C(40)-Si(3A)-O(13)-C(38)	-23.6(4)
C(42)-Si(3A)-O(13)-C(38)	-143.7(3)
C(6)-Si(1)-O(1)-C(7)	-134.8(3)
C(5)-Si(1)-O(1)-C(7)	-15.6(4)
C(1)-Si(1)-O(1)-C(7)	107.9(3)

C(36)-O(12)-C(35)-O(11)	-174.1(3)
C(36)-O(12)-C(35)-C(34)	6.6(3)
O(10)-C(31)-C(32)-C(33)	58.2(3)
O(10)-C(31)-C(32)-C(38)	-179.1(2)
C(30)-O(8)-C(27)-C(26)	-116.3(2)
C(30)-O(8)-C(27)-C(28)	-0.6(3)
O(8)-C(27)-C(28)-C(29)	5.2(3)
C(26)-C(27)-C(28)-C(29)	123.1(2)
O(8)-C(27)-C(28)-C(17)	-117.8(2)
C(26)-C(27)-C(28)-C(17)	0.1(3)
Si(1)-O(1)-C(7)-C(8)	-13.7(4)
Si(1)-O(1)-C(7)-C(9)	-138.4(3)
Si(1)-O(1)-C(7)-C(14)	113.9(3)
O(8)-C(27)-C(26)-C(18)	92.0(3)
C(28)-C(27)-C(26)-C(18)	-23.3(3)
Si(3A)-O(13)-C(38)-C(39)	57.4(4)
Si(3B)-O(13)-C(38)-C(39)	25.0(18)
Si(3A)-O(13)-C(38)-C(37)	-67.9(4)
Si(3B)-O(13)-C(38)-C(37)	-100.3(18)
Si(3A)-O(13)-C(38)-C(32)	-178.5(3)
Si(3B)-O(13)-C(38)-C(32)	149.1(18)
C(31)-C(32)-C(38)-O(13)	-49.6(3)
C(33)-C(32)-C(38)-O(13)	78.9(2)
C(31)-C(32)-C(38)-C(39)	73.0(3)
C(33)-C(32)-C(38)-C(39)	-158.5(2)
C(31)-C(32)-C(38)-C(37)	-165.5(2)
C(33)-C(32)-C(38)-C(37)	-37.0(3)
O(6)-C(16)-C(17)-C(18)	-179.3(2)
O(6)-C(16)-C(17)-C(28)	57.8(3)
C(29)-C(28)-C(17)-C(16)	35.6(4)

C(27)-C(28)-C(17)-C(16)	150.0(2)
C(29)-C(28)-C(17)-C(18)	-91.2(3)
C(27)-C(28)-C(17)-C(18)	23.2(3)
Si(2)-O(7)-C(18)-C(19)	6.0(4)
Si(2)-O(7)-C(18)-C(26)	-119.9(3)
Si(2)-O(7)-C(18)-C(17)	130.9(2)
C(27)-C(26)-C(18)-O(7)	-75.7(3)
C(27)-C(26)-C(18)-C(19)	158.8(2)
C(27)-C(26)-C(18)-C(17)	37.1(3)
C(16)-C(17)-C(18)-O(7)	-52.3(3)
C(28)-C(17)-C(18)-O(7)	75.9(2)
C(16)-C(17)-C(18)-C(19)	72.5(3)
C(28)-C(17)-C(18)-C(19)	-159.2(2)
C(16)-C(17)-C(18)-C(26)	-165.4(2)
C(28)-C(17)-C(18)-C(26)	-37.2(2)
C(27)-C(28)-C(29)-C(30)	-7.5(3)
C(17)-C(28)-C(29)-C(30)	107.1(3)
C(35)-O(12)-C(36)-C(37)	-118.2(2)
C(35)-O(12)-C(36)-C(33)	-0.8(3)
C(27)-O(8)-C(30)-O(9)	177.4(3)
C(27)-O(8)-C(30)-C(29)	-4.6(3)
C(28)-C(29)-C(30)-O(9)	-174.4(3)
C(28)-C(29)-C(30)-O(8)	7.8(3)
O(12)-C(36)-C(37)-C(38)	102.9(3)
C(33)-C(36)-C(37)-C(38)	-14.2(3)
O(13)-C(38)-C(37)-C(36)	-81.8(3)
C(39)-C(38)-C(37)-C(36)	153.6(2)
C(32)-C(38)-C(37)-C(36)	31.3(3)
C(31)-C(32)-C(33)-C(34)	40.6(3)
C(38)-C(32)-C(33)-C(34)	-86.1(3)

C(31)-C(32)-C(33)-C(36)	155.2(2)
C(38)-C(32)-C(33)-C(36)	28.5(3)
O(12)-C(36)-C(33)-C(34)	-5.0(3)
C(37)-C(36)-C(33)-C(34)	115.4(2)
O(12)-C(36)-C(33)-C(32)	-129.2(2)
C(37)-C(36)-C(33)-C(32)	-8.8(3)
O(1)-C(7)-C(14)-C(15)	-56.3(3)
C(8)-C(7)-C(14)-C(15)	70.2(3)
C(9)-C(7)-C(14)-C(15)	-167.6(2)
O(1)-C(7)-C(14)-C(13)	70.7(3)
C(8)-C(7)-C(14)-C(13)	-162.8(3)
C(9)-C(7)-C(14)-C(13)	-40.5(3)
C(10)-C(13)-C(14)-C(15)	156.2(3)
C(12)-C(13)-C(14)-C(15)	42.4(4)
C(10)-C(13)-C(14)-C(7)	26.9(3)
C(12)-C(13)-C(14)-C(7)	-86.9(3)
O(11)-C(35)-C(34)-C(33)	171.1(3)
O(12)-C(35)-C(34)-C(33)	-9.7(3)
C(32)-C(33)-C(34)-C(35)	123.6(2)
C(36)-C(33)-C(34)-C(35)	8.5(3)
C(10)-O(2)-C(11)-O(3)	175.0(3)
C(10)-O(2)-C(11)-C(12)	-6.8(4)
C(7)-C(14)-C(15)-O(4)	-72.8(3)
C(13)-C(14)-C(15)-O(4)	164.9(2)
C(11)-O(2)-C(10)-C(9)	-112.8(3)
C(11)-O(2)-C(10)-C(13)	3.2(3)
C(12)-C(13)-C(10)-O(2)	1.6(3)
C(14)-C(13)-C(10)-O(2)	-120.9(3)
C(12)-C(13)-C(10)-C(9)	120.0(3)
C(14)-C(13)-C(10)-C(9)	-2.5(3)

O(7)-Si(2)-C(22)-C(23)	59.5(2)
C(21)-Si(2)-C(22)-C(23)	-54.2(2)
C(20)-Si(2)-C(22)-C(23)	-173.4(2)
O(7)-Si(2)-C(22)-C(24)	178.74(18)
C(21)-Si(2)-C(22)-C(24)	65.0(2)
C(20)-Si(2)-C(22)-C(24)	-54.2(2)
O(7)-Si(2)-C(22)-C(25)	-61.1(2)
C(21)-Si(2)-C(22)-C(25)	-174.88(19)
C(20)-Si(2)-C(22)-C(25)	65.9(2)
O(3)-C(11)-C(12)-C(13)	-174.4(3)
O(2)-C(11)-C(12)-C(13)	7.6(4)
C(10)-C(13)-C(12)-C(11)	-5.1(3)
C(14)-C(13)-C(12)-C(11)	109.1(3)
O(2)-C(10)-C(9)-C(7)	93.1(3)
C(13)-C(10)-C(9)-C(7)	-23.1(3)
O(1)-C(7)-C(9)-C(10)	-72.5(3)
C(8)-C(7)-C(9)-C(10)	162.8(2)
C(14)-C(7)-C(9)-C(10)	39.3(3)
O(13)-Si(3A)-C(42)-C(43)	59.7(3)
C(41)-Si(3A)-C(42)-C(43)	177.0(3)
C(40)-Si(3A)-C(42)-C(43)	-63.6(3)
O(13)-Si(3A)-C(42)-C(45)	-178.1(3)
C(41)-Si(3A)-C(42)-C(45)	-60.7(4)
C(40)-Si(3A)-C(42)-C(45)	58.6(4)
O(13)-Si(3A)-C(42)-C(44)	-59.7(3)
C(41)-Si(3A)-C(42)-C(44)	57.6(3)
C(40)-Si(3A)-C(42)-C(44)	177.0(3)
O(1)-Si(1)-C(1)-C(3)	59.4(4)
C(6)-Si(1)-C(1)-C(3)	-55.8(4)
C(5)-Si(1)-C(1)-C(3)	-174.8(3)

O(1)-Si(1)-C(1)-C(2)	-60.5(3)
C(6)-Si(1)-C(1)-C(2)	-175.7(3)
C(5)-Si(1)-C(1)-C(2)	65.3(4)
O(1)-Si(1)-C(1)-C(4)	179.1(2)
C(6)-Si(1)-C(1)-C(4)	64.0(3)
C(5)-Si(1)-C(1)-C(4)	-55.1(3)

Symmetry transformations used to generate equivalent atoms: